ASTROCYTES Ca^{2+} SIGNALING IN THE MODULATION OF NEURAL NETWORKS EXCITABILITY AND SYNAPTIC TRANSMISSIONS

EDITED BY: Wannan Tang, Leonid Savtchenko, Yu-Wei Wu and Rolf Sprengel
PUBLISHED IN: Frontiers in Cellular Neuroscience

frontiers Research Topics

ISSN 1664-8714
ISBN 978-2-88976-101-2
DOI 10.3389/978-2-88976-101-2

About Frontiers

Frontiers is more than just an open-access publisher of scholarly articles: it is a pioneering approach to the world of academia, radically improving the way scholarly research is managed. The grand vision of Frontiers is a world where all people have an equal opportunity to seek, share and generate knowledge. Frontiers provides immediate and permanent online open access to all its publications, but this alone is not enough to realize our grand goals.

Frontiers Journal Series

The Frontiers Journal Series is a multi-tier and interdisciplinary set of open-access, online journals, promising a paradigm shift from the current review, selection and dissemination processes in academic publishing. All Frontiers journals are driven by researchers for researchers; therefore, they constitute a service to the scholarly community. At the same time, the Frontiers Journal Series operates on a revolutionary invention, the tiered publishing system, initially addressing specific communities of scholars, and gradually climbing up to broader public understanding, thus serving the interests of the lay society, too.

Dedication to Quality

Each Frontiers article is a landmark of the highest quality, thanks to genuinely collaborative interactions between authors and review editors, who include some of the world's best academicians. Research must be certified by peers before entering a stream of knowledge that may eventually reach the public - and shape society; therefore, Frontiers only applies the most rigorous and unbiased reviews.
Frontiers revolutionizes research publishing by freely delivering the most outstanding research, evaluated with no bias from both the academic and social point of view. By applying the most advanced information technologies, Frontiers is catapulting scholarly publishing into a new generation.

What are Frontiers Research Topics?

Frontiers Research Topics are very popular trademarks of the Frontiers Journals Series: they are collections of at least ten articles, all centered on a particular subject. With their unique mix of varied contributions from Original Research to Review Articles, Frontiers Research Topics unify the most influential researchers, the latest key findings and historical advances in a hot research area! Find out more on how to host your own Frontiers Research Topic or contribute to one as an author by contacting the Frontiers Editorial Office: frontiersin.org/about/contact

ASTROCYTES Ca^{2+} SIGNALING IN THE MODULATION OF NEURAL NETWORKS EXCITABILITY AND SYNAPTIC TRANSMISSIONS

Topic Editors:
Wannan Tang, Norwegian University of Science and Technology, Norway
Leonid Savtchenko, University College London, United Kingdom
Yu-Wei Wu, Institute of Molecular Biology, Academia Sinica, Taiwan
Rolf Sprengel, Max Planck Institute for Medical Research (MPIMF), Germany

Citation: Tang, W., Savtchenko, L., Wu, Y.-W., Sprengel, R., eds. (2022). Astrocytes Ca^{2+} Signaling in the Modulation of Neural Networks Excitability and Synaptic Transmissions. Lausanne: Frontiers Media SA. doi: 10.3389/978-2-88976-101-2

Table of Contents

frontiers in Cellular Neuroscience

MINI REVIEW
published: 26 November 2020
doi: 10.3389/fncel.2020.609947

The Paradox of Astroglial Ca^{2+} Signals at the Interface of Excitation and Inhibition

Laura C. Caudal†‡, Davide Gobbo†‡, Anja Scheller‡ and Frank Kirchhoff‡*

Department of Molecular Physiology, Center for Integrative Physiology and Molecular Medicine, University of Saarland, Homburg, Germany

OPEN ACCESS

Edited by:
Wannan Tang,
University of Oslo, Norway

Reviewed by:
Yuriy Pankratov,
University of Warwick,
United Kingdom
Hyungju Park,
Korea Brain Research Institute,
South Korea

****Correspondence:***
Frank Kirchhoff
frank.kirchhoff@uks.eu

† These authors have contributed equally to this work

‡ORCID:
Laura C. Caudal
orcid.org/0000-0003-2165-281X
Davide Gobbo
orcid.org/0000-0002-4076-2697
Anja Scheller
orcid.org/0000-0001-8955-2634
Frank Kirchhoff
orcid.org/0000-0002-2324-2761

Specialty section:
This article was submitted to Non-Neuronal Cells, a section of the journal Frontiers in Cellular Neuroscience

Received: *24 September 2020*
Accepted: *03 November 2020*
Published: *26 November 2020*

Citation:
Caudal LC, Gobbo D, Scheller A and Kirchhoff F (2020) The Paradox of Astroglial Ca^{2+} Signals at the Interface of Excitation and Inhibition. Front. Cell. Neurosci. 14:609947. doi: 10.3389/fncel.2020.609947

Astroglial networks constitute a non-neuronal communication system in the brain and are acknowledged modulators of synaptic plasticity. A sophisticated set of transmitter receptors in combination with distinct secretion mechanisms enables astrocytes to sense and modulate synaptic transmission. This integrative function evolved around intracellular Ca^{2+} signals, by and large considered as the main indicator of astrocyte activity. Regular brain physiology meticulously relies on the constant reciprocity of excitation and inhibition (E/I). Astrocytes are metabolically, physically, and functionally associated to the E/I convergence. Metabolically, astrocytes provide glutamine, the precursor of both major neurotransmitters governing E/I in the central nervous system (CNS): glutamate and γ-aminobutyric acid (GABA). Perisynaptic astroglial processes are structurally and functionally associated with the respective circuits throughout the CNS. Astonishingly, in astrocytes, glutamatergic as well as GABAergic inputs elicit similar rises in intracellular Ca^{2+} that in turn can trigger the release of glutamate and GABA as well. Paradoxically, as gliotransmitters, these two molecules can thus strengthen, weaken or even reverse the input signal. Therefore, the net impact on neuronal network function is often convoluted and cannot be simply predicted by the nature of the stimulus itself. In this review, we highlight the ambiguity of astrocytes on discriminating and affecting synaptic activity in physiological and pathological state. Indeed, aberrant astroglial Ca^{2+} signaling is a key aspect of pathological conditions exhibiting compromised network excitability, such as epilepsy. Here, we gather recent evidence on the complexity of astroglial Ca^{2+} signals in health and disease, challenging the traditional, neuro-centric concept of segregating E/I, in favor of a non-binary, mutually dependent perspective on glutamatergic and GABAergic transmission.

Keywords: astrocyte, Ca^{2+}, glutamate, γ-aminobutyric acid, epilepsy, gliotransmission, network plasticity

INTRODUCTION

The path that led the scientific community to agree upon the role of astrocytes in actively tuning and modulating brain activity has been one of the most challenging and fertile fields in neuroscience for the last decades. It is now widely accepted that astrocytes can sense, react to and modify the extracellular transmitter *milieu* both quantitatively and qualitatively, thus contributing to neural network excitability and functioning. Nevertheless, little is still known about the exact molecular mechanisms of the astrocytic response and contribution to synaptic transmission. Most studies

have been characterizing astrocytes in terms of their inputs and outputs, without precise knowledge of their inner working, thus regarding them as *black boxes*. Nowadays, internal Ca^{2+} oscillations are by far considered the main read-out of astrocytic activity (Bazargani and Attwell, 2016) and are known to be induced, among others, by binding of neurotransmitters to astroglial membrane receptors and to eventually lead to the release of gliotransmitters in the extracellular space. These include glutamate (Parpura et al., 1994; Pasti et al., 1997; Kang et al., 1998; Parri et al., 2001; Angulo et al., 2004; Fellin et al., 2004), ATP (Pascual et al., 2005; Serrano et al., 2006), D-serine (Henneberger et al., 2010) and γ-aminobutyric acid (GABA; Liu et al., 2000; Kozlov et al., 2006; Lee et al., 2010; Jiménez-González et al., 2011). In this review we point out that a pile of evidence is building up against a simplistic way of considering astrocytic Ca^{2+} response as a linear and stereotypical process. In order to understand the brain, it is essential to regard astrocytes as active information integrators and processors.

ASTROGLIAL Ca^{2+} DYNAMICS AT THE INTERFACE OF GLUTAMATERGIC AND GABAERGIC SIGNALING

The astroglial role as mere responders to neuronal firing was challenged by the fact that astrocytes exhibited internal Ca^{2+} oscillations in hippocampal slice preparations even in presence of the neuronal voltage-gated Na^+ channel blocker tetrodotoxin (Nett et al., 2002). This confirmed previous *in vitro* evidence of neuron-independent Ca^{2+} activity (Araque et al., 1999; Parri et al., 2001). These results were then similarly obtained using genetically encoded Ca^{2+} indicators (GECIs; Haustein et al., 2014; Bindocci et al., 2017). Several lines of evidence suggested that the spontaneous opening of a member of the transient receptor potential (TRP) family, TRPA1, and possibly of other cation channels of the same family, contribute to resting astroglial Ca^{2+} levels and at least a fraction of their intrinsic fluctuations (Shigetomi et al., 2011, 2013; Agarwal et al., 2017). However, neither specific TRPA1 mRNA or protein was so far detected in astrocytes (Verkhratsky et al., 2014). In line with these observations, 0 mM $[Ca^{2+}]_o$ reduced the Ca^{2+} transient frequency of the gliapil by up to 75% and the knockout of the inositol triphosphate type 2 receptor (IP3R2) spared around 10% of somatic and around 40% of gliapil fluctuations without affecting the frequency of the latter (Srinivasan et al., 2015). Since tetrodotoxin prevents action potential generation and not neurotransmission itself, these results can, at least partially, be attributed to astroglial responses elicited by spontaneous neurotransmitter release, as shown for the activation of cortical astrocytes by glutamate and ATP (Palygin et al., 2010; Lalo et al., 2011).

Indeed, astroglial Ca^{2+} oscillations driven by extracellular inputs superimpose on and integrate intrinsic Ca^{2+} activity, thus making astrocytes active partners of network functioning. With some notable exceptions (Jennings et al., 2017; Xin et al., 2019), activation of G-protein coupled receptors (GPCRs) leads to intracellular Ca^{2+} elevations (Kofuji and Araque, 2020) not only upon stimulation with molecules commonly considered excitatory, such as glutamate, but also with the canonical inhibitory neurotransmitter GABA (Perea et al., 2016; Mariotti et al., 2018; Mederos and Perea, 2019; Nagai et al., 2019). In line with these observations and contrary to their neuronal counterpart (Huang and Thathiah, 2015), *in vivo* chemogenetic activation of both G_q and $G_{i/o}$ DREADDs elicited Ca^{2+} increases in astrocytes (Durkee et al., 2019), thus challenging the long-established concept of E/I as mutually interplaying and yet still discernable processes (Isaacson and Scanziani, 2011). $[Ca^{2+}]_i$ increase can lead to the release of glutamate (Parpura et al., 1994; Pasti et al., 1997; Kang et al., 1998; Parri et al., 2001; Angulo et al., 2004; Fellin et al., 2004) as well as of GABA (Liu et al., 2000; Kozlov et al., 2006; Lee et al., 2010; Jiménez-González et al., 2011). Notably, contrary to Ca^{2+} uncaging or inositol-1,4,5-trisphosphate (IP3) application, G_q-coupled receptor activation does not necessarily induce the release of gliotransmitters (Wang et al., 2013) and different G_q-coupled receptors can exert gliotransmitter release with different efficiencies (Shigetomi et al., 2008). This challenges the idea that astrocytes may act as a redundant layer that responds similarly to GPCR-mediated inputs (Guerra-Gomes et al., 2017) and suggests that astrocytes can discriminate metabotropic signaling upstream of internal Ca^{2+} oscillations.

The astroglial membrane receptome, responsible for transmitter-triggered Ca^{2+} signaling is highly diverse and is far from being fully characterized (**Figure 1A**). In the following, we focus on glutamatergic and GABAergic signaling, representing by far the major emblems of the black-and-white E/I dichotomy. Astrocytes can express various types of ionotropic Ca^{2+} permeable glutamate receptors: AMPA receptors in cortex and cerebellum (Schipke et al., 2001; Lalo et al., 2006; Saab et al., 2012) and NMDA receptors in the cortex (Schipke et al., 2001; Lalo et al., 2006; Kirchhoff, 2017), although their expression in the hippocampus is still unclear (Matthias et al., 2003; Verkhratsky and Kirchhoff, 2007; Serrano et al., 2008; Letellier et al., 2016). Kainate receptors may be absent from astroglial membranes under physiological conditions, but were reported to be inducible in a mouse model of temporal lobe epilepsy (TLE; Das et al., 2012; Vargas et al., 2013). Among metabotropic glutamate receptors, G_q-coupled mGluR5 activation results in IP_3-mediated Ca^{2+} increase through the phospholipase C pathway (Panatier and Robitaille, 2016). mGluR5 contribution to Ca^{2+} oscillations seems to be restricted, at least in the adult brain, to the fine perisynaptic processes (Sun et al., 2013, 2014; Haustein et al., 2014). Astrocytes express also the $G_{i/o}$-coupled mGluR2/3, whose activation leads to inhibition of adenylate cyclase (Aronica et al., 2003; Sun et al., 2013; **Figure 1A**).

With respect to GABAergic signaling, astrocytes display internal Ca^{2+} increases following $GABA_A$ receptor-mediated depolarization through voltage-gated Ca^{2+} channels (VGCCs; Nilsson et al., 1993; Verkhratsky and Steinhäuser, 2000; Meier et al., 2008; Parpura et al., 2011; Verkhratsky et al., 2012). However, given the low membrane input resistance of mature astrocytes, the contribution of $GABA_A$ receptors to Ca^{2+} responses *in vivo* remains controversial. Metabotropic

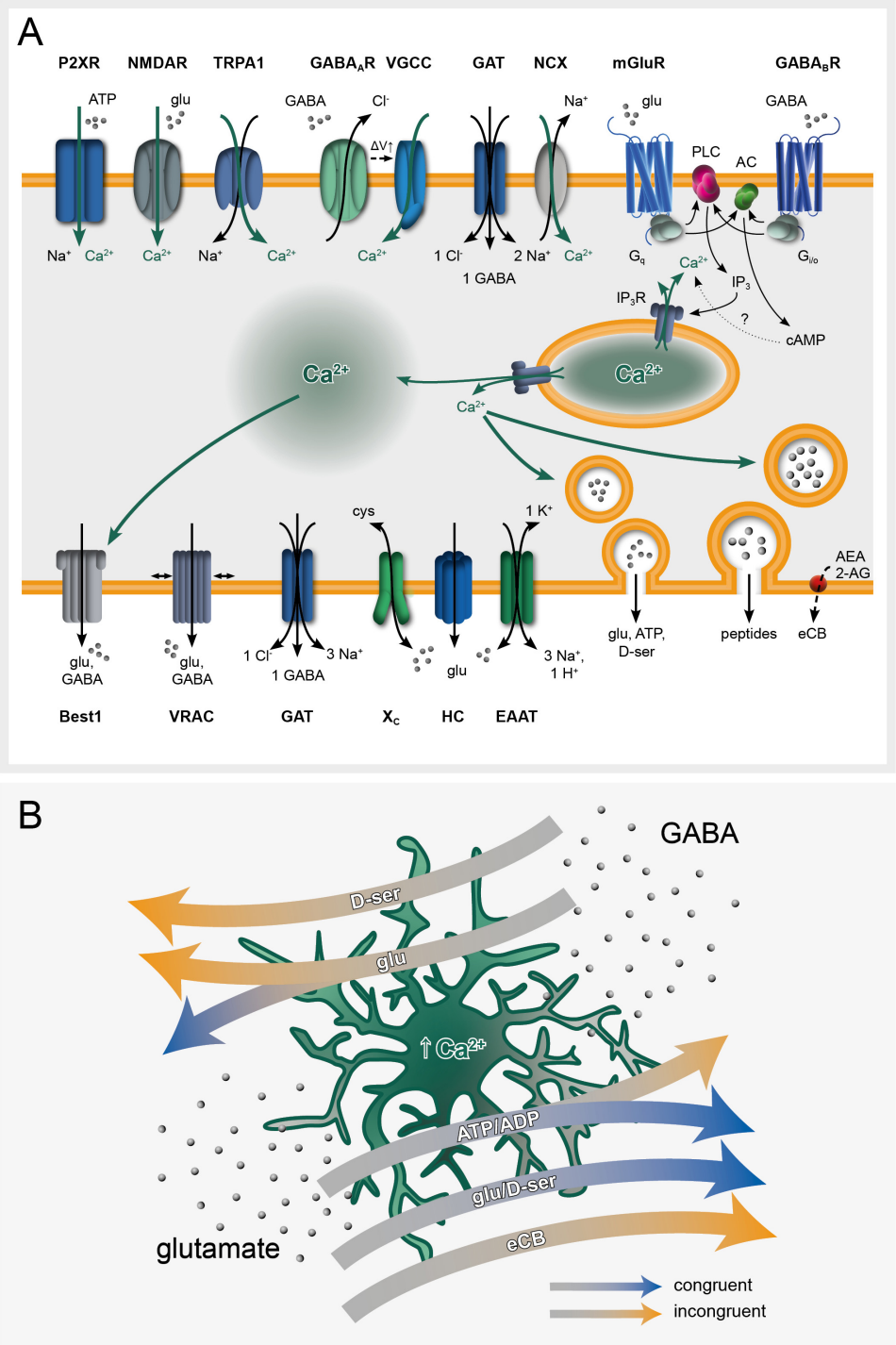

FIGURE 1 | Ca^{2+} signaling at the core of astroglial *black box* operations. **(A)** Astroglial receptome coordinates glutamate and GABA-induced intracellular Ca^{2+} signaling and subsequent gliotransmitter release. **(B)** Glutamate and GABA elicit Ca^{2+}-dependent gliotransmitter-mediated congruent and incongruent modulation of network plasticity. Congruent signaling refers to contexts in which GABA and glutamate as initial stimuli exert inhibitory or excitatory effects on the neuronal network, respectively. *Vice versa*, incongruent signaling designates scenarios in which GABA has an excitatory and glutamate an inhibitory final impact on the network. Both congruent and incongruent signaling may involve the same gliotransmitters (highlighted on the arrows). 2-AG, 2-arachidonoylglycerol; AC, adenylate cyclase; ADP/ATP, adenosine di/tri-phosphate; AEA, anandamide; Best1, bestrophin-1 channel; cAMP, cyclic AMP; cys, cysteine; D-ser, D-serine; EAAT, excitatory amino acid transporter; eCB, endocannabinoids; GABA, γ-aminobutyric acid; GABA$_A$R/GABA$_B$R, GABA receptors; GAT, GABA transporter; glu, glutamate; HC, hemichannel; IP$_3$, inositol triphosphate; IP$_3$R, inositol triphosphate receptor; mGluR, metabotropic glutamate receptor; NCX, sodium-calcium exchanger; NMDAR, N-methyl-D-aspartate receptor; P2XR, purinergic transmitter-gated ion channels; PLC, phospholipase C; TRPA1, transient receptor potential A1; VGCC, voltage-gated calcium channel; VRAC, volume-regulated anion channel; X$_C$, cysteine-glutamate antiporter; ΔV, membrane potential.

$G_{i/o}$-coupled $GABA_B$ receptors were extensively reported to induce intracellular Ca^{2+} rises in an IP_3-dependent manner (Mariotti et al., 2016; Nagai et al., 2019) followed by gliotransmitter release (Serrano et al., 2006; Perea et al., 2016; Durkee et al., 2019). Although their role in the cortical astroglial response is unclear, GABA transporter (GAT)-mediated Na^+ symport increases intracellular Ca^{2+} through the Na^+/Ca^{2+} exchanger (Doengi et al., 2009; Boddum et al., 2016), as previously suggested for glutamate transporters (Schummers et al., 2008). Synergistic activation of different pathways is likely to occur upon GABAergic signaling, thus potentially introducing an additional level of up-stream signal discrimination (Matos et al., 2018; **Figure 1A**).

There is plenty of evidence that gliotransmitter release occurs (Parpura et al., 1994; Jeftinija et al., 1997; Bezzi et al., 1998) and that it is, at least partially, a Ca^{2+} dependent mechanism (Bezzi et al., 2004; Perea and Araque, 2005; Araque and Navarrete, 2010; Schwarz et al., 2017; Bohmbach et al., 2018; Savtchouk and Volterra, 2018). Glutamate release occurs through several pathways, including reverse operation of plasma membrane glutamate transporters (Longuemare and Swanson, 1997; Rossi et al., 2000), cystine-glutamate Xc- antiporter (Cavelier and Attwell, 2005), volume-regulated anion channels (VRACs; Kimelberg et al., 1990; Mongin and Kimelberg, 2005; Abdullaev et al., 2006; Liu et al., 2006; Ramos-Mandujano et al., 2007), $P2X_7$ receptors (Duan et al., 2003), the Ca^{2+} activated anion channel bestrophin 1 (Best1; Park et al., 2009; Woo et al., 2012), hemichannels (Ye et al., 2003) and vesicular exocytosis (Jeftinija et al., 1997; Bezzi et al., 2004; Montana et al., 2006; Bowser and Khakh, 2007; Xu et al., 2007; Parpura and Zorec, 2010; Schwarz et al., 2017). In contrast to glutamate, GABA release mechanisms were less extensively addressed and remain elusive. Vesicular release of GABA seems unlikely due to the lack of GABA-containing synaptic vesicles in astrocytes (Yoon and Lee, 2014). *Ex vivo* electrophysiological studies using acute brain slices suggested that VRACs (Kozlov et al., 2006; Le Meur et al., 2012) as well as GATs (Barakat and Bordey, 2002; Richerson and Wu, 2003; Lee et al., 2011) can mediate GABA release. GAT2/3 are indeed involved in astroglial GABA release (Héja et al., 2012; Unichenko et al., 2013), as well as Best1 (Lee et al., 2010). Although still under debate, both GATs and Best1 could be responsible for tonic as well as phasic GABAergic astroglial signaling under physiological conditions. Remarkably, reactive astrocytes show aberrant and abundant tonic GABA release through Best1 in mouse models of Alzheimer's disease (Jo et al., 2014). In a mouse model of TLE, the astrocyte-specific rescue of Best1 could restore tonic GABAergic inhibition and suppressed seizure susceptibility in Best1 complete knock-out mice (Pandit et al., 2020).

THE PARADOX OF ASTROGLIAL *BLACK BOX* FUNCTION IN THE NEURAL NETWORK

The astrocytes' *black box* operations typically involve an initial stimulus (most commonly synaptically released neurotransmitters), an astroglial receptor inducing an intracellular signaling cascade leading to Ca^{2+} elevations, a released gliotransmitter and finally the net effect on the neuronal network: excitation or inhibition. Assuming that GABA as initial stimulus would exert an inhibitory (congruent) rather than excitatory (incongruent) and glutamate an excitatory (congruent) rather than inhibitory (incongruent) effect on the network, several scenarios co-exist along this information processing thread (**Figure 1B** and **Table 1**).

Congruent Signaling Preserves Input–Output Polarity

In the simplest case, initial stimulus and net result are congruent as it has been observed frequently across brain regions. Cortical, hippocampal and thalamic astrocytes stimulated by glutamate release glutamate and in turn induce NMDA receptor-dependent slow inward currents (SICs) in adjacent neurons (D'Ascenzo et al., 2007; Ding et al., 2007; Pirttimaki et al., 2011; Sasaki et al., 2011; Gómez-Gonzalo et al., 2017), resulting in neuronal synchronization and an elevated network excitability (Fellin et al., 2004). However, a congruent net result can also be obtained when the released gliotransmitter is neither glutamate nor GABA. Within the hippocampal network, both glutamate and GABA, as neurotransmitters, can stimulate ATP release from astrocytes and thereby evoke congruent consequences for the neuronal environment. Glutamate-induced ATP release enhances basal synaptic transmission at pyramidal cells (Panatier et al., 2011), while GABA-induced ATP release generates (hetero-) synaptic depression (Serrano et al., 2006; Andersson et al., 2007; Chen et al., 2013; Covelo and Araque, 2018) or up-regulation of inhibitory transmission (Matos et al., 2018). Alternatively, glutamate can stimulate astrocytes to release the NMDA receptor co-agonist D-serine, being an essential component of hippocampal long-term potentiation (LTP; Henneberger et al., 2010; Sherwood et al., 2017). Most strikingly, GABAergic stimulation can lead to astroglial release of glutamate, anticipating a reversal of the initial stimulus' nature, yet still exhibiting a net dampening effect on the hippocampal network through potentiated inhibitory postsynaptic currents (IPSCs; Kang et al., 1998) or heterosynaptic depression (Andersson et al., 2007). Astrocytes therefore can convey the initial message of the primary stimulus to the network, sometimes via alternative routes (ATP, D-serine) and even by switching from an "inhibitory" GABAergic stimulation to glutamate release (**Figure 1B** and **Table 1**).

Incongruent Signaling Reverses Input–Output Polarity

Astrocytes can change the nature of the initial stimulus with respect to the output to the network. The most evident way to achieve this is to perform a switch between the main inhibitory and the main excitatory transmitter. Indeed, GABAergic stimulation of astrocytes can be turned into glutamatergic excitation and thereby potentiate excitatory transmission at the CA3-CA1 microcircuit (Mariotti et al., 2016;

TABLE 1 | Summary of congruent and incongruent signaling pathways evoked by glutamate and GABA, according to brain region, released gliotransmitter, and principal neuronal targets.

	Region	Gliotransmitter	Neuronal target	Net effect	References	
GLU	Hc	D-ser	NMDAR	LTP	Henneberger et al., 2010; Sherwood et al., 2017	Congruent
	Hc	glu		SIC	Fellin et al., 2004; D'Ascenzo et al., 2007; Ding et al., 2007; Sasaki et al., 2011; Gómez-Gonzalo et al., 2017	
	Vb th					
	Ctx					
	Nac					
	Hc	ATP	presynaptic A2AR	increased basal synaptic transmission	Panatier et al., 2011	
	Hc	eCB	CB1R	heterosynaptic depression	Smith et al., 2020	Incongruent
	Ht	ATP	P2XR	LTP of GABAergic synapses	Crosby et al., 2018	
	Str	ATP/ADP	A1R	LTD of cortico-striatal synapses	Cavaccini et al., 2020	
	Hc	glu	AMPAR/ NMDAR	potentiated mIPSCs	Kang et al., 1998	
GABA	Hc	glu	mGluR 2/3	(transient) heterosynaptic depression	Andersson et al., 2007	Congruent
	Hc	ATP	presynaptic A1R		Serrano et al., 2006; Chen et al., 2013; Covelo and Araque, 2018; Matos et al., 2018	
	Hc	glu	Presynaptic mGluR 1	potentiation of excitatory transmission	Perea et al., 2016; Covelo and Araque, 2018	Incongruent
	Ssctx		NMDAR	SIC	Mariotti et al., 2016	
	MNTB	glu + D-ser			Reyes-Haro et al., 2010	

A1R, adenosine 1 receptor; A2AR, adenosine 2A receptor; ADP/ATP, adenosine di/tri-phosphate; CB1R, cannabinoid receptor 1; Ctx, cortex; D*-ser,* D*-serine; eCB, endocannabinoids; GABA, γ-aminobutyric acid; glu, glutamate; Hc, hippocampus; Ht, hypothalamus; LTD, long-term depression; LTP, long-term potentiation; mGluR, metabotropic glutamate receptor; MNTB, medial nucleus of the trapezoid body; Nac, nucleus accumbens; NMDAR, N-methyl-*D*-aspartate receptor; SIC, slow inward current; Str, striatum; Ssctx, somatosensory cortex; Vb th, ventro-basal thalamus.*

Perea et al., 2016; Covelo and Araque, 2018). Likewise, an astroglial switch is attained by including impartial transmitters in the information processing thread. Hypothalamic astrocytes receiving concomitant glutamatergic input and cholecystokinin stimulation release ATP. Acting on P2X-receptors, this astrocyte-derived purinergic stimulation is crucial for LTP of local GABAergic synapses, thereby augmenting the inhibitory tone of the network (Crosby et al., 2018). Moreover, striatal astrocytes also switch a glutamatergic input into long-term depression (LTD) mediated via purines (Cavaccini et al., 2020). Similarly, endocannabinoids released after glutamatergic activation mediate transient hippocampal heterosynaptic depression (Smith et al., 2020). Conversely, GABA-evoked astroglial Ca^{2+}-transients induce the co-release of glutamate and D-Serine, thereby producing NMDA receptor-dependent SICs in principal neurons of the medial nucleus of the trapezoid body (MNTB, ascending auditory pathway) (Reyes-Haro et al., 2010). In contrast to hippocampal pyramidal neurons, however, the postsynaptic principal neurons of the MNTB are less susceptible to SIC-mediated synchronization. Moreover, astroglial switches modulating synaptic plasticity operate at various timescales. In contrast to mechanisms such as LTP and (transient) heterosynaptic depression acting within minutes, striatal astrocytes increase the number of excitatory synapses and enhance excitatory transmission upon GABAergic stimulation, prevailing for at least 48 h. Mechanistically, the activation of the G_i-pathway downstream of the astroglial $GABA_B$ receptor leads to an upregulation of the synaptogenic multi-domain matrix glycoprotein thrombospondin-1 *in vivo* (Nagai et al., 2019).

Astrocytes therefore can reverse the initial message of the primary stimulus to the network with the same mechanisms employed to convey a congruent message: by switching from an "inhibitory" GABAergic stimulation to glutamate release, using alternative routes (ATP, D-serine, endocannabinoids), but oppositely even by reproducing the initial stimulus (glutamate-induced glutamate release) (**Figure 1B** and **Table 1**). For sake of simplicity, here the concept of congruent and incongruent signaling has been mainly reduced to contexts involving glutamate or GABA as initial stimulus, followed by Ca^{2+}-dependent gliotransmitter release. However, gliotransmitters' impact on neuronal signaling encompasses several additional levels of complexity. Glia-driven purinergic signaling for example can induce down regulation of neuronal $GABA_A$ (Lalo et al., 2014) as well as NMDA receptors (Lalo et al., 2016), thereby potentially acting in both congruent and incongruent ways. Furthermore, astroglial Ca^{2+}-sensitive Best-1 channels have been shown to release glutamate and GABA, in a region-dependent manner. While hippocampal astrocytes predominantly release glutamate (Woo et al., 2012), putatively due to a lack of GABA content (Yoon et al., 2011), cerebellar astrocytes do contain and release GABA (Lee et al., 2010).

Generalizing the gathered evidence, stimulation of the same astroglial receptor can lead to the release of different gliotransmitters. Stimulation of different receptors can have

the same output and the same gliotransmitter can finally have different actions on the network. This paradoxical feature of astrocytes can be partially resolved by dissecting the information processing steps attributed to the astrocyte function itself or the context it is embedded in.

Astroglial Ca^{2+} Bottleneck: Upstream and Downstream Signal Discrimination and Processing

Astrocyte-mediated neuronal plasticity starts with the detection and discrimination of a stimulus. At the multipartite synapse, astroglial processes frequently interact with GABAergic interneurons and glutamatergic principal neurons. Specifically, cortical as well as hippocampal astroglia have the capacity to engage in interneuron-type specific interactions. Remarkably, they are more responsive to somatostatin compared to parvalbumin interneuron stimulation, based on the co-release of the neuropeptide somatostatin (Mariotti et al., 2018). Subsequently, the selective sensitivity to somatostatin interneurons is integrated and translated into an astroglia-mediated up-regulation of the synaptic inhibition of pyramidal neurons (Matos et al., 2018). Moreover, neuronal activity is also decoded in spatiotemporal patterns of circuit association, firing duration and frequency. Astrocytes are capable of discriminating synaptic activity of different neuronal circuits within the hippocampus, even if the same transmitter is released. This is likely due to distinct patterns of receptor expression and the existence of subcellular functional domains (Perea and Araque, 2005; Shigetomi et al., 2008). In the hippocampus, neuronal firing rates can be correlated with astroglial Ca^{2+} signals, i.e., high frequency synaptic activity depresses and low frequency increases Ca^{2+} signals (Perea and Araque, 2005). Moreover, neuronal firing patterns lead to distinct gliotransmitter release profiles, differentially affecting the neuronal network. While low or brief interneuron stimulation evokes glutamate release, high or sustained interneuron stimulation provokes the co-release of glutamate and purines (Covelo and Araque, 2018).

At the core of the astroglial *black box*, intracellular Ca^{2+}-signals remain loosely defined. Even though a variety of Ca^{2+} signals have been mapped according to their spatiotemporal properties, still analysis and interpretation remain a major challenge (Nimmerjahn et al., 2009; Khakh and Sofroniew, 2015; Rusakov, 2015; Bazargani and Attwell, 2016; Bindocci et al., 2017; Stobart et al., 2018; Semyanov et al., 2020). So far, distinct Ca^{2+}-signals have not been associated to specific intracellular signaling cascades or the nature of synaptic plasticity. The current consensus, however, states that spatially restrained Ca^{2+} signals will likely induce homosynaptic modulation while larger, propagating Ca^{2+} signals intervene in heterosynaptic and territorial synaptic plasticity (Araque et al., 2014). In particular, the integrative function of astrocytes, i.e., the computation of simultaneously converging signaling pathways in a probably non-linear fashion, remains to be elucidated (Durkee and Araque, 2019). Similarly, only few classes of Ca^{2+} signals could be clearly attributed to a functional correlate such as sensory stimulation (Wang et al., 2009; Stobart et al., 2018) or locomotion and startle responses (Paukert et al., 2014).

Downstream of intracellular Ca^{2+} signal integration, astrocytes can modulate gliotransmitter release and thereby determine the final impact on neuronal plasticity. Recent work supports the concept that the same astrocyte can release different gliotransmitters based on the existence of individual vesicle populations containing different gliotransmitters, operating through distinct v-SNARE proteins and oppositely regulating synaptic plasticity (Schwarz et al., 2017; Covelo and Araque, 2018). A further level of complexity arises from the coexistence of different mechanisms of gliotransmission with specific Ca^{2+}-dependency. Vesicular release of gliotransmitters is threshold-based and requires relatively high intracellular Ca^{2+} elevations (Kreft et al., 2003; Parpura and Zorec, 2010). Ca^{2+}-dependent opening of large conductance anion channels like Best1 is sigmoidal and has an EC50 for $[Ca^{2+}]_i$ of about 150 nM (Lee et al., 2010), thus making it a suitable mechanism of gliotransmitter release even at resting conditions or in response to minute Ca^{2+} elevations (Clapham, 2007).

Finally, the net outcome of astroglial *black box* operations depends on the context of targeted neuronal receptors and the connectivity of the local circuitry. Especially in glutamatergic and purinergic transmission, the stimulus nature can be switched if presynaptic rather than postsynaptic receptors are activated (Serrano et al., 2006; Andersson et al., 2007; Hulme et al., 2014; Cavaccini et al., 2020). The connectivity of local circuits plays a major role when inhibitory transmission is potentiated by an excitatory transmitter (Kang et al., 1998; Crosby et al., 2018; Mederos and Perea, 2019), inhibitory transmission is inhibited, or excitatory transmission is disinhibited (Liu et al., 2004; Yarishkin et al., 2015). Associated to specific local circuits, distinct astroglial subpopulations (Zhang and Barres, 2010; Liddelow et al., 2017; Morel et al., 2017) interact with designated neuronal subtypes or circuits such as the striatal dopaminergic D1/D2 pathways (Martín et al., 2015; Martin-Fernandez et al., 2017). Given the kaleidoscopic complexity added to brain and network function, the astroglial syncytium holds a multitude of targets to be explored in health and disease.

ABERRANT Ca^{2+} SIGNALING AND NETWORK EXCITABILITY DISRUPTION IN EPILEPSY

The (im-) balance of E/I is a central element in the pathophysiology of epilepsy. More specifically, large populations of neurons become hyperexcitable and are more likely to engage in synchronous firing episodes. Accordingly, a great proportion of anti-epileptic drugs aim at enhancing GABA-mediated inhibition and decreasing glutamate-mediated excitation (Treiman, 2001; Czapiński et al., 2005). Astrocytes are portrayed as key players in epilepsy due to their diverse roles in the modulation of neuronal excitability and synchrony (Coulter and Steinhäuser, 2015; Robel and Sontheimer, 2016). A central property in this context is Ca^{2+}-dependent astroglial glutamate release, driving NMDA receptor-induced neuronal

excitation and favoring neuronal synchrony (Parri et al., 2001; Angulo et al., 2004; Fellin et al., 2004; Tian et al., 2005; Poskanzer and Yuste, 2011; Sasaki et al., 2014). Importantly, astroglial Ca^{2+} signals themselves are generally perturbed under neuropathological conditions (Kuchibhotla et al., 2009; Jiang et al., 2016; Mizuno et al., 2018; Shigetomi et al., 2019). Tonic long-lasting Ca^{2+} elevations result at least partially from excitotoxic spilling of glutamate, GABA and ATP from dying cells (Shigetomi et al., 2019).

Astrocyte (dys-) functions have been causally linked to the etiology of TLE (Bedner et al., 2015; Steinhäuser et al., 2016; Deshpande et al., 2020). On a cellular and molecular level, this is paralleled by a selective vulnerability of GABAergic interneurons (Sanon et al., 2005; Upadhya et al., 2019) and reduced glutamate decarboxylase (GAD) as well as glutamine synthetase (GS) activity in astrocytes (Robel and Sontheimer, 2016; Chan et al., 2019), leading to reduced vesicular GABA levels in neurons and subsequently reduced inhibitory input on hippocampal pyramidal neurons (Liang et al., 2006). However, glutamate levels also increase (Luna-Munguia et al., 2011) and a re-emergence of astroglial mGluR5 receptors can be observed (Umpierre et al., 2019). Recent lines of evidence also support a role for purinergic signaling in the etiology and progression of epilepsy and therefore further suggest that astrocytes actively contribute to this pathological scenario as modulators of the ATP/adenosine signaling (Boison, 2016; Beamer et al., 2017; Boison and Steinhäuser, 2018). Astroglial Ca^{2+} signals are pivotal for understanding the pathophysiology of epilepsy (Carmignoto and Haydon, 2012). *Ex vivo*, focal, seizure-like discharge onset and maintenance are associated with substantial astroglial Ca^{2+} transients, generating recurrent excitatory loops with neurons (Gómez-Gonzalo et al., 2010; Álvarez-Ferradas et al., 2015). *In vivo*, astroglial Ca^{2+} signals promote the propagation of epileptiform activity in the hippocampus. In fact, at seizure onset astrocytes display Ca^{2+} elevations prior to neurons and the suppression of those preceeding signals in $Itpr2^{-/-}$ mice reduces seizure activity (Heuser et al., 2018). These data suggest a modulatory, pro-epileptic effect of astroglial Ca^{2+} signals (Fellin et al., 2006; Heuser et al., 2018). Finally, seizure termination by spreading depolarization (SD) is accompanied by large Ca^{2+} waves in astrocytes, whose importance has been largely overlooked so far (Seidel et al., 2016; Heuser et al., 2018).

As it is for TLE, both glutamatergic- and GABAergic signaling are intimately involved in the generation and spreading of slow-wave discharges (SWDs) normally occurring in the thalamocortical network during sleep and pathologically in absence epilepsy (Tanaka et al., 1997; Tancredi et al., 2000; Crunelli and Leresche, 2002; Melø et al., 2006; Gould et al., 2014). *In vivo* astroglial Ca^{2+} activity temporally precedes the rhythmic and synchronized neocortical slow oscillations (∼1 Hz) which are typical for sleep. Indeed, optogenetic activation of astrocytes can induce this slow-oscillation state, possibly through glutamate transients (Poskanzer and Yuste, 2016). In line with this, neuronal firing reliably follows astroglial network synchronization during slow-wave activity. The fraction of astrocytes and neurons involved in the synchronous slow-wave state decreases both after astroglial uncoupling and intracellular Ca^{2+} chelation using EGTA (Szabó et al., 2017). Moreover, astroglial Ca^{2+} signaling is involved in the *in vivo* mGluR2-dependent disinhibition of neurons of the thalamic ventro-basal nucleus, thus playing a key role in sensory information processing (Copeland et al., 2017). On the other hand, dampening of astroglial Ca^{2+} oscillations in the striatum was linked to the upregulation of GAT3 expression and the resulting GABA uptake, thus reducing tonic inhibition and exacerbating neuronal excitability (Yu et al., 2018). The role of astrocytic Ca^{2+} transients in network synchronization and pathology is therefore still controversial.

CONCLUSION

Neuronal network plasticity can be simplified in terms of E/I, represented by glutamate and GABA, respectively. Including the discriminatory and integrative function of astrocytes into the equation reveals a profound entanglement of E/I, making these traditional labels insufficient. Astrocytes can preserve (*congruence*) or reverse (*incongruence*) neuronal inputs based on the engagement of distinct receptor arrays as well as the integration of converging Ca^{2+} signaling cascades and orchestrated gliotransmitter release. Furthermore, the association of astroglial subpopulations to specific neuronal circuits adds a further layer of complexity. To date, further efforts are required in order to understand astroglial *black box* operations and link them to Ca^{2+} signal heterogeneity. Advances in decoding astroglial Ca^{2+} signaling could reveal the untapped therapeutic potential in pathologies emerging from network excitability dysregulation, as suggested by the collectively acknowledged role of astroglial Ca^{2+} in epilepsy.

AUTHOR CONTRIBUTIONS

LC and DG equally contributed to the review, screened the literature, wrote the first draft, conceptualized the table, designed the figure with AS, and finalized the manuscript. AS and FK reviewed and finalized manuscript and figure. All authors approved on the final version of the manuscript.

FUNDING

This project has received funding from the European Union's Horizon 2020 Research and Innovation Programme under the Marie Skłodowska-Curie grant agreement No. 722053 and from the Deutsche Forschungsgemeinschaft DFG (SFB 894, SFB 1158, SPP 1757, FOR 2289, and Open Access Publishing funds).

ACKNOWLEDGMENTS

We thank the members of the department for fruitful discussions, particularly Wenhui Huang and Jens Grosche (Effigos AG) for his contribution to **Figure 1A**.

REFERENCES

Abdullaev, I. F., Rudkouskaya, A., Schools, G. P., Kimelberg, H. K., and Mongin, A. A. (2006). Pharmacological comparison of swelling-activated excitatory amino acid release and Cl- currents in cultured rat astrocytes. *J. Physiol.* 572, 677–689. doi: 10.1113/jphysiol.2005.103820

Agarwal, A., Wu, P. H., Hughes, E. G., Fukaya, M., Tischfield, M. A., Langseth, A. J., et al. (2017). Transient opening of the mitochondrial permeability transition pore induces microdomain calcium transients in astrocyte processes. *Neuron* 93, 587–605.e7.

Álvarez-Ferradas, C., Morales, J. C., Wellmann, M., Nualart, F., Roncagliolo, M., Fuenzalida, M., et al. (2015). Enhanced astroglial Ca2+ signaling increases excitatory synaptic strength in the epileptic brain. *Glia* 63, 1507–1521. doi: 10.1002/glia.22817

Andersson, M., Blomstrand, F., and Hanse, E. (2007). Astrocytes play a critical role in transient heterosynaptic depression in the rat hippocampal CA1 region. *J. Physiol.* 585, 843–852. doi: 10.1113/jphysiol.2007.142737

Angulo, M. C., Kozlov, A. S., Charpak, S., and Audinat, E. (2004). Glutamate released from glial cells synchronizes neuronal activity in the hippocampus. *J. Neurosci.* 24, 6920–6927. doi: 10.1523/jneurosci.0473-04.2004

Araque, A., Carmignoto, G., Haydon, P. G., Oliet, S. H., Robitaille, R., and Volterra, A. (2014). Gliotransmitters travel in time and space. *Neuron* 81, 728–739. doi: 10.1016/j.neuron.2014.02.007

Araque, A., and Navarrete, M. (2010). Glial cells in neuronal network function. *Philos. Trans. R. Soc. Lond. B Biol. Sci.* 365, 2375–2381. doi: 10.1098/rstb.2009.0313

Araque, A., Parpura, V., Sanzgiri, R. P., and Haydon, P. G. (1999). Tripartite synapses: glia, the unacknowledged partner. *Trends Neurosci.* 22, 208–215. doi: 10.1016/s0166-2236(98)01349-6

Aronica, E., Gorter, J. A., Ijlst-Keizers, H., Rozemuller, A. J., Yankaya, B., Leenstra, S., et al. (2003). Expression and functional role of mGluR3 and mGluR5 in human astrocytes and glioma cells: opposite regulation of glutamate transporter proteins. *Eur. J. Neurosci.* 17, 2106–2118. doi: 10.1046/j.1460-9568.2003.02657.x

Barakat, L., and Bordey, A. (2002). GAT-1 and reversible GABA transport in Bergmann glia in slices. *J. Neurophysiol.* 88, 1407–1419. doi: 10.1152/jn.2002.88.3.1407

Bazargani, N., and Attwell, D. (2016). Astrocyte calcium signaling: the third wave. *Nat. Neurosci.* 19, 182–189. doi: 10.1038/nn.4201

Beamer, E., Fischer, W., and Engel, T. (2017). The ATP-Gated P2X7 receptor as a target for the treatment of drug-resistant epilepsy. *Front. Neurosci.* 11:21. doi: 10.3389/fnins.2017.00021

Bedner, P., Dupper, A., Hüttmann, K., Müller, J., Herde, M. K., Dublin, P., et al. (2015). Astrocyte uncoupling as a cause of human temporal lobe epilepsy. *Brain* 138, 1208–1222. doi: 10.1093/brain/awv067

Bezzi, P., Carmignoto, G., Pasti, L., Vesce, S., Rossi, D., Rizzini, B. L., et al. (1998). Prostaglandins stimulate calcium-dependent glutamate release in astrocytes. *Nature* 391, 281–285. doi: 10.1038/34651

Bezzi, P., Gundersen, V., Galbete, J. L., Seifert, G., Steinhäuser, C., Pilati, E., et al. (2004). Astrocytes contain a vesicular compartment that is competent for regulated exocytosis of glutamate. *Nat. Neurosci.* 7, 613–620. doi: 10.1038/nn1246

Bindocci, E., Savtchouk, I., Liaudet, N., Becker, D., Carriero, G., and Volterra, A. (2017). Three-dimensional Ca(2+) imaging advances understanding of astrocyte biology. *Science* 356:eaai8185. doi: 10.1126/science.aai8185

Boddum, K., Jensen, T. P., Magloire, V., Kristiansen, U., Rusakov, D. A., Pavlov, I., et al. (2016). Astrocytic GABA transporter activity modulates excitatory neurotransmission. *Nat. Commun.* 7:13572.

Bohmbach, K., Schwarz, M. K., Schoch, S., and Henneberger, C. (2018). The structural and functional evidence for vesicular release from astrocytes in situ. *Brain Res. Bull.* 136, 65–75. doi: 10.1016/j.brainresbull.2017.01.015

Boison, D. (2016). Adenosinergic signaling in epilepsy. *Neuropharmacology* 104, 131–139. doi: 10.1016/j.neuropharm.2015.08.046

Boison, D., and Steinhäuser, C. (2018). Epilepsy and astrocyte energy metabolism. *Glia* 66, 1235–1243. doi: 10.1002/glia.23247

Bowser, D. N., and Khakh, B. S. (2007). Vesicular ATP is the predominant cause of intercellular calcium waves in astrocytes. *J. Gen. Physiol.* 129, 485–491. doi: 10.1085/jgp.200709780

Carmignoto, G., and Haydon, P. G. (2012). Astrocyte calcium signaling and epilepsy. *Glia* 60, 1227–1233. doi: 10.1002/glia.22318

Cavaccini, A., Durkee, C., Kofuji, P., Tonini, R., and Araque, A. (2020). Astrocyte signaling gates long-term depression at corticostriatal synapses of the direct pathway. *J. Neurosci.* 40, 5757–5768. doi: 10.1523/jneurosci.2369-19.2020

Cavelier, P., and Attwell, D. (2005). Tonic release of glutamate by a DIDS-sensitive mechanism in rat hippocampal slices. *J. Physiol.* 564, 397–410. doi: 10.1113/jphysiol.2004.082131

Chan, F., Lax, N. Z., Voss, C. M., Aldana, B. I., Whyte, S., Jenkins, A., et al. (2019). The role of astrocytes in seizure generation: insights from a novel in vitro seizure model based on mitochondrial dysfunction. *Brain* 142, 391–411. doi: 10.1093/brain/awy320

Chen, J., Tan, Z., Zeng, L., Zhang, X., He, Y., Gao, W., et al. (2013). Heterosynaptic long-term depression mediated by ATP released from astrocytes. *Glia* 61, 178–191. doi: 10.1002/glia.22425

Clapham, D. E. (2007). Calcium signaling. *Cell* 131, 1047–1058.

Copeland, C. S., Wall, T. M., Sims, R. E., Neale, S. A., Nisenbaum, E., Parri, H. R., et al. (2017). Astrocytes modulate thalamic sensory processing via mGlu2 receptor activation. *Neuropharmacology* 121, 100–110. doi: 10.1016/j.neuropharm.2017.04.019

Coulter, D. A., and Steinhäuser, C. (2015). Role of astrocytes in epilepsy. *Cold Spring Harb. Perspect. Med.* 5:a022434.

Covelo, A., and Araque, A. (2018). Neuronal activity determines distinct gliotransmitter release from a single astrocyte. *eLife* 7:e32237.

Crosby, K. M., Murphy-Royal, C., Wilson, S. A., Gordon, G. R., Bains, J. S., and Pittman, Q. J. (2018). Cholecystokinin switches the plasticity of GABA synapses in the dorsomedial hypothalamus via astrocytic ATP release. *J. Neurosci.* 38, 8515–8525. doi: 10.1523/jneurosci.0569-18.2018

Crunelli, V., and Leresche, N. (2002). Childhood absence epilepsy: genes, channels, neurons and networks. *Nat. Rev. Neurosci.* 3, 371–382. doi: 10.1038/nrn811

Czapiński, P., Blaszczyk, B., and Czuczwar, S. J. (2005). Mechanisms of action of antiepileptic drugs. *Curr. Top. Med. Chem.* 5, 3–14.

Das, A., Wallace, G. C., Holmes, C., McDowell, M. L., Smith, J. A., Marshall, J. D., et al. (2012). Hippocampal tissue of patients with refractory temporal lobe epilepsy is associated with astrocyte activation, inflammation, and altered expression of channels and receptors. *Neuroscience* 220, 237–246. doi: 10.1016/j.neuroscience.2012.06.002

D'Ascenzo, M., Fellin, T., Terunuma, M., Revilla-Sanchez, R., Meaney, D. F., Auberson, Y. P., et al. (2007). mGluR5 stimulates gliotransmission in the nucleus accumbens. *Proc. Natl. Acad. Sci. U.S.A.* 104, 1995–2000. doi: 10.1073/pnas.0609408104

Deshpande, T., Li, T., Henning, L., Wu, Z., Müller, J., Seifert, G., et al. (2020). Constitutive deletion of astrocytic connexins aggravates kainate-induced epilepsy. *Glia* 68, 2136–2147. doi: 10.1002/glia.23832

Ding, S., Fellin, T., Zhu, Y., Lee, S.-Y., Auberson, Y. P., Meaney, D. F., et al. (2007). Enhanced astrocytic Ca2+ signals contribute to neuronal excitotoxicity after status epilepticus. *J. Neurosci.* 27, 10674–10684. doi: 10.1523/jneurosci.2001-07.2007

Doengi, M., Hirnet, D., Coulon, P., Pape, H. C., Deitmer, J. W., and Lohr, C. (2009). GABA uptake-dependent Ca(2+) signaling in developing olfactory bulb astrocytes. *Proc. Natl. Acad. Sci. U.S.A.* 106, 17570–17575. doi: 10.1073/pnas.0809513106

Duan, S., Anderson, C. M., Keung, E. C., Chen, Y., and Swanson, R. A. (2003). P2X7 receptor-mediated release of excitatory amino acids from astrocytes. *J. Neurosci.* 23, 1320–1328. doi: 10.1523/jneurosci.23-04-01320.2003

Durkee, C. A., and Araque, A. (2019). Diversity and specificity of astrocyte-neuron communication. *Neuroscience* 396, 73–78. doi: 10.1016/j.neuroscience.2018.11.010

Durkee, C. A., Covelo, A., Lines, J., Kofuji, P., Aguilar, J., and Araque, A. (2019). Gi/o protein-coupled receptors inhibit neurons but activate astrocytes and stimulate gliotransmission. *Glia* 67, 1076–1093. doi: 10.1002/glia.23589

Fellin, T., Gomez-Gonzalo, M., Gobbo, S., Carmignoto, G., and Haydon, P. G. (2006). Astrocytic glutamate is not necessary for the generation of epileptiform neuronal activity in hippocampal slices. *J. Neurosci.* 26, 9312–9322. doi: 10.1523/jneurosci.2836-06.2006

Fellin, T., Pascual, O., Gobbo, S., Pozzan, T., Haydon, P. G., and Carmignoto, G. (2004). Neuronal synchrony mediated by astrocytic glutamate through

activation of extrasynaptic NMDA receptors. *Neuron* 43, 729–743. doi: 10.1016/j.neuron.2004.08.011

Gómez-Gonzalo, M., Losi, G., Chiavegato, A., Zonta, M., Cammarota, M., Brondi, M., et al. (2010). An excitatory loop with astrocytes contributes to drive neurons to seizure threshold. *PLoS Biol.* 8:e1000352. doi: 10.1371/journal.pbio.1000352

Gómez-Gonzalo, M., Martin-Fernandez, M., Martínez-Murillo, R., Mederos, S., Hernández-Vivanco, A., Jamison, S., et al. (2017). Neuron-astrocyte signaling is preserved in the aging brain. *Glia* 65, 569–580. doi: 10.1002/glia.23112

Gould, T., Chen, L., Emri, Z., Pirttimaki, T., Errington, A. C., Crunelli, V., et al. (2014). GABA(B) receptor-mediated activation of astrocytes by gamma-hydroxybutyric acid. *Philos. Trans. R. Soc. Lond. B Biol. Sci.* 369:20130607. doi: 10.1098/rstb.2013.0607

Guerra-Gomes, S., Sousa, N., Pinto, L., and Oliveira, J. F. (2017). Functional roles of astrocyte calcium elevations: from synapses to behavior. *Front. Cell Neurosci.* 11:427. doi: 10.3389/fncel.2017.00427

Haustein, M. D., Kracun, S., Lu, X. H., Shih, T., Jackson-Weaver, O., Tong, X., et al. (2014). Conditions and constraints for astrocyte calcium signaling in the hippocampal mossy fiber pathway. *Neuron* 82, 413–429. doi: 10.1016/j.neuron.2014.02.041

Héja, L., Nyitrai, G., Kékesi, O., Dobolyi, A., Szabó, P., Fiáth, R., et al. (2012). Astrocytes convert network excitation to tonic inhibition of neurons. *BMC Biol.* 10:26. doi: 10.1186/1741-7007-10-26

Henneberger, C., Papouin, T., Oliet, S. H., and Rusakov, D. A. (2010). Long-term potentiation depends on release of D-serine from astrocytes. *Nature* 463, 232–236. doi: 10.1038/nature08673

Heuser, K., Nome, C. G., Pettersen, K. H., Åbjørsbråten, K. S., Jensen, V., Tang, W., et al. (2018). Ca2+ signals in astrocytes facilitate spread of epileptiform activity. *Cereb. Cortex* 28, 4036–4048. doi: 10.1093/cercor/bhy196

Huang, Y., and Thathiah, A. (2015). Regulation of neuronal communication by G protein-coupled receptors. *FEBS Lett.* 589, 1607–1619. doi: 10.1016/j.febslet.2015.05.007

Hulme, S. R., Jones, O. D., Raymond, C. R., Sah, P., and Abraham, W. C. (2014). Mechanisms of heterosynaptic metaplasticity. *Philos. Trans. R. Soc. Lond. B Biol. Sci.* 369:20130148. doi: 10.1098/rstb.2013.0148

Isaacson, J. S., and Scanziani, M. (2011). How inhibition shapes cortical activity. *Neuron* 72, 231–243. doi: 10.1016/j.neuron.2011.09.027

Jeftinija, S. D., Jeftinija, K. V., and Stefanovic, G. (1997). Cultured astrocytes express proteins involved in vesicular glutamate release. *Brain Res.* 750, 41–47. doi: 10.1016/s0006-8993(96)00610-5

Jennings, A., Tyurikova, O., Bard, L., Zheng, K., Semyanov, A., Henneberger, C., et al. (2017). Dopamine elevates and lowers astroglial Ca. *Glia* 65, 447–459. doi: 10.1002/glia.23103

Jiang, R., Diaz-Castro, B., Looger, L. L., and Khakh, B. S. (2016). Dysfunctional calcium and glutamate signaling in striatal astrocytes from Huntington's disease model mice. *J. Neurosci.* 36, 3453–3470. doi: 10.1523/jneurosci.3693-15.2016

Jiménez-González, C., Pirttimaki, T., Cope, D. W., and Parri, H. R. (2011). Non-neuronal, slow GABA signalling in the ventrobasal thalamus targets δ-subunit-containing GABA(A) receptors. *Eur. J. Neurosci.* 33, 1471–1482. doi: 10.1111/j.1460-9568.2011.07645.x

Jo, S., Yarishkin, O., Hwang, Y. J., Chun, Y. E., Park, M., Woo, D. H., et al. (2014). GABA from reactive astrocytes impairs memory in mouse models of Alzheimer's disease. *Nat. Med.* 20, 886–896. doi: 10.1038/nm.3639

Kang, J., Jiang, L., Goldman, S. A., and Nedergaard, M. (1998). Astrocyte-mediated potentiation of inhibitory synaptic transmission. *Nat. Neurosci.* 1, 683–692. doi: 10.1038/3684

Khakh, B. S., and Sofroniew, M. V. (2015). Diversity of astrocyte functions and phenotypes in neural circuits. *Nat. Neurosci.* 18, 942–952. doi: 10.1038/nn.4043

Kimelberg, H. K., Goderie, S. K., Higman, S., Pang, S., and Waniewski, R. A. (1990). Swelling-induced release of glutamate, aspartate, and taurine from astrocyte cultures. *J. Neurosci.* 10, 1583–1591. doi: 10.1523/jneurosci.10-05-01583.1990

Kirchhoff, F. (2017). Analysis of functional NMDA receptors in astrocytes. *Methods Mol. Biol.* 1677, 241–251. doi: 10.1007/978-1-4939-7321-7_13

Kofuji, P., and Araque, A. (2020). G-protein-coupled receptors in astrocyte-neuron communication. *Neuroscience* [Epub ahead of print],

Kozlov, A. S., Angulo, M. C., Audinat, E., and Charpak, S. (2006). Target cell-specific modulation of neuronal activity by astrocytes. *Proc. Natl. Acad. Sci. U.S.A.* 103, 10058–10063. doi: 10.1073/pnas.0603741103

Kreft, M., Stenovec, M., Rupnik, M., Grilc, S., Krzan, M., Milisav, I., et al. (2003). Calcium-dependent exocytosis in cultured astrocytes. *Glia* 46, 437–445.

Kuchibhotla, K. V., Lattarulo, C. R., Hyman, B. T., and Bacskai, B. J. (2009). Synchronous hyperactivity and intercellular calcium waves in astrocytes in Alzheimer mice. *Science* 323, 1211–1215. doi: 10.1126/science.1169096

Lalo, U., Palygin, O., North, R. A., Verkhratsky, A., and Pankratov, Y. (2011). Age-dependent remodelling of ionotropic signalling in cortical astroglia. *Aging Cell* 10, 392–402. doi: 10.1111/j.1474-9726.2011.00682.x

Lalo, U., Palygin, O., Rasooli-Nejad, S., Andrew, J., Haydon, P. G., and Pankratov, Y. (2014). Exocytosis of ATP from astrocytes modulates phasic and tonic inhibition in the neocortex. *PLoS Biol.* 12:e1001747. doi: 10.1371/journal.pbio.1001747

Lalo, U., Palygin, O., Verkhratsky, A., Grant, S. G., and Pankratov, Y. (2016). ATP from synaptic terminals and astrocytes regulates NMDA receptors and synaptic plasticity through PSD-95 multi-protein complex. *Sci. Rep.* 6:33609.

Lalo, U., Pankratov, Y., Kirchhoff, F., North, R. A., and Verkhratsky, A. (2006). NMDA receptors mediate neuron-to-glia signaling in mouse cortical astrocytes. *J. Neurosci.* 26, 2673–2683. doi: 10.1523/jneurosci.4689-05.2006

Le Meur, K., Mendizabal-Zubiaga, J., Grandes, P., and Audinat, E. (2012). GABA release by hippocampal astrocytes. *Front. Comput. Neurosci.* 6:59. doi: 10.3389/fncom.2012.00059

Lee, M., Schwab, C., and McGeer, P. L. (2011). Astrocytes are GABAergic cells that modulate microglial activity. *Glia* 59, 152–165. doi: 10.1002/glia.21087

Lee, S., Yoon, B. E., Berglund, K., Oh, S. J., Park, H., Shin, H. S., et al. (2010). Channel-mediated tonic GABA release from glia. *Science* 330, 790–796. doi: 10.1126/science.1184334

Letellier, M., Park, Y. K., Chater, T. E., Chipman, P. H., Gautam, S. G., Oshima-Takago, T., et al. (2016). Astrocytes regulate heterogeneity of presynaptic strengths in hippocampal networks. *Proc. Natl. Acad. Sci. U.S.A.* 113, E2685–E2694.

Liang, S. L., Carlson, G. C., and Coulter, D. A. (2006). Dynamic regulation of synaptic GABA release by the glutamate-glutamine cycle in hippocampal area CA1. *J. Neurosci.* 26, 8537–8548. doi: 10.1523/jneurosci.0329-06.2006

Liddelow, S. A., Guttenplan, K. A., Clarke, L. E., Bennett, F. C., Bohlen, C. J., Schirmer, L., et al. (2017). Neurotoxic reactive astrocytes are induced by activated microglia. *Nature* 541, 481–487.

Liu, H. T., Tashmukhamedov, B. A., Inoue, H., Okada, Y., and Sabirov, R. Z. (2006). Roles of two types of anion channels in glutamate release from mouse astrocytes under ischemic or osmotic stress. *Glia* 54, 343–357. doi: 10.1002/glia.20400

Liu, Q.-S., Xu, Q., Kang, J., and Nedergaard, M. (2004). Astrocyte activation of presynaptic metabotropic glutamate receptors modulates hippocampal inhibitory synaptic transmission. *Neuron Glia Biol.* 1, 307–316. doi: 10.1017/s1740925x05000190

Liu, Q. Y., Schaffner, A. E., Chang, Y. H., Maric, D., and Barker, J. L. (2000). Persistent activation of GABA(A) receptor/Cl(-) channels by astrocyte-derived GABA in cultured embryonic rat hippocampal neurons. *J. Neurophysiol.* 84, 1392–1403. doi: 10.1152/jn.2000.84.3.1392

Longuemare, M. C., and Swanson, R. A. (1997). Net glutamate release from astrocytes is not induced by extracellular potassium concentrations attainable in brain. *J. Neurochem.* 69, 879–882. doi: 10.1046/j.1471-4159.1997.69020879.x

Luna-Munguia, H., Orozco-Suarez, S., and Rocha, L. (2011). Effects of high frequency electrical stimulation and R-verapamil on seizure susceptibility and glutamate and GABA release in a model of phenytoin-resistant seizures. *Neuropharmacology* 61, 807–814. doi: 10.1016/j.neuropharm.2011.05.027

Mariotti, L., Losi, G., Lia, A., Melone, M., Chiavegato, A., Gómez-Gonzalo, M., et al. (2018). Interneuron-specific signaling evokes distinctive somatostatin-mediated responses in adult cortical astrocytes. *Nat. Commun.* 9:82.

Mariotti, L., Losi, G., Sessolo, M., Marcon, I., and Carmignoto, G. (2016). The inhibitory neurotransmitter GABA evokes long-lasting Ca(2+) oscillations in cortical astrocytes. *Glia* 64, 363–373. doi: 10.1002/glia.22933

Martín, R., Bajo-Grañeras, R., Moratalla, R., Perea, G., and Araque, A. (2015). Circuit-specific signaling in astrocyte-neuron networks in basal ganglia pathways. *Science* 349, 730–734. doi: 10.1126/science.aaa7945

Martin-Fernandez, M., Jamison, S., Robin, L. M., Zhao, Z., Martin, E. D., Aguilar, J., et al. (2017). Synapse-specific astrocyte gating of amygdala-related behavior. *Nat. Neurosci.* 20, 1540–1548. doi: 10.1038/nn.4649

Matos, M., Bosson, A., Riebe, I., Reynell, C., Vallée, J., Laplante, I., et al. (2018). Astrocytes detect and upregulate transmission at inhibitory synapses of somatostatin interneurons onto pyramidal cells. *Nat. Commun.* 9:4254.

Matthias, K., Kirchhoff, F., Seifert, G., Hüttmann, K., Matyash, M., Kettenmann, H., et al. (2003). Segregated expression of AMPA-type glutamate receptors and glutamate transporters defines distinct astrocyte populations in the mouse hippocampus. *J. Neurosci.* 23, 1750–1758. doi: 10.1523/jneurosci.23-05-01750.2003

Mederos, S., and Perea, G. (2019). GABAergic-astrocyte signaling: a refinement of inhibitory brain networks. *Glia* 67, 1842–1851. doi: 10.1002/glia.23644

Meier, S. D., Kafitz, K. W., and Rose, C. R. (2008). Developmental profile and mechanisms of GABA-induced calcium signaling in hippocampal astrocytes. *Glia* 56, 1127–1137. doi: 10.1002/glia.20684

Melø, T. M., Sonnewald, U., Touret, M., and Nehlig, A. (2006). Cortical glutamate metabolism is enhanced in a genetic model of absence epilepsy. *J. Cereb. Blood Flow Metab.* 26, 1496–1506. doi: 10.1038/sj.jcbfm.9600300

Mizuno, G. O., Wang, Y., Shi, G., Sun, J., Papadopoulos, S., Broussard, G. J., et al. (2018). Aberrant calcium signaling in astrocytes inhibits neuronal excitability in a human down syndrome stem cell model. *Cell Rep.* 24, 355–365. doi: 10.1016/j.celrep.2018.06.033

Mongin, A. A., and Kimelberg, H. K. (2005). ATP regulates anion channel-mediated organic osmolyte release from cultured rat astrocytes via multiple Ca2+-sensitive mechanisms. *Am. J. Physiol. Cell Physiol.* 288, C204–C213.

Montana, V., Malarkey, E. B., Verderio, C., Matteoli, M., and Parpura, V. (2006). Vesicular transmitter release from astrocytes. *Glia* 54, 700–715. doi: 10.1002/glia.20367

Morel, L., Chiang, M. S. R., Higashimori, H., Shoneye, T., Iyer, L. K., Yelick, J., et al. (2017). Molecular and functional properties of regional astrocytes in the adult brain. *J. Neurosci.* 37, 8706–8717. doi: 10.1523/jneurosci.3956-16.2017

Nagai, J., Rajbhandari, A. K., Gangwani, M. R., Hachisuka, A., Coppola, G., Masmanidis, S. C., et al. (2019). Hyperactivity with disrupted attention by activation of an astrocyte synaptogenic cue. *Cell* 177, 1280–1292.e20.

Nett, W. J., Oloff, S. H., and McCarthy, K. D. (2002). Hippocampal astrocytes in situ exhibit calcium oscillations that occur independent of neuronal activity. *J. Neurophysiol.* 87, 528–537. doi: 10.1152/jn.00268.2001

Nilsson, M., Eriksson, P. S., Rönnbäck, L., and Hansson, E. (1993). GABA induces Ca2+ transients in astrocytes. *Neuroscience* 54, 605–614. doi: 10.1016/0306-4522(93)90232-5

Nimmerjahn, A., Mukamel, E. A., and Schnitzer, M. J. (2009). Motor behavior activates Bergmann glial networks. *Neuron* 62, 400–412. doi: 10.1016/j.neuron.2009.03.019

Palygin, O., Lalo, U., Verkhratsky, A., and Pankratov, Y. (2010). Ionotropic NMDA and P2X1/5 receptors mediate synaptically induced Ca2+ signalling in cortical astrocytes. *Cell Calcium* 48, 225–231. doi: 10.1016/j.ceca.2010.09.004

Panatier, A., and Robitaille, R. (2016). Astrocytic mGluR5 and the tripartite synapse. *Neuroscience* 323, 29–34. doi: 10.1016/j.neuroscience.2015.03.063

Panatier, A., Vallée, J., Haber, M., Murai, K. K., Lacaille, J. C., and Robitaille, R. (2011). Astrocytes are endogenous regulators of basal transmission at central synapses. *Cell* 146, 785–798. doi: 10.1016/j.cell.2011.07.022

Pandit, S., Neupane, C., Woo, J., Sharma, R., Nam, M. H., Lee, G. S., et al. (2020). Bestrophin1-mediated tonic GABA release from reactive astrocytes prevents the development of seizure-prone network in kainate-injected hippocampi. *Glia* 68, 1065–1080. doi: 10.1002/glia.23762

Park, H., Oh, S. J., Han, K. S., Woo, D. H., Mannaioni, G., Traynelis, S. F., et al. (2009). Bestrophin-1 encodes for the Ca2+-activated anion channel in hippocampal astrocytes. *J. Neurosci.* 29, 13063–13073. doi: 10.1523/jneurosci.3193-09.2009

Parpura, V., Basarsky, T. A., Liu, F., Jeftinija, K., Jeftinija, S., and Haydon, P. G. (1994). Glutamate-mediated astrocyte neuron signaling. *Nature* 369, 744–747.

Parpura, V., Grubišiæ, V., and Verkhratsky, A. (2011). Ca(2+) sources for the exocytotic release of glutamate from astrocytes. *Biochim. Biophys. Acta* 1813, 984–991. doi: 10.1016/j.bbamcr.2010.11.006

Parpura, V., and Zorec, R. (2010). Gliotransmission: exocytotic release from astrocytes. *Brain Res. Rev.* 63, 83–92. doi: 10.1016/j.brainresrev.2009.11.008

Parri, H. R., Gould, T. M., and Crunelli, V. (2001). Spontaneous astrocytic Ca2+ oscillations in situ drive NMDAR-mediated neuronal excitation. *Nat. Neurosci.* 4, 803–812. doi: 10.1038/90507

Pascual, O., Casper, K. B., Kubera, C., Zhang, J., Revilla-Sanchez, R., Sul, J. Y., et al. (2005). Astrocytic purinergic signaling coordinates synaptic networks. *Science* 310, 113–116. doi: 10.1126/science.1116916

Pasti, L., Volterra, A., Pozzan, T., and Carmignoto, G. (1997). Intracellular calcium oscillations in astrocytes: a highly plastic, bidirectional form of communication between neurons and astrocytes in situ. *J. Neurosci.* 17, 7817–7830. doi: 10.1523/jneurosci.17-20-07817.1997

Paukert, M., Agarwal, A., Cha, J., Doze, V. A., Kang, J. U., and Bergles, D. E. (2014). Norepinephrine controls astroglial responsiveness to local circuit activity. *Neuron* 82, 1263–1270. doi: 10.1016/j.neuron.2014.04.038

Perea, G., and Araque, A. (2005). Properties of synaptically evoked astrocyte calcium signal reveal synaptic information processing by astrocytes. *J. Neurosci.* 25, 2192–2203. doi: 10.1523/jneurosci.3965-04.2005

Perea, G., Gómez, R., Mederos, S., Covelo, A., Ballesteros, J. J., Schlosser, L., et al. (2016). Activity-dependent switch of GABAergic inhibition into glutamatergic excitation in astrocyte-neuron networks. *eLife* 5:e20362.

Pirttimaki, T. M., Hall, S. D., and Parri, H. R. (2011). Sustained neuronal activity generated by glial plasticity. *J. Neurosci.* 31, 7637–7647. doi: 10.1523/jneurosci.5783-10.2011

Poskanzer, K. E., and Yuste, R. (2011). Astrocytic regulation of cortical UP states. *Proc. Natl. Acad. Sci. U.S.A.* 108, 18453–18458. doi: 10.1073/pnas.1112378108

Poskanzer, K. E., and Yuste, R. (2016). Astrocytes regulate cortical state switching in vivo. *Proc. Natl. Acad. Sci. U.S.A.* 113, E2675–E2684.

Ramos-Mandujano, G., Vázquez-Juárez, E., Hernández-Benítez, R., and Pasantes-Morales, H. (2007). Thrombin potently enhances swelling-sensitive glutamate efflux from cultured astrocytes. *Glia* 55, 917–925. doi: 10.1002/glia.20513

Reyes-Haro, D., Müller, J., Boresch, M., Pivneva, T., Benedetti, B., Scheller, A., et al. (2010). Neuron-astrocyte interactions in the medial nucleus of the trapezoid body. *J. Gen. Physiol.* 135, 583–594. doi: 10.1085/jgp.200910354

Richerson, G. B., and Wu, Y. (2003). Dynamic equilibrium of neurotransmitter transporters: not just for reuptake anymore. *J. Neurophysiol.* 90, 1363–1374. doi: 10.1152/jn.00317.2003

Robel, S., and Sontheimer, H. (2016). Glia as drivers of abnormal neuronal activity. *Nat. Neurosci.* 19, 28–33. doi: 10.1038/nn.4184

Rossi, D. J., Oshima, T., and Attwell, D. (2000). Glutamate release in severe brain ischaemia is mainly by reversed uptake. *Nature* 403, 316–321. doi: 10.1038/35002090

Rusakov, D. A. (2015). Disentangling calcium-driven astrocyte physiology. *Nat. Rev. Neurosci.* 16, 226–233. doi: 10.1038/nrn3878

Saab, A. S., Neumeyer, A., Jahn, H. M., Cupido, A., Šimek, A. A., Boele, H. J., et al. (2012). Bergmann glial AMPA receptors are required for fine motor coordination. *Science* 337, 749–753. doi: 10.1126/science.1221140

Sanon, N., Carmant, L., Emond, M., Congar, P., and Lacaille, J. C. (2005). Short-term effects of kainic acid on CA1 hippocampal interneurons differentially vulnerable to excitotoxicity. *Epilepsia* 46, 837–848. doi: 10.1111/j.1528-1167.2005.21404.x

Sasaki, T., Ishikawa, T., Abe, R., Nakayama, R., Asada, A., Matsuki, N., et al. (2014). Astrocyte calcium signalling orchestrates neuronal synchronization in organotypic hippocampal slices. *J. Physiol.* 592, 2771–2783. doi: 10.1113/jphysiol.2014.272864

Sasaki, T., Kuga, N., Namiki, S., Matsuki, N., and Ikegaya, Y. (2011). Locally synchronized astrocytes. *Cereb. Cortex* 21, 1889–1900. doi: 10.1093/cercor/bhq256

Savtchouk, I., and Volterra, A. (2018). Gliotransmission: beyond black-and-white. *J. Neurosci.* 38, 14–25. doi: 10.1523/jneurosci.0017-17.2017

Schipke, C. G., Ohlemeyer, C., Matyash, M., Nolte, C., Kettenmann, H., and Kirchhoff, F. (2001). Astrocytes of the mouse neocortex express functional N-methyl-D-aspartate receptors. *FASEB J.* 15, 1270–1272. doi: 10.1096/fj.00-0439fje

Schummers, J., Yu, H., and Sur, M. (2008). Tuned responses of astrocytes and their influence on hemodynamic signals in the visual cortex. *Science* 320, 1638–1643. doi: 10.1126/science.1156120

Schwarz, Y., Zhao, N., Kirchhoff, F., and Bruns, D. (2017). Astrocytes control synaptic strength by two distinct v-SNARE-dependent release pathways. *Nat. Neurosci.* 20, 1529–1539. doi: 10.1038/nn.4647

Seidel, J. L., Escartin, C., Ayata, C., Bonvento, G., and Shuttleworth, C. W. (2016). Multifaceted roles for astrocytes in spreading depolarization: a target

for limiting spreading depolarization in acute brain injury? *Glia* 64, 5–20. doi: 10.1002/glia.22824

Semyanov, A., Henneberger, C., and Agarwal, A. (2020). Making sense of astrocytic calcium signals - from acquisition to interpretation. *Nat. Rev. Neurosci.* 21, 551–564. doi: 10.1038/s41583-020-0361-8

Serrano, A., Haddjeri, N., Lacaille, J. C., and Robitaille, R. (2006). GABAergic network activation of glial cells underlies hippocampal heterosynaptic depression. *J. Neurosci.* 26, 5370–5382. doi: 10.1523/jneurosci.5255-05.2006

Serrano, A., Robitaille, R., and Lacaille, J. C. (2008). Differential NMDA-dependent activation of glial cells in mouse hippocampus. *Glia* 56, 1648–1663. doi: 10.1002/glia.20717

Sherwood, M. W., Arizono, M., Hisatsune, C., Bannai, H., Ebisui, E., Sherwood, J. L., et al. (2017). Astrocytic IP. *Glia* 65, 502–513.

Shigetomi, E., Bowser, D. N., Sofroniew, M. V., and Khakh, B. S. (2008). Two forms of astrocyte calcium excitability have distinct effects on NMDA receptor-mediated slow inward currents in pyramidal neurons. *J. Neurosci.* 28, 6659–6663. doi: 10.1523/jneurosci.1717-08.2008

Shigetomi, E., Bushong, E. A., Haustein, M. D., Tong, X., Jackson-Weaver, O., Kracun, S., et al. (2013). Imaging calcium microdomains within entire astrocyte territories and endfeet with GCaMPs expressed using adeno-associated viruses. *J. Gen. Physiol.* 141, 633–647. doi: 10.1085/jgp.201210949

Shigetomi, E., Saito, K., Sano, F., and Koizumi, S. (2019). Aberrant calcium signals in reactive astrocytes: a key process in neurological disorders. *Int. J. Mol. Sci.* 20:996. doi: 10.3390/ijms20040996

Shigetomi, E., Tong, X., Kwan, K. Y., Corey, D. P., and Khakh, B. S. (2011). TRPA1 channels regulate astrocyte resting calcium and inhibitory synapse efficacy through GAT-3. *Nat. Neurosci.* 15, 70–80. doi: 10.1038/nn.3000

Smith, N. A., Bekar, L. K., and Nedergaard, M. (2020). Astrocytic endocannabinoids mediate hippocampal transient heterosynaptic depression. *Neurochem. Res.* 45, 100–108. doi: 10.1007/s11064-019-02834-0

Srinivasan, R., Huang, B. S., Venugopal, S., Johnston, A. D., Chai, H., Zeng, H., et al. (2015). Ca(2+) signaling in astrocytes from Ip3r2(-/-) mice in brain slices and during startle responses in vivo. *Nat. Neurosci.* 18, 708–717. doi: 10.1038/nn.4001

Steinhäuser, C., Grunnet, M., and Carmignoto, G. (2016). Crucial role of astrocytes in temporal lobe epilepsy. *Neuroscience* 323, 157–169. doi: 10.1016/j.neuroscience.2014.12.047

Stobart, J. L., Ferrari, K. D., Barrett, M. J. P., Glück, C., Stobart, M. J., Zuend, M., et al. (2018). Cortical circuit activity evokes rapid astrocyte calcium signals on a similar timescale to neurons. *Neuron* 98, 726–735.e4.

Sun, M. Y., Devaraju, P., Xie, A. X., Holman, I., Samones, E., Murphy, T. R., et al. (2014). Astrocyte calcium microdomains are inhibited by bafilomycin A1 and cannot be replicated by low-level Schaffer collateral stimulation in situ. *Cell Calcium* 55, 1–16. doi: 10.1016/j.ceca.2013.10.004

Sun, W., McConnell, E., Pare, J.-F., Xu, Q., Chen, M., Peng, W., et al. (2013). Glutamate-dependent neuroglial calcium signaling differs between young and adult brain. *Science* 339, 197–200. doi: 10.1126/science.1226740

Szabó, Z., Héja, L., Szalay, G., Kékesi, O., Füredi, A., Szebényi, K., et al. (2017). Extensive astrocyte synchronization advances neuronal coupling in slow wave activity in vivo. *Sci. Rep.* 7:6018.

Tanaka, K., Watase, K., Manabe, T., Yamada, K., Watanabe, M., Takahashi, K., et al. (1997). Epilepsy and exacerbation of brain injury in mice lacking the glutamate transporter GLT-1. *Science* 276, 1699–1702. doi: 10.1126/science.276.5319.1699

Tancredi, V., Biagini, G., D'Antuono, M., Louvel, J., Pumain, R., and Avoli, M. (2000). Spindle-like thalamocortical synchronization in a rat brain slice preparation. *J. Neurophysiol.* 84, 1093–1097. doi: 10.1152/jn.2000.84.2.1093

Tian, G. F., Azmi, H., Takano, T., Xu, Q. W., Peng, W. G., Lin, J., et al. (2005). An astrocytic basis of epilepsy. *Nat. Med.* 11, 973–981.

Treiman, D. M. (2001). GABAergic mechanisms in epilepsy. *Epilepsia* 42(Suppl. 3), 8–12. doi: 10.1046/j.1528-1157.2001.042suppl.3008.x

Umpierre, A. D., West, P. J., White, J. A., and Wilcox, K. S. (2019). Conditional knock-out of mGluR5 from astrocytes during epilepsy development impairs high-frequency glutamate uptake. *J. Neurosci.* 39, 727–742. doi: 10.1523/jneurosci.1148-18.2018

Unichenko, P., Dvorzhak, A., and Kirischuk, S. (2013). Transporter-mediated replacement of extracellular glutamate for GABA in the developing murine neocortex. *Eur. J. Neurosci.* 38, 3580–3588. doi: 10.1111/ejn.12380

Upadhya, D., Kodali, M., Gitai, D., Castro, O. W., Zanirati, G., Upadhya, R., et al. (2019). A model of chronic temporal lobe epilepsy presenting constantly rhythmic and robust spontaneous seizures, co-morbidities and hippocampal neuropathology. *Aging Dis.* 10, 915–936. doi: 10.14336/ad.2019.0720

Vargas, J. R., Takahashi, D. K., Thomson, K. E., and Wilcox, K. S. (2013). The expression of kainate receptor subunits in hippocampal astrocytes after experimentally induced status epilepticus. *J. Neuropathol. Exp. Neurol.* 72, 919–932. doi: 10.1097/nen.0b013e3182a4b266

Verkhratsky, A., and Kirchhoff, F. (2007). NMDA receptors in glia. *Neuroscientist* 13, 28–37. doi: 10.1177/1073858406294270

Verkhratsky, A., Reyes, R. C., and Parpura, V. (2014). TRP channels coordinate ion signalling in astroglia. *Rev. Physiol. Biochem. Pharmacol.* 166, 1–22. doi: 10.1007/112_2013_15

Verkhratsky, A., Rodríguez, J. J., and Parpura, V. (2012). Calcium signalling in astroglia. *Mol. Cell Endocrinol.* 353, 45–56. doi: 10.1016/j.mce.2011.08.039

Verkhratsky, A., and Steinhäuser, C. (2000). Ion channels in glial cells. *Brain Res. Brain Res. Rev.* 32, 380–412. doi: 10.1016/s0165-0173(99)00093-4

Wang, F., Smith, N. A., Xu, Q., Goldman, S., Peng, W., Huang, J. H., et al. (2013). Photolysis of caged Ca2+ but not receptor-mediated Ca2+ signaling triggers astrocytic glutamate release. *J. Neurosci.* 33, 17404–17412. doi: 10.1523/jneurosci.2178-13.2013

Wang, X., Takano, T., and Nedergaard, M. (2009). Astrocytic calcium signaling: mechanism and implications for functional brain imaging. *Methods Mol. Biol.* 489, 93–109. doi: 10.1007/978-1-59745-543-5_5

Woo, D. H., Han, K. S., Shim, J. W., Yoon, B. E., Kim, E., Bae, J. Y., et al. (2012). TREK-1 and Best1 channels mediate fast and slow glutamate release in astrocytes upon GPCR activation. *Cell* 151, 25–40. doi: 10.1016/j.cell.2012.09.005

Xin, W., Schuebel, K. E., Jair, K. W., Cimbro, R., De Biase, L. M., Goldman, D., et al. (2019). Ventral midbrain astrocytes display unique physiological features and sensitivity to dopamine D2 receptor signaling. *Neuropsychopharmacology* 44, 344–355. doi: 10.1038/s41386-018-0151-4

Xu, J., Peng, H., Kang, N., Zhao, Z., Lin, J. H., Stanton, P. K., et al. (2007). Glutamate-induced exocytosis of glutamate from astrocytes. *J. Biol. Chem.* 282, 24185–24197. doi: 10.1074/jbc.m700452200

Yarishkin, O., Lee, J., Jo, S., Hwang, E. M., and Lee, C. J. (2015). Disinhibitory action of astrocytic GABA at the perforant path to dentate gyrus granule neuron synapse reverses to inhibitory in Alzheimer's disease model. *Exp. Neurobiol.* 24, 211–218. doi: 10.5607/en.2015.24.3.211

Ye, Z. C., Wyeth, M. S., Baltan-Tekkok, S., and Ransom, B. R. (2003). Functional hemichannels in astrocytes: a novel mechanism of glutamate release. *J. Neurosci.* 23, 3588–3596. doi: 10.1523/jneurosci.23-09-03588.2003

Yoon, B. E., Jo, S., Woo, J., Lee, J. H., Kim, T., Kim, D., et al. (2011). The amount of astrocytic GABA positively correlates with the degree of tonic inhibition in hippocampal CA1 and cerebellum. *Mol. Brain* 4:42. doi: 10.1186/1756-6606-4-42

Yoon, B. E., and Lee, C. J. (2014). GABA as a rising gliotransmitter. *Front. Neural Circuits* 8:141. doi: 10.3389/fncir.2014.00141

Yu, X., Taylor, A. M. W., Nagai, J., Golshani, P., Evans, C. J., Coppola, G., et al. (2018). Reducing astrocyte calcium signaling in vivo alters striatal microcircuits and causes repetitive behavior. *Neuron* 99, 1170–1187.e9.

Zhang, Y., and Barres, B. A. (2010). Astrocyte heterogeneity: an underappreciated topic in neurobiology. *Curr. Opin. Neurobiol.* 20, 588–594. doi: 10.1016/j.conb.2010.06.005

Conflict of Interest: The authors declare that the research was conducted in the absence of any commercial or financial relationships that could be construed as a potential conflict of interest.

frontiers in Cellular Neuroscience

REVIEW
published: 25 February 2021
doi: 10.3389/fncel.2021.645691

Astrocytes, Noradrenaline, α1-Adrenoreceptors, and Neuromodulation: Evidence and Unanswered Questions

Jérôme Wahis[1,2,3]* *and Matthew G. Holt*[1,2,3]*

[1] Laboratory of Glia Biology, VIB-KU Leuven Center for Brain and Disease Research, Leuven, Belgium, [2] Department of Neurosciences, KU Leuven, Leuven, Belgium, [3] Leuven Brain Institute, Leuven, Belgium

Noradrenaline is a major neuromodulator in the central nervous system (CNS). It is released from varicosities on neuronal efferents, which originate principally from the main noradrenergic nuclei of the brain – the locus coeruleus – and spread throughout the parenchyma. Noradrenaline is released in response to various stimuli and has complex physiological effects, in large part due to the wide diversity of noradrenergic receptors expressed in the brain, which trigger diverse signaling pathways. In general, however, its main effect on CNS function appears to be to increase arousal state. Although the effects of noradrenaline have been researched extensively, the majority of studies have assumed that noradrenaline exerts its effects by acting directly on neurons. However, neurons are not the only cells in the CNS expressing noradrenaline receptors. Astrocytes are responsive to a range of neuromodulators – including noradrenaline. In fact, noradrenaline evokes robust calcium transients in astrocytes across brain regions, through activation of α1-adrenoreceptors. Crucially, astrocytes ensheath neurons at synapses and are known to modulate synaptic activity. Hence, astrocytes are in a key position to relay, or amplify, the effects of noradrenaline on neurons, most notably by modulating inhibitory transmission. Based on a critical appraisal of the current literature, we use this review to argue that a better understanding of astrocyte-mediated noradrenaline signaling is therefore essential, if we are ever to fully understand CNS function. We discuss the emerging concept of astrocyte heterogeneity and speculate on how this might impact the noradrenergic modulation of neuronal circuits. Finally, we outline possible experimental strategies to clearly delineate the role(s) of astrocytes in noradrenergic signaling, and neuromodulation in general, highlighting the urgent need for more specific and flexible experimental tools.

Keywords: α1-adrenoceptor, α1-adrenergic receptors, noradrenaline (NA), norepinephrine (NE), neuromodulation, astrocyte–neuron interaction, astrocyte calcium

OPEN ACCESS

Edited by:
Wannan Tang,
University of Oslo, Norway

Reviewed by:
Yuriy Pankratov,
University of Warwick,
United Kingdom
Robert Zorec,
University of Ljubljana, Slovenia

***Correspondence:**
Jérôme Wahis
Jerome.Wahis@kuleuven.be
Matthew G. Holt
Matthew.Holt@kuleuven.be

Specialty section:
This article was submitted to Non-Neuronal Cells, a section of the journal Frontiers in Cellular Neuroscience

Received: *23 December 2020*
Accepted: *03 February 2021*
Published: *25 February 2021*

Citation:
Wahis J and Holt MG (2021) Astrocytes, Noradrenaline, α1-Adrenoreceptors, and Neuromodulation: Evidence and Unanswered Questions. Front. Cell. Neurosci. 15:645691. doi: 10.3389/fncel.2021.645691

INTRODUCTION

Astrocytes are a major cell type in the central nervous system (CNS), found across brain regions, generally in a non-overlapping fashion (Nimmerjahn and Bergles, 2015). Astrocytes possess many thin membraneous processes, which extend out from the cell body into the parenchyma, where they contact neurons at synapses, physically isolating these structures. This so-called tripartite synapse

structure is remarkably common, with up to 90% of mouse cortical synapses being associated with an astrocyte process (Genoud et al., 2006). Not only are astrocytes necessary for synapse formation and maintenance, they have also been shown to perform key roles in the maintenance of local synaptic homeostasis, such as regulating extracellular K^+ and neurotransmitter levels (Verkhratsky and Nedergaard, 2018). While these important functions are well established, the past decades have seen an upsurge in astrocyte-oriented neuroscience research, fueled largely by the emergence of new technologies (Yu et al., 2020), revealing that astrocytes are not simple housekeeping cells, which passively service the needs of neurons. In fact, numerous studies have shown that astrocytes are actually a dynamic cell type, which respond to a wide range of stimuli, most notably neurotransmitters and neuromodulators, for which they express a large repertoire of receptors (Verkhratsky and Nedergaard, 2018). Astrocytes respond to stimuli in an active fashion, often measured as transient changes in intracellular calcium ($[Ca^{2+}]_i$) (Rusakov, 2015; Bazargani and Attwell, 2016; Shigetomi et al., 2016), and can in turn release active signaling molecules (gliosignals) (Vardjan and Zorec, 2015), which induce responses in their target cells (Perea and Araque, 2005; Verkhratsky and Nedergaard, 2018). At the synapse, these small neuroactive molecules have been shown to act on both neuronal and glial cell surface receptors to modulate circuit activity and are more commonly referred to as gliotransmitters (Durkee and Araque, 2019). Changes in astrocyte activity can also modulate their K^+ buffering capacity, with important consequences for local neuronal excitability (Beckner, 2020). Astrocytes are also central players in CNS energy production, through lactate production and secretion, which is influenced by the activation state of the cell (Magistretti and Allaman, 2018). Moreover, astrocyte morphology often changes in response to stimuli, and such changes affect the interactions of astrocytes with neurons at the tripartite synapse (Zhou et al., 2019; Henneberger et al., 2020). Furthermore, astrocytes are coupled into functional networks via gap junctions, allowing crosstalk between otherwise unrelated and relatively distant synapses, a process referred to as lateral regulation of synaptic activity (Covelo and Araque, 2016).

Interestingly, similar effects on CNS circuits have also been attributed to neuromodulators (Pacholko et al., 2020). Indeed, neuromodulators often exert effects on numerous, otherwise unrelated, synapses to change global CNS activity, in response to specific environmental or internal stimuli (Avery and Krichmar, 2017). Over the past several years, there has been accumulating evidence that several neuromodulators may well exert their effects through astrocytes (Ma et al., 2016; Papouin et al., 2017; Robin et al., 2018; Corkrum et al., 2019, 2020; Mu et al., 2019; Wahis et al., 2021b), a subject which is also reviewed in Pacholko et al. (2020). In this review, we focus on noradrenergic neuromodulation through α1-adrenoreceptor (α1-NAR) signaling, as this G Protein Coupled Receptor (GPCR) is highly expressed in astrocytes and is Gq-coupled, leading to intracellular Ca^{2+} release following noradrenaline receptor (NAR) activation.

We organize this review according to the sequence of events involved in astrocyte α1-NAR signaling, starting with the release of noradrenaline (NA) and its action on NARs. We then discuss the evidence indicating that α1-NAR activation is not only modulated by prior cellular activation history, but may also 'prime' astrocytes to be more sensitive to synaptic inputs. Next, we review the known effects α1-NAR signaling has on astrocyte functions, followed by a discussion of how this then impacts the activity of brain circuits. Furthermore, we advance a hypothesis linking astrocytes and inhibitory neurons as a functional unit in α1-NAR signaling. Key concepts discussed are shown schematically in **Figure 1**. We also discuss these issues in light of recent advances in our understanding of astrocyte heterogeneity (Pestana et al., 2020), and how this might impact noradrenergic neuromodulation through astrocytes. Finally, we highlight an ensemble of technical approaches that might be relevant in helping us understand, in greater detail, how astrocytes and NA interact to modulate different brain circuits in the CNS.

NA RELEASE IN THE CNS

Noradrenaline (also known as norepinephrine) is a catecholamine synthesized from the amino acid tyrosine and is a direct derivative of the neurotransmitter dopamine. It is produced in several groups of neurons, amongst which the brain stem locus coeruleus (LC) is the principal source of noradrenergic afferences in the CNS (Samuels and Szabadi, 2008; Schwarz and Luo, 2015). LC neurons display different firing patterns, consisting either of tonic spikes or phasic bursts of action potentials, which have been associated with the control of wakefulness. Changes in LC firing patterns usually predict changes in behavioral state, with increased tonic firing being correlated with increased arousal, and phasic bursting with the response to salient sensory stimuli (Berridge and Waterhouse, 2003). NA is thought to act on brain function by changing the gain of neuronal circuits, allowing animals to quickly adapt their behavior to changing environmental conditions (Bouret and Sara, 2005; Sara and Bouret, 2012). An interesting feature of noradrenergic transmission is the mode of NA release. Indeed, 20% (or less) of varicosities on monoaminergic (noradrenergic) axons (Vizi et al., 2010), seem to form typical neuronal synapses, while the remainder preferentially face astrocytic processes and release neuromodulators into the extracellular space, which then act as so-called volume transmitters (**Figure 1A**) (Cohen et al., 1997; Descarries and Mechawar, 2000; Hirase et al., 2014; Fuxe et al., 2015). Crucially, in the case of noradrenergic neurons this figure appears to be lower, with up to 95% of NA varicosities being devoid of synaptic contacts in cortex (Vizi et al., 2010). This morphological evidence is a key component of the hypothesis that astrocytes are important targets of noradrenergic signaling (Stone and Ariano, 1989; Hirase et al., 2014; Fuxe et al., 2015; Pacholko et al., 2020).

NORADRENERGIC RECEPTORS IN THE CNS

Noradrenaline acts on three functional groups of NARs, all of which belong to the GPCR superfamily. α1-NAR are coupled

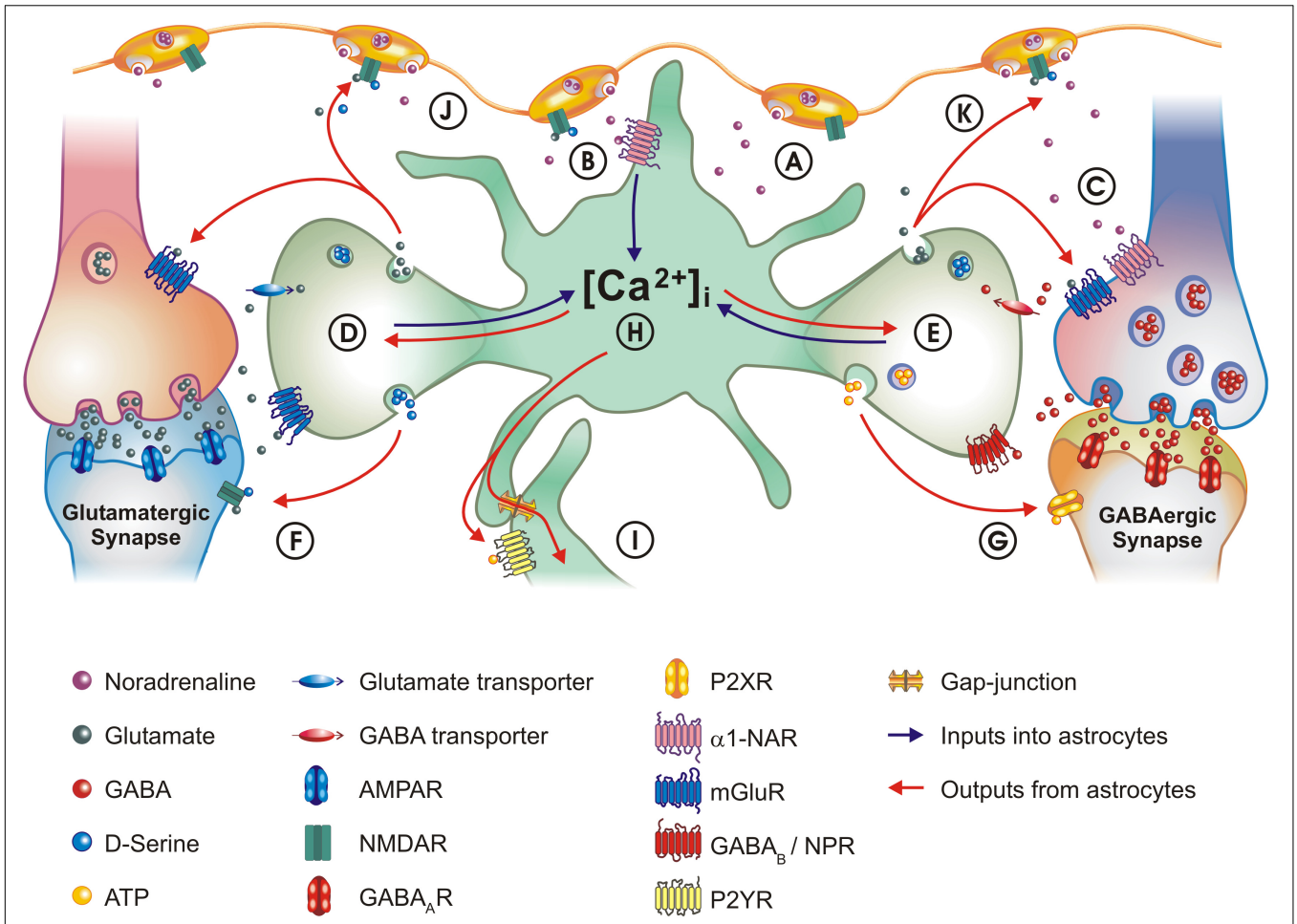

FIGURE 1 | Schematic of astrocyte – neuron interactions and the role of α1-NAR signaling. **(A)** NA is released from LC varicosities into the extracellular space. **(B)** Activation of α1-NAR on astrocytes elicits $[Ca^{2+}]_i$ transients. **(C)** GABAergic interneurons also express α1-NAR. **(D)** Astrocytes appear capable of integrating information across signaling modalities: α1-NAR signaling 'primes' astrocytes to local glutamatergic synapse activity. **(E)** Astrocytes also integrate activity at GABAergic synapses, through co-activation of neuropeptide receptors (NPR) and $GABA_B$ receptors. **(F)** One consequence of astrocyte stimulation is modulation of synaptic activity: one major mechanism by which this occurs is the release of glutamate and D-serine, which activate NMDA receptors, as well as pre-synaptic metabotropic glutamate receptors (mGluR) on neurons. **(G)** Astrocytes can downregulate $GABA_A$ currents by releasing ATP which acts on neuronal P2X receptors. **(H)** Astrocytes can transform inhibitory activity at a GABAergic synapse into excitatory signaling at a glutamatergic synapse – a concept known as lateral regulation. **(I)** The concept of lateral regulation also extends to when functionally coupled astrocytes act as bridges, allowing communication between distant synapses. Mechanisms used are either paracrine secretion (local purinergic signaling), or direct transfer of the $[Ca^{2+}]_i$ signal (or metabolites) through gap-junctions. **(J)** Integrating synaptic activity with α1-NAR signaling allows astrocytes to participate in the "Glutamate Amplifies Noradrenergic Effects" (GANE) mechanism, in which astrocytes act in a positive feedback loop releasing glutamate, which acts on receptors located in LC axons to stimulate further noradrenaline release. **(K)** A mechanism analogous to "GANE" may also act at GABAergic synapses, with astrocytes transforming GABAergic activity into glutamate release. For purposes of clarity, the size of the different elements are not drawn to scale. In the legend key, R, receptor.

to Gq signaling pathways, α2-NAR to Gi and β1-3-NAR to Gs. Each functional group is further composed of three subclasses, each corresponding to a different gene product: α1A-, α1B-, α1D-NAR; α2A-, α2B-, α2C-NAR; β1-, β2-, β3-NAR. These three functional groups of NAR have different affinities for NA, from highest to lowest: α2 (∼50 nM), α1 (∼300 nM), and β1-3 (∼800 nM), suggesting that cells show different responses depending on the local NA concentration they are exposed to, in combination with the repertoire of NARs expressed (Ramos and Arnsten, 2007; Atzori et al., 2016). In their review, Atzori et al. (2016) build an interesting hypothesis based on this simple starting premise: they argue that activation of the different NARs effectively follows the firing patterns of LC neurons. During sleep, the LC is not firing and no NAR are activated; during quiet wakefulness, increases in both tonic and phasic firing of LC neurons promote activation of α2- and α1-NAR, while β-NAR are only ever activated in "fight or flight" behavioral states, correlated to low phasic firing and a sustained tonic release (Atzori et al., 2016). An interesting *in vivo* imaging study, which reinforces this hypothesis, found that α1-NAR are indeed activated during quiet wakefulness, when significant behavioral stimuli emerge (i.e., when a facial air puff startles the animal). This activation

is linked to phasic activity in NAergic neurons. In contrast, β-NAR are only activated during long-lasting aversive stimuli (i.e., repetitive foot-shocks) linked to continual phasic activity of NA axons (Oe et al., 2020). This provides a framework of how NA signaling functions and encodes environmental information relevant for the animal: cells (co)-express various NARs, and their different affinities for NA help the cell distinguish between different levels of extracellular NA, which are a function of the rate and mode of LC axon firing. Interestingly, the cell type that was studied by Oe et al. (2020), and found to respond to activation of both α1- and β-NAR, is the astrocyte. These *in vivo* results confirmed an earlier report showing similar modes of NA signaling in cultured rat astrocytes (Horvat et al., 2016). While these studies clearly demonstrate functional responses of astrocytes to both α1- and β-NAR signaling, other cell types in the CNS also express NARs, which complicates the entire issue of how cell-type specific effects of NA impact on CNS function. Indeed, NAR expression profiles remain a matter of debate and are only being slowly clarified. This is probably due to the difficulties of obtaining reliable antibodies for adrenoreceptors, as well as the shortcomings of genetic models generally used to study this question (in which overexpression of reporter genes, driven by a fragment of the endogenous promoter, might not precisely recapitulate the cellular expression profile of a given NAR; Perez, 2020).

Astrocytes and α1-NAR

Assessing all the literature on NAR expression patterns in the CNS would constitute a review in itself. As astrocyte Ca^{2+} signaling is central to the modulation of synaptic transmission and neural network excitability (Khakh and McCarthy, 2015; Bazargani and Attwell, 2016), we will focus on the role of α1-NAR signaling in these cells. Indeed, it has been clear for several decades that astrocyte α1-NAR are a prime target of NA (Salm and McCarthy, 1989, 1992; Stone and Ariano, 1989; Shao and Sutin, 1992). α1-NAR are coupled into Gq signaling pathways, which trigger increases in $[Ca^{2+}]_i$ in astrocytes, following startling stimuli or the activation of LC neurons using electrical stimulation (**Figure 1B**) (Bekar et al., 2008; Ding et al., 2013; Paukert et al., 2014; Oe et al., 2020). Recent transcriptome studies confirmed mouse astrocytes express transcripts encoding α1A- (*Adra1a*), α1B- (*Adra1b*), and α1D-NAR (*Adra1d*), as well as transcripts for α2- and β-NAR (Cahoy et al., 2008; Hertz et al., 2010; Batiuk et al., 2020). While one of these studies (Hertz et al., 2010) argues for astrocyte-specific expression of α1-NAR, it should be noted that other single cell RNA sequencing studies have found that (inter)neurons also express significant amounts of the various α1-NAR transcripts (**Figure 1C**) (Zhang et al., 2014; Zeisel et al., 2015). The majority of single cell transcriptome studies, however, are in agreement that α1A-NAR and α1B-NAR appear to be the main α1-NAR subtypes expressed in cortical astrocytes, with α1D-NAR found in much lower amounts, effectively confirming earlier work using transgenic models and radioligand binding (Perez, 2020). Two recent studies independently generated transgenic mouse lines with *LoxP* sites flanking *Adra1a*, allowing conditional deletion of the gene in astrocytes by crossing to appropriate Cre drivers. Both found a loss of calcium transients evoked by enforced locomotion (i.e., a form of startling), or noxious stimuli, in cerebellar (Ye et al., 2020) and spinal cord astrocytes (Kohro et al., 2020), respectively. This is consistent with the transcriptome data from astrocytes isolated from these regions (Anderson et al., 2016; Boisvert et al., 2018). Interestingly, deletion of *Adra1a* was sufficient to result in a loss of NA induced $[Ca^{2+}]_i$ elevations in both cerebellar and spinal cord astrocytes, despite the expression of *Adra1b* transcripts. This indicates that in these brain regions, the increase in $[Ca^{2+}]_i$ elicited by α1-NAR activation is mediated principally through the α1A-NAR subtype. Whether this holds true in other brain regions awaits clarification. While these data were all obtained in rodents, the importance of α1-NAR signaling through astrocytes seems evolutionary conserved. Indeed, tyramine and octopamine, the invertebrate equivalents of NA, also signal to astrocyte-like cells in *Drosophila melanogaster*. Moreover, tyramine-octopamine evoked astrocyte $[Ca^{2+}]_i$ transients are crucial for neuromodulation. Interestingly, the fact that these $[Ca^{2+}]_i$ transients can be blocked by application of terazosin, an antagonist of vertebrate α1-NAR, highlights the conservation of the basic building blocks used by invertebrates and vertebrates to construct key signaling pathways (Ma et al., 2016). More recently, it was also found that zebrafish α1B-NAR are expressed in radial astrocytes and are essential for NA-mediated responses generated by repeated behavioral (locomotor) failures. Human data are scarce, but indicate that the α1-NAR mRNA expression patterns observed in mouse astrocytes and neurons are essentially conserved (Zhang et al., 2016), while data from the human protein atlas confirm that glial cells are the main cell type expressing *ADRA1A* in human cortex[1] (Thul et al., 2017). This indicates noradrenergic signaling, through astrocytic α1-NAR, has been conserved throughout evolution, highlighting its importance.

α1-NAR TRIGGERED CALCIUM SIGNALING IN ASTROCYTES: A SWITCH FOR SIGNAL INTEGRATION?

In this section, we will evaluate evidence indicating that astrocytic $[Ca^{2+}]_i$ transients evoked by α1-NAR activation can be modulated by interactions with other signaling pathways, and argue that this represents a form of complex signal integration in astrocytes.

Astrocytes Encode Levels of NA

Phasic release of NA reliably provokes Ca^{2+} transients in astrocytes (Slezak et al., 2019), through α1-NAR signaling (Bekar et al., 2008; Ding et al., 2013; Paukert et al., 2014; Oe et al., 2020). Interestingly, another study found this response is dependent on the degree of NAergic neuron firing. Indeed, Mu et al. (2019) found that zebrafish radial astrocytes encode the number of behavioral (locomotor) failures through successive bouts of

[1]https://www.proteinatlas.org/ENSG00000120907-ADRA1A/tissue/cerebral+cortex#imid_8462679

NAergic neuron activity and the accumulation of astrocyte $[Ca^{2+}]_i$ following α1-NAR activation; once a $[Ca^{2+}]_i$ threshold is reached, GABAergic neurons are then activated by astrocytes, leading to a change in behavioral state. However, the molecular mechanisms by which astrocytes encode the history of α1-NAR activation and modulate GABAergic neuron activity are currently unclear (Mu et al., 2019). However, insights into the possible mechanism(s) can be found in other studies. Nuriya et al. (2017) found that background levels of NA (500 nM) facilitate the astrocyte $[Ca^{2+}]_i$ response evoked by a short pulse of NA designed to mimic local release from LC varicosities (20 μM). Interestingly, this background 'priming' was shown to occur via β-NAR activation and an associated increase in intracellular cAMP levels; in contrast, the astrocyte $[Ca^{2+}]_i$ response was shown to occur through an α1-NAR-dependent mechanism (Nuriya et al., 2017). Although seemingly counterintuitive, when considering NAR affinities alone, there are a number of plausible explanations accounting for this 'priming'. β-NAR signaling occurs on a slower timescale than α1-NAR activation (Horvat et al., 2016; Oe et al., 2020). Furthermore, synergistic actions between Gs and Gq-coupled signaling pathways have been reported (Delumeau et al., 1991; Cordeaux and Hill, 2002; Ahuja et al., 2014; Horvat et al., 2016). Hence, low levels of β-NAR signaling may act synergistically with α1-NAR signaling to facilitate astrocyte $[Ca^{2+}]_i$. Interestingly, β-NAR activation can also increase α1A-NAR expression, probably via post-transcriptional mechanisms, increasing mesenchymal stromal cell sensitivity to NA (Tyurin-Kuzmin et al., 2016). If the same holds true for astrocytes, this could also increase the sensitivity of cells to α1A-NAR activation. Interestingly, the two mechanisms postulated are not mutually exclusive and may act in tandem.

These last studies demonstrate that astrocytes can encode extracellular NA levels, likely through the synergistic effects of different NAR signaling pathways. This would allow astrocytes to encode salient behavioral stimuli (α1-NAR signaling through phasic NA release) with a different weight (encoded in the $[Ca^{2+}]_i$) depending on the wakefulness state (encoded in the ambient NA levels due to tonic NA release). Importantly, however, it would also incorporate aspects of behavioral history, taking into account the number of prior "startling" stimuli and the associated phasic release of NA.

Astrocytes Integrate Synaptic Activity Through α1-NAR Signaling

There is also *in vivo* evidence that astrocyte responses to phasic NA release, through α1-NAR signaling, are influenced by local synaptic activity. Paukert et al. (2014) found that Ca^{2+} transients elicited in mouse Bergmann glia by enforced locomotion are fully abolished by an α1-NAR antagonist. However, the transients are also diminished in amplitude when α-amino-3-hydroxy-5-methyl-4-isoxazolepropionic acid (AMPA) and *N*-methyl-D-aspartate (NMDA) receptor antagonists are applied, indicating the involvement of glutamatergic signaling in amplifying astrocyte responses to α1-NAR activation. Furthermore, the authors also found that visual cortex astrocytes do not reliably respond to visual stimuli during periods of quiet wakefulness, but that astrocyte $[Ca^{2+}]_i$ responses to enforced locomotion (through α1-NAR activation) are amplified if mice are simultaneously presented with a simple visual stimulus (light flash). This indicates that astrocytes integrate sensory inputs dependent on the behavioral state of the animal (Paukert et al., 2014). This result was later confirmed by work demonstrating that visual cortex astrocytes respond to moving visual stimuli in a retinotopic fashion but only when mice are locomoting, an effect which is linked to the presence of NA (Slezak et al., 2019) (although it should be noted that a recent study found contrasting results, with evidence for α1-NAR-mediated $[Ca^{2+}]_i$ signaling masking astrocyte responses to visual stimuli in mouse; Sonoda et al., 2018). Nonetheless, results similar to those obtained by Paukert et al. (2014) and Slezak et al. (2019) were obtained in zebrafish. Mu et al. (2019) observed that radial astrocytes in the lateral medulla oblongata do not reliably respond to neuronal activity during swimming. However, if NA neurons are optogenetically activated during swimming, radial astrocytes encode swimming-related neuronal activity in the form of robust $[Ca^{2+}]_i$ transients larger than those evoked by stimulation of NA neurons alone (Mu et al., 2019). This indicates a mechanism, seemingly conserved in vertebrates, in which the noradrenergic system gates, or at least greatly amplifies, the response of astrocytes to local synaptic inputs, through α1-NAR signaling. The mechanisms behind this gating phenomenon remain to be explored, but the data of Paukert et al. (2014) implicate glutamatergic ionotropic receptors. Whether these receptors are expressed alongside α1-NAR on astrocytes, or whether they are expressed independently on other (interacting) cell types, remains unclear at present. It should also be noted that none of the studies performed in mouse visual cortex that we cite unambiguously demonstrate the direct activation of astrocyte α1-NAR to be central to the observed effects. Even if this is the most likely explanation, it remains to be explored in future studies, likely employing the *Adra1a*-floxed mouse lines that were recently reported (Kohro et al., 2020; Ye et al., 2020).

Taken together, these reports clearly indicate that astrocyte responses to α1-NAR are complex, and are capable of integrating information based on recent circuit activity (**Figure 1D**). It is worth mentioning that signal integration by astrocytes also exists outside the frame of NA signaling. For instance, the $[Ca^{2+}]_i$ transients induced in mouse cortical astrocytes by GABA released from somatostatin interneurons are potentiated by the co-release of somatostatin that occurs when these neurons are subject to intense activation. However, the activity of parvalbumin interneurons, or somatostatin interneurons when somatostatin receptors are pharmacologically blocked, depresses astrocyte $[Ca^{2+}]_i$ responses triggered by $GABA_B$ receptor activation (Mariotti et al., 2018). Moreover, somatostatin is also able to potentiate the response of cultured striatal astrocytes to α1-NAR activation (Marin et al., 1993). A similar result was observed with another neuropeptide co-released with GABA from interneurons, vasoactive intestinal peptide (VIP). In this study, VIP receptor stimulation in astrocyte

cultures could essentially reduce the threshold to evoke $[Ca^{2+}]_i$ transients through α1-NAR activation, again indicating a synergistic action of the two receptor pathways (Fatatis et al., 1994). This indicates α1-NAR signaling can further be amplified at tripartite synapses involving somatostatin or VIP expressing GABAergic interneurons (**Figure 1E**, see also section "Astrocytes and α1-NAR: A System Tailored to Regulate Inhibition?").

So far, it remains unclear how the complex integration of synaptic activity with α1-NAR signaling affects the functional output(s) of vertebrate astrocytes. However, we believe it likely that it allows astrocytes to fine tune the activity of CNS circuits (discussed in sections "α1-NAR Signaling: Effects on Astrocyte Function" and "α1-NAR Signaling in Astrocytes: Relevance for Neuromodulation").

α1-NAR SIGNALING: EFFECTS ON ASTROCYTE FUNCTION

α1-NAR signaling has been linked to modulation of many known astrocyte functions, which may or may not involve increases in $[Ca^{2+}]_i$. However, the majority of these studies did not use cell-type specific manipulations, or were performed using reductionist *in vitro* models, hindering the extrapolation of results to the *in vivo* situation. Nonetheless, they provide interesting perspectives on how α1-NAR signaling could impact on astrocyte functions, with potentially important consequences for α1-NAR mediated neuromodulation.

For instance, activation of α1-NAR has been linked to increases in lactate formation and oxidative metabolism (Subbarao and Hertz, 1991), although most studies attribute α2-and β-NAR activation to metabolic regulation in astrocytes (Hertz et al., 2010), most notably glycogen metabolism (Subbarao and Hertz, 1990; Coggan et al., 2018; Oe et al., 2020). The role of astrocytes in production of lactate and its transport from astrocytes to neurons is an intense area of astrocyte research; it is clearly linked to noradrenergic signaling, but again, is mostly related to β-NAR activation (Magistretti and Allaman, 2018; Zuend et al., 2020). The regulation of astrocyte-mediated energy metabolism by α1-NAR might also be indirect, for instance by its action on glutamate uptake and the consequent increase in its metabolite, α-ketoglutarate (Alexander et al., 1997; Hertz et al., 2010). Interested readers are directed to more extensive recent reviews covering this topic (Dienel and Cruz, 2016; Alberini et al., 2018). The role α1-NARs play in regulating glutamate uptake into astrocytes might be especially relevant when it comes to controlling levels of (local) neuronal activity. Interestingly, increases in the rate of glutamate uptake following NA release seem to be solely linked to α1-NAR activity, while activation of β-NARs is thought to specifically increase the rate of GABA uptake into astrocytes (Hansson and Rönnbäck, 1989, 1992). This hints at potentially opposing roles for these two receptors, with α1-NAR activation decreasing excitatory glutamatergic signaling, and β-NAR decreasing inhibitory GABAergic signaling.

Another key homeostatic function of astrocytes is the maintenance of extracellular potassium levels ($[K^+]_e$). Following action potential firing, astrocytes remove K^+ from the extracellular space, using both active and passive mechanisms, and redistribute it through the (gap-junction coupled) astrocyte network, facilitating further action potential firing (Beckner, 2020). A recent study found that NA, likely acting through astrocytes, increases the speed at which $[K^+]_e$ reverts to basal levels following neuronal stimulation, and dampens the maximal increase of $[K^+]_e$ reached during high frequency neuronal activity (Wotton et al., 2020). Yet a possible role for α1-NAR in controlling $[K^+]_e$ remains unclear and requires further study. Indeed, most reports indicate a role for β-NAR in increasing K^+ uptake in astrocytes; in contrast, one study shows that phenylephrine, an α1-NAR agonist, reduces K^+ uptake in cultured astrocytes (Åkerman et al., 1988; Wotton et al., 2020).

α1-NAR receptors are also involved in controlling the level of gap-junction coupling between astrocytes. α1-NAR activation in cultured astrocytes leads to the phosphorylation and redistribution of connexins and loss of functional coupling (Giaume et al., 1991; Nuriya et al., 2018). This is in agreement with a study showing that α1-NAR signaling can decrease the propagation of $[Ca^{2+}]_i$ waves through an astrocyte network (Muyderman et al., 1998). In contrast, activation of β-NARs appears to have opposite actions, opening gap junctions and increasing permeability (Giaume et al., 1991; Scemes et al., 2017). This has potentially important consequences on neuronal function, as gap-junction-mediated communication between astrocytes plays a role in the functional and metabolic coupling of astrocytes and neurons (Pannasch and Rouach, 2013; Mayorquin et al., 2018).

Cultured astrocytes change morphology on exposure to NA, adopting a more compact, less branched structure (Bar El et al., 2018), although the NAR mediating this effect remains unknown. Other studies found that β-NAR signaling has the opposite effect, promoting astrocyte stellation in cultures (Vardjan et al., 2014; Koppel et al., 2018) and increasing astrocyte volume in tissue slices. These changes in astrocyte volume will directly impact the size of the extracellular space (Sherpa et al., 2016), impacting on neuronal excitability, by affecting the ability of astrocytes to regulate extracellular neurotransmitter and K^+ levels (Zhou et al., 2019; Henneberger et al., 2020).

Another function in which the precise role of α1-NAR versus β-NAR signaling in astrocytes remains unclear is the synthesis and secretion of trophic factors, such as brain-derived neurotrophic factor (BDNF) (Juric et al., 2008; Koppel et al., 2018), which are induced by NA.

To summarize, there is substantial evidence suggesting α1-NAR signaling in astrocytes has major functional effects. However, these need to be confirmed *in vivo*, for example, by conditional deletion of α1-NAR from astrocytes (see also section "Noradrenergic Receptors in the CNS" and "Future Strategies to Decipher the Role of NAR Signaling in Heterogenous Astrocyte Populations"). As there seems to be a close relationship to the functional consequences of α1-, α2-, and β-NAR activation, which either elicit opposing or reinforcing effects, a detailed

dissection of the role played by each NAR will be necessary to fully understand the consequences of NA signaling on individual astrocytes and, by extension, on CNS circuits.

α1-NAR SIGNALING IN ASTROCYTES: RELEVANCE FOR NEUROMODULATION

There is abundant literature on the roles of α1-NAR in neuromodulation, which was recently reviewed (Perez, 2020). Most studies highlight a role for α1-NAR in modulating synaptic efficacy and plasticity – and ultimately memory (Perez, 2020). Reports are sometimes contradictory at first glance. For example, one study found that α1-NAR signaling increases long-term potentiation (LTP) at CA3-CA1 synapses in the hippocampus (Izumi and Zorumski, 1999), while another found it increases long-term depression (LTD) at the same synapses (Dyer-Reaves et al., 2019). These discrepancies can likely be attributed to the different experimental protocols and tools used, but what is clear is that α1-NAR signaling affects the plasticity of neuronal circuits, with a common theme being effects on inhibitory transmission (Perez, 2020; and see section "Astrocytes and α1-NAR: A System Tailored to Regulate Inhibition?"). However, a common weakness amongst these studies is again the lack of cell-type specificity in the manipulations used. For example, the majority of studies employ small molecule agonists/antagonists that act on α1-NAR irrespective of the cell type expressing them; some studies use a transgenic mouse model expressing a constitutively active α1-NAR, which potentially does not recapitulate the precise expression profile of the endogenous receptor (see section "Noradrenergic Receptors in the CNS") (Perez, 2020). In addition to these obvious experimental caveats, most studies on α1-NAR neuromodulation simply (and erroneously in our opinion) assume that NA exerts its actions through direct modulation of neuronal activity. However, astrocytes have a clear role in plasticity mechanisms (Wahis et al., 2021a) and a few (key) studies have made a case for the importance of astrocyte α1-NAR signaling in NA-mediated neuromodulation, most notably in the control of synaptic plasticity.

For example, work in chicks, using metabolic inhibitors to impair astrocyte function, strongly argues for a role of astrocytic α1-NAR signaling in memory consolidation (Gibbs and Bowser, 2010). Another study reports that in the mouse periaqueductal gray, NA promotes arousal through the activation of α1-NAR, which are enriched in astrocytes in this brain region. Interestingly, activating a Gq-coupled Designer Drug Activated by a Designer Receptor (hM3Dq-DREADD), specifically expressed in astrocytes, was sufficient to mimic the positive effects of α1-NAR in this region, reinforcing a role for astrocytes in NA-mediated arousal modulation (Porter-Stransky et al., 2019). Pankratov and Lalo (2015) used several technical approaches to demonstrate that astrocytic α1-NAR signaling is essential for plasticity in the mouse cortex. They found that activation of α1A-NAR, using a subtype-selective agonist, induces the release of both ATP and D-serine in cortical slices. This effect is abolished in mice overexpressing a soluble SNARE protein fragment in astrocytes (dn-SNARE line), which acts in a dominant negative fashion to impair vesicular release of gliotransmitters, by preventing the formation of a productive SNARE core complex necessary for membrane fusion (Scales et al., 2000; Pascual et al., 2005; Jahn and Scheller, 2006; Guček et al., 2016), but note that the astrocyte specificity of dn-SNARE expression is debated (Fujita et al., 2014). They further show that NA induces an increase in the frequency of synaptic currents evoked in pyramidal neurons by purines, an effect abolished both in the dn-SNARE mouse model and when astrocytes are infused with tetanus toxin, a SNARE-specific protease (Holt et al., 2008), which acts to acutely block vesicular release of gliotransmitters. Finally, they found that astrocytic α1-NAR signaling, promoting ATP release in tissue slices, is crucial for LTP induction in visual cortex, which again was blocked by dominant negative SNARE expression or tetanus toxin treatment in astrocytes. Note that earlier work in hypothalamic astrocytes already hinted at a role for astrocytic α1-NAR in eliciting ATP release with subsequent modulation of synaptic activity (Gordon et al., 2005). Monai et al. (2016) demonstrated that transcranial direct current stimulation (tDCS)-induced potentiation of visual responses in cortex is abolished when an antagonist for α1-NAR is applied. Crucially, they found these effects to be dependent on astrocyte Gq signaling, since tDCS is equally ineffective in a transgenic mouse line in which the astrocyte-specific IP_3R2 receptor is genetically ablated (knocked out: KO), and α1-NAR evoked Ca^{2+} transients are consequently impaired (Srinivasan et al., 2015; Monai et al., 2016). This clearly hints at a core role for astrocytes in conveying the effects of α1-NAR signaling. To date, the strongest evidence for a role of astrocytic α1A-NAR in neuromodulation has been obtained using a recently created *Adra1a*-floxed mouse line, allowing conditional deletion of α1A-NAR in a subset of astrocytes located in the superficial laminae of the spinal cord (Kohro et al., 2020). These astrocytes respond directly to descending noradrenergic projections through α1A-NAR activation. This α1A-NAR-mediated activation of astrocytes is sufficient to potentiate nociceptive inputs, lowering the threshold to mechanical pain in mice, an effect mimicked by astrocyte-specific expression of hM3Dq-DREADDs. This DREADD effect was lost in both IP_3R2 KO and astrocyte-specific dn-SNARE mice, indicating that both Gq evoked $[Ca^{2+}]_i$ increases and SNARE-mediated vesicular release from astrocytes were involved. To reveal the signaling pathways mediating astrocyte to neuron communication, the authors blocked several receptors known to be activated by gliotransmitters. While antagonists of P2 purinergic receptors and AMPA receptors did not alter the effects of hM3Dq-DREADD activation on the mechanical pain threshold, 5,7-dichlorokynurenic acid, an antagonist targeting the NMDA receptor co-agonist binding site, did produce effects. This antagonist similarly impaired the nociceptive hypersensitivity induced by the α1-NAR agonist, phenylephrine. This implicates activation of the NMDA receptor co-agonist binding site in α1-NAR-mediated effects on mechanical pain hypersensitivity. Next, the authors identified D-serine, an endogenous (NMDA) receptor co-agonist, as the most likely gliotransmitter involved, as direct injection of D-serine in wild type mice dose-dependently mimicked the effect of α1-NAR activation on mechanical pain threshold. These results indicate

the gating of neuronal NMDA receptors, probably through astrocyte-mediated increases in extracellular D-serine, to be the likely mode of astrocyte-to-neuron communication following astrocyte α1A-NAR activation (**Figure 1F**) (Kohro et al., 2020). This conclusion is in agreement with other studies, which found D-serine levels and neuronal NMDA currents increase in an astrocyte-dependent manner following α1A-NAR activation in mouse cortical slices (Pankratov and Lalo, 2015; Lalo et al., 2018), and that NMDA receptors are implicated in the α1-NAR and astrocyte-dependent potentiation of visually evoked potentials in mice subjected to tDCS (Monai et al., 2016). However, we want to highlight that the study from Kohro et al. (2020) is the only one, to the best of our knowledge, that establishes a clear link between astrocytic α1A-NAR activation and the effects of NA on local circuit function. While other studies suggest a role for α1-NAR signaling in astrocytes, sometimes using multiple lines of evidence (Pankratov and Lalo, 2015), we believe cell-type specific gene ablation approaches are the cleanest way to understand the role of α1-NAR signaling in the CNS. We believe that the recent publication of two *Adra1a*-floxed mouse lines, enabling such experiments (Kohro et al., 2020; Ye et al., 2020), will prove crucial in this endeavor and be a valuable resource for the neuroscience community.

ASTROCYTES AND α1-NAR : A SYSTEM TAILORED TO REGULATE INHIBITION?

A shared trait among neuromodulators is their effects on inhibitory neurotransmission in the CNS, notably in the cortex (Pacholko et al., 2020). By acting on the inhibitory system, neuromodulators change the gain of specific inputs into cortical circuits, affecting the signal-to-noise ratio of relevant information perceived in the environment (Aston-Jones and Cohen, 2005), shifting the global brain state (Lee and Dan, 2012), and ultimately affecting behavior (Berridge and Waterhouse, 2003). NA-mediated neuromodulation is almost the prototypical example of this model. Indeed, phasic NA release, induced by salient stimuli, will momentarily change the gain of inhibitory circuits (Salgado et al., 2016), which, for instance, will lead to an inhibition of horizontal inputs in the visual cortex, changing the signal-to-noise ratio of sensory inputs (Kobayashi et al., 2000). Crucially, the study by Kobayashi et al. (2000) found these effects to be elicited by α1-NAR activation. There is accumulating evidence that α1-NAR activation increases the activity of GABAergic neurons (directly or indirectly) in multiple CNS regions, including in the hippocampus (Alreja and Liu, 1996; Bergles et al., 1996; Hillman et al., 2009), cortex (Marek and Aghajanian, 1996; Kawaguchi and Shindou, 1998; Kobayashi et al., 2000; Kobayashi, 2007; Lei et al., 2007; Dinh et al., 2009), basolateral amygdala (Braga et al., 2004), spinal cord (Yuan et al., 2009; Seibt and Schlichter, 2015), the bed nucleus of the stria terminalis (Dumont and Williams, 2004), cerebellum (Herold et al., 2005; Hirono and Obata, 2006), nucleus ambiguus (Boychuk et al., 2011), and olfactory bulb (Zimnik et al., 2013). Some of these studies actually used α1-NAR subtype selective antagonists and mostly identified the α1A-NAR as being responsible for mediating responses in GABAergic neurons (Alreja and Liu, 1996; Braga et al., 2004; Hillman et al., 2009; Yuan et al., 2009; Zimnik et al., 2013), with one study reporting effects mediated by α1B-NAR (Marek and Aghajanian, 1996).

From this evidence, it seems that the control of inhibitory transmission through α1-NAR, and probably the α1A-NAR subtype, is a ubiquitous mechanism in the CNS. However, none of these studies could conclusively show which cell type(s) expressed α1A-NAR and were activated by NA. We have already noted that astrocytes are increasingly recognized as the targets of various neuromodulators (Kjaerby et al., 2017; Kastanenka et al., 2020; Pacholko et al., 2020), including NA (O'Donnell et al., 2012), and direct astrocyte activation seems to mimic the shifts in brain state produced by neuromodulators (Poskanzer and Yuste, 2016). The most plausible explanation is that α1A-NAR are expressed by both astrocytes and interneurons, with the functional effects of NA being linked to the concerted activation of both cell types. Indeed, recent single-cell RNA sequencing studies report that both interneurons and astrocytes express *Adra1a* (see section "Noradrenergic Receptors in the CNS").

Therefore, we hypothesize that α1A-NAR signaling in the CNS might simultaneously activate astrocytes and interneurons, which effectively form a functional unit through which NA exerts its actions. While studies of synaptic regulation typically focus on excitatory (glutamatergic) synapses, there is an increasing number of studies reporting that astrocytes are instrumental in regulating inhibitory (GABAergic) signaling in the CNS (reviewed in Losi et al., 2014; Mederos and Perea, 2019). In particular, three recent studies highlight the importance of astrocytes in the modulation of GABAergic networks, demonstrating that they control the formation of GABAergic synapses through expression of neuronal cell adhesion molecule (NRCAM; Takano et al., 2020), that activation of astrocytic $GABA_B$ receptors is crucial for controlling inhibition in cortical circuits and ultimately goal-directed behaviors (Mederos et al., 2021), and that activity of the astrocyte GABA transporter is crucial for the function of circuits in the striatum (Yu et al., 2018). Astrocytes also modulate the activity of GABAergic synapses by releasing the gliotransmitter ATP. Acting through post-synaptic P2X4 receptors, this astrocyte-released ATP decreases the amplitude of both tonic and post-synaptic $GABA_A$ currents in neurons (Lalo et al., 2014; **Figure 1G**). This effect likely plays a key role in regulating astrocytic α1A-NAR-mediated plasticity (Pankratov and Lalo, 2015; and see "α1-NAR Signaling in Astrocytes: Relevance for Neuromodulation"), since P2X4 KO mice have defects in LTP induction (Lalo et al., 2016) and NA-mediated release of ATP by astrocytes has been implicated in experience-dependent metaplasticity (Lalo et al., 2018).

However, the interactions between astrocytes and GABAergic neurons show additional layers of complexity. First, and somewhat counter-intuitively, astrocytes can transform inhibitory signals into excitatory ones in the hippocampus, with astrocytic $GABA_B$ receptor activation inducing glutamate release from astrocytes, which potentiates synapses by acting on pre-synaptic metabotropic glutamate receptors (mGluR) (Perea et al., 2016; Mederos et al., 2021). Another study reports that increased activity of the astrocytic GABA transporter,

GAT3, following repetitive firing of neuropeptide Y (NPY) positive GABAergic interneurons, elevates $[Ca^{2+}]_i$ in astrocytes inducing glutamate release, which in turn acts on neuronal $mGluR_1$ to modify the spiking patterns of NPY expressing interneurons (Deemyad et al., 2018), in effect creating a feedback loop. Second, a single astrocyte can detect different levels of GABAergic activity and respond by releasing distinct gliotransmitters, with different and opposing effects on synaptic activity (Covelo and Araque, 2018). Activation of astrocytic $GABA_B$ receptors, in response to low levels of neuronal activity, potentiates excitatory transmission through a $mGluR_1$-based mechanism. However, high levels of interneuron activity over prolonged periods eventually leads to synaptic depression, mediated by activation of neuronal A_1 receptors, probably following astrocytic release of ATP with subsequent degradation into adenosine. Moreover, this biphasic modulation could be induced by artificially manipulating the $[Ca^{2+}]_i$ in a single astrocyte. This notion of biphasic modulation of synaptic transmission by astrocytes is further reinforced by studies demonstrating that ATP and D-serine, which are known to be released by astrocytes following α1A-NAR activation (Pankratov and Lalo, 2015), also have opposing actions on synaptic activity. D-serine (and glutamate) gate the activation of NMDA receptors, increasing overall excitability and boosting LTP; in contrast, ATP activates neuronal P2X receptors depressing the extent of LTP induction. Mechanistically, it appears this astrocyte-dependent activation of P2X receptors leads to a down-regulation of NMDA receptors at excitatory synapses (Lalo et al., 2016, 2018).

Taken together, these studies reinforce the concept of lateral regulation of synaptic transmission by astrocytes. According to this concept, one astrocyte receiving inputs from an inhibitory interneuron can also modulate an excitatory synapse, and vice versa (**Figure 1H**, blue and red arrows). This phenomenon can be extended to incorporate distant synapses, with the activation of one astrocyte being relayed to other cells through either paracrine or gap-junction-based intercellular communication (**Figure 1I**; Covelo and Araque, 2016). These numerous mechanisms exemplify the complexity of astrocyte-neuron interactions, and show that astrocytes can modulate circuits in multiple ways depending on the patterns of activity they detect at synapses, as well as the presence of neuromodulators. For interested readers, these last issues are discussed in depth in a parallel publication in this edition of Frontiers in Cellular Neuroscience (Caudal et al., 2020).

We believe that the concomitant activation of astrocytes and interneurons by NA through α1-NAR might harness the mechanisms we have discussed in this section to convey (at least some of) the effects of NA. Other signaling mechanisms, namely the synergistic effects of synaptic signaling and cellular 'priming' by NA in astrocytes (see section "α1-NAR Triggered Calcium Signaling in Astrocytes: A Switch for Signal Integration?"), are also likely to participate in the mechanisms underlying astrocyte-interneuron crosstalk. However, the relative contributions of these two cell types to the effects elicited by NA remains to be elucidated. This will, no doubt, require precise cell-type (and perhaps even cell subtype) specific manipulation of NA signaling, coupled to readouts of functional effects (also see sections "NA Signaling Through Astrocytes: The Impact of Cell Heterogeneity" and "Future Strategies to Decipher the Role of NAR Signaling in Heterogenous Astrocyte Populations").

ASTROCYTE–NEURON INTERACTIONS FOLLOWING α1-NAR SIGNALING: POSITIVE FEEDBACK MECHANISMS FOR NA RELEASE?

The complexity of astrocyte-neuron interactions underlying NA signaling might have a further layer of complexity. Indeed, Mather et al. (2016) have proposed an interesting model, which they term "Glutamate Amplifies Noradrenergic Effects" (GANE). In this model, NA release is amplified at sites of high activity, by the action of synaptically released glutamate. This glutamate accumulates and activates receptors expressed on NA varicosities located in proximity to the active synapse, evoking further release of NA from active LC axons. Elevated concentrations of NA then activate post-synaptic β-NAR, increasing synaptic weight. Astrocytes can be factored into this model in several ways. First, astrocytes may respond to the presence of either, or both, released neurotransmitters and NA by releasing glutamate and D-serine, further boosting NA release (**Figure 1J**). Second, as astrocytes activated by GABAergic signaling can release glutamate, they may also potentiate activity at active GABAergic synapses by increasing NA release from LC varicosities in close proximity (**Figure 1K**). Third, high local concentrations of NA may activate astrocytic β-NAR, leading to increased production and secretion of L-lactate, which is known to increase the firing rate of LC axons, leading to further NA release (Tang et al., 2014). Finally, astrocytes function as "signal integrators" (see section "α1-NAR Triggered Calcium Signaling in Astrocytes: A Switch for Signal Integration?"): in this case, α1A-NAR activation in astrocytes is likely to be enhanced by GABA and somatostatin release from α1A-NAR expressing interneurons (Marin et al., 1993; Hillman et al., 2009; Mariotti et al., 2018). This will lead to increased astrocyte $[Ca^{2+}]_i$ and the subsequent release of glutamate, which will itself lead to increased NA release. It is interesting to speculate that the astrocytic release of ATP, associated with high levels of interneuron activity (Covelo and Araque, 2018), might serve as a brake in this system, acting to limit (or inhibit) release of NA from varicosities by activating A_1 receptors following extracellular degradation to adenosine. Similarly, astrocyte-released ATP, signaling through neuronal P2X receptors, may lead to the down-regulation of NMDA-mediated currents (Lalo et al., 2016) limiting neuronal excitability.

Many unanswered (and exciting) questions remain in this area. For example, what are the relative roles of astrocyte-interneuron interactions in mediating the effects of NA on circuits? One area of increasing importance to the astrocyte field is the issue of cellular heterogeneity (see section "NA Signaling

Through Astrocytes: The Impact of Cell Heterogeneity"): it will be crucial for our understanding of CNS function to know if astrocytes express or respond to α1-NAR activation in a homogeneous or heterogeneous function and how this impacts circuit activity.

NA SIGNALING THROUGH ASTROCYTES: THE IMPACT OF CELL HETEROGENEITY

Analysis of single cell transcriptome data shows that the *Adra1a* transcript is one of the few that is detectable in all cortical astrocytes (see section "Noradrenergic Receptors in the CNS"). This finding corroborates the results of several functional studies, which have found that application of phenylephrine, an α1-NAR agonist, reliably evokes $[Ca^{2+}]_i$ responses in the majority (if not all) cortical astrocytes (Ding et al., 2013; Srinivasan et al., 2015, 2016). However, in a recent study from our own lab, we found that the dynamics of the α1-NAR evoked Ca^{2+} transients differ between cortical layers (Batiuk et al., 2020). Astrocytes in different cortical layers have also been shown to have different morphologies (Lanjakornsiripan et al., 2018) and molecular profiles (Bayraktar et al., 2020), which we hypothesize drive differential $[Ca^{2+}]_i$ signaling (Semyanov et al., 2020) and functional outputs (Bagur and Hajnóczky, 2017). We regard this as interesting because NA is known to have layer-specific effects on inhibitory transmission in the cortex (Salgado et al., 2016), suggesting that α1A-NAR signaling in otherwise heterogeneous astrocyte populations might produce different downstream effects on neuronal function(s). Yet further evidence supporting a role for functionally specialized cortical astrocyte subtypes is work demonstrating that activation of astrocytes specifically in supragranular layers is important for neuronal reactivation, following loss of sensory inputs into the visual cortex after monocular enucleation (Hennes et al., 2020). As there is increasing evidence that astrocytes show anatomical, molecular and physiological specialization across brain regions (reviewed in Bayraktar et al., 2015; Farmer and Murai, 2017; Dallérac et al., 2018; Khakh and Deneen, 2019; Pestana et al., 2020), we expect astrocyte heterogeneity will emerge as a major factor contributing to the complex, differential actions of NA in the CNS (O'Donnell et al., 2012; Perez, 2020). In fact, α1-NAR signaling seems a uniform property of astrocytes, with evidence for phenylephrine-evoked $[Ca^{2+}]_i$ transients in multiple brain regions, including in striatum (Yu et al., 2018), hippocampus (Duffy and MacVicar, 1995), cerebellum (Kulik et al., 1999), ventrolateral medulla (Schnell et al., 2016), hypothalamus (Gordon et al., 2005), and spinal cord (Kohro et al., 2020). However, consistent with our hypothesis, α1A-NAR signaling appears to elicit differing Ca^{2+} responses in regionally distinct cells, with Pham et al. (2020) uncovering differences between hypothalamic and cortical astrocytes. Unfortunately, the complex molecular signatures of astrocyte subtypes identified to date means that new genetic tools will likely be required to fully probe the functional roles of α1A-NAR expressing subtypes (see section "Future Strategies to Decipher the Role of NAR Signaling in Heterogenous Astrocyte Populations").

FUTURE STRATEGIES TO DECIPHER THE ROLE OF NAR SIGNALING IN HETEROGENOUS ASTROCYTE POPULATIONS

In our opinion, the ability to target functional astrocyte subtypes will likely need the use of intersectional genetics. This typically uses simultaneous activation of multiple promoters to achieve selective transgene expression in the desired cell subtype. An obvious example is the split Cre system (Hirrlinger et al., 2009), which could, for example, be used in combination with *Adra1a*-floxed mice to delete α1A-NAR in specific astrocyte subtypes (Kohro et al., 2020; Ye et al., 2020), or induce expression of a fluorescent protein (or genetically encoded sensor) in cells using existing mouse lines (such as GCaMP6f in the Ai95D line[2]).

Obtaining the genetic fingerprint of spatially resolved and functionally distinct cell populations remains difficult. At the time of publication, spatial transcriptomic approaches, based on *in situ* sequencing, lack single cell resolution (Ståhl et al., 2016; Ortiz et al., 2020). Although somewhat cumbersome, it is, however, possible to map back unique cell subtypes, identified using single cell RNA-seq approaches, to their anatomical positions, using highly multiplexed *in situ* hybridization techniques, as we demonstrated in recent publications (Batiuk et al., 2020; Bayraktar et al., 2020). Unique transcripts, defining cell subtypes, can then theoretically be used to identify promoters for use in intersectional approaches. It should be noted, however, that promoter mapping is notoriously difficult, and in some cases even 500 bp of sequence is sufficient to completely change the pattern of gene expression (Miller et al., 2019). Given the need to screen multiple promoter fragments, to ensure the endogenous gene expression profile is faithfully recapitulated, we anticipate the manufacture of transgenic mouse lines will prove too laborious and costly for many questions of interest. The use of viral vectors offers an attractive alternative (Beckervordersandforth et al., 2010, 2014), although these typically suffer from limited capacity (Luo et al., 2018) and may not be able to incorporate the full regulatory sequence required to recapitulate the endogenous pattern of gene expression (Regan et al., 2007). To overcome these limitations, our lab is developing a PiggyBac-based system, misPiggy, for flexible gene expression in the CNS, based on *in utero* electroporation (Slezak et al., 2018: pre-print). This simple, one plasmid solution can be easily used to perform rapid analysis of putative promoter sequences based on fluorescent protein expression (Wang et al., 2007), while its large cargo capacity allows the incorporation of multiple independent expression modules, making it ideal for intersectional genetics. We expect this system will allow us to make substantial progress in deciphering the contribution

[2]https://www.jax.org/strain/024105

of unique astrocyte subtypes to NA-mediated control of local circuit function.

Understanding the biology of α1-NAR signaling in astrocytes (as well as that of other NAR types) will benefit from further advances in the development of genetically encoded biosensors. Changes in astrocyte $[Ca^{2+}]_i$ are still considered the best measure of astrocyte activity (Verkhratsky and Nedergaard, 2018; Caudal et al., 2020). New genetically encoded calcium indicators (GECIs), such as the jGCaMP7 series, are under intense development, and benefit from improved properties, such as signal-to-noise ratio and steady-state brightness (Dana et al., 2019). Other developments include red-shifted GECIs (Dana et al., 2016), which allow simultaneous dual color (green-red) imaging in astrocytes and neurons (including LC axons) (Bindocci et al., 2017; Oe et al., 2020). Of importance, the use of red-shifted GECIs can also be combined with optogenetic tools, allowing precise cell stimulation (Forli et al., 2018). However, as discussed earlier (see section "α1-NAR Signaling: Effects on Astrocyte Function"), Ca^{2+} is not the only important secondary messenger, or metabolite, whose level changes following astrocyte stimulation with NA. Examples include cAMP, whose levels can be measured using the red-shifted sensor PinkFlamindo (Oe et al., 2020), as well as lactate, which can be measured using the Laconic system (San Martín et al., 2013; Mächler et al., 2016; Zuend et al., 2020). Furthermore, genetically encoded sensors exist for the measurement of various neurotransmitters and neuromodulators (including NA; Patriarchi et al., 2018; Feng et al., 2019; Oe et al., 2020 and further reviewed in Leopold et al., 2019). New genetically encoded sensors are constantly being developed (Leopold et al., 2019) and will undoubtedly bring new insights in the mechanisms of NA release. When these are combined with sensors for cell-type specific second messenger detection, we will be able to dissect out the mechanisms by which NA exerts its actions across CNS cell types. Measurements of ionic species beyond calcium is also possible, with genetically encoded fluorescent sensors for K^+ (Shen et al., 2019), H^+ and Cl^- (Germond et al., 2016) currently available.

Finally, to understand the role(s) of astrocytes in neuromodulation and beyond, there is a clear need for tools allowing precise and reproducible cell activation. Optogenetic control of astrocytes, using different channelrhodopsin variants or proton pumps, has already been attempted (Figueiredo et al., 2014; Xie et al., 2015; Cho et al., 2016). However, the mechanism(s) through which a light-sensitive cation channel can evoke $[Ca^{2+}]_i$ transients in astrocytes remain unclear (Figueiredo et al., 2014; Octeau et al., 2019); in fact, channelrhodopsins have recently been criticized as having unwanted effects, such as promoting increases in $[K^+]_e$ (Octeau et al., 2019), which lead to secondary increases in neuronal activity that compound the interpretation of experimental data. It is now becoming clear that a much better approach to optical control of astrocyte function is the use of light-gated GPCRs, such as the Gq-GPCR Optoα1AR. This chimeric receptor is actually based on the intracellular amino acid sequence of the α1A-NAR (Airan et al., 2009), and has recently been used to elicit Gq signaling in astrocytes (Adamsky et al., 2018; Iwai et al., 2020: pre-print). An example of a naturally occurring protein that has been repurposed is the Gq-coupled photopigment melanopsin, which has been used to study the role of astrocytes in GABAergic transmission (Mederos et al., 2019, 2021). Optogenetics has the important advantage of allowing fine spatial and temporal control of cell activation, which is harder to attain when using chemogenetic (DREADD-based) approaches, which are limited by the pharmacodynamics of their synthetic agonists. However, DREADDs have the advantage of allowing simultaneous activation of cells across a broad tissue area, without the need for invasive implantation of optical devices. As such, they are being increasingly used in neuroscience research (Roth, 2016), with particular success in helping elucidate the roles played by astrocytes in the control of CNS circuits (Adamsky et al., 2018; Hennes et al., 2020; Erickson et al., 2021).

We believe that the use of these tools in innovative and imaginative combinations will undoubtedly bring new insights into astrocyte functions in the CNS, including (and importantly) their role(s) in NAR signaling.

CONCLUSION

With this review, we aimed to provide an overview of the current state of the art on α1-NAR signaling in astrocytes, and how this relates to NA-mediated neuromodulation. We believe that α1-NAR signaling is a major signaling pathway in astrocytes, which switches the cell into a more sensitive state, effectively 'priming' it to integrate signals originating from other cells in the immediate environment. We advance the hypothesis that both GABAergic interneurons and astrocytes are involved in α1A-NAR signaling, with the two cell types forming a functional unit, through which NA exerts its neuromodulatory effects. We argue that these issues will need to be considered in light of the fact that astrocytes show considerable heterogeneity in morphology, transcriptome/proteome and physiology, and discuss tools to potentially solve these issues. For brevity, we deliberately chose not to discuss aspects of astrocyte α1-NAR signaling that are potentially involved in response to developmental deficits (D'Adamo et al., 2021), injury (Vardjan et al., 2016) or disease (Zorec et al., 2018). However, given the presence of astrocytes throughout the CNS and their ubiquitous responses to NA, it is likely that aberrant NA-mediated Ca^{2+} signaling plays a central role in many conditions. Therefore, understanding α1-NAR signaling and how it modulates astrocyte functions (including interactions with other cell types) will not only lead to a better understanding of CNS function in the healthy brain, it will likely provide insights into the mechanisms underlying injury and disease.

AUTHOR CONTRIBUTIONS

JW and MGH participated equally in the writing of this review. Both authors contributed to the article and approved the submitted version.

FUNDING

JW was supported by a post-doctoral fellowship from the Fund for Scientific Research Flanders (FWO, 12V7519N). This work was further supported by FWO grants to MGH (1523014N, G066715N, G088415N, and G080821N), KU Leuven Research Council grants to MGH (C14/20/071 and CELSA/19/036), as well as a European Research Council Starting Grant (AstroFunc: 281961) and VIB Institutional Funding to MGH.

ACKNOWLEDGMENTS

We would like to thank Dr. Araks Martirosyan for advice regarding interpretation of transcriptome-based studies. Some figure elements are adapted from illustrations provided by Servier Medical Art (https://smart.servier.com/). Medical Art by Servier is licensed under a Creative Commons Attribution 3.0 Unported License. The final figure was prepared by David Pennington (penningtonArt.co.uk).

REFERENCES

Adamsky, A., Kol, A., Kreisel, T., Doron, A., Ozeri-Engelhard, N., Melcer, T., et al. (2018). Astrocytic activation generates de novo neuronal potentiation and memory enhancement. *Cell* 174, 59.e14–71.e14. doi: 10.1016/j.cell.2018.05.002

Ahuja, M., Jha, A., Maléth, J., Park, S., and Muallem, S. (2014). cAMP and Ca^{2+} signaling in secretory epithelia: crosstalk and synergism. *Cell Calcium* 55, 385–393. doi: 10.1016/j.ceca.2014.01.006

Airan, R. D., Thompson, K. R., Fenno, L. E., Bernstein, H., and Deisseroth, K. (2009). Temporally precise in vivo control of intracellular signalling. *Nature* 458, 1025–1029. doi: 10.1038/nature07926

Åkerman, K. E. O., Enkvist, M. O. K., and Holopainen, I. (1988). Activators of protein kinase C and phenylephrine depolarize the astrocyte membrane by reducing the K^+ permeability. *Neurosci. Lett.* 92, 265–269. doi: 10.1016/0304-3940(88)90600-3

Alberini, C. M., Cruz, E., Descalzi, G., Bessières, B., and Gao, V. (2018). Astrocyte glycogen and lactate: new insights into learning and memory mechanisms. *Glia* 66, 1244–1262. doi: 10.1002/glia.23250

Alexander, G. M., Grothusen, J. R., Gordon, S. W., and Schwartzman, R. J. (1997). Intracerebral microdialysis study of glutamate reuptake in awake, behaving rats. *Brain Res.* 766, 1–10. doi: 10.1016/s0006-8993(97)00519-2

Alreja, M., and Liu, W. (1996). Noradrenaline induces IPSCs in rat medial septal/diagonal band neurons: involvement of septohippocampal GABAergic neurons. *J. Physiol.* 494, 201–215. doi: 10.1113/jphysiol.1996.sp021485

Anderson, M. A., Burda, J. E., Ren, Y., Ao, Y., O'Shea, T. M., Kawaguchi, R., et al. (2016). Astrocyte scar formation aids central nervous system axon regeneration. *Nature* 532, 195–200. doi: 10.1038/nature17623

Aston-Jones, G., and Cohen, J. D. (2005). An integrative theory of locus coeruleus-norepinephrine function: adaptive gain and optimal performance. *Annu. Rev. Neurosci.* 28, 403–450. doi: 10.1146/annurev.neuro.28.061604.135709

Atzori, M., Cuevas-Olguin, R., Esquivel-Rendon, E., Garcia-Oscos, F., Salgado-Delgado, R. C., Saderi, N., et al. (2016). Locus ceruleus norepinephrine release: a central regulator of CNS spatio-temporal activation? *Front. Synaptic Neurosci.* 8:25. doi: 10.3389/fnsyn.2016.00025

Avery, M. C., and Krichmar, J. L. (2017). Neuromodulatory systems and their interactions: a review of models, theories, and experiments. *Front. Neural Circuits* 11:108. doi: 10.3389/fncir.2017.00108

Bagur, R., and Hajnóczky, G. (2017). Intracellular Ca^{2+} sensing: its role in calcium homeostasis and signaling. *Mol. Cell* 66, 780–788. doi: 10.1016/j.molcel.2017.05.028

Bar El, Y., Kanner, S., Barzilai, A., and Hanein, Y. (2018). Activity changes in neuron-astrocyte networks in culture under the effect of norepinephrine. *PLoS One* 13:e0203761. doi: 10.1371/journal.pone.0203761

Batiuk, M. Y., Martirosyan, A., Wahis, J., de Vin, F., Marneffe, C., Kusserow, C., et al. (2020). Identification of region-specific astrocyte subtypes at single cell resolution. *Nat. Commun.* 11:1220. doi: 10.1038/s41467-019-14198-8

Bayraktar, O. A., Bartels, T., Holmqvist, S., Kleshchevnikov, V., Martirosyan, A., Polioudakis, D., et al. (2020). Astrocyte layers in the mammalian cerebral cortex revealed by a single-cell in situ transcriptomic map. *Nat. Neurosci.* 23, 500–509. doi: 10.1038/s41593-020-0602-1

Bayraktar, O. A., Fuentealba, L. C., Alvarez-Buylla, A., and Rowitch, D. H. (2015). Astrocyte development and heterogeneity. *Cold Spring Harb. Perspect. Biol.* 7:a020362. doi: 10.1101/cshperspect.a020362

Bazargani, N., and Attwell, D. (2016). Astrocyte calcium signaling: the third wave. *Nat. Neurosci.* 19, 182–189. doi: 10.1038/nn.4201

Beckervordersandforth, R., Deshpande, A., Schäffner, I., Huttner, H. B., Lepier, A., Lie, D. C., et al. (2014). In vivo targeting of adult neural stem cells in the dentate gyrus by a split-cre approach. *Stem Cell Rep.* 2, 153–162. doi: 10.1016/j.stemcr.2014.01.004

Beckervordersandforth, R., Tripathi, P., Ninkovic, J., Bayam, E., Lepier, A., Stempfhuber, B., et al. (2010). In vivo fate mapping and expression analysis reveals molecular hallmarks of prospectively isolated adult neural stem cells. *Cell Stem Cell* 7, 744–758. doi: 10.1016/j.stem.2010.11.017

Beckner, M. E. (2020). A roadmap for potassium buffering/dispersion via the glial network of the CNS. *Neurochem. Int.* 136:104727. doi: 10.1016/j.neuint.2020.104727

Bekar, L. K., He, W., and Nedergaard, M. (2008). Locus coeruleus α-adrenergic-mediated activation of cortical astrocytes in vivo. *Cereb. Cortex* 18, 2789–2795. doi: 10.1093/cercor/bhn040

Bergles, D., Doze, V., Madison, D., and Smith, S. (1996). Excitatory actions of norepinephrine on multiple classes of hippocampal CA1 interneurons. *J. Neurosci.* 16, 572–585. doi: 10.1523/JNEUROSCI.16-02-00572.1996

Berridge, C. W., and Waterhouse, B. D. (2003). The locus coeruleus–noradrenergic system: modulation of behavioral state and state-dependent cognitive processes. *Brain Res. Rev.* 42, 33–84. doi: 10.1016/S0165-0173(03)00143-7

Bindocci, E., Savtchouk, I., Liaudet, N., Becker, D., Carriero, G., and Volterra, A. (2017). Three-dimensional Ca^{2+} imaging advances understanding of astrocyte biology. *Science* 356:eaai8185. doi: 10.1126/science.aai8185

Boisvert, M. M., Erikson, G. A., Shokhirev, M. N., and Allen, N. J. (2018). The aging astrocyte transcriptome from multiple regions of the mouse brain. *Cell Rep.* 22, 269–285. doi: 10.1016/j.celrep.2017.12.039

Bouret, S., and Sara, S. J. (2005). Network reset: a simplified overarching theory of locus coeruleus noradrenaline function. *Trends Neurosci.* 28, 574–582. doi: 10.1016/j.tins.2005.09.002

Boychuk, C. R., Bateman, R. J., Philbin, K. E., and Mendelowitz, D. (2011). α_1-adrenergic receptors facilitate inhibitory neurotransmission to cardiac vagal neurons in the nucleus ambiguus. *Neuroscience* 193, 154–161. doi: 10.1016/j.neuroscience.2011.07.024

Braga, M. F. M., Aroniadou-Anderjaska, V., Manion, S. T., Hough, C. J., and Li, H. (2004). Stress impairs α_{1A} adrenoceptor-mediated noradrenergic facilitation of GABAergic transmission in the basolateral amygdala. *Neuropsychopharmacology* 29, 45–58. doi: 10.1038/sj.npp.1300297

Cahoy, J. D., Emery, B., Kaushal, A., Foo, L. C., Zamanian, J. L., Christopherson, K. S., et al. (2008). A transcriptome database for astrocytes, neurons, and oligodendrocytes: a new resource for understanding brain development and function. *J. Neurosci.* 28, 264–278. doi: 10.1523/JNEUROSCI.4178-07.2008

Caudal, L. C., Gobbo, D., Scheller, A., and Kirchhoff, F. (2020). The paradox of astroglial Ca^{2+} signals at the interface of excitation and inhibition. *Front. Cell. Neurosci.* 14:947. doi: 10.3389/fncel.2020.609947

Cho, W.-H., Barcelon, E., and Lee, S. J. (2016). Optogenetic glia manipulation: possibilities and future prospects. *Exp. Neurobiol.* 25, 197–204. doi: 10.5607/en.2016.25.5.197

Coggan, J. S., Keller, D., Calì, C., Lehväslaiho, H., Markram, H., Schürmann, F., et al. (2018). Norepinephrine stimulates glycogenolysis in astrocytes to fuel neurons with lactate. *PLoS Comput. Biol.* 14:e1006392. doi: 10.1371/journal.pcbi.1006392

Cohen, Z., Molinatti, G., and Hamel, E. (1997). Astroglial and vascular interactions of noradrenaline terminals in the rat cerebral cortex. *J. Cereb. Blood Flow Metab.* 17, 894–904. https://journals.sagepub.com/doi/full/10.1097/00004647-199708000-00008

Cordeaux, Y., and Hill, S. J. (2002). Mechanisms of cross-talk between G-protein-coupled receptors. *Neurosignals* 11, 45–57. doi: 10.1159/000057321

Corkrum, M., Covelo, A., Lines, J., Bellocchio, L., Pisansky, M., Loke, K., et al. (2020). Dopamine-evoked synaptic regulation in the nucleus accumbens requires astrocyte activity. *Neuron* 105, 1036.e5–1047.e5. doi: 10.1016/j.neuron.2019.12.026

Corkrum, M., Rothwell, P. E., Thomas, M. J., Kofuji, P., and Araque, A. (2019). Opioid-mediated astrocyte–neuron signaling in the nucleus accumbens. *Cells* 8:586. doi: 10.3390/cells8060586

Covelo, A., and Araque, A. (2016). Lateral regulation of synaptic transmission by astrocytes. *Neuroscience* 323, 62–66. doi: 10.1016/j.neuroscience.2015.02.036

Covelo, A., and Araque, A. (2018). Neuronal activity determines distinct gliotransmitter release from a single astrocyte. *eLife* 7:e32237. doi: 10.7554/eLife.32237

D'Adamo, P., Horvat, A., Gurgone, A., Mignogna, M. L., Bianchi, V., Masetti, M., et al. (2021). Inhibiting glycolysis rescues memory impairment in an intellectual disability *Gdi1*-null mouse. *Metabolism* 116:154463. doi: 10.1016/j.metabol.2020.154463

Dallérac, G., Zapata, J., and Rouach, N. (2018). Versatile control of synaptic circuits by astrocytes: where, when and how? *Nat. Rev. Neurosci.* 19, 729–743. doi: 10.1038/s41583-018-0080-6

Dana, H., Mohar, B., Sun, Y., Narayan, S., Gordus, A., Hasseman, J. P., et al. (2016). Sensitive red protein calcium indicators for imaging neural activity. *eLife* 5, 1–24. doi: 10.7554/eLife.12727

Dana, H., Sun, Y., Mohar, B., Hulse, B. K., Kerlin, A. M., Hasseman, J. P., et al. (2019). High-performance calcium sensors for imaging activity in neuronal populations and microcompartments. *Nat. Methods* 16, 649–657. doi: 10.1038/s41592-019-0435-6

Deemyad, T., Lüthi, J., and Spruston, N. (2018). Astrocytes integrate and drive action potential firing in inhibitory subnetworks. *Nat. Commun.* 9:4336. doi: 10.1038/s41467-018-06338-3

Delumeau, J. C., Marin, P., Cordier, J., Glowinski, J., and Premont, J. (1991). Synergistic effects in the α_1- and β_1-adrenergic regulations of intracellular calcium levels in striatal astrocytes. *Cell. Mol. Neurobiol.* 11, 263–276. doi: 10.1007/BF00769039

Descarries, L., and Mechawar, N. (2000). Ultrastructural evidence for diffuse transmission by monoamine and acetylcholine neurons of the central nervous system. *Prog. Brain Res.* 125, 27–47. doi: 10.1016/S0079-6123(00)25005-X

Dienel, G. A., and Cruz, N. F. (2016). Aerobic glycolysis during brain activation: adrenergic regulation and influence of norepinephrine on astrocytic metabolism. *J. Neurochem.* 138, 14–52. doi: 10.1111/jnc.13630

Ding, F., O'Donnell, J., Thrane, A. S., Zeppenfeld, D., Kang, H., Xie, L., et al. (2013). α1-Adrenergic receptors mediate coordinated Ca^{2+} signaling of cortical astrocytes in awake, behaving mice. *Cell Calcium* 54, 387–394. doi: 10.1016/j.ceca.2013.09.001

Dinh, L., Nguyen, T., Salgado, H., and Atzori, M. (2009). Norepinephrine homogeneously inhibits α-amino-3-hydroxyl-5-methyl-4-isoxazole-propionate- (AMPAR-) mediated currents in all layers of the temporal cortex of the rat. *Neurochem. Res.* 34, 1896–1906. doi: 10.1007/s11064-009-9966-z

Duffy, S., and MacVicar, B. (1995). Adrenergic calcium signaling in astrocyte networks within the hippocampal slice. *J. Neurosci.* 15, 5535–5550. doi: 10.1523/JNEUROSCI.15-08-05535.1995

Dumont, E. C., and Williams, J. T. (2004). Noradrenaline triggers $GABA_A$ inhibition of bed nucleus of the stria terminalis neurons projecting to the ventral tegmental area. *J. Neurosci.* 24, 8198–8204. doi: 10.1523/JNEUROSCI.0425-04.2004

Durkee, C. A., and Araque, A. (2019). Diversity and specificity of astrocyte–neuron communication. *Neuroscience* 396, 73–78. doi: 10.1016/j.neuroscience.2018.11.010

Dyer-Reaves, K., Goodman, A. M., Nelson, A. R., and McMahon, L. L. (2019). Alpha1-adrenergic receptor mediated long-term depression at CA3-CA1 synapses can be induced via accumulation of endogenous norepinephrine and is preserved following noradrenergic denervation. *Front. Synaptic Neurosci.* 11:27. doi: 10.3389/fnsyn.2019.00027

Erickson, E. K., DaCosta, A. J., Mason, S. C., Blednov, Y. A., Mayfield, R. D., and Harris, R. A. (2021). Cortical astrocytes regulate ethanol consumption and intoxication in mice. *Neuropsychopharmacology* 46, 500–508. doi: 10.1038/s41386-020-0721-0

Farmer, W. T., and Murai, K. (2017). Resolving astrocyte heterogeneity in the CNS. *Front. Cell. Neurosci.* 11:300. doi: 10.3389/fncel.2017.00300

Fatatis, A., Holtzclaw, L. A., Avidor, R., Brenneman, D. E., and Russell, J. T. (1994). Vasoactive intestinal peptide increases intracellular calcium in astroglia: synergism with alpha-adrenergic receptors. *Proc. Natl. Acad. Sci. U.S.A.* 91, 2036–2040. doi: 10.1073/pnas.91.6.2036

Feng, J., Zhang, C., Lischinsky, J. E., Jing, M., Zhou, J., Wang, H., et al. (2019). A genetically encoded fluorescent sensor for rapid and specific in vivo detection of norepinephrine. *Neuron* 102, 745.e8–761.e8. doi: 10.1016/j.neuron.2019.02.037

Figueiredo, M., Lane, S., Stout, R. F., Liu, B., Parpura, V., Teschemacher, A. G., et al. (2014). Comparative analysis of optogenetic actuators in cultured astrocytes. *Cell Calcium* 56, 208–214. doi: 10.1016/j.ceca.2014.07.007

Forli, A., Vecchia, D., Binini, N., Succol, F., Bovetti, S., Moretti, C., et al. (2018). Two-photon bidirectional control and imaging of neuronal excitability with high spatial resolution in vivo. *Cell Rep.* 22, 3087–3098. doi: 10.1016/j.celrep.2018.02.063

Fujita, T., Chen, M. J., Li, B., Smith, N. A., Peng, W., Sun, W., et al. (2014). Neuronal transgene expression in dominant-negative snare mice. *J. Neurosci.* 34, 16594–16604. doi: 10.1523/JNEUROSCI.2585-14.2014

Fuxe, K., Agnati, L. F., Marcoli, M., and Borroto-Escuela, D. O. (2015). Volume transmission in central dopamine and noradrenaline neurons and its astroglial targets. *Neurochem. Res.* 40, 2600–2614. doi: 10.1007/s11064-015-1574-5

Genoud, C., Quairiaux, C., Steiner, P., Hirling, H., Welker, E., and Knott, G. W. (2006). Plasticity of astrocytic coverage and glutamate transporter expression in adult mouse cortex. *PLoS Biol.* 4:e343. doi: 10.1371/journal.pbio.0040343

Germond, A., Fujita, H., Ichimura, T., and Watanabe, T. M. (2016). Design and development of genetically encoded fluorescent sensors to monitor intracellular chemical and physical parameters. *Biophys. Rev.* 8, 121–138. doi: 10.1007/s12551-016-0195-9

Giaume, C., Marin, P., Cordier, J., Glowinski, J., and Premont, J. (1991). Adrenergic regulation of intercellular communications between cultured striatal astrocytes from the mouse. *Proc. Natl. Acad. Sci. U.S.A.* 88, 5577–5581. doi: 10.1073/pnas.88.13.5577

Gibbs, M. E., and Bowser, D. N. (2010). Astrocytic adrenoceptors and learning: α_1-adrenoceptors. *Neurochem. Int.* 57, 404–410. doi: 10.1016/j.neuint.2010.03.020

Gordon, G. R. J., Baimoukhametova, D. V., Hewitt, S. A., Rajapaksha, W. R. A. K. J. S., Fisher, T. E., and Bains, J. S. (2005). Norepinephrine triggers release of glial ATP to increase postsynaptic efficacy. *Nat. Neurosci.* 8, 1078–1086. doi: 10.1038/nn1498

Guček, A., Jorgačevski, J., Singh, P., Geisler, C., Lisjak, M., Vardjan, N., et al. (2016). Dominant negative SNARE peptides stabilize the fusion pore in a narrow, release-unproductive state. *Cell. Mol. Life Sci.* 73, 3719–3731. doi: 10.1007/s00018-016-2213-2

Hansson, E., and Rönnbäck, L. (1989). Regulation of glutamate and GABA transport by adrenoceptors in primary astroglial cell cultures. *Life Sci.* 44, 27–34. doi: 10.1016/0024-3205(89)90214-2

Hansson, E., and Rönnbäck, L. (1992). Adrenergic receptor regulation of amino acid neurotransmitter uptake in astrocytes. *Brain Res. Bull.* 29, 297–301. doi: 10.1016/0361-9230(92)90060-B

Henneberger, C., Bard, L., Panatier, A., Reynolds, J. P., Kopach, O., Medvedev, N. I., et al. (2020). LTP induction boosts glutamate spillover by driving withdrawal of perisynaptic astroglia. *Neuron* 108, 919.e11–936.e11. doi: 10.1016/j.neuron.2020.08.030

Hennes, M., Lombaert, N., Wahis, J., Van den Haute, C., Holt, M. G., and Arckens, L. (2020). Astrocytes shape the plastic response of adult cortical neurons to vision loss. *Glia* 68, 2102–2118. doi: 10.1002/glia.23830

Herold, S., Hecker, C., Deitmer, J. W., and Brockhaus, J. (2005). α1-Adrenergic modulation of synaptic input to Purkinje neurons in rat cerebellar brain slices. *J. Neurosci. Res.* 82, 571–579. doi: 10.1002/jnr.20660

Hertz, L., Lovatt, D., Goldman, S. A., and Nedergaard, M. (2010). Adrenoceptors in brain: cellular gene expression and effects on astrocytic metabolism and $[Ca^{2+}]_i$. *Neurochem. Int.* 57, 411–420. doi: 10.1016/j.neuint.2010.03.019

Hillman, K. L., Lei, S., Doze, V. A., and Porter, J. E. (2009). Alpha-1A adrenergic receptor activation increases inhibitory tone in CA1 hippocampus. *Epilepsy Res.* 84, 97–109. doi: 10.1016/j.eplepsyres.2008.12.007

Hirase, H., Iwai, Y., Takata, N., Shinohara, Y., and Mishima, T. (2014). Volume transmission signalling via astrocytes. *Philos. Trans. R. Soc. L. B Biol. Sci.* 369:20130604. doi: 10.1098/rstb.2013.0604

Hirono, M., and Obata, K. (2006). α-adrenoceptive dual modulation of inhibitory GABAergic inputs to Purkinje cells in the mouse cerebellum. *J. Neurophysiol.* 95, 700–708. doi: 10.1152/jn.00711.2005

Hirrlinger, J., Scheller, A., Hirrlinger, P. G., Kellert, B., Tang, W., Wehr, M. C., et al. (2009). Split-cre complementation indicates coincident activity of different genes in vivo. *PLoS One* 4:e4286. doi: 10.1371/journal.pone.0004286

Holt, M., Riedel, D., Stein, A., Schuette, C., and Jahn, R. (2008). Synaptic vesicles are constitutively active fusion machines that function independently of Ca^{2+}. *Curr. Biol.* 18, 715–722. doi: 10.1016/j.cub.2008.04.069

Horvat, A., Zorec, R., and Vardjan, N. (2016). Adrenergic stimulation of single rat astrocytes results in distinct temporal changes in intracellular Ca^{2+} and cAMP-dependent PKA responses. *Cell Calcium* 59, 156–163. doi: 10.1016/j.ceca.2016.01.002

Iwai, Y., Ozawa, K., Yahagi, K., Tanaka, M., Itohara, S., and Hirase, H. (2020). Transient astrocytic Gq signaling underlies remote memory enhancement. *bioRxiv* [Preprint]. doi: 10.1101/753095

Izumi, Y., and Zorumski, C. F. (1999). Norepinephrine promotes long-term potentiation in the adult rat hippocampus in vitro. *Synapse* 31, 196–202. doi: 10.1002/(SICI)1098-2396(19990301)31:3<196::AID-SYN4>3.0.CO;2-K

Jahn, R., and Scheller, R. H. (2006). SNAREs - engines for membrane fusion. *Nat. Rev. Mol. Cell Biol.* 7, 631–643. doi: 10.1038/nrm2002

Jurič, D. M., Lončar, D., and Čarman-Kržan, M. (2008). Noradrenergic stimulation of BDNF synthesis in astrocytes: mediation via α_1- and β_1/β_2-adrenergic receptors. *Neurochem. Int.* 52, 297–306. doi: 10.1016/j.neuint.2007.06.035

Kastanenka, K. V., Moreno-Bote, R., De Pittà, M., Perea, G., Eraso-Pichot, A., Masgrau, R., et al. (2020). A roadmap to integrate astrocytes into Systems Neuroscience. *Glia* 68, 5–26. doi: 10.1002/glia.23632

Kawaguchi, Y., and Shindou, T. (1998). Noradrenergic excitation and inhibition of GABAergic cell types in rat frontal cortex. *J. Neurosci.* 18, 6963–6976. doi: 10.1523/JNEUROSCI.18-17-06963.1998

Khakh, B. S., and Deneen, B. (2019). The emerging nature of astrocyte diversity. *Annu. Rev. Neurosci.* 42, 187–207. doi: 10.1146/annurev-neuro-070918-050443

Khakh, B. S., and McCarthy, K. D. (2015). Astrocyte calcium signaling: from observations to functions and the challenges therein. *Cold Spring Harb. Perspect. Biol.* 7:a020404. doi: 10.1101/cshperspect.a020404

Kjaerby, C., Rasmussen, R., Andersen, M., and Nedergaard, M. (2017). Does global astrocytic calcium signaling participate in awake brain state transitions and neuronal circuit function? *Neurochem. Res.* 42, 1810–1822. doi: 10.1007/s11064-017-2195-y

Kobayashi, M. (2007). Differential regulation of synaptic transmission by adrenergic agonists via protein kinase A and protein kinase C in layer V pyramidal neurons of rat cerebral cortex. *Neuroscience* 146, 1772–1784. doi: 10.1016/j.neuroscience.2007.04.001

Kobayashi, M., Imamura, K., Sugai, T., Onoda, N., Yamamoto, M., Komai, S., et al. (2000). Selective suppression of horizontal propagation in rat visual cortex by norepinephrine. *Eur. J. Neurosci.* 12, 264–272. doi: 10.1046/j.1460-9568.2000.00917.x

Kohro, Y., Matsuda, T., Yoshihara, K., Kohno, K., Koga, K., Katsuragi, R., et al. (2020). Spinal astrocytes in superficial laminae gate brainstem descending control of mechanosensory hypersensitivity. *Nat. Neurosci.* 23, 1376–1387. doi: 10.1038/s41593-020-00713-4

Koppel, I., Jaanson, K., Klasche, A., Tuvikene, J., Tiirik, T., Pärn, A., et al. (2018). Dopamine cross-reacts with adrenoreceptors in cortical astrocytes to induce BDNF expression, CREB signaling and morphological transformation. *Glia* 66, 206–216. doi: 10.1002/glia.23238

Kulik, A., Haentzsch, A., Lückermann, M., Reichelt, W., and Ballanyi, K. (1999). Neuron–glia signaling via α_1 adrenoceptor-mediated Ca^{2+} release in bergmann glial cells in situ. *J. Neurosci.* 19, 8401–8408. doi: 10.1523/JNEUROSCI.19-19-08401.1999

Lalo, U., Bogdanov, A., and Pankratov, Y. (2018). Diversity of astroglial effects on aging- and experience-related cortical metaplasticity. *Front. Mol. Neurosci.* 11:239. doi: 10.3389/fnmol.2018.00239

Lalo, U., Palygin, O., Rasooli-Nejad, S., Andrew, J., Haydon, P. G., and Pankratov, Y. (2014). Exocytosis of ATP from astrocytes modulates phasic and tonic inhibition in the neocortex. *PLoS Biol.* 12:e1001747. doi: 10.1371/journal.pbio.1001747

Lalo, U., Palygin, O., Verkhratsky, A., Grant, S. G. N., and Pankratov, Y. (2016). ATP from synaptic terminals and astrocytes regulates NMDA receptors and synaptic plasticity through PSD-95 multi-protein complex. *Sci. Rep.* 6:33609. doi: 10.1038/srep33609

Lanjakornsiripan, D., Pior, B.-J., Kawaguchi, D., Furutachi, S., Tahara, T., Katsuyama, Y., et al. (2018). Layer-specific morphological and molecular differences in neocortical astrocytes and their dependence on neuronal layers. *Nat. Commun.* 9, 1623. doi: 10.1038/s41467-018-03940-3

Lee, S. H., and Dan, Y. (2012). Neuromodulation of brain states. *Neuron* 76, 209–222. doi: 10.1016/j.neuron.2012.09.012

Lei, S., Deng, P.-Y., Porter, J. E., and Shin, H.-S. (2007). Adrenergic facilitation of GABAergic transmission in rat entorhinal cortex. *J. Neurophysiol.* 98, 2868–2877. doi: 10.1152/jn.00679.2007

Leopold, A. V., Shcherbakova, D. M., and Verkhusha, V. V. (2019). Fluorescent biosensors for neurotransmission and neuromodulation: engineering and applications. *Front. Cell. Neurosci.* 13:474. doi: 10.3389/fncel.2019.00474

Losi, G., Mariotti, L., and Carmignoto, G. (2014). GABAergic interneuron to astrocyte signalling: a neglected form of cell communication in the brain. *Philos. Trans. R. Soc. B Biol. Sci.* 369:20130609. doi: 10.1098/rstb.2013.0609

Luo, L., Callaway, E. M., and Svoboda, K. (2018). Genetic dissection of neural circuits: a decade of progress. *Neuron* 98, 256–281. doi: 10.1016/j.neuron.2018.03.040

Ma, Z., Stork, T., Bergles, D. E., and Freeman, M. R. (2016). Neuromodulators signal through astrocytes to alter neural circuit activity and behaviour. *Nature* 539, 428–432. doi: 10.1038/nature20145

Mächler, P., Wyss, M. T., Elsayed, M., Stobart, J., Gutierrez, R., Von Faber-Castell, A., et al. (2016). In vivo evidence for a lactate gradient from astrocytes to neurons. *Cell Metab.* 23, 94–102. doi: 10.1016/j.cmet.2015.10.010

Magistretti, P. J., and Allaman, I. (2018). Lactate in the brain: from metabolic end-product to signalling molecule. *Nat. Rev. Neurosci.* 19, 235–249. doi: 10.1038/nrn.2018.19

Marek, G. J., and Aghajanian, G. K. (1996). α_{1B}-Adrenoceptor-mediated excitation of piriform cortical interneurons. *Eur. J. Pharmacol.* 305, 95–100. doi: 10.1016/0014-2999(96)00158-6

Marin, P., Tencé, M., Delumeau, J.-C., Glowinski, J., and Prémont, J. (1993). Adenosine and somatostatin potentiate the α_1-adrenergic activation of phospholipase C in striatal astrocytes through a mechanism involving arachidonic acid and glutamate. *Biochem. Soc. Trans.* 21, 1114–1119. doi: 10.1042/bst0211114

Mariotti, L., Losi, G., Lia, A., Melone, M., Chiavegato, A., Gómez-Gonzalo, M., et al. (2018). Interneuron-specific signaling evokes distinctive somatostatin-mediated responses in adult cortical astrocytes. *Nat. Commun.* 9:82. doi: 10.1038/s41467-017-02642-6

Mather, M., Clewett, D., Sakaki, M., and Harley, C. W. (2016). Norepinephrine ignites local hotspots of neuronal excitation: how arousal amplifies selectivity in perception and memory. *Behav. Brain Sci.* 39:e200. doi: 10.1017/S0140525X15000667

Mayorquin, L. C., Rodriguez, A. V., Sutachan, J.-J., and Albarracín, S. L. (2018). Connexin-mediated functional and metabolic coupling between astrocytes and neurons. *Front. Mol. Neurosci.* 11:118. doi: 10.3389/fnmol.2018.00118

Mederos, S., Hernández-Vivanco, A., Ramírez-Franco, J., Martín-Fernández, M., Navarrete, M., Yang, A., et al. (2019). Melanopsin for precise optogenetic activation of astrocyte-neuron networks. *Glia* 67, 915–934. doi: 10.1002/glia.23580

Mederos, S., and Perea, G. (2019). GABAergic-astrocyte signaling: a refinement of inhibitory brain networks. *Glia* 67, 1842–1851. doi: 10.1002/glia.23644

Mederos, S., Sánchez-Puelles, C., Esparza, J., Valero, M., Ponomarenko, A., and Perea, G. (2021). GABAergic signaling to astrocytes in the prefrontal cortex sustains goal-directed behaviors. *Nat. Neurosci.* 24, 82–92. doi: 10.1038/s41593-020-00752-x

Miller, S. J., Philips, T., Kim, N., Dastgheyb, R., Chen, Z., Hsieh, Y.-C., et al. (2019). Molecularly defined cortical astroglia subpopulation modulates neurons via secretion of Norrin. *Nat. Neurosci.* 22, 741–752. doi: 10.1038/s41593-019-0366-7

Monai, H., Ohkura, M., Tanaka, M., Oe, Y., Konno, A., Hirai, H., et al. (2016). Calcium imaging reveals glial involvement in transcranial direct current stimulation-induced plasticity in mouse brain. *Nat. Commun.* 7:11100. doi: 10.1038/ncomms11100

Mu, Y., Bennett, D. V., Rubinov, M., Narayan, S., Yang, C.-T., Tanimoto, M., et al. (2019). Glia accumulate evidence that actions are futile and suppress unsuccessful behavior. *Cell* 178, 27.e19–43.e19. doi: 10.1016/J.CELL.2019.05.050

Muyderman, H., Nilsson, M., Blomstrand, F., Khatibi, S., Olsson, T., Hansson, E., et al. (1998). Modulation of mechanically induced calcium waves in hippocampal astroglial cells. Inhibitory effects of α_1-adrenergic stimulation. *Brain Res.* 793, 127–135. doi: 10.1016/S0006-8993(98)00151-6

Nimmerjahn, A., and Bergles, D. E. (2015). Large-scale recording of astrocyte activity. *Curr. Opin. Neurobiol.* 32, 95–106. doi: 10.1016/j.conb.2015.01.015

Nuriya, M., Morita, A., Shinotsuka, T., Yamada, T., and Yasui, M. (2018). Norepinephrine induces rapid and long-lasting phosphorylation and redistribution of connexin 43 in cortical astrocytes. *Biochem. Biophys. Res. Commun.* 504, 690–697. doi: 10.1016/j.bbrc.2018.09.021

Nuriya, M., Takeuchi, M., and Yasui, M. (2017). Background norepinephrine primes astrocytic calcium responses to subsequent norepinephrine stimuli in the cerebral cortex. *Biochem. Biophys. Res. Commun.* 483, 732–738. doi: 10.1016/j.bbrc.2016.12.073

Octeau, J. C., Gangwani, M. R., Allam, S. L., Tran, D., Huang, S., Hoang-Trong, T. M., et al. (2019). Transient, consequential increases in extracellular potassium ions accompany Channelrhodopsin2 excitation. *Cell Rep* 27, 2249.e7–2261.e7. doi: 10.1016/j.celrep.2019.04.078

O'Donnell, J., Zeppenfeld, D., McConnell, E., Pena, S., and Nedergaard, M. (2012). Norepinephrine: a neuromodulator that boosts the function of multiple cell types to optimize CNS performance. *Neurochem. Res.* 37, 2496–2512. doi: 10.1007/s11064-012-0818-x

Oe, Y., Wang, X., Patriarchi, T., Konno, A., Ozawa, K., Yahagi, K., et al. (2020). Distinct temporal integration of noradrenaline signaling by astrocytic second messengers during vigilance. *Nat. Commun.* 11:471. doi: 10.1038/s41467-020-14378-x

Ortiz, C., Navarro, J. F., Jurek, A., Märtin, A., Lundeberg, J., and Meletis, K. (2020). Molecular atlas of the adult mouse brain. *Sci. Adv.* 6:eabb3446. doi: 10.1126/sciadv.abb3446

Pacholko, A. G., Wotton, C. A., and Bekar, L. K. (2020). Astrocytes—The ultimate effectors of long-range neuromodulatory networks? *Front. Cell. Neurosci.* 14:1075. doi: 10.3389/fncel.2020.581075

Pankratov, Y., and Lalo, U. (2015). Role for astroglial α1-adrenoreceptors in gliotransmission and control of synaptic plasticity in the neocortex. *Front. Cell. Neurosci.* 9:230. doi: 10.3389/fncel.2015.00230

Pannasch, U., and Rouach, N. (2013). Emerging role for astroglial networks in information processing: from synapse to behavior. *Trends Neurosci.* 36, 405–417. doi: 10.1016/j.tins.2013.04.004

Papouin, T., Dunphy, J. M., Tolman, M., Dineley, K. T., and Haydon, P. G. (2017). Septal cholinergic neuromodulation tunes the astrocyte-dependent gating of hippocampal NMDA receptors to wakefulness. *Neuron* 94, 840.e7–854.e7. doi: 10.1016/j.neuron.2017.04.021

Pascual, O., Casper, K. B., Kubera, C., Zhang, J., Revilla-Sanchez, R., Sul, J.-Y., et al. (2005). Astrocytic purinergic signaling coordinates synaptic networks. *Science* 310, 113–116. doi: 10.1126/science.1116916

Patriarchi, T., Cho, J. R., Merten, K., Howe, M. W., Marley, A., Xiong, W.-H., et al. (2018). Ultrafast neuronal imaging of dopamine dynamics with designed genetically encoded sensors. *Science* 360:eaat4422. doi: 10.1126/science.aat4422

Paukert, M., Agarwal, A., Cha, J., Doze, V. A., Kang, J. U., and Bergles, D. E. (2014). Norepinephrine controls astroglial responsiveness to local circuit activity. *Neuron* 82, 1263–1270. doi: 10.1016/j.neuron.2014.04.038

Perea, G., and Araque, A. (2005). Glial calcium signaling and neuron-glia communication. *Cell Calcium* 38, 375–382. doi: 10.1016/j.ceca.2005.06.015

Perea, G., Gómez, R., Mederos, S., Covelo, A., Ballesteros, J. J., Schlosser, L., et al. (2016). Activity-dependent switch of GABAergic inhibition into glutamatergic excitation in astrocyte-neuron networks. *eLife* 5, 1–26. doi: 10.7554/eLife.20362

Perez, D. M. (2020). α_1-Adrenergic receptors in neurotransmission, synaptic plasticity, and cognition. *Front. Pharmacol.* 11:1098. doi: 10.3389/fphar.2020.581098

Pestana, F., Edwards-Faret, G., Belgard, T. G., Martirosyan, A., and Holt, M. G. (2020). No longer underappreciated: the emerging concept of astrocyte heterogeneity in neuroscience. *Brain Sci.* 10, 1–21. doi: 10.3390/brainsci10030168

Pham, C., Moro, D. H., Mouffle, C., Didienne, S., Hepp, R., Pfrieger, F. W., et al. (2020). Mapping astrocyte activity domains by light sheet imaging and spatio-temporal correlation screening. *Neuroimage* 220:117069. doi: 10.1016/j.neuroimage.2020.117069

Porter-Stransky, K. A., Centanni, S. W., Karne, S. L., Odil, L. M., Fekir, S., Wong, J. C., et al. (2019). Noradrenergic transmission at alpha1-adrenergic receptors in the ventral periaqueductal gray modulates arousal. *Biol. Psychiatry* 85, 237–247. doi: 10.1016/j.biopsych.2018.07.027

Poskanzer, K. E., and Yuste, R. (2016). Astrocytes regulate cortical state switching in vivo. *Proc. Natl. Acad. Sci. U.S.A.* 113, E2675–E2684. doi: 10.1073/pnas.1520759113

Ramos, B. P., and Arnsten, A. F. T. (2007). Adrenergic pharmacology and cognition: focus on the prefrontal cortex. *Pharmacol. Ther.* 113, 523–536. doi: 10.1016/j.pharmthera.2006.11.006

Regan, M. R., Huang, Y. H., Kim, Y. S., Dykes-Hoberg, M. I., Jin, L., Watkins, A. M., et al. (2007). Variations in promoter activity reveal a differential expression and physiology of glutamate transporters by glia in the developing and mature CNS. *J. Neurosci.* 27, 6607–6619. doi: 10.1523/JNEUROSCI.0790-07.2007

Robin, L. M., Oliveira da Cruz, J. F., Langlais, V. C., Martin-Fernandez, M., Metna-Laurent, M., Busquets-Garcia, A., et al. (2018). Astroglial CB_1 receptors determine synaptic D-Serine availability to enable recognition memory. *Neuron* 98, 935.e5–944.e5. doi: 10.1016/j.neuron.2018.04.034

Roth, B. L. (2016). DREADDs for neuroscientists. *Neuron* 89, 683–694. doi: 10.1016/j.neuron.2016.01.040

Rusakov, D. A. (2015). Disentangling calcium-driven astrocyte physiology. *Nat. Rev. Neurosci.* 16, 226–233. doi: 10.1038/nrn3878

Salgado, H., Treviño, M., and Atzori, M. (2016). Layer- and area-specific actions of norepinephrine on cortical synaptic transmission. *Brain Res.* 1641, 163–176. doi: 10.1016/j.brainres.2016.01.033

Salm, A. K., and McCarthy, K. D. (1989). Expression of beta-adrenergic receptors by astrocytes isolated from adult rat cortex. *Glia* 2, 346–352. doi: 10.1002/glia.440020507

Salm, A. K., and McCarthy, K. D. (1992). The evidence for astrocytes as a target for central noradrenergic activity: expression of adrenergic receptors. *Brain Res. Bull.* 29, 265–275. doi: 10.1016/0361-9230(92)90056-4

Samuels, E. R., and Szabadi, E. (2008). Functional neuroanatomy of the noradrenergic locus coeruleus: its roles in the regulation of arousal and autonomic function part I: principles of functional organisation. *Curr. Neuropharmacol.* 6, 235–253. doi: 10.2174/157015908785777229

San Martín, A., Ceballo, S., Ruminot, I., Lerchundi, R., Frommer, W. B., and Barros, L. F. (2013). A genetically encoded FRET lactate sensor and its use to detect the warburg effect in single cancer cells. *PLoS One* 8:e57712. doi: 10.1371/journal.pone.0057712

Sara, S. J., and Bouret, S. (2012). Orienting and reorienting: the locus coeruleus mediates cognition through arousal. *Neuron* 76, 130–141. doi: 10.1016/j.neuron.2012.09.011

Scales, S. J., Chen, Y. A., Yoo, B. Y., Patel, S. M., Doung, Y. C., and Scheller, R. H. (2000). SNAREs contribute to the specificity of membrane fusion. *Neuron* 26, 457–464. doi: 10.1016/S0896-6273(00)81177-0

Scemes, E., Stout, R. F., and Spray, D. C. (2017). "Adrenergic receptors on astrocytes modulate gap junctions," in *Noradrenergic Signaling and Astroglia*, eds R. Zorec and N. Vardjan (Amsterdam: Elsevier), 127–144. doi: 10.1016/B978-0-12-805088-0.00006-2

Schnell, C., Negm, M., Driehaus, J., Scheller, A., and Hülsmann, S. (2016). Norepinephrine-induced calcium signaling in astrocytes in the respiratory network of the ventrolateral medulla. *Respir. Physiol. Neurobiol.* 226, 18–23. doi: 10.1016/j.resp.2015.10.008

Schwarz, L. A., and Luo, L. (2015). Organization of the locus coeruleus-norepinephrine system. *Curr. Biol.* 25, R1051–R1056. doi: 10.1016/j.cub.2015.09.039

Seibt, F., and Schlichter, R. (2015). Noradrenaline-mediated facilitation of inhibitory synaptic transmission in the dorsal horn of the rat spinal cord involves interlaminar communications. *Eur. J. Neurosci.* 42, 2654–2665. doi: 10.1111/ejn.13077

Semyanov, A., Henneberger, C., and Agarwal, A. (2020). Making sense of astrocytic calcium signals — from acquisition to interpretation. *Nat. Rev. Neurosci.* 21, 551–564. doi: 10.1038/s41583-020-0361-8

Shao, Y., and Sutin, J. (1992). Expression of adrenergic receptors in individual astrocytes and motor neurons isolated from the adult rat brain. *Glia* 6, 108–117. doi: 10.1002/glia.440060205

Shen, Y., Wu, S. Y., Rancic, V., Aggarwal, A., Qian, Y., Miyashita, S. I., et al. (2019). Genetically encoded fluorescent indicators for imaging intracellular potassium ion concentration. *Commun. Biol.* 2, 1–10. doi: 10.1038/s42003-018-0269-2

Sherpa, A. D., Xiao, F., Joseph, N., Aoki, C., and Hrabetova, S. (2016). Activation of β-adrenergic receptors in rat visual cortex expands astrocytic processes and reduces extracellular space volume. *Synapse* 70, 307–316. doi: 10.1002/syn.21908

Shigetomi, E., Patel, S., and Khakh, B. S. (2016). Probing the complexities of astrocyte calcium signaling. *Trends Cell Biol.* 26, 300–312. doi: 10.1016/j.tcb.2016.01.003

Slezak, M., de Vin, F., Shinmyo, Y., Batiuk, M. Y., Rincon, M. Y., Pando, C. M., et al. (2018). Flexible, fast and selective genetic manipulation of the vertebrate CNS with misPiggy. *bioRxiv* [Preprint]. doi: 10.1101/481580

Slezak, M., Kandler, S., Van Veldhoven, P. P., Van den Haute, C., Bonin, V., and Holt, M. G. (2019). Distinct mechanisms for visual and motor-related astrocyte responses in mouse visual cortex. *Curr. Biol.* 29, 3120.e5–3127.e5. doi: 10.1016/j.cub.2019.07.078

Sonoda, K., Matsui, T., Bito, H., and Ohki, K. (2018). Astrocytes in the mouse visual cortex reliably respond to visual stimulation. *Biochem. Biophys. Res. Commun.* 505, 1216–1222. doi: 10.1016/j.bbrc.2018.10.027

Srinivasan, R., Huang, B. S., Venugopal, S., Johnston, A. D., Chai, H., Zeng, H., et al. (2015). Ca^{2+} signaling in astrocytes from $IP_3R2^{-/-}$ mice in brain slices and during startle responses in vivo. *Nat. Neurosci.* 18, 708–717. doi: 10.1038/nn.4001

Srinivasan, R., Lu, T., Chai, H., Xu, J., Huang, B. S., Golshani, P., et al. (2016). New transgenic mouse lines for selectively targeting astrocytes and studying calcium signals in astrocyte processes in situ and in vivo. *Neuron* 92, 1181–1195. doi: 10.1016/j.neuron.2016.11.030

Ståhl, P. L., Salmén, F., Vickovic, S., Lundmark, A., Navarro, J. F., Magnusson, J., et al. (2016). Visualization and analysis of gene expression in tissue sections by spatial transcriptomics. *Science* 353, 78–82. doi: 10.1126/science.aaf2403

Stone, E. A., and Ariano, M. A. (1989). Are glial cells targets of the central noradrenergic system? A review of the evidence. *Brain Res. Rev.* 14, 297–309. doi: 10.1016/0165-0173(89)90015-5

Subbarao, K. V., and Hertz, L. (1990). Effect of adrenergic agonists on glycogenolysis in primary cultures of astrocytes. *Brain Res.* 536, 220–226. doi: 10.1016/0006-8993(90)90028-A

Subbarao, K. V., and Hertz, L. (1991). Stimulation of energy metabolism by α-adrenergic agonists in primary cultures of astrocytes. *J. Neurosci. Res.* 28, 399–405. doi: 10.1002/jnr.490280312

Takano, T., Wallace, J. T., Baldwin, K. T., Purkey, A. M., Uezu, A., Courtland, J. L., et al. (2020). Chemico-genetic discovery of astrocytic control of inhibition in vivo. *Nature* 588, 296–302. doi: 10.1038/s41586-020-2926-0

Tang, F., Lane, S., Korsak, A., Paton, J. F. R., Gourine, A. V., Kasparov, S., et al. (2014). Lactate-mediated glia-neuronal signalling in the mammalian brain. *Nat. Commun.* 5:3284. doi: 10.1038/ncomms4284

Thul, P. J., Åkesson, L., Wiking, M., Mahdessian, D., Geladaki, A., Ait Blal, H., et al. (2017). A subcellular map of the human proteome. *Science* 356:eaal3321. doi: 10.1126/science.aal3321

Tyurin-Kuzmin, P. A., Fadeeva, J. I., Kanareikina, M. A., Kalinina, N. I., Sysoeva, V. Y., Dyikanov, D. T., et al. (2016). Activation of β-adrenergic receptors is required for elevated α1A-adrenoreceptors expression and signaling in mesenchymal stromal cells. *Sci. Rep.* 6:32835. doi: 10.1038/srep32835

Vardjan, N., Horvat, A., Anderson, J. E., Yu, D., Croom, D., Zeng, X., et al. (2016). Adrenergic activation attenuates astrocyte swelling induced by hypotonicity and neurotrauma. *Glia* 64, 1034–1049. doi: 10.1002/glia.22981

Vardjan, N., Kreft, M., and Zorec, R. (2014). Dynamics of β-adrenergic/cAMP signaling and morphological changes in cultured astrocytes. *Glia* 62, 566–579. doi: 10.1002/glia.22626

Vardjan, N., and Zorec, R. (2015). Excitable astrocytes: Ca^{2+}- and cAMP-Regulated exocytosis. *Neurochem. Res.* 40, 2414–2424. doi: 10.1007/s11064-015-1545-x

Verkhratsky, A., and Nedergaard, M. (2018). Physiology of astroglia. *Physiol. Rev.* 98, 239–389. doi: 10.1152/physrev.00042.2016

Vizi, E., Fekete, A., Karoly, R., and Mike, A. (2010). Non-synaptic receptors and transporters involved in brain functions and targets of drug treatment. *Br. J. Pharmacol.* 160, 785–809. doi: 10.1111/j.1476-5381.2009.00624.x

Wahis, J., Hennes, M., Arckens, L., and Holt, M. G. (2021b). Star power: the emerging role of astrocytes as neuronal partners during cortical plasticity. *Curr. Opin. Neurobiol.* 67, 174–182. doi: 10.1016/j.conb.2020.12.001

Wahis, J., Baudon, A., Althammer, F., Kerspern, D., Goyon, S., Hagiwara, D., et al. (2021a). Astrocytes mediate the effect of oxytocin in the central amygdala on neuronal activity and affective states in rodents. *Nat. Neurosci.* doi: 10.1038/s41593-021-00800-0

Wang, X., Qiu, R., Tsark, W., and Lu, Q. (2007). Rapid promoter analysis in developing mouse brain and genetic labeling of young neurons by doublecortin-DsRed-express. *J. Neurosci. Res.* 85, 3567–3573. doi: 10.1002/jnr.21440

Wotton, C. A., Cross, C. D., and Bekar, L. K. (2020). Serotonin, norepinephrine, and acetylcholine differentially affect astrocytic potassium clearance to modulate somatosensory signaling in male mice. *J. Neurosci. Res.* 98, 964–977. doi: 10.1002/jnr.24597

Xie, A. X., Petravicz, J., and McCarthy, K. D. (2015). Molecular approaches for manipulating astrocytic signaling in vivo. *Front. Cell. Neurosci.* 9:144. doi: 10.3389/fncel.2015.00144

Ye, L., Orynbayev, M., Zhu, X., Lim, E. Y., Dereddi, R. R., Agarwal, A., et al. (2020). Ethanol abolishes vigilance-dependent astroglia network activation in mice by inhibiting norepinephrine release. *Nat. Commun.* 11:6157. doi: 10.1038/s41467-020-19475-5

Yu, X., Nagai, J., and Khakh, B. S. (2020). Improved tools to study astrocytes. *Nat. Rev. Neurosci.* 21, 121–138. doi: 10.1038/s41583-020-0264-8

Yu, X., Taylor, A. M. W., Nagai, J., Golshani, P., Evans, C. J., Coppola, G., et al. (2018). Reducing astrocyte calcium signaling in vivo alters striatal microcircuits and causes repetitive behavior. *Neuron* 99, 1170.e9–1187.e9. doi: 10.1016/j.neuron.2018.08.015

Yuan, W.-X., Chen, S.-R., Chen, H., and Pan, H.-L. (2009). Stimulation of α_1-adrenoceptors reduces glutamatergic synaptic input from primary afferents through $GABA_A$ receptors and T-type Ca^{2+} channels. *Neuroscience* 158, 1616–1624. doi: 10.1016/j.neuroscience.2008.11.022

Zeisel, A., Muñoz-Manchado, A. B., Codeluppi, S., Lönnerberg, P., La Manno, G., Juréus, A., et al. (2015). Cell types in the mouse cortex and hippocampus revealed by single-cell RNA-seq. *Science* 347, 1138–1142. doi: 10.1126/science.aaa1934

Zhang, Y., Chen, K., Sloan, S. A., Bennett, M. L., Scholze, A. R., O'Keeffe, S., et al. (2014). An RNA-sequencing transcriptome and splicing database of glia, neurons, and vascular cells of the cerebral cortex. *J. Neurosci.* 34, 11929–11947. doi: 10.1523/JNEUROSCI.1860-14.2014

Zhang, Y., Sloan, S. A., Clarke, L. E., Caneda, C., Plaza, C. A., Blumenthal, P. D., et al. (2016). Purification and characterization of progenitor and mature human astrocytes reveals transcriptional and functional differences with mouse. *Neuron* 89, 37–53. doi: 10.1016/j.neuron.2015.11.013

Zhou, B., Zuo, Y.-X., and Jiang, R.-T. (2019). Astrocyte morphology: diversity, plasticity, and role in neurological diseases. *CNS Neurosci. Ther.* 25, 665–673. doi: 10.1111/cns.13123

Zimnik, N. C., Treadway, T., Smith, R. S., and Araneda, R. C. (2013). α_{1A}-Adrenergic regulation of inhibition in the olfactory bulb. *J. Physiol.* 591, 1631–1643. doi: 10.1113/jphysiol.2012.248591

Zorec, R., Parpura, V., and Verkhratsky, A. (2018). Preventing neurodegeneration by adrenergic astroglial excitation. *FEBS J.* 285, 3645–3656. doi: 10.1111/febs.14456

Zuend, M., Saab, A. S., Wyss, M. T., Ferrari, K. D., Hösli, L., Looser, Z. J., et al. (2020). Arousal-induced cortical activity triggers lactate release from astrocytes. *Nat. Metab.* 2, 179–191. doi: 10.1038/s42255-020-0170-4

Conflict of Interest: The authors declare that the research was conducted in the absence of any commercial or financial relationships that could be construed as a potential conflict of interest.

frontiers in Cellular Neuroscience

ORIGINAL RESEARCH
published: 01 March 2021
doi: 10.3389/fncel.2021.617989

Spontaneous Ca^{2+} Fluctuations Arise in Thin Astrocytic Processes With Real 3D Geometry

László Héja[1], Zsolt Szabó[1], Márton Péter[1,2] and Julianna Kardos[1]*

[1]*Functional Pharmacology Research Group, Institute of Organic Chemistry, Research Centre for Natural Sciences, Hungarian Academy of Sciences (MTA), Budapest, Hungary,* [2]*Hevesy György PhD School of Chemistry, ELTE Eötvös Loránd University, Budapest, Hungary*

Fluctuations of cytosolic Ca^{2+} concentration in astrocytes are regarded as a critical non-neuronal signal to regulate neuronal functions. Although such fluctuations can be evoked by neuronal activity, rhythmic astrocytic Ca^{2+} oscillations may also spontaneously arise. Experimental studies hint that these spontaneous astrocytic Ca^{2+} oscillations may lie behind different kinds of emerging neuronal synchronized activities, like epileptogenic bursts or slow-wave rhythms. Despite the potential importance of spontaneous Ca^{2+} oscillations in astrocytes, the mechanism by which they develop is poorly understood. Using simple 3D synapse models and kinetic data of astrocytic Glu transporters (EAATs) and the Na^+/Ca^{2+} exchanger (NCX), we have previously shown that NCX activity alone can generate markedly stable, spontaneous Ca^{2+} oscillation in the astrocytic leaflet microdomain. Here, we extend that model by incorporating experimentally determined real 3D geometries of 208 excitatory synapses reconstructed from publicly available ultra-resolution electron microscopy datasets. Our simulations predict that the surface/volume ratio (SVR) of peri-synaptic astrocytic processes prominently dictates whether NCX-mediated spontaneous Ca^{2+} oscillations emerge. We also show that increased levels of intracellular astrocytic Na^+ concentration facilitate the appearance of Ca^{2+} fluctuations. These results further support the principal role of the dynamical reshaping of astrocyte processes in the generation of intrinsic Ca^{2+} oscillations and their spreading over larger astrocytic compartments.

Keywords: astrocyte, Ca^{2+} oscillation, NCX (sodium–calcium exchanger), astrocyte morphology, real geometry, simulation

OPEN ACCESS

Edited by:
Leonid Savtchenko, University College London, United Kingdom

Reviewed by:
Alexey Brazhe, Lomonosov Moscow State University, Russia
Maurizio De Pittà, Basque Center for Applied Mathematics, Spain

****Correspondence:***
László Héja
heja.laszlo@ttk.mta.hu

Specialty section:
This article was submitted to Non-Neuronal Cells, a section of the journal Frontiers in Cellular Neuroscience

Received: *15 October 2020*
Accepted: *18 January 2021*
Published: *01 March 2021*

Citation:
Héja L, Szabó Z, Péter M and Kardos J (2021) Spontaneous Ca^{2+} Fluctuations Arise in Thin Astrocytic Processes With Real 3D Geometry. Front. Cell. Neurosci. 15:617989. doi: 10.3389/fncel.2021.617989

INTRODUCTION

Over the past three decades, astrocytes have emerged as crucial regulators of synaptic function (Zhang et al., 2016). On the cellular scale, many of these regulatory functions operate by controlling the extracellular concentration of various substances pivotal to synaptic activity (Somogyi et al., 1990; Harris et al., 1992; Rusakov et al., 1997, 1998, 1999; Rusakov and Kullmann, 1998a,b; Araque et al., 1999; Bergles et al., 1999; Ventura and Harris, 1999; Newman, 2004; Matsui et al., 2005; Savtchenko and Rusakov, 2007; Heller et al., 2020). One of such classical astrocyte-mediated regulatory function is the uptake of synaptically released glutamate. Glial glutamate uptake by the Na^+/Glu symporter, Glu transporters (EAATs), in turn, alters astrocytic intracellular Na^+ concentration, leading to the activation of diverse Na^+-symporters, like GABA and Gln transporters or Na^+/K^+-ATPase (NKA) and $Na^+/K^+/2Cl^-$ (NKCC1; Lenart et al., 2004; Héja et al., 2009, 2012, 2019; Pál et al., 2013, 2015; Kirischuk et al., 2016; Gerkau et al., 2019; Henneberger et al., 2020; Lerchundi et al., 2020).

Another consequence of the altered astrocytic Na^+ concentration is the triggering of coupled Ca^{2+} fluctuations (Mergenthaler et al., 2019) mediated mainly by the Na^+/Ca^{2+} exchanger (NCX; Brazhe et al., 2018). Since NCX operates close to its equilibrium, it can be easily switched between forward and reverse operations (Kirischuk et al., 2016). Moreover, intracellular fluctuations of Na^+ concentration in the synapse-covering astrocytic microdomain can be intensified by local Na^+ inhomogeneity due to surface retention of cations by the dipole heads of negatively charged membrane lipids (Breslin et al., 2018). Therefore, EAAT-mediated Glu/Na^+ symport may easily give rise to local Ca^{2+} fluctuations.

We and others conjectured different Ca^{2+} signaling mechanisms at perisynaptic astrocytic processes (PAPs) and their relevance for the regulation of the tripartite synapses (Kékesi et al., 2015; Kovács et al., 2015; Savtchenko et al., 2015; Kirischuk et al., 2016; Szabó et al., 2017; De Pittà, 2020; Héja and Kardos, 2020; Semyanov et al., 2020). Using a simplified tripartite synapse model built up by geometric modules we have previously shown that NCX alone can generate spontaneous calcium fluctuations, enhanced by glutamate taken up through EAATs (Héja and Kardos, 2020). However, local Na^+ and Ca^{2+} dynamics in these very thin processes heavily depend on the actual geometry of PAPs. Moreover, this geometry is known to be dynamically changing due to astrocyte activation (Henneberger et al., 2020). Therefore, in the current work, we explored whether NCX activity may introduce rhythmic Ca^{2+} dynamics in real excitatory tripartite synapses using a public annotated database of 1,700 real synapses reconstructed from serial electron microscopic sections (Kasthuri et al., 2015).

MATERIALS AND METHODS

Obtaining Real Geometry of Tripartite Synapses

Real geometry of synapses and surrounding astrocytic processes were obtained from the high-resolution ($6 \times 6 \times 30$ nm) reconstruction of a 1,500 μm^3 volume of mouse neocortex (Kasthuri et al., 2015), containing 1,700 identified and characterized synapses. In the first step, 208 "single" excitatory synapses with individual glutamatergic axon terminal synapsed to single postsynaptic dendritic spines were selected for simulation. Geometry of segmented cells in $1.2 \times 1.2 \times 1.2$ μm volumes ($201 \times 201 \times 41$ pixels) around each post-synaptic density centroid were imported from the database to Matlab using the VAST Lite 1.2.1 software and custom-written Matlab scripts.

To correct geometry for fixation-induced swelling, we shrunk the segmented cells by 6 nm and extended the extracellular space (ECS) to this volume. This way, a fraction of the ECS in the synaptic environment was increased from $11.2 \pm 3.0\%$ to $18.2 \pm 3.3\%$ that is closer to physiological values (Van Harreveld and Khattab, 1968; Harreveld and Fifkova, 1975; Korogod et al., 2015; Pallotto et al., 2015).

Astrocytic coverage of the presynaptic axon terminal (bouton) and the postsynaptic dendritic spine was calculated by counting the number of surface pixels of boutons and spines having close contact with astrocytes. The surface/volume ratio (SVR) was determined by dividing the number of surface pixels counted according to the above method by the number of all pixels belonging to astrocyte processes.

Simulation of Astrocytic $[Ca^{2+}]$ and Synaptic Glu Release

Extracellular concentrations of relevant ions ($[Na^+]_e$ = 140 mM; $[K^+]_e$ = 3 mM; $[Ca^{2+}]_e$ = 2 mM) as well as astrocytic $[K^+]_i$ (130 mM) and $[Glu]_i$ (3 mM) were kept constant during the simulation, while $[Glu]_e$ (0.3 μM), $[Na^+]_i$ (15 mM) and $[Ca^{2+}]_i$ (100 nM) were allowed to change due to Glu release, intracellular Ca^{2+} diffusion and activation of EAATs and NCX (Héja and Kardos, 2020). It is to note that $[Glu]_e$ is difficult to measure and rather different estimates are reported in the literature. Electrophysiological measurements suggest tens of nanomolar concentrations (Herman et al., 2011) based on receptor activation, while microdialysis studies measure tens of micromolar for $[Glu]_e$ (Baker et al., 2002). Furthermore, EC_{50} values of postsynaptic glutamate receptor (382 μM; Jonas and Sakmann, 1992; Li et al., 2002) and astrocytic glutamate transporter (14.8 μM; Levy et al., 1998; Herman and Jahr, 2007) indicate effective activation of postsynaptic receptors and extrasynaptic transporters at above 100 μM and 3 μM glutamate, respectively. These glutamate concentration ranges are far beyond the $[Glu]_e$ of 0.4 ± 0.1 μM (Kékesi et al., 2000) allowing for receptor/transporter activation. Our *in vivo* microdialysis data also validates the mean of these values as being 0.4 ± 0.1 μM (Kékesi et al., 2000). Therefore, 0.3 μM $[Glu]_e$, used in this study seems a reliable estimate.

Markovian kinetic models of astrocytic EAATs and NCX were constructed according to published rate constants based on experimental data. Glutamate uptake by EAATs was modeled by a 13-step cycle comprised of separate bindings and unbindings of 3 Na^+, 1H^+, 1 K^+, and 1 Glu molecules (Bergles et al., 2002). NCX activity was modeled by a 6-step cycle according to Chu et al. (2016). 10,800/μm^2 EAAT (Lehre and Danbolt, 1998) and 500/μm^2 NCX (Chu et al., 2016) molecules were distributed randomly on the astrocytic surface.

Before starting the simulation, EAAT and NCX randomly populated the available states and we allowed them to reach steady-state distribution for 30 ms at the above concentrations. Simulations began with a further 10 ms baseline activity before initiating single synaptic glutamate release (5,000 Glu molecules) at the synapse centroid as determined by Kasthuri et al. (2015). The diffusion of independent glutamate molecules in the 3D ECS was estimated by random walks at 1 μs intervals. The diffusion coefficient of glutamate was set to 0.33 μm^2/ms (Gavrilov et al., 2018).

Each time steps (1 μs) was comprised of the following functions: (1) position of extracellular glutamate molecules and intracellular Ca^{2+} ions were updated by moving them with normally distributed random distances around their mean square displacement values. If a particle moved outside of the sample volume, it was removed from the available pool, except if $[Glu]_e$, $[Na^+]_i$ or $[Ca^{2+}]_i$ dropped below the baseline level, in

EAAT

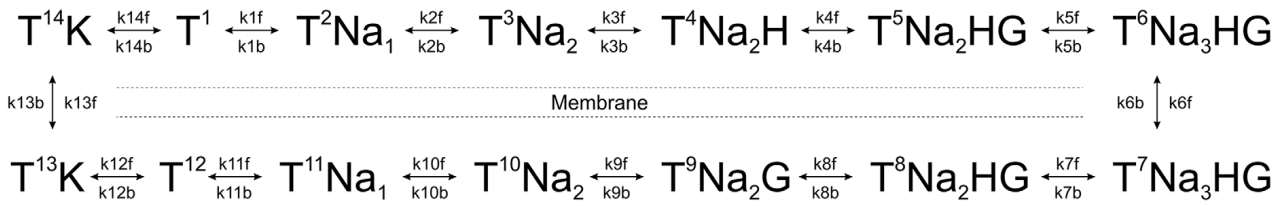

$k1f=10^4\ M^{-1}s^{-1}$	$k1b=10^2\ s^{-1}$
$k2f=10^4\ M^{-1}s^{-1}$	$k2b=5\times10^2\ s^{-1}$
$k3f=6\times10^{11}\ M^{-1}s^{-1}$	$k3b=7\times10^2\ s^{-1}$
$k4f=6\times10^6\ s^{-1}$	$k4b=5\times10^2\ s^{-1}$
$k5f=10^4\ M^{-1}s^{-1}$	$k5b=10^3\ s^{-1}$
$k6f=2\times10^3\ s^{-1}$	$k6b=1.9\times10^3\ s^{-1}$
$k7f=10^3\ s^{-1}$	$k7b=4\times10^4\ s^{-1}$
$k8f=3\times10^3\ s^{-1}$	$k8b=9\times10^{10}\ M^{-1}s^{-1}$
$k9f=3\times10^3\ s^{-1}$	$k9b=10^5\ M^{-1}s^{-1}$
$k10f=10^5\ s^{-1}$	$k10b=2\times10^7\ M^{-1}s^{-1}$
$k11f=10^5\ s^{-1}$	$k11b=10^8\ M^{-1}s^{-1}$
$k12f=10^6\ M^{-1}s^{-1}$	$k12b=10^3\ s^{-1}$
$k13f=40\ s^{-1}$	$k13b=10\ s^{-1}$
$k14f=2\times10^4\ s^{-1}$	$k14b=10^6\ M^{-1}s^{-1}$

NCX

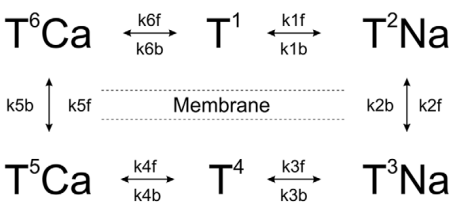

$k1f=4.325\times10^{10}\ M^{-3}s^{-1}$	$k1b=1.0524\times10^4\ s^{-1}$
$k2f=1.0781\times10^4\ s^{-1}$	$k2b=3.3541\times10^3\ s^{-1}$
$k3f=1.408\times10^4\ s^{-1}$	$k3b=2.8692\times10^9\ s^{-1}$
$k4f=4.024\times10^8\ s^{-1}$	$k4b=7.3916\times10^3\ s^{-1}$
$k5f=7.1389\times10^3\ s^{-1}$	$k5b=9.4959\times10^3\ s^{-1}$
$k6f=4.5134\times10^3\ s^{-1}$	$k6b=1.0691\times10^{10}\ M^{-1}s^{-1}$

SCHEME 1 | Kinetic schemes and rates of astrocytic Glu transporters (EAAT) and Na^+/Ca^{2+} exchanger (NCX).

which case it was moved back to its previous position. Particles moving out of their compartment (astrocyte, dendrite, axon terminal, or ECS) were also placed back to their previous position. (2) Transition states of EAAT and NCX molecules were determined according to their rate constants and dynamic rate constants based on the current intra- and extracellular concentrations of relevant ions (**Scheme 1**). In the case of EAAT kinetics, local $[Glu]_e$ in the surrounding $50 \times 50 \times 50$ nm^3 extracellular microdomain of each EAAT molecule was used instead of the average extracellular glutamate concentration. Local $[Glu]_e$ was determined by counting the freely diffusing Glu molecules in the $50 \times 50 \times 50$ nm^3 ECS around each EAATs in each time frame. Transition rates were corrected for $Q_{10} = 3$ to account for temperature dependence. Astrocyte membrane potential was set to −70 mV. (3) Glutamate molecules bound to the extracellularly faced EAAT were removed from the available pool until they were released back by reverse operation of the transporter. Ca^{2+} ions bound to the intracellularly faced NCX were removed from the available pool until they were released back by reverse operation of the transporter.

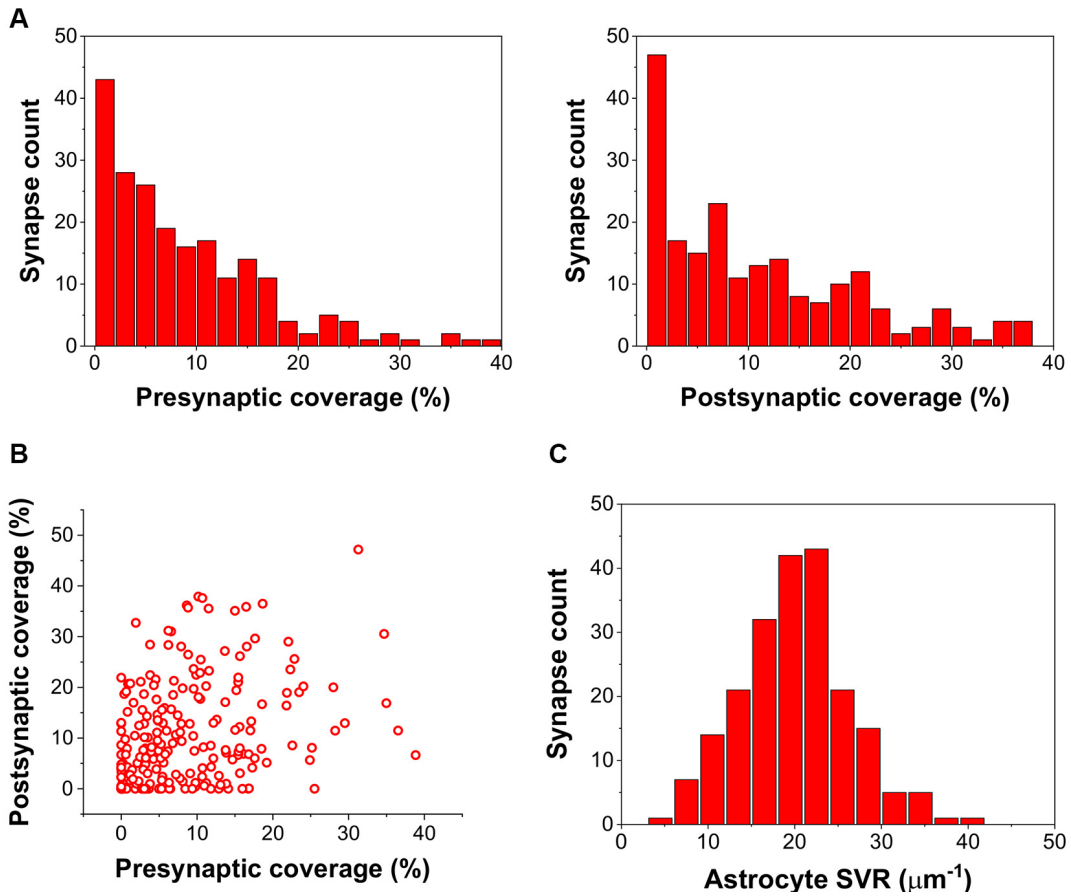

FIGURE 1 | Astrocyte related geometric parameters of the 208 investigated synapses. **(A)** Distribution of pre-and postsynaptic coverage of synapses by astrocyte processes. **(B)** Correlation of pre-and postsynaptic coverage of synapses by astrocyte processes. **(C)** Distribution of the astrocytic surface/volume ratio (SVR) in the 1.2 × 1.2 × 1.2 μm volume surrounding each synapse.

All simulations were done in Matlab using custom-written scripts[1]. Reconstructed and segmented EM stacks of real synapses were downloaded and handled by the VAST Lite 1.2.1 software[2] (Kasthuri et al., 2015) and the VastTools Matlab package. Processed data of synapses containing 3D geometries and calculated surfaces and volumes in Matlab file format as well as tools to reproduce the simulations can be downloaded at http://downloadables.ttk.hu/heja/Front_CellNeurosci2021. Synapses were visualized using Cinema4D.

Data are shown as mean ± SEM and were analyzed with one-way analysis of variances (ANOVAs, OriginPro 2018). Statistical significance was considered at $p < 0.05$.

RESULTS

To simulate Ca^{2+} oscillations in real astrocyte processes, we used the saturated reconstruction of a 1,500 μm^3 volume of mouse neocortex (Kasthuri et al., 2015). The dataset contains 1,700 identified and morphologically characterized synapses. We explored volumes of 1.2 × 1.2 × 1.2 μm around these synapses to investigate the potential of astrocytic processes to readout synaptic activity.

Due to the applied glutaraldehyde and paraformaldehyde fixative, the ECS of the sample was found to occupy only 6% of the total volume around the synapses (Kasthuri et al., 2015). Since ECS fraction was found to be between 15% and 25% in frozen tissues (Van Harreveld and Khattab, 1968; Harreveld and Fifkova, 1975; Korogod et al., 2015; Pallotto et al., 2015) where fixation-issued swelling is not present, we modified the original segmentation by replacing the outer 6 nm surface of each cellular segment with ECS. This modification also allowed free diffusion of the released glutamate in the ECS, which would otherwise be hindered due to the direct connection of segmented cells.

To simulate spontaneous and glutamate-release associated, NCX activity-linked Ca^{2+} changes in real glutamatergic tripartite synapses, we selected 208 "classical" synapses out of the 1,700 identified synapses (Kasthuri et al., 2015) based on the following criteria: (1) axon type is excitatory; (2) axon terminal is present, i.e., it is not an en-passant synapse; (3) axon bouton

[1]https://github.com/hejalaszlo/Astrocyte-leaflet-simulation
[2]https://lichtman.rc.fas.harvard.edu/vast/

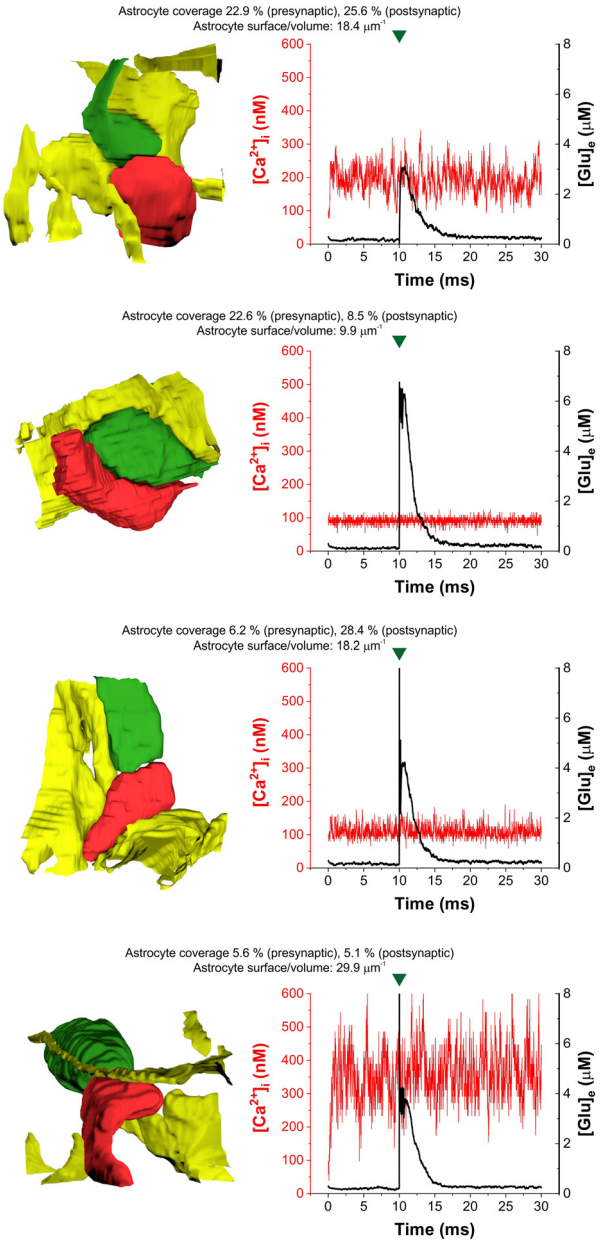

FIGURE 2 | Heterogeneity of astrocytic intracellular Ca^{2+} oscillations ($[Ca^{2+}]i$) during the control period (1–10 ms) and following glutamate release (10–30 ms) in four selected real tripartite synapses showing different levels of astrocytic coverage and astrocyte SVR. The dynamics of astrocytic Ca^{2+} concentration is shown in red, extracellular [Glu] ($[Glu]_e$) is shown in the black trace. Astrocytes are colored yellow, presynaptic terminals are green and postsynaptic spines are red in images showing real 3D geometry of each synapse. Green marks indicate release events.

is not multi-synaptic; (4) the postsynaptic element is a spine, not a shaft; and (5) astrocytic volume fraction is at least 2% in the 1.2 × 1.2 × 1.2 μm volume. Astrocytic Ca^{2+}, extracellular glutamate concentrations following synaptic Glu release, as well as dynamics of astrocytic Glu transporters (EAAT) and NCX were simulated as previously described (Héja and Kardos, 2020).

By calculating the ratio of the axon terminal and spine surfaces that are in contact with astrocytic processes, we found many presynaptic axon terminals and postsynaptic spines with little or no astrocytic coverage at all (**Figure 1A**). Also, astrocytic coverage of pre- and postsynaptic elements showed a high degree of heterogeneity (**Figure 1B**). Although many of the synapses were equally covered by astrocytes at the axon terminal and the dendritic spine, highly asymmetric astrocytic coverage was also abundant. Besides, we also determined the surface to volume ratio (SVR) of astrocytic processes in the surrounding of the 208 selected synapses. Following previous observations (Gavrilov et al., 2018), the distribution of SVR followed normal distributions with a mean between 20 and 25 μm^{-1}, corresponding to astrocytic leaflets that are known to cover synapses (Gavrilov et al., 2018; **Figure 1C**).

In agreement with previous findings (Héja and Kardos, 2020), we found that astrocytic oscillatory Ca^{2+} dynamics spontaneously emerged in different kinds of realistic astrocytic leaflets characterized by various pre- or postsynaptic contacts (**Figure 2**). The incidence of Ca^{2+} fluctuations strongly depends on the astrocytic SVR and also correlates with pre- and postsynaptic astrocytic coverage (**Figure 2**). High astrocytic SVR frequently correlated with large amplitude fluctuations of astrocytic Ca^{2+} concentration both spontaneously and following glutamate release (**Figure 2**). Medium SVR in conjunction with high coverage of both presynaptic axon terminal and postsynaptic dendritic spine is characterized by the medium intensity of Ca^{2+} fluctuations that is unaffected by glutamate release (**Figure 2**). On the other hand, no astrocytic Ca^{2+} fluctuations emerge at low SVR (**Figure 2**).

To quantify the extent of NCX-mediated astrocytic Ca^{2+} oscillations, we calculated the power spectral density of the Ca^{2+} signal and summed its power in a wide range between 100 and 500 Hz. The power of these high-frequency Ca^{2+} oscillations showed a direct correlation with increasing SVR, i.e., it is more apparent in thin astrocytic processes (**Figure 3A**). By contrast, the power of high-frequency Ca^{2+} fluctuations does not depend on either pre- or postsynaptic astrocytic coverage (**Figures 3B,C**).

Furthermore, we also investigated whether synaptic glutamate release alters the spontaneous NCX-mediated Ca^{2+} fluctuations. To this end, we compared the oscillatory powers of the Ca^{2+} concentration signals in the 100–500 Hz range in two different conditions: (1) simulating baseline Ca^{2+} fluctuations when only NCX was allowed to operate and no synaptic glutamate release occurred; and (2) simulating Ca^{2+} fluctuations according to our original conditions, releasing 5,000 glutamate molecule after 10 ms of baseline activity and letting EAATs function. The powers of the 100–500 Hz range of the Ca^{2+} concentration signals were compared in the 12–21 ms period. In some synapses, glutamate release significantly increased the 100–500 Hz power. As an example, 100–500 Hz power increased from −23.85 ± 0.20 dB to −22.72 ± 0.27 dB due to synaptic glutamate release (n = 5 simulation runs, p = 0.01) in a synapse with high SVR (22.4 μm^{-1}; **Figure 4A**). However, although a slight increase was also observed on the population

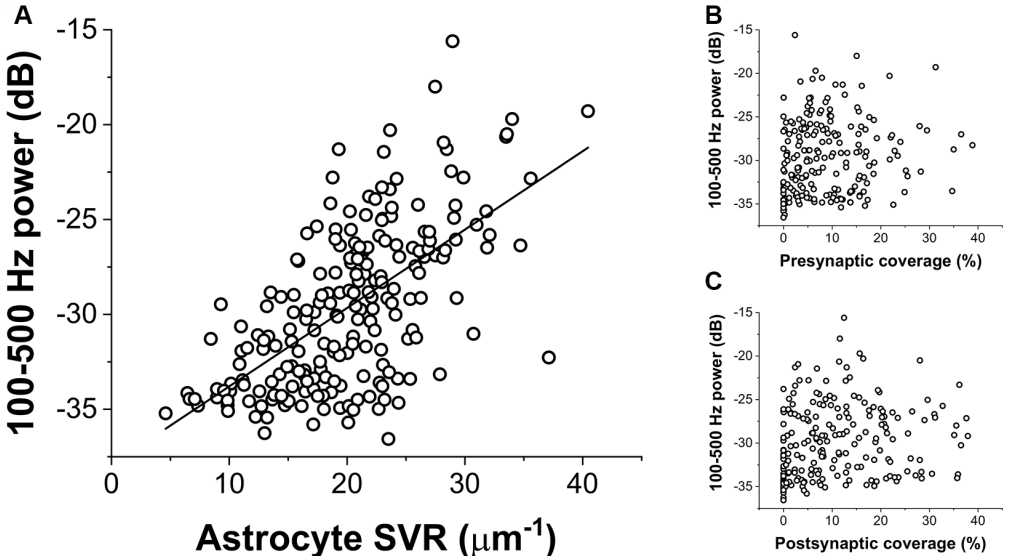

FIGURE 3 | Correlation of the power of astrocytic Ca^{2+} oscillations (100–500 Hz) with geometric characteristics of the astrocyte processes. **(A)** Ca^{2+} oscillation is more pronounced in thin astrocytic processes characterized by a high SVR. The black line shows linear regression fitted to the data (R^2 = 0.38). **(B,C)** Astrocytic Ca^{2+} oscillation shows no correlation with the extent of pre-or postsynaptic coverage by astrocytes.

level, this increase was not significant (−29.73 ± 0.29 dB vs. −29.61 ± 0.29 dB, n = 208 synapses, p = 0.09). Therefore, we investigated whether synapses characterized by different SVR of the surrounding astrocytes may respond differently to Glu release. Resolution of Glu release-induced changes in the power of astrocytic Ca^{2+} fluctuations by astrocyte SVRs, however, still did not reveal a significant effect of Glu release (**Figure 4B**). Since single Glu release events only slightly increase astrocytic Na^+ concentration, we investigated whether more pronounced (but still physiological) changes in astrocytic Na^+ concentration may significantly affect NCX-mediated Ca^{2+} fluctuations. Changing astrocytic Na^+ concentration from the original 15 mM to 10 or 20 mM, indeed, markedly altered Ca^{2+} oscillatory power (**Figure 4C**). Increasing astrocytic Na^+ concentration enhances Ca^{2+} fluctuations in general, and consequently allows the emergence of such oscillations in thicker processes characterized by smaller SVR.

DISCUSSION

Spontaneous astroglial Ca^{2+} fluctuations, mediated by NCX in real excitatory tripartite synapses appear to be primarily dependent on astrocytic SVR. In our simulations, more pronounced NCX-operated Ca^{2+} fluctuations are associated with high SVR, suggesting that thin astrocytic processes are capable to spontaneously generate astrocytic Ca^{2+} signals. Although, we found that NCX mediated spontaneous Ca^{2+} fluctuations are not significantly modulated by single Glu release events and corresponding Na^+ entry through plasma membrane glutamate transporters, we showed that increasing astrocytic Na^+ concentration in the physiological range markedly enhances Ca^{2+} fluctuations in real tripartite synapses, especially in those, characterized by high SVR. Therefore, we hypothesize that bursting synaptic activity or simultaneous activation of multiple synapses in the domain of a single astrocyte may significantly contribute to the emergence and enhancement of Ca^{2+} fluctuations by increasing astrocytic Na^+ concentration. The scenario with Na^+ threshold and mechanistic explanation, however, remains to be clarified. Importantly, astrocytic Ca^{2+} concentration can also be directly increased by the activation of astrocytic NMDA receptors (Ziemens et al., 2019) that are currently not included in our model.

It is evident from our simulations that the appearance of fast Ca^{2+} fluctuations is correlated to the high surface-to-volume ratio of PAPs. Unfortunately, neither spatial nor temporal resolution of current experimental techniques allows the direct observation of such fast (>100 Hz) Ca^{2+} signals in tiny processes (d < 2–300 nm, SVR > 10; Rusakov, 2015). Therefore, we can only speculate about how these spontaneous Ca^{2+} events, triggered by Ca^{2+} entry through NCX can propagate into astrocytic branchlets and can be amplified and propagated as a result of various downstream mechanisms, including Ca^{2+}-dependent Ca^{2+} release in association with activation of inositol 1,4,5-trisphosphate receptors (IP_3R) or mitochondrial permeability transition pores (Semyanov et al., 2020). It was experimentally observed, however, that the appearance and frequency of slower spontaneous Ca^{2+} events in somewhat larger astrocytic processes (characterized by SVR < 3) depend on SVR (Wu et al., 2019). Also, compartmentalized Ca^{2+} waves as predicted by the dynamically rich repertoire of distinct Ca^{2+}-dependent Ca^{2+} release dynamics (Matrosov et al., 2019) may travel and act by modulating local spontaneous Ca^{2+} fluctuations. Indeed, the shape of the slow Ca^{2+} wave with fast Ca^{2+} fluctuations (Savtchenko et al., 2018; SI Figure 12) may indicate the superimposition of slow waves and fast Ca^{2+} fluctuations locally. It is to mention, that fast astrocytic Ca^{2+}

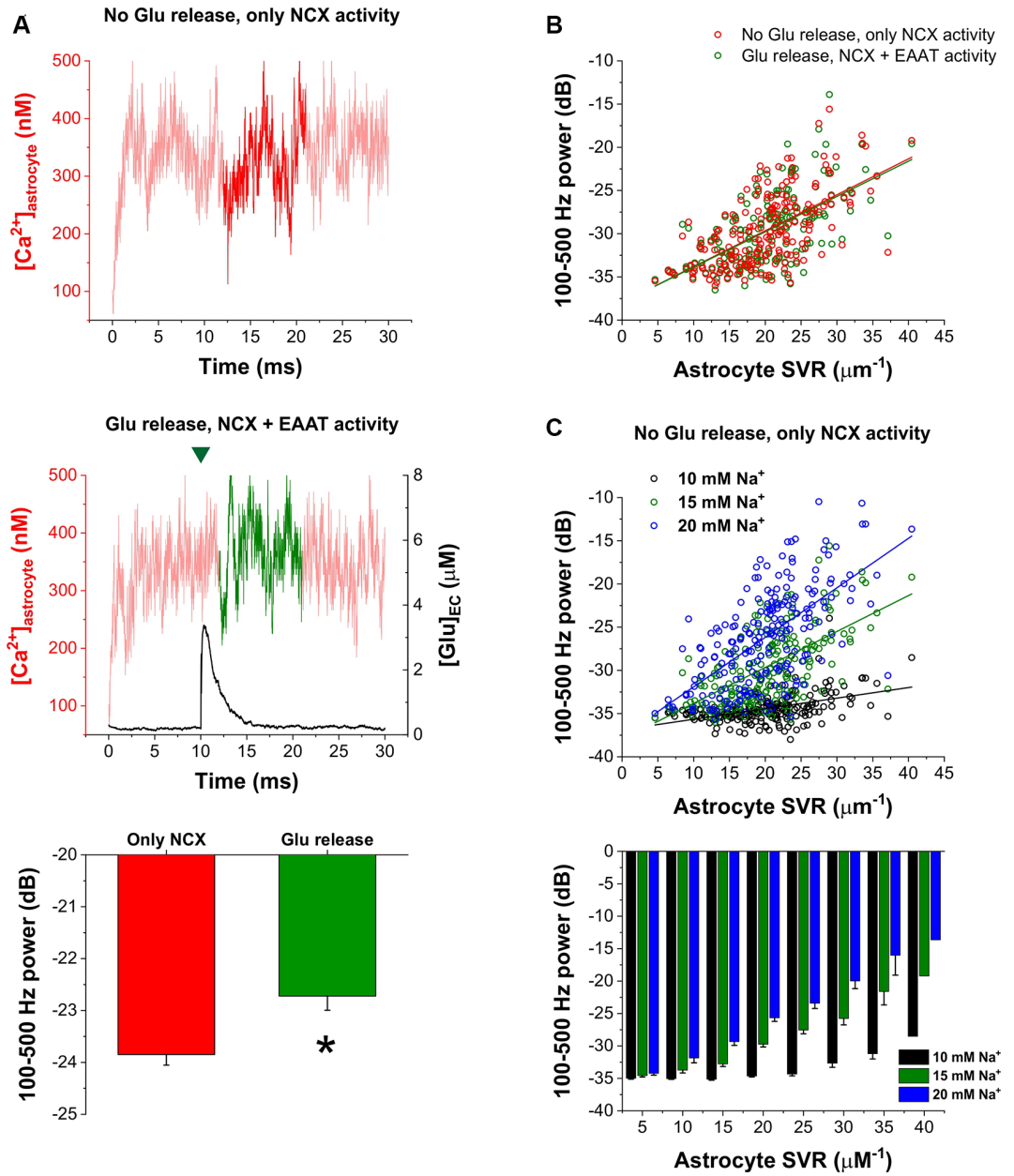

FIGURE 4 | Increased astrocytic Na^+ concentration enhances astrocytic Ca^{2+} oscillations. **(A)** Representative traces of astrocytic Ca^{2+} concentration in the astrocytic processes surrounding a synapse with high SVR (22.4 μm^{-1}). Dark traces represent the analyzed period during which 100–500 Hz power was calculated when no glutamate release occurred and only NCX activity was allowed (*top*) or when 5,000 molecules of glutamate were released at 10 ms. The green mark indicates the release event (*middle*). Power of the 100–500 Hz range increased from −23.85 ± 0.20 dB to −22.72 ± 0.27 dB due to synaptic glutamate release in this synapse (n = 5 simulation runs, p = 0.01; asterisk means significant difference, *bottom*). **(B)** Correlation of 100–500 Hz powers with astrocytic SVR with (green) and without (red) synaptic glutamate release in the 12–21 ms period in all the investigated 208 synapses. Green and red lines show linear regression fitted to the data (R^2 = 0.38 for both lines). **(C)** Correlation of 100–500 Hz powers with astrocytic SVR at different astrocytic Na^+ concentrations in the 12–21 ms period in all the investigated 208 synapses. No glutamate release was initiated, only NCX activity was considered. Black, green and blue lines show linear regression fitted to the data (R^2 = 0.20, R^2 = 0.38 and R^2 = 0.39 respectively; *top*). Grouping of power vs. astrocyte SVR data shows that increasing astrocytic Na^+ concentration enables the emergence of Ca^{2+} oscillations in thicker processes (*bottom*).

signaling with mean onset time as rapid as that of neurons is not unprecedented (Kékesi et al., 2015; Pál et al., 2015; Lind et al., 2018; Stobart et al., 2018; Semyanov et al., 2020). Assessing the true impact of spontaneously emerging, local high-frequency Ca^{2+} fluctuations on the evolution of cellular- and network-scale Ca^{2+} oscillations necessitates further studies, that include models describing downstream Ca^{2+} stores and Ca^{2+} buffers (Savtchenko et al., 2018; Matrosov et al., 2019), as well as simulate

Ca^{2+} dynamics in multiple, neighboring synapses contacted by the same astrocyte. We may also conjecture that the structural plasticity of astrocytic processes may serve as a *de novo* signal generator, independently of its role in regulating glutamate spillover, K^+ buffering, or other indirect forms of modulation of neuronal activity (Henneberger et al., 2020). These findings suggest a prominent role for dynamically changing PAPs in neuro-glial coupling.

DATA AVAILABILITY STATEMENT

Raw data is available to download at http://downloadables.ttk.hu/heja/Front_Cell_Neurosci_2021. Matlab scripts used to process the data can be downloaded at https://github.com/hejalaszlo/Astrocyte-leaflet-simulation.

AUTHOR CONTRIBUTIONS

LH: conceptualization, data curation, formal analysis, funding acquisition, methodology, software, supervision, validation, visualization, roles/writing—original draft, writing—review and editing. ZS and MP: data curation, methodology, validation, roles/writing—original draft, writing—review and editing. JK: conceptualization, investigation, methodology, supervision, roles/writing—original draft, writing—review and editing. All authors contributed to the article and approved the submitted version.

FUNDING

This work was supported by National Research, Development, and Innovation Office grant OTKA K124558. LH is a recipient of the János Bolyai Scholarship of the Hungarian Academy of Sciences.

ACKNOWLEDGMENTS

We thank Péter Somogyi FRS, FMedSci, Professor of Neurobiology, Department of Pharmacology, University of Oxford for valuable discussions.

REFERENCES

Araque, A., Parpura, V., Sanzgiri, R. P., and Haydon, P. G. (1999). Tripartite synapses: glia, the unacknowledged partner. *Trends Neurosci.* 22, 208–215. doi: 10.1016/s0166-2236(98)01349-6

Baker, D. A., Shen, H., and Kalivas, P. W. (2002). Cystine/glutamate exchange serves as the source for extracellular glutamate: modifications by repeated cocaine administration. *Amino Acids* 23, 161–162. doi: 10.1007/s00726-001-0122-6

Bergles, D. E., Diamond, J. S., and Jahr, C. E. (1999). Clearance of glutamate inside the synapse and beyond. *Curr. Opin. Neurobiol.* 9, 293–298. doi: 10.1016/s0959-4388(99)80043-9

Bergles, D. E., Tzingounis, A. V., and Jahr, C. E. (2002). Comparison of coupled and uncoupled currents during glutamate uptake by GLT-1 transporters. *J. Neurosci.* 22, 10153–10162. doi: 10.1523/JNEUROSCI.22-23-10153.2002

Brazhe, A. R., Verisokin, A. Y., Verveyko, D. V., and Postnov, D. E. (2018). Sodium-calcium exchanger can account for regenerative Ca^{2+} entry in thin astrocyte processes. *Front. Cell. Neurosci.* 12:250. doi: 10.3389/fncel.2018.00250

Breslin, K., Wade, J. J., Wong-Lin, K., Harkin, J., Flanagan, B., Van Zalinge, H., et al. (2018). Potassium and sodium microdomains in thin astroglial processes: A computational model study. *PLoS Comput. Biol.* 14:e1006151. doi: 10.1371/journal.pcbi.1006151

Chu, L., Greenstein, J. L., and Winslow, R. L. (2016). Modeling Na^+-Ca^{2+} exchange in the heart: allosteric activation, spatial localization, sparks and excitation-contraction coupling. *J. Mol. Cell. Cardiol.* 99, 174–187. doi: 10.1016/j.yjmcc.2016.06.068

De Pittà, M. (2020). "Neuron-glial interactions," in *Encyclopedia of Computational Neuroscience*. New York, NY: Springer New York, 1–30.

Gavrilov, N., Golyagina, I., Brazhe, A., Scimemi, A., Turlapov, V., and Semyanov, A. (2018). Astrocytic coverage of dendritic spines, dendritic shafts and axonal boutons in hippocampal neuropil. *Front. Cell. Neurosci.* 12:248. doi: 10.3389/fncel.2018.00248

Gerkau, N. J., Lerchundi, R., Nelson, J. S. E., Lantermann, M., Meyer, J., Hirrlinger, J., et al. (2019). Relation between activity-induced intracellular sodium transients and ATP dynamics in mouse hippocampal neurons. *J. Physiol.* 597, 5687–5705. doi: 10.1113/JP278658

Harris, K. M., Jensen, F. E., and Tsao, B. (1992). Three-dimensional structure of dendritic spines and synapses in rat hippocampus (CA1) at postnatal day 15 and adult ages: Implications for the maturation of synaptic physiology and long-term potentiation. *J. Neurosci.* 12, 2685–2705. doi: 10.1523/JNEUROSCI.12-07-02685.1992

Héja, L., Barabás, P., Nyitrai, G., Kékesi, K. A. K. A., Lasztóczi, B., Toke, O., et al. (2009). Glutamate uptake triggers transporter-mediated GABA release from astrocytes. *PLoS One* 4:e7153. doi: 10.1371/journal.pone.0007153

Héja, L., and Kardos, J. (2020). NCX activity generates spontaneous Ca^{2+} oscillations in the astrocytic leaflet microdomain. *Cell Calcium* 86:102137. doi: 10.1016/j.ceca.2019.102137

Héja, L., Nyitrai, G., Kékesi, O., and Dobolyi, Á. (2012). Astrocytes convert network excitation to tonic inhibition of neurons. *BMC Biol.* 10:26. doi: 10.1186/1741-7007-10-26

Héja, L., Simon, Á., Szabó, Z., and Kardos, J. (2019). Feedback adaptation of synaptic excitability *via* Glu:Na^+ symport driven astrocytic GABA and Gln release. *Neuropharmacology* 161:107629. doi: 10.1016/j.neuropharm.2019.05.006

Heller, J. P., Odii, T., Zheng, K., and Rusakov, D. A. (2020). Imaging tripartite synapses using super-resolution microscopy. *Methods* 174, 81–90. doi: 10.1016/j.ymeth.2019.05.024

Henneberger, C., Bard, L., Panatier, A., Reynolds, J. P., Kopach, O., Medvedev, N. I., et al. (2020). LTP induction boosts glutamate spillover by driving withdrawal of perisynaptic astroglia. *Neuron* 108, e11919–e11936. doi: 10.1016/j.neuron.2020.08.030

Herman, M. A., and Jahr, C. E. (2007). Extracellular glutamate concentration in hippocampal slice. *J. Neurosci.* 27, 9736–9741. doi: 10.1523/JNEUROSCI.3009-07.2007

Herman, M. A., Nahir, B., and Jahr, C. E. (2011). Distribution of extracellular glutamate in the neuropil of hippocampus. *PLoS One* 6:e26501. doi: 10.1371/journal.pone.0026501

Jonas, P., and Sakmann, B. (1992). Glutamate receptor channels in isolated patches from CA1 and CA3 pyramidal cells of rat hippocampal slices. *J. Physiol.* 455, 143–171. doi: 10.1113/jphysiol.1992.sp019294

Kasthuri, N., Hayworth, K. J., Berger, D. R., Schalek, R. L., Conchello, J. A., Knowles-Barley, S., et al. (2015). Saturated reconstruction of a volume of neocortex. *Cell* 162, 648–661. doi: 10.1016/j.cell.2015.06.054

Kékesi, O., Ioja, E. E., Szabó, Z., Kardos, J., and Héja, L. (2015). Recurrent seizure-like events are associated with coupled astroglial synchronization. *Front. Cell. Neurosci.* 9:215. doi: 10.3389/fncel.2015.00215

Kékesi, K. A., Szilágyi, N., Nyitrai, G., Árpád, D., Skuban, N., and Kardos, J. (2000). Persistent depolarization and Glu uptake inhibition operate distinct

osmoregulatory mechanisms in the mammalian brain. *Neurochem. Int.* 37, 171–178. doi: 10.1016/s0197-0186(00)00020-6

Kirischuk, S., Héja, L., Kardos, J., and Billups, B. (2016). Astrocyte sodium signaling and the regulation of neurotransmission. *Glia.* 64, 1655–1666. doi: 10.1002/glia.22943

Korogod, N., Petersen, C. C. H., and Knott, G. W. (2015). Ultrastructural analysis of adult mouse neocortex comparing aldehyde perfusion with cryo fixation. *eLife* 4:e05793. doi: 10.7554/eLife.05793

Kovács, Z., Kékesi, K. A., Juhász, G., Barna, J., Héja, L., Lakatos, R., et al. (2015). Non-adenosine nucleoside inosine, guanosine and uridine as promising antiepileptic drugs: a summary of current literature. *Mini Rev. Med. Chem.* 14, 1033–1042. doi: 10.2174/1389557514666141107120226

Lehre, K. P., and Danbolt, N. C. (1998). The number of glutamate transporter subtype molecules at glutamatergic synapses: chemical and stereological quantification in young adult rat brain. *J. Neurosci.* 18, 8751–8757. doi: 10.1523/JNEUROSCI.18-21-08751.1998

Lenart, B., Kintner, D. B., Shull, G. E., and Sun, D. (2004). Na-K-Cl cotransporter-mediated intracellular Na^+ accumulation affects Ca^{2+} signaling in astrocytes in an in vitro ischemic model. *J. Neurosci.* 24, 9585–9597. doi: 10.1523/JNEUROSCI.2569-04.2004

Lerchundi, R., Huang, N., and Rose, C. R. (2020). Quantitative imaging of changes in astrocytic and neuronal adenosine triphosphate using two different variants of ATeam. *Front. Cell. Neurosci.* 14:80. doi: 10.3389/fncel.2020.00080

Levy, L. M., Warr, O., and Attwell, D. (1998). Stoichiometry of the glial glutamate transporter GLT-1 expressed inducibly in a Chinese hamster ovary cell line selected for low endogenous Na^+-dependent glutamate uptake. *J. Neurosci.* 18, 9620–9628. doi: 10.1523/JNEUROSCI.18-23-09620.1998

Li, H., Nowak, L. M., Gee, K. R., and Hess, G. P. (2002). Mechanism of glutamate receptor-channel function in rat hippocampal neurons investigated using the laser-pulse photolysis (LaPP) technique. *Biochemistry* 41, 4753–4759. doi: 10.1021/bi0118916

Lind, B. L., Jessen, S. B., Lønstrup, M., Joséphine, C., Bonvento, G., and Lauritzen, M. (2018). Fast Ca^{2+} responses in astrocyte end-feet and neurovascular coupling in mice. *Glia* 66, 348–358. doi: 10.1002/glia.23246

Matrosov, V., Gordleeva, S., Boldyreva, N., Ben-Jacob, E., Kazantsev, V., and De Pittà, M. (2019). "Emergence of regular and complex calcium oscillations by inositol 1,4,5-trisphosphate signaling in astrocytes," in *Computational Glioscience*, eds M. De Pittà and H. Berry (Cham: Springer), 151–176.

Matsui, K., Jahr, C. E., and Rubio, M. E. (2005). High-concentration rapid transients of glutamate mediate neural-glial communication *via* ectopic release. *J. Neurosci.* 25, 7538–7547. doi: 10.1523/JNEUROSCI.1927-05.2005

Mergenthaler, K., Oschmann, F., and Obermeyer, K. (2019). "Glutamate uptake by astrocytic transporters," in *Computational Glioscience* (Cham: Springer), 329–361.

Newman, E. A. (2004). A dialogue between glia and neurons in the retina: modulation of neuronal excitability. *Neuron Glia Biol.* 1, 245–252. doi: 10.1017/S1740925X0500013X

Pál, I., Kardos, J., Dobolyi, Á., and Héja, L. (2015). Appearance of fast astrocytic component in voltage-sensitive dye imaging of neural activity. *Mol. Brain* 8:35. doi: 10.1186/s13041-015-0127-9

Pál, I., Nyitrai, G., Kardos, J., and Héja, L. (2013). Neuronal and astroglial correlates underlying spatiotemporal intrinsic optical signal in the rat hippocampal slice. *PLoS One* 8:e57694. doi: 10.1371/journal.pone.0057694

Pallotto, M., Watkins, P. V., Fubara, B., Singer, J. H., and Briggman, K. L. (2015). Extracellular space preservation aids the connectomic analysis of neural circuits. *eLife* 4:e08206. doi: 10.7554/eLife.08206

Rusakov, D. A. (2015). Disentangling calcium-driven astrocyte physiology. *Nat. Rev. Neurosci.* 16, 226–233. doi: 10.1038/nrn3878

Rusakov, D. A., and Kullmann, D. M. (1998a). Extrasynaptic glutamate diffusion in the hippocampus: ultrastructural constraints, uptake and receptor activation. *J. Neurosci.* 18, 3158–3170. doi: 10.1523/JNEUROSCI.18-09-03158.1998

Rusakov, D. A., and Kullmann, D. M. (1998b). Geometric and viscous components of the tortuosity of the extracellular space in the brain. *Proc. Natl. Acad. Sci. U S A* 95, 8975–8980. doi: 10.1073/pnas.95.15.8975

Rusakov, D. A., Davies, H. A., Harrison, E., Diana, G., Richter-Levin, G., Bliss, T. V. P., et al. (1997). Ultrastructural synaptic correlates of spatial learning in rat hippocampus. *Neuroscience.* 80, 69–77. doi: 10.1016/s0306-4522(97)00125-5

Rusakov, D. A., Harrison, E., and Stewart, M. G. (1998). Synapses in hippocampus occupy only 1-2% of cell membranes and are spaced less than half-micron apart: a quantitative ultrastructural analysis with discussion of physiological implications. in *Neuropharmacology* 37, 513–521. doi: 10.1016/s0028-3908(98)00023-9

Rusakov, D. A., Kullmann, D. M., and Stewart, M. G. (1999). Hippocampal synapses: do they talk to their neighbours? *Trends Neurosci.* 22, 382–388. doi: 10.1016/s0166-2236(99)01425-3

Savtchenko, L. P., and Rusakov, D. A. (2007). The optimal height of the synaptic cleft. *Proc. Natl. Acad. Sci. U S A* 104, 1823–1828. doi: 10.1073/pnas.0606636104

Savtchenko, L. P., Bard, L., Jensen, T. P., Reynolds, J. P., Kraev, I., Medvedev, N., et al. (2018). Disentangling astroglial physiology with a realistic cell model in silico. *Nat. Commun.* 9:3554. doi: 10.1038/s41467-018-05896-w

Savtchenko, L., Megalogeni, M., Rusakov, D. A., Walker, M. C., and Pavlov, I. (2015). Synaptic GABA release prevents GABA transporter type-1 reversal during excessive network activity. *Nat. Commun.* 6:6597. doi: 10.1038/ncomms7597

Semyanov, A., Henneberger, C., and Agarwal, A. (2020). Making sense of astrocytic calcium signals—from acquisition to interpretation. *Nat. Rev. Neurosci.* 21, 551–564. doi: 10.1038/s41583-020-0361-8

Somogyi, P., Eshhar, N., Teichberg, V. I., and Roberts, J. D. B. (1990). Subcellular localization of a putative kainate receptor in Bergmann glial cells using a monoclonal antibody in the chick and fish cerebellar cortex. *Neuroscience* 35, 9–30. doi: 10.1016/0306-4522(90)90116-l

Stobart, J. L., Ferrari, K. D., Barrett, M. J. P., Glück, C., Stobart, M. J., Zuend, M., et al. (2018). Cortical circuit activity evokes rapid astrocyte calcium signals on a similar timescale to neurons. *Neuron* 98, e4726–e4735. doi: 10.1016/j.neuron.2018.03.050

Szabó, Z., Héja, L., Szalay, G., Kékesi, O., Füredi, A., Szebényi, K., et al. (2017). Extensive astrocyte synchronization advances neuronal coupling in slow wave activity *in vivo*. *Sci. Rep.* 7:6018. doi: 10.1007/s11356-020-09610-6

Harreveld, A. V., and Fifkova, E. (1975). Rapid freezing of deep cerebral structures for electron microscopy. *Anat. Rec.* 182, 377–385. doi: 10.1002/ar.1091820311

Van Harreveld, A., and Khattab, F. I. (1968). Chloride movements during perfusion fixation with glutaraldehyde. *Anat. Rec.* 162, 467–477. doi: 10.1002/ar.1091620408

Ventura, R., and Harris, K. M. (1999). Three-dimensional relationships between hippocampal synapses and astrocytes. *J. Neurosci.* 19, 6897–6906. doi: 10.1523/JNEUROSCI.19-16-06897.1999

Wu, Y.-W., Gordleeva, S., Tang, X., Shih, P.-Y., Dembitskaya, Y., and Semyanov, A. (2019). Morphological profile determines the frequency of spontaneous calcium events in astrocytic processes. *Glia.* 67, 246–262. doi: 10.1002/glia.23537

Zhang, Y., Sloan, S. A., Clarke, L. E., Caneda, C., Plaza, C. A., Blumenthal, P. D., et al. (2016). Purification and characterization of progenitor and mature human astrocytes reveals transcriptional and functional differences with mouse. *Neuron* 89, 37–53. doi: 10.1016/j.neuron.2015.11.013

Ziemens, D., Oschmann, F., Gerkau, N. J., and Rose, C. R. (2019). Heterogeneity of activity-induced sodium transients between astrocytes of the mouse hippocampus and neocortex: mechanisms and consequences. *J. Neurosci.* 39, 2620–2634. doi: 10.1523/JNEUROSCI.2029-18.2019

Conflict of Interest: The authors declare that the research was conducted in the absence of any commercial or financial relationships that could be construed as a potential conflict of interest.

frontiers in Cellular Neuroscience

ORIGINAL RESEARCH
published: 05 March 2021
doi: 10.3389/fncel.2021.645068

Modeling of Astrocyte Networks: Toward Realistic Topology and Dynamics

Andrey Yu. Verisokin[1], *Darya V. Verveyko*[1], *Dmitry E. Postnov*[2] *and Alexey R. Brazhe*[3,4]*

[1] Department of Theoretical Physics, Kursk State University, Kursk, Russia, [2] Department of Optics and Biophotonics, Saratov State University, Saratov, Russia, [3] Department of Biophysics, Biological Faculty, Lomonosov Moscow State University, Moscow, Russia, [4] Department of Molecular Neurobiology, Institute of Bioorganic Chemistry RAS, Russian Federation, Moscow, Russia

Neuronal firing and neuron-to-neuron synaptic wiring are currently widely described as orchestrated by astrocytes—elaborately ramified glial cells tiling the cortical and hippocampal space into non-overlapping domains, each covering hundreds of individual dendrites and hundreds thousands synapses. A key component to astrocytic signaling is the dynamics of cytosolic Ca^{2+} which displays multiscale spatiotemporal patterns from short confined elemental Ca^{2+} events (puffs) to Ca^{2+} waves expanding through many cells. Here, we synthesize the current understanding of astrocyte morphology, coupling local synaptic activity to astrocytic Ca^{2+} in perisynaptic astrocytic processes and morphology-defined mechanisms of Ca^{2+} regulation in a distributed model. To this end, we build simplified realistic data-driven spatial network templates and compile model equations as defined by local cell morphology. The input to the model is spatially uncorrelated stochastic synaptic activity. The proposed modeling approach is validated by statistics of simulated Ca^{2+} transients at a single cell level. In multicellular templates we observe regular sequences of cell entrainment in Ca^{2+} waves, as a result of interplay between stochastic input and morphology variability between individual astrocytes. Our approach adds spatial dimension to the existing astrocyte models by employment of realistic morphology while retaining enough flexibility and scalability to be embedded in multiscale heterocellular models of neural tissue. We conclude that the proposed approach provides a useful description of neuron-driven Ca^{2+}-activity in the astrocyte syncytium.

Keywords: calcium signaling, cell morphology, noise-driven dynamics, astrocytes, modeling

OPEN ACCESS

Edited by:
Leonid Savtchenko, University College London, United Kingdom

Reviewed by:
Kerstin Lenk, Tampere University, Finland
Sara Mederos, Cajal Institute (CSIC), Spain

***Correspondence:**
Alexey R. Brazhe
brazhe@biophys.msu.ru

Specialty section:
This article was submitted to Non-Neuronal Cells, a section of the journal Frontiers in Cellular Neuroscience

Received: *22 December 2020*
Accepted: *09 February 2021*
Published: *05 March 2021*

Citation:
Verisokin AY, Verveyko DV, Postnov DE and Brazhe AR (2021) Modeling of Astrocyte Networks: Toward Realistic Topology and Dynamics. Front. Cell. Neurosci. 15:645068. doi: 10.3389/fncel.2021.645068

1. INTRODUCTION

Astrocytes of the cortical and hippocampal gray matter are important actors in a number of information processing processes, including synaptic plasticity, long-term potentiation, and synchronization of neuronal firing (Haydon, 2001; Lee et al., 2014; De Pitta et al., 2016; Poskanzer and Yuste, 2016) as well as in coupling neuronal activity to blood flow changes (Otsu et al., 2015). Recent evidence converges on a close connection of these functions with whole-brain processes and systemic regulation pathways. Thus, astrocytes respond to and are able to regulate systemic blood pressure (Marina et al., 2020); they significantly (up to 60%) change their volume during sleep or under anesthesia (Xie et al., 2013); astrocytes play an important role in the clearance of

beta-amyloids, a process with mechanisms that are now being actively discussed (Iliff et al., 2012; Abbott et al., 2018; Semyachkina-Glushkovskaya et al., 2018; Mestre et al., 2020); both intracellular and network-level activity of astrocytes are significantly different in sleep and during wakefulness, and activates with locomotion (Bojarskaite et al., 2020; Ingiosi et al., 2020; McCauley et al., 2020). It is important to note that many of the mentioned astrocyte functions are not directly related to neural activity, but are governed by their own regulatory pathways (O'Donnell et al., 2015). Some of these functions are tightly linked to dynamic regulation of astrocyte morphology and volume and depend, for example, on the circadian rhythm of aquaporin expression (Hablitz et al., 2020).

In summary, this frames a new mindset for understanding the function of astrocytes and at the same time poses a challenge for modeling studies. Namely, the morphological features should now be considered as a specific control parameter that significantly contribute to the both single-cell dynamics and network activity patterns. This problem breaks down into three specific tasks: (i) to provide tractable, but still biologically reasonable mathematical account for contribution of subcellular morphological features to intracellular calcium dynamics; (ii) to further develop approaches to modeling of Ca^{2+} dynamics on data-driven irregular structures, both for an individual cell and for a network; (iii) to reveal how realistic morphological features are manifested in the spatiotemporal patterns of the calcium dynamics.

We address these tasks in more detail in the rest of the Introduction.

1.1. Calcium Signaling in Astrocytes

With plasma membranes enriched in a variety of potassium channels and lacking voltage-gated sodium channels, astrocytes are not electrically excitable (Verkhratsky and Nedergaard, 2018). On the other hand, they display a rich repertoire of Ca^{2+}-activity at multiple spatial and temporal scales (Lind et al., 2013; Volterra et al., 2014; Wu et al., 2014; Bindocci et al., 2017). Although astrocytic Ca^{2+} transients can occur spontaneously, their frequency is modulated by neuronal activity (Stobart et al., 2018), changes in local tissue oxygenation (Mathiesen et al., 2013; Marina et al., 2020), and other factors (Semyanov et al., 2020). As outputs, Ca^{2+}-activity in astrocytes leads to release of signaling molecules: gliotransmitters, such as GABA, D-serine, and glutamate, as well as vasoactive metabolites (Serrano et al., 2006; Henneberger et al., 2010; Bazargani and Attwell, 2016). This has been summarized in a concept of "tripartite synapse," i.e., sensing of synaptic neurotransmitter release by perisynaptic astrocyte processes, encoding this information in Ca^{2+} signals and response with secretion of neuroactive molecules (Araque et al., 2014). There is still however an ongoing debate on the mechanisms involved in generating Ca^{2+} transients in astrocytes and the extent of effect of astrocyte-derived molecules on synaptic plasticity, e.g., on LTP (Fiacco and McCarthy, 2018; Savtchouk and Volterra, 2018).

Recent experimental evidence obtained with genetically encoded or pipette-loaded Ca^{2+} indicators (Tong et al., 2013; Rungta et al., 2016) heralds functional segregation between the less frequent global internal store-operated Ca^{2+} transients at the level of cell soma and primary branches, and the more frequent spatially limited microdomain Ca^{2+} transients in the thin mesh of astrocytic leaflets—ramified nanoscopic processes, also known as perisynaptic processes (PAPs) due to their proximity to synaptic connections between neurons. The transients located in the leaflets primarily rely on influx of Ca^{2+} through plasma membrane, in part because of the high surface-to-volume ratio in this region and in part because the leaflets are often devoid of organelles including ER (Patrushev et al., 2013) and thus can not support exchange with intracellular stores.

The coupling from synaptic activity to local Ca^{2+} transients in PAPs and from the latter to global Ca^{2+} events is an area of active research. As reviewed in Savtchouk and Volterra (2018), early works attributed this to activation of G-protein coupled receptors to glutamate, but later this pathway has been put to question due to apparent lack of mGluR5 receptor expression in adult astrocytes. Alternative sources of microdomain transients have been proposed, such as via TRP channels (Shigetomi et al., 2011), from mitochondria (Agarwal et al., 2017), etc. One plausible alternative causal pathway can be formulated as follows (Rojas et al., 2007; Verkhratsky et al., 2012; Kirischuk et al., 2016; Parpura et al., 2016): neurotransmitters, released from the presynaptic membranes, primarily glutamate, but also GABA, are cleared from the extracellular space by astrocytic transporters utilizing Na^+ gradient to drive the neurotransmitters into the cell. This leads to build up of Na^+ ions in the cytosol, which can lead to temporary reversal of Na^+/Ca^{2+}-exchanger allowing for Ca^{2+} entry via this transporter. Conceivably, if this local Ca^{2+} influx happens near the ER and coincides with an increase in inositol trisphosphate (IP_3) production by phospholipase C, it can trigger Ca^{2+}-induced release of Ca^{2+} from intracellular stores via IP_3 receptors (IP_3Rs) of the ER.

The release of calcium from ER is spatially inhomogeneous due to the non-uniform, clustered, distribution of IP_3 receptors (Smith et al., 2009; Taufiq-Ur-Rahman et al., 2009; Ross, 2012), with clusters spaced at about 0.5–5 μm apart. At a detailed level, calcium release from the receptor clusters has a stochastic character. The effect of the stochastic activation of IP_3R clusters on the calcium dynamics has been investigated by Shuai and Jung both in point and distributed models (Shuai and Jung, 2002, 2003). In the case of a large enough number of clusters, Ca^{2+} release events can be averaged to a lumped deterministic description. Particularly, the increase in IP_3 level transforms stochastic calcium increases into regular waves.

Recapitulating, calcium signaling mechanisms are inhomogeneous across the cell and depend on local morphological parameters, which has to be taken into account in modeling. It seems practical to introduce a metaparameter to describe the relative inputs of store-related and plasma membrane-related Ca^{2+} pathways. This metaparameter can reflect local surface-to-volume ratio or the dominant size of processes and can empirically be linked to the astrocyte cytoplasm volume fraction parameter, which can be estimated directly from fluorescent images.

1.2. Cell Morphology and Network Connectivity

Astrocytes have intricate and highly complex morphology, which raises computational issues and demands an elaborate approach to modeling. The contribution of the astrocytic spatial segregation and coupling to brain physiology and functions is still not sufficiently understood, especially taking into account that astrocyte-to-neuron and astrocyte-to-astrocyte interaction mechanisms are diverse and depend on brain region. The existence of intercellular Ca^{2+} waves traveling across the network of astrocytes suggests a distinct mechanism for long-distance signaling (Cornell-Bell et al., 1990) and plasticity, which operates in parallel to and at much slower time scales than neuronal synaptic transmission (Pirttimaki and Parri, 2013; Sims et al., 2015).

The size of cliques of cortical astrocytes coupled within a local network is estimated around 60–80 cells (Haas et al., 2006; Houades et al., 2006, 2008), but several networks can also connect via a limited number of "hub" astrocytes (Carmignoto, 2000). The implications of inter-astrocyte connectivity have been analyzed in a modeling study by Lallouette et al. (2014) with the main conclusion that sparse short-range connections can promote Ca^{2+} wave propagation along the network. This allows to conjecture that once initiated, a wave of excitation can propagate over long distances in the brain cortex and affect (activate or inhibit) postsynaptic neurons at distant synaptic terminals, although most Ca^{2+} events are confined to a single astrocyte spatial domain. Propagating calcium waves can travel distances of more than 100 μm with speed from 7 to 27 μm/s in culture and brain slices (Dani et al., 1992). However, the waves observed *in vivo* rarely spread more than 80 μm (Hoogland et al., 2009; Brazhe et al., 2013), although this observation can be influenced by imaging protocol, as Kuga and colleagues reported large-scale Ca^{2+} glissandi *in vivo* that were only observable under low laser intensity (Kuga et al., 2011).

It follows that for meso-scale problems related to brain tissue physiology, it is computationally cumbersome to build a ground-up model starting from individual processes. We propose a more pragmatic approach based on texture-like volume segmentation to classes such as "soma," "large branches," and "gliapil" or a mesh of unresolved thin processes. This rasterization radically simplifies model implementation and scales to large networks. At the same time, by defining morphology-based spatial distribution of a metaparameter, one can study the effects of spatial heterogeneity at different scales. Indeed, the spatial distributions used for simulations are ideally data-driven. Because it is not always possible to infer the astrocytic network structure or even individual domain boundaries from experimental data, and because the networks can be variable anyway, it seems inviting to generate variable astrocytic tilings from images of individual cells.

1.3. Modeling Studies

Models of IP_3-mediated Ca^{2+} oscillations have been extensively reviewed both in general (Dupont et al., 2011) and in application to astrocytes (Riera et al., 2011; Manninen and Havela, 2017; Oschmann et al., 2017a), which included both point- and spatially extended models. In particular, the De Young–Keizer model stemmed several currently popular models of Ca^{2+} dynamics in literature. This model allows to simulate IP_3-sensitive calcium dynamics in cytoplasm and ER occurring at the constant level of IP_3 including also a variant of the model with the positive-feedback mechanism of Ca^{2+} on IP_3 production (De Young and Keizer, 1992). Li and Rinzel (1994) reduced De Young–Keizer model to a two-variable system introducing the experimentally observed time scale difference between fast and slow inactivation of IP_3 receptor by Ca^{2+}. Adding the dynamics for $[IP_3]$ with synthesis dependent on activation of metabotropic glutamate receptors and $[Ca^{2+}]$ degradation leads to a three variable model (Ullah et al., 2006). Also building on Li–Rinzel model and providing a more detailed description of IP_3 degradation, De Pitta and co-authors proposed a three-variable model for glutamate-induced intracellular calcium dynamics caused by the synaptic activity in astrocytes (De Pitta et al., 2009).

One of the first models for intercellular propagation of calcium waves has been described in (Sneyd et al., 1994) by adding diffusion of IP_3 and cytosolic Ca^{2+} to the two-pool Ca^{2+} model. The effect of Ca^{2+} diffusion rate on spatiotemporal patterns of Ca^{2+} signaling was studied by Shuai and Jung (2003) in a lattice-based model. Later, Kang and Othmer (2009) regarded networked astroglial Ca^{2+} signaling in a 2D model using spatial patterns in form of sparsely connected irregularly branching cells with simplified morphology. Both intracellular diffusion of IP_3 via gap-junctions and extracellular purinergic signaling was regarded as a mechanism of intercellular communication in Kang and Othmer (2009), Edwards and Gibson (2010); intercellular Ca^{2+} diffusion was however disregarded in most modeling studies, e.g., Ullah et al., 2006; Kang and Othmer, 2009; Edwards and Gibson, 2010, primarily based on the notion of a much faster diffusion of IP_3 than Ca^{2+}, see Allbritton et al., 1992, and small permeability of gap junctions to Ca^{2+}. More recently Savtchenko et al. (2018) suggested an advanced NEURON-based modeling environment for detailed spatially extended models of astrocytes. However, they did not address full calcium dynamics models or morphology-defined variations of mechanisms. Specifically, the relative weights of plasma membrane-dependent mechanisms (IP_3 synthesis and Ca^{2+} influx) and store-dependent mechanisms scale with astrocytic process morphology, as defined by surface to volume ratio, cytoplasm volume fraction and the physical presence of ER in the process. This has been studied in point-models by Oschmann et al. (2017b) and in 1D extended model by Wu et al. (2018). Recently, Brazhe et al. (2018) studied the implications of the spatial segregation between IP_3 synthesis and plasma membrane exchange and the IP_3-mediated ER exchange in discrete spatial templates of variable complexity.

The tripartite synapse concept and the computational role of astrocytes in neural network activity has early attracted the attention of modeling studies, pioneered by papers by Nadkarni and Jung (2004, 2007). Understanding of the tripartite synapse from the viewpoint of non-linear dynamics and functional models have been developed in works of Postnov et al. (2007, 2008, 2011), and Tewari and Majumdar (2012). Later, tripartite

synapses have been adopted in more formal neural network models (Alvarellos-González et al., 2012; Sajedinia and Hélie, 2018; Lenk et al., 2020). Because there is still no consensus based on experimental evidence on mechanisms of Ca^{2+} transients in PAPs and gliotransmission effects (Savtchouk and Volterra, 2018), it is hard to formulate a comprehensive model that would include all conceivable pathways and still remain tractable. While at this stage refraining from closing the loop from astrocytes to neurons, we believe it is important to understand the spatiotemporal patterning of astrocytic Ca^{2+} signaling at levels from microdomains to networks.

1.4. The Proposed Modeling Approach

Our main motivation in this study is to learn if uncorrelated background synaptic activity, when sensed by astrocytes, will be shaped into morphology-defined patterns of Ca^{2+} signaling. We present a model of multi-cellular network of astrocytes based on realistic spatial templates. We start from a single-cell model, which is considerably simpler than in Savtchenko et al. (2018), allowing for smaller computational costs, and move on to connect separate cells together to obtain a network model.

We focus on the implications of the morphology-dependent spatial segregation of the Ca^{2+} signaling mechanisms between astrocytic leaflets and branches. We follow the lines set out in Brazhe et al. (2018) toward more realistic and larger scale spatial templates, ranging from single astrocytes to networks. In contrast to astrocytes in culture or retina *in vivo*, cortex astrocytes are non-flat and occupy some volume in 3D space. Nevertheless, we chose to reduce dimensions to 2D and flatten astrocyte images used as spatial templates. One reason for this was to reduce computational cost, especially when addressing network models. Another reason that most existing Ca^{2+} imaging data are obtained as time series in single focal plane, and the experimentally obtained dynamics is confined to flat 2D anyway. The work of Bindocci et al. (2017) demonstrated the richness of Ca^{2+} dynamics within the whole astrocytic domain in 3D, but volumetric imaging is not yet widely used in the context of astrocytes. We therefore contemplated that using 2D templates for simulations would not restrict us from observing diverse and physiologically relevant Ca^{2+} signaling patterns, event if real astrocytes have more degrees of freedom. The rest of the paper is organized as follows: we start from a description of the proposed model in a top-down order: the general concept is followed by proposed algorithm of creating spatial templates for modeling and then continues with description of the differential equations for dynamics of intracellular and ER Ca^{2+}, intracellular IP_3, and extracellular glutamate concentrations. Having defined the model, we test its plausibility on single-astrocyte templates and after quantification of Ca^{2+} event statistics we proceed to behavior of astrocyte networks, where we observe noise-driven regular activation patterns.

2. MODEL

2.1. Model Design and Overview

In this work we aim to conceptualize our current understanding of spatial organization of the astrocytic Ca^{2+} dynamics in a form of a spatially detailed model of individual and networked astrocytes excited by stochastic background neuronal activity. In the light of the striking differences between Ca^{2+} signaling in astrocytic leaflets and thin processes on the one hand and global somatic signaling on the other, we start with segregation of the modeling space into three major classes as shown in **Figure 1**: astrocyte soma with thick branches (I), a mesh of astrocytic thin processes (II) and extracellular space (III). The continuum between the two extreme classes I and II is defined as local fraction of astrocytic cytoplasm volume (AVF) and a related parameter—local surface-to-volume ratio (SVR) of the astrocytic processes. In extreme class I regions, such as soma, Ca^{2+} dynamics are dominated by exchange with intracellular stores, and a unit of modeled space (template pixel/voxel) contains only astrocyte, while in extreme class II regions (leaflets), Ca^{2+} dynamics is dominated by exchange with plasma membrane and each modeled pixel contains a mesh of extremely thin astrocyte processes tangled with neuropil. We thus define a mapping of each pixel in the spatial model template to either class III (no astrocyte) or to a continuous variable between the extreme cases of class I and II with implications in local calcium dynamics and diffusion.

With regard to the local calcium dynamics, the extreme complexity and sheer number of cellular pathways involved, makes the detailed and comprehensive modeling of every Ca^{2+}-related mechanism extremely challenging. Not surprisingly, there is a substantial body of published models that aim to account for the essential features of calcium dynamics in astrocytes, which do not completely agree with each other (Manninen and Havela, 2017). To choose the best model we build upon a model proposed by Ullah et al. (2006) as a prototype, while other models could fit in the proposed approach as well, for example the "ChI" model by De Pitta et al. (2009), which is similar to that of Ullah et al.

2.1.1. Spatial Structure

To represent astrocyte networks with realistic geometry of the regions I–III, one needs to create such templates algorithmically or, alternatively, obtain them from experimental data. Each of the two variants has its benefits and drawbacks. To provide just two examples, the experiment-based approach was employed in Wallach et al. (2014) and an algorithmic creation of network templates was employed in Postnov et al. (2009). Here, we draw advantages from both approaches by suggesting a simple stochastic data-driven algorithm to create realistic surrogate spatial templates of astrocyte networks. Specifically, we use experimental images of astrocytes obtained from a public database, and arrange network structure using Voronoi partition and simple geometrical transformations (see section 2.2.1).

2.1.2. Neuronal Activity

We assume that astrocytic Ca^{2+} response to local neuronal activity is primarily driven by the transporter-mediated uptake of neurotransmitters released from presynaptic membranes. One of the possible coupling mechanisms is the reversal of the Na^+/Ca^{2+}-exchanger transport due to an increase in $[Na^+]$ allowing for a Ca^{2+} influx. Here, we sacrifice biophysical details in favor of model simplicity and assume that astrocyte calcium

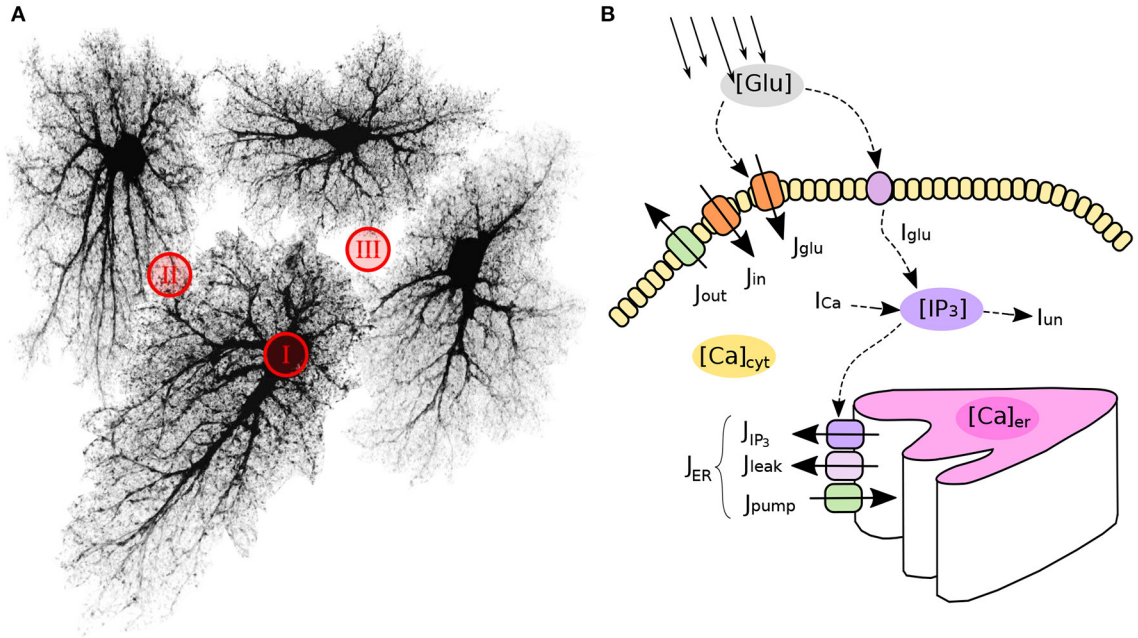

FIGURE 1 | Model structure and molecular mechanisms. **(A)** Astrocytic network is segmented in three spatial compartments: I—cell bodies and thick branches; II—the mesh of thin branches; III—extracellular space. **(B)** Model variables (in colored ovals) and main regulatory pathways of intra-astrocyte calcium dynamics.

dynamics is excited directly by glutamate released from the presynaptic terminals, causing transient fluxes of Ca^{2+} through the plasma membrane. A typical cortex astrocyte is associated with 300–400 individual dendrites and is in contact with about 10^4–10^5 synapses (Bushong et al., 2002; Halassa et al., 2007). Judging by these numbers and taking into account sparsity of neuronal signaling in the cortex it seems safe to treat each pixel in the distributed model template as associated with a single or just a few individual synapses. For as long as we are not focused on information processing in the cortex, we can assume independent stochastic nature of spiking activity in any of the presynaptic units and describe local activity only statistically, neglecting any complex spike timing patterns. Consequently, we describe the synaptic glutamate drive to the model in each pixel as triggered by presynaptic spike trains drawn from independent homogeneous Poisson process $\xi_p(t)$ with intensity p Hz.

2.2. Astrocyte Network Topology

2.2.1. Data-Driven Network Generation

Astrocytes, like neurons, have complex morphology. Ideally, an algorithm to create spatial templates should provide means to "grow" realistic branching 3D shapes of astrocytes from a set of randomly placed "seed" locations. Indeed, there are many experimental and modeling studies of the branching patterns for various types of neurons (Ascoli et al., 2007; Donohue and Ascoli, 2008; Cuntz et al., 2010; Polavaram et al., 2014), providing means for creation of realistic surrogate shapes of as many neurons as needed. However, unlike neurons, there is less data available on the statistics of astrocyte branching, which makes it harder to create surrogate spatial templates of astrocyte networks. This hindrance can be circumvented by using a public database of microscopic images of cortical and hippocampal astrocytes (Martone et al., 2002, 2008).

To create a library of realistic spatial templates for individual cells, we downloaded a set of 27 fluorescent confocal 3D stacks of hippocampal astrocytes (4-week old rats, microinjection loaded with lucifer yellow in acute slices) (Bushong et al., 2004). The stacks have average lateral resolution of $\approx$ 0.07 μm/px and vertical (Z-axis) resolution of 0.2 μm; there are 45-60 Z-planes in each stack, thus encompassing the thickness of about 10 μm along the Z-axis. Because our model is set in two-dimensional space, the stacks were flattened along the Z-axis by max-projection, **Figure 2**. The projections were downsampled 4$\times$ before simulations, resulting in lateral resolution of $\approx$ 0.28 μm/px. Each of the experimental astrocyte images then serves as a progenitor of randomized offsprings obtained by applying 250 random rotations (from 0° to 360°, shearings and stretchings (within $\pm$20% of original size, uniform distribution), which results in a collection of 6,750 randomized pseudo-experimental astrocyte templates, used to tile the model space. Such data set expansion from a limited number of "real-world" objects is a popular approach in machine learning (Simard et al., 2003; Krizhevsky et al., 2012) helping to prevent overfitting and providing for transformation-invariant feature learning.

Inspired by the fact that astrocytes establish distinct non-overlapping territories, we employ an algorithm based on Voronoi partitioning and active contours to tile the model space with astrocytes. First, we create a lattice of "seed points" regularly spaced at some intervals corresponding to average cell density, typically around 50 μm, shown in light gray in

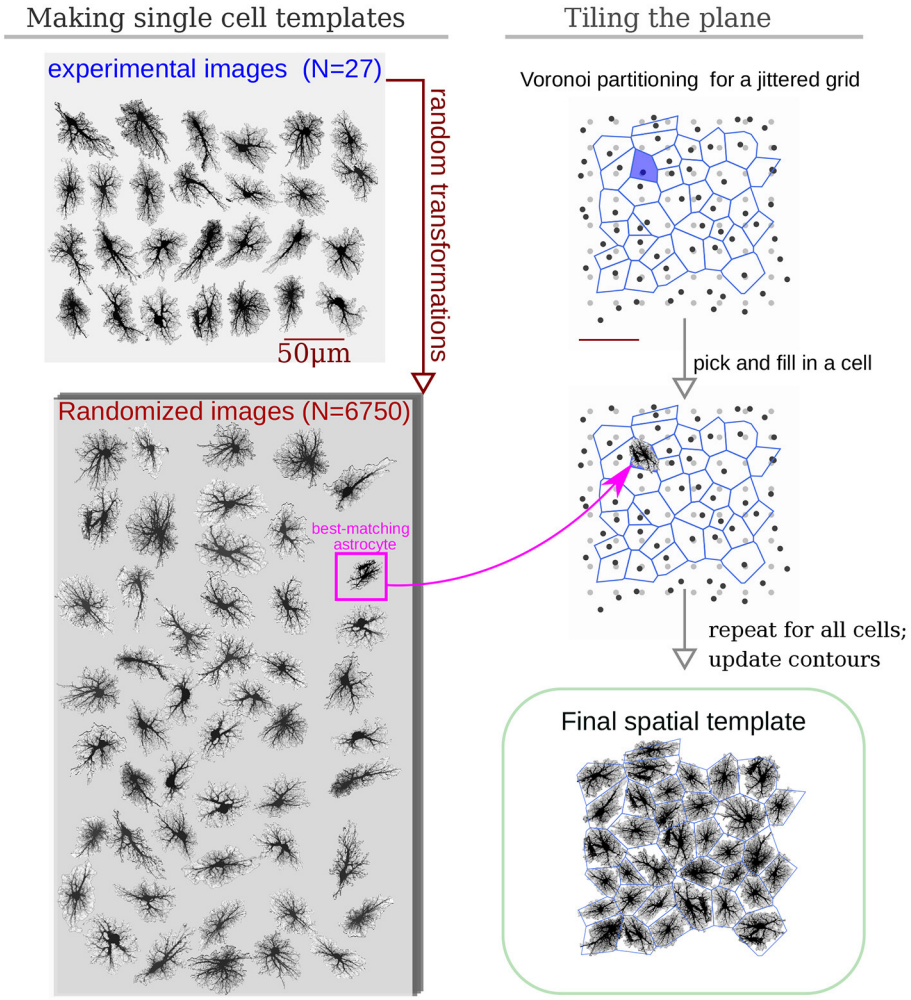

FIGURE 2 | Algorithm to create surrogate templates of astrocyte network. First, a set of seeding points on a regular grid (light-gray) is perturbed with random shifts (dark-gray points). Voronoi diagram is then drawn for these points (blue lines). Each patch in the Voronoi partitioning is then filled with the best shape-matching template from an augmented collection of astrocyte images. The lookup collection is created from a set of experimental images taken from CCDB (Martone et al., 2002, 2008) by applying multiple different random rotations and shears to each experimental image.

Figure 2. The resulting regular grid is then deformed by jittering x and y coordinates of every point by a random displacement value drawn from Gaussian distribution with $\sigma = 10\,\mu$m (dark gray points in **Figure 2**). Different values of spacing and jitter can be used, the ones used here tended to give the most realistic tiling results. Next, a Voronoi diagram, which for each seed point delineates territories closer to it than to any other seed point, is drawn for the jittered points. We then iteratively pick a polygonal area patch from the Voronoi partitioning, look up a template astrocyte from the randomized collection, with a convex hull best matching the shape of the given Voronoi patch, and place this template into the model space. Repeated for all patches in the Voronoi partition, this creates a preliminary tiling with partially overlapping domains of neighboring astrocytes and occasional empty spaces. Next, this draft tiling is optimized with an active deformable model: the perimeter of each cell template is treated as an elastic two-dimensional curve, which optimizes an energy functional designed to promote repulsion between overlapping regions and adhesion between neighboring cells, with a penalization of the major cell shape deformation. After all domain boundaries are settled, the spatial templates are interpolated into the deformed contours. The described process of the network template creation is visualized in **Supplementary Video 1**.

2.2.2. Computational Design

Our simulations are based on compiling an encoded raster image representation (a template) of the model space to region-specific equations. For the sake of computational simplicity, we use two-dimensional spatial layout—each pixel of the spatial template can be interpreted as a thin slab, occupied either exclusively (e.g., in the soma) or partly by astrocyte cytosol; or as belonging to extracellular space. As follows from this approach, each pixel in the model space has to be assigned

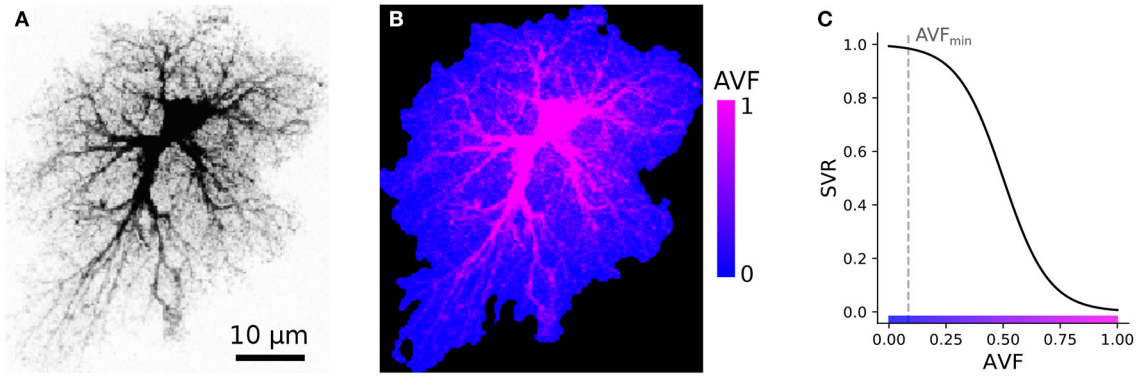

FIGURE 3 | Example of AVF color-coding. **(A)** Maximal projection of a confocal image of a cortical astrocyte. **(B)** color-coded template ready for simulation; regions with non-zero blue channel delineate astrocyte domain, while intensity of the red channel encodes AVF. **(C)** Link between color-coded AVF and SVR parameters.

to either astrocyte-free space (class III) or astrocyte-occupied space, ranging from class I, astrocyte soma and thick branches, to class II, i.e., elements of volume containing a tangle of thin astrocyte processes and unresolved neuronal structures, e.g., synaptic boutons. We account for a graded transition from thick branches to thin processes to leaflets by introducing a local astrocyte volume fraction (AVF) parameter, which defines the landscape of how much of each pixel volume is occupied by astrocyte in the 3D prototype. AVF here is defined as a ratio between local fluorescence intensity of the template and the intensity at the soma AVF $= \max(I/I_{\max}, \mathrm{AVF}_{\min})$. An example of the described mapping from image intensity to AVF is shown in **Figures 3A,B**, where the colormap in **Figure 3B** is such that the non-zero blue channel delineates the presence of astrocyte cytoplasm (non-zero AVF), and the intensity of the red channel encodes the AVF value. To describe the relative input of the store-operated calcium flux and plasma membrane flux, we introduce a surface-volume ratio (SVR) parameter, which inversely depends on AVF (**Figure 3C**). The SVR value is maximal at the edges of the leaflets and minimal in the soma. Accordingly, a simple raster RGB image serves as a spatial template to encode the model space. Specifically, non-zero values in the blue channel define astrocyte-occupied pixels, while intensity in the red channel encodes AVF and ranges from minimal value $\mathrm{AVF}_{\min}$ (class II) to 1 (class I). Thus, one can set up computation for a specific spatial template by simply drawing it algorithmically or with an indexed palette using a graphical editor.

At each integration step the master program module optionally compiles the provided image into a set of equations by mapping each pixel color to equation set following the color-coded dictionary. For each pixel first the point dynamics are applied, i.e., right-hand terms are evaluated. Next, diffusion of ions and molecules and any other short-range interactions is taken into account based on the class of the neighboring pixels. This approach is flexible, but has an overhead of compiling the color-to-equation mapping. To improve the computational performance we employ NVIDIA CUDA, a parallel GPU-based computing technology.

2.3. Intracellular Calcium Dynamics: Principal Quantities and Flows

The model for local Ca^{2+} dynamics is based on that of Ullah et al. (2006) with a few modifications previously introduced in Brazhe et al. (2018), which sum up to treating ER calcium as a dynamic variable, adding neurotransmitter-dependent calcium influx via plasma membrane, and segregation between thick and thin processes. Below we describe the proposed model, focusing on the differences with the Ullah et al. (2006) model; equations and parameters that are the same here as in the Ullah model are omitted.

The principal variables of the model are (i) the cytosolic calcium concentration $[Ca^{2+}]_c$, (ii) calcium concentration in the endoplasmic reticulum $[Ca^{2+}]_{ER}$, (iii) inositol trisphosphate concentration in the cytosol $[IP_3]$ and (iv) extracellular glutamate concentration [Glu].

To account for the morphology-based spatial heterogeneity of astrocytes, we introduce a parameter $r \in (0 < r_{\min} \ldots 1]$—a scalar quantity, roughly representing local AVF. This parameter also defines a linked parameter s representing local SVR of the astrocyte processes; SVR is inversely related to AVF: $s = 1/(1 - \exp[0.1(r - 0.5)])$. SVR scales relative inputs of Ca^{2+} exchange through plasma membrane and with ER as described below, while AVF scales effective diffusion coefficients for Ca^{2+} and IP_3.

The equation set for the principal variables reads:

$$\frac{d[Ca^{2+}]_c}{dt} = (1-s)J_{ER} + sJ_{pm} + J_{diff}, \quad (1)$$

$$\frac{d[Ca^{2+}]_{ER}}{dt} = -\frac{1-s}{c_1}J_{ER}, \quad (2)$$

$$\frac{d[IP_3]}{dt} = s(I_{Glu} + I_{Ca}) - I_{eq} + I_{diff}, \quad (3)$$

$$\frac{d[Glu]}{dt} = \frac{[Glu]_{amb} - [Glu]}{\tau_{Glu}} + \xi_p(t) + G_{diff}, \quad (4)$$

where J_{ER} is the total flow of calcium ions in exchange between the cytosol and endoplasmic reticulum; J_{pm} is the total flow

of calcium ions through the plasma membrane in exchange between the cytosol and extracellular space; I_{Glu} and I_{Ca} stand for glutamate- and calcium-dependent inositol trisphosphate production mechanisms, mediated by phospholipases β and δ; I_{eq} is a simplified first-order equilibration of inositol trisphosphate concentration to the basal level $[IP_3]_0$; $[\mathrm{Glu}]_{amb}$ is the ambient concentration of extracellular glutamate, and τ_{Glu} is the timescale of its clearance and return to the baseline level; $\xi_p(t)$ is stochastic source of glutamate from nearby located neuronal synapses triggered by Poisson spike trains in each pixel. Additionally, J_{diff}, I_{diff}, and G_{diff} describe the finite-element approximation of diffusion of cytosolic Ca^{2+}, IP_3 and extracellular glutamate, respectively and are described below.

The weighting coefficient s accounts for the stratification of intracellular dynamics according to **Figure 3**: in the leaflets $r = r_{\min} \ll 1$ and $s \approx 1$, while for deep cytosol locations $r = 1$ and $s \approx 0$. With this we (i) describe that input from all plasma membrane calcium currents is maximal in the leaflets and (ii) assume that endoplasmic reticulum does not invade leaflets much, thus ER exchange is large only in thicker branches and soma. We also assume that all IP_3 is produced in the plasma membrane by means of G-protein coupled phospholipase β or Ca^{2+}-dependent phospholipase δ.

2.3.1. Calcium Exchange Between the Cytosol and ER

Total calcium flow across the endoplasmic membrane is composed of IP_3R-mediated current J_{IP_3}, leak of Ca^{2+} from endoplasmic reticulum J_{leak}, and contribution of ER membrane Ca^{2+} pump J_{pump}:

$$J_{ER} = J_{IP_3} + J_{\mathrm{leak}} - J_{\mathrm{pump}}. \tag{5}$$

Ca^{2+} current via IP_3 receptors J_{IP_3} is modeled in the same way as in Ullah et al. (2006) (Equations 2, 4, 5, 9–12). Two other terms in Equation (5) stand for the leak of calcium from *ER*, and for the pumping it back, respectively, following Equations (3,6) in Ullah et al. (2006).

2.3.2. Transmembrane Calcium Flows

Transmembrane calcium exchange J_{pm} consists of three flows:

$$J_{\mathrm{pm}} = J_{in} + J_{\mathrm{Glu}} - J_{out}, \tag{6}$$

where J_{in} describes the sum of background constant Ca^{2+} influx and agonist-dependent IP_3-stimulated Ca^{2+} influx across plasma membrane from the extracellular space and J_{out} is an extrusion current (eqs. 7–8 in Ullah et al.); $J_{\mathrm{Glu}} = \gamma[\mathrm{Glu}]$ describes the direct effect of extracellular glutamate on additional calcium influx.

2.3.3. Inositol Trisphosphate Turnover

The dynamics for IP_3 concentration from Equation (3) has the following terms: first, we use a lumped first-order description of $[IP_3]$ equilibration to a resting level $[IP_3]_0$:

$$I_{eq} = \frac{[\mathrm{IP_3}] - [\mathrm{IP_3}]_0}{\tau_{\mathrm{IP_3}}}; \tag{7}$$

second, we account for the Ca^{2+}-stimulated IP_3 production in the same way as in Ullah et al. (2006), (eq. 14), and third, we account for glutamate-driven IP_3 production I_{Glu} following Ullah et al. (2006), (eq. 15).

2.3.4. Synaptic Glutamate Drive

Stochastic glutamate source $\xi_p(t)$ in each pixel is modeled as quantal release triggered by a spike train drawn from a homogeneous Poisson process with intensity p, which agrees with statistics of neuronal firing (Softky and Koch, 1993). Accordingly, the $\xi_p(t)$ term in Equation (4) is given by

$$\xi_p(t) = \sum_k A\delta(t - t_k), \tag{8}$$

where A is the instantaneous increase in glutamate release rate associated with each presynaptic event and t_k are times of presynaptic spikes in the given pixel following Poisson process with intensity p_{syn}.

2.4. Intracellular Diffusion

Elevated cytoplasmic Ca^{2+} can remain confined to the spatial domain of a single astrocyte, but can also spread to the neighboring astrocytes (Nedergaard, 1994; Carmignoto, 2000; Falcke, 2004) in a wavelike manner. The involvement of a large number of cells into a wave is still not fully understood though it may be an important aspect of information processing in the brain (Haas et al., 2006). At least two main mechanisms can account for the intercellular wave propagation: (i) secretion and diffusion of *extracellular* ATP and its action on P2Y receptors on astrocytic membranes and (ii) diffusion of *intracellular* IP_3 and Ca^{2+} between contacting astrocytic leaflets, via gap junctions. Relative input of the two mechanisms differs across brain regions and for the cortical astrocytes the one mediated by the gap junctions has been reported to prevail (Haas et al., 2006). The current work is therefore focused on the latter mechanism. Accordingly, astrocytes in the model are networked by an analog of gap junctions dispersed over the parts of the cell perimeter and simulated as the connection of areas with low AVF.

Here we employ a rather simplified description of diffusion in the cytoplasm where the region occupied by astrocyte is considered as a continuous space. As corroborated by evidence for autologous gap junctions between the processes of the same astrocyte (Wolff et al., 1998; Nagy and Rash, 2003; Genoud et al., 2015), astrocyte cytosolic volume can be described as a porous sponge-like medium rather than a branched structure or acyclic graph. Thus, possible hindrance to IP_3 or Ca^{2+} diffusion through the intricate mesh of astrocytic processes due to tortuosity and porosity of the astrocytic volume can be accounted for by a simple scaling of the apparent diffusion coefficient. Though an interesting issue, a detailed account for intracellular diffusion and connectivity between neighboring points in an astrocyte is outside the scope of the current study and here we resort to a rather minimalistic description.

Following the study of diffusion coefficients of IP_3 and Ca^{2+} in *Xenopus laevis* oocytes (Allbritton et al., 1992), most modeling studies assume a much faster diffusion of IP_3 ($\approx$ 300 $\mu m^2/s$)

TABLE 1 | Model parameters.

Param.	Value	Units	Remarks
c_0	Not used		Total [Ca^{2+}] in terms of cytosolic vol
v_4	0.1 (0.4)	$\mu M/s$,	Max rate of Ca^{2+}-stimulated IP_3 production
v_5	0.01 (0.025)	$\mu M/s$,	Rate of Ca^{2+} Leak across plasma membrane
k_1	1.0 (0.5)	1/s,	Rate constant of Ca^{2+} extrusion
k_3	0.05 (0.1)	μM,	Activation constant for Ca^{2+}-pump
τ_{Glu}	0.1	$\mu M/s$	Rate constant for perisynaptic glutamate uptake
p_{syn}	0.005–0.01	Hz	Rate of Poisson process, for glutamate release
A	27	μM	Instantaneous rise in glutamate release rate
$[Glu]_{amb}$	0	μM	Ambient extracellular glutamate
D_{Ca}	10	$\mu m^2/s$	Diffusion coefficient for cytoplasmic Ca^{2+}
D_{IP3}	10	$\mu m^2/s$	Diffusion coefficient for cytoplasmic IP_3
D_{Glu}	0.02	$\mu m^2/s$	Diffusion coefficient for extracellular glutamate
r_{min}	0.085	Dimensionless	Minimal value of the AVF

Values in parentheses are the corresponding parameter values in Ullah et al. (2006).

than Ca^{2+} ($\approx$ 10 $\mu m^2/s$) due to Ca^{2+} buffering and often disregard Ca^{2+} diffusion altogether. However, the effective rate of IP_3 diffusion can occur on a much slower timescale (Dickinson et al., 2016), equalizing the signaling range and speed of the two signaling factors. Moreover, gap junctions formed by connexin43, characteristic for astrocytes, are permeable to Ca^{2+} (De Bock et al., 2012). We thus account for intra- and intercellular diffusion of both IP_3 and Ca^{2+} in the model with the same effective diffusion coefficients. This includes exchange at borders between neighboring astrocytes to imitate the function of gap junctions, which is supported by evidence that IP_3 can diffuse through the gap junctions along with Ca^{2+} (Yule et al., 1996).

Specifically, the diffusive term in Equation (1), e.g., for Ca^{2+} reads:

$$J_{diff} = D^*_{Ca}(\sum_{i}^{N} [Ca^{2+}]^i_c - N[Ca^{2+}]_c) \,, \tag{9}$$

where D^*_{Ca} is the diffusion rate defined as the diffusion coefficient for Ca^{2+} scaled by spatial grid step δx and local AVF value r: $D^*_{Ca} = r^2 D_{Ca}/\delta x^2$, and i enumerates the N nearest neighboring astrocyte-containing units. Here, we regard diffusion in porous media and assume that larger AVF is associated with larger cross-sectional area open for diffusion, as the astrocyte process diameter increases, and simultaneously with less tortuous paths taken up by diffusing molecules as the processes become less entangled. This leads to approximately quadratic scaling of D^* with r. The diffusive term for IP_3 is defined in a similar way.

Finally, neighboring pixels with different AVF values obviously contain unequal volumes of astrocyte cytoplasm; hence, small concentration changes in areas with high AVF should cause larger diffusion-mediated concentration changes in the neighboring pixels with low AVF. This was accounted for by scaling the concentration rates of change due to diffusive exchange by the ratio of the AVF values of the two neighboring pixels.

2.5. Model Parameters and Numerical Details

The basic set of model parameters is given in **Table 1**. Only new parameters and values different from that in Ullah et al. (2006) are shown. For convenience, the full set of parameters is provided in **Supplementary Table 1**. The few values that are different were adjusted in order to provide the reasonable dynamics with the introduced treatment of $[Ca^{2+}]_{ER}$ as a variable in our model and the spatially extended layout. Diffusion coefficient for Ca^{2+} is taken as a lower-bound estimate in Allbritton et al. (1992). Slow diffusion coefficient of IP_3 is based on Dickinson et al. (2016). We also added new parameters, specifically, A, τ_{Glu}, and D_{Glu}. The latter was chosen as a small value to describe only minimal spillover from a release site and buffering by binding to transporters. The pair of parameters describing instantaneous glutamate release rate and slower decay could be varied, because it is hard to assess the actual transmitter concentration and decay time as sensed by astrocyte leaflets. Extracellular glutamate transients occurring due do quantal synaptic release as estimated by fluorescent glutamate sensor have decay timescale in close to 100 ms (Jensen et al., 2019), and this value was used for the simulations shown below. This led to local glutamate transients peaking at 1.2 μM and decaying within 200 ms. We note that qualitatively similar Ca^{2+} signaling dynamics could be obtained with a shorter τ_{Glu} value, compensated by higher release rate A.

Numerical integration of the model differential equations is done in an explicit scheme (4th order Runge–Kutta method adopted for stochastic differential equations with a fixed timestep dt = 0.002 s) implemented in AGEOM–CUDA software (Postnov et al., 2012). Spatial grid step was δx = 0.275 μm/pixel for single-cell templates and δx = 0.55 μm/pixel for network templates. For reproducibilty, a reference implementation of spatial template generation and model simulation is available at https://zenodo.org/record/4552726#.YDAz1nUzZQ8 in form of Jupyter notebooks, Python and C code.

To quantify spatiotemporal properties of the simulated Ca^{2+} dynamics, we examined complementary cumulative distribution functions (CCDF) of areas and lifetimes of individual Ca^{2+} transients in all single-cell spatial templates to avoid selection bias. Ca^{2+} transients were thresholded at 25% change from the local baseline level. The resulting contiguous *TXY* volumes of suprathreshold Ca^{2+} concentration were treated as discrete events. CCDF $\bar{F}_X(x)$ of some random variable X is defined as the probability P that X is greater than some x value: $\bar{F}_X(x) = P[X > x]$. We present the CCDF curves in double logarithmic coordinates to test if they can be approximated by a straight line, implying a power-law behavior. If a given variable is distributed according to a power law with probability density function (PDF) $P_X(x) \propto x^{-\alpha}$, then the CCDF also has a power-law behavior, but with a smaller exponent $\bar{F}_X(x) \propto x^{-(\alpha-1)}$.

3. RESULTS

The proposed model, including the modifications to the local calcium dynamics and spatial mapping, was tested in a number of simulation experiments with different parameter settings and different spatial templates (which we call "cells" for shorthand below). To test for agreement between model behavior and the experimentally observed dynamics, first, we looked at the effect of the level of mean neuronal firing rate (local rate of the Poisson point process in terms of our model) on spatio-temporal dynamics of astrocytic calcium, and second, we tested whether the artificial spatial templates could provide for realistic intercellular calcium waves or other collective variants of astrocytic calcium dynamics.

3.1. Wave Patterns in Single-Cell Templates

Figure 4 summarizes simulations of the 27 single-cell templates shown in **Figure 2**. At low excitation ($p_{syn} = 0.005$ Hz) most Ca^{2+} events were spatially confined and tended to start at a small number of sites, as shown with max-span contours and red labeling in **Figure 4A** (left) for 25 largest events. At higher excitation ($p_{syn} = 0.01$ Hz) many Ca^{2+} events spread to occupy the whole cell domain and again tended to initiate at the same sites. Synaptic signaling events were integrated into a spatial glutamate profile as shown in **Figure 4A** (bottom): local surges of extracellular glutamate are sparse at low excitation, while their instantaneous spatial density increases at high excitation, with a tendency of nearby sparks to blend.

The tendency, exemplified by a single template in **Figure 4A**, was supported by the majority of single-cell templates (**Figure 4B**): the number of events (during 2,500 s simulation time) covering more than 25% of the cell area increased with excitation for nearly all cells except six, which were incapable of generating whole-cell transients at $p_{syn} = 0.01$ Hz. There were no obvious differences between these cells and all the others in overall morphology or AVF statistics. All cells did generate whole-cell transients at a higher excitation of $p_{syn} = 0.02$ Hz. Most cells demonstrated a decline in the number of small events, covering less than 25% of the cell area with excitation, as a larger proportion of events was enabled to spread over larger areas, while the rate of event initiation could remain stable. The area of large ($> 25\%$) events increased for all cells which generate large events under low drive conditions except the three, which did not generate large events at all, apart from other cells. The average area of the small ($< 25\%$) events increased with excitation strength for all cells.

Stochastic local glutamate surges initiate two parallel processes: fast localized Ca^{2+} transients and slower IP_3 production. Both integrate over time to steady-state levels of the model variables. Because the relative input of plasma membrane transport is defined by AVF in our model, we expected that the steady state levels and the probability of Ca^{2+} event initiation should depend on AVF as well. Steady-state values of $[Ca^{2+}]$ and $[IP_3]$ decreased with growing AVF (**Figures 4C,D**), forming an uneven spatial profile. Calcium, as well as IP_3 levels, were higher in the periphery and lower near the soma, which is due to Ca^{2+} entry during the synaptic excitation and due to higher IP_3 production in the regions with lower AVF. Different cells varied in steady-state levels of the variables, while intensified stimulation lead on average to a slight elevation of steady-state $[Ca^{2+}]_i$, due to increased Ca^{2+} entry and did not affect $[IP_3]_i$, as the increase in $[Ca^{2+}]_i$ was insufficient for activation of PLC_δ.

An example of a single large Ca^{2+}-event is shown in **Figure 4E**. The expanding wave of elevated $[Ca^{2+}]_i$ initiates in a small location and spreads over the whole spatial domain (top row). Due to the large range of steady-state $[IP_3]_i$ concentrations, the event is unclear in absolute $[IP_3]_i$ values (middle row), but is obvious in the relative scale (bottom row).

Despite the stochastic nature of excitation, Ca^{2+} activity in most cells is self-organized in a repeated pattern of Ca^{2+} transient initiation and spreading (**Figure 5**); event initiation sites were tightly clustered. Interestingly, activation in some clusters lead to spatially confined events, unlinked to activity in the rest of the cell, while transients originating in other sites tended to spread over the whole spatial domain in a repeated fashion. This is illustrated in **Figures 5A–D** for an example spatial template (see also **Supplementary Video 2**). This cell is markedly anisotropic, which defines the dominant wave spreading properties. The two active initiation sites labeled as #1 and #2 display different properties: events, starting in the site #1 often spread over large portions of the cell, as shown for a line-scan path in **Figure 5B**, while line-scan along the path starting in #2 was either activated by a wave coming from #1 or—very locally and with a higher frequency—by confined transients initiating in #2. Averaging small temporal windows around Ca^{2+} spikes at the origin of path #1 shows that activation along this path is time-locked to activation of the initiation site. On the other hand, averaging similar temporal windows triggered by Ca^{2+} spike at the origin of path #2 did not reveal any structured activation patterns. **Figure 5D** shows max-span contours of 25 largest events with their initiation sites mapped in red, as well as 5 peak-delay maps for a repeated pattern of activation. In these maps color indicates delay in seconds between the Ca^{2+} peak at the initiation site and the Ca^{2+} peak at each point of the cell. The precise wave initiation site could vary within 3–5μm, but the overall spatiotemporal pattern remained similar, with activation spreading mainly along the long thick processes toward the soma. Additional examples

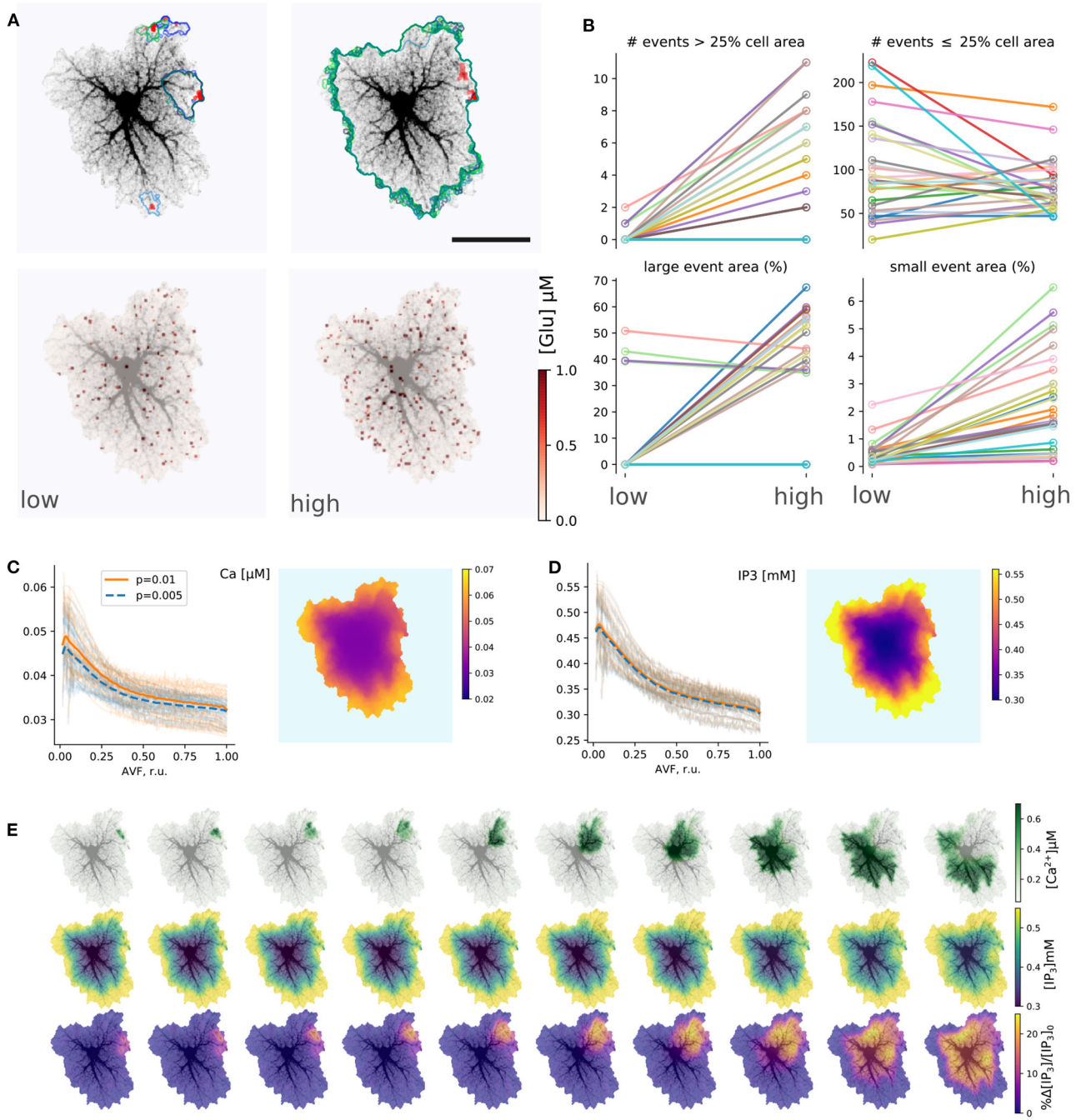

FIGURE 4 | Simulations of single-astrocyte spatial templates. **(A)** top row: Ca^{2+} transient initiation sites (red) and maximum span contours at low (left, $p_{syn} = 0.005$ Hz) and high (right, $p_{syn} = 0.01$ Hz) synaptic drive, in both cases 25 largest events are shown, at high drive all such events span the whole template; bottom row: snapshots of instantaneous extracellular glutamate concentrations at low and high synaptic drive parameters. Scale bar: 25 μm. **(B)** Effect of synaptic drive on Ca^{2+} transient frequency and sizes ($n = 27$ templates, simulation time 2,500 s after burn-in period of 2,000 s); top row: number of events covering more than 25% of cell area ("large" events) increases with excitation strength (left), number of events covering less than 25% of cell area ("small" events) decreases (right); bottom row: average areas of both "large" (left) and "small" (right) events increases with excitation strength in most templates. **(C)** Distribution of baseline $[Ca^{2+}]_i$ levels with AVF parameter at low and high stimulation drives (left) and an example of spatial distribution (right). Each transparent line corresponds to one template, thick lines: average. **(D)** Same as in **(C)**, but for $[IP_3]_i$. **(E)** Evolution of a single Ca^{2+} transient starting in top-right corner of the template; top row: $[Ca^{2+}]_i$, middle row: $[IP_3]_i$, bottom row: relative change in $[IP_3]_i$.

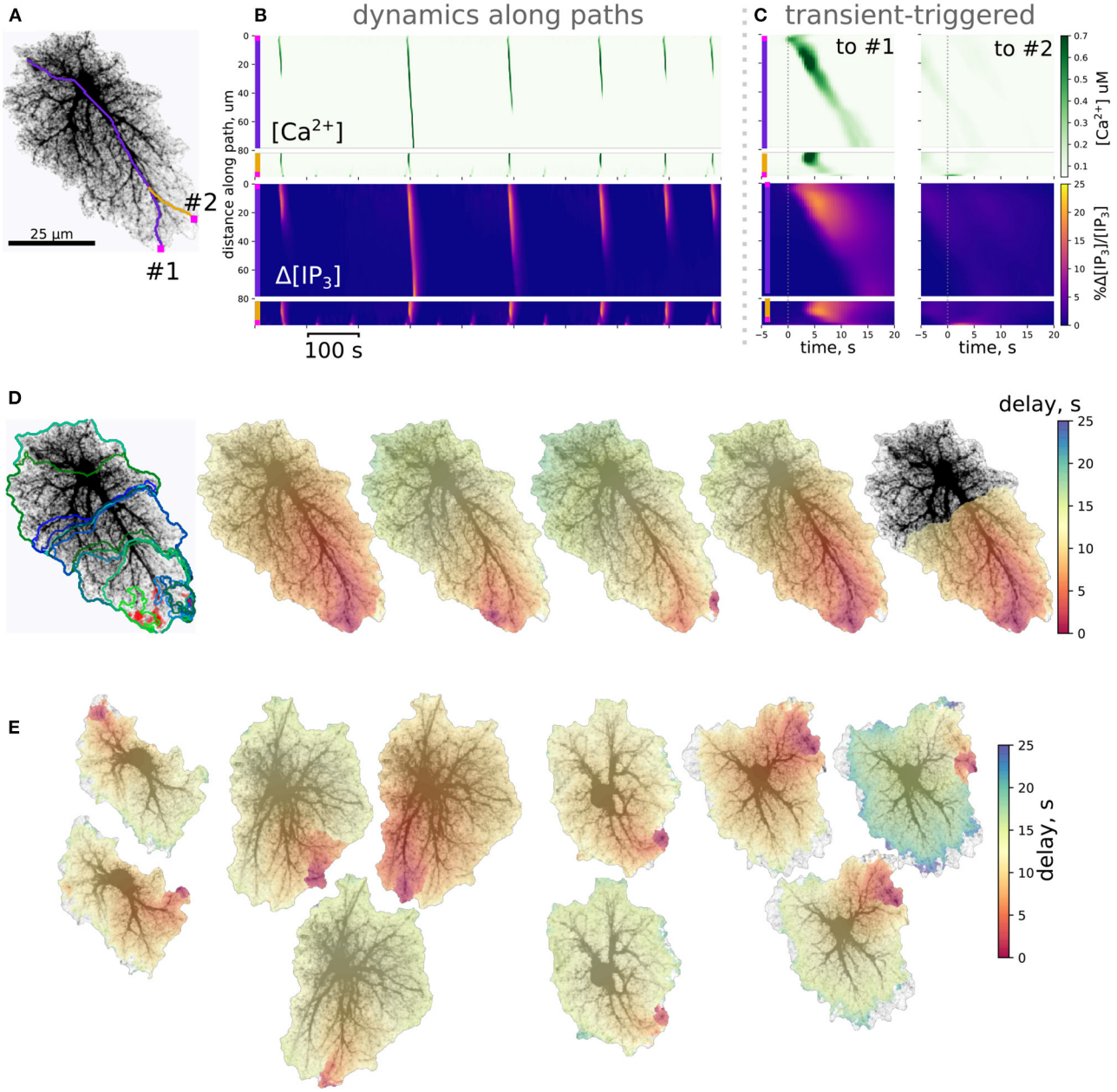

FIGURE 5 | Ca^{2+} dynamics in single-cell templates self-organizes in repeatable spatiotemporal patterns. **(A)** A spatial template for simulation and 2 path-scans (#1, purple and #2, yellow) used for rasters in **(B)**; **(B)** Rasters of $[Ca^{2+}]_i$ and relative change in $[IP_3]_i$ along paths; path starting points are shown as magenta squares. **(C)** Transient-triggered averages, linked to the $[Ca^{2+}]_i$ peaks at the origin of path #1 (left) and to the $[Ca^{2+}]_i$ peaks at the origin of path #2 (right); initiation of a $[Ca^{2+}]_i$ peak at the origin of path #1 typically leads to a full-cell $[Ca^{2+}]_i$ wave, while $[Ca^{2+}]_i$ transients emerging at the origin of path #2 remained localized. **(D)** Left: clustered initiation points (red) and contours of 25 biggest $[Ca^{2+}]_i$ waves; right: 5 "large" $[Ca^{2+}]_i$ waves with color-coded delay before reaching the peak in $[Ca^{2+}]_i$ show a tendency to start in the same area and spread with similar spatiotemporal profiles. **(E)** Examples of repeated spatiotemporal patterns in 4 other spatial templates: in some cells there was more than one preferred initiation site, the full delay before initiation and waning of the wave also varied.

of repeated patterns for other cells are provided in **Figure 5E**. In some cells preferred wave initiation sites could alternate between two polar positions or a few neighboring regions. There was also some scatter in the maximum delay between the initiation of the wave and its full expansion.

Though localized Ca^{2+} events could be initiated in the low-AVF regions due to direct influx through the plasma membrane, these event seeds needed to reach a tip of a thicker branch with higher AVF to be amplified by IP_3-mediated ER exchange. Thus, initialization of a global Ca^{2+} wave critically depends on a coincidence of exactly the right spot in the AVF profile—allowing both for a high enough $[IP_3]_i$ baseline and sufficient ER exchange—and a wide and long enough cluster of glutamate release due to local increase in synaptic activity. Areas containing

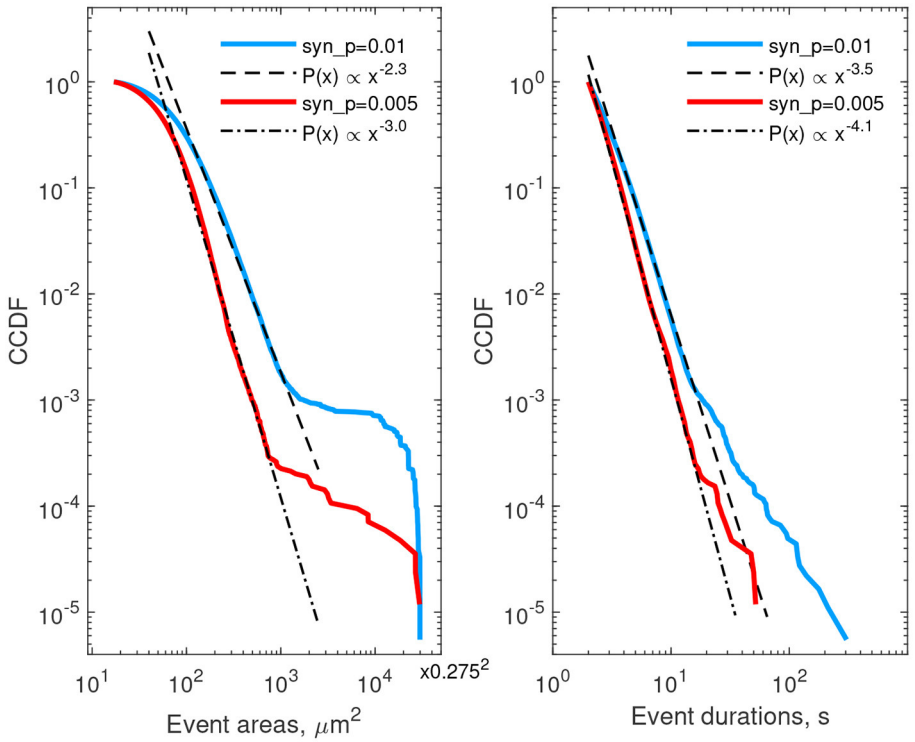

FIGURE 6 | Complementary cumulative distribution functions for areas **(left)** and durations **(right)** of Ca^{2+} events in all single-cell templates. Red lines—low excitation (p_{syn} = 0.005 Hz), blue lines—high excitation (p_{syn} = 0.01 Hz). Event area CCDFs: slopes of the fits for the low and high excitations are 3.0 and 2.3, correspondingly; the bend at the large areas corresponds to transition to whole-cell activation. Event duration CCDFs: slopes of the fits are 4.1 and 3.5 for the low and high excitations, correspondingly.

only thin processes with low AVF will display only frequent local Ca^{2+} sparks, unable to invade the neighboring regions and thus will primarily set the baseline levels of $[Ca^{2+}]_i$ and $[IP_3]$ due to diffusion. Indeed, astrocytes in hippocampal slices display frequent localized Ca^{2+} events in the cell periphery, often termed "microdomains," with a characteristic size of high-Ca^{2+} spots much smaller than the cell size and originating in the thin processes region (Rungta et al., 2016). At the same time, the "lifespan" of the Ca^{2+} wavefront increases with the already invaded area of the thick branch region due to regenerative Ca^{2+} release, which in turn relies on background $[IP_3]$ level. Thus, the specific topology of the cell template predicts the "hot spots" for the probability of Ca^{2+} wave seeding.

We next describe statistics of areas and lifetimes of individual Ca^{2+} transients (thresholded at 25% deviation from baseline). The left column of **Figure 6** provides CCDF of areas, covered by individual events, while the right column describes durations of calcium events. Red curves correspond to the case of low neuron activity, the blue ones correspond to high neuron activity. In both cases the CCDF curves are presented in double logarithmic coordinates and can be approximated by a straight line within some ranges of event areas or durations, suggesting a power-law behavior in agreement with experimental data (Wu et al., 2014). After recalculating from CCDF to PDF exponents, the resulting parameters were different from that reported in Wu et al. (2014): for areas, $\alpha \approx 3.3 \ldots 4.0$ in the model vs. $\alpha \approx 2.1 \ldots 2.4$ in cultured astrocytes, and for durations $\alpha \approx 4.5 \ldots 5.1$ in the model vs. $\alpha \approx 1.97 \ldots 2.16$. These discrepancies can be explained by imperfection of the model and the 2D spatial embedding in the model. Defining model parameters that govern the shape of the event size and duration distributions is a potentially interesting outlook for further studies. Increase in synaptic excitation favored larger areas occupied by waves and longer durations of each event. The kinks in the CCDFs for event areas correspond to transition to whole-cell waves, i.e., events covering more than 30–50 μm^2 were likely to expand further and cover the whole cell.

We so far examined Ca^{2+} transients in 2D spatial templates, which we use to generate astrocytic network in the next section to reduce computational load. We note however that the presented modeling approach is extendable to 3D with minimal modifications. An example of simulation for a 3D single-cell spatial template is presented in **Supplementary Video 3**. The features reported above for 2D templates remain in 3D: there are Ca^{2+} transients at different spatial and temporal scales, waves that expand toward soma and vice versa, there are visible repeated patterns of activation.

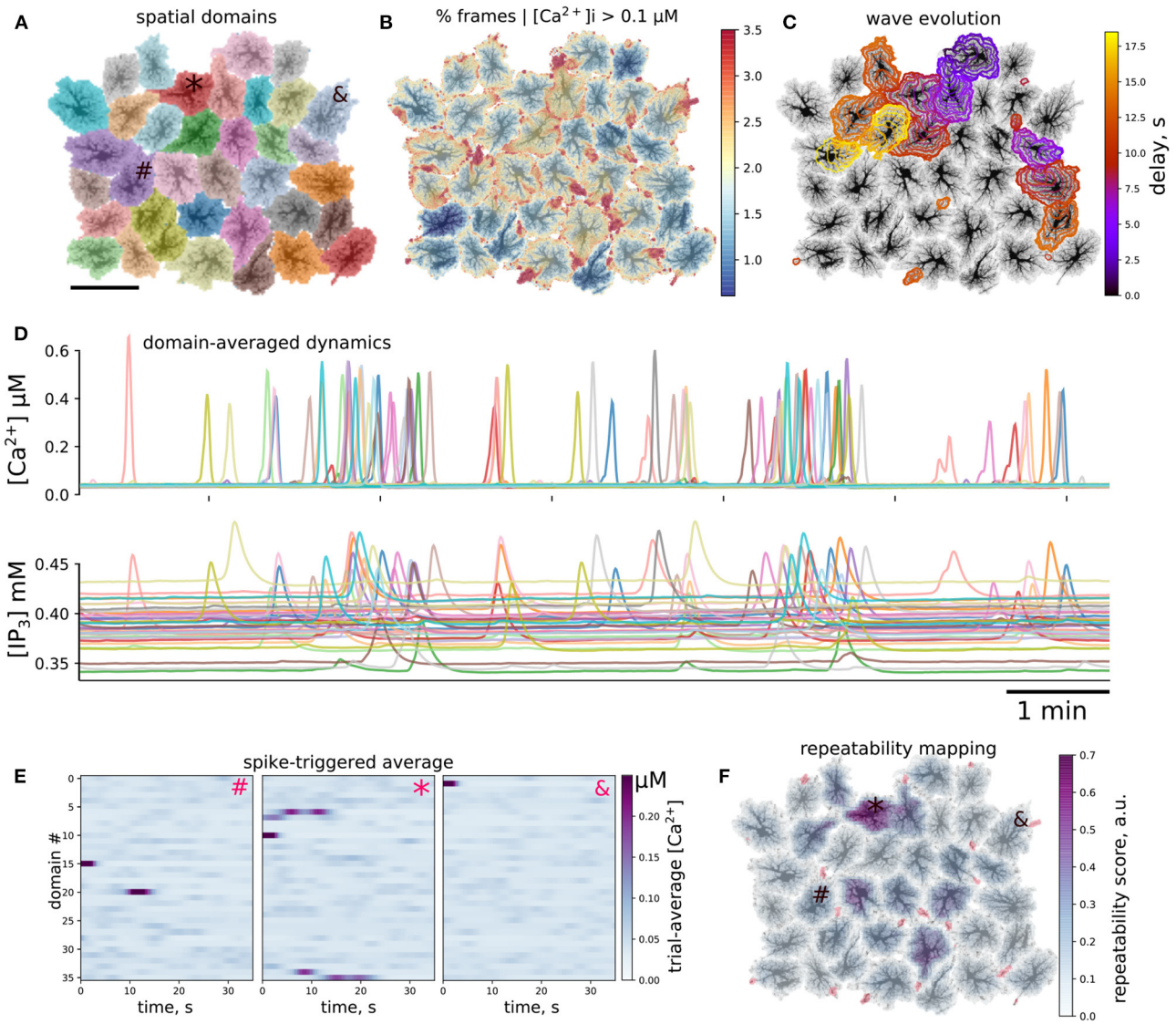

FIGURE 7 | Ca^{2+} activity in multicellular template. **(A)** Layout of individual spatial domains, each cell is color-coded. **(B)** Activity level is not uniform: color-coded percentage of time that each pixel had $[Ca^{2+}]_i$ above 0.1μM. Domain periphery is more active than somatic regions. **(C)** Example of spatiotemporal evolution of two co-occurring waves. Contours are separated by 1 s, time delay since the first contour is color-coded. **(D)** Cellwise dynamics: Ca^{2+} and IP_3 values averaged over individual cell domains, line color corresponds to the map in **(A)**, visible are single-cell events as well as packed Ca^{2+} transients representing multi-cellular waves. **(E,F)** Repeated patterns of cell activation. **(E)** Spike-triggered averages of cellwise $[Ca^{2+}]_i$ profiles initiated by the cells indicated as #, *, and & in **(A,F)**; activity of the first cell is time-locked to activation of a single other cell, Ca^{2+} transient the second cell consistently leads to activation of several cells, while the third cell does not participate in repeatable patterns. **(F)** Local score of activation pattern repeatability based on approach shown in **(E)** (see text for more details); activation of a subpopulation of cells leads to repeated activation of its neighbors; red regions denote wave initiation sites as in **Figure 4A**.

3.2. Collective Dynamics of Astrocytes

After testing model behavior at microdomain and single-cell level, we turned to ensembles of connected cells. Collective dynamics of astrocytes was simulated using spatial templates containing about 40 cells as shown in **Figure 7A**; see also **Supplementary Video 4**. The simulated network is smaller than the size of cliques or networks of connected astrocytes in the neocortex (Houades et al., 2008), but still at the same order of magnitude. Simulations of larger spatial network templates are also possible but are more computationally demanding. Ca^{2+} activity was not uniform across the spatial template: there were active "hot" brims in the periphery of most of the cell domains and some cells were less active than others, as shown in **Figure 7B**. We observed Ca^{2+} transients originating in some astrocytes and expanding to their neighbors in a wavelike manner, an example of such a wave is shown in **Figure 7C** as a sequence of contours of elevated $[Ca^{2+}]_i$, separated by 1 s.

To simplify the description of emerging spatiotemporal patterns, each cell can be considered as an element that "fires," i.e., producing a global whole-cell spike, or remains silent. This cell-wise activity is shown for $[Ca^{2+}]_i$ and $[IP_3]_i$ in **Figure 7D**, where line colors correspond to domain colors in **Figure 7A**. We observed individual cell spikes as well as packs of tightly grouped spikes corresponding to multi-cellular waves. A considerable scatter is clear in the baseline levels of IP_3, which reflects individual properties of each cell. IP_3 concentration peaks are wider and occur with a small delay in comparison to Ca^{2+} peaks, which reflects the slower kinetics of IP_3 production timescale and a lag due to diffusion of IP_3 from the periphery to the somatic region.

A large Ca^{2+} transient in one astrocyte can spread to other cells. In single cell templates we observed self-organized repeated patterns of activation. We were curious, if there will also emerge repeated patterns of intercellular dynamics at a network level. As a simple test for repeatable patterns, we calculated averages of the domain-averaged Ca^{2+} rasters in a short time window, triggered by Ca^{2+} spikes in different domains. We collected Ca^{2+} traces, where each spatial domain served as a large region of interest (ROI), selected one cell as a seed, created time windows around Ca^{2+} spikes in this cell and averaged Ca^{2+} dynamics snapshots in all other ROIs across the time windows. In the case of stable activation sequence, the spikes appear with the same time-lag relative to the seeding astrocyte, and are thus visible in the raster plot, while if spiking in other astrocytes is not time-locked to the seeding astrocyte, the average Ca^{2+} signal will be faint. Examples of such spike-triggered averages are shown in **Figure 7E** for three cells labeled as "#," "⋆," and "&" in **Figure 7A** used to center the time windows. Here, Ca^{2+} spikes in cell "#" was time-locked to activation of a single other cell, activation of cell "⋆" lead to repeated activation of several other cells with a stable delay, while activation of cell "&" did not repeatedly lead to activation of other cells.

Inspired by this cell-wide "repeatability" measure based on the contrast of spike-triggered averages, we defined a similar score for more a detailed mapping of whether activation in some region repeatedly lead to activation in other areas with stable time lags. To this end, we split the spatial domain into overlapping square windows of size $5\times5\,\mu$m and extracted Ca^{2+} dynamics from these patches. We then selected the patches where there were more than 10 Ca^{2+} spikes reaching at least $0.5\,\mu$M $[Ca^{2+}]_i$ and created spike-triggered 50 s-long averages from the raster of Ca^{2+} signals in all patches. Percentage of all points with $[Ca^{2+}]_i > 0.2\,\mu$M in such spike-triggered windows was used as the repeatability score for a given patch. The patches were then projected back onto the spatial template, with averaging of the values in overlapping areas between patches. This resulted in an automated mapping of areas leading to repeated downstream activation at the network level, revealing cells, serving as hubs in spreading multicellular events (**Figure 7F**). As suggested in Brazhe et al. (2018) for a simpler model, some spatial configurations of thick branches and leaflets can trigger persistent pacemaker-like activity, taking over the control of dynamics at the network level. We thus tested if alterations to the spatial template could lead to self-organization in a different spatial pattern of the centers of high repeatability (**Figure 8**). The cell labeled as "⋆" in **Figure 7** was often activated from its direct neighbor to the right. Unlinking this cell from the network by setting to zero all contacts at domain boundaries (**Figure 7A**) lead to a change in the repeatability map, decreasing the score for the cell "⋆" and increasing it for the three cells in the center. Unlinking the cell "⋆" from the network effectively silenced it, leaving only three cells with relatively high repeatability scores in the template.

A subtler alteration of the spatial template can be directed at the sites of frequent Ca^{2+} transient initiation sites shown in red in **Figure 8**. Substituting the natural AVF profile at these sites with the average AVF value (**Figure 8C**) or ablating cell content from these areas (**Figure 8D**) lead to a dramatic reorganization of the Ca^{2+} initiation sites and the centers of high repeatability. In both cases the number of initiation sites was reduced, with some of the former sites being silenced and some new sites formed in the neighborhood of the previous sites. Also in both cases the inequality of repeatability score was increased, with a few cells showing very high values. We attribute this to the reduced number of initiation sites, leading to a more repeated activation sequences.

4. DISCUSSION

We proposed a spatially detailed model of astrocytic calcium activity, which reflects current understanding of the two distinct mechanisms of Ca^{2+} dynamics: excitable IP_3-mediated exchange with ER in astrocyte soma and branches and plasma membrane exchange in the fine astrocytic processes and leaflets, sensitive to external conditions. Specifically, we suggest (i) an algorithm for data-based generation of 2D spatial templates matching realistic astrocyte morphology, and (ii) morphology-dependent spatially non-uniform parameter landscape for the calcium dynamics. To this end, we introduce the AVF parameter, which sets locally the relative input of the plasma membrane and ER based pathways and scales effective intracellular diffusion coefficients. The central idea underlying this separation is that astrocytes "sense" synaptic activity with fine processes, and it is where Ca^{2+} transients are relying on extracellular Ca^{2+} rather than intracellular stores, and where the bulk of IP_3 can be produced, while thicker branches and somata provide the positive feedback gain mechanism for IP_3-mediated Ca^{2+}-induced Ca^{2+} release from ER. This mechanism separation is directly mapped to cell morphology in our approach.

We tested the suggested framework both at individual cell level and for algorithmically created multicellular astrocytic network templates. Our results show that the model is able to reproduce characteristic spatiotemporal patterns of Ca^{2+} dynamics driven by synaptic activity, represented by spatially uncorrelated point-sources of glutamate release coupled to focal Ca^{2+} entry, triggered by independent stochastic Poisson spike trains. At the single-cell level, the statistics of Ca^{2+} event durations and expansion areas turned out to have a power-law distribution resembling experimental data (Wu et al., 2014). Power-law statistics of the Ca^{2+} transients does not directly

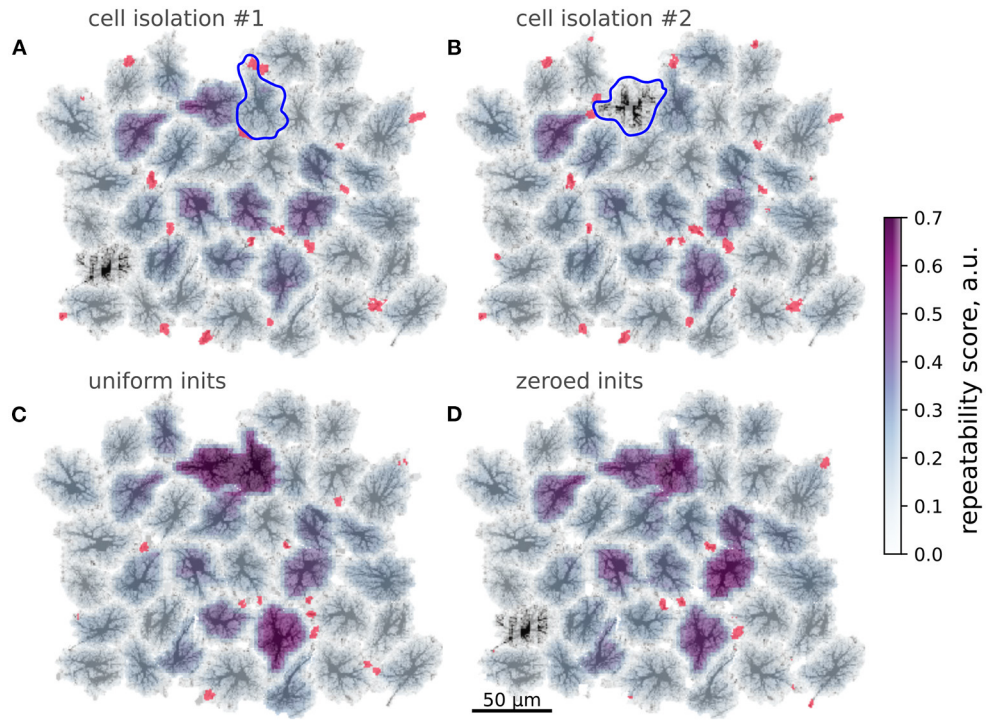

FIGURE 8 | Modification of spatial templates changes activation patterns. Color-coding: repeatability score, red: wave initiation sites. **(A,B)** Unlinking single cells from the neighbors; Blue contours—isolated cells, red regions denote wave initiation sites as in **Figure 4A**. Isolation of the cell often activated the cell denoted "*" in **Figure 7** lowers repeatability of the latter. **(B)** Isolation effectively silences the cell denoted "*" in **Figure 7**, which was a center of repeated patterns before. **(C,D)** Modifications of wave initiation sites. **(C)** Averaging AVF values within the activation sites increases repeatability of the waves, starting at the cells, isolated in **(A,B)** and one other cell. **(D)** Removing cell content from the spatial template within active initiation sites leads to a lower number of wave initiation sites and increased repeatability in several cells.

follow from the model equations and is an emergent property of the interplay between astrocyte morphology and Ca^{2+} dynamics.

The presented model is a rather simplified representation of native astrocyte morphology and Ca^{2+} dynamics. It is less detailed, but also less computationally demanding than the framework proposed by Savtchenko et al. (2018), allowing for simulations on a GPU-equipped laptop rather than on a supercomputer or a cloud. A major simplification of our model, dictating its limitations, is the reduction of real 3D astrocytic morphology to flat 2D spatial templates. The flattening was primarily done for the sake of computational tractability, but also conceptually matches single-plane imaging regime. The emergence of repeated activation patterns should not depend on the embedding space dimensionality, although the repeated propagation patterns can become more complex and elaborate in 3D; one can also expect different expansion rates and initiation probabilities for Ca^{2+} events in 3D. Notwithstanding, we argue that using 2D patterns can be a useful approximation. First, some astrocyte network systems can be regarded as effectively two-dimensional, e.g., astrocyte cultures or retinal astrocyte networks. Second, "true" astrocyte morphology can be regarded as less than three-dimensional, with the degrees of freedom limited by branching connectivity of the astrocytic processes, creating more or less independent astrocyte lobes and sub-domains. A 2D morphology-based modeling approach has earlier been employed by Kang and Othmer (2009) to study calcium waves in retinal astrocytes. Our interpretation of astrocyte morphology is however different from the one in Kang and Othmer (2009) in several key aspects. First, Kang and Othmer used a GFAP-positive immunostained micrograph of retinal astrocytes, but GFAP stains only a small fraction of astrocyte cytosol volume, while the rest, especially the mesh of thin processes, got excluded from consideration of calcium dynamics, leading for the reconstructed morphology to resemble that of cultured astrocytes (see e.g., Wu et al., 2014 for comparison of morphology). On the other hand, an account for spatial segregation of calcium activity in fine astrocytic processes and thick branches was key to this study. Second, we account for a morphology-based balance between Ca^{2+} entry via plasma membrane and from ER, which is absent in the work of Kang and Othmer. Third, we use a larger spatial template and describe Ca^{2+} dynamics on a larger spatial scale. Our model is also more focused on intercellular communication through gap junctions, as we do not account for extracellular purinergic signaling to explain Ca^{2+} wave propagation, which was done in earlier works focused on retinal astrocytes (Kang and Othmer, 2009; Edwards and Gibson, 2010), keeping in mind that the role of the extracellular pathway can be more pronounced in the retina than in neocortex.

Another limitation comes from our approximation of the 3D mesh of fine astropil sponge by a continuous active medium, parameterized by astrocytic cytosol volume fraction. Effectively, we "glue" together the individual branches and leaflets, assuming that they are at least partly interconnected by autologous gap junctions and branch-to-branch loops. The idea of "loopy" or sponge-like organization of the astropil has experimental support (Wolff et al., 1998; Genoud et al., 2015; Arizono et al., 2020), and we therefore adopt the AVF framework to represent unresolved astrocyte processes, also accounting for the tortuosity of the sponge by AVF-dependent scaling diffusion coefficients.

Indeed, the mentioned simplifications are expected to limit the predictive power of the model with regard to event frequencies, scaling characteristics and propagation speed. On the other hand, the simulated patterns of single-cell calcium transients are qualitatively similar to that observed in a single focal plane, which suggests that this reduction seems to preserve main features of astrocyte dynamics, while it is worth to be investigated further at sub-cellular spatial scales in future work. A proof-of-concept possibility to use the proposed modeling framework to simulate Ca^{2+} signaling in 3D is presented in **Supplementary Video 3**.

A notable feature of simulated Ca^{2+} dynamics in this system is spontaneously emerging stable patterns in both initiation and propagation of calcium transients, in tune to the co-active neuronal and astrocytic cells or repeating sequences of neuronal activation reported in slices (Sasaki et al., 2011, 2014). In agreement with Brazhe et al. (2018) we observed morphology-dependent emergence of hotspots with persistent pacemaker-like activity, taking over control of the dynamics at larger scales. In single-cell templates these preferred initiation sites could lead to activation of either spatially confined microdomains or larger expanding Ca^{2+} areas, covering up to the whole cell. In multicellular systems we observed self-organized patterns of repeated calcium activity involving multiple cells. All cells in the template sharing the same equations and parameters, local differences in morphology of single astrocytes and geometry of astrocyte-to-astrocyte contacts favored initiation of multicellular Ca^{2+} waves in some cells, followed by repeated sequences of cell activation as the Ca^{2+} wave sweeped across the network. Excluding some cells from the original template caused dramatic reshaping of repeating activation patterns; removing or mashing up cell content in event initiation hotspots effectively reduced the number of active initiation sites and led to more stereotyped network activity. Our simulations showed that different cells in the network templates had different levels of activity and could develop patterns of Ca^{2+} events with preferred directionality. Recently, Wang et al. (2019) have demonstrated heterogeneity of individual neocortical astrocytes with respect to the properties of their Ca^{2+} activity. They also report a tendency for anatomical directionality during network-wide bursts of Ca^{2+} activity, accompanying locomotion and presumed to result from adrenergic input from locus coeruleus. In the light of the present study, it is interesting to ask, whether the experimentally observed heterogeneity of astrocytic signaling is defined by different patterning and levels of local synaptic activity or by individual astrocyte morphology, or the interplay of both? At a larger spatial scale it is interesting whether the observed population-wide directionality is a product of the afferentation delays from locus coeruleus or some previously unstudied anatomic directionality of astrocyte morphology? Going even further, it seems an exciting possibility that—if Ca^{2+} activity indeed affects LTP and Ca^{2+} activity patterns are shaped by astrocytic morphology template—some part of memory in the neural network can be engraved in the fingerprint of astrocyte morphology. We conclude that with the same parameter set, the specific dynamical regime and role of an individual cell within astrocytic network is to a large extent defined by its morphology and this may have implications for computational performance of the underlying neuronal network.

The concept of spatially segregated oscillator regarded in (Brazhe et al., 2018) attracts growing interest as a new class of bio-inspired dynamic models. For example, Vanag (2020) explores a model of spatially segregated Belousov-Zhabotinsky oscillating reaction, where the catalyst (analogous to calcium induced calcium release in Ca^{2+} models) is confined to small beads, whereas the rest chemical components of the reaction can diffuse freely, which leads to complex dynamical regimes and interaction between neighboring beads with immobilized catalyst. Another similar concept is that of volume transmission and intercellular communication via diffusing signaling molecules secreted by excitable cells (Sykova and Nicholson, 2008). There also appears to be an interesting connection between the self-organizing Ca^{2+} signaling in coupled astrocytes and the concept of "reaction-diffusion computing" or "chemical computing" based on oscillatory chemical (e.g., Belousov-Zhabotinsky) systems in coupled reactor volumes, e.g., microemulsions (Adamatzky et al., 2005; Epstein et al., 2012; Showalter and Epstein, 2015; Torbensen et al., 2017; Vanag, 2019; Proskurkin et al., 2020). It is conceivable that astrocytes can provide a substrate for such Ca^{2+}-based reaction-diffusion computing in parallel to, and organizing sparse network-based neuronal connectivity. Interestingly, it is common for self-organizing spatially distributed chemical systems to rely on inhibitory diffusive coupling (Li et al., 2015), while only excitatory coupling of neighboring astrocytes was modeled. Finding a mechanism for negative diffusive coupling, competing with the excitatory one can be an interesting outlook stemming from this analogy. Finally, it is inviting to believe that a combination of "analog" chemical computing approaches and "digital" neuronal ones, as well as a combination of graph-based and neighbor-based connectivity will inspire new algorithms for machine learning.

DATA AVAILABILITY STATEMENT

The model code and data, used for network spatial template generation and simulations are available for download at https://zenodo.org/record/4552726#.YDAz1nUzZQ8 (doi: 10.5281/zenodo.4552726).

AUTHOR CONTRIBUTIONS

DV: computer simulations, analysis of simulation results, figure preparation. AV: computer simulations, analysis of

simulation results, figure preparation, writing the manuscript. DP: program design and architecture for simulations, writing the manuscript. AB: conceptualization of the model, network generation algorithm, figure preparation, writing the manuscript. All authors contributed to the article and approved the submitted version.

ACKNOWLEDGMENTS

DP and AB acknowledge the support from the Russian Foundation for Basic Research, grant 19-515-55016, which covered the development of the modeling approach for spatial segmentation of inter-astrocyte functions. AV and AB acknowledge support from Russian Science Foundation, grant 17-74-20089, which covered development of the numeric algorithm for creation of realistic spatial templates, biophysical interpretation of the model, and the collective astrocyte signaling analysis. AB also acknowledges support from Interdisciplinary Scientific and Educational School of Moscow University Molecular Technologies of the Living Systems and Synthetic Biology, which covered 3D model simulations. DV acknowledges support from the Russian Foundation for Basic Research, grant 16-32-50221 for mobility of young scientists, which covered model interpretation in terms of non-linear dynamics, CUDA-based simulations of the model, and analysis of single-cell dynamics.

SUPPLEMENTARY MATERIAL

The Supplementary Material for this article can be found online at: https://www.frontiersin.org/articles/10.3389/fncel.2021.645068/full#supplementary-material

REFERENCES

Abbott, N. J., Pizzo, M. E., Preston, J. E., Janigro, D., and Thorne, R. G. (2018). The role of brain barriers in fluid movement in the CNS: is there a "glymphatic" system? *Acta Neuropathol*. 135, 387–407. doi: 10.1007/s00401-018-1812-4

Adamatzky, A., De Lacy Costello, B., and Asai, T. (2005). *Reaction-Diffusion Computers*. Amsterdam: Elsevier.

Agarwal, A., Wu, P. H., Hughes, E. G., Fukaya, M., Tischfield, M. A., Langseth, A. J., et al. (2017). Transient opening of the mitochondrial permeability. transition pore induces microdomain calcium transients in astrocyte processes. *Neuron* 93, 587.e7–605.e7. doi: 10.1016/j.neuron.2016.12.034

Allbritton, N. L., Meyer, T., and Stryer, L. (1992). Range of messenger action of calcium ion and inositol 1,4,5-trisphosphate. *Science* 258, 1812–1815. doi: 10.1126/science.1465619

Alvarellos-González, A., Pazos, A., and Porto-Pazos, A. (2012). Computational models of neuron-astrocyte interactions lead to improved efficacy in the performance of neural networks. *Comput. Math. Methods Med*. 2012:476324. doi: 10.1155/2012/476324

Araque, A., Carmignoto, G., Haydon, P. G., Oliet, S. H., Robitaille, R., and Volterra, A. (2014). Gliotransmitters travel in time and space. *Neuron* 81, 728–739. doi: 10.1016/j.neuron.2014.02.007

Arizono, M., Inavalli, V., Panatier, A., Pfeiffer, T., Angibaud, J., Levet, F., et al. (2020). Structural basis of astrocytic Ca. *Nat. Commun*. 11:1906. doi: 10.1038/s41467-020-15648-4

Ascoli, G. A., Donohue, D. E., and Halavi, M. (2007). Neuromorpho.org: a central resource for neuronal morphologies. *J. Neurosci*. 27, 9247–9251. doi: 10.1523/JNEUROSCI.2055-07.2007

Bazargani, N., and Attwell, D. (2016). Astrocyte calcium signaling: the third wave. *Nat. Neurosci*. 19, 182–189. doi: 10.1038/nn.4201

Bindocci, E., Savtchouk, I., Liaudet, N., Becker, D., Carriero, G., and Volterra, A. (2017). Three-dimensional Ca^{2+} imaging advances understanding of astrocyte biology. *Science* 356:eaai8185. doi: 10.1126/science.aai8185

Bojarskaite, L., Bjoernstad, D. M., Pettersen, K. H., Cunen, C., Hermansen, G. H., Aabjoersbraaten, K. S., et al. (2020). Astrocytic ca2+ signaling is reduced during sleep and is involved in the regulation of slow wave sleep. *Nat. Commun*. 11:3240. doi: 10.1038/s41467-020-17062-2

Brazhe, A., Mathiesen, C., and Lauritzen, M. (2013). Multiscale vision model highlights spontaneous glial calcium waves recorded by 2-photon imaging in brain tissue. *Neuroimage* 68, 192–202. doi: 10.1016/j.neuroimage.2012.11.024

Brazhe, A. R., Postnov, D. E., and Sosnovtseva, O. (2018). Astrocyte calcium signaling: interplay between structural and dynamical patterns. *Chaos* 28:106320. doi: 10.1063/1.5037153

Bushong, E. A., Martone, M. E., and Ellisman, M. H. (2004). Maturation of astrocyte morphology and the establishment of astrocyte domains during postnatal hippocampal development. *Int. J. Dev. Neurosci*. 22, 73–86. doi: 10.1016/j.ijdevneu.2003.12.008

Bushong, E. A., Martone, M. E., Jones, Y. Z., and Ellisman, M. H. (2002). Protoplasmic astrocytes in ca1 stratum radiatum occupy separate anatomical domains. *J. Neurosci*. 22, 183–192. doi: 10.1523/JNEUROSCI.22-01-00183.2002

Carmignoto, G. (2000). Reciprocal communication systems between astrocytes and neurones. *Prog. Neurobiol*. 62, 561–581. doi: 10.1016/S0301-0082(00)00029-0

Cornell-Bell, A. H., Finkbeiner, S. M., Cooper, M. S., and Smith, S. J. (1990). Glutamate induces calcium waves in cultured astrocytes: long-range glial signaling. *Science* 247, 470–473. doi: 10.1126/science.1967852

Cuntz, H., Forstner, F., Borst, A., and Hausser, M. (2010). One rule to grow them all: a general theory of neuronal branching and its practical application. *PLoS Comput. Biol*. 6:e1000877. doi: 10.1371/journal.pcbi.1000877

Dani, J. W., Chernjavsky, A., and Smith, S. J. (1992). Neuronal activity triggers calcium waves in hippocampal astrocyte networks. *Neuron* 8, 429–440. doi: 10.1016/0896-6273(92)90271-E

De Bock, M., Wang, N., Bol, M., Decrock, E., Ponsaerts, R., Bultynck, G., et al. (2012). Connexin 43 hemichannels contribute to cytoplasmic ca2+ oscillations by providing a bimodal ca2+-dependent ca2+ entry pathway. *J. Biol. Chem*. 287, 12250–12266. doi: 10.1074/jbc.M111.299610

De Pitta, M., Brunel, N., and Volterra, A. (2016). Astrocytes: Orchestrating synaptic plasticity? *Neuroscience*. 323, 43–61. doi: 10.1016/j.neuroscience.2015.04.001

De Pitta, M., Goldberg, M., Volman, V., Berry, H., and Ben-Jacob, E. (2009). Glutamate regulation of calcium and ip_3 oscillating and pulsating dynamics in astrocytes. *J. Biol. Phys*. 35, 383–411. doi: 10.1007/s10867-009-9155-y

De Young, G. W., and Keizer, J. (1992). A single-pool inositol 1,4,5-trisphosphate-receptor-based model for agonist-stimulated oscillations in Ca^{2+} concentration. *Proc. Natl. Acad. Sci. U.S.A*. 89, 9895–9899. doi: 10.1073/pnas.89.20.9895

Dickinson, G. D., Ellefsen, K. L., Dawson, S. P., Pearson, J. E., and Parker, I. (2016). Hindered cytoplasmic diffusion of inositol trisphosphate restricts its cellular range of action. *Sci. Signal*. 9:ra108. doi: 10.1126/scisignal.aag1625

Donohue, D. E., and Ascoli, G. A. (2008). A comparative computer simulation of dendritic morphology. *PLoS Comput. Biol*. 4:e1000089. doi: 10.1371/journal.pcbi.1000089

Dupont, G., Combettes, L., Bird, G. S., and Putney, J. W. (2011). Calcium oscillations. *Cold Spring Harb Perspect Biol*. 3:a004226. doi: 10.1101/cshperspect.a004226

Edwards, J. R., and Gibson, W. G. (2010). A model for ca2+ waves in networks of glial cells incorporating both intercellular and extracellular communication pathways. *J. Theor. Biol*. 263, 45–58. doi: 10.1016/j.jtbi.2009.12.002

Epstein, I. R., Vanag, V. K., Balazs, A. C., Kuksenok, O., Dayal, P., and Bhattacharya, A. (2012). Chemical oscillators in structured media. *Acc. Chem. Res.* 45, 2160–2168. doi: 10.1021/ar200251j

Falcke, M. (2004). Reading the patterns in living cells the physics of Ca^{2+} signaling. *Adv. Phys.* 53, 255–440. doi: 10.1080/00018730410001703159

Fiacco, T. A., and McCarthy, K. D. (2018). Multiple lines of evidence indicate that gliotransmission does not occur under physiological conditions. *J. Neurosci.* 38, 3–13. doi: 10.1523/JNEUROSCI.0016-17.2017

Genoud, C., Houades, V., Kraftsik, R., Welker, E., and Giaume, C. (2015). Proximity of excitatory synapses and astroglial gap junctions in layer IV of the mouse barrel cortex. *Neuroscience* 291, 241–249. doi: 10.1016/j.neuroscience.2015.01.051

Haas, B., Schipke, C. G., Peters, O., Söhl, G., Willecke, K., and Kettenmann, H. (2006). Activity-dependent ATP-waves in the mouse neocortex are independent from astrocytic calcium waves. *Cereb. Cortex* 16, 237–246. doi: 10.1093/cercor/bhi101

Hablitz, L. M., Plá, V., Giannetto, M., Vinitsky, H. S., Stæger, F. F., Metcalfe, T., et al. (2020). Circadian control of brain glymphatic and lymphatic fluid flow. *Nat. Commun.* 11, 1–11. doi: 10.1038/s41467-020-18115-2

Halassa, M. M., Fellin, T., Takano, H., Dong, J. H., and Haydon, P. G. (2007). Synaptic islands defined by the territory of a single astrocyte. *J. Neurosci.* 27, 6473–6477. doi: 10.1523/JNEUROSCI.1419-07.2007

Haydon, P. G. (2001). Glia: listening and talking to the synapse. *Nat. Rev. Neurosci.* 2, 185–193. doi: 10.1038/35058528

Henneberger, C., Papouin, T., Oliet, S. H., and Rusakov, D. A. (2010). Long-term potentiation depends on release of D-serine from astrocytes. *Nature* 463, 232–236. doi: 10.1038/nature08673

Hoogland, T. M., Kuhn, B., Göbel, W., Huang, W., Nakai, J., Helmchen, F., et al. (2009). Radially expanding transglial calcium waves in the intact cerebellum. *Proc. Natl. Acad. Sci. U.S.A.* 106, 3496–3501. doi: 10.1073/pnas.0809269106

Houades, V., Koulakoff, A., Ezan, P., Seif, I., and Giaume, C. (2008). Gap junction-mediated astrocytic networks in the mouse barrel cortex. *J. Neurosci.* 28, 5207–5217. doi: 10.1523/JNEUROSCI.5100-07.2008

Houades, V., Rouach, N., Ezan, P., Kirchhoff, F., Koulakoff, A., and Giaume, C. (2006). Shapes of astrocyte networks in the juvenile brain. *Neuron Glia Biol.* 2, 3–14. doi: 10.1017/S1740925X06000081

Iliff, J. J., Wang, M., Liao, Y., Plogg, B. A., Peng, W., Gundersen, G. A., et al. (2012). A paravascular pathway facilitates csf flow through the brain parenchyma and the clearance of interstitial solutes, including amyloid β. *Sci. Transl. Med.* 4:147ra111. doi: 10.1126/scitranslmed.3003748

Ingiosi, A. M., Hayworth, C. R., Harvey, D. O., Singletary, K. G., Rempe, M. J., Wisor, J. P., et al. (2020). A role for astroglial calcium in mammalian sleep and sleep regulation. *Curr. Biol.* 30, 4373–4383.e7. doi: 10.1016/j.cub.2020.08.052

Jensen, T. P., Zheng, K., Cole, N., Marvin, J. S., Looger, L. L., and Rusakov, D. A. (2019). Multiplex imaging relates quantal glutamate release to presynaptic Ca. *Nat. Commun.* 10:1414. doi: 10.1038/s41467-019-09216-8

Kang, M., and Othmer, H. (2009). Spatiotemporal characteristics of calcium dynamics in astrocytes. *Chaos* 19:037116. doi: 10.1063/1.3206698

Kirischuk, S., Heja, L., Kardos, J., and Billups, B. (2016). Astrocyte sodium signaling and the regulation of neurotransmission. *Glia* 64, 1655–1666. doi: 10.1002/glia.22943

Krizhevsky, A., Sutskever, I., and Hinton, G. E. (2012). "ImageNet classification with deep convolutional neural networks," in *Advances in Neural Information Processing Systems 25*, eds F. Pereira, C. J. C. Burges, L. Bottou, and K. Q. Weinberger (New York, NY: Curran Associates, Inc.), 1097–1105.

Kuga, N., Sasaki, T., Takahara, Y., Matsuki, N., and Ikegaya, Y. (2011). Large-scale calcium waves traveling through astrocytic networks *in vivo*. *J. Neurosci.* 31, 2607–2614. doi: 10.1523/JNEUROSCI.5319-10.2011

Lallouette, J., De Pitta, M., Ben-Jacob, E., and Berry, H. (2014). Sparse short-distance connections enhance calcium wave propagation in a 3D model of astrocyte networks. *Front. Comput. Neurosci.* 8:45. doi: 10.3389/fncom.2014.00045

Lee, H. S., Ghetti, A., Pinto-Duarte, A., Wang, X., Dziewczapolski, G., Galimi, F., et al. (2014). Astrocytes contribute to gamma oscillations and recognition memory. *Proc. Natl. Acad. Sci. U.S.A.* 111, E3343–E3352. doi: 10.1073/pnas.1410893111

Lenk, K., Satuvuori, E., Lallouette, J., Ladron-de Guevara, A., Berry, H., and Hyttinen, J. (2020). A computational model of interactions between neuronal and astrocytic networks: the role of astrocytes in the stability of the neuronal firing rate. *Front. Comput. Neurosci.* 13:92. doi: 10.3389/fncom.2019.00092

Li, N., Tompkins, N., Gonzalez-Ochoa, H., and Fraden, S. (2015). Tunable diffusive lateral inhibition in chemical cells. *Eur. Phys. J. E Soft. Matter* 38:18. doi: 10.1140/epje/i2015-15018-3

Li, Y., and Rinzel, J. (1994). Equations for insp3 receptor-mediated [ca2+]i oscillations derived from a detailed kinetic model: a hodgkin-huxley like formalism. *Proc. Natl. Acad. Sci. U.S.A.* 166, 461–473. doi: 10.1006/jtbi.1994.1041

Lind, B. L., Brazhe, A. R., Jessen, S. B., Tan, F. C., and Lauritzen, M. J. (2013). Rapid stimulus-evoked astrocyte ca2+ elevations and hemodynamic responses in mouse somatosensory cortex *in vivo*. *Proc. Natl. Acad. Sci. U.S.A.* 110, E4678–E4687. doi: 10.1073/pnas.1310065110

Manninen, T., and Havela, R., andLinne, M.-L. (2017). Reproducibility and comparability of computational models for astrocyte calcium excitability. *Front. Neuroinform.* 11:11. doi: 10.3389/fninf.2017.00011

Marina, N., Christie, I. N., Korsak, A., Doronin, M., Brazhe, A., Hosford, P. S., et al. (2020). Astrocytes monitor cerebral perfusion and control systemic circulation to maintain brain blood flow. *Nat. Commun.* 11, 1–9. doi: 10.1038/s41467-019-13956-y

Martone, M. E., Gupta, A., Wong, M., Qian, X., Sosinsky, G., Ludascher, B., et al. (2002). A cell-centered database for electron tomographic data. *J. Struct. Biol.* 138, 145–155. doi: 10.1016/S1047-8477(02)00006-0

Martone, M. E., Tran, J., Wong, W. W., Sargis, J., Fong, L., Larson, S., et al. (2008). The cell centered database project: an update on building community resources for managing and sharing 3D imaging data. *J. Struct. Biol.* 161, 220–231. doi: 10.1016/j.jsb.2007.10.003

Mathiesen, C., Brazhe, A., Thomsen, K., and Lauritzen, M. (2013). Spontaneous calcium waves in bergman glia increase with age and hypoxia and may reduce tissue oxygen. *J. Cereb. Blood Flow Metab.* 33, 161–169. doi: 10.1038/jcbfm.2012.175

McCauley, J. P., Petroccione, M. A., D'Brant, L. Y., Todd, G. C., Affinnih, N., Wisnoski, J. J., et al. (2020). Circadian modulation of neurons and astrocytes controls synaptic plasticity in hippocampal area Ca1. *Cell Rep.* 33:108255. doi: 10.1016/j.celrep.2020.108255

Mestre, H., Mori, Y., and Nedergaard, M. (2020). The brain's glymphatic system: Current controversies. *Trends Neurosci.* 43, 458–466. doi: 10.1016/j.tins.2020.04.003

Nadkarni, S., and Jung, P. (2004). Dressed neurons: modeling neural-glial interactions. *Phys. Biol.* 1, 35–41. doi: 10.1088/1478-3967/1/1/004

Nadkarni, S., and Jung, P. (2007). Modeling synaptic transmission of the tripartite synapse. *Phys. Biol.* 4:1. doi: 10.1088/1478-3975/4/1/001

Nagy, J. I., and Rash, J. E. (2003). Astrocyte and oligodendrocyte connexins of the glial syncytium in relation to astrocyte anatomical domains and spatial buffering. *Cell Commun. Adhes* 10, 401–406. doi: 10.1080/cac.10.4-6.401.406

Nedergaard, M. (1994). Direct signaling from astrocytes to neurons in cultures of mammalian brain cells. *Science* 263, 1768–1771. doi: 10.1126/science.8134839

O'Donnell, J., Ding, F., and Nedergaard, M. (2015). Distinct functional states of astrocytes during sleep and wakefulness: is norepinephrine the master regulator? *Curr. Sleep Med. Rep.* 1, 1–8. doi: 10.1007/s40675-014-0004-6

Oschmann, F., Berry, H., Obermayer, K., and Lenk, K. (2017a). From in silico astrocyte cell models to neuron-astrocyte network models: a review. *Brain Res. Bull.* 1–9. doi: 10.1016/j.brainresbull.2017.01.027

Oschmann, F., Mergenthaler, K., Jungnickel, E., and Obermayer, K. (2017b). Spatial separation of two different pathways accounting for the generation of calcium signals in astrocytes. *PLoS Comput. Biol.* 13:e1005377. doi: 10.1371/journal.pcbi.1005377

Otsu, Y., Couchman, K., Lyons, D. G., Collot, M., Agarwal, A., Mallet, J.-M., et al. (2015). Calcium dynamics in astrocyte processes during neurovascular coupling. *Nat. Neurosci.* 18, 210–218. doi: 10.1038/nn.3906

Parpura, V., Sekler, I., and Fern, R. (2016). Plasmalemmal and mitochondrial na(+) -ca(2+) exchange in neuroglia. *Glia* 64, 1646–1654. doi: 10.1002/glia.22975

Patrushev, I., Gavrilov, N., Turlapov, V., and Semyanov, A. (2013). Subcellular location of astrocytic calcium stores favors extrasynaptic neuron-astrocyte communication. *Cell Calcium* 54, 343–349. doi: 10.1016/j.ceca.2013.08.003

Pirttimaki, T. M., and Parri, H. R. (2013). Astrocyte plasticity: implications for synaptic and neuronal activity. *Neuroscientist* 19, 604–615. doi: 10.1177/1073858413504999

Polavaram, S., Gillette, T. A., Parekh, R., and Ascoli, G. A. (2014). Statistical analysis and data mining of digital reconstructions of dendritic morphologies. *Front. Neuroanat.* 8:138. doi: 10.3389/fnana.2014.00138

Poskanzer, K. E., and Yuste, R. (2016). Astrocytes regulate cortical state switching *in vivo*. *Proc. Natl. Acad. Sci. U.S.A.* 113, E2675–E2684. doi: 10.1073/pnas.1520759113

Postnov, D., Ryazanova, L., Brazhe, N., Brazhe, A., Maximov, G., Mosekilde, E., et al. (2008). Giant glial cell: new insight through mechanism-based modeling. *J. Biol. Phys.* 34, 441–457. doi: 10.1007/s10867-008-9070-7

Postnov, D. E., Brazhe, N. A., and Sosnovtseva, O. V. (2011). "Functional modeling of neural-glial interaction," in *Biosimulation in Biomedical Research, Health Care and Drug Development*, eds E. Mosekilde, O. Sosnovtseva, and A. Rostami-Hodjegan (Vienna: Springer), 133–151. doi: 10.1007/978-3-7091-0418-7_6

Postnov, D. E., Koreshkov, R. N., Brazhe, N. A., Brazhe, A. R., and Sosnovtseva, O. V. (2009). Dynamical patterns of calcium signaling in a functional model of neuron-astrocyte networks. *J. Biol. Phys.* 35, 425–445. doi: 10.1007/s10867-009-9156-x

Postnov, D. E., Postnov, D. D., and Zhirin, R. (2012). *The "AGEOM_CUDA" Software for Simulation of Oscillatory and Wave Processes in Two-Dimensional Media of Arbitrary Geometry on the Basis of High-Speed Parallel Computing on Graphics Processing Unit Technology CUDA*. RF registration certificate #2012610085 from 10.01.2012 (in russian), Moscow.

Postnov, D. E., Ryazanova, L. S., and Sosnovtseva, O. V. (2007). Functional modeling of neural-glial interaction. *Biosystems* 89, 84–91. doi: 10.1016/j.biosystems.2006.04.012

Proskurkin, I. S., Smelov, P. S., and Vanag, V. K. (2020). Experimental verification of an opto-chemical "neurocomputer". *Phys. Chem. Chem. Phys.* 22, 19359–19367. doi: 10.1039/D0CP01858A

Riera, J., Hatanaka, R., Ozaki, T., and Kawashima, R. (2011). Modeling the spontaneous Ca^{2+} oscillations in astrocytes: Inconsistencies and usefulness. *J. Integr. Neurosci.* 10, 439–473. doi: 10.1142/S0219635211002877

Rojas, H., Colina, C., Ramos, M., Benaim, G., Jaffe, E. H., Caputo, C., et al. (2007). Na^+ entry via glutamate transporter activates the reverse Na^+/Ca^{2+} exchange and triggers $Ca(i)^{2+}$-induced Ca^{2+} release in rat cerebellar type-1 astrocytes. *J. Neurochem.* 100, 1188–1202. doi: 10.1111/j.1471-4159.2006.04303.x

Ross, W. (2012). Understanding calcium waves and sparks in central neurons. *Nat. Rev. Neurosci.* 13, 157–168. doi: 10.1038/nrn3168

Rungta, R. L., Bernier, L. P., Dissing-Olesen, L., Groten, C. J., LeDue, J. M., Ko, R., et al. (2016). Ca^{2+} transients in astrocyte fine processes occur via Ca^{2+} influx in the adult mouse hippocampus. *Glia* 64, 2093–2103. doi: 10.1002/glia.23042

Sajedinia, Z., and Hélie, S. (2018). A new computational model for astrocytes and their role in biologically realistic neural networks. *Comput. Intell. Neurosci.* 2018, 1–10. doi: 10.1155/2018/3689487

Sasaki, T., Ishikawa, T., Abe, R., Nakayama, R., Asada, A., Matsuki, N., et al. (2014). Astrocyte calcium signalling orchestrates neuronal synchronization in organotypic hippocampal slices. *J. Physiol.* 592, 2771–2783. doi: 10.1113/jphysiol.2014.272864

Sasaki, T., Kuga, N., Namiki, S., Matsuki, N., and Ikegaya, Y. (2011). Locally synchronized astrocytes. *Cereb. Cortex* 21, 1889–1900. doi: 10.1093/cercor/bhq256

Savtchenko, L. P., Bard, L., Jensen, T. P., Reynolds, J. P., Kraev, I., Medvedev, N., et al. (2018). Disentangling astroglial physiology with a realistic cell model *in silico*. *Nat. Commun.* 9:3554. doi: 10.1038/s41467-018-05896-w

Savtchouk, I., and Volterra, A. (2018). Gliotransmission: beyond black-and-white. *J. Neurosci.* 38, 14–25. doi: 10.1523/JNEUROSCI.0017-17.2017

Semyachkina-Glushkovskaya, O., Postnov, D., and Kurths, J. (2018). Blood-brain barrier, lymphatic clearance, and recovery: Ariadne's thread in labyrinths of hypotheses. *Int. J. Mol. Sci.* 19:3818. doi: 10.3390/ijms19123818

Semyanov, A., Henneberger, C., and Agarwal, A. (2020). Making sense of astrocytic calcium signals - from acquisition to interpretation. *Nat. Rev. Neurosci.* 21, 551–564. doi: 10.1038/s41583-020-0361-8

Serrano, A., Haddjeri, N., Lacaille, J. C., and Robitaille, R. (2006). Gabaergic network activation of glial cells underlies hippocampal heterosynaptic depression. *J. Neurosci.* 26, 5370–5382. doi: 10.1523/JNEUROSCI.5255-05.2006

Shigetomi, E., Tong, X., Kwan, K. Y., Corey, D. P., and Khakh, B. S. (2011). Trpa1 channels regulate astrocyte resting calcium and inhibitory synapse efficacy through gat-3. *Nat. Neurosci.* 15, 70–80. doi: 10.1038/nn.3000

Showalter, K., and Epstein, I. R. (2015). From chemical systems to systems chemistry: patterns in space and time. *Chaos* 25:097613. doi: 10.1063/1.4918601

Shuai, J. W., and Jung, P. (2002). Stochastic properties of ca(2+) release of inositol 1,4,5-trisphosphate receptor clusters. *Biophys. J.* 83, 87–97. doi: 10.1016/S0006-3495(02)75151-5

Shuai, J. W., and Jung, P. (2003). Selection of intracellular calcium patterns in a model with clustered ca2+ release channels. *Phys. Rev. E Stat. Nonlin. Soft Matter Phys. 67(3 Pt* 1):031905. doi: 10.1103/PhysRevE.67.031905

Simard, P. Y., Steinkraus, D., and Platt, J. C. (2003). "Best practices for convolutional neural networks applied to visual document analysis," in *International Conference on Document Analysis and Recognition* (Washington, DC: IEEE Computer Society), 958–962.

Sims, R. E., Butcher, J. B., Parri, H. R., and Glazewski, S. (2015). Astrocyte and neuronal plasticity in the somatosensory system. *Neural Plast* 2015:732014. doi: 10.1155/2015/732014

Smith, I. F., Wiltgen, S. M., Shuai, J., and Parker, I. (2009). Ca^{2+} puffs originate from preestablished stable clusters of inositol trisphosphate receptors. *Sci. Signal.* 2:ra77. doi: 10.1126/scisignal.2000466

Sneyd, J., Charles, A. C., and Sanderson, M. J. (1994). A model for the propagation of intercellular calcium waves. *Am. J. Physiol. 266(1 Pt 1):C293–C302*. doi: 10.1152/ajpcell.1994.266.1.C293

Softky, W. R., and Koch, C. (1993). The highly irregular firing of cortical cells is inconsistent with temporal integration of random EPSPs. *J. Neurosci.* 13, 334–350. doi: 10.1523/JNEUROSCI.13-01-00334.1993

Stobart, J. L., Ferrari, K. D., Barrett, M., Gluck, C., Stobart, M. J., Zuend, M., et al. (2018). Cortical circuit activity evokes rapid astrocyte calcium signals on a similar timescale to neurons. *Neuron* 98, 726.e4–735.e4. doi: 10.1016/j.neuron.2018.03.050

Sykova, E., and Nicholson, C. (2008). Diffusion in brain extracellular space. *Physiol. Rev.* 88, 1277–1340. doi: 10.1152/physrev.00027.2007

Taufiq-Ur-Rahman, Skupin, A., Falcke, M., and Taylor, C. W. (2009). Clustering of InsP3 receptors by InsP3 retunes their regulation by InsP3 and Ca^{2+}. *Nature* 458, 655–659. doi: 10.1038/nature07763

Tewari, S. G., and Majumdar, K. K. (2012). A mathematical model of the tripartite synapse: astrocyte-induced synaptic plasticity. *J. Biol. Phys.* 38, 465–496. doi: 10.1007/s10867-012-9267-7

Tong, X., Shigetomi, E., Looger, L. L., and Khakh, B. S. (2013). Genetically encoded calcium indicators and astrocyte calcium microdomains. *Neuroscientist* 19, 274–291. doi: 10.1177/1073858412468794

Torbensen, K., Rossi, F., Ristori, S., and Abou-Hassan, A. (2017). Chemical communication and dynamics of droplet emulsions in networks of belousov-zhabotinsky micro-oscillators produced by microfluidics. *Lab Chip* 17, 1179–1189. doi: 10.1039/C6LC01583B

Ullah, G., Jung, P., and Cornell-Bell, A. (2006). Anti-phase calcium oscillations in astrocytes via inositol (1, 4, 5)-trisphosphate regeneration. *Cell Calcium* 39, 197–208. doi: 10.1016/j.ceca.2005.10.009

Vanag, V. K. (2019). Hierarchical network of pulse coupled chemical oscillators with adaptive behavior: chemical neurocomputer. *Chaos* 29:083104. doi: 10.1063/1.5099979

Vanag, V. K. (2020). Size- and position-dependent bifurcations of chemical microoscillators in confined geometries. *Chaos* 30:013112. doi: 10.1063/1.5126404

Verkhratsky, A., and Nedergaard, M. (2018). Physiology of astroglia. *Physiol. Rev.* 98, 239–389. doi: 10.1152/physrev.00042.2016

Verkhratsky, A., Rodriguez, J. J., and Parpura, V. (2012). Calcium signalling in astroglia. *Mol. Cell Endocrinol.* 353, 45–56. doi: 10.1016/j.mce.2011.08.039

Volterra, A., Liaudet, N., and Savtchouk, I. (2014). Astrocyte Ca^{2+} signalling: an unexpected complexity. *Nat. Rev. Neurosci.* 15, 327–335. doi: 10.1038/nrn3725

Wallach, G., Lallouette, J., Herzog, N., De Pitta, M., Ben Jacob, E., Berry, H., et al. (2014). Glutamate mediated astrocytic filtering of neuronal activity. *PLoS Comput. Biol.* 10:e1003964. doi: 10.1371/journal.pcbi.1003964

Wang, Y., DelRosso, N. V., Vaidyanathan, T. V., Cahill, M. K., Reitman, M. E., Pittolo, S., et al. (2019). Accurate quantification of astrocyte and neurotransmitter fluorescence dynamics for single-cell and population-level physiology. *Nat. Neurosci.* 22, 1936–1944. doi: 10.1038/s41593-019-0492-2

Wolff, J. R., Stuke, K., Missler, M., Tytko, H., Schwarz, P., Rohlmann, A., et al. (1998). Autocellular coupling by gap junctions in cultured astrocytes: a new view on cellular autoregulation during process formation. *Glia* 24, 121–140. doi: 10.1002/(SICI)1098-1136(199809)24:1<121::AID-GLIA12>3.0.CO;2-T

Wu, Y.-W., Gordleeva, S., Tang, X., Shih, P.-Y., Dembitskaya, Y., and Semyanov, A. (2018). Morphological profile determines the frequency of spontaneous calcium events in astrocytic processes. *bioRxiv*. 67, 246–262. doi: 10.1101/410076

Wu, Y. W., Tang, X., Arizono, M., Bannai, H., Shih, P. Y., Dembitskaya, Y., et al. (2014). Spatiotemporal calcium dynamics in single astrocytes and its modulation by neuronal activity. *Cell Calcium* 55, 119–129. doi: 10.1016/j.ceca.2013.12.006

Xie, L., Kang, H., Xu, Q., Chen, M. J., Liao, Y., Thiyagarajan, M., et al. (2013). Sleep drives metabolite clearance from the adult brain. *Science* 342, 373–377. doi: 10.1126/science.1241224

Yule, D. I., Stuenkel, E., and Williams, J. A. (1996). Intercellular calcium waves in rat pancreatic acini: mechanism of transmission. *Am. J. Physiol.* 271(4 Pt 1), C1285–C1294. doi: 10.1152/ajpcell.1996.271.4.C1285

Conflict of Interest: The authors declare that the research was conducted in the absence of any commercial or financial relationships that could be construed as a potential conflict of interest.

frontiers in Cellular Neuroscience

ORIGINAL RESEARCH
published: 31 March 2021
doi: 10.3389/fncel.2021.631485

Modeling Working Memory in a Spiking Neuron Network Accompanied by Astrocytes

Susanna Yu. Gordleeva[1,2*], *Yuliya A. Tsybina*[1], *Mikhail I. Krivonosov*[1], *Mikhail V. Ivanchenko*[1], *Alexey A. Zaikin*[1,3,4], *Victor B. Kazantsev*[1,2,5] *and Alexander N. Gorban*[1,6]

[1] *Scientific and Educational Mathematical Center "Mathematics of Future Technology," Lobachevsky State University of Nizhny Novgorod, Nizhny Novgorod, Russia,* [2] *Neuroscience and Cognitive Technology Laboratory, Center for Technologies in Robotics and Mechatronics Components, Innopolis University, Innopolis, Russia,* [3] *Center for Analysis of Complex Systems, Sechenov First Moscow State Medical University, Sechenov University, Moscow, Russia,* [4] *Institute for Women's Health and Department of Mathematics, University College London, London, United Kingdom,* [5] *Neuroscience Research Institute, Samara State Medical University, Samara, Russia,* [6] *Department of Mathematics, University of Leicester, Leicester, United Kingdom*

OPEN ACCESS

Edited by:
Yu-Wei Wu,
Academia Sinica, Taiwan

Reviewed by:
Randy Franklin Stout,
New York Institute of Technology, United States
Mahmood Amiri,
Kermanshah University of Medical Sciences, Iran
Jun Ma,
Lanzhou University of Technology, China

****Correspondence:***
Susanna Yu. Gordleeva
gordleeva@neuro.nnov.ru

Specialty section:
This article was submitted to Non-Neuronal Cells, a section of the journal Frontiers in Cellular Neuroscience

Received: *20 November 2020*
Accepted: *04 March 2021*
Published: *31 March 2021*

Citation:
Gordleeva SY, Tsybina YA, Krivonosov MI, Ivanchenko MV, Zaikin AA, Kazantsev VB and Gorban AN (2021) Modeling Working Memory in a Spiking Neuron Network Accompanied by Astrocytes. Front. Cell. Neurosci. 15:631485. doi: 10.3389/fncel.2021.631485

We propose a novel biologically plausible computational model of working memory (WM) implemented by a spiking neuron network (SNN) interacting with a network of astrocytes. The SNN is modeled by synaptically coupled Izhikevich neurons with a non-specific architecture connection topology. Astrocytes generating calcium signals are connected by local gap junction diffusive couplings and interact with neurons via chemicals diffused in the extracellular space. Calcium elevations occur in response to the increased concentration of the neurotransmitter released by spiking neurons when a group of them fire coherently. In turn, gliotransmitters are released by activated astrocytes modulating the strength of the synaptic connections in the corresponding neuronal group. Input information is encoded as two-dimensional patterns of short applied current pulses stimulating neurons. The output is taken from frequencies of transient discharges of corresponding neurons. We show how a set of information patterns with quite significant overlapping areas can be uploaded into the neuron-astrocyte network and stored for several seconds. Information retrieval is organized by the application of a cue pattern representing one from the memory set distorted by noise. We found that successful retrieval with the level of the correlation between the recalled pattern and ideal pattern exceeding 90% is possible for the multi-item WM task. Having analyzed the dynamical mechanism of WM formation, we discovered that astrocytes operating at a time scale of a dozen of seconds can successfully store traces of neuronal activations corresponding to information patterns. In the retrieval stage, the astrocytic network selectively modulates synaptic connections in the SNN leading to successful recall. Information and dynamical characteristics of the proposed WM model agrees with classical concepts and other WM models.

Keywords: spiking neural network, astrocyte, neuron-astrocyte interaction, working memory, delayed activity

1. INTRODUCTION

In neuroscience, the understanding of the functional role of astrocytes in the central nervous system (CNS) is still open to debate (Savtchouk and Volterra, 2018), but now there is accumulating evidence demonstrating the involvement of astrocytes in local synaptic plasticity and the coordination of network activity (Durkee and Araque, 2019), and as a result in information processing and memory encoding (Santello et al., 2019). Astrocytes sense synaptic activity and respond to it with the transient elevation of intracellular Ca^{2+} concentration (lasting from hundreds of a millisecond to dozens of seconds). Such Ca^{2+} signals in astrocytes have been observed in different brain regions and also in the cortex, appearing there in response to mechanic sensory stimulation (Wang X. et al., 2006; Takata et al., 2011; Stobart et al., 2018) and visual sensory stimulation (Schummers et al., 2008; Chen et al., 2012; Perea et al., 2014). Ca^{2+} activation can trigger the release of gliotransmitters from astrocytes, which in turn affect the dynamics of presynaptic and postsynaptic terminals resulting in modulations of synaptic transmission (Araque et al., 2014). The gliotransmitter-mediated synaptic modulation lasts from a dozen seconds (Jourdain et al., 2007; Perea et al., 2014) to a dozen minutes (Stellwagen and Malenka, 2006; Perea and Araque, 2007; Navarrete et al., 2012) contributing to both short- and long-term synaptic plasticity.

Obviously, there is a qualitative coincidence between the time scales of astrocyte-mediated synaptic modulation and the working memory (WM) timings during decision making. Based on this and the other following facts of astrocytes participation in neuronal signaling, we hypothesized that astrocytes may be involved in WM formation. In particular, recent *in vivo* studies have shown the participation of astrocytes in the synchronization of certain cortical network activities (Takata et al., 2011; Chen et al., 2012; Paukert et al., 2014; Perea et al., 2014), cognitive functions, and behaviors (Poskanzer and Yuste, 2016; Sardinha et al., 2017). Experimental evidence shows that astrocyte pathology in the medium prefrontal cortex (PFC) impairs WM and learning functions (Lima et al., 2014), increasing astrocyte density enhances short-term memory performance (Luca et al., 2020), and recognition memory performance and disruption of WM depend on gliotransmitter release from astrocytes in the hippocampus (Han et al., 2012; Robin et al., 2018). Despite these numerous experimental insights of the contribution of astrocytes to synaptic modulations in neuronal signaling, the possible role of astrocytes in information processing and learning is still a subject of discussion (Kanakov et al., 2019; Kastanenka et al., 2019).

Considering the significance of WM processes and the challenge of finding alternative mechanisms and experimental evidence of the astrocytic role in information processing in CNS, it is interesting to study astrocyte-induced modulation of synaptic transmission in WM organization. Specifically, we assume that the potentiation of excitatory synapses induced by Ca^{2+} elevation-mediated glutamate release from astrocytes (Fellin et al., 2004; Perea and Araque, 2007; Navarrete and Araque, 2008, 2010; Chen et al., 2012) plays an essential role in WM. To test this hypothesis, we developed a novel neuron-astrocyte network model for visual WM to reflect experimental data on the structure, connectivity, and neurophysiology of the neuron-astrocytic interaction in underlying cortical tissue. We focused on the implementation of a multi-item WM task in a delayed matching to sample (DMS) framework representing a classical neuropsychological paradigm (Miller et al., 1996). During the experiment, a test animal was given a sample stimulus, which it had to remember for several seconds until it could begin executing a certain task. For example, a stimulus was followed by a sequence of several test stimuli and the animal was rewarded for indicating when one of the test stimuli. matched the original sample. The DMS paradigm was previously studied using a recurrent neural network (Brunel and Wang, 2001; Amit, 2003; Amit et al., 2013; Fiebig and Lansner, 2016). The novelty of our model is that we associate memory with item-specific patterns of astrocyte-induced enhancement of excitatory synaptic transmission. We present a new case of how the biologically relevant neuron-astrocyte network model implements loading, storage, and cued retrieval of multiple items with significant overlapping. The memory items are encoded in neuronal populations in the form of discrete high-frequency bursts rather than persistent spiking.

In this paper, we review some related works (section 2), describe the proposed model and methods in detail (section 3), present the results (section 4), and finally, we conclude this work in section 5.

2. RELATED WORK

The concept of WM implies the ability to temporarily store and process information in goal-directed behavior. WM is crucial in the generation of higher cognitive functions for both humans and other animals (Baddeley, 1986, 2012; Conway et al., 2003). In primates, visual WM has been studied in delay tasks, such as DMS, which require a memory to be held during a brief delay period lasting for several seconds (Miller et al., 1996). Recordings in the monkeys' PFCs during the delay task showed that some neurons displayed persistent and stimulus-specific delay-period activity (Fuster and Alexander, 1971; Funahashi et al., 1989; Shafi et al., 2007; Barak et al., 2010; Funahashi, 2017). Delay persistent activity is considered the neural correlate of WM (Goldman-Rakic, 1995; Constantinidis et al., 2018).

The classical theoretical memory models suggest that an information item can be stored with sustained neural activity which emerges via activation of stable activity patterns in the network (e.g., attractors) (Hopfield, 1982; Amit, 1995; Wang, 2001; Wimmer et al., 2014) recently reviewed by Zylberberg and Strowbridge (2017) and Chaudhuri and Fiete (2016). These WM models propose that the generation of persistent activity can be the result of an intrinsic property of the neurons [including the generation of the bistability mediated by the voltage-gated inward currents (Kass and Mintz, 2005) and Ca^{2+}-triggered long-term changes in neuronal excitability (Fransén et al., 2006)] and can be induced by the connectivity within the neural circuit with feed-forward (Ganguli and Latham, 2009; Goldman, 2009) or recurrent architecture (Koulakov et al., 2002; Kilpatrick et al.,

2013). In such models, memory recall is impossible from a silent inactive state. For many WM models of persistent activity based on recurrent connectivity, small deviations in the network structure destroy the persistence. Moreover, a spiking form of information storage is energetically unfavorable because of the high metabolic value of action potentials (Attwell and Laughlin, 2001).

In theoretical studies, a concept of oscillatory sub-cycles storing 7 ± 2 in oscillatory neuronal networks was proposed by Lisman and Idiart (1995). Other models employ oscillatory activity of spiking neuron networks after depolarization to memorize a set of information patterns at different phases of rhythmic oscillations (Klinshov and Nekorkin, 2008; Borisyuk et al., 2013).

Recently, the persistent activity hypothesis has been undergoing critical reviews (Lundqvist et al., 2018) based on the experimental findings in rodents and primates showing that the robust persistent activity does not last for the entire delay period, but rather sequential neuronal firing is observed during the delay period suggesting that the PFC neural network may support WM based on dynamically changing neuronal activity (Fujisawa et al., 2008; Lundqvist et al., 2016; Runyan et al., 2017; Park et al., 2019; Ozdemir et al., 2020). Despite the considerable progress that has been made in identifying the neurophysiological mechanisms contributing to WM in mammals (D'Esposito and Postle, 2015; Zylberberg and Strowbridge, 2017), the ongoing debate focuses on the generation mechanisms of the delay period activity that appears to underlie WM (Constantinidis et al., 2018; Sreenivasan and D'Esposito, 2019).

Currently, one of the recognized experimentally based hypotheses of the WM mechanism underlining the delay activity (not necessarily persistent) is the synaptic plasticity in the PFC (Tsodyks and Markram, 1997; Hempel et al., 2000; Wang Y. et al., 2006; Erickson et al., 2010). Synaptic plasticity implies a rapid regulation of the strengths of individual synapses in response to specific patterns of correlated synaptic activity and contributes to the activity-dependent refinement of neural circuitry. Following these findings, alternative synaptic-based WM models have been proposed (Mongillo et al., 2008; Barak and Tsodyks, 2014; Koutsikou et al., 2018; Manohar et al., 2019). In these models, memory items are stored by stimulus-specific patterns of synaptic facilitation in a neuronal circuit. Synaptic plasticity does not require neurons to show a persistent activity for the entire period of the memory task, which results in a robust and more metabolically efficient mechanism. Some synaptic WM models based on short-term non-associative synaptic facilitation (Mongillo et al., 2008; Lundqvist et al., 2011; Mi et al., 2017) allow for reading out and refreshing existing representations maintained in the synaptic structure. Others have proposed fast Hebbian activity-dependent synaptic plasticity (Sandberg et al., 2003; Fiebig and Lansner, 2016) for encoding and maintenance of novel associations.

Despite the numerous models describing the astrocytic impact on signaling in neuronal networks (see Oschmann et al., 2018 for a recent review) (Makovkin et al., 2020), there are few attempts to theoretically investigate the role of astrocyte-induced modulation of synaptic transmission in memory formation. Shen and Wilde (2007) demonstrate one of the first results of simulating the coupling of a Hopfield neural network, astrocytes, and cerebrovascular activity. Although this is not yet a true biophysical model, the results suggest that a modification of the synapse strengths allows the neuronal firing and the cerebrovascular flow to be compatible on a meso-scale; with astrocyte signaling added, limit cycles exist in the coupled networks. Tewari and Parpura (2013) and Wade et al. (2011) study how bidirectional coupling between astrocytes and neurons in small neuron-astrocyte ensembles mediates learning and dynamic coordination in the brain. A recent interesting theoretical study proposes a self-repairing spiking astrocyte-neural network combined with a novel learning rule based on the spike-timing-dependent plasticity and Bienenstock, Cooper, and Munro learning rule (Liu et al., 2019).

3. MATERIALS AND METHODS

3.1. Neuron-Astrocyte Network Model

Even though the balance of inhibition and excitation was shown to play an important role in WM stabilization and can influence WM capacity (Barak and Tsodyks, 2014), we focus on the properties of astrocyte-induced modulation of excitatory synaptic transmission in the PFC. We take spiking neuronal network with dimension $W \times H$ consisting of synaptically coupled excitatory neurons formed by the Izhikevich model (Izhikevich, 2003). Neurons in the network are connected randomly with the connection length determined by the exponential distribution.

It has been experimentally estimated that there is some overlap in the spatial territories occupied by individual astrocytes in the cortex (Halassa et al., 2007). An individual cortical astrocyte contacts on average 4-8 neuronal somata and 300–600 neuronal dendrites (Halassa et al., 2007). A cortical astrocyte has a "bushy" ramified structure in fine perisynaptic processes, which cover most of the neuronal membranes within their reach (Allen and Eroglu, 2017). This allows the astrocyte to integrate and coordinate a unique volume of synaptic activity. Following the experimental data, the astrocytic network compartment of our model is organized into a two-dimensional square lattice with only nearest-neighbor connectivity. Each astrocyte interacts with the neuronal ensemble of N_a neurons with some overlapping. We consider bidirectional communication between neuronal and astrocytic networks. The scheme of the network topology is shown in **Figure 1**.

Model equations are integrated using the Runge-Kutta fourth-order method with a fixed time step, $\Delta t = 0.1$ ms. A detailed list of model parameters and values can be found in **Table 1** (neural network model), **Table 2** (astrocytic network parameters), **Table 3** (neuron-astrocytic interaction parameters), and **Table 4** (stimulation and recall testing). The code is available at: https://github.com/altergot/neuro-astro-network.

3.2. Neuronal Network

There are many available biophysical models of neuronal membrane potential dynamics (Morris and Lecar, 1981; Hodgkin and Huxley, 1990; Xu et al., 2020a,b; Zhang et al., 2020). For our purpose we chose the Izhikevich model as it is quite functional and computationally effective for network simulations

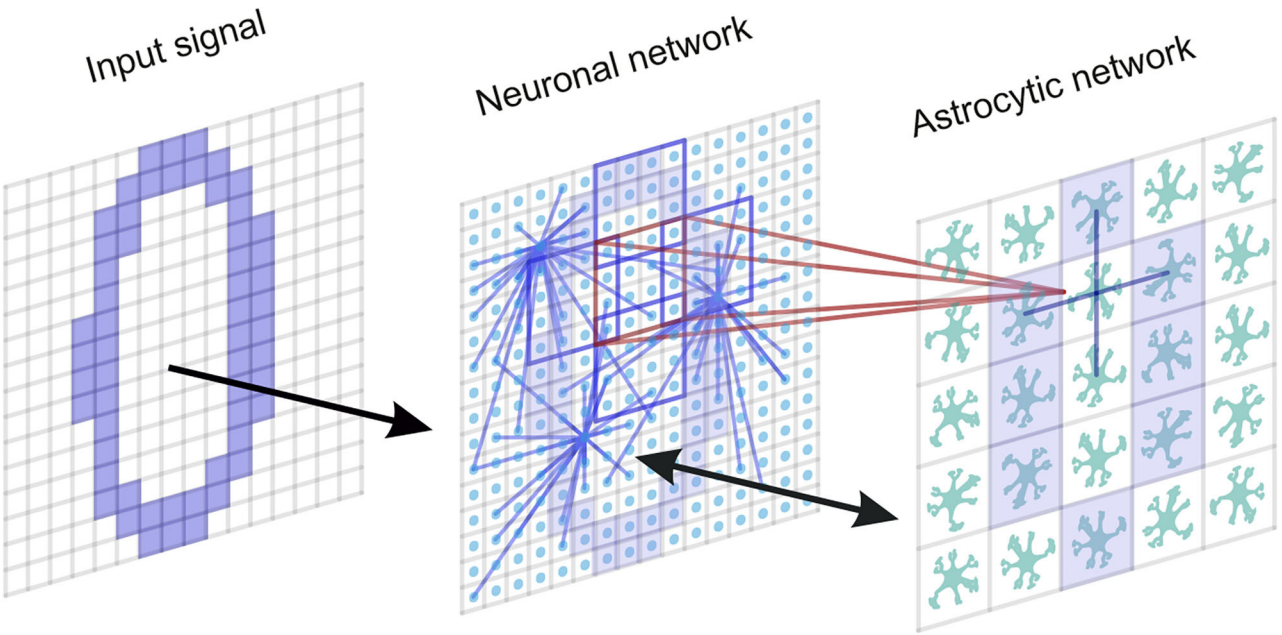

FIGURE 1 | A neuron-astrocyte network topology. The neuron-astrocyte network consists of two interacting layers: a neural network layer and an astrocytic layer. The neuronal network with dimension $W \times H$ (79 × 79) consists of synaptically coupled excitatory neurons modeled by the Izhikevich neuron. Neurons in the network are connected randomly. The astrocytic network consists of diffusely connected astrocytes with dimension $M \times N$ (26 × 26). Blue lines show connections between elements in each layer. We consider the bidirectional interaction between the neuronal and astrocytic layers. Each astrocyte is interconnected with a neuronal ensemble of $N_a = 16$ neurons with dimensions 4 × 4 (red lines) with overlapping in one row (violet lines). The input signal is fed to the neural network.

TABLE 1 | Neural network parameters Izhikevich (2003), Kazantsev and Asatryan (2011).

Parameter	Parameter description	Value
$W \times H$	Neural network grid size	79 × 79
a	Time scale of the recovery variable	0.1
b	Sensitivity of the recovery variable to the sub-threshold fluctuations of the membrane potential	0.2
c	After-spike reset value of the membrane potential	−65 mV
d	After-spike reset value of the recovery variable	2
η	Synaptic weight without astrocytic influence	0.025
E_{syn}	Synaptic reversal potential for excitatory synapses	0 mV
k_{syn}	Slope of the synaptic activation function	0.2 mV
N_{out}	Number of output connections per each neuron	40
λ	Rate of the exponential distribution of synaptic connections distance	5

(Izhikevich, 2003):

$$\begin{aligned} \frac{dV^{(i,j)}}{dt} &= 0.04V^{(i,j)^{(2)}} + 5V^{(i,j)} - U^{(i,j)} + 140 + I_{\text{app}}^{(i,j)} + I_{\text{syn}}^{(i,j)}; \\ \frac{dU^{(i,j)}}{dt} &= a(bV^{(i,j)} - U^{(i,j)}); \end{aligned} \tag{1}$$

with the auxiliary after-spike resetting

$$\text{if } V^{(i,j)} \geq 30 \text{ mV, then } \begin{cases} V^{(i,j)} \leftarrow c \\ U^{(i,j)} \leftarrow U^{(i,j)} + d, \end{cases} \tag{2}$$

where the superscripts ($i = 1, \ldots, 79, j = 1, \ldots, 79$) correspond to a neuronal index, the transmembrane potential V is given in mV and time t in ms. The applied currents $I_{\text{app}}^{(i,j)}$ simulate the input signal. Neurons receive a number of synaptic currents from other presynaptic neurons in the network, $N_{in}^{(i,j)}$, which are summed at the membrane according to the following equation (Kazantsev and Asatryan, 2011; Esir et al., 2018):

$$I_{\text{syn}}^{(i,j)} = \sum_{k=1}^{N_{in}^{(i,j)}} \frac{g_{\text{syn}}^{(i,j)}(E_{\text{syn}} - V^{(i,j)})}{1 + \exp(\frac{-V_{\text{pre}}^{k}}{k_{\text{syn}}})}; \tag{3}$$

Parameter $g_{\text{syn}}^{(i,j)}$ describes the synaptic weight, $g_{\text{syn}}^{(i,j)} = \eta + \nu_{Ca}^{(m,n)}$. The astrocyte (m, n) modulates the synaptic currents of the neuron (i, j). The variable ν_{Ca} introduces the astrocyte-induced modulation of synaptic strength and will be discussed below. In this study, we concentrate exclusively on the role of astrocyte-induced modulation of synaptic transmission and did not include mechanisms of synaptic plasticity in the model. The synaptic reversal potential for excitatory synapses is taken with $E_{\text{syn}} = 0$. V_{pre} denotes the membrane potential of the presynaptic neuron. For simplicity, we neglect the axonal and synaptic delays.

TABLE 2 | Astrocytic network parameters Ullah et al. (2006).

Parameter	Parameter description	Value
$M \times N$	Astrocytic network grid size	26 × 26
c_0	Total Ca^{2+} in terms of cytosolic vol	2.0 μM
c_1	(ER vol)/(cytosolic vol)	0.185
v_1	Max Ca^{2+} channel flux	6 s^{-1}
v_2	Ca^{2+} leak flux constant	0.11 s^{-1}
v_3	Max Ca^{2+} uptake	2.2 μM s^{-1}
v_6	Maximum rate of activation-dependent calcium influx	0.2 μM s^{-1}
k_1	Rate constant of calcium extrusion	0.5 s^{-1}
k_2	Half-saturation constant for agonist-dependent calcium entry	1 μM
k_3	Activation constant for ATP-Ca^{2+} pump	0.1 μM
d_1	Dissociation constant for IP_3	0.13 μM
d_2	Dissociation constant for Ca^{2+} inhibition	1.049 μM
d_3	Receptor dissociation constant for IP_3	943.4 nM
d_5	Ca^{2+} activation constant	82 nM
α		0.8
v_4	Max rate of IP_3 production	0.3 μM s^{-1}
$1/\tau_r$	Rate constant for loss of IP_3	0.14 s^{-1}
$IP_3{}^*$	Steady state concentration of IP_3	0.16 μM
k_4	Dissociation constant for Ca^{2+} stimulation of IP_3 production	1.1 μM
d_{Ca}	Ca^{2+} diffusion rate	0.05 s^{-1}
d_{IP_3}	IP_3 diffusion rate	0.1 s^{-1}

TABLE 3 | Neuron-astrocytic interaction parameters Gordleeva et al. (2012).

Parameter	Parameter description	Value
N_a	Number of neurons interacting with one astrocyte	16, 4 × 4
α_{glu}	Glutamate clearance constant	10 s^{-1}
k_{glu}	Efficacy of the glutamate release	600 μM s^{-1}
A_{glu}	Rate of IP_3 production through glutamate	5 μM s^{-1}
t_{glu}	Duration of IP_3 production through glutamate	60 ms
G_{thr}	Threshold concentration of glutamate for IP_3 production	0.7
F_{act}	Fraction of synchronously spiking neurons required for the emergence of Ca^{2+} elevation	0.5
F_{astro}	Fraction of synchronously spiking neurons required for the emergence of astrocytic modulation of synaptic transmission	0.375
ν^*_{Ca}	Strength of the astrocyte-induced modulation of synaptic weight	0.5
$[Ca^{2+}]_{thr}$	Threshold concentration of Ca^{2+} for the astrocytic modulation of the synapse	0.15 μM
τ_{astro}	Duration of the astrocyte-induced modulation of the synapse	250 ms

The architecture of synaptic connections between neurons is non-specific (random) with the following parameters. The number of output connections per each neuron is fixed at $N_{out} = 40$. Each neuron innervates N_{out} local postsynaptic targets, which are randomly chosen in polar coordinates. The distances between neurons r are determined according to the exponential distribution $f_R(r)$ and the angles ϕ are chosen from the uniform distribution in the range $[0; 2\pi]$:

$$f_R(r) = \begin{cases} 1/\lambda \exp(-(1/\lambda)r), r \geq 0, \\ 0, r < 0. \end{cases} \quad (4)$$

In this way, the coordinates of postsynaptic neurons are computed as follows:

$$x_{post} = \lceil x_{pre} + r\cos(\phi) \rceil, y_{post} = \lceil y_{pre} + r\sin(\phi) \rceil, \quad (5)$$

where x_{pre}, y_{pre} denote the coordinates of the presynaptic neuron, x_{post}, y_{post} are coordinates of the postsynaptic neurons. Coordinates are picked repeatedly in case of a duplicated connection.

TABLE 4 | Stimulation protocol and recall testing parameters.

Parameter	Parameter description	Value
f_{bg}	Background activity rate	1.5 Hz
A_{stim}	Stimulation amplitude	10 μA
t_{stim}	Stimulation duration	200 ms
	Noise level in sample	5%
A_{test}	Cue stimulation amplitude	8 μA
t_{test}	Cue stimulation length	150 ms
	Noise level in cue	20%

3.3. Astrocytic Network

In the model, we try to implement the biologically plausible organization of the astrocytic network and neuron-astrocyte interaction. The astrocytic network is configured in the form of a two-dimensional square lattice with dimension $M \times N$. Cortical astrocytes are coupled via Cx43 gap junctions mostly permeable to inositol 1,4,5-trisphosphate (IP_3) (Yamamoto et al., 1990; Nagy and Rash, 2000). Hence, in the model, we consider local diffusive coupling. Besides, each astrocyte is interconnected with a neuronal ensemble of N_a neurons. It was experimentally shown that the sensory stimulation evokes fast intracellular Ca^{2+} signals in fine processes of cortical astrocytes in response to local synaptic activity in the neuronal circuit (Wang X. et al., 2006; Takata et al., 2011; Stobart et al., 2018). Multiple rapid spatially restricted Ca^{2+} events in the astrocytic process are induced by intense neuronal firing. Local events are spatially and temporally integrated by the astrocytic cell, which results in a global long lasting Ca^{2+} event. In turn, this event induces the release of gliotransmitters affecting synaptic transmission in the local territory of individual astrocytes (Bekar et al., 2008; Henneberger et al., 2010; Araque et al., 2014). For simplicity, we did not model the detailed process of spatial-temporal integration of the rapid Ca^{2+} signals in the morphological structure of astrocytes modeled earlier by Gordleeva et al. (2018, 2019) and Wu et al. (2018). Here we employ a mean-field approach to describe the emergence of a global Ca^{2+} signal and its impact on the synchronization of neuronal ensemble controlled by a certain astrocyte.

As pyramidal neurons generate the spike, glutamate is released from the presynaptic terminal into the synaptic cleft (**Figures 3B,D**). The amount of glutamate, G, that was diffused from the synaptic cleft and reached the astrocytic process can be described by the following equation (Gordleeva et al., 2012; Pankratova et al., 2019):

$$\frac{dG^{(i,j)}}{dt} = -\alpha_{\text{glu}} G^{(i,j)} + k_{\text{glu}} \Theta(V^{(i,j)} - 30mV), \tag{6}$$

here α_{glu} is the glutamate clearance constant, k_{glu} is the efficacy of the release, Θ denotes the Heaviside step function, and $V^{(i,j)}$ is the membrane potential of the corresponding presynaptic neuron (i, j). Binding of glutamate to metabotropic glutamate receptors (mGluR) on the astrocytic membrane, which is located close to the synapse, triggers the production of IP_3 in the astrocytes (**Figure 3E**). We use the approaches from earlier studies to describe the dynamics of the intracellular concentration of IP_3 in astrocytes (Nadkarni and Jung, 2003; Ullah et al., 2006):

$$\frac{dIP_3^{(m,n)}}{dt} = \frac{IP_3^* - IP_3^{(m,n)}}{\tau_{IP3}} + J_{\text{PLC}\delta}^{(m,n)} + J_{\text{glu}}^{(m,n)} + \text{diff}_{IP3}^{(m,n)}, \tag{7}$$

with $m = 1, \ldots, 26$, $n = 1, \ldots, 26$. Parameter IP_3^* denotes the steady state concentration of the IP_3 and $J_{\text{PLC}\delta}$ describes the IP_3 production by phospholipase Cδ (PLCδ) (Ullah et al., 2006):

$$J_{\text{PLC}\delta} = \frac{\nu_4([Ca^{2+}] + (1-\alpha)k_4)}{[Ca^{2+}] + k_4} \tag{8}$$

The variable J_{glu} describes the glutamate-induced production of the IP_3 in response to neuronal activity and is modeled as a rectangular-shaped pulse with amplitude A_{glu} μM and duration t_{glu} ms:

$$J_{\text{glu}} = \begin{cases} A_{\text{glu}}, & \text{if} \quad t_0 < t \le t_0 + t_{\text{glu}}, \\ 0, & \text{otherwise}; \end{cases} \tag{9}$$

here t_0 denotes the periods when the total level of glutamate in all synapses associated with this astrocyte reaches a threshold:

$$\left(\frac{1}{N_a} \sum_{(i,j) \in N_a} [G^{(i,j)} > G_{\text{thr}}] \right) > F_{act}, \tag{10}$$

here we use the parameter $G_{\text{thr}} = 0.7$. $[x]$ denotes the Iverson bracket. F_{act} is the fraction of synchronously spiking neurons of the neuronal ensemble corresponding to the astrocyte. For the emergence of the calcium, elevation $F_{\text{act}} = 0.5$ is required. In other words, according to the experimental data (Bindocci et al., 2017), activation of the production term, J_{glu}, which results in the generation of a calcium signal in the astrocyte, can be induced only when correlated activity in the neuronal ensemble interacting with the astrocyte reaches a sufficient level of coherence.

Increase of IP_3 concentration in the astrocytes induces the release of Ca^{2+} from internal stores, mostly from the endoplasmic reticulum (ER), to cytosol. For a simplified description of the biophysical mechanism underlying the calcium dynamics in astrocytes, we use the Ullah model (Ullah et al., 2006). Changes of the intracellular Ca^{2+} concentration, $[Ca^{2+}]$, are described by the following equations:

$$\begin{aligned} \frac{d[Ca^{2+}]^{(m,n)}}{dt} &= J_{\text{ER}}^{(m,n)} - J_{\text{pump}}^{(m,n)} + J_{\text{leak}}^{(m,n)} + J_{\text{in}}^{(m,n)} - J_{\text{out}}^{(m,n)} \\ &\quad + \text{diff}_{Ca}^{(m,n)}; \\ \frac{dh^{(m,n)}}{dt} &= a_2 \left(d_2 \frac{IP_3^{(m,n)} + d_1}{IP_3^{(m,n)} + d_3} (1 - h^{m,n}) - [Ca^{2+}]^{(m,n)} h^{(m,n)} \right); \end{aligned} \tag{11}$$

where h is the fraction of the activated IP_3 receptors (IP_3Rs) on the ER surface. Flux J_{ER} is Ca^{2+} flux from the ER to the cytosol through IP_3Rs, J_{pump} is the Ca^{2+} flux pumped back into ER via the sarco/ER Ca^{2+}-ATPase (SERCA), and J_{leak} is the leakage flux from the ER to the cytosol. Fluxes J_{in} and J_{out} describe the calcium exchange with extracellular space. The fluxes are expressed as follows:

$$\begin{aligned} J_{\text{ER}} &= c_1 \nu_1 [Ca^{2+}]^3 h^3 IP_3^3 \frac{(c_0/c_1 - (1 + 1/c_1)[Ca^{2+}])}{((IP_3 + d_1)([Ca^{2+}] + d_5)^3}; \\ J_{\text{pump}} &= \frac{\nu_3 [Ca^{2+}]^2}{k_3^2 + [Ca^{2+}]^2}; \\ J_{\text{leak}} &= c_1 \nu_2 (c_0/c_1 - (1 + 1/c_1)[Ca^{2+}]); \\ J_{\text{in}} &= \frac{\nu_6 IP_3^2}{k_2^2 + IP_3^2}; \\ J_{\text{out}} &= k_1 [Ca^{2+}]; \end{aligned} \tag{12}$$

Biophysical meaning of all parameters in Equations (7), (8), (11), (12) and their experimentally determined values can be found in Li and Rinzel (1994), Ullah et al. (2006) and **Table 2**.

Cortical astrocytes are coupled by Cx43 gap junctions (Yamamoto et al., 1990; Nagy and Rash, 2000; Nimmerjahn et al., 2004). Thus, the diffusion of active chemicals becomes possible between the neighboring astrocytes. Currents diff_{Ca} and diff_{IP_3} describe the diffusion of Ca^{2+} ions and IP_3 molecules via gap junctions between the astrocytes in the network and can be expressed as follows:

$$\begin{aligned} \text{diff}_{Ca}^{(m,n)} &= d_{Ca} (\Delta [Ca^{2+}])^{(m,n)}; \\ \text{diff}_{IP3}^{(m,n)} &= d_{IP3} (\Delta IP_3)^{(m,n)}; \end{aligned} \tag{13}$$

where parameters d_{Ca} and d_{IP_3} describe the Ca^{2+} and IP_3 diffusion rates, respectively. Following experimental data, we assume that Cx43 is less permeable to Ca^{2+} than to IP_3. We consider that each astrocyte is diffusively coupled with only four nearest-neighbors. $(\Delta [Ca^{2+}])^{(m,n)}$ and $(\Delta IP_3)^{(m,n)}$ are the discrete Laplace operators:

$$\begin{aligned} (\Delta [Ca^{2+}])^{(m,n)} &= ([Ca^{2+}]^{(m+1,n)} + [Ca^{2+}]^{(m-1,n)} \\ &\quad + [Ca^{2+}]^{(m,n+1)} + [Ca^{2+}]^{(m,n-1)} \\ &\quad - 4[Ca^{2+}]^{(m,n)}). \end{aligned} \tag{14}$$

Equations (7)–(9), (11)–(13) predict that the synchronized activity in the neuronal ensemble trigger astrocytic Ca^{2+} signals, and in the absence of neuronal stimulus in the astrocytic network, steady state Ca^{2+} concentration is maintained.

Next, we account for the effect of the enhancement of excitatory synaptic transmission through the action of the glutamate released from astrocytes. We consider that the astrocytic glutamate-induced potentiation of the synapse consists in NMDAR-dependent postsynaptic slow inward currents (SICs) generation (Fellin et al., 2004; Chen et al., 2012) and mGluR-dependent heterosynaptic facilitation of presynaptic glutamate release (Perea and Araque, 2007; Navarrete and Araque, 2008, 2010). In the model, we propose that global events of Ca^{2+} elevation in astrocytes result in glutamate release, which can modulate the synaptic strength of all synapses corresponding to the morphological territory of a given astrocyte. For simplicity, the relationship between the astrocyte Ca^{2+} concentration and synaptic weight of the affected synapses g_{syn}, is described as follows:

$$\begin{aligned} g_{\text{syn}} &= \eta + \nu_{Ca}, \\ \nu_{Ca} &= \nu^{*}_{Ca}\Theta([Ca^{2+}]^{(m,n)} - [Ca^{2+}]_{\text{thr}}), \end{aligned} \tag{15}$$

where the parameter ν^{*}_{Ca} denotes the strength of the astrocyte-induced modulation of the synaptic weight and $\Theta(x)$ is the Heaviside step-function. The feedback from the astrocytes to the neurons is activated when the astrocytic Ca^{2+} concentration is larger than $[Ca^{2+}]_{\text{thr}}$ and the fraction of synchronously spiking neurons of the neuronal ensemble corresponding to the astrocyte F_{astro} during the time period of $\tau_{\text{syn}} = 10$ ms. According to the experimental data on the kinetics of NMDAr-dependent SICs that is evoked by glutamate released from astrocytes (Fellin et al., 2004), the duration of the astrocyte-induced facilitation of synaptic transmission is fixed and is equal to $\tau_{\text{astro}} = 250$ ms.

3.4. Stimulation Protocol

The term I_{app} in Equation (1) represents specific and non-specific external inputs. A non-specific noisy input simulates input signals from networks of other brain areas and is applied continuously to all neurons in the form of independent Poisson pulse trains of a certain rate, f_{bg}, with amplitudes randomly and uniformly distributed in the interval $[-10, 10]$ μA. This input evokes a background network state with low-rate spontaneous spiking.

Specific input contains training samples in the form of binary spatial patterns. The patterns represent different spatial distributions relative to background state with non-specific input only. The average size of a sample is 1,078 neurons (18% of the network) stimulated by the specific input, with an average 35.2% overlapping in the population. For a visual representation of samples, we take binary images of numerals (0,1,2,3,4,..) with size $W \times H$ pixels, where each pixel corresponds to a neuron in the neuronal layer. Neurons corresponding to the shape of the numerals receive a rectangular excitatory pulse with length t_{stim} and amplitude A_{stim}. The shape of each sample was spatially distorted by 5% random noise such as "salt and pepper noise." Then transient inputs were applied to simulate the nonmatching test items and the cue (length t_{test}, and amplitude A_{test}). In the cued recall for simulating the loss in saliency, we applied a shorter input with lower amplitude and a higher level (20%) of random noise. **Figure 2** illustrates the time course of a training and test protocol used in the WM paradigm.

3.5. Memory Performance Metrics

To measure the memory performance of the system we calculate the correlation of a recalled pattern with the ideal item in the following way:

$$\begin{aligned} M_{ij}(t) &= I\left[\left(\sum_{k=t-w}^{t} I[V_{ij}(k) > thr]\right) > 0\right], \\ C(t) &= \frac{1}{2}\left(\frac{1}{|P|}\sum_{(i,j)\in P} M_{ij}(t) + \frac{1}{W\cdot H - |P|}\sum_{(i,j)\notin P}(1 - M_{ij}(t))\right), \\ C_P &= \frac{1}{|T_P|}\max_{t\in T_P} C(t); \end{aligned} \tag{16}$$

here $w = 10$ frames $= 1$ ms, P—a set of pixels belonging ideal pattern, W, H—network dimensions, thr—spike threshold, I—indicator function, and T_P—a set of frames in the tracking range of pattern P. In a sense, this correlation metric can be associated with $1 - d$ averaged between the pattern and background, where d is the Hamming distance.

4. RESULTS

Let us show how the neuron-astrocyte network model exhibits memory formation. First, we will consider a simple single-item memory task illustrating information loading, storage, and retrieval. Next, we will demonstrate how the network can be successfully trained to memorize and recall several patterns with significant overlaps. Finally, we will analyze model performance metrics, capacity, and characteristics of pattern remembering on different parameters.

4.1. Single-Item WM

First, we will test the neuron-astrocyte network in the most common experimental paradigm of WM studies—the DMS task. This task requires a single item to be held in memory during a brief delay period. Before specific stimulation, the neural network demonstrates irregular, low-rate background activity (see activity beginning in **Figure 4**). At the 500 ms mark, we load an item by applying transient external input to the corresponding neuronal population for 200 ms (**Figures 3A**, **4**). During training, each astrocyte tracks the activity of the neuronal subnetwork associated with it. As soon as the extracellular concentration of glutamate (**Figures 3B,D**) and correlated firing in neurons achieve a certain level, which satisfies the condition Equation (10), Ca^{2+} concentration in matching astrocytes elevates (**Figure 3E**). In accordance with the experimental data (Bindocci et al., 2017), we tuned the model parameters in such a way that the onset of calcium elevation in the astrocytes induced by synchronous neuronal discharge had a delay of ≤ 2 s. Following the increased firing in the stimulus-specific

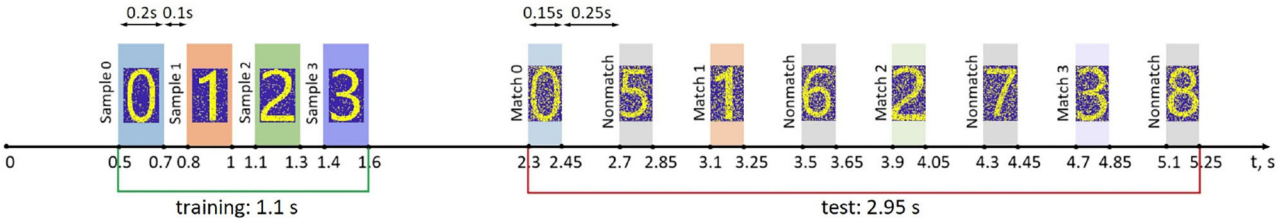

FIGURE 2 | Time course of a training and test protocol in the multi-item WM paradigm used. During training the samples were loaded sequentially by applying external inputs of 200 ms durations with 100 ms inter-item intervals. After a 700 ms training stimulus was applied, we tested the maintenance of the memory by applying matching and non-matching items of 150 ms durations and 250 ms inter-item intervals.

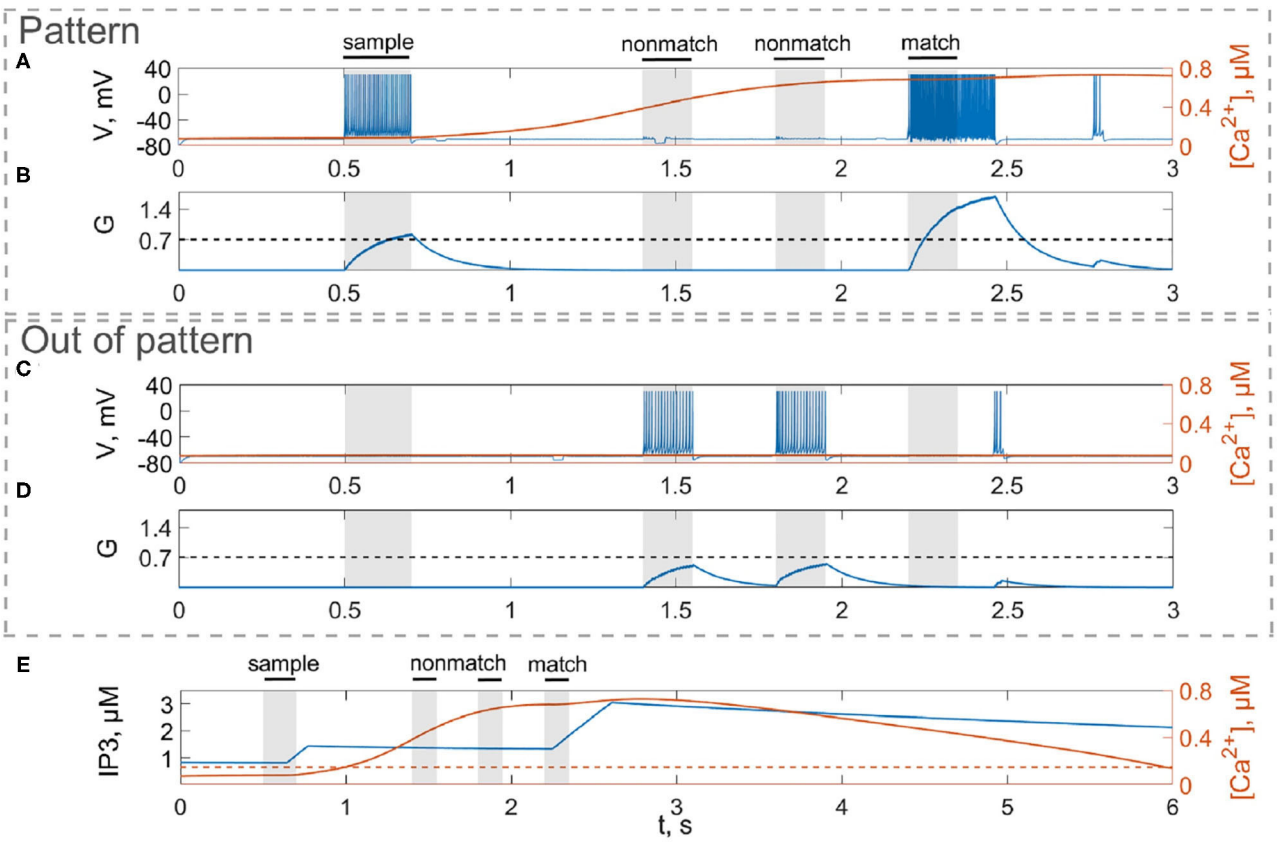

FIGURE 3 | Model of neuron-astrocyte interaction. **(A)** Spike train and **(B)** concentration of the neurotransmitter, $G(t)$, of the stimulus-specific neuron. **(C,D)** Same as in **(A,B)** but for an unspecific neuron. **(E)** Intracellular concentration of Ca^{2+} and IP_3 in a stimulus-specific astrocyte. Black bars at the top indicate periods when each of the stimuli (training stimulus—sample, nonmatching test items—nonmatch, test cue—match) were presented. In response to the presynaptic spike train **(A,C)**, the neurotransmitter, glutamate, G releases **(B,D)** into extracellular space and the concentration of IP_3 increases in the astrocyte (**E**, blue line) inducing the elevation of intracellular Ca^{2+} (**E**, red line).

part of the neuronal network upon reaching a threshold of 0.15 μM, the astrocytes release gliotransmitters modulating the synaptic strengths in corresponding locations (**Figure 3**). The calcium pulse in astrocytes lasts for several seconds. Its duration determines the length of the delay interval in the DMS task, during which the item is maintained in the memory. After the training stimulus ends, we test maintenance of the single-item memory by applying two non-matching items and cue item with t_{test} durations and 250 ms inter-item intervals (**Figures 3**, **4**). Because the astrocytic feedback also depends on the activity of the neuronal subnetwork, the model responds differently to the applied items. A short presentation of the cue to the neural network evokes the astrocytic-induced increase in the synaptic strength between stimulus-specific neurons and results in a local spatial synchronization in the whole stimulus-specific neuronal population (see **Figure 3A** in comparison to **Figure 3C**). Similar

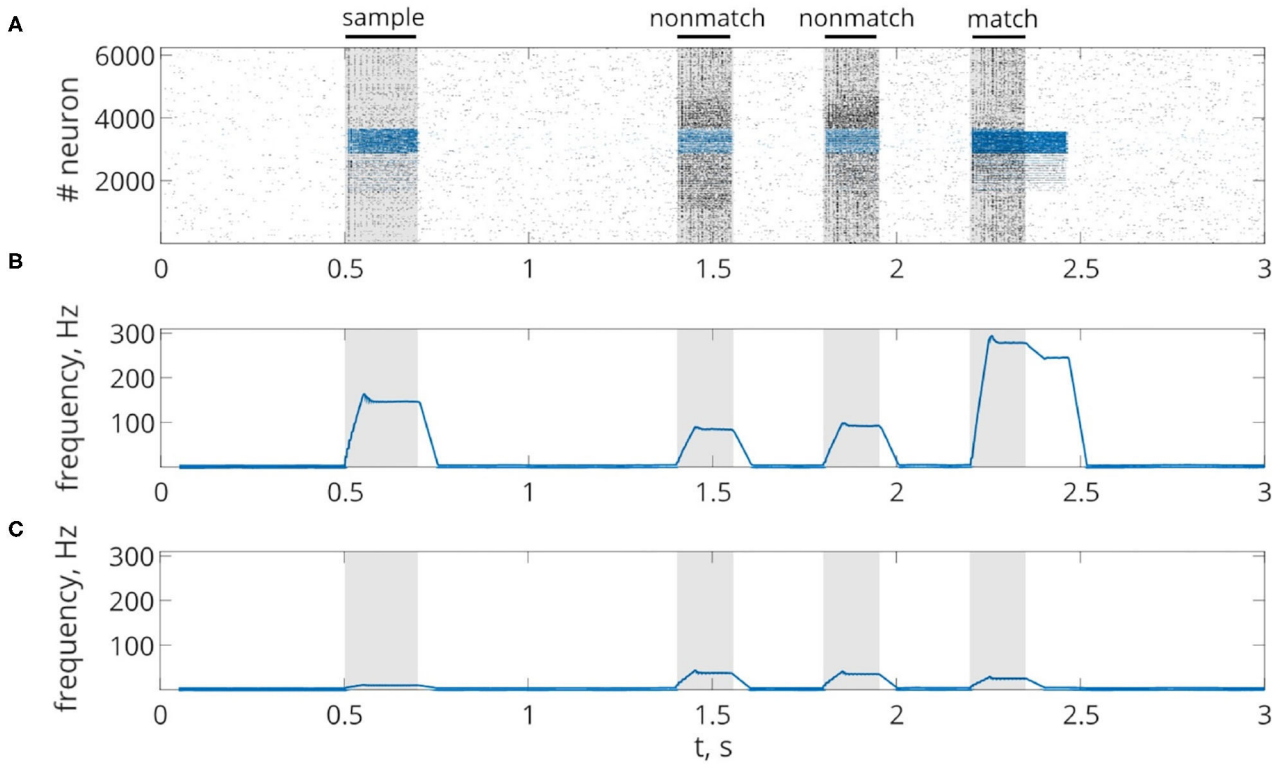

FIGURE 4 | Delayed matching to sample WM task. **(A)** One trial of the task simulated in the network. Spike raster of the neuronal network showing sample-selective delay activity. Neurons belonging to the stimulus-specific population are indicated by blue color. Black bars at the top indicate periods when each of the stimuli (training stimulus—sample, nonmatching test items—non-match, test cue—match) were presented. **(B,C)** The averaged firing rate of the stimulus-specific and unspecific neurons over time, respectively (20 ms bins).

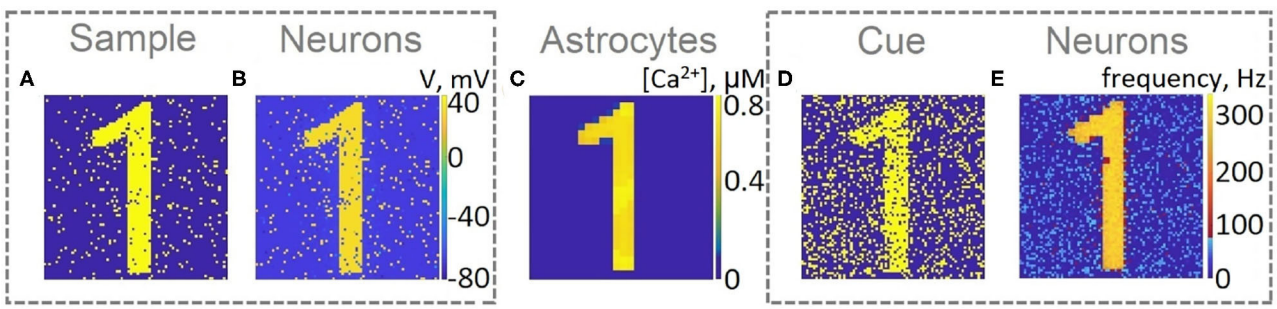

FIGURE 5 | Snapshots of the training **(A–C)** and testing **(D,E)** of the neuron-astrocyte network in the single-item working memory task. **(A)** Training sample. **(B)** Response of the neuronal network to the sample. The values of the membrane potentials are shown. **(C)** Intracellular Ca^{2+} concentrations in the astrocytic layer. **(D)** Testing item with 20% salt and pepper noise. **(E)** Cued recall in the neuronal network. The averaged firing rate on the test time interval for each neuron is shown.

to experimental data (Miller et al., 1996), delay activity in our model is sample-selective. We observe that the pattern-specific firing rate in the neuronal network increases and is equal to 270 Hz in comparison with the response to a non-specific stimulus (80 Hz) (**Figure 4B**). Such a high frequency is determined by the choice of a fast-spiking neuron model (Izhikevich, 2003). The firing rates in simulations with a regular spiking neuron model (Izhikevich, 2003) are almost 10 times lower: 30 Hz for stimulus-specific and 4.5 Hz for non-specific stimulus. The elevation of the frequency in the stimulus-specific neuronal population can continue after the end of the cue, which is determined by the duration of the astrocyte-induced enhancement of the synaptic weight.

For a visual representation of memory formation, we follow the space-time distribution of sample-selective delay activity. **Figure 5** illustrates the spatial distribution of activity in neuronal

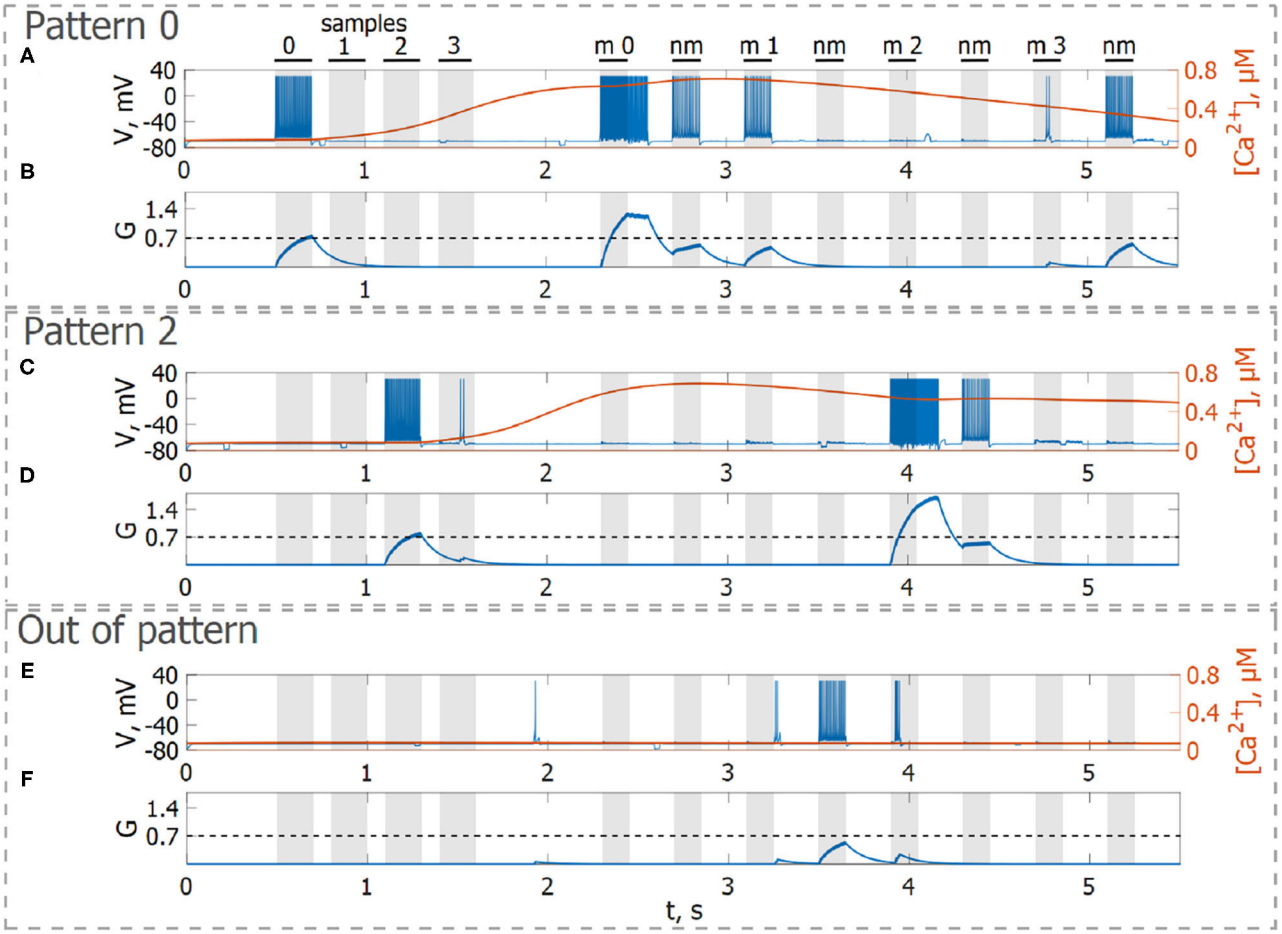

FIGURE 6 | Neuron-astrocyte network simulation with four loaded memory items. **(A,C,E)** Spike train and **(B,D,F)** concentration of the neurotransmitter, $G(t)$, of three neurons belonging to different stimulus-specific populations. **(A,B)** Stimulus-specific neuron to sample 0. **(C,D)** Stimulus-specific neuron to sample 2. **(E,F)** Neuron unspecific to all samples. Black bars at the top indicate periods when each of the stimuli (training stimulus—sample, non-matching test items—nm, match cue—m) were presented.

and astrocytic layers at the different moments of training and cued recall for the same single-item memory task as presented in **Figure 4**. Training induces the emergence of synchronized calcium activity of spatially clustered astrocytes (**Figure 5C**). Note that locally synchronized astrocytes have been found in the neocortex and hippocampus *in situ* and *in vivo* (Takata and Hirase, 2008; Sasaki et al., 2011). Such calcium activity correlated in time and space can lead to spatial-temporal synchronization in the neuronal network (Araque et al., 2014). This mechanism of neuron-astrocyte network interaction underlies the sample selectivity and pattern retrieval in the model. Note that 20 % of noisy cue items (**Figure 5D**) can be identified and cleared from noise by the neuronal network due to the astrocyte-induced feedback (**Figure 5E**). In other words, the spiking neuronal network accompanied by astrocytes can filter a cue pattern distorted by noise. Video of the single-item memory encoding and cued recall in the neuron-astrocyte network can be found in the **Supplementary Material**.

4.2. Multi-Item WM

Next, we consider the multi-item WM formation. In this case, we loaded four items, images of numerals 0, 1, 2, 3 in the following way. The images were loaded sequentially by applying external inputs of t_{stim} durations with 100 ms inter-item intervals (see **Figures 2**, **6**, **7A**, **8**). Due to the coincidence of different stimulus-specific neuronal populations in space, the spatial calcium patterns in astrocytic layers for different items overlap significantly (**Figure 8H**). After a 700 ms training stimulus was applied, we tested the maintenance of the memory by applying matching and non-matching items of t_{test} durations and 250 ms inter-item intervals (**Figures 2**, **6**, **7A**, **8**). The images were distorted by 20% noise. The astrocyte-mediated feedback modulating coherent neuronal activity provided the selectivity of the model response. The system remembered the correct image. Thus, we observed that all items were successfully filtered only in the cued recall. Needless to say that firing rate increases significantly in the cued recall due to the selective increase of

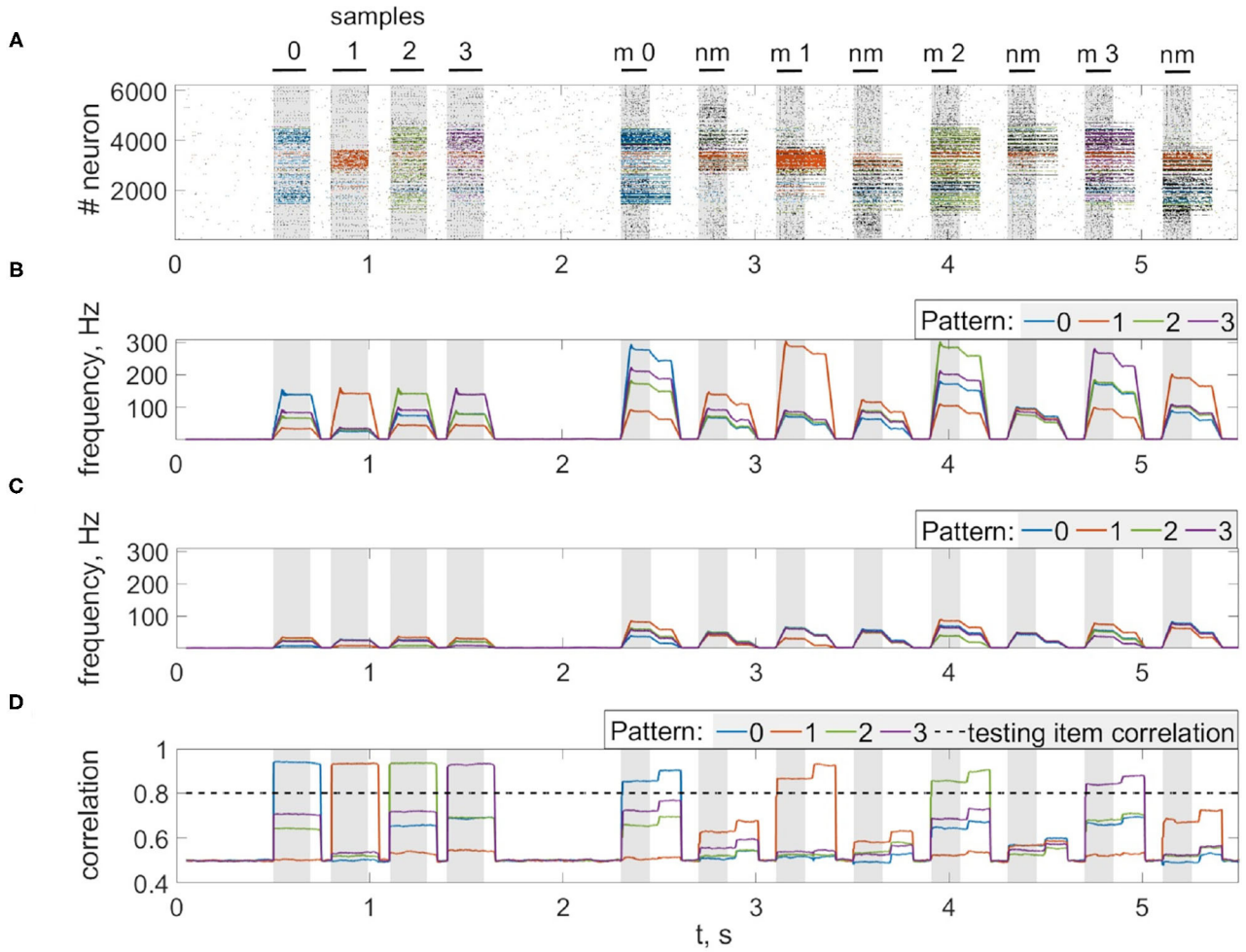

FIGURE 7 | Multi-item WM in the neuron-astrocyte network. **(A)** Spike raster of the neuronal network with four training patterns. Neurons are colored according to their pattern selectivity. Pattern overlapping in neuronal populations is 35.2% on average for four patterns. Black bars indicate periods when each of the stimuli were presented. **(B,C)** The averaged firing rate of the stimulus-specific and unspecific neurons over time, respectively (20 ms bins). **(D)** Correlation of filtered items. The different colors correspond to the correlations with different ideal samples. The dotted line shows the correlation of the testing item (for 20% noise level in test). Black bars at the top indicate periods when each of the stimuli (training stimulus—sample, non-matching test items—nm, match cue—m) were presented.

synaptic strengths (**Figures 7B,C**). To evaluate the performance of the neuron-astrocyte WM, we used the correlation between recalled item and the ideal item during the multi-item WM task as a metric (see section 3.5; **Figure 7D**). It is important to note, that during multi-item remembering, spurious correlations never dominate in that sense as accuracy of our system is always equal to 100%. There was an increase in correlation with the target image and no attraction to the wrong image or chimeras. Maximum correlation reached 95% in training and 93% in testing sets on average for four samples. Also note that the model is quite robust to the type of binary images input (images of numerals, letters, etc.). Video of the multi-item WM in the neuron-astrocyte network can be found in **Supplementary Material 2**.

To characterize the quality of memory formation in the model, we examined the dependencies of correlation of retrieval pattern in cued recall on variable parameters of the input patterns and astrocytic, synaptic, and network structure (**Figures 9**, **10**). First, we investigated its dependence on noise parameters. The dependence of correlation of recalled pattern on the noise level in training and test experiments is shown in **Figure 9A**. Specifically, the correlation difference between the recalled pattern and noisy input is presented. In other words, the model can improve test images depending on noise in training and testing. Training the network with samples with a low noise level (up to 25%) provides a high correlation. The elevation of the noise level in the training sample induces a random activity pattern in the astrocytic network, which in turn leads to noisy recall.

The morpho-functional structure of connections between neurons and astrocytes can affect pattern retrieval in the model (**Figures 9B,C**). The key parameters determining this structure are the fraction of synchronously spiking neurons of the neuronal ensemble corresponding to the astrocyte required

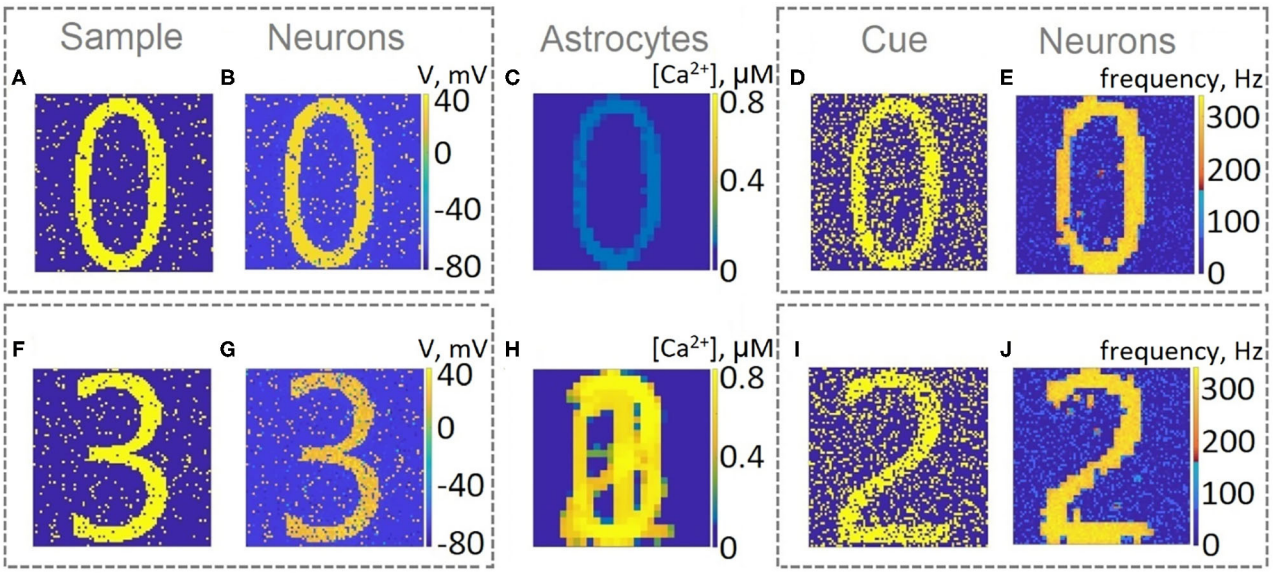

FIGURE 8 | Snapshots of the training **(A,B,C,F,G,H)** and testing **(D,E,I,J)** of the neuron-astrocyte network in the multi-item working memory task. We used the following training set consisting of four samples: 0,1,2,3. **(A,F)** The example of the first and last training samples, respectively. **(B,G)** The response of the neuronal network to samples. The values of the membrane potentials are shown. **(C,H)** The intracellular Ca^{2+} concentrations in the astrocytic layer. **(D,I)** The testing items with 20% salt and pepper noise. **(E,J)** The cued recalls in the neuronal network. The firing rate averaged on the test time interval for each neuron is shown.

for the emergence of calcium elevation in the astrocyte, F_{act}, and the fraction of synchronously spiking neurons of the neuronal ensemble corresponding to the astrocyte required for the emergence of astrocyte-induced enhancement of synaptic transmission, F_{astro}. Here we do not account for various spatiotemporal properties of gliotransmitter release and astrocyte Ca^{2+} signals evoked by different levels of neuronal activity (Araque et al., 2014). We assume that simultaneous activation of synapses induces multiple Ca^{2+} events at different processes of the astrocyte, which are spatially and temporally integrated and result in the generation of a global long-lasting Ca^{2+} elevation (Bindocci et al., 2017) that can affect synaptic transmission in the territory of individual astrocytes. For this purpose, parameters F_{act} and F_{astro} estimate the correlation level of synapse activity in the model. The optimal range of F_{astro} for correlation of recalled pattern is [0.4–0.6] (**Figure 9B**). Smaller values of the parameter, F_{astro}, lead to the effect of astrocyte-induced synchronization initiated even by non-stimulus specific uncorrelated noise activity in a small ensemble of neurons. On the contrary, the use of larger F_{astro} values implies that a highly correlated activity of almost all neurons located in the territory of a given astrocyte is required for the existence of astrocytic modulation of synapses. Hence, the neuron-astrocytic network can not perform a correct recall of noisy cue. Another point is that **Figure 9B** was obtained for a training set with a low 5% noise level and did not reveal the dependence of the correlation of recalled pattern on the parameter F_{act}. We studied the influence of the parameter F_{act} on the correlation in the simulations with different noise in training samples (**Figure 9C**). For lower noise level in training samples, the network memorizes items regardless of the value of the parameter, F_{act}. Increasing the level of noise in the training samples for small values of the parameter, F_{act}, leads to Ca^{2+} elevation in randomly distributed astrocytes first, and then in the whole astrocytic layer. Nevertheless, such non-stimulus-specific astrocytic activation can result in a high correlation of recalled pattern because of the moderate noise level in the cue and optimally chosen value of the parameter F_{astro}. On the contrary, for a larger value of the $F_{act} > 0.85$ Ca^{2+} signal in astrocytes can only be evoked by a relatively "clean" sample with a small percentage of noise $< 5\%$, therefore increasing the level of noise in training samples results in poor correlation (**Figure 9C**). We found that the range of $F_{act} = 0.8 - 0.85$ was optimal for performing the WM tasks by the neuron-astrocyte network. In this range, astrocyte activations were stimulus-specific and the astrocyte layer could memorize training samples with a low noise level. The obtained high value of optimal F_{act} denotes that correct functioning of WM in the neuron-astrocyte network dependent on the generation of global Ca^{2+} signals in astrocytes required highly correlated activity in corresponding neuronal ensembles as confirmed by recent experimental work (Bindocci et al., 2017).

Next, we studied the influence of synaptic connectivity architecture in the neural network, specifically the number, weight, and distribution of synaptic connections, on the correlation in the multi-item WM task (**Figure 10**). The minimal number of synaptic connections, N_{out}, required for the existence of cued recall is 20 (**Figure 10A**). A smaller number of connections is not enough to activate all the neurons from the stimulus-specific population. Simultaneous increase of weights and number of connections induces the generation of large synaptic currents resulting in self-sustained

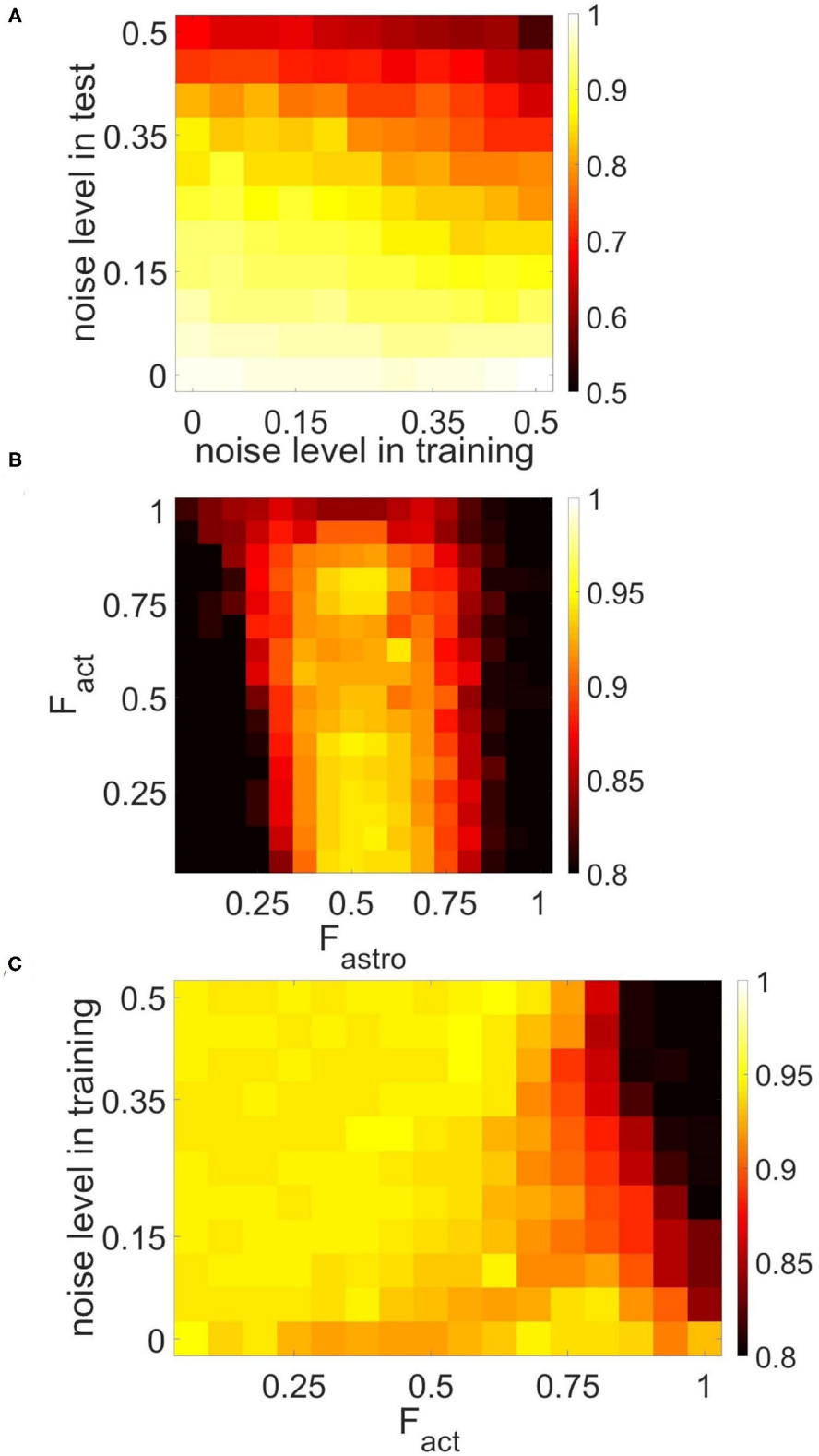

FIGURE 9 | Correlation between recalled pattern (see section 3.5) and ideal item in a multi-item WM task performed by the neuron-astrocyte network. The correlation averaged over four patterns is shown. **(A)** Noise-resistance of the model. Dependence of correlation on the noise level in training and testing. The correlation

(Continued)

FIGURE 9 | difference between cued recall pattern and noisy input is shown. **(B,C)** The influence of the neuron-astrocytic interaction structure. **(B)** Dependence of correlation on the number of spiking neurons required for the calcium elevation in the astrocyte, F_{act}, and on the number of spiking neurons required for the emergence of astrocyte-induced enhancement synaptic transmission, F_{astro}. **(C)** Dependence of correlation on noise level in training samples and on the parameter, F_{act}. $F_{astro} = 0.5$. For **(B,C)** noise level in cue is 20%.

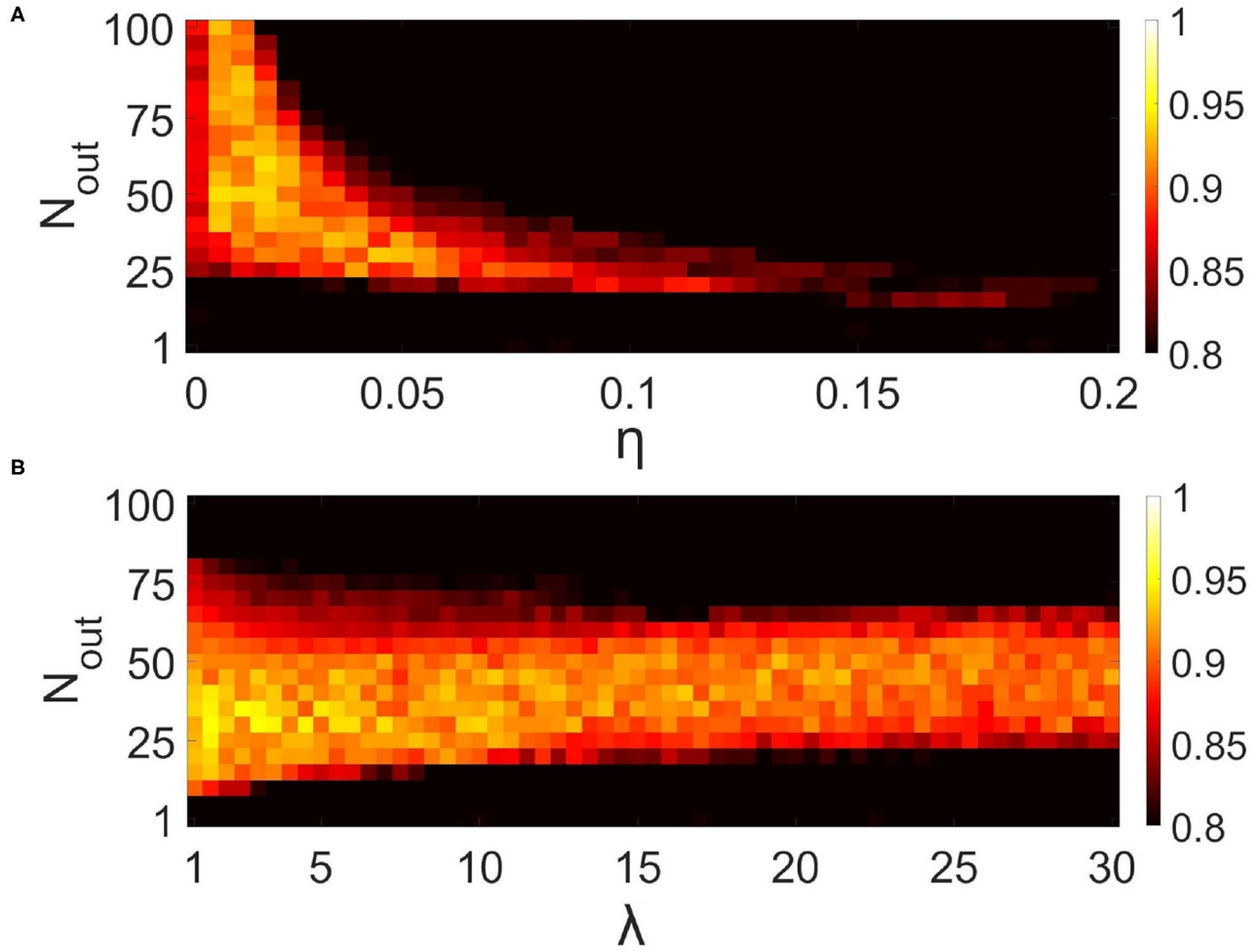

FIGURE 10 | Influence of synaptic connectivities architecture in the neural network on the correlation of recalled pattern in the multi-item WM task performed by the neuron-astrocyte network. The correlation averaged over four patterns is shown. **(A)** Dependence of correlation on the number of output synaptic connections for each neuron, N_{out}, and synaptic weight, η. $\lambda = 5$. **(B)** Dependence of correlation on the number of output synaptic connections for each neuron, N_{out}, and synaptic connection distribution parameter, λ Equation (4). $\eta = 0.025$.

overactivation of the neuron-astrocyte network. Therefore there exists an optimal range of synaptic weight values to ensure high correlation. We found that for our model this range is $\eta \in [0.005 - 0.05]$. **Figure 10B** illustrates the dependence of correlation on the number of output synaptic connections and their distribution. The smaller the parameter λ from Equation (4), the lower the probability of long-distance connections. The highest correlation was observed for local connections, $\lambda < 7$, due to the fact that short-range connections do not lead to blurring of the pattern retrieval boundaries in the neural network. **Figure 10B** also determined the optimal range for the number of synaptic connections: $N_{\text{out}} \in [25, 55]$.

The key parameters, which determine WM capacity in the proposed neuron-astrocyte network, are the duration of calcium signals in astrocytes and duration of the astrocyte-induced modulation of synaptic transmission. Duration of astrocytic calcium elevations is determined by the intrinsic mechanisms of the IP_3-evoked Ca^{2+}-induced Ca^{2+} release from the astrocyte endoplasmic reticulum stores, which is described by the biophysical model (Li and Rinzel, 1994) used in this study. Fragmentary experimental data on duration of

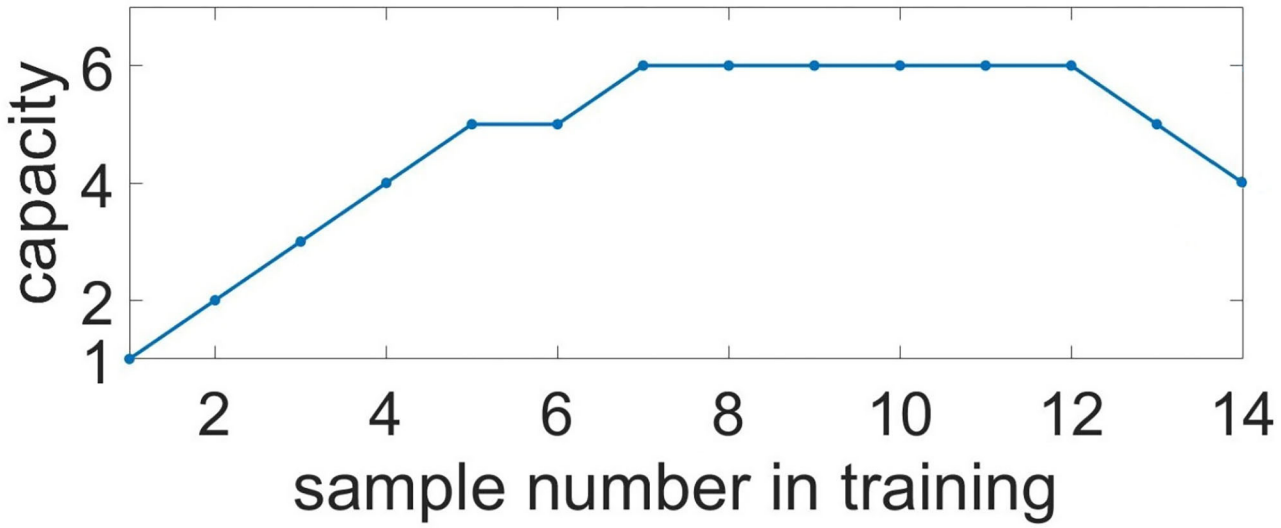

FIGURE 11 | Capacity of the multi-item WM in the neuron-astrocyte network. Capacity as a function of the sample number in training. The number of images with a correlation of recalled pattern higher than 90% is shown.

the gliotransmitter-induced modulation of synaptic transmission shows that the short-lived version of this modulation lasts from fractions of a second to a few minutes, while long-term plasticity can last for tens of minutes (for review see Pittà et al., 2016). In this study we have chosen the duration of astrocytic effect on synaptic transmission in accordance with the kinetics of SICs triggered by astrocytic glutamate (Fellin et al., 2004).

To characterize memory capacity, we subjected it to longer trains of samples. Samples were applied to neuronal ensembles with an average 35.2% overlapping in population. To check the memorization, we presented cue items in reverse order compared to the learning mode (e.g., learning: $0, 1, 2, ..., 7, 8$; test: $8, 7, ..., 2, 1, 0$). The number of items with a correlation of recalled pattern higher than 90% indicated the capacity of the system. **Figure 11** shows the capacity as a function of the sample number in the training sequence. For a chosen set of parameters, the capacity of WM ranges from five to six. It is interesting that such a limited capacity coincides with psychological studies indicating that human ability to keep information in readily accessible WM is limited, ranging between three and five items for the majority of healthy people (Cowan, 2010). However, it is obvious that the organization of the WM in the human brain involves the coordinated work of a much larger number of cells and even several CNS regions. We investigated the influence of the duration of astrocyte-induced modulation of synaptic transmission, τ_{astro}, on the capacity of WM. The number of items stored in the system memory is maximum for parameter values in the range: $\tau_{\text{astro}} \in [60, 660]$ ms. For small values of τ_{astro}, excitation does not have time to spread to the stimulus-specific neural population; for long astrocytic modulation the different items in cued recalls interfered with each other.

The capacity of WM in the proposed neuron-astrocyte network is primarily limited by the duration of the astrocytic Ca^{2+} event τ_{Ca} and does not depend on the number of neurons or astrocytes in the network. In the protocol of our testing session, the duration of the Ca^{2+} signal is sufficient to keep six samples only, and after that it starts forgetting the images received at the beginning. So, the maximum capacity of the model is six. In case more than 12 items are applied, the network starts dumping them and chimeras appear (**Figure 11**). So, the system begins to make mistakes and the capacity of the network shrinks (here the capacity is understood as the number of the retrieval items with a correlation level with the sample of more than 90%). This is valid for the case considered in the paper when a stimulus is applied to the whole network and different stimuli overlap strongly in neuronal subnetworks. For this case, the capacity does not depend on the number of neurons and astrocytes.

If we consider the case of applying items to different unique non-overlapping neuronal subpopulations, an increase in the size of the network will result in increased capacity. The WM capacity of each subnetwork in this case is unequivocally determined by the duration of the calcium signal and can be obtained analytically. We estimated the Ca^{2+} signal duration to be $\tau_{Ca} = 3.8$ s. We consider the case of training on K samples in a fixed order: $1, 2, ..., K$. During the test, we look at a permutation p consisting of K patterns. For the permutation, we estimate the number of correctly recalled patterns, K_p. The pattern is considered correctly recalled if no more than τ_{astro} has passed since its presentation. The average capacity, C, for this case is defined as the average number of correctly recalled patterns over all possible permutations p. According to this description, the average capacity can be calculated by the

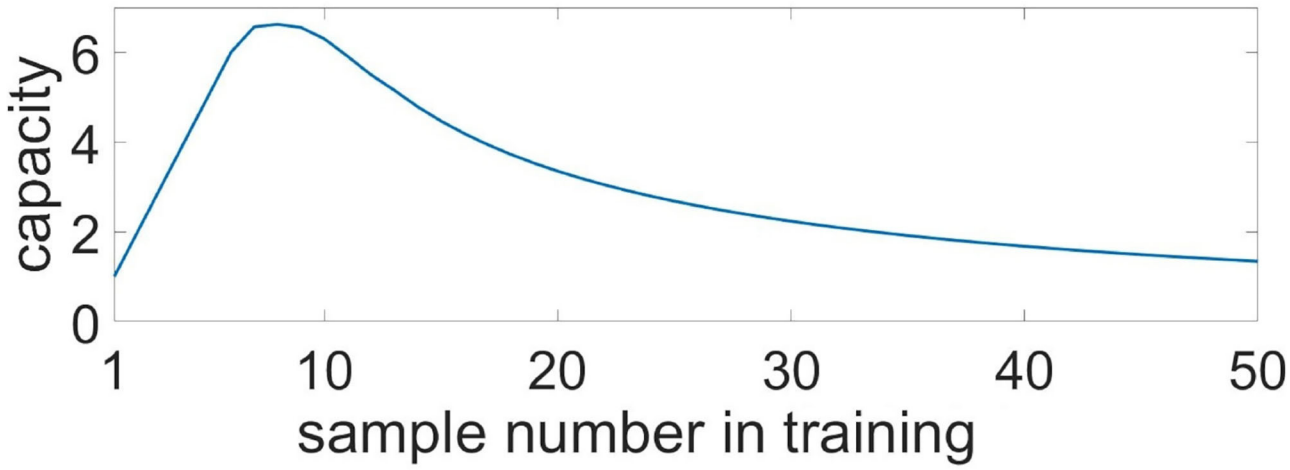

FIGURE 12 | Capacity of the multi-item WM in the neuron-astrocyte network in the case of non-overlapping neuronal populations obtained analytically. Capacity as a function of the sample number in the training sequence.

following equation:

$$
\begin{aligned}
&t^{i}_{train} = i \cdot \tau_{11} + (i-1)\tau_{12},\\
&t^{j,i}_{test} = t^{i}_{train} + \tau_{shift} + j \cdot \tau_{21} + (j-1)\tau_{22},\\
&C = \frac{1}{K!}\sum_{p}\sum_{1}^{K}\left[t^{p_i,i}_{test} - t^{i}_{train} < \tau_{Ca}\right] =\\
&\frac{1}{K!}\sum_{1}^{K}\sum_{p}\left[t^{p_i,i}_{test} - t^{i}_{train} < \tau_{Ca}\right] =\\
&\frac{(K-1)!}{K!}\sum_{1}^{K}\sum_{j=1}^{K}\left[t^{j,i}_{test} - t^{i}_{train} < \tau_{Ca}\right],
\end{aligned}
\tag{17}
$$

where τ_{11}—train sample duration, τ_{12}—duration between train samples, τ_{21}—test sample duration, τ_{22}—duration between test samples, τ_{shift}—delay between train and test, τ_{Ca}—calcium event duration, t^{i}_{train}—time of i-th train sample finishes, $t^{j,i}_{test}$. **Figure 12** shows the capacity as a function of the sample number, K. After it reaches a maximum of 6.6 for 8 samples, the capacity begins to decrease monotonically, while the number of samples increases.

5. DISCUSSION

We proposed a new biologically motivated spiking neuron network model accompanied by astrocytes that demonstrates working memory formation. The model acts at multiple timescales: at a millisecond scale of firing neurons and the second scale of calcium dynamics in astrocytes. The neuronal network consists of randomly sparsely connected excitatory spiking neurons with non-plastic synapses. Astrocyte-induced activity-dependent short-term synaptic plasticity results in local spatial synchronization in neuronal ensembles. The WM realized by such astrocytic modulation is characterized by one-shot learning and is maintained for seconds. The astrocyte influence on the synaptic connections during the elevation of calcium concentration implements Hebbian-like synaptic plasticity differentiating between specific and non-specific activations. Note that the proposed model is crucially different from the attractor-based network memory models (Hopfield, 1982; Amit, 1995; Wang, 2001; Wimmer et al., 2014) and works similarly to WM models based on synaptic plasticity (Mongillo et al., 2008; Lundqvist et al., 2011; Mi et al., 2017; Manohar et al., 2019). In particular, in its functionality, the model is quite close to short-term associative (Hebbian) synaptic facilitation (Sandberg et al., 2003; Fiebig and Lansner, 2016).

The concept of our WM model operation is schematically summarized in **Figure 13**. Composed of two building blocks, e.g., fast-spiking neurons and slow astrocytes, the proposed memory architecture eventually demonstrated synergetic functionality in loading information and its readout by the neuronal block and storage implemented by the astrocytes. In contrast with solely neuronal circuit models where memory is encoded in synaptic connections and their plasticity, which inevitably leads to the problem of overlapping, our model splits functionality using astrocytes as a pool for stored patterns. Even with significant overlaps, they can be successfully retrieved due to coherent synaptic modulations by the astrocytes and synchronous neuron firing, which provide the selectivity. When the memory is maintained at the time scale of calcium elevation in astrocytes, the synapses are not specifically modulated and theoretically can be employed for other tasks. Note also that the memory is transient with no long-lasting changes in structure and parameters. Thus, new information can be successfully uploaded and stored without interference of traces of previously memorized information. Complete memory overwrite interval is estimated at several seconds and is also defined by the duration of astrocyte activations. The circuit in **Figure 13** can be also treated as a building block for functional spiking neuron networks (SNN) which are now intensively discussed in the IT

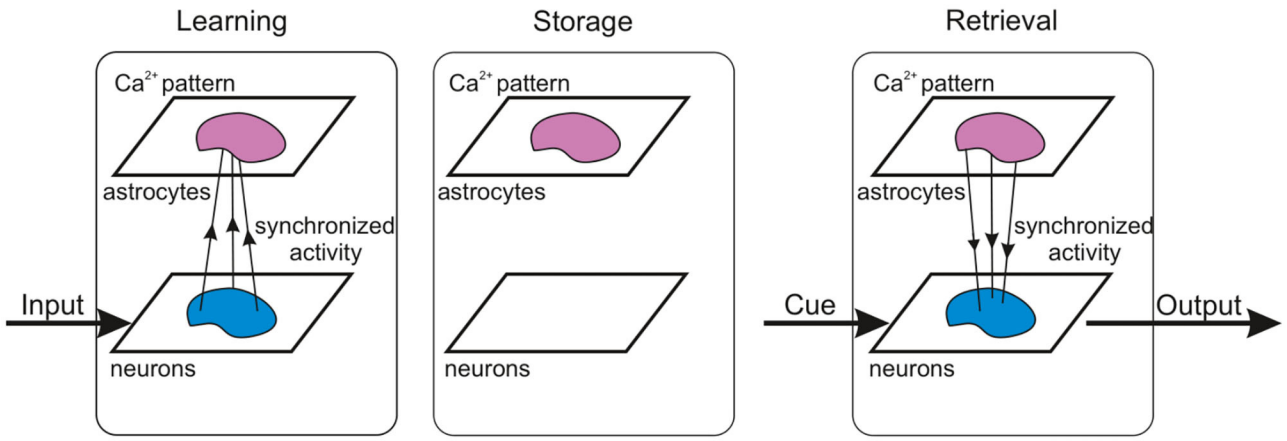

FIGURE 13 | Concept of WM operation in the spiking neuron network model accompanied by astrocytes.

community as an alternative to artificial neural networks (ANNs) used in machine learning and artificial intelligence. Theoretically, SNNs as more accurate models of brain circuits are believed to be much more powerful than traditional formal networks in processing efficiency. However, learning and memory algorithms working well in ANNs can not be directly translated to spiking neurons representing, in fact, analogous dynamical systems. We hypothesized that astrocytes may be a missing block in the implementation of learning and memory in SNNs as systems to solve information processing tasks.

The proposed model clearly confirms the theoretical hypothesis that astrocytic modulation of synaptic transmission can be involved in the formation of functional cortical WM. We show that the potentiation of excitatory synapses induced by the glutamate released from astrocytes could serve as a possible molecular mechanism for WM. Stages of multi-item WM, which include loading, storage, and cued recall, manifest in brief oscillatory bursts, which are functionally similar to WM activity in nonhuman primate PFC (Lundqvist et al., 2016) rather than sustained neuron spiking. Interestingly, the activity of the neuron-astrocyte network corresponding to a memorized pattern exhibits a sufficient degree of stability, which ensures memory retention despite the presence of significant overlaps in the stimulus-specific subnetworks.

Needless to say the astrocyte-induced modulation of synaptic transmission proposed in this study as a mechanism for WM organization does not exclude but rather complements other synaptic and neural plasticity mechanisms (fast Hebbian synaptic plasticity/short-term synaptic plasticity, facilitation, augmentation, dendritic voltage bistability, etc.) and may well act in parallel to them.

On the one hand, there has been much experimental evidence that astrocytes contribute to synaptic plasticity, coordination of neural network oscillatory activity, and memory function (Santello et al., 2019). It was shown recently that astrocytic impact is circuit-specific (Martin et al., 2015) and stimulus-specific (Mariotti et al., 2018). Improved Ca^{2+} imaging approaches have identified a spatiotemporal diversity of astrocytic signals that may underlie the capacity of astrocytes to encode and process different patterns of activation (Bindocci et al., 2017; Stobart et al., 2018). Besides, the temporal scale of the astrocytic calcium dynamics and dynamics of the neuron-astrocyte bidirectional communication including the effects of astrocytic influence on synaptic plasticity fit very well in the timing required in WM processes.

On the other hand, the ongoing intense debate about principles of WM organization challenges the canonical theory of persistent delay activity in network attractors with recurrent excitation (Bouchacourt and Buschman, 2019) and offers alternative models incorporating different biophysical network mechanisms of WM (Barak and Tsodyks, 2014; Lundqvist et al., 2018). The principal reasons for such a debate are the reexamination of experimental data, which show a large heterogeneity in delay neuronal activity during WM tasks (Stokes et al., 2013). A non-classical WM model includes short-term synaptic plasticity (Mongillo et al., 2008; Hansel and Mato, 2013), the balance of inhibition and excitation (Boerlin et al., 2013), NMDA currents affecting on the neuronal excitability (Durstewitz, 2009), and other parameters. These models, however, have a number of shortcomings: inability to describe encoding of novel associations in synaptic facilitation-based models; unclear mechanisms for achieving precise tuning of recurrent excitation and inhibition; and the time constant of the NMDA receptor is appropriate to maintain memories for 1–5 s, but not for longer. The investigation of the synaptic mechanisms underlying WM is an ongoing process. Therefore, incorporation of astrocytes as spatiotemporal integrators and modulators of synaptic transmission in neural network models may help advance the theoretical framework of WM encoding and maintenance mechanisms.

Our simulations in a biologically relevant but still quite general model have eventually illustrated the hypothesis of astrocytes participation in WM functioning. This hypothesis emerged from several experimental facts on the astrocyte

contributions to the cognitive functions and their impairments (Santello et al., 2019; Gordleeva et al., 2020; Whitwell et al., 2020). Indeed, in many of these cases, the understanding of the precise mechanisms of the astrocytic involvement is quite fragmentary and more work on the specific role of astrocytic action in the memory processes is needed. We believe that our model demonstrating WM functionality based on a quite clear mechanism of inter-coordination between fast spiking neuronal circuits and an astrocyte reservoir will be helpful in further experimental research including cellular and *in vivo* studies. In particular, depressing or facilitating the neuron-astrocyte interaction by specific drug injections can be used to monitor behavior impairments in animal studies.

To conclude, the recent controversies in the field of WM and the constant growth of experimental evidence about the participation of astrocytes in information processing, cognitive function, and dysfunction open up questions about mechanisms of astrocyte involvement in memory formation. Using a computational model, we demonstrated that the astrocyte-induced facilitation of excitatory transmission in PFC is a plausible mechanism for WM organization. The proposed model accounts for the astrocytic modulation of synaptic transmission in a spiking neural network. The biologically relevant neuron-astrocytic network implements loading, storage, and cued retrieval of multiple items presented to the neuronal populations with significant overlapping. The mechanism of WM functioning in the model is based on coherent neuronal firing in response to sensory inputs which are coordinated by astrocytes in time, serving as a "memory reservoir" and in space serving as a "signal bridge" providing a certain level of synchrony.

Future research in the framework of the proposed WM model in the neuron-astrocyte network will be focused on the interplay of excitation and inhibition that can stabilize WM (Boerlin et al., 2013); the effects of synaptic plasticity (Mongillo et al., 2008; Hansel and Mato, 2013) namely associative short-term potentiation (a fast-expressing form of Hebbian synaptic plasticity) that can provide an encoding of novel associations (Fiebig and Lansner, 2016); the subcellular calcium dynamics in astrocytes (Bindocci et al., 2017; Gordleeva et al., 2019); and on the structure of the cortical microcircuit reflecting the columnar organization of the neocortex.

DATA AVAILABILITY STATEMENT

The raw data supporting the conclusions of this article will be made available by the authors, without undue reservation.

AUTHOR CONTRIBUTIONS

All authors jointly worked on all aspects of the study and the preparation of the manuscript. The literature analysis, coding, and data gathering were mainly done by YT, MK, SG. The manuscript was mainly written by SG and VK. AZ, MI and AG supervised the work.

FUNDING

This research was supported by the Ministry of Science and Higher Education of the Russian Federation (project no. 075-15-2020-808).

ACKNOWLEDGMENTS

AZ acknowledged support from MRC Grant no. MR/R02524X/1.

SUPPLEMENTARY MATERIAL

The Supplementary Material for this article can be found online at: https://www.frontiersin.org/articles/10.3389/fncel.2021.631485/full#supplementary-material

REFERENCES

Allen, N. J., and Eroglu, C. (2017). Cell biology of astrocyte-synapse interactions. *Neuron* 96, 697–708. doi: 10.1016/j.neuron.2017.09.056

Amit, D. (1995). *Modeling Brain Functions: The World of Attractor Neural Networks*. Cambridge, UK: Cambridge University Press.

Amit, D. (2003). Multiple-object working memory-a model for behavioral performance. *Cereb. Cortex* 13, 435–443. doi: 10.1093/cercor/13.5.435

Amit, Y., Yakovlev, V., and Hochstein, S. (2013). Modeling behavior in different delay match to sample tasks in one simple network. *Front. Hum. Neurosci.* 7:408. doi: 10.3389/fnhum.2013.00408

Araque, A., Carmignoto, G., Haydon, P. G., Oliet, S. H., Robitaille, R., and Volterra, A. (2014). Gliotransmitters travel in time and space. *Neuron* 81, 728–739. doi: 10.1016/j.neuron.2014.02.007

Attwell, D., and Laughlin, S. B. (2001). An energy budget for signaling in the grey matter of the brain. *J. Cereb. Blood Flow Metab*. 21, 1133–1145. doi: 10.1097/00004647-200110000-00001

Baddeley, A. (2012). Working memory: theories, models, and controversies. *Annu. Rev. Psychol.* 63, 1–29. doi: 10.1146/annurev-psych-120710-100422

Baddeley, A. D. (1986). *Working Memory*. New York, NY: Oxford University Press; Clarendon Press.

Barak, O., and Tsodyks, M. (2014). Working models of working memory. *Curr. Opin. Neurobiol.* 25, 20–24. doi: 10.1016/j.conb.2013.10.008

Barak, O., Tsodyks, M., and Romo, R. (2010). Neuronal population coding of parametric working memory. *J. Neurosci*. 30, 9424–9430. doi: 10.1523/jneurosci.1875-10.2010

Bekar, L. K., He, W., and Nedergaard, M. (2008). Locus coeruleus α-adrenergic–mediated activation of cortical astrocytes *in vivo*. *Cereb. Cortex* 18, 2789–2795. doi: 10.1093/cercor/bhn040

Bindocci, E., Savtchouk, I., Liaudet, N., Becker, D., Carriero, G., and Volterra, A. (2017). Three-dimensional ca2+imaging advances understanding of astrocyte biology. *Science* 356:eaai8185. doi: 10.1126/science.aai8185

Boerlin, M., Machens, C. K., and Denève, S. (2013). Predictive coding of dynamical variables in balanced spiking networks. *PLoS Comput. Biol*. 9:e1003258. doi: 10.1371/journal.pcbi.1003258

Borisyuk, R., Chik, D., Kazanovich, Y., and da Silva Gomes, J. (2013). Spiking neural network model for memorizing sequences with forward and backward recall. *Biosystems* 112, 214–223. doi: 10.1016/j.biosystems.2013.03.018

Bouchacourt, F., and Buschman, T. J. (2019). A flexible model of working memory. *Neuron* 103, 147–160.e8. doi: 10.1016/j.neuron.2019.04.020

Brunel, N., and Wang, X.-J. (2001). Effects of neuromodulation in a cortical network model of object working memory dominated by recurrent inhibition. *J. Comput. Neurosci.* 11, 63–85. doi: 10.1023/a:1011204814320

Chaudhuri, R., and Fiete, I. (2016). Computational principles of memory. *Nat. Neurosci.* 19, 394–403. doi: 10.1038/nn.4237

Chen, N., Sugihara, H., Sharma, J., Perea, G., Petravicz, J., Le, C., et al. (2012). Nucleus basalis-enabled stimulus-specific plasticity in the visual cortex is mediated by astrocytes. *Proc. Natl. Acad. Sci. U.S.A.* 109, E2832–E2841. doi: 10.1073/pnas.1206557109

Constantinidis, C., Funahashi, S., Lee, D., Murray, J. D., Qi, X.-L., Wang, M., et al. (2018). Persistent spiking activity underlies working memory. *J. Neurosci.* 38, 7020–7028. doi: 10.1523/jneurosci.2486-17.2018

Conway, A. R., Kane, M. J., and Engle, R. W. (2003). Working memory capacity and its relation to general intelligence. *Trends Cogn. Sci.* 7, 547–552. doi: 10.1016/j.tics.2003.10.005

Cowan, N. (2010). The magical mystery four. *Curr. Direct. Psychol. Sci.* 19, 51–57. doi: 10.1177/0963721409359277

D'Esposito, M., and Postle, B. R. (2015). The cognitive neuroscience of working memory. *Annu. Rev. Psychol.* 66, 115–142. doi: 10.1146/annurev-psych-010814-015031

Durkee, C. A., and Araque, A. (2019). Diversity and specificity of astrocyte–neuron communication. *Neuroscience* 396, 73–78. doi: 10.1016/j.neuroscience.2018.11.010

Durstewitz, D. (2009). Implications of synaptic biophysics for recurrent network dynamics and active memory. *Neural Netw.* 22, 1189–1200. doi: 10.1016/j.neunet.2009.07.016

Erickson, M. A., Maramara, L. A., and Lisman, J. (2010). A single brief burst induces (glur)1-dependent associative short-term potentiation: a potential mechanism for short-term memory. *J. Cogn. Neurosci.* 22, 2530–2540. doi: 10.1162/jocn.2009.21375

Esir, P. M., Gordleeva, S. Y., Simonov, A. Y., Pisarchik, A. N., and Kazantsev, V. B. (2018). Conduction delays can enhance formation of up and down states in spiking neuronal networks. *Phys. Rev. E* 98:052401. doi: 10.1103/physreve.98.052401

Fellin, Pascual, Gobbo, Pozzan, Haydon, andFellin, T., Pascual, O., Gobbo, S., Pozzan, T., Haydon, P. G., and Carmignoto, G. (2004). Neuronal synchrony mediated by astrocytic glutamate through activation of extrasynaptic NMDA receptors. *Neuron* 43, 729–743. doi: 10.1016/j.neuron.2004.08.011

Fiebig, F., and Lansner, A. (2016). A spiking working memory model based on hebbian short-term potentiation. *J. Neurosci.* 37, 83–96. doi: 10.1523/jneurosci.1989-16.2016

Fransén, E., Tahvildari, B., Egorov, A. V., Hasselmo, M. E., and Alonso, A. A. (2006). Mechanism of graded persistent cellular activity of entorhinal cortex layer v neurons. *Neuron* 49, 735–746. doi: 10.1016/j.neuron.2006.01.036

Fujisawa, S., Amarasingham, A., Harrison, M. T., and Buzsáki, G. (2008). Behavior-dependent short-term assembly dynamics in the medial prefrontal cortex. *Nat. Neurosci.* 11, 823–833. doi: 10.1038/nn.2134

Funahashi, S. (2017). Working memory in the prefrontal cortex. *Brain Sci.* 7:49. doi: 10.3390/brainsci7050049

Funahashi, S., Bruce, C. J., and Goldman-Rakic, P. S. (1989). Mnemonic coding of visual space in the monkey's dorsolateral prefrontal cortex. *J. Neurophysiol.* 61, 331–349. doi: 10.1152/jn.1989.61.2.331

Fuster, J. M., and Alexander, G. E. (1971). Neuron activity related to short-term memory. *Science* 173, 652–654. doi: 10.1126/science.173.3997.652

Ganguli, S., and Latham, P. (2009). Feedforward to the past: the relation between neuronal connectivity, amplification, and short-term memory. *Neuron* 61, 499–501. doi: 10.1016/j.neuron.2009.02.006

Goldman, M. S. (2009). Memory without feedback in a neural network. *Neuron* 61, 621–634. doi: 10.1016/j.neuron.2008.12.012

Goldman-Rakic, P. (1995). Cellular basis of working memory. *Neuron* 14, 477–485. doi: 10.1016/0896-6273(95)90304-6

Gordleeva, S., Kanakov, O., Ivanchenko, M., Zaikin, A., and Franceschi, C. (2020). Brain aging and garbage cleaning. *Semin. Immunopathol.* 42, 647–665. doi: 10.1007/s00281-020-00816-x

Gordleeva, S. Y., Ermolaeva, A. V., Kastalskiy, I. A., and Kazantsev, V. B. (2019). Astrocyte as spatiotemporal integrating detector of neuronal activity. *Front. Physiol.* 10:294. doi: 10.3389/fphys.2019.00294

Gordleeva, S. Y., Lebedev, S. A., Rumyantseva, M. A., and Kazantsev, V. B. (2018). Astrocyte as a detector of synchronous events of a neural network. *JETP Lett.* 107, 440–445. doi: 10.1134/s0021364018070032

Gordleeva, S. Y., Stasenko, S. V., Semyanov, A. V., Dityatev, A. E., and Kazantsev, V. B. (2012). Bi-directional astrocytic regulation of neuronal activity within a network. *Front. Comput. Neurosci.* 6:92. doi: 10.3389/fncom.2012.00092

Halassa, M. M., Fellin, T., Takano, H., Dong, J.-H., and Haydon, P. G. (2007). Synaptic islands defined by the territory of a single astrocyte. *J. Neurosci.* 27, 6473–6477. doi: 10.1523/jneurosci.1419-07.2007

Han, J., Kesner, P., Metna-Laurent, M., Duan, T., Xu, L., Georges, F., et al. (2012). Acute cannabinoids impair working memory through astroglial CB1 receptor modulation of hippocampal LTD. *Cell* 148, 1039–1050. doi: 10.1016/j.cell.2012.01.037

Hansel, D., and Mato, G. (2013). Short-term plasticity explains irregular persistent activity in working memory tasks. *J. Neurosci.* 33, 133–149. doi: 10.1523/jneurosci.3455-12.2013

Hempel, C. M., Hartman, K. H., Wang, X.-J., Turrigiano, G. G., and Nelson, S. B. (2000). Multiple forms of short-term plasticity at excitatory synapses in rat medial prefrontal cortex. *J. Neurophysiol.* 83, 3031–3041. doi: 10.1152/jn.2000.83.5.3031

Henneberger, C., Papouin, T., Oliet, S. H. R., and Rusakov, D. A. (2010). Long-term potentiation depends on release of d-serine from astrocytes. *Nature* 463, 232–236. doi: 10.1038/nature08673

Hodgkin, A., and Huxley, A. (1990). A quantitative description of membrane current and its application to conduction and excitation in nerve. *Bull. Math. Biol.* 52, 25–71. doi: 10.1016/s0092-8240(05)80004-7

Hopfield, J. J. (1982). Neural networks and physical systems with emergent collective computational abilities. *Proc. Natl. Acad. Sci. U.S.A.* 79, 2554–2558. doi: 10.1073/pnas.79.8.2554

Izhikevich, E. (2003). Simple model of spiking neurons. *IEEE Trans. Neural Netw.* 14, 1569–1572. doi: 10.1109/tnn.2003.820440

Jourdain, P., Bergersen, L. H., Bhaukaurally, K., Bezzi, P., Santello, M., Domercq, M., et al. (2007). Glutamate exocytosis from astrocytes controls synaptic strength. *Nat. Neurosci.* 10, 331–339. doi: 10.1038/nn1849

Kanakov, O., Gordleeva, S., Ermolaeva, A., Jalan, S., and Zaikin, A. (2019). Astrocyte-induced positive integrated information in neuron-astrocyte ensembles. *Phys. Rev. E* 99:012418. doi: 10.1103/physreve.99.012418

Kass, J. I., and Mintz, I. M. (2005). Silent plateau potentials, rhythmic bursts, and pacemaker firing: three patterns of activity that coexist in quadristable subthalamic neurons. *Proc. Natl. Acad. Sci. U.S.A.* 103, 183–188. doi: 10.1073/pnas.0506781102

Kastanenka, K. V., Moreno-Bote, R., Pittà, M. D., Perea, G., Eraso-Pichot, A., Masgrau, R., et al. (2019). A roadmap to integrate astrocytes into systems neuroscience. *Glia* 68, 5–26. doi: 10.1002/glia.23632

Kazantsev, V. B., and Asatryan, S. Y. (2011). Bistability induces episodic spike communication by inhibitory neurons in neuronal networks. *Phys. Rev. E* 84:031913. doi: 10.1103/physreve.84.031913

Kilpatrick, Ermentrout, andKilpatrick, Z. P., Ermentrout, B., and Doiron, B. (2013). Optimizing working memory with heterogeneity of recurrent cortical excitation. *J. Neurosci.* 33, 18999–19011. doi: 10.1523/jneurosci.1641-13.2013

Klinshov, V. V., and Nekorkin, V. I. (2008). Working memory in the network of neuron-like units with noise. *Int. J. Bifurcat. Chaos* 18, 2743–2752. doi: 10.1142/s0218127408021968

Koulakov, A. A., Raghavachari, S., Kepecs, A., and Lisman, J. E. (2002). Model for a robust neural integrator. *Nat. Neurosci.* 5, 775–782. doi: 10.1038/nn893

Koutsikou, S., Merrison-Hort, R., Buhl, E., Ferrario, A., Li, W.-C., Borisyuk, R., et al. (2018). A simple decision to move in response to touch reveals basic sensory memory and mechanisms for variable response times. *J. Physiol.* 596, 6219–6233. doi: 10.1113/jp276356

Li, Y.-X., and Rinzel, J. (1994). Equations for InsP3 receptor-mediated [ca2+]i oscillations derived from a detailed kinetic model: a Hodgkin-Huxley like formalism. *J. Theor. Biol.* 166, 461–473. doi: 10.1006/jtbi.1994.1041

Lima, A., Sardinha, V. M., Oliveira, A. F., Reis, M., Mota, C., Silva, M. A., et al. (2014). Astrocyte pathology in the prefrontal cortex impairs the cognitive function of rats. *Mol. Psychiatry* 19, 834–841. doi: 10.1038/mp.2013.182

Lisman, J., and Idiart, M. (1995). Storage of 7 ± 2 short-term memories in oscillatory subcycles. *Science* 267, 1512–1515. doi: 10.1126/science.7878473

Liu, J., McDaid, L. J., Harkin, J., Karim, S., Johnson, A. P., Millard, A. G., et al. (2019). Exploring self-repair in a coupled spiking astrocyte neural network. *IEEE Trans. Neural Netw. Learn. Syst*. 30, 865–875. doi: 10.1109/tnnls.2018.2854291

Luca, S. N. D., Soch, A., Sominsky, L., Nguyen, T.-X., Bosakhar, A., and Spencer, S. J., (2020). Glial remodeling enhances short-term memory performance in Wistar rats. *J. Neuroinflamm*. 17:52. doi: 10.1186/s12974-020-1729-4

Lundqvist, M., Herman, P., and Lansner, A. (2011). Theta and gamma power increases and alpha/beta power decreases with memory load in an attractor network model. *J. Cogn. Neurosci*. 23, 3008–3020. doi: 10.1162/jocn_a_00029

Lundqvist, M., Herman, P., Miller, E. K., (2018). Working memory: delay activity, yes! Persistent activity? Maybe not. *J. Neurosci*. 38, 7013–7019. doi: 10.1523/jneurosci.2485-17.2018

Lundqvist, M., Rose, J., Herman, P., Brincat, S. L., Buschman, T. J., and Miller, E. K. (2016). Gamma and beta bursts underlie working memory. *Neuron* 90, 152–164. doi: 10.1016/j.neuron.2016.02.028

Makovkin, S. Y., Shkerin, I. V., Gordleeva, S. Y., and Ivanchenko, M. V. (2020). Astrocyte-induced intermittent synchronization of neurons in a minimal network. *Chaos Solitons Fract*. 138:109951. doi: 10.1016/j.chaos.2020.109951

Manohar, S. G., Zokaei, N., Fallon, S. J., Vogels, T. P., and Husain, M. (2019). Neural mechanisms of attending to items in working memory. *Neurosci. Biobehav. Rev*. 101, 1–12. doi: 10.1016/j.neubiorev.2019.03.017

Mariotti, Losi, Lia, Melone, Chiavegato,Mariotti, L., Losi, G., Lia, A., Melone, M., Chiavegato, A., Gómez-Gonzalo, M., et al. (2018). Interneuron-specific signaling evokes distinctive somatostatin-mediated responses in adult cortical astrocytes. *Nat. Commun*. 9:82. doi: 10.1038/s41467-017-02642-6

Martin, R., Bajo-Graneras, R., Moratalla, R., Perea, G., and Araque, A. (2015). Circuit-specific signaling in astrocyte-neuron networks in basal ganglia pathways. *Science* 349, 730–734. doi: 10.1126/science.aaa7945

Mi, Y., Katkov, M., and Tsodyks, M. (2017). Synaptic correlates of working memory capacity. *Neuron* 93, 323–330. doi: 10.1016/j.neuron.2016.12.004

Miller, E. K., Erickson, C. A., and Desimone, R. (1996). Neural mechanisms of visual working memory in prefrontal cortex of the macaque. *J. Neurosci*. 16, 5154–5167. doi: 10.1523/jneurosci.16-16-05154.1996

Mongillo, G., Barak, O., and Tsodyks, M. (2008). Synaptic theory of working memory. *Science* 319, 1543–1546. doi: 10.1126/science.1150769

Morris, C., and Lecar, H. (1981). Voltage oscillations in the barnacle giant muscle fiber. *Biophys. J*. 35, 193–213. doi: 10.1016/s0006-3495(81)84782-0

Nadkarni, S., and Jung, P. (2003). Spontaneous oscillations of dressed neurons: a new mechanism for epilepsy? *Phys. Rev. Lett*. 91(26 Pt 1):268101. doi: 10.1103/physrevlett.91.268101

Nagy, J. I., and Rash, J. E. (2000). Connexins and gap junctions of astrocytes and oligodendrocytes in the CNS. *Brain Res. Rev*. 32, 29–44. doi: 10.1016/s0165-0173(99)00066-1

Navarrete, M., and Araque, A. (2008). Endocannabinoids mediate neuron-astrocyte communication. *Neuron* 57, 883–893. doi: 10.1016/j.neuron.2008.01.029

Navarrete, M., and Araque, A. (2010). Endocannabinoids potentiate synaptic transmission through stimulation of astrocytes. *Neuron* 68, 113–126. doi: 10.1016/j.neuron.2010.08.043

Navarrete, M., Perea, G., de Sevilla, D. F., Gómez-Gonzalo, M., Núñez, A., Martín, E. D., et al. (2012). Astrocytes mediate *in vivo* cholinergic-induced synaptic plasticity. *PLoS Biol*. 10:e1001259. doi: 10.1371/journal.pbio.1001259

Nimmerjahn, A., Kirchhoff, F., Kerr, J. N. D., and Helmchen, F. (2004). Sulforhodamine 101 as a specific marker of astroglia in the neocortex *in vivo*. *Nat. Methods* 1, 31–37. doi: 10.1038/nmeth706

Oschmann, F., Berry, H., Obermayer, K., and Lenk, K., (2018). From *in silico* astrocyte cell models to neuron-astrocyte network models: a review. *Brain Res. Bull*. 136, 76–84. doi: 10.1016/j.brainresbull.2017.01.027

Ozdemir, A. T., Lagler, M., Lagoun, S., Malagon-Vina, H., Lasztóczi, B., and Klausberger, T. (2020). Unexpected rule-changes in a working memory task shape the firing of histologically identified delay-tuned neurons in the prefrontal cortex. *Cell Rep*. 30, 1613–1626.e4. doi: 10.1016/j.celrep.2019.12.102

Pankratova, E. V., Kalyakulina, A. I., Stasenko, S. V., Gordleeva, S. Y., Lazarevich, I. A., and Kazantsev, V. B. (2019). Neuronal synchronization enhanced by neuron–astrocyte interaction. *Nonlin. Dyn*. 97, 647–662. doi: 10.1007/s11071-019-05004-7

Park, J. C., Bae, J. W., Kim, J., and Jung, M. W. (2019). Dynamically changing neuronal activity supporting working memory for predictable and unpredictable durations. *Sci. Rep*. 9:15512. doi: 10.1038/s41598-019-52017-8

Paukert, M., Agarwal, A., Cha, J., Doze, V. A., Kang, J. U., and Bergles, D. E. (2014). Norepinephrine controls astroglial responsiveness to local circuit activity. *Neuron* 82, 1263–1270. doi: 10.1016/j.neuron.2014.04.038

Perea, G., and Araque, A. (2007). Astrocytes potentiate transmitter release at single hippocampal synapses. *Science* 317, 1083–1086. doi: 10.1126/science.1144640

Perea, G., Yang, A., Boyden, E. S., and Sur, M. (2014). Optogenetic astrocyte activation modulates response selectivity of visual cortex neurons *in vivo*. *Nat. Commun*. 5:3262. doi: 10.1038/ncomms4262

Pittà, M. D., Brunel, N., and Volterra, A. (2016). Astrocytes: orchestrating synaptic plasticity? *Neuroscience* 323, 43–61. doi: 10.1016/j.neuroscience.2015.04.001

Poskanzer, K. E., and Yuste, R. (2016). Astrocytes regulate cortical state switching *in vivo*. *Proc. Natl. Acad. Sci. U.S.A*. 113, E2675–E2684. doi: 10.1073/pnas.1520759113

Robin, L. M., da Cruz, J. F. O., Langlais, V. C., Martin-Fernandez, M., Metna-Laurent, M., Busquets-Garcia, A., et al. (2018). Astroglial CB1 receptors determine synaptic d-serine availability to enable recognition memory. *Neuron* 98, 935–944.e5. doi: 10.1016/j.neuron.2018.04.034

Runyan, C. A., Piasini, E., Panzeri, S., and Harvey, C. D., (2017). Distinct timescales of population coding across cortex. *Nature* 548, 92–96. doi: 10.1038/nature23020

Sandberg, A., Tegnér, J., and Lansner, A., (2003). A working memory model based on fast Hebbian learning. *Network Comput. Neural Syst*. 14, 789–802. doi: 10.1088/0954-898x_14_4_309

Santello, M., Toni, N., and Volterra, A. (2019). Astrocyte function from information processing to cognition and cognitive impairment. *Nat. Neurosci*. 22, 154–166. doi: 10.1038/s41593-018-0325-8

Sardinha, V. M., Guerra-Gomes, S., Caetano, I., Tavares, G., Martins, M., Reis, J. S., et al. (2017). Astrocytic signaling supports hippocampal-prefrontal theta synchronization and cognitive function. *Glia* 65, 1944–1960. doi: 10.1002/glia.23205

Sasaki, T., Kuga, N., Namiki, S., Matsuki, N., and Ikegaya, Y. (2011). Locally synchronized astrocytes. *Cereb. Cortex* 21, 1889–1900. doi: 10.1093/cercor/bhq256

Savtchouk, I., and Volterra, A. (2018). Gliotransmission: beyond black-and-white. *J. Neurosci*. 38, 14–25. doi: 10.1523/jneurosci.0017-17.2017

Schummers, J., Yu, H., and Sur, M. (2008). Tuned responses of astrocytes and their influence on hemodynamic signals in the visual cortex. *Science* 320, 1638–1643. doi: 10.1126/science.1156120

Shafi, M., Zhou, Y., Quintana, J., Chow, C., Fuster, J., and Bodner, M. (2007). Variability in neuronal activity in primate cortex during working memory tasks. *Neuroscience* 146, 1082–1108. doi: 10.1016/j.neuroscience.2006.12.072

Shen, X., and Wilde, P. D. (2007). Long-term neuronal behavior caused by two synaptic modification mechanisms. *Neurocomputing* 70, 1482–1488. doi: 10.1016/j.neucom.2006.05.011

Sreenivasan, K. K., and D'Esposito, M. (2019). The what, where and how of delay activity. *Nat. Rev. Neurosci*. 20, 466–481. doi: 10.1038/s41583-019-0176-7

Stellwagen, D., and Malenka, R. C. (2006). Synaptic scaling mediated by glial TNF-α. *Nature* 440, 1054–1059. doi: 10.1038/nature04671

Stobart, J. L., Ferrari, K. D., Barrett, M. J., Glück, C., Stobart, M. J., Zuend, M., et al. (2018). Cortical circuit activity evokes rapid astrocyte calcium signals on a similar timescale to neurons. *Neuron* 98, 726–735.e4. doi: 10.1016/j.neuron.2018.03.050

Stokes, M. G., Kusunoki, M., Sigala, N., Nili, H., Gaffan, D., and Duncan, J. (2013). Dynamic coding for cognitive control in prefrontal cortex. *Neuron* 78, 364–375. doi: 10.1016/j.neuron.2013.01.039

Takata, N., and Hirase, H. (2008). Cortical layer 1 and layer 2/3 astrocytes exhibit distinct calcium dynamics *in vivo*. *PLoS ONE* 3:e2525. doi: 10.1371/journal.pone.0002525

Takata, N., Mishima, T., Hisatsune, C., Nagai, T., Ebisui, E., Mikoshiba, K., et al. (2011). Astrocyte calcium signaling transforms cholinergic modulation to cortical plasticity *in vivo*. *J. Neurosci*. 31, 18155–18165. doi: 10.1523/jneurosci.5289-11.2011

Tewari, S., and Parpura, V. (2013). A possible role of astrocytes in contextual memory retrieval: an analysis obtained using a quantitative framework. *Front. Comput. Neurosci*. 7:145. doi: 10.3389/fncom.2013.00145

Tsodyks, M. V., and Markram, H. (1997). The neural code between neocortical pyramidal neurons depends on neurotransmitter release probability. *Proc. Natl. Acad. Sci. U.S.A*. 94, 719–723. doi: 10.1073/pnas.94.2.719

Ullah, G., Jung, P., and Cornell-Bell, A. (2006). Anti-phase calcium oscillations in astrocytes via inositol (1, 4, 5)-trisphosphate regeneration. *Cell Calcium* 39, 197–208. doi: 10.1016/j.ceca.2005.10.009

Wade, J. J., McDaid, L. J., Harkin, J., Crunelli, V., and Kelso, J. A. S. (2011). Bidirectional coupling between astrocytes and neurons mediates learning and dynamic coordination in the brain: a multiple modeling approach. *PLoS ONE* 6:e29445. doi: 10.1371/journal.pone.0029445

Wang, X., Lou, N., Xu, Q., Tian, G.-F., Peng, W. G., Han, X., et al. (2006). Astrocytic ca2+ signaling evoked by sensory stimulation *in vivo*. *Nat. Neurosci.* 9, 816–823. doi: 10.1038/nn1703

Wang, X.-J. (2001). Synaptic reverberation underlying mnemonic persistent activity. *Trends Neurosci*. 24, 455–463. doi: 10.1016/s0166-2236(00)01868-3

Wang, Y., Markram, H., Goodman, P. H., Berger, T. K., Ma, J., and Goldman-Rakic, P. S. (2006). Heterogeneity in the pyramidal network of the medial prefrontal cortex. *Nat. Neurosci.* 9, 534–542. doi: 10.1038/nn1670

Whitwell, H. J., Bacalini, M. G., Blyuss, O., Chen, S., Garagnani, P., Gordleeva, S. Y., et al. (2020). The human body as a super network: Digital methods to analyze the propagation of aging. *Front. Aging Neurosci*. 12:136. doi: 10.3389/fnagi.2020.00136

Wimmer, K., Nykamp, D. Q., Constantinidis, C., and Compte, A. (2014). Bump attractor dynamics in prefrontal cortex explains behavioral precision in spatial working memory. *Nat. Neurosci*. 17, 431–439. doi: 10.1038/nn.3645

Wu, Y.-W., Gordleeva, S., Tang, X., Shih, P.-Y., Dembitskaya, Y., and Semyanov, A. (2018). Morphological profile determines the frequency of spontaneous calcium events in astrocytic processes. *Glia* 67, 246–262. doi: 10.1002/glia.23537

Xu, Y., Guo, Y., Ren, G., and Ma, J. (2020a). Dynamics and stochastic resonance in a thermosensitive neuron. *Appl. Math. Comput*. 385:125427. doi: 10.1016/j.amc.2020.125427

Xu, Y., Liu, M., Zhu, Z., and Ma, J. (2020b). Dynamics and coherence resonance in a thermosensitive neuron driven by photocurrent. *Chin. Phys. B* 29:098704. doi: 10.1088/1674-1056/ab9dee

Yamamoto, T., Ochalski, A., Hertzberg, E. L., and Nagy, J. I. (1990). On the organization of astrocytic gap junctions in rat brain as suggested by LM and EM immunohistochemistry of connexin43 expression. *J. Compar. Neurol.* 302, 853–883. doi: 10.1002/cne.903020414

Zhang, Y., Xu, Y., Yao, Z., and Ma, J. (2020). A feasible neuron for estimating the magnetic field effect. *Nonlin. Dyn*. 102, 1849–1867. doi: 10.1007/s11071-020-05991-y

Zylberberg, J., and Strowbridge, B. W. (2017). Mechanisms of persistent activity in cortical circuits: possible neural substrates for working memory. *Annu. Rev. Neurosci.* 40, 603–627. doi: 10.1146/annurev-neuro-070815-014006

Conflict of Interest: The authors declare that the research was conducted in the absence of any commercial or financial relationships that could be construed as a potential conflict of interest.

frontiers in Cellular Neuroscience

ORIGINAL RESEARCH
published: 30 April 2021
doi: 10.3389/fncel.2021.640217

Extracellular ATP-Induced Alterations in Extracellular H^+ Fluxes From Cultured Cortical and Hippocampal Astrocytes

Ji-in Vivien Choi[1,2], *Boriana K. Tchernookova*[1], *Wasan Kumar*[1], *Lech Kiedrowski*[1,3], *Calla Goeke*[4,5], *Marina Guizzetti*[4,5], *John Larson*[6], *Matthew A. Kreitzer*[7] *and Robert Paul Malchow*[1,8]*

[1] *Department of Biological Sciences, University of Illinois at Chicago, Chicago, IL, United States,* [2] *Stritch School of Medicine, Loyola University, Maywood, IL, United States,* [3] *Spot Cells LLC, Chicago, IL, United States,* [4] *VA Portland Health Care System, Portland, OR, United States,* [5] *Department of Behavioral Neuroscience, Oregon Health & Science University, Portland, OR, United States,* [6] *Department of Psychiatry, University of Illinois at Chicago, Chicago, IL, United States,* [7] *Department of Biology, Indiana Wesleyan University, Marion, IN, United States,* [8] *Department Ophthalmology and Visual Sciences, University of Illinois at Chicago, Chicago, IL, United States*

OPEN ACCESS

Edited by:
Yu-Wei Wu,
Academia Sinica, Taiwan

Reviewed by:
Shefeeq Theparambil,
University College London, United Kingdom
Ana Lucia Marques Ventura,
Fluminense Federal University, Brazil

***Correspondence:**
Robert Paul Malchow
paulmalc@uic.edu

Specialty section:
This article was submitted to Non-Neuronal Cells, a section of the journal Frontiers in Cellular Neuroscience

Received: *10 December 2020*
Accepted: *19 March 2021*
Published: *30 April 2021*

Citation:
Choi JV, Tchernookova BK, Kumar W, Kiedrowski L, Goeke C, Guizzetti M, Larson J, Kreitzer MA and Malchow RP (2021) Extracellular ATP-Induced Alterations in Extracellular H^+ Fluxes From Cultured Cortical and Hippocampal Astrocytes. Front. Cell. Neurosci. 15:640217. doi: 10.3389/fncel.2021.640217

Small alterations in the level of extracellular H^+ can profoundly alter neuronal activity throughout the nervous system. In this study, self-referencing H^+-selective microelectrodes were used to examine extracellular H^+ fluxes from individual astrocytes. Activation of astrocytes cultured from mouse hippocampus and rat cortex with extracellular ATP produced a pronounced increase in extracellular H^+ flux. The ATP-elicited increase in H^+ flux appeared to be independent of bicarbonate transport, as ATP increased H^+ flux regardless of whether the primary extracellular pH buffer was 26 mM bicarbonate or 1 mM HEPES, and persisted when atmospheric levels of CO_2 were replaced by oxygen. Adenosine failed to elicit any change in extracellular H^+ fluxes, and ATP-mediated increases in H^+ flux were inhibited by the P2 inhibitors suramin and PPADS suggesting direct activation of ATP receptors. Extracellular ATP also induced an intracellular rise in calcium in cultured astrocytes, and ATP-induced rises in both calcium and H^+ efflux were significantly attenuated when calcium re-loading into the endoplasmic reticulum was inhibited by thapsigargin. Replacement of extracellular sodium with choline did not significantly reduce the size of the ATP-induced increases in H^+ flux, and the increases in H^+ flux were not significantly affected by addition of EIPA, suggesting little involvement of Na^+/H^+ exchangers in ATP-elicited increases in H^+ flux. Given the high sensitivity of voltage-sensitive calcium channels on neurons to small changes in levels of free H^+, we hypothesize that the ATP-mediated extrusion of H^+ from astrocytes may play a key role in regulating signaling at synapses within the nervous system.

Keywords: astrocyte, pH, H^+, ATP, glia, calcium

INTRODUCTION

An ever-increasing number of studies suggest strongly that glial cells are far more than the "passive" or "filler" elements originally envisaged years ago when christened "glue" by Rudolf Virchow (Ndubaku and de Bellard, 2008). In addition to their now well-established roles in providing nutrients and scaffolding critical for neuronal growth, proper development, and continued function, glia are now recognized as active participants in the "tripartite synapse," modulating and regulating signal transmission between neurons and among themselves (Halassa et al., 2007, 2009; Papouin et al., 2017). The removal by glia of neurotransmitter released by neurons is one key mechanism well-known to play an essential role in regulating the extent of neuronal excitation and inhibition (cf. Allen, 2014; Kardos et al., 2017; Malik and Willnow, 2019; Valtcheva and Venance, 2019; Belov Kirdajova et al., 2020 for review). In addition, it has long been suspected that elevations in glial intracellular calcium also lead to modulation of synaptic transfer at synapses, but the precise nature and molecular mechanism(s) of such regulation by glial cells is currently an area of contentious debate (cf. Khakh and McCarthy, 2015; Bazargani and Attwell, 2016; Guerra-Gomes et al., 2017; Fiacco and McCarthy, 2018; Savtchouk and Volterra, 2018; Ashhad and Narayanan, 2019; Kofuji and Araque, 2020; Semyanov et al., 2020).

A number of chemical agents including glutamate, adenosine, serine and GABA have been suggested to act as "gliotransmitters" and act as potential modulators of neuronal activity, although the molecular mechanisms by which these gliotransmitters are released remains controversial (Sahlender et al., 2014; Durkee and Araque, 2019). However, an additional powerful but commonly overlooked mechanism for regulation of synaptic transmission is small changes in levels of extracellular acidity (H^+). As extracellular acidity increases, protons bind to neuronal calcium channels, reducing the peak calcium influx through these proteins as well as inducing a rightward shift in the transmembrane voltage required to activate these voltage-gated channels (Barnes and Bui, 1991; Barnes et al., 1993). Indeed, in experiments conducted by Stephen Barnes and colleagues using the retina of the tiger salamander, altering extracellular pH to 7.0 completely abolished postsynaptic responses from photoreceptors to second order horizontal cells and was as effective in reducing neurotransmission as 100 μM cadmium, an agent known to potently block calcium influx through voltage-gated calcium channels and to also effectively eliminate all synaptic transmission at this concentration (Barnes et al., 1993). A similar dramatic cessation of neurotransmission from photoreceptors to horizontal cells was reported by Kleinschmidt (1991) upon reducing extracellular pH to 7.2 in the retina of the salamander.

Recent experiments examining radial glial cells isolated from the vertebrate retina (Müller cells) have shown that activation of these glia by extracellular ATP induces a marked increase in extracellular H^+ flux, acidifying the extracellular milieu (Tchernookova et al., 2018). This ATP-induced extracellular increase in H^+ flux was detected from Müller cells isolated from a wide range of evolutionarily distant species, ranging from lamprey, skate, tiger salamander, rat, monkey, and human, suggesting a highly evolutionarily conserved response. Further experiments examining the molecular mechanisms responsible for the ATP-elicited H^+ flux from tiger salamander Müller cells suggested that the response arose from activation of a G-protein coupled ATP receptor and that the H^+ flux required an increase in calcium released from intracellular stores. It was suggested that this release of H^+ from Müller cells might play a role in regulating release of neurotransmitter from retinal neurons.

In the present set of experiments, we used H^+-selective microelectrodes in a self-referencing fashion to show that ATP applied extracellularly to astrocytes cultured from the hippocampus and cortex also elicits a pronounced increase in extracellular H^+ flux. We also found that the extracellular H^+ flux is similarly dependent upon an increase in the release of calcium from intracellular stores. We propose that the ATP-mediated increase in extracellular H^+ flux is likely to be a general property of many types of glia and that this may be a common mechanism by which glial cells modulate neurotransmitter release from neurons throughout the nervous system.

MATERIALS AND METHODS

Preparation of Cell Cultures

All animals were treated in accordance with the protocols approved by the Animal Care Committee (ACC), the Institutional Animal Care and Use Committee (IACUC) of the University of Illinois at Chicago and the federal guidelines listed in the Public Health Service Policy on Humane Care and Use of Laboratory Animals. CD-1 mice pups were purchased from Charles River Laboratories (Wilmington, Massachusetts) and were bred and maintained by the Biological Resources Laboratory (BRL) of the University of Illinois at Chicago. Gestational day 15 pregnant female Sprague-Dawley rats were purchased from Charles River Laboratories (Wilmington, Massachusetts).

Astrocyte cultures were prepared from the hippocampus of postnatal day (PD) 0–1 CD-1 mice or from the cortex of PD 0–1 rats of either sex based on protocols previously described (Guizzetti et al., 1996; Chen et al., 2013). The hippocampi (mice) and cortices (rats) were dissected in 10 ml of HBSS solution (Gibco) containing 10 mM HEPES (pH 7.5), 1 unit/mL penicillin/streptomycin (Invitrogen), and 1 mM of pyruvic acid and cut into smaller pieces and collected into a new tube containing 10 mL of fresh HBSS solution. After two additional washes in 10 mL HBSS solution, hippocampal, or cortical pieces were digested in sterile enzyme solution containing 0.75 mM EDTA, 1.5 mM $CaCl_2$, and 25 units/mL of papain for 30 min at 37°C under gentle shaking. The enzymatically digested brain pieces were washed with 5 mL of DMEM (Gibco) containing 1 unit/mL of penicillin/streptomycin (Invitrogen) and 10% fetal bovine serum (complete glial medium) twice, 10 mL of HBSS twice, and again with 5 mL of glial medium twice. About 3 mL of the glial medium from the final wash was discarded and the brain tissues in remaining 2 mL of glial medium were mechanically triturated through a 1 mL pipette. Astrocytes were

plated in complete medium at a concentration of 40,000–65,000 cells/mL in 35 mm dishes (Falcon 3001) for H^+ flux recording and incubated at 37°C in a humified atmosphere of 5% CO_2-95% air. The medium was replaced a day after the dissociation, and then every other day after that. In some experiments, cryopreserved cortical astrocyte cultures from Sprague-Dawley rats were purchased from Spot Cells LLC. These cells were thawed and plated using a protocol provided by the manufacturer and cultured as described above for freshly obtained tissue.

For imaging of intracellular calcium alterations, cells were plated on glass coverslips mounted in Petri dish inserts (Spot Cells LLC). Glass coverslips were coated with 50 μg/mL of poly-D-lysine (Sigma) for at least 2 h, rinsed twice with distilled water and air dried before plating cells on them.

Staining for GFAP

Astrocytic cultures were fixed with 4% formaldehyde in phosphate buffered saline (PBS) and treated with blocking buffer containing 0.3% Triton X-100 and 3% goat serum in PBS. The cells were then incubated with a primary monoclonal anti-GFAP mouse antibody (1:500, Sigma) and stored in a refrigerator overnight at 4°C. After rinsing with PBS, the cells were incubated with a secondary FITC-labeled anti-rabbit IgG antibody (1:500, Sigma) in blocking buffer for 2 h at room temperature. After washing the cells with PBS, fluorescent staining was analyzed under standard FITC settings (488 nm excitation, 585 nm emission) using digital fluorescence microscopy. Cell dishes not exposed to the primary antibody were used as negative controls.

H^+-Selective Electrode Preparation

The procedure used to prepare H^+-selective microelectrodes was similar to the protocol described by Smith et al. (1999), Smith and Trimarchi (2001), and Molina et al. (2004). Glass capillary tubes with outer diameter of 1.65 mm and inner diameter of 1.15 mm (King Precision Glass) were pulled to tip diameters of 2–4 μm using a model P-97 Sutter Instruments pipette puller. Pulled pipettes were placed on a metal screen rack tip-side-up; the rack full of pulled pipettes was placed on a glass petri dish, covered with a glass beaker and placed in an oven located in a laboratory safety hood and heated at 200°C for at least 24 h for drying. The micropipettes were then silanized with the vapor produced by adding a 0.1 mL drop of N, N-dimethyltrimethylsilyalamine (Sigma) onto the bottom of the glass Petri dish. After 30 min, the beaker covering the pipettes was rotated 180 degrees to allow vapor to escape into the air hood, and the silanized micropipettes were taken out of the oven and set aside to cool down for several minutes. Cooled pipettes were stored in a glass desiccator with desiccant to prevent moisture formation inside. Silanized micropipettes were then back-filled with 100 mM KCl (pH 7.4) buffered with 10 mM HEPES, and a positive pressure applied through a syringe filled with air to fill the tip all the way to the end of the micropipette with fluid. Using an inverted microscope, the tip of the pipette was then placed in contact with a silanized glass pipette of greater diameter containing the highly selective H^+ resin, hydrogen ionophore 1-cocktail B (Fluka), and about 30 μm of H^+ ionophore was drawn into the smaller silanized pipette tip. H^+-selective microelectrodes were calibrated with standard pH 6.0, 7.0, and 8.0 solutions (Fisher Scientific). Only microelectrodes with Nernstian voltage slopes of 45–60 mV/per pH unit were used in experiments. Control experiments were also conducted to ensure that drugs at the concentrations applied did not alter the sensitivity of the H^+ sensors.

Solutions

For most H^+ flux experiments, solutions contained 1 mM of the pH buffer HEPES along with 140 mM of NaCl, 5 mM KCl, 2.5 mM $CaCl_2$, 2 mM $MgCl_2$, and 15 mM glucose and were adjusted to pH 7.4 using NaOH. In some experiments, bicarbonate buffer solutions containing 124 mM NaCl, 4 mM KCl, 1.25 mM KH_2PO_4, 1.25 mM $CaCl_2$, 1.5 mM $MgSO_4$, 26 mM $NaHCO_3$, and 10 mM glucose were used; this was bubbled with 95% O_2 and 5% CO_2 to achieve a pH of 7.4. Recordings were made in a cell dish containing 4 mL of solution, and during each solution exchange, 20 mL of the next solution was exchanged to ensure near complete washout of previous solution, followed by a short period of time to allow the solutions to once again become mechanically quiet and to allow the H^+ gradient to be restored. The self-referencing technique relies on the presence of an H^+ concentration gradient between the two points being measured (see below). Continual superfusion of solutions over the cell would eliminate this concentration gradient. A home-built superfusion chamber, described fully in Kreitzer et al. (2017), was employed to exchange solutions and apply pharmaceutical agents; this same chamber allowed maintenance of the 95% O_2/5% CO_2 mix used in experiments with bicarbonate as the primary extracellular pH buffer, and also allowed the maintenance of a 100% oxygen atmosphere in experiments designed to eliminate potential contributions from CO_2 in the normal room air.

H^+ Flux Recordings

To make self-referencing recordings from isolated cells, the culture medium in a dish containing cells was first replaced by a recording saline and placed on the stage of a Zeiss 40CFL inverted microscope resting on an air isolation table and enclosed in a Faraday cage to reduce electrical interference. A ground electrode made from a capillary tube filled with 3% agar and 3 M NaCl was placed in the dish and connected to the head stage of the self-referencing amplifier via a sintered silver/silver chloride electrode (WPI). The electronics, software, and mechanical control of electrode movement were the same as described in Molina et al. (2004) and Kreitzer et al. (2017) and were products of the BioCurrents Research Center, Woods Hole MA.

For self-referencing measurements of extracellular H^+ flux, a H^+-selective microelectrode was first positioned about 1–2 μm away from an isolated cell, a voltage was recorded, and the electrode then moved to a second position 30 μm away and another reading taken at this background location. An H^+-dependent differential voltage signal was then obtained by subtracting the voltage signal at the distant position from the position adjacent to the cell membrane. This differential measurement is at the heart of self-referencing, and removes much of the inherent slow electrical drift that is present in virtually all ion-selective electrodes. An important assumption

of the technique is that the frequency of movement of the microelectrode between the two points (0.3 Hz in these studies) is fast enough so that the electrical drift is virtually identical at the two points, but not fast enough to significantly stir the solution and disturb the diffusional H^+ gradient being measured from the cell. This differential measurement combined with signal averaging is estimated to increase the sensitivity of the ion-selective microelectrodes by 1,000 times (Somieski and Nagel, 2001). As noted in prior publications (Smith and Trimarchi, 2001; Molina et al., 2004; Kreitzer et al., 2007, 2017), the signals generated by the self-referencing H^+-selective microelectrodes used in these experimental conditions are not likely to arise from surface potentials or other stray sources of extracellular voltages. For example, extracellular voltage fields generated by isolated cells are usually in the nanovolt range and below the sensitivity of ion-selective self-referencing probes (Kuhtreiber and Jaffe, 1990; Smith et al., 1999), and electrical potentials from local boundary conditions associated with membrane surface charges (McLaughlin et al., 1971, 1981) drop with the Debye length and do not extend into the medium by more than tens of angstroms (cf. Cevc, 1990); our H^+-selective microelectrodes were located at least 1 μm away from the surface of cells. Finally, at the end of every recording, control background differential signals were measured at a position 600 μm away from the cell in the Z-plane; at this location, the levels of H^+ should be the same at the two positions of electrode movement, resulting in a differential signal near zero. Recordings from which the differential signal differed by more than 25 μV from the expected zero value were discarded.

Calcium Imaging

Intracellular [Ca^{2+}] was assessed using the Ca^{2+}-sensitive fluorescent indicator Fura-2 AM (Grynkiewicz et al., 1985). Astrocytes growing in Spot Cells' Petri dish inserts were loaded with Fura-2, by filling the inserts with 50 μl of 4 μM Fura-2AM in cell culture medium and incubating (37°C, 5% CO2) for 10 min. The inserts were then transferred to chambers that fit a microscope stage (Kiedrowski and Feinerman, 2018), where they were superfused with 1 mM HEPES saline buffer solution to remove the extracellular Fura-2 AM. Intracellular Fura-2 fluorescence imaging was carried out using a digital fluorescence imaging system with DIC optics. The system included a 20× Zeiss Fluar 20×, NA 0.75 objective, a Zeiss AxioObserver D1 microscope (Zeiss, Göttingen, Germany), and excitation/emission filter wheels (Sutter Instrument, Novato CA) controlled by MetaFluor 7.7.8 software (Molecular Devices LLC, Sunnyvale, CA, USA). Agents of interest were applied onto the cells via superfusion that was conducted using a MPRE-8 manifold and 8-channel valve switch, cFlow8 (Cell MicroControls, Norfolk, VA, USA). Images of fluorescence (4 × 4 binning) emitted at 510 nm and excited at 340 and 380 nm were taken every 10 s for off line analysis. The F340/F380 ratio was measured in regions of interest (ROIs) and used as an indicator of intracellular [Ca^{2+}]. At the end of each experiment, cells were exposed to 10 μM of ionomycin and 3 μM of FCCP for saturation of Fura-2 with Ca^{2+}. For data analysis, background fluorescence measured in cell-free regions was subtracted from raw fluorescence values at F340 and F380 measured in the ROIs.

Data Analysis

For most self-referencing isolated cell recordings, differential voltage values quickly reached new plateau levels, and the mean value of the last 90 points were used in data analysis. In some cases (e.g., in response to application of glutamate), cellular responses to a solution exchange were rather transient. For these cases, the first 20 points out of 100 were used in data analysis. The Wilcoxon signed-rank test was used to determine the level of statistical significance in experiments for which the N was 5. For all other experiments, mean ± standard error of the mean (SEM) and *P*-values were calculated using Prism software (GraphPad), and Student's paired *t*-tests were used to determine statistical significance. In histograms, a single asterisk indicates *P*-values between 0.01 and 0.05, two asterisks indicate $P < 0.01$.

RESULTS

Experiments were carried out on primary cell cultures prepared from rat cortex and mouse hippocampus using culturing conditions designed to limit the growth of neurons and microglia. To confirm that the cells in culture had characteristics of astrocytes, cell cultures were immune-stained with an antibody specific for glial fibrillary acidic protein (GFAP), an intermediate filament protein typically expressed at high concentrations in astrocytes (Dixon et al., 2004; Sofroniew and Vinters, 2010; Zhang et al., 2017). **Figure 1A** shows a photomicrograph illustrating the extensive and intense staining for GFAP detected in cells prepared from mouse hippocampus in a dish with a nearly confluent cell culture, with almost all cells observed displayed high levels of GFAP.

Figure 1B shows a photomicrograph depicting the typical recording arrangement used to measure H^+ fluxes from single cells. Recordings were made in dishes plated at a lower density of cells than shown in **Figure 1A**. Under such conditions, cells tended to be large and flat with extensive broad extensions, a morphology typical of cells also identified as astrocytes in previous studies (Fawthrop and Evans, 1987; Schildge et al., 2013). Plating at a lower density ensured that there was ample open area free of cells for at least several hundred microns away from the edges of a cell identified for recording, a key requirement for the self-referencing recordings used here to examining extracellular H^+ fluxes. Once a cell with appropriate morphology and ample spacing had been identified, an H^+-selective microelectrode was positioned ∼1–2 μm from the edge of the membrane of the cell as well as about 1–2 μm from the bottom of the dish, as shown in **Figure 1B**. An initial reading was first obtained from the H^+-selective microelectrode at this position; the electrode was then translated laterally to a background reference location 30 μm away into the open area devoid of cells, and a second reading from the H^+-selective microelectrode taken (for further details associated with data collection, please see methods). The reading obtained at the background location was then subtracted from that obtained at the edge of the

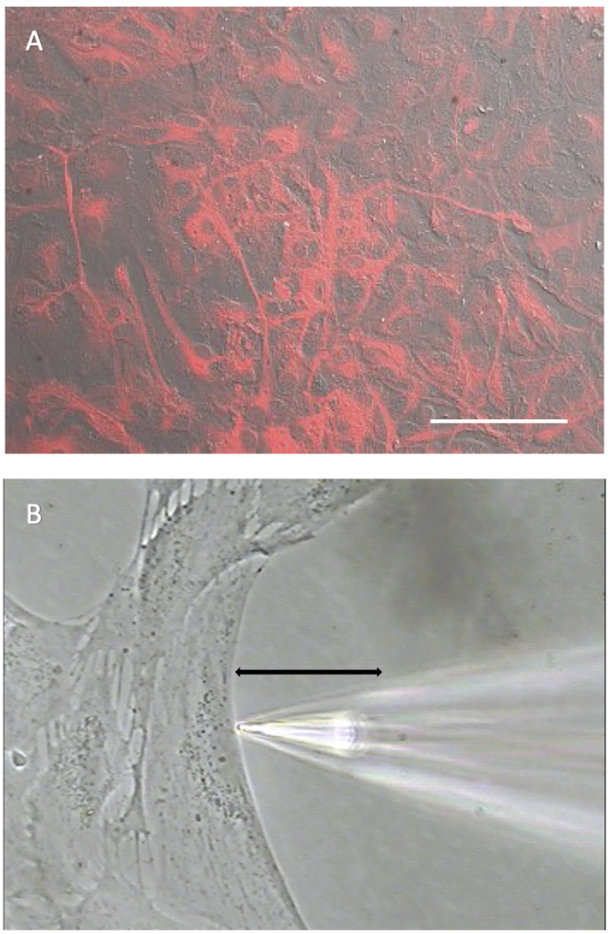

FIGURE 1 | Cells cultured from mouse hippocampus display robust staining for the glial cell marker GFAP. **(A)** Low power photomicrograph combining DIC image with fluorescent staining for GFAP in a confluent dish of cells cultured for 11 days from mouse hippocampus. Red indicates signal from GFAP. The signal was not observed in negative controls (not shown). White scale bar indicates 100 μm. **(B)** High power photomicrograph depicting positioning of an H^+ selective microelectrode adjacent to a cell cultured from mouse hippocampus. Black line indicates the 30 μm lateral movement the H^+ selective electrode would travel from the near pole adjacent to the plasma membrane (pictured) to a background location 30 μm away.

cell, resulting in a signal that reflects an extracellular H^+ flux. A key advantage of this self-referencing approach is that it effectively eliminates the slow electrical drift inherent in all ion-selective electrodes, which can otherwise be large enough to significantly obscure measurements of H^+ efflux from single cells (Smith and Trimarchi, 2001).

A characteristic feature of astrocytes is the presence of H^+-dependent transporters for the neurotransmitter glutamate, and activation of these transport proteins leads to an extracellular alkalinization (Rose and Ransom, 1996; Rose et al., 2017). We therefore initially examined alterations in H^+ flux from cells cultured from mouse hippocampus that were bathed in a Ringer's solution containing 1 mM HEPES and then challenged with 500 μM glutamate. Prior to stimulation, a standing differential signal of 129 ± 22 μV was detected from seven cells, indicating that the solution adjacent to the plasma membrane of the cell was more acidic than the point 30 μm away. Following a control application of a bolus of the same Ringer's solution bathing the cell, the standing H^+ flux was virtually unchanged at 123 ± 21 μV ($P = 0.32$). Upon application of 500 μM glutamate, the differential H^+ signal declined to 69 ± 22 μV, indicating a significant drop in the level of acidity adjacent to the membrane as compared to the originally detected standing H^+ flux ($P = 0.004$), consistent with what would be expected from the transport of glutamate into the cell.

We next examined the effects of the addition of extracellular ATP on H^+ flux from cells cultured from mouse hippocampus. **Figure 2A** shows a response from one cell typical of those obtained when recordings were made with cells bathed in a solution containing 26 mM bicarbonate, the primary buffer for extracellular pH under normal physiological conditions. The initial portion of the trace shows a small standing differential signal which we refer to as the standing H^+ flux prior to stimulation. Upon exchange of the normal bicarbonate Ringer's solution with one containing 100 μM ATP, a significant increase in the signal associated with H^+ flux was detected. Replacement of the ATP containing solution with the normal bicarbonate Ringer's solution lacking ATP resulted in an H^+ flux similar in magnitude to the standing H^+ flux initially detected. At about 1,250 s into the recording, the electrode was elevated to a position 600 μm above the cell and a control set of differential measurements was made until the end of the recording (marked by the asterisk in this and in other recordings). With the electrode at this control location, the concentration of H^+ in the solution should be identical at the two locations of electrode movement. The output of the H^+-selective electrode should thus be the same at the two locations of electrode movement and the differential signal should be close to zero, which is what was observed. This control was done in all recordings obtained in the present work.

Figure 2B shows the quantitative results obtained for H^+ flux from seven cells cultured from mouse hippocampus and bathed in the Ringer's solution in which the primary buffer was 26 mM bicarbonate. Under these conditions, cells had an average standing H^+ flux prior to stimulation of 53 ± 21 μV. Challenging the cells with 100 μM ATP led to an increase in total H^+ flux to 125 ± 25 μV, a significant increase in the overall differential signal detected ($P = 0.0004$). Upon restoration of normal Ringer's solution lacking ATP, the flux decreased to 44 ± 14 μV, a value statistically indistinguishable from the initial standing flux ($P = 0.40$). Extracellular ATP induced similar increases in extracellular H^+ flux from cells cultured from rat cortex possessing astroglial-like characteristics. 100 μM ATP significantly increased the size of the H^+ signal from a standing value of 43 ± 18 μV to 186 ± 39 μV in six cells examined ($P = 0.004$).

When stimulated by extracellular ATP, radial glial cells of the retina, known as Müller cells, demonstrate a significantly increased H^+ efflux that is not dependent on the presence of extracellular bicarbonate or bicarbonate transport mechanisms. To test whether the ATP-induced response from cells cultured from hippocampus was similarly independent of extracellular

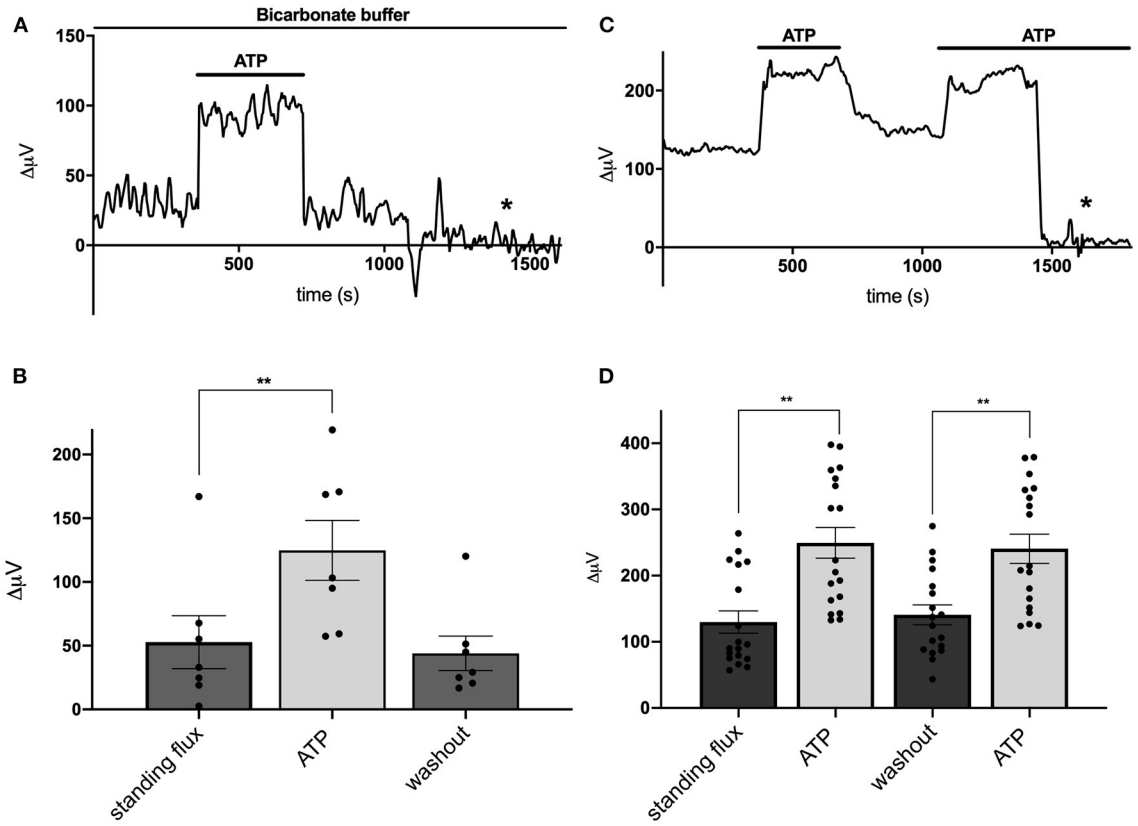

FIGURE 2 | Responses of cells identified as astrocytes cultured from mouse hippocampus to applications of 100 μM ATP. **(A)** Response from one cell bathed in saline buffered with 26 mM bicarbonate to 100 μM ATP. A standing H^+ flux of about 30 μV was observed prior to stimulation. Addition of 100 μM ATP to the bath solution induced a detectable increase in H^+ flux. Upon removal of ATP, the H^+ flux signal returned to its pre-stimulus baseline. From about 1,250 s until the end of the trace (indicated by the asterisk), the electrode was moved to a position 600 μm above the cell, a location where the differential response should be close to 0 μV. **(B)** Average H^+ flux from seven cells bathed in 26 mM bicarbonate saline before, during and after the application of 100 μM ATP; $N = 7$. **(C)** Response from one cell bathed in saline containing 1 mM HEPES as the primary extracellular pH buffer to applications of 100 μM ATP. Prior to challenge with ATP, the cell displayed a standing H^+ flux signal of abut 120 μV. Addition of 100 μM ATP induced an increase in the H^+ flux signal. Removal of ATP resulted in the return of the H^+ flux signal near to its original pre stimulus level. A second application of 100 μM ATP again led to a marked increase in H^+ flux. At about 1,450 s, the electrode was repositioned 600 μm above the cell (designated by the asterisk); at this background location, sampling between two points 30 μm apart gave a differential signal close to 0 μV. **(D)** Average H^+ flux signals from cells bathed in saline containing 1 mM HEPES as the primary extracellular pH buffer; $N = 18$. **indicates $P < 0.01$.

bicarbonate, recordings from cells cultured from mouse hippocampus were obtained using a solution in which 1 mM HEPES was used as the primary extracellular pH buffer and to which no bicarbonate was added. **Figure 2C** shows a sample trace from one cell recorded under these conditions. A standing H^+ flux was again detected prior to stimulation. Application of 100 μM ATP to the extracellular solution induced a notable increase in the overall differential H^+ flux. Removal of ATP brought the flux back to near the original standing H^+ flux, and a second stimulation with 100 μM ATP again increased the size of the detected signal from the H^+-selective microelectrode. The later portion of the trace again reflects a control recording with the electrode placed at 600 μm above the cell resulting in a differential H^+ signal close to zero. **Figure 2D** shows the averaged signals obtained from 18 cells and reveals a standing H^+ flux from unstimulated cells and a significant and repeatable increase in H^+ flux upon addition of 100 μM ATP ($P < 0.0001$). Removal of ATP again led to return of the H^+ flux signal to levels similar to the initial standing H^+ flux. A second application of ATP again increased the H^+ flux signal detected ($P < 0.0001$). The size of this second increase was statistically indistinguishable from the initial response to ATP ($P = 0.14$).

Astrocytes have been shown to possess a sodium-dependent bicarbonate transporter with particularly high affinity, such that the low levels of bicarbonate resulting from CO_2 in the normal atmosphere could potentially provide sufficient substrate for this transporter to function (Theparambil et al., 2014, 2017; Theparambil and Deitmer, 2015). Activation of this transporter could also lead to an alteration in detected levels of H^+ adjacent to the membrane of a cell even in the absence of added bicarbonate. To test whether this mechanism might account for H^+ fluxes initiated by extracellular ATP, we recorded from mouse hippocampal astrocytes immersed in solutions containing 1 mM of the pH buffer HEPES that had been bubbled continuously

with 100% oxygen for at least 15 min, to drive off possible contributions from CO_2 in the air. **Figure 3** shows individual responses and averaged data from cells recorded in normal air and a separate population of cells bathed in 100% oxygen. **Figure 3A** depicts the standing H^+ flux signal, response to 100 μM ATP, and return of the H^+ flux signal upon removal of ATP from a single cell maintained in normal air. **Figure 3B** shows quantitative data averaged from six cells maintained in normal air. In this cell population, the average H^+ flux prior to stimulation was 31 ± 2 μV and addition of 100 μM ATP increased the overall H^+ flux signal to 140 ± 4 μV ($P < 0.0001$). **Figure 3C** shows a recording from one cell maintained in 100% oxygen demonstrating that 100 μM ATP induced a clear increase in H^+ flux in cells in this condition. **Figure 3D** shows results from a separate population of cells recorded in solutions with 100% oxygen. In seven cells examined in Ringer's solution containing 100% oxygen, 100 μM ATP increased the H^+ signal from a standing H^+ flux of 29 ± 3 μV to 157 ± 5 μV ($P < 0.0001$). Thus, ATP elicited H^+ fluxes from cells recorded in oxygen and no atmospheric CO_2 were actually marginally larger in magnitude compared to cells maintained in normal air by about 17% ($P = 0.02$).

Figure 4 shows that the ATP-elicited extracellular H^+ fluxes from cells cultured from mouse hippocampus were dependent upon the dose of extracellular ATP applied. **Figure 4A** shows a sample trace from a cell first exposed to 100 μM ATP and then when challenged with 1 mM ATP. **Figure 4B** shows the average response from five cells to applications of extracellular ATP as concentrations were raised from 100 nM up to 100 μM, and **Figure 4C** shows averaged results from an additional set of five cells when challenged with 100 μM followed by 1 mM ATP.

Extracellular ATP is known to be broken down to adenosine by the action of ecto-ATPase enzymes, and activation of adenosine receptors is known to be a potent modulator of the activity of many cells in the nervous system (Wilson and Mustafa, 2009). We therefore tested the effects of adenosine on cells cultured from mouse hippocampus and identified as astroglial in nature. **Figure 5A** shows a trace from a single cell that was unresponsive to application of 100 μM adenosine but showed a notable increase in H^+ flux when challenged by 100 μM ATP. **Figure 5B** shows averaged results from six cells. In this population, the average H^+ flux in the presence of 100 μM adenosine was 76 ± 27 μV, statistically indistinguishable from the standing H^+ signal of 88 ± 31 μV observed prior to challenge with adenosine. In these same cells, 100 μM ATP increased the H^+ flux signal to 160 ± 35 μV, a statistically significant increase compared to the standing flux ($P = 0.002$). While adenosine was ineffective in inducing an increase in H^+ flux, chemicals known to block ATP receptors were effective in significantly reducing the H^+ flux induced by ATP. **Figure 5C** shows a trace from one cell challenged with 100 μM ATP with the cells bathed in a solution containing 500 μM suramin and 500 μM PPADS, agents known for their ability to block P2 ATP-activated receptors. The mean response from six cells to 100 μM ATP in the presence of PPADS and suramin was 65 ± 23 μV, which was not significantly different from the standing flux (61 ± 23 μV) observed in the presence of those blockers ($P = 0.68$). Following washout of PPADS and suramin, 100 μM ATP increased the H^+ flux signal from a new standing flux value of 72 ± 20 μV to 131 ± 29 μV (shown graphically in **Figure 5D**). A similar block of ATP-elicited increases in H^+ flux by suramin was observed in cells cultured from rat cortex. The mean H^+ flux signal detected in response to application of 50 μM ATP in the presence of 1 mM suramin was 33 ± 4 μV in five such cells, which was not significantly different from the standing flux of 24 ± 9 μV observed in the presence of the blocker alone ($P = 0.19$). Following washout of both suramin and ATP, these cells displayed a standing H^+ flux signal of 39 ± 5 μV, and application of 50 μM ATP then increased the size of the H^+ flux signal to 159 ± 29 μV ($P = 0.006$).

Extracellular ATP has been shown to increase intracellular calcium in astrocytes via activation of G-protein-linked ATP receptors that result in the release of calcium from intracellular stores (cf. Agulhon et al., 2008; Wang et al., 2009; Bazargani and Attwell, 2016; Guerra-Gomes et al., 2017 for review). We therefore tested whether the ATP-initiated H^+ flux detected with self-referencing H^+ selective electrodes similarly required increases of intracellular calcium. Ratiometric measurements of fluorescence changes in cells loaded with Fura-2AM and excited at 340 and 380 nm were used to examine alterations in intracellular calcium and plotted as a percentage of the saturating fluorescence change induced by addition of the calcium ionophore ionomycin. **Figure 6A** shows the change in the fluorescent ratio with time averaged from 12 astrocytes cultured from mouse hippocampus and monitored simultaneously during one such experiment. Following challenge with 100 μM ATP, a significant increase in the ratio of 340/380 induced fluorescence was detected, indicating a significant elevation of intracellular calcium as expected; the standing fluorescence ratio prior to stimulation was 26 ± 2% of the maximal signal, compared to a ratio of 51 ± 3% in the presence of 100 μM ATP ($P < 0.001$) (shown graphically in **Figure 6B**). ATP thus produced an ∼100% increase in the fluorescent ratio. ATP was then washed off, and 1 μM thapsigargin, an agent known to prevent re-accumulation of calcium into intracellular stores, was added for several minutes. Cells were then challenged again with 100 μM ATP, and as can be seen in the figure, ATP now failed to elicit a significant rise in intracellular calcium. The standing fluorescence ratio in the presence of 1 μM thapsigargin was 29 ± 2%; upon addition of 100 μM ATP, the fluorescence ratio remained at 29 ± 1% ($P = 0.84$). In contrast, in control experiments conducted in the absence of thapsigargin, a second application of 100 μM ATP produced an alteration in the fluorescent ratio that was 71% the size of the initial application of ATP ($N = 11$); the inset to **Figure 6A** shows one example of a control experiment in which ATP was applied multiple times. Thus, thapsigargin was able to significantly depress the rise in intracellular calcium normally initiated by ATP.

The same concentration of thapsigargin that effectively eliminated ATP-induced increases in intracellular calcium also potently inhibited ATP-induced increases in H^+ flux. **Figure 6C** shows the H^+ flux signal obtained from one astrocyte cultured from cryopreserved hippocampal cells. Application of 100 μM ATP produced a clear increase in H^+ flux. 1 μM thapsigargin was then added to the bath and ATP removed several seconds

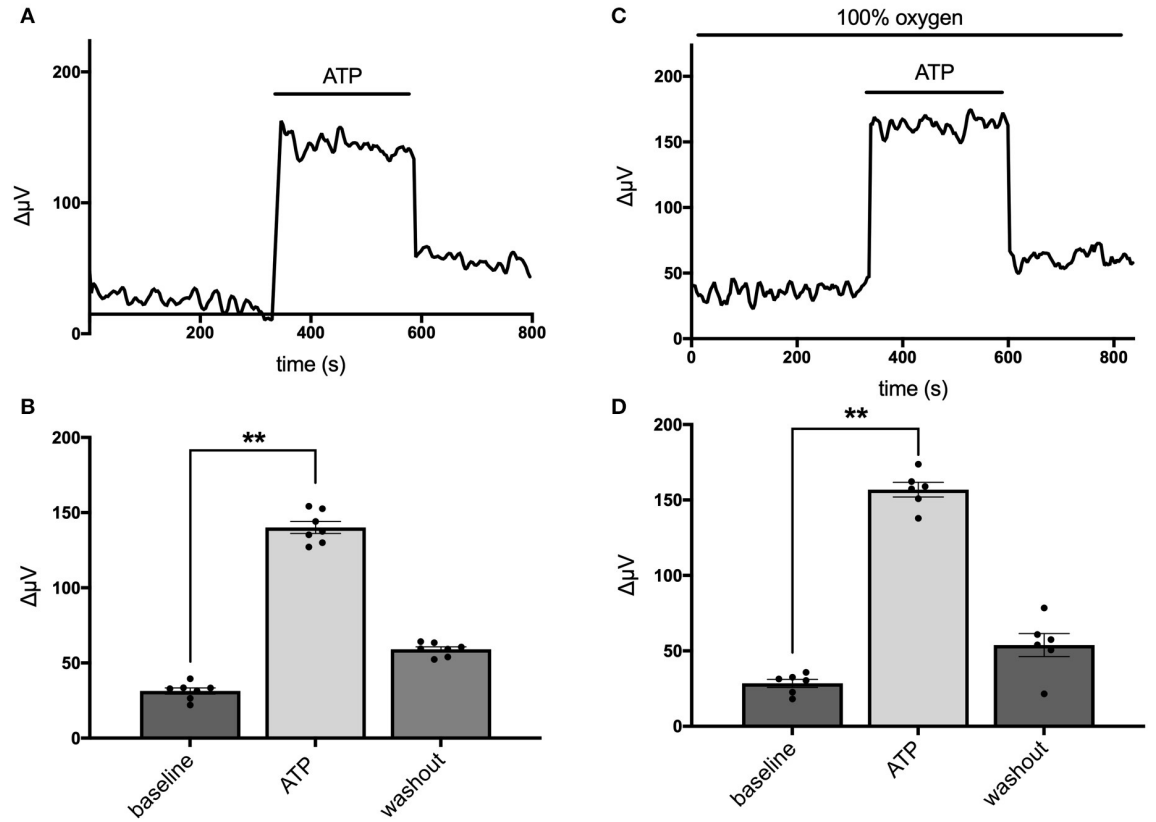

FIGURE 3 | Responses of cells from cryopreserved mouse hippocampal cultures to 100 μM ATP bathed in a saline solution containing 1 mM HEPES and saturated either with normal air or 100% oxygen. **(A)** Trace from one cell maintained in normal air in standing saline followed by application and then removal of 100 μM ATP. **(B)** Quantitative data averaged from cells in normal air; $N = 6$. **(C)** Trace of H^+ flux signal from one cell maintained in 100% oxygen. **(D)** Quantitative data of H^+ signals obtained from cells in saline containing 100% oxygen; $N = 7$. **indicates $P < 0.01$.

after, and the H^+ flux signal returned to its pre-stimulus level. Challenge of the cell with 100 μM ATP several minutes later with thapsigargin still present now failed to induce a large increase in the H^+ flux signal. **Figure 6D** shows averaged responses from six cells cultured from cryopreserved mouse hippocampal cells. 100 μM ATP increased the H^+ flux signal from a pre-stimulus level of 36 ± 1 μV to 178 ± 1 μV ($P < 0.0001$). In the presence of 1 μM thapsigargin, 100 μM ATP failed to induce a significant increase in the same set of cells. After several minutes in thapsigargin, the standing H^+ flux signal from these cells was at 45 ± 2 μV; addition of 100 μM ATP in the continued presence of thapsigargin now resulted in an H^+ flux signal of 49 ± 3 μV, not significantly different from the pre-stimulus standing flux detected in the presence of thapsigargin alone ($P = 0.081$).

Recent work examining the molecular mechanisms underlying ATP-induced H^+ extrusion from retinal Müller glia suggests that the majority of acid is provided by Na^+/H^+ exchange activity (Tchernookova et al., 2021). Consequently, we sought to determine if this was also the case for the ATP-induced extrusion of H^+ from brain astrocytes. To explore this question, we examined H^+ fluxes under conditions in which extracellular sodium was removed and replaced with an equivalent amount of choline, a large cation that cannot substitute for sodium in Na^+/H^+ exchange. **Figure 7A** shows the result of this ionic substitution protocol on the response from one astrocyte cultured from mouse hippocampus. With the cell bathed in 0 mM extracellular sodium (all sodium replaced by equimolar choline), 100 μM ATP still produced a sizable increase in extracellular H^+ flux as measured with a self-referencing H^+-selective electrode and washing out the ATP brought the H^+ flux signal back near to its original size. Restoration of extracellular sodium to normal levels resulted in an increase in the standing H^+ flux signal, and addition of 100 μM ATP produced a further increase in H^+ flux. Panel B of **Figure 7** shows quantitative results averaged from nine such cells. With cells bathed in 0 mM sodium, addition of 100 μM ATP increased the H^+ flux signal from an initial standing flux value of 65 ± 10 μV to 185 ± 31 μV, a statistically significant increase in the size of the flux ($P = 0.009$). Washing out the ATP with the cell still in 0 mM sodium brought the signal back close to its initial level (68 ± 12 μV). Replacement of the 0 sodium/choline solution with normal extracellular sodium Ringer's solution increased the standing H^+ flux signal to 137 ± 16 μV, significantly larger than the standing flux observed in 0 sodium Ringer's solution ($P = 0.0003$). Addition of 100 μM ATP

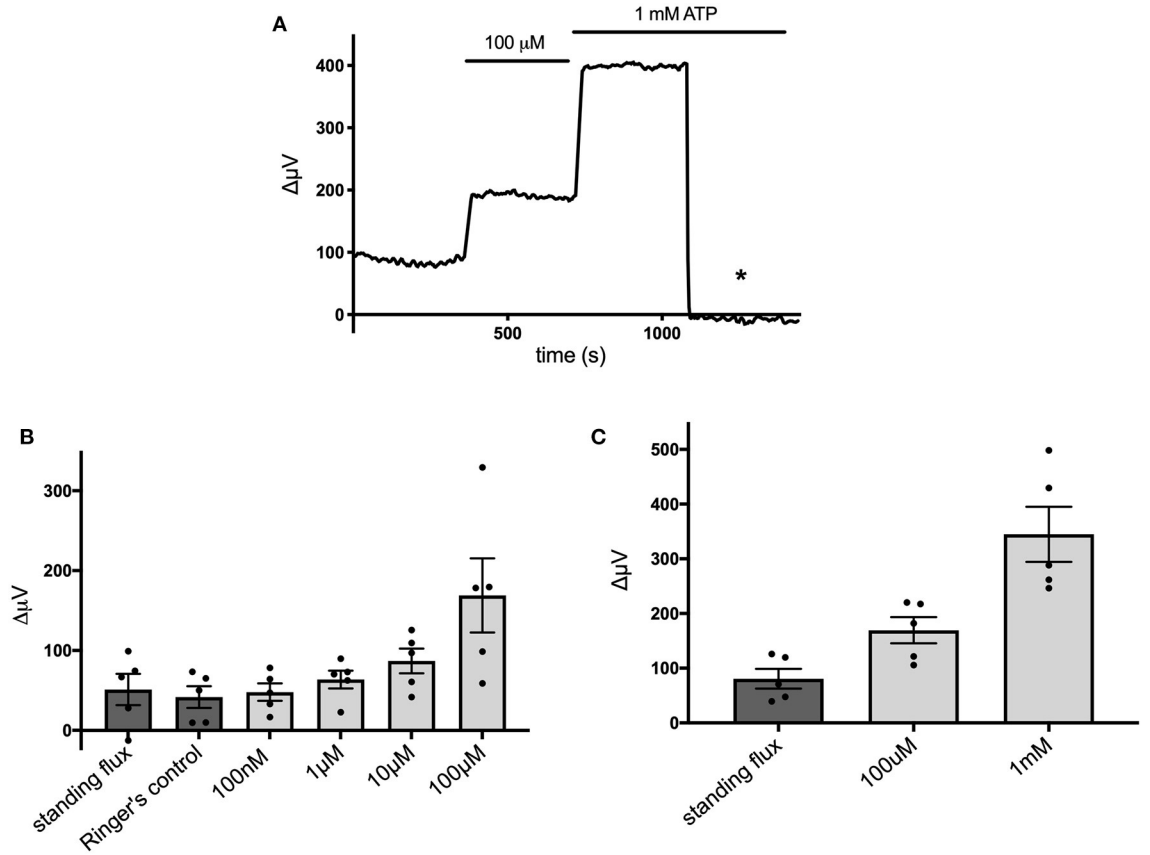

FIGURE 4 | Responses of cells cultured from hippocampus to different concentrations of extracellular ATP. **(A)** Response of one cell in saline solution containing 1 mM HEPES to application of 100 μM and 1 mM ATP. **(B)** Average responses of cells to concentrations of extracellular ATP ranging from 100 nM to 100 μM; $N = 5$. **(C)** Average responses of additional cells to 100 μM and 1 mM extracellular ATP; $N = 5$.

to the same cells further increased the H^+ flux signal to 249 ± 41 μV, a significant increase compared to the standing H^+ flux observed upon restoration of normal extracellular sodium ($P = 0.037$). In order to determine the effect of sodium specifically on ATP-induced increases in H^+, the size of the ATP-induced signals were compared after having subtracted out the value for the standing H^+ flux. This is shown in **Figure 7C** and plots the average amplitude of the ATP-induced H^+ flux signal in the same nine cells after having subtracted out the value for the standing flux prior to ATP application. The increase in H^+ flux due to addition of 100 μM ATP was 120 ± 35 μV with cells bathed in 0 mM sodium and 112 ± 35 μV in normal sodium solution, values that were not statistically different from one another ($P = 0.57$) and arguing against a large role for Na^+/H^+ exchange in mediating ATP-elicited increases in H^+ flux.

We also examined the effects of EIPA, a potent pharmacological inhibitor of Na^+/H^+ exchange, on the ATP-induced increases in H^+ flux. EIPA has been reported to have an IC50 of ∼0.02–2.5 μM in inhibiting the activity of isoforms NHE1, NHE2, NHE3, and NHE5 (Attaphitaya et al., 1999; Masereel et al., 2003). **Figure 8A** shows the response from one astrocyte cultured from mouse hippocampus to applications of 100 μM ATP in the presence and then absence of 200 μM EIPA. An obvious increase in the size of the H^+ flux upon addition of 100 μM ATP was apparent in both conditions. **Figure 8B** shows the size of the H^+ flux signals averaged from nine such cells. 100 μM ATP increased the H^+ flux from a standing value of 10 ± 21μV to 187 ± 25 μV ($P = 0.0009$) in the presence of EIPA. Following washout of the EIPA, 100 μM ATP increased the H^+ flux from a standing value of 118 ± 16 μV to 182 ± 24 μV ($P = 0.002$). The size of the ATP-induced responses in the presence and absence of EIPA were not statistically significantly different ($P = 0.75$).

DISCUSSION

The data presented here demonstrate that extracellular ATP applied to cells cultured from mouse hippocampus and rat cortex possessing characteristics typical of astrocytes induces an increase in the flux of acid (H^+) from the cells. Extracellular ATP also induces an increase in levels of intracellular calcium, and this calcium appears to be required for the increase in H^+ flux, since abolishment of ATP-induced rises in intracellular calcium using thapsigargin also eliminate the increase in H^+ flux measured with self-referencing H^+ selective electrodes.

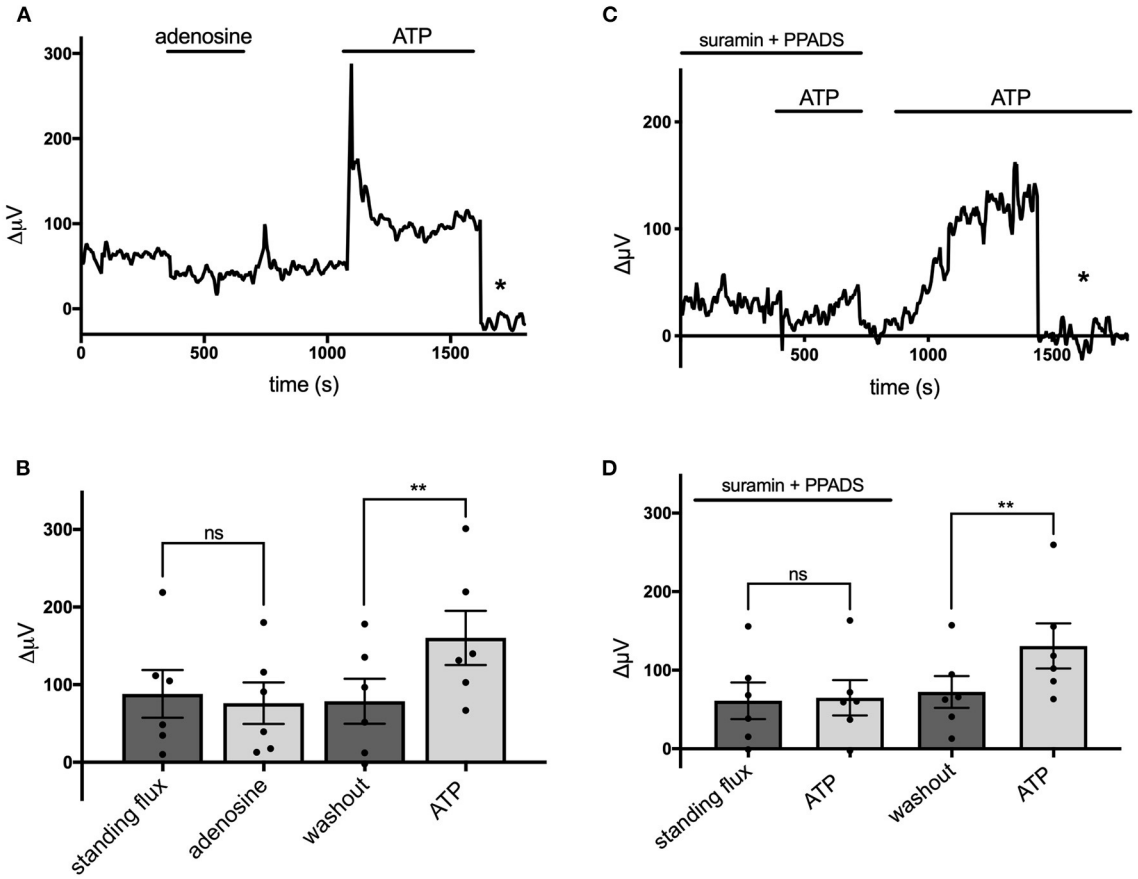

FIGURE 5 | Adenosine does not alter H^+ flux signals while suramin and PPADS reduce H^+ flux. **(A)** Response of a single cell cultured from mouse hippocampus to 100 μM adenosine and 100 μM ATP. Asterisk indicates signal obtained when the H^+-selective electrode had been moved to a control position 600 μm above the cell. **(B)** Quantitative results to the applications of 100 μM adenosine and 100 μM ATP from cells ($N = 6$). **(C)** Response of a single cell to 100 μM ATP first in the presence of 500 μM suramin and 500 μM PPADS and then again to 100 μM ATP following removal of suramin and PPADS. Asterisk again indicates recordings of the H^+-selective electrode when at a control position 600 μm above the cell. **(D)** Quantitative results averaged from cells to 100 μM ATP in the presence of 500 μM suramin and 500 μM PPADS and response to 100 μM ATP following removal of suramin and PPADS; $N = 6$. **indicates $P < 0.01$; ns indicates not significantly different ($P > 0.05$).

H^+ fluxes monitored from mouse hippocampal and rat cortical astrocytes using self-referencing electrodes have a number of features that are similar to H^+ fluxes previously examined from isolated retinal radial glia commonly referred to as Müller cells using similar self-referencing techniques (Tchernookova et al., 2018). Brain-derived astrocytes and retinal radial glia both display small standing H^+ fluxes prior to activation that are likely associated with the removal of internal H^+ generated by normal metabolism, and ATP applied extracellularly promotes a sizable increase in H^+ efflux from both cell types. The increase in H^+ flux induced by extracellular ATP likely results from activation of metabotropic P2 ATP receptors known to be present on both sets of cells, as judged by the ability of the response to be significantly reduced by the ATP receptor blockers suramin and PPADS. H^+ flux responses from both cultured astrocytes and isolated retinal radial glia are not altered by application of adenosine, and the ATP-elicited increase in H^+ flux from both sets of cells require a rise in intracellular calcium as judged by the ability of thapsigargin to eliminate both ATP-initiated increases in intracellular calcium and ATP-induced alterations in H^+ flux. ATP-induced increases in H^+ flux are also detected from both cultured astrocytes and Müller cells regardless of whether the primary extracellular pH buffer is provided by physiologically relevant concentrations of bicarbonate or 1 mM HEPES (Tchernookova et al., 2018).

Both astrocytes and Müller cells extend fine processes that wrap and envelop nearby synaptic complexes established by neurons (Wang et al., 2017; cf. Vasile et al., 2017; Zhou et al., 2019). Both sets of cells are thus in an ideal position to be able to detect chemical signals released by neurons at synapses and to modulate release of neurotransmitter at these crucial neuronal connections. Given the high sensitivity of voltage-gated calcium channels to small changes in extracellular acidity (Barnes et al., 1993; Tombaugh and Somjen, 1996; Shah et al., 2001; Doering and McRory, 2007; Saegusa et al., 2011; Han et al., 2017), we propose that the ATP-initiated increase in H^+ efflux from

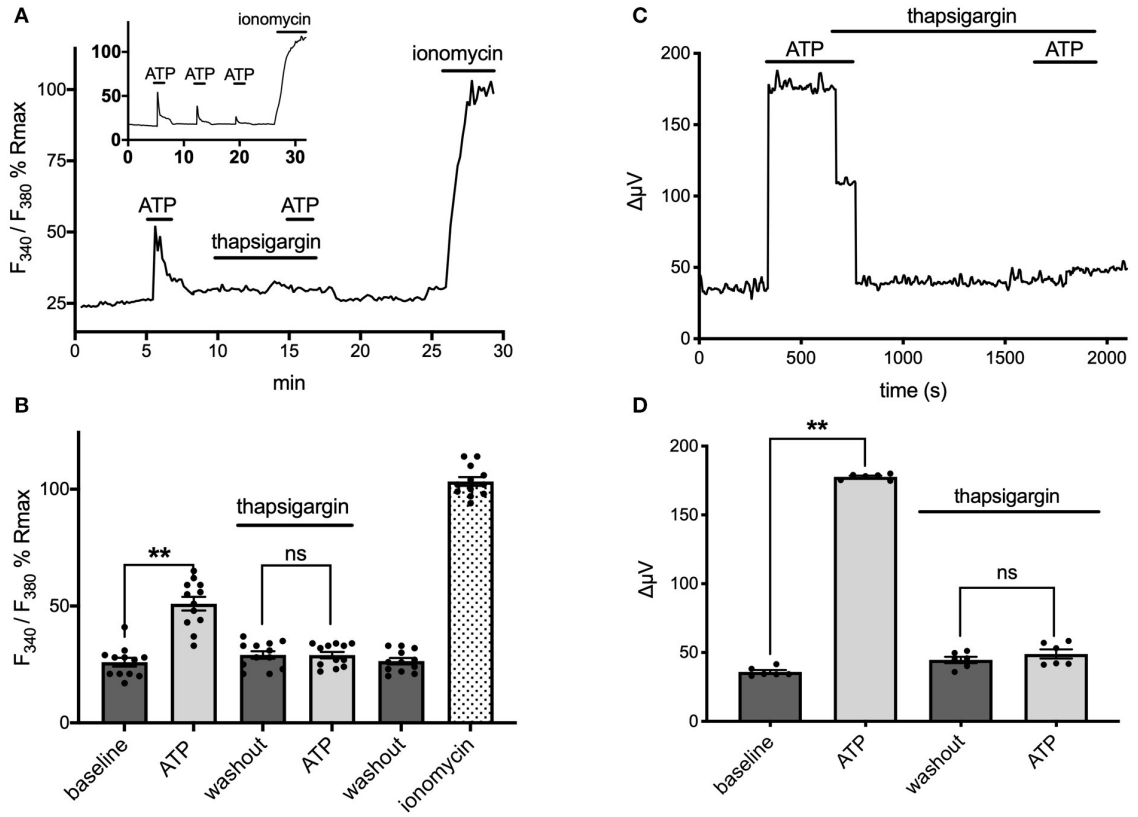

FIGURE 6 | ATP-induced alterations in H^+ flux require increases in intracellular calcium. **(A)** Measurements of changes in intracellular calcium from cells cultured from mouse hippocampus as reported by the calcium indicator fura-2. Trace shows averaged percentage change in the ratio of Fura-2 fluorescence from 12 astrocytes imaged simultaneously plotted as a percentage of the maximal change in ratio observed upon addition of the calcium ionophore ionomysin. Challenge of the cells with 100 μM ATP resulted in an increase in the ratio of Fura-2 fluorescence indicative of an increase in intracellular calcium. Following washout of the ATP and return of the signal to baseline, cells were superfused with 1 μM thapsigargin for several minutes and then challenged a second time with 100 μM ATP, which now induced little change in the Fura-2 ratio. The thapsigargin and ATP were then removed from the dish; after several additional minutes, the calcium ionophore ionomycin was added to determine a maximal change in fluorescent ratio. Inset shows typical response to multiple applications of ATP under control conditions with no thapsigargin present. **(B)** Data from the same cells presented in histogram format, again as a percentage of the maximal induced change in ratio induced by application of ionomycin; $N = 12$. **(C)** Self-referencing trace from a single cell cultured from cryopreserved mouse hippocampal cells showing alteration in H^+ flux to 100 μM ATP. The cell was then bathed in 1 μM thapsigargin, ATP washed off, and the cell left to sit in thapsigargin for several minutes. A second application of 100 μM ATP now produced little change in the H^+ flux signal. **(D)** Effects of thapsigargin on H^+ flux signal; $N = 6$. **indicates $P < 0.01$; ns indicates not significantly different ($P > 0.05$).

both astrocytes and Müller cells may well be a key mechanism regulating neurotransmitter release by neurons, acting as an inhibitory feedback loop to reduce release of neurotransmitter. Vesicles in neurons containing neurotransmitter are also known to contain ATP and release that ATP upon fusion with the plasma membrane (cf. Zimmermann, 1994; Pankratov et al., 2006; Abbracchio et al., 2009; Burnstock and Verkhratsky, 2012 for review). We propose that the fusion of neuronal vesicles with the plasma membrane results in the release of both neurotransmitter and ATP, and that the released ATP activates ATP metabotropic receptors on the glia. This would result in an increase in intracellular calcium released from intracellular stores in glia, which ultimately results in the increased extrusion of H^+ from the glia. According to this hypothesis, H^+ released by glia would bind to calcium channels on neurons, reducing the peak amount of calcium entering through the channel as well as shifting the voltage-dependent opening of the channels to more depolarized values. The resulting decrease in the influx of calcium into the neurons would result in a decrease in the calcium-dependent fusion of vesicles to the plasma membrane and a consequent decrease in neurotransmitter release by the neurons.

A second important impact likely to result from the extrusion of acid from glial cells is enhanced removal of neurotransmitter from the extracellular milieu by H^+-dependent transporters known to be present in glia and neurons (Grewer and Rauen, 2005; Soto et al., 2018). For example, hippocampal astrocytes are known to possess transport proteins for the key neurotransmitter glutamate that act by ferrying three sodium ions and one proton along with glutamate into the cell while also exporting one potassium ion (Nicholls and Attwell, 1990; Owe et al., 2006; Vandenberg and Ryan, 2013; Rose et al., 2017). The removal of neuronally-released glutamate by uptake into astrocytes thus leads to an extracellular alkalinization, and is indeed what we and others have detected from cultured astrocytes upon application of

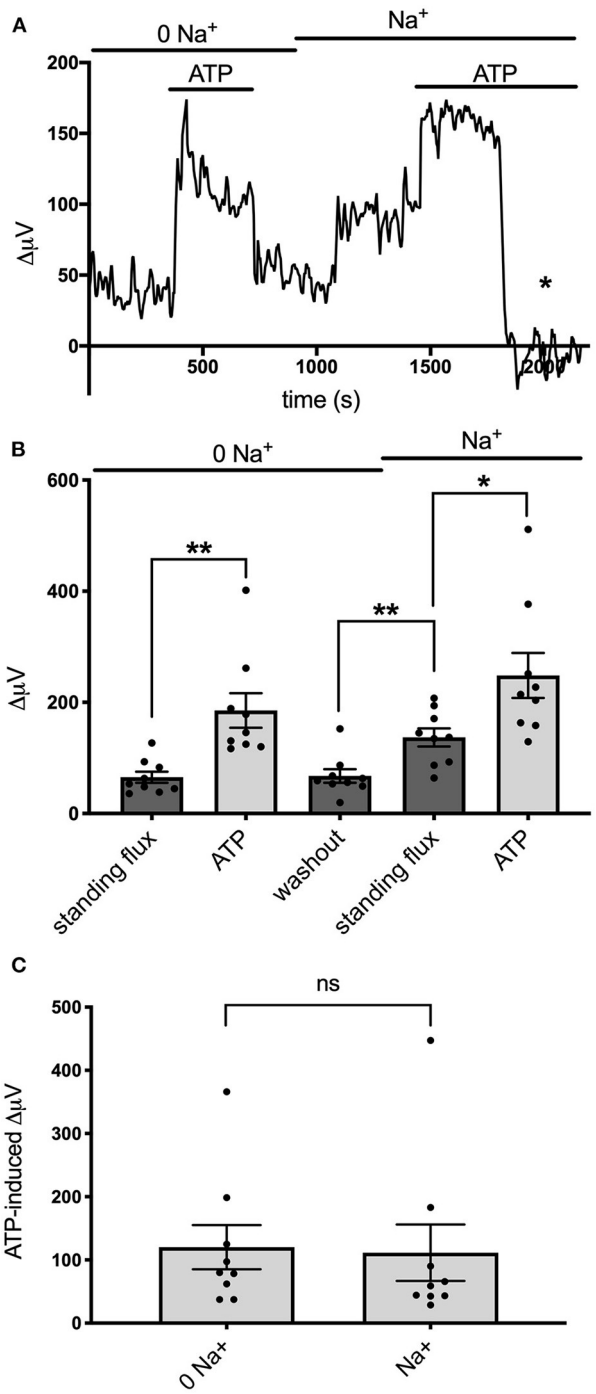

FIGURE 7 | Effects of alterations in extracellular sodium on ATP-induced increases in H^+ flux. **(A)** Trace showing H^+ flux signals in response to 100 μM ATP from a single cell cultured from mouse hippocampus first when bathed in 0 mM extracellular sodium and then when extracellular sodium was restored to normal levels. Restoration of sodium induced a notable increase in the standing H^+ flux. Asterisk indicates response of self-referencing H^+-selective electrode when in a control location 600 μm above the cell. **(B)** Quantitative results averaged from cultured mouse hippocampal cells showing H^+ flux in cells first bathed in 0 mM sodium and then when normal levels of sodium were restored; $N = 9$. *indicates $0.01 < P < 0.05$; **indicates $P < 0.01$. **(C)** Responses to ATP from the same cells when the contribution of the standing H^+ flux observed prior to application of ATP was subtracted out; $N = 9$. ns, indicates not significantly different ($P > 0.05$).

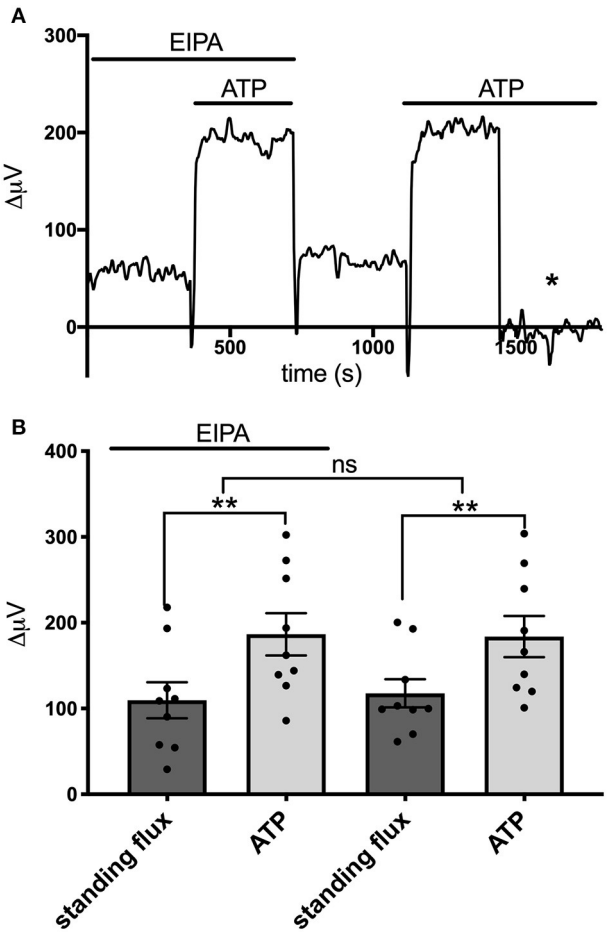

FIGURE 8 | Lack of effect of the Na^+/H^+ inhibitor EIPA on H^+ flux. **(A)** Trace showing H^+ flux signal from a single astrocyte cultured from mouse hippocampus upon application of 100 μM ATP first in the presence of 200 μM EIPA and then again after the EIPA had been removed from the bath. **(B)** H^+ flux signals averaged from cells cultured from mouse hippocampus in the presence of EIPA and following washout of the drug; $N = 9$. **indicates $P < 0.01$; ns indicates not significantly different ($P > 0.05$).

glutamate. The co-release of ATP with glutamate from neuronal vesicles would activate H^+ extrusion from the glia into the extracellular fluid, a process that would supply much needed substrate for the further removal of glutamate from the synaptic cleft. In a careful examination of flux coupling of the EAAT3 glutamate transporter, Zerangue and Kavanaugh (1996) reported an affinity constant for H^+ of 26 nM during glutamate transport, corresponding to a pH of about 7.58. This value implies that small changes of extracellular H^+ around normal physiological levels of pH could indeed significantly impact the transport of glutamate into cells. The expected enhancement of the removal of neurotransmitter via addition of H^+ extruded by astrocytes, coupled with the reduction in the release of neurotransmitter due to H^+-mediated decrease of calcium into neurons, would both result in inhibiting the flow of neuronal information transfer at the synapse.

Studies examining the three dimensional pattern of calcium dynamics in both awake animals and brain slices

suggest that calcium increases in individual astrocytes are scattered throughout the cell, highly compartmentalized within predominantly local regions, and heterogeneously distributed regionally and locally (Bindocci et al., 2017; Savtchouk et al., 2018). Moreover, these same studies also indicate that astrocytes can respond locally to quite minimal axonal firing with time-correlated changes in intracellular calcium. These data suggest that potential regulation of neurotransmitter release by H^+ into the extracellular fluid could be highly localized, and that extrusion of H^+ initiated by local increases in calcium may modulate synaptic strength at a synapse-by-synapse scale. The thousands of fine processes from astrocytes wrapping various separate synapses could thus potentially act independently from one another, with ATP released at just that synapse acting to locally influence synaptic strength by highly localized release of H^+.

ATP can also be released from the glial cells themselves, a phenomenon that has been implicated in the production of waves of intracellular calcium across many glia (Arcuino et al., 2002; Coco et al., 2003; Koizumi et al., 2003; Anderson et al., 2004; Scemes and Giaume, 2006; Bowser and Khakh, 2007; Halassa et al., 2007). Release of ATP from glial cells has also been shown to have effects on synaptic signaling and neuronal activity (Newman, 2003, 2015; Illes et al., 2019). While the mechanism by which glial cells release ATP remains a matter of considerable contention, a number of studies have provided evidence that the release is dependent upon a rise in intracellular calcium. We suggest that H^+ efflux from glial cells mediated via waves of ATP across multiple glia may represent a key component underlying the phenomenon known as "spreading depression," characterized as a slow wave of depression of electrical activity observed in many areas of the nervous system (Kunkler and Kraig, 1998; Torrente et al., 2014; Cozzolino et al., 2018; Wu et al., 2018). We hypothesize that the associated depression of electrical activity results from the release of H^+ from the glial cells, acting on the neuronal calcium channels to reduce the amount of neurotransmitter released.

The ATP-elicited H^+ fluxes from cultured astrocytes did not appear to be highly dependent upon extracellular sodium. That observation and the fact that fluxes were not significantly reduced in solutions designed to reduce contributions of CO_2 from the air (by bubbling solutions with 100% oxygen) make it highly likely that the ATP-induced H^+ fluxes we report here are not due to the activity of a high affinity sodium-dependent bicarbonate transporter. The ATP-initiated increases in H^+ flux were also not significantly reduced by EIPA, an agent known to be a potent inhibitor of Na^+/H^+ exchange activity. The lack of dependence on extracellular sodium and the inability of Na^+/H^+ inhibitors to reduce the flux differ from the ATP-induced alteration in H^+ flux previously detected in the radial glial cells (Müller cells) isolated from the retina of the tiger salamander. Upon removal of extracellular sodium, ATP-initiated H^+ fluxes from Müller cells were reduced by about 70%, and ATP-initiated H^+ fluxes were also inhibited by several pharmacological agents known to interfere with Na^+/H^+ exchange (Tchernookova et al., 2021). These differences suggest that the molecular mechanism mediating the majority of H^+ flux in astrocytes cells is likely to be different from that in the retinal radial glial cells. One attractive potential alternative candidate remaining is the activity of monocarboxylate transporters, which are thought to play an important role in enabling astrocytes to provide lactate to neurons for their energy needs and which require co-transport of lactate with H^+ (Pierre and Pellerin, 2005; Jha and Morrison, 2018, 2020). The release of lactate would likely be greatest when neuronal activity is highest, which would coincide with the highest levels of extracellular ATP co-released with neurotransmitter when numerous vesicles fuse. Future studies will be required to determine the particular protein(s) mediating H^+ efflux as well as other steps involved in the ATP-initiated signal transduction cascade.

The hydrolysis of ATP to ADP and an additional phosphate group by ecto-ATPases has been suggested to lead to an acidification of the extracellular solution within synapses of the nervous system (Vroman et al., 2014). However, the extracellular acidifications measured here are unlikely to be caused by such a mechanism. The ATP-induced increase in H^+ flux was virtually abolished by 1 μM thapsigargin, a compound that exerts its effects by blocking the reuptake of intracellular calcium into internal stores, and by the addition of the P2 receptor blockers suramin and PPADS. Neither of these agents is known to have any effect on ecto-ATPases. If the ATP-elicited increase in extracellular H^+ flux was due to the acidifying actions of an ecto-ATPase, then our H^+-selective self-referencing probes should still have detected an increase in ATP-induced extracellular H^+ flux when either thapsigargin or the P2 receptor blocking agents were added to the bath.

The amplitude of the ATP-induced H^+ flux signal detected from cells in 1 mM HEPES was similar to that obtained with cells bathed in 26 mM HCO_3. While the overall bulk buffering capacity of the 26 mM bicarbonate solution is expected to be greater than the solution containing 1 mM HEPES, the kinetics of the bicarbonate buffering system in the absence of carbonic anhydrase is also relatively slow and can be rate-limiting, with interconversion between CO_2 and HCO_3 taking 30 s or more to reach equilibrium (Maren, 1988; Spitzer et al., 2002). The combination of the slow kinetics of bicarbonate buffering coupled with the very close positioning of the H^+-selective microelectrode ($\sim$ 1 μm) to the source of H^+ extrusion from the plasma membrane makes it likely that relatively few protons interact with bicarbonate ions to produce CO_2 prior to being detected by the H^+-selective sensor. In an unbuffered solution the diffusion coefficient for H^+ has been reported to be $9.3 * 10^{-5}$ $cm^2 * sec^{-1}$, and even within the cytoplasm of a cell containing a mixture of immobile buffering agents along with mobile bicarbonate ions, the diffusion coefficient of H^+ has been estimated to be $1.4–2.1 * 10^{-6}$ $cm^2 * sec^{-1}$ (Al-Baldawi and Abercrombie, 1992; Spitzer et al., 2002). In the latter condition, the time it takes for a proton to travel 1 μm (the distance of the H^+-selective sensor used in these experiments from the plasma membrane of the cell) is about 2 ms (Al-Baldawi and Abercrombie, 1992). Thus, because of the limited degree of H^+ buffering expected to take place over this short time and distance, it is perhaps not surprising

that the size of the H^+ flux signals from cells in solutions buffered with bicarbonate or HEPES are likely to be similar in overall magnitude.

A previous study examining acid efflux from astrocytes cultured from the neopallium of 1 day old rats using microphysiometry, an entirely different technique (McConnell et al., 1992), also suggests that extracellular ATP induces acid efflux (Dixon et al., 2004). In that study, it was noted that cariporide, an inhibitor of Na^+/H^+ exchange, suppressed the initial portion of ATP-induced H^+ efflux, and the authors argued for a role for Na^+/H^+ transport in this process. However, the 5 μM cariporide used in that study depressed the ATP-elicited H^+ efflux measured by microphysiometry by a maximum of only about 30%, indicating that the majority of acid release was not due to extrusion by NHE1 exchange. One challenge with the interpretation of microphysiometry results is the requirement in those experiments for responses from very large numbers of cells. While an indication of the exact number of cells used in each microphysiometry experiment was not listed, with techniques employed at the time, on the order of 10^6 cells or more were needed to obtain reliable signals with this technique (McConnell et al., 1992). The authors note that ∼99% of cultured cells in their cultures expressed abundant GFAP and had morphological characteristics similar to those expected to astrocytes, but also note that the cultures used did have small numbers of cells with other characteristics. Given the nature of the microphysiometry experiments (measuring the sum of acid released by all the cells present), it is possible that some portion of the measured H^+ fluxes may have come from cells other than astrocytes. One major advantage of the self-referencing H^+ microelectrode method used here is the ability to restrict measurements to alterations in extracellular H^+ fluxes from single cells possessing a clear astrocytic morphology. On the other hand, the high spatial resolution of H^+-selective microelectrodes also means that we might have consistently positioned the sensors at regions of the cell low in Na^+/H^+ activity and could have missed higher levels in other locations around the cell. Another difference in methodology is that the experiments conducted with microphysiometry were done on confluent cell cultures grown for 11 days, while in the present set of experiments cells were examined at earlier times prior to confluence, and it may well be that the physiological properties of the astrocytes are different in the two sets of culturing conditions. One feature that both methods have in common, however, is the difficulty of attempting to estimate what the actual change in extracellular H^+ concentration might be under normal physiological conditions where astrocytes wrap and envelop neuronal synapses. As noted by Dixon et al. (2004), extrapolation of results from cell cultures to the brain requires consideration of the buffering properties and geometric characteristics of the intact tissue, including the distance of astrocytic process from the synapse and the location and density of the transporters exporting H^+ from the astrocytes.

Given the very high sensitivity of neuronal transmission in response to quite small changes in extracellular H^+, and the observations demonstrating H^+ efflux from astrocytes when activated by ATP in the present work, experiments to directly measure changes at the level of synapses in the intact brain mediated by activation of astrocytes are clearly called for. A number of important issues remain to be addressed by such future studies. For example, a recent study has suggested that activation of glial P2Y receptors results in the release of bicarbonate from astrocytes (Theparambil et al., 2020) and has been proposed as a mechanism to moderate alterations in H^+ in the nervous system. The production of H^+ and HCO_3 are intimately related, with both resulting from the interaction of CO_2 with water that is greatly facilitated by the enzyme carbonic anhydrase, and many glial cells have been reported to have high concentrations of this enzyme (cf. Cammer and Tansey, 1988; Nagelhus, 2005; Theparambil et al., 2017, 2020). It seems likely, then, that activation of glial P2Y receptors leads to the production and release of both H^+ and HCO_3. The overall impact of these two chemical species on synaptic activity will depend upon the specific location of H^+ and HCO_3 transporters as well as on the level of extracellular carbonic anhydrase present within the synaptic cavity. Our previous studies on H^+ efflux from retinal radial glial (Müller) cells suggest release of protons from areas likely to be associated with synaptic connections, while sodium coupled HCO_3 transporters on these same cells are much more abundantly expressed in the basal end foot of the cell close to the vitreous humor, suggesting potential differential impacts from the spatial inhomogeneity of release of H^+ and HCO_3 produced within the cell (Newman, 1996; Kreitzer et al., 2017; Tchernookova et al., 2018). Also, as noted earlier, the uncatalyzed conversion of HCO_3 to CO_2 is quite slow. Even if H^+ and HCO_3 were released at the same subcellular location, the effects of H^+ could be swift, significant, and relatively prolonged if little carbonic anhydrase were present in the synaptic cavity. The impact of concomitantly released HCO_3 on the time course of extracellular acidification could be dramatically altered if significant concentrations of carbonic anhydrase, which can speed the conversion reaction by a factor of $\sim 10^6$, were present. The overall time course and magnitude of the effects of H^+ released by glia will thus depend critically on the concentration, spatial location, and variant of extracellular carbonic anhydrase present.

The pharmacological profile of ATP-initiated H^+ release by glial cells in the intact nervous system is also an area worthy of future investigation that has the potential to be challenging and complicated. Our own experiments on astrocytes cultured from hippocampus and cortex strongly implicate activation of a P2Y receptor, since the ATP-initiated H^+ flux could be largely abolished by thapsigargin, suggesting that release of calcium from intracellular stores is an essential step in the signal transduction pathway. The block of ATP-initiated H^+ efflux by thapsigargin along with its elimination of ATP-elicited changes in intracellular calcium would appear to eliminate the possibility that calcium influx through a P2X receptor plays a significant role, since extracellular calcium was still present when ATP was applied in the presence of thapsigargin. Studies of ATP-elicited H^+ efflux from retinal radial glia (Müller) cells strongly suggest activation of a PLC-dependent pathway leading to release of calcium stores, and similar studies should be

done with the astrocyte cultures to solidify this portion of the transduction pathway. The specific subtype(s) of P2Y receptor initiating the signal transduction pathway is also a question worth pursuing, but also has the potential to be difficult to cleanly interpret. For example, data from retinal Müller cells of the tiger salamander suggest the possibility that six different subtypes of P2Y receptors are expressed by these cells (Reifel Saltzberg et al., 2003), and there is also the possibility of splice variants of P2Y receptors. Astrocytes in different parts of the nervous system are also likely to differ subtly from one another in their physiological and pharmacological profiles as neurons in different parts of the nervous system do (Batiuk et al., 2020; Borggrewe et al., 2020; Pestana et al., 2020), necessitating the careful determination of individual profiles of each subtype of astrocyte.

The experiments reported here demonstrate ATP-initiated H^+ efflux from cells identified as astrocytes cultured without the presence of neurons. Several recently developed methods are likely to help shine light in future experiments designed to examine the role that H^+ extrusion by glial cells plays in modulating neuronal activity in the intact nervous system. Molecular biological tools now allow selective activation of glial cell intracellular signaling cascade pathways using DREADDs (designer receptors exclusively activated by designer drugs), avoiding the potential problem of direct activation of ATP receptors also present on neurons in the intact nervous system (Xie et al., 2015; Bang et al., 2016; Losi et al., 2017; Yu et al., 2020). Such selective activation of glial cells coupled with the use of sensors such as CalipHluorin that allow measurement of changes in extracellular pH within intact individual synapses (Wang et al., 2014) could help to provide a much better understanding of the role that H^+ efflux by glial cells plays in modulating neuronal activity. A key challenge in the interpretation of such studies will be in determining how similar the pattern of activation of alterations in intracellular calcium by DREADDs are compared to naturally occurring pathways both in magnitude and spatial pattern. Further experiments will also be needed for direct functional characterization of the effects of glial-related H^+ on the inhibition of the release of neurotransmitters mediated by the block of calcium influx into neuronal axon terminals, as well as the extent to which such changes in glial-mediated alterations in extracellular acidity alter H^+-dependent uptake of neurotransmitters. Our demonstration in this study of the direct release of H^+ from astrocytes opens the door to a complex array of future studies needed to better understand the molecular mechanisms by which astrocytes may modulate neuronal activity.

DATA AVAILABILITY STATEMENT

The raw data supporting the conclusions of this article will be made available by the authors, without undue reservation.

ETHICS STATEMENT

All animals were treated in accordance with the protocols and approved by the Animal Care Committee (ACC), the Institutional Animal Care and Use Committee (IACUC) of the University of Illinois at Chicago and the federal guidelines listed in the Public Health Service Policy on Humane Care and Use of Laboratory Animals.

AUTHOR CONTRIBUTIONS

JC, MK, and RM conceptualized the study, conducted experiments, analyzed resulting data, created figures, and discussed and wrote the manuscript. BT, WK, LK, and JL conducted experiments, analyzed resulting data, made suggestions for the direction of the study, and discussed and edited the manuscript. CG and MG contributed to the initial discussion about the design of the experiments using *in vitro* astrocyte cultures, provided cells for the study, helped guide preparation and culture of cells, and discussed and edited the manuscript. MK and RM wrote the grant applications that resulted in financial support for this work. All authors contributed to manuscript revision, read, and approved the submitted version.

FUNDING

This work was supported by National Science Foundation (NSF) Grants 1557820 and 1557725, grant R01AA022948 from NIH/NIAAA, a grant from the UICenter for Drug Development, an LAS award for Faculty in the Natural Sciences from the University of Illinois at Chicago, an Indiana Wesleyan University Hodson Research Institute award, an Indiana Wesleyan University Scholar award, and a gift from the estate of John C. Hagensick.

ACKNOWLEDGMENTS

We thank the two reviewers for their thoughts and comments in improving the initial draft of the manuscript and Ms. Wenping Li for help and guidance in the preparation of astrocyte cell cultures.

REFERENCES

Abbracchio, M. P., Burnstock, G., Verkhratsky, A., and Zimmermann, H. (2009). Purinergic signalling in the nervous system: an overview. *Trends Neurosci.* 32, 19–29. doi: 10.1016/j.tins.2008.10.001

Agulhon, C., Petravicz, J., McMullen, A. B., Sweger, E. J., Minton, S. K., Taves, S. R., et al. (2008). What is the role of astrocyte calcium in neurophysiology? *Neuron* 59, 932–946. doi: 10.1016/j.neuron.2008.09.004

Al-Baldawi, N. F., and Abercrombie, R. F. (1992). Cytoplasmic hydrogen ion diffusion coefficient. *Biophys. J.* 61, 1470–1479. doi: 10.1016/S0006-3495(92)81953-7

Allen, N. J. (2014). Astrocyte regulation of synaptic behavior. *Annu. Rev. Cell Dev. Biol.* 30, 439–463. doi: 10.1146/annurev-cellbio-100913-013053

Anderson, C. M., Bergher, J. P., and Swanson, R. A. (2004). ATP-induced ATP release from astrocytes. *J. Neurochem.* 88, 246–256. doi: 10.1111/j.1471-4159.2004.02204.x

Arcuino, G., Lin, J. H.-C., Takano, T., Liu, C., Jiang, L., Gao, Q., et al. (2002). Intercellular calcium signaling mediated by point-source burst release of ATP. *Proc. Natl. Acad. Sci. U.S.A.* 99, 9840–9845. doi: 10.1073/pnas.152588599

Ashhad, S., and Narayanan, R. (2019). Stores, channels, glue, and trees: active glial and active dendritic physiology. *Mol. Neurobiol.* 56, 2278–2299. doi: 10.1007/s12035-018-1223-5

Attaphitaya, S., Park, K., and Melvin, J. E. (1999). Molecular cloning and functional expression of a rat Na^+/H^+ exchanger (NHE5) highly expressed in brain. *J. Biol. Chem.* 274, 4383–4388. doi: 10.1074/jbc.274.7.4383

Bang, J., Kim, H. Y., and Lee, H. (2016). Optogenetic and chemogenetic approaches for studying astrocytes and gliotransmitters. *Exp. Neurobiol.* 25, 205–221. doi: 10.5607/en.2016.25.5.205

Barnes, S., and Bui, Q. (1991). Modulation of calcium-activated chloride current via pH-induced changes of calcium-channel properties in cone photoreceptors. *J. Neurosci.* 11, 4015–4023. doi: 10.1523/JNEUROSCI.11-12-04015.1991

Barnes, S., Merchant, V., and Mahmud, F. (1993). Modulation of transmission gain by protons at the photoreceptor output synapse. *Proc. Natl. Acad. Sci. U.S.A.* 90, 10081–10085. doi: 10.1073/pnas.90.21.10081

Batiuk, M. Y., Martirosyan, A., Wahis, J., de Vin, F., Marneffe, C., Kusserow, C., et al. (2020). Identification of region-specific astrocyte subtypes at single cell resolution. *Nat. Commun.* 11:1220. doi: 10.1038/s41467-019-14198-8

Bazargani, N., and Attwell, D. (2016). Astrocyte calcium signaling: the third wave. *Nat. Neurosci.* 19, 182–189. doi: 10.1038/nn.4201

Belov Kirdajova, D., Kriska, J., Tureckova, J., and Anderova, M. (2020). Ischemia-triggered glutamate excitotoxicity from the perspective of glial cells. *Front. Cell. Neurosci.* 14:51. doi: 10.3389/fncel.2020.00051

Bindocci, E., Savtchouk, I., Liaudet, N., Becker, D., Carriero, G., and Volterra, A. (2017). Three-dimensional Ca^{2+} imaging advances understanding of astrocyte biology. *Science* 356:eaai8185. doi: 10.1126/science.aai8185

Borggrewe, M., Grit, C., Vainchtein, I. D., Brouwer, N., Wesseling, E. M., Laman, J. D., et al. (2020). Regionally diverse astrocyte subtypes and their heterogeneous response to EAE. *Glia.* 69, 1140–1154. doi: 10.1002/glia.23954

Bowser, D. N., and Khakh, B. S. (2007). Vesicular ATP is the predominant cause of intercellular calcium waves in astrocytes. *J. Gen. Physiol.* 129, 485–491. doi: 10.1085/jgp.200709780

Burnstock, G., and Verkhratsky, A. (2012). *Purinergic Signalling and the Nervous System*. Berlin, Heidelberg: Sprinber Verlag Berlin Heidelberg. doi: 10.1007/978-3-642-28863-0

Cammer, W., and Tansey, F. A. (1988). Carbonic anhydrase immunostaining in astrocytes in the rat cerebral cortex. *J. Neurochem.* 50, 319–322. doi: 10.1111/j.1471-4159.1988.tb13267.x

Cevc, G. (1990). Membrane electrostatics. *Biochim. Biophys. Acta* 1031, 311–382. doi: 10.1016/0304-4157(90)90015-5

Chen, J., Zhang, X., Kusumo, H., Costa, L. G., and Guizzetti, M. (2013). Cholesterol efflux is differentially regulated in neurons and astrocytes: implications for brain cholesterol homeostasis. *Biochim. Biophys. Acta* 1831, 263–275. doi: 10.1016/j.bbalip.2012.09.007

Coco, S., Calegari, F., Pravettoni, E., Pozzi, D., Taverna, E., Rosa, P., et al. (2003). Storage and release of ATP from astrocytes in culture. *J. Biol. Chem.* 278, 1354–1362. doi: 10.1074/jbc.M209454200

Cozzolino, O., Marchese, M., Trovato, F., Pracucci, E., Ratto, G. M., Buzzi, M. G., et al. (2018). Understanding spreading depression from headache to sudden unexpected death. *Front. Neurol.* 9:19. doi: 10.3389/fneur.2018.00019

Dixon, S. J., Yu, R., Panupinthu, N., and Wilson, J. X. (2004). Activation of P2 nucleotide receptors stimulates acid efflux from astrocytes. *Glia* 47, 367–376. doi: 10.1002/glia.20048

Doering, C. J., and McRory, J. E. (2007). Effects of extracellular pH on neuronal calcium channel activation. *Neuroscience* 146, 1032–1043. doi: 10.1016/j.neuroscience.2007.02.049

Durkee, C. A., and Araque, A. (2019). Diversity and specificity of astrocyte-neuron communication. *Neuroscience* 396, 73–78. doi: 10.1016/j.neuroscience.2018.11.010

Fawthrop, D. J., and Evans, R. J. (1987). Morphological changes in cultured astrocytes following exposure to calcium ionophores. *Neurosci. Lett.* 81, 250–256. doi: 10.1016/0304-3940(87)90391-0

Fiacco, T. A., and McCarthy, K. D. (2018). Multiple lines of evidence indicate that gliotransmission does not occur under physiological conditions. *J. Neurosci.* 38, 3–13. doi: 10.1523/JNEUROSCI.0016-17.2017

Grewer, C., and Rauen, T. (2005). Electrogenic glutamate transporters in the CNS: molecular mechanism, pre-steady-state kinetics, and their impact on synaptic signaling. *J. Membr. Biol.* 203, 1–20. doi: 10.1007/s00232-004-0731-6

Grynkiewicz, G., Poenie, M., and Tsien, R. T. (1985). A new generation of Ca^{2+} indicators with greatly improved fluorescence properties. *J. Biol. Chem.* 260, 3440–3450. doi: 10.1016/S0021-9258(19)83641-4

Guerra-Gomes, S., Sousa, N., Pinto, L., and Oliveira, J. F. (2017). Functional roles of astrocyte calcium elevations: from synapses to behavior. *Front. Cell. Neurosci.* 11:427. doi: 10.3389/fncel.2017.00427

Guizzetti, M., Costa, P., Peters, J., and Costa, L. G. (1996). Acetylcholine as a mitogen: muscarinic receptor-mediated proliferation of rat astrocytes and human astrocytoma cells. *Eur. J. Pharmacol.* 297, 265–273. doi: 10.1016/0014-2999(95)00746-6

Halassa, M. M., Fellin, T., and Haydon, P. G. (2007). The tripartite synapse: roles for gliotransmission in health and disease. *Trends Mol. Med.* 13, 54–63. doi: 10.1016/j.molmed.2006.12.005

Halassa, M. M., Fellin, T., and Haydon, P. G. (2009). Tripartite synapses: roles for astrocytic purines in the control of synaptic physiology and behavior. *Neuropharmacol* 57, 343–346. doi: 10.1016/j.neuropharm.2009.06.031

Han, J.-E., Cho, J.-H., Choi, I.-S., Kim, D.-Y., and Jang, I.-S. (2017). Effects of acidic pH on voltage-gated ion channels in rat trigeminal mesencephalic nucleus neurons. *Korean J. Physiol. Pharmacol.* 21, 215–223. doi: 10.4196/kjpp.2017.21.2.215

Illes, P., Burnstock, G., and Tang, Y. (2019). Astroglia-derived ATP modulates CNS neuronal circuits. *Trends Neurosci.* 42, 885–898. doi: 10.1016/j.tins.2019.09.006

Jha, M. K., and Morrison, B. M. (2018). Glia-neuron energy metabolism in health and diseases: new insights into the role of nervous system metabolic transporters. *Exp. Neurol.* 309, 23–31. doi: 10.1016/j.expneurol.2018.07.009

Jha, M. K., and Morrison, B. M. (2020). Lactate transporters mediate glia-neuron metabolic crosstalk in homeostasis and disease. *Front. Cell. Neurosci.* 14:589582. doi: 10.3389/fncel.2020.589582

Kardos, J., Héja, L., Jemnitz, K., Kovács, R., and Palkovits, M. (2017). The nature of early astroglial protection-Fast activation and signaling. *Prog Neurobiol.* 153, 86–99. doi: 10.1016/j.pneurobio.2017.03.005

Khakh, B. S., and McCarthy, K. D. (2015). Astrocyte calcium signaling: from observations to functions and the challenges therein. *Cold Spring Harb. Perspect. Biol.* 7:a020404. doi: 10.1101/cshperspect.a020404

Kiedrowski, L., and Feinerman, A. (2018). Medium-retaining Petri dish insert to grow and image cultured cells. *J. Neurosci. Methods* 294, 111–115. doi: 10.1016/j.jneumeth.2017.11.007

Kleinschmidt, J. (1991). Signal transmission at the photoreceptor synapse. role of calcium ions and protons. *Ann. N. Y. Acad. Sci.* 635, 468–470. doi: 10.1111/j.1749-6632.1991.tb36529.x

Kofuji, P., and Araque, A. (2020). G-protein-coupled receptors in astrocyte-neuron communication. *Neuroscience* 456, 71–84. doi: 10.1016/j.neuroscience.2020.03.025

Koizumi, S., Fujishita, K., Tsuda, M., Shigemoto-Mogami, Y., and Inoue, K. (2003). Dynamic inhibition of excitatory synaptic transmission by astrocyte-derived ATP in hippocampal cultures. *Proc. Natl. Acad. Sci. U.S.A.* 100, 11023–11028. doi: 10.1073/pnas.1834448100

Kreitzer, M. A., Collis, L. P., Molina, A. J. A., Smith, P. J. S., and Malchow, R. P. (2007). Modulation of extracellular proton fluxes from retinal horizontal cells of the catfish by depolarization and glutamate. *J. Gen. Physiol.* 130, 169–182. doi: 10.1085/jgp.200709737

Kreitzer, M. A., Swygart, D., Osborn, M., Skinner, B., Heer, C., Kaufman, R., et al. (2017). Extracellular H^+ fluxes from tiger salamander Müller (glial) cells measured using self-referencing H^+-selective microelectrodes. *J. Neurophysiol.* 118, 3132–3143. doi: 10.1152/jn.00409.2017

Kuhtreiber, W. M., and Jaffe, L. F. (1990). Detection of extracellular calcium gradients with a calcium-specific vibrating electrode. *J. Cell Biol.* 110, 1565–1573. doi: 10.1083/jcb.110.5.1565

Kunkler, P. E., and Kraig, R. P. (1998). Calcium waves precede electrophysiological changes of spreading depression in hippocampal organ cultures. *J. Neurosci.* 18, 3416–3425. doi: 10.1523/JNEUROSCI.18-09-03416.1998

Losi, G., Mariotti, L., Sessolo, M., and Carmignoto, G. (2017). New tools to study astrocyte Ca^{2+} signal dynamics in brain networks *in vivo*. *Front. Cell. Neurosci.* 11:134. doi: 10.3389/fncel.2017.00134

Malik, A. R., and Willnow, T. E. (2019). Excitatory amino acid transporters in physiology and disorders of the central nervous system. *Int. J. Mol. Sci.* 20:5671. doi: 10.3390/ijms20225671

Maren, T. H. (1988). The kinetics of HCO3- synthesis related to fluid secretion, pH control, and CO2 elimination. *Annu. Rev. Physiol.* 50, 695–717. doi: 10.1146/annurev.ph.50.030188.003403

Masereel, B., Pochet, L., and Laeckmann, D. (2003). An overview of inhibitors of Na^+/H^+ exchanger. *Eur. J. Med. Chem.* 38, 547–554. doi: 10.1016/S0223-5234(03)00100-4

McConnell, H. M., Owicki, J. C., Parce, J. W., Miller, D. L., Baxter, G. T., Wada, H. G., et al. (1992). The cytosensor microphysiometer: biological applications of silicon technology. *Science* 257, 1906–1912. doi: 10.1126/science.1329199

McLaughlin, S., Mulrine, N., Gresalfi, T., Vaio, G., and McLaughlin, A. (1981). Adsorption of divalent cations to bilayer membranes containing phosphatidylserine. *J. Gen. Physiol.* 77, 445–473. doi: 10.1085/jgp.77.4.445

McLaughlin, S. G., Szabo, G., and Eisenman, G. (1971). Divalent ions and the surface potential of charged phospholipid membranes. *J. Gen. Physiol.* 58, 667–687. doi: 10.1085/jgp.58.6.667

Molina, A. J. A., Verzi, M. P., Birnbaum, A. D., Yamoah, E. N., Hammar, K., Smith, P. J. S., et al. (2004). Neurotransmitter modulation of extracellular H^+ fluxes from isolated retinal horizontal cells of the skate. *J. Physiol.* 560, 639–657. doi: 10.1113/jphysiol.2004.065425

Nagelhus, E. A. (2005). Carbonic anhydrase XIV is enriched in specific membrane domains of retinal pigment epithelium, Müller cells, and astrocytes. *Proc. Natl. Acad. Sci. U.S.A.* 102, 8030–8035. doi: 10.1073/pnas.0503021102

Ndubaku, U., and de Bellard, M. E. (2008). Glial cells: old cells with new twists. *Acta Histochem.* 110, 182–195. doi: 10.1016/j.acthis.2007.10.003

Newman, E. A. (1996). Acid efflux from retinal glial cells generated by sodium bicarbonate cotransport. *J. Neurosci.* 16, 159–168. doi: 10.1523/JNEUROSCI.16-01-00159.1996

Newman, E. A. (2003). Glial cell inhibition of neurons by release of ATP. *J. Neurosci.* 23, 1659–1666. doi: 10.1523/JNEUROSCI.23-05-01659.2003

Newman, E. A. (2015). Glial cell regulation of neuronal activity and blood flow in the retina by release of gliotransmitters. *Philos. Trans. R Soc. Lond. B Biol. Sci.* 370, 20140195–20140199. doi: 10.1098/rstb.2014.0195

Nicholls, D., and Attwell, D. (1990). The release and uptake of excitatory amino acids. *Trends Pharmacol. Sci.* 11, 462–468. doi: 10.1016/0165-6147(90)90129-V

Owe, S. G., Marcaggi, P., and Attwell, D. (2006). The ionic stoichiometry of the GLAST glutamate transporter in salamander retinal glia. *J. Physiol.* 577, 591–599. doi: 10.1113/jphysiol.2006.116830

Pankratov, Y., Lalo, U., Verkhratsky, A., and North, R. A. (2006). Vesicular release of ATP at central synapses. *Pflugers Arch.* 452, 589–597. doi: 10.1007/s00424-006-0061-x

Papouin, T., Dunphy, J., Tolman, M., Foley, J. C., and Haydon, P. G. (2017). Astrocytic control of synaptic function. *Philos. Trans. R Soc. Lond. B Biol. Sci.* 372, 20160154–20160158. doi: 10.1098/rstb.2016.0154

Pestana, F., Edwards-Faret, G., Belgard, T. G., Martirosyan, A., and Holt, M. G. (2020). No longer underappreciated: the emerging concept of astrocyte heterogeneity in neuroscience. *Brain Sci.* 10:168. doi: 10.3390/brainsci10030168

Pierre, K., and Pellerin, L. (2005). Monocarboxylate transporters in the central nervous system: distribution, regulation and function. *J. Neurochem.* 94, 1–14. doi: 10.1111/j.1471-4159.2005.03168.x

Reifel Saltzberg, J. M., Garvey, K. A., and Keirstead, S. A. (2003). Pharmacological characterization of P2Y receptor subtypes on isolated tiger salamander Muller cells. *Glia* 42, 149–159. doi: 10.1002/glia.10198

Rose, C. R., Felix, L., Zeug, A., Dietrich, D., Reiner, A., and Henneberger, C. (2017). Astroglial glutamate signaling and uptake in the hippocampus. *Front. Mol. Neurosci.* 10:451. doi: 10.3389/fnmol.2017.00451

Rose, C. R., and Ransom, B. R. (1996). Mechanisms of H^+ and Na^+ changes induced by glutamate, kainate, and D-aspartate in rat hippocampal astrocytes. *J. Neurosci.* 16, 5393–5404. doi: 10.1523/JNEUROSCI.16-17-05393.1996

Saegusa, N., Moorhouse, E., Vaughan-Jones, R. D., and Spitzer, K. W. (2011). Influence of pH on Ca^{2+} current and its control of electrical and Ca^{2+} signaling in ventricular myocytes. *J. Gen. Physiol.* 138, 537–559. doi: 10.1085/jgp.201110658

Sahlender, D. A., Savtchouk, I., and Volterra, A. (2014). What do we know about gliotransmitter release from astrocytes? *Philos. Trans. R. Soc. Lond. B Biol. Sci.* 369:20130592. doi: 10.1098/rstb.2013.0592

Savtchouk, I., Carriero, G., and Volterra, A. (2018). Studying axon-astrocyte functional interactions by 3D two-photon Ca^{2+} imaging: a practical guide to experiments and "Big Data" analysis. *Front. Cell. Neurosci.* 12:98. doi: 10.3389/fncel.2018.00098

Savtchouk, I., and Volterra, A. (2018). Gliotransmission: beyond black-and-white. *J. Neurosci.* 38, 14–25. doi: 10.1523/JNEUROSCI.0017-17.2017

Scemes, E., and Giaume, C. (2006). Astrocyte calcium waves: what they are and what they do. *Glia* 54, 716–725. doi: 10.1002/glia.20374

Schildge, S., Bohrer, C., Beck, K., and Schachtrup, C. (2013). Isolation and culture of mouse cortical astrocytes. *J. Vis. Exp.* 19:50079. doi: 10.3791/50079

Semyanov, A., Henneberger, C., and Agarwal, A. (2020). Making sense of astrocytic calcium signals - from acquisition to interpretation. *Nat. Rev. Neurosci.* 19:182. doi: 10.1038/s41583-020-0361-8

Shah, M. J., Meis, S., Munsch, T., and Pape, H. C. (2001). Modulation by extracellular pH of low- and high-voltage-activated calcium currents of rat thalamic relay neurons. *J. Neurophysiol.* 85, 1051–1058. doi: 10.1152/jn.2001.85.3.1051

Smith, P., Hammar, K., and Porterfield, D. M. (1999). Self-referencing, non-invasive, ion selective electrode for single cell detection of trans-plasma membrane calcium flux. *Microscop. Res. Techn.* 46, 398–417. doi: 10.1002/(SICI)1097-0029(19990915)46:6<398::AID-JEMT8>3.0.CO;2-H

Smith, P., and Trimarchi, J. (2001). Noninvasive measurement of hydrogen and potassium ion flux from single cells and epithelial structures. *Am. J. Physiol. Cell Physiol.* 280, C1–C11. doi: 10.1152/ajpcell.2001.280.1.C1

Sofroniew, M. V., and Vinters, H. V. (2010). Astrocytes: biology and pathology. *Acta Neuropathol.* 119, 7–35. doi: 10.1007/s00401-009-0619-8

Somieski, P., and Nagel, W. (2001). Measurement of pH gradients using an ion-sensitive vibrating probe technique (IP). *Pflugers Arch.* 442, 142–149. doi: 10.1007/s004240000505

Soto, E., Ortega-Ramírez, A., and Vega, R. (2018). Protons as messengers of intercellular communication in the nervous system. *Front. Cell. Neurosci.* 12:342. doi: 10.3389/fncel.2018.00342

Spitzer, K. W., Skolnick, R. L., Peercy, B. E., Keener, J. P., and Vaughan Jones, R. D. (2002). Facilitation of intracellular H(+) ion mobility by CO(2)/HCO(3)(-) in rabbit ventricular myocytes is regulated by carbonic anhydrase. *J. Physiol.* 541, 159–167. doi: 10.1113/jphysiol.2001.013268

Tchernookova, B. K., Gongwer, M. W., George, A., Goeglein, B., Powell, A. M., Caringal, H. L., et al. (2021). ATP-mediated increase in H^+ flux from retinal Müller cells: a role for Na^+/H^+ exchange. *J. Neurophysiol.* 125, 184–198. doi: 10.1152/jn.00546.2020

Tchernookova, B. K., Heer, C., Young, M., Swygart, D., Kaufman, R., Gongwer, M., et al. (2018). Activation of retinal glial (Müller) cells by extracellular ATP induces pronounced increases in extracellular H^+ flux. *PLoS ONE* 13:e0190893. doi: 10.1371/journal.pone.0190893

Theparambil, S. M., and Deitmer, J. W. (2015). High effective cytosolic H^+ buffering in mouse cortical astrocytes attributable to fast bicarbonate transport. *Glia* 63, 1581–1594. doi: 10.1002/glia.22829

Theparambil, S. M., Hosford, P. S., Ruminot, I., Kopach, O., Reynolds, J. R., Sandoval, P. Y., et al. (2020). Astrocytes regulate brain extracellular pH via a neuronal activity-dependent bicarbonate shuttle. *Nat. Commun.* 11:5073. doi: 10.1038/s41467-020-18756-3

Theparambil, S. M., Naoshin, Z., Defren, S., Schmaelzle, J., Weber, T., Schneider, H.-P., et al. (2017). Bicarbonate sensing in mouse cortical astrocytes during extracellular acid/base disturbances. *J. Physiol.* 595, 2569–2585. doi: 10.1113/JP273394

Theparambil, S. M., Ruminot, I., Schneider, H.-P., Shull, G. E., and Deitmer, J. W. (2014). The electrogenic sodium bicarbonate cotransporter NBCe1 is a high-affinity bicarbonate carrier in cortical astrocytes. *J. Neurosci.* 34, 1148–1157. doi: 10.1523/JNEUROSCI.2377-13.2014

Tombaugh, G. C., and Somjen, G. G. (1996). Effects of extracellular pH on voltage-gated Na^+, K^+ and Ca^{2+} currents in isolated rat CA1 neurons. *J. Physiol.* 493, 719–732. doi: 10.1113/jphysiol.1996.sp021417

Torrente, D., Mendes-da-Silva, R. F., Lopes, A. A. C., González, J., Barreto, G. E., and Guedes, R. C. A. (2014). Increased calcium influx triggers and accelerates

cortical spreading depression *in vivo* in male adult rats. *Neurosci. Lett.* 558, 87–90. doi: 10.1016/j.neulet.2013.11.004

Valtcheva, S., and Venance, L. (2019). Control of long-term plasticity by glutamate transporters. *Front. Synaptic Neurosci.* 11:10. doi: 10.3389/fnsyn.2019.00010

Vandenberg, R. J., and Ryan, R. M. (2013). Mechanisms of glutamate transport. *Physiol. Rev.* 93, 1621–1657. doi: 10.1152/physrev.00007.2013

Vasile, F., Dossi, E., and Rouach, N. (2017). Human astrocytes: structure and functions in the healthy brain. *Brain Struct. Funct* 222, 2017–2029. doi: 10.1007/s00429-017-1383-5

Vroman, R., Klaassen, L. J., Howlett, M. H. C., Cenedese, V., Klooster, J., Sjoerdsma, T., et al. (2014). Extracellular ATP hydrolysis inhibits synaptic transmission by increasing pH buffering in the synaptic cleft. *PLoS Biol.* 12:e1001864. doi: 10.1371/journal.pbio.1001864

Wang, J., O'Sullivan, M. L., Mukherjee, D., Puñal, V. M., Farsiu, S., and Kay, J. N. (2017). Anatomy and spatial organization of Müller glia in mouse retina. *J. Comp. Neurol.* 525, 1759–1777. doi: 10.1002/cne.24153

Wang, T.-M., Holzhausen, L. C., and Kramer, R. H. (2014). Imaging an optogenetic pH sensor reveals that protons mediate lateral inhibition in the retina. *Nat. Neurosci.* 17, 262–268. doi: 10.1038/nn.3627

Wang, X., Takano, T., and Nedergaard, M. (2009). Astrocytic calcium signaling: mechanism and implications for functional brain imaging. *Methods Mol. Biol.* 489, 93–109. doi: 10.1007/978-1-59745-543-5_5

Wilson, C. N., and Mustafa, S. J. (2009). *Adenosine Receptors in Health and Disease*. Heidelberg: Springer Science & Business Media. doi: 10.1007/978-3-540-89615-9

Wu, D. C., Chen, R. Y.-T., Cheng, T.-C., Chiang, Y.-C., Shen, M.-L., Hsu, L.-L., et al. (2018). Spreading depression promotes astrocytic calcium oscillations and enhances gliotransmission to hippocampal neurons. *Cereb. Cortex* 28, 3204–3216. doi: 10.1093/cercor/bhx192

Xie, A. X., Petravicz, J., and McCarthy, K. D. (2015). Molecular approaches for manipulating astrocytic signaling *in vivo*. *Front. Cell. Neurosci.* 9:144. doi: 10.3389/fncel.2015.00144

Yu, X., Nagai, J., and Khakh, B. S. (2020). Improved tools to study astrocytes. *Nat. Rev. Neurosci.* 21, 121–138. doi: 10.1038/s41583-020-0264-8

Zerangue, N., and Kavanaugh, M. P. (1996). Flux coupling in a neuronal glutamate transporter. *Nature* 383, 634–637. doi: 10.1038/383634a0

Zhang, S., Wu, M., Peng, C., Zhao, G., and Gu, R. (2017). GFAP expression in injured astrocytes in rats. *Exp. Ther. Med.* 14, 1905–1908. doi: 10.3892/etm.2017.4760

Zhou, B., Zuo, Y. X., and Jiang, R. T. (2019). Astrocyte morphology: diversity, plasticity, and role in neurological diseases. *CNS Neurosci. Ther.* 25, 665–673. doi: 10.1111/cns.13123

Zimmermann, H. (1994). Signalling via ATP in the nervous system. *Trends Neurosci.* 17, 420–426. doi: 10.1016/0166-2236(94)90016-7

Conflict of Interest: LK declares his involvement with Spot Cells LLC.

The remaining authors declare that the research was conducted in the absence of any commercial or financial relationships that could be construed as a potential conflict of interest.

frontiers in Cellular Neuroscience

REVIEW
published: 20 May 2021
doi: 10.3389/fncel.2021.644126

Ion Channels and Electrophysiological Properties of Astrocytes: Implications for Emergent Stimulation Technologies

*Jessica McNeill, Christopher Rudyk, Michael E. Hildebrand and Natalina Salmaso**

Department of Neuroscience, Carleton University, Ottawa, ON, Canada

Astrocytes comprise a heterogeneous cell population characterized by distinct morphologies, protein expression and function. Unlike neurons, astrocytes do not generate action potentials, however, they are electrically dynamic cells with extensive electrophysiological heterogeneity and diversity. Astrocytes are hyperpolarized cells with low membrane resistance. They are heavily involved in the modulation of K^+ and express an array of different voltage-dependent and voltage-independent channels to help with this ion regulation. In addition to these K^+ channels, astrocytes also express several different types of Na^+ channels; intracellular Na^+ signaling in astrocytes has been linked to some of their functional properties. The physiological hallmark of astrocytes is their extensive intracellular Ca^{2+} signaling cascades, which vary at the regional, subregional, and cellular levels. In this review article, we highlight the physiological properties of astrocytes and the implications for their function and influence of network and synaptic activity. Furthermore, we discuss the implications of these differences in the context of optogenetic and DREADD experiments and consider whether these tools represent physiologically relevant techniques for the interrogation of astrocyte function.

Keywords: glia, physiology, ion channels, calcium, potassium, sodium, optogenetics, DREADDs

OPEN ACCESS

Edited by:
Wannan Tang,
University of Oslo, Norway

Reviewed by:
Hyungju Park,
Korea Brain Research Institute, South Korea
Frank Kirchhoff,
Saarland University, Germany

***Correspondence:**
Natalina Salmaso
natalina.salmaso@carleton.ca

Specialty section:
This article was submitted to Non-Neuronal Cells, a section of the journal Frontiers in Cellular Neuroscience

Received: *20 December 2020*
Accepted: *26 April 2021*
Published: *20 May 2021*

Citation:
McNeill J, Rudyk C, Hildebrand ME and Salmaso N (2021) Ion Channels and Electrophysiological Properties of Astrocytes: Implications for Emergent Stimulation Technologies. Front. Cell. Neurosci. 15:644126. doi: 10.3389/fncel.2021.644126

INTRODUCTION

Astrocytes comprise a heterogeneous population of macroglial cells that are the most abundant neural cell type in the central nervous system (CNS). Similar to both neurons and oligodendrocytes, astrocytes arise from the neural stem cell pool (Sloan and Barres, 2014). The process of gliogenesis in rodents begins around embryonic day 16–18 with the majority of cortical astrogliogenesis likely occurring in the postnatal period where a substantial increase in glial numbers are observed during the second and third postnatal weeks (Abney et al., 1981; Qian et al., 2000; Bushong et al., 2004; Freeman, 2010). The extensive morphological and functional heterogeneity of astrocytes is in part driven by their place of birth and neuronal neighbors during the course of development (Lanjakornsiripan et al., 2018; Bayraktar et al., 2020). This may be mediated, in part, through the release of specific neurotransmitters or neurotrophic factors from these nearby neurons. At least in cortical development, neuronal heterogeneity induces differential astroglial phenotypes (Bayraktar et al., 2020).

Morphologically, astrocytes can take many forms, though they are perhaps best known for their protoplasmic shape; a smaller soma surrounded by numerous processes that extend outwards (Sofroniew and Vinters, 2010), giving them a "star-like" shape for which they are named. In addition to these protoplasmic astrocytes, which predominantly exist in gray matter, there are fibrous astrocytes which are found throughout the white matter (Sofroniew and Vinters, 2010). The somata of these cells orient themselves in perpendicular rows between the axon bundles while their processes make connections to nodes of Ranvier (Oberheim et al., 2009). These two dominant morphological types of astrocytes are by no means an exhaustive list; velate astrocytes of the olfactory bulb and cerebellum, Bergmann glia of the cerebellum, Müller glia in the retina, pituicytes of the neurohypophysis, radial glia, and Gomori astrocytes of the hypothalamus all represent morphologically-distinct classes of astrocytes (Verkhratsky and Nedergaard, 2018; Khakh and Deneen, 2019).

Astrocytes display even greater diversity in their functional roles. Previously believed to only provide structural support to neurons, it is now well-established that astrocytes are key regulators of CNS homeostasis. Some of these homeostatic functions include the buffering of ions like potassium (K^+), sodium (Na^+), and protons (H^+), and the regulation of neurotransmitters. Astrocytes form an integral part of the tripartite synapse; their processes encompass the synapse, allowing them to remove excess neurotransmitters from the cleft. This is particularly important for the excitatory neurotransmitter, glutamate: astrocytes are responsible for removing and breaking down almost all central extracellular glutamate (Mahmoud et al., 2019). These glutamatergic transporters are also critical for modulating neuronal plasticity; for example, downregulation of the glutamate-1 transporter has been shown to impair long-term potentiation (LTP; Li Y.-K. et al., 2012).

In addition, astrocytes contribute to CNS homeostasis by forming an integral part of the blood-brain barrier; their endfeet surround the cerebral capillaries as part of the neurovascular unit (Liedtke et al., 1996; Wilhelm et al., 2016). Thus, they play a key role in modulating the entry of molecules into the CNS; permitting access for essential substances like nutrients while preventing access of potentially harmful agents like oxidants (Wilhelm et al., 2016). Astrocytes are also crucial for regulating pH levels, modulating oxidative stress, and providing energy substrates to neurons. For example, astrocytes are key metabolizers of glucose, the main source of energy (ATP) production in the brain (Prebil et al., 2011).

Astrocytes are also key players in CNS injury response, undergoing morphological and functional changes in a process known as reactive astrogliosis. Their response differs according to the extent and cause of the injury and includes molecular, morphological, and physiological changes (Sofroniew and Vinters, 2010). Reactive astrocytes can produce neurotoxic or neuroprotective effects. Two distinct classifications of reactive astrocytes, termed "A1" and "A2" (neurotoxic and neuroprotective, respectively) have recently been characterized (Liddelow et al., 2017), though it is likely more phenotypes exist.

Despite the accumulating evidence demonstrating the extensive regional and sub-regional diversity of astrocytes, there remains very little understanding of how the electrophysiological properties of astrocytes may diverge across these subpopulations. A large body of evidence in the field suggests that astrocytes may not be as "electrically silent" as previously believed, so characterizing differences in these electrophysiological properties will be important for understanding the functional differences of astroglial cells. Moreover, the increased use of technologies such as designer receptors activated by designer drugs (DREADDs) and optogenetics in astrocytes, augments the need to understand the physiological properties of astrocytes as these properties will be critical for the future application of these tools to this cell population. A greater knowledge of astrocyte physiology will inform experimental design, determine the physiological relevance (or not) of specific electrical stimulation experiment(s) and help with acknowledging the limitations of each. In the remainder of this review, we will highlight the regional differences in astrocyte physiology, and discuss the implications for optogenetic and DREADD manipulation of astrocytes.

HETEROGENEITY OF ASTROCYTE MEMBRANE POTENTIAL, RESISTANCE AND CURRENT PATTERNS UNDER BASAL AND REACTIVE CONDITIONS

Astrocytes Are Electrically Active Cells

Though neurons are the main excitable cell type of the brain, astrocytes are not "electrically silent" cells. Astrocytes have a hyperpolarized membrane (Du et al., 2016) that typically rests below that of neurons (see section below; Bolton et al., 2006; Zhou et al., 2006), in contrast to the majority of non-excitable cells that have relatively depolarized membrane potentials. Though they cannot generate an action potential, astrocytes are able to respond biochemically to stimuli within their environment, especially ions and neurotransmitters. Astrocytic membranes are rich with several cation and anion channels (including both voltage-dependent and voltage-independent channels), which help with the regulation of ions such as Na^+, K^+, Ca^{2+} and Cl^-, in addition to contributing to the resting membrane potential (RMP), resting conductance and intracellular signaling within astrocytes (Parpura et al., 2011; Ryoo and Park, 2016). Several of these channels have permeability properties that are independent of voltage (i.e., TWIK 1, TREK 1—see "Voltage-Independent K^+ Channels Contribute to Passive Conductance" section), but many are voltage-dependent (such as delayed–rectifying potassium channels—see "Voltage-Dependent K^+ Channels Have Distinct Subcellular Localization" section). Therefore, astrocytes are a dynamic cell type with functional and signaling properties that vary with changes in membrane potential. In addition to ion-permeable channels, astrocytes also express several electrogenic transporters to help facilitate the exchange of ions across their membrane. For example, the Na^+-K^+-ATPase pump exchanges three Na^+ ions out for every two K^+ ions in, and the

Na^+-K^+-$2Cl^-$-cotransporter pump exchanges Na^+, K^+, and Cl^-, with an accompanying influx of water into the cell (Bellot-Saez et al., 2017). These ion channels and transporters represent an important facet of astrocyte physiology; astrocytic Ca^{2+} signaling represents another.

Calcium signaling in astrocytes plays an important role in facilitating the bidirectional communication between neurons and astrocytes at the synapse (for a more complete review on neuron-astrocyte interactions at the synapse, see Allen and Eroglu, 2017). Astrocytes express a plethora of ionotropic and metabotropic receptors, enabling a diverse set of responses to neurotransmitters such as glutamate, serotonin, dopamine, and GABA (Verkhratsky et al., 2019). Neurotransmitter binding to astrocytes can induce intracellular Ca^{2+} signals, and the magnitude, localization and time course of these signals vary significantly depending on the stimulus and synaptic network involved (Araque et al., 2014). However, this neuron to astrocyte communication is not the only form of interaction between these cell types. Astrocytes are able to modulate neuronal activity through the release of several active factors such as glutamate, ATP and D-serine in a process known as gliotransmission (Parpura et al., 1994; Cotrina et al., 2000; Henneberger et al., 2010; Araque et al., 2014; Perez et al., 2017). This process is partly mediated by intracellular Ca^{2+} signaling pathways (Araque et al., 2014). The release of these gliotransmitters from astrocytes is known to regulate synaptic transmission and plasticity. Changes in the frequency of miniature and spontaneous excitatory postsynaptic currents (EPSCs) and inhibitory postsynaptic currents (IPSCs), and the modulation of both LTP and long-term depression (LTD) have all been observed following the release of gliotransmitters from astrocytes across several different brain regions including the hippocampus, cortex and cerebellum (Kang et al., 1998; Brockhaus and Deitmer, 2002; Takata et al., 2011; Navarrete et al., 2012; Araque et al., 2014). Calcium signaling in astrocytes has also been shown to stimulate the Na^+-K^+-ATPase pump, leading to a decrease in extracellular K^+ and subsequent neuronal hyperpolarization and suppression of baseline excitatory activity (Wang et al., 2012).

Astrocytes Display a Highly Negative Resting Membrane Potential

Compared to their neuronal counterparts, astrocytes display a more hyperpolarized, or negative, RMP (Bolton et al., 2006). While neuronal membranes typically rest at between approximately −50 mV and −70 mV (Zaitzev et al., 2012; Shen et al., 2018; Fernandez et al., 2019), the RMP of astrocytes is typically lower. However, specific astrocyte RMP values vary substantially across the CNS. For example, mature astrocytes of the CA1 region of the hippocampus have an RMP of about −80 mV (Tang et al., 2009; Deemyad et al., 2018), whereas astrocytes of the optic nerve have an average RMP of −62 mV (Butt and Jennings, 1994). A comparison between telencephalic astrocytes found that those of the *stratum oriens* and *stratum pyramidale* regions of the hippocampus had a significantly more negative (RMP of −90 mV) average membrane potential compared to those of the layers V and VI of the cortex (with an RMP of about −85 mV; Mishima and Hirase, 2010).

There is also extensive heterogeneity of astrocytes within the *same* region; astrocytes of the optic nerve have an RMP ranging from −25 to −80 mV (Bolton et al., 2006) whereas those in the ventral tegmental area (VTA) ranged from −60 to −90 mV (Xin et al., 2019). The hippocampus has proven to have a diverse pool of astrocytes; astrocytes in this area have RMPs ranging from −80 mV in the CA1 and *stratum radiatum* subregions (Zhong et al., 2016; Deemyad et al., 2018) to a more negative RMP (−90 mV) in the *stratum oriens* and *stratum pyramidale* (Mishima and Hirase, 2010).

In neurons, the RMP is important for setting the threshold, propensity, and frequency of action potentials. In astrocytes, which lack action potentials, the highly negative (hyperpolarized) RMP is critical for enabling and regulating homeostatic functions such as K^+ buffering and even neurotransmitter reuptake (Zhou et al., 2006; Ryoo and Park, 2016). Variability in astrocytic RMPs throughout the CNS may therefore reflect differences in (some) astrocytic functions.

The underlying reason(s) for differences in astrocyte RMP across brain regions and subtypes have not been fully elucidated, but it is likely a result of a complex interplay between numerous extrinsic and intrinsic factors. An astrocyte's immediate environment and neuronal input may drive heterogeneity in RMP values across the CNS. The morphological characteristics of individual astrocytes may also play a role in determining RMP. For example, a heavily branched astrocyte with numerous processes and greater membrane surface area may have a higher number of ion channels, particularly leak channels (i.e., K^+), that could in part explain some of the differences in astrocyte RMP (relationships between morphology, RMP heterogeneity, and differential astrocytic Ca^{2+} signaling- *are further discussed in "Ca^{2+} signaling pathways in astrocytes"*). However, as specific morphological classes of astrocytes have not been linked with particular ranges of RMPs, it is highly probable that several other factors also influence the RMP of an astrocyte, such as intracellular signaling pathways (see **Figure 1**).

One intracellular signaling cascade that may influence the RMP of astrocytes is the cAMP/PKA pathway. Bolton et al. (2006) demonstrated that incubation of astrocytes with a cAMP analog (to activate adenylate cyclase) hyperpolarized their mean RMP. The addition of a PKA inhibitor caused a significant depolarization of the astrocytic membrane, but this effect was only partially reversed with the cAMP analog, suggesting that cAMP influences astrocytic RMP *via* both PKA-dependent and—independent pathways (Bolton et al., 2006). Therefore, the variability of astrocytic RMP may be mediated by differences in intracellular cAMP/PKA signaling. In astrocytes, this cAMP/PKA pathway has been linked to changes in cell morphology and gene expression. A recent study found that over 6,000 astroglial gene transcripts were differentially regulated by cAMP signaling; gene ontology revealed associations with pathways controlling antioxidant activity, cell metabolism, and ion transporters (Paco et al., 2016). For example, numerous ion channels, pumps and transporters such as Kcn2 (for K^+) and ATP2a2 (for Ca^{2+}) were all upregulated by cAMP (Paco et al., 2016). Given the critical role of cAMP in these various functions,

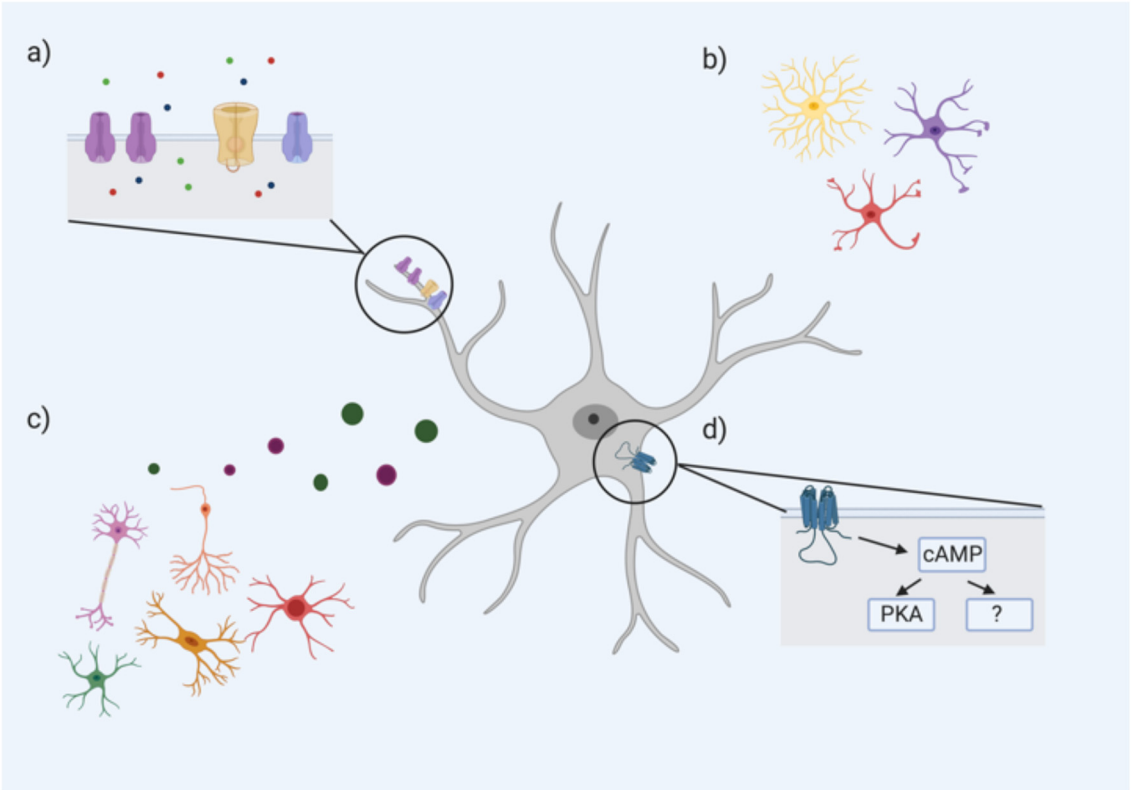

FIGURE 1 | An astrocyte's resting membrane potential (RMP) is likely influenced by multiple extrinsic and intrinsic factors including **(A)** ion channel subtype expression and density, particularly Ca^{2+}, Na^{+}, and K^{+} channels (ions represented by green, red, and blue circles, respectively); **(B)** astrocyte morphology; **(C)** neighboring cells including neurons, oligodendrocytes, microglia, and other astrocytes through the release of neurotransmitters, gliotransmitters, and other factors; **(D)** intracellular astrocyte signaling cascades such as the cAMP pathway. cAMP PKA-dependent and PKA-independent mechanisms have been proposed to influence astrocyte RMP (Bolton et al., 2006).

the differences in astrocyte RMP may be an electrophysiological hallmark of critical differences in cAMP signaling of astrocytes between and within regions (see **Figure 1**).

Astrocytes Are Characterized by Low Membrane Resistance

In addition to their negative RMP state, astrocytes typically have a dramatically lower membrane input resistance than neurons under basal conditions (Zhou et al., 2006; Ma et al., 2014; Du et al., 2015; Xin et al., 2019), suggesting a relatively high overall permeability to ions at rest. The low input resistance of astrocytes makes it particularly challenging to study their biophysical properties using electrophysiological approaches (for example, the low membrane resistance can cause a large portion of the voltage drop to occur across the electrode tip rather than across the cell membrane change; Ma et al., 2014). Nonetheless, the available data suggests astrocytic membrane resistance differs across brain regions, and even within the same region. For example, VTA astrocytes have, on average, a significantly lower membrane resistance compared to those of the cortex or hippocampus (approximately 1 MΩ in the VTA compared to approximately 3 MΩ in the cortex and hippocampus; Xin et al., 2019), though no differences have been noted between cortical and hippocampal astrocytes (Mishima and Hirase, 2010; Xin et al., 2019). However, several studies have found differences in membrane resistance amongst astrocytes within the hippocampus (Isokawa and McKhann, 2005; Zhong et al., 2016), suggesting that the membrane resistance of only some hippocampal astrocytes are comparable to those in the cortex. In one study, two distinct electrophysiological phenotypes of astrocytes were identified in the *stratum radiatum*; one subclass was defined by a variable input resistance with an overall mean input resistance significantly higher than the other subclass (Zhong et al., 2016).

Precisely what these differences mean is not fully understood, however, because input resistance is inversely proportional to overall ion permeability across the membrane, these differences might represent variability in the capacity of astrocytes to conduct/transport ions in and out of the cell. Therefore, differences in membrane resistance could offer significant insight into the ability of astrocytes to buffer various ions as well as resultant downstream intracellular signaling pathways driven by these ions.

It is also important to consider how morphology, and specifically, membrane surface area, may influence membrane resistance. An increase in the number or length of astrocytic

processes and therefore, membrane surface area, will lead to an increase in leak channels (if channel density is equal across these membrane processes), and thus an increase in overall membrane conductance. An increase in membrane conductance will directly result in a decrease in membrane resistance. While differences in morphology alone may be insufficient to explain the heterogeneity in astrocytic membrane resistance, it is likely that it is a contributing factor.

Challenges to the CNS have also been noted to influence membrane resistance in astrocytes, though these changes are variable and appear to depend on the type and extent of the challenge. Following a unilateral entorhinal cortex lesion, astrocytes of the denervated layer in the dentate gyrus had an increase in membrane resistance that persisted for up to 10 days post-lesion (Schröder et al., 1999). Another study observed changes of membrane resistance in some astrocytes, but not others, following incubation with high $[K^+]$, a model of early astrocyte activation (Neprasova et al., 2007). A decrease in the membrane resistance of hippocampal astrocytes in slice was noted following exposure to ammonium (a model of hepatic encephalopathy; Stephan et al., 2012).

In a cortical freeze lesion model, changes in the membrane resistance of astrocytes were noted though these changes varied significantly depending on the relative location of the astrocytes to the injury site (Bordey et al., 2001). Increased membrane resistance was noted in layer I astrocytes of a lesioned cortex compared to controls but astrocytes in the "hyperexcitable" zone (characterized by the epileptiform activity of neurons upon stimulation) showed virtually no changes in membrane resistance (Bordey et al., 2001). Additionally, this model induced a proliferative zone; an area surrounding the lesion characterized by proliferating astrocytes (Bordey et al., 2001). Interestingly, astrocytes in this proliferative zone had a mean membrane resistance that was significantly higher than astrocytes of the hyperexcitable zone under both control and lesioned conditions (Bordey et al., 2001).

The changes in astrocytic membrane resistance following disturbances to the CNS may represent compensatory mechanisms. A low membrane resistance, such as the one typically seen in astrocytes, suggests increased ionic permeability across the astrocyte's membranes. The initial increase in input resistance following a unilateral entorhinal cortex lesion (Schröder et al., 1999) suggests a reduced ability of ion conduction across the membrane in the proliferative zone. This might represent a mechanism to help regulate ion homeostasis during times of CNS perturbations. On the contrary, this increase in membrane resistance could also represent a mechanism that perpetuates CNS damage. If an increase in membrane resistance corresponds to a reduced ability to transport ions across the membrane, this could mean a reduced ability to maintain extracellular ion homeostasis, thus causing further damage.

These injury-induced changes in astrocyte membrane resistance may correspond with the changes in astrocyte morphology that characterizes reactive astrogliosis. Following CNS injury, hypertrophy of astrocytes occurs in levels correlative to the severity of the injury (Sofroniew and Vinters, 2010). Retraction of astrocytic processes and a hypertrophied cell soma means a smaller membrane surface area (and potentially fewer leak channels), which could explain an increase in membrane resistance. As astrocytes closer to the site of injury tend to undergo greater hypertrophy, this could partially explain why the membrane resistance of astrocytes might vary across different zones of the injury site. In the case of localized CNS damage (such as a lesion or ischemic event), the location of astrocytes relative to the damage may represent a significant factor in determining whether the membrane resistance increases, decreases, or remains the same. In Bordey et al.'s (2001) study, the physiological changes differed significantly amongst the different zones of the injury, suggesting this may be an important factor influencing astrocyte physiology under reactive conditions.

Reactive astrogliosis has long been recognized as a process that induces morphological, molecular and physiological changes. Data from studies that have induced CNS damage (Schröder et al., 1999; Bordey et al., 2001; Neprasova et al., 2007; Stephan et al., 2012) demonstrate clearly that the basic electrophysiological properties of astrocytes (i.e., membrane resistance) also change in response to perturbations in the CNS, though in many contexts, these changes are not well characterized and understood. As the perspective of astrocyte heterogeneity continues to develop, under basal and reactive conditions, it will be essential for the perspective of astrocyte electrophysiology to do the same.

Electrophysiological Properties of Astrocytes Across Development

Further contributing to the complexity of astrocyte physiology is that many of the other basic electrophysiological properties of astrocytes such as their membrane potential change across development (Zhou et al., 2006; Zhong et al., 2016). One study found that neonatal astrocytes (P1–P3) of the *stratum radiatum* had a more negative membrane potential compared to mature astrocytes ($P > 21$) of the same region (approximately −85 mV and −80.9 mV, respectively; Zhong et al., 2016). These changes across development highlight the caution that must be taken when generalizing electrophysiological data across studies and across timepoints.

It is currently unknown what drives these changes in the electrophysiological properties of astrocytes throughout development. In the cortex, morphological and functional heterogeneity of astrocytes is influenced greatly by neuronal heterogeneity *via* the release of specific neurotransmitters, ions, and neurotrophic factors (Verkhratsky and Nedergaard, 2018; Bayraktar et al., 2020); it is likely that this is also the case for the electrophysiological features of astrocytes. It is also possible these changes reflect shifts in the expression of ion transporters. For example, the K^+-Cl^-- cotransporter (KCC2) helps modulate Cl^- levels in neurons through the export of 1 K^+ and 1 Cl^- across the membrane (Annunziato et al., 2013). An increase in the neuronal expression of KCC2 early in development is believed to drive the shift of GABA from an excitatory to an inhibitory neurotransmitter (Moore et al., 2019). However, KCC2 is also expressed in astrocytes (Annunziato et al., 2013; Rurak et al., 2020), and this expression increases

across development (Rurak et al., 2020). Perhaps the increase in KCC2 expression in astrocytes, and subsequent changes in intracellular K^+ and Cl^+ levels and reversal potentials, is what drives the changes in the electrophysiological properties such as RMP over development. Moreover, increased ion transport across the membrane *via* transporters such as KCC2 could also influence the input resistance of astrocytes. Developmental changes in transporter expression may represent one potential mechanism that drives changes in astrocyte electrophysiology across the lifespan.

It is clear from the literature that astrocytes differ tremendously in many of their basic electrophysiological properties such as their RMP, membrane resistance, membrane currents, and selective ion permeability. The literature also shows that these properties differ significantly at both the regional and sub-regional levels. There remains a large gap in knowledge about the relationship between the specific electrophysiology properties of astrocyte subpopulations and how these properties correspond to their morphological, biochemical, and functional properties. It is likely that future studies on astrocyte electrophysiology, will result in new methods for classifying and modulating signaling within astrocyte subtypes.

Astrocyte Electrophysiology: Convergence Across Species

The evidence presented thus far for the heterogeneity of astrocyte electrophysiology is primarily derived from studies utilizing *in vitro* or *in vivo* rodent models. However, whether the electrophysiological properties of astrocytes are conserved across species is not well characterized. Furthermore, while rodent astrocytes appear to exhibit extensive heterogeneity in their electrophysiology, it is unknown whether (or to what extent) human astrocytes show similar heterogeneity in *their* electrophysiological properties. However, it is well established that rodent and human astrocytes do differ in many of their characteristics (Oberheim et al., 2009; Dossi et al., 2018; Miller, 2018).

Morphological and transcriptional analyses have revealed differences between astrocytes across species. For example, several studies have demonstrated that human astrocytes tend to exhibit larger soma with a greater number of processes compared to their rodent counterparts (Oberheim et al., 2006, 2009; Zhang et al., 2016). Transcriptional differences have also been noted; one study found over 600 genes enriched in human astrocytes that were not enriched in mouse astrocytes (Zhang et al., 2016). Given this divergence between species, it is possible that human astrocytes also differ in terms of their electrophysiological properties.

Few studies have been conducted that evaluate the electrophysiological properties of human astrocytes. Early studies of human astrocytes measured comparable RMPs to those observed in rodents (Bordey and Sontheimer, 1998; O'Connor et al., 1998; Hinterkeuser et al., 2000). One of these studies noted a higher membrane capacitance in human astrocytes (Bordey and Sontheimer, 1998), which is perhaps expected given the larger surface area of human astrocytes (Bedner et al., 2020). Interestingly though, this study did note a high input resistance (Bordey and Sontheimer, 1998). However, there is contention over whether these early studies successfully analyzed astrocytes, or whether they had actually identified NG2+ glial cells (Bedner et al., 2020). A more recent study of hippocampal astrocytes from patients with temporal lobe epilepsy revealed they exhibited a passive conductance and an RMP, membrane resistance and capacitance similar to rodent astrocytes of the same region (Bedner et al., 2015, 2020). This suggests that some electrophysiological properties of astrocytes are, in fact, conserved between rodents and humans (Bedner et al., 2020). However, there lacks sufficient studies/evidence to draw any strong conclusions.

Given the heterogeneity of astrocytes in the rodent brain, it is possible that a similar diversity in electrophysiological properties exists in human astrocytes. Studies involving direct comparisons across species will also be critical; this is particularly important because of the observed differences in species morphology, and the link between morphology and membrane capacitance. Any differences between rodent and human astrocyte electrophysiology could potentially be explained by differences in morphology. However, one study did show comparable membrane capacitance values between mouse and human astrocytes (Bedner et al., 2015, 2020), which could mean other factors are influencing human astrocyte physiology such as the density of ion channel expression. At this time, too few studies have been conducted to reach reliable conclusions as to if, and to what extent, human astrocyte electrophysiology differs from their rodent counterparts.

An additional caveat of astrocyte electrophysiology research is the extensive differences in the experimental protocol. Although *in vitro* (i.e., cell culture and slice) and *in vivo* data suggests comparable findings across experimental paradigms, few, if any, studies have directly compared electrophysiological properties of astrocytes from culture, slice and *in vivo* samples. Therefore, this calls for caution when interpreting and extrapolating electrophysiological data across paradigms.

ASTROCYTES ARE KEY REGULATORS OF K^+ HOMEOSTASIS

Astroglial K^+ Spatial Buffering Mediated Through $K_{ir}4.1$ Subtype

The combination of a highly negative RMP and a low membrane resistance make astrocytes particularly well suited for buffering potassium (K^+; Du et al., 2015), one of their most critical homeostatic functions within the CNS. The extracellular concentration of K^+ ($[K^+]_o$) rests at approximately 3.0 mM, and is critical in establishing the RMP of both neurons and astrocytes (Anderson et al., 1995; Bellot-Saez et al., 2017). Interestingly, the average RMP of astrocytes is close to the equilibrium potential of K^+ (Somjen, 1979; Guatteo et al., 1996), thus reflecting a high resting conductance for the ion (Somjen, 1979; Dallérac et al., 2013).

Changes in $[K^+]_o$ can be indicative of increased neuronal activity (Neprasova et al., 2007). Increases in $[K^+]_o$ occur following neuronal excitation whereby K^+ clearance from the neuron is used to co-transport Na^+ ions out of the cell following periods of high action potential-mediated Na^+ influx (Hertz and Chen, 2016). Thus, regulation and uptake of extracellular K^+ is essential in maintaining a homeostatic balance within the CNS. While both neurons and astrocytes are capable of regulating K^+ levels, this function is typically associated with astroglial cells. Several mechanisms of K^+ maintenance have been identified including passive spatial buffering and uptake mediated through active transporters.

The concept of K^+ spatial buffering was first proposed decades ago (Walz, 1982; Verkhratsky and Nedergaard, 2018). In the proposed model, K^+ enters astrocytes *via* K^+-permeable membrane channels and diffuses to areas of lower K^+ concentration in the glial network *via* gap junctions connecting the glial syncytium (Higashi et al., 2001; Verkhratsky and Nedergaard, 2018). This occurs without additional energy requirements (Orkand et al., 1966; Bellot-Saez et al., 2017). The initial uptake of extracellular K^+ prior to its redistribution throughout the glial syncytium is mediated through many subtypes of K^+-permeable channels, including both voltage-dependent (i.e., inward-rectifying and Kv families) and independent (i.e., two-pore domain or "leak" family, see next section) K^+ channels. Each of these families of channels express several subtypes including TREK 1, TWIK 1, and Kv 3.4 and 4.3 (this is not an exhaustive list but will be the focus in the remainder of this section). Of the variants of voltage-dependent K^+ channels, the inward-rectifying K^+ channels are a family consisting of 16 channels, subdivided into seven subfamilies (Bellot-Saez et al., 2017). The $K_{ir}4.1$ subtype, a weakly inward-rectifying K^+ channel, is the predominant subtype expressed on astrocytes (Kofuji and Newman, 2004; Brasko et al., 2017).

The robust expression of the $K_{ir}4.1$ subtype is believed to contribute to the high resting conductance of K^+ in astrocytes (Tang et al., 2009). However, expression of the $K_{ir}4.1$ subtype within astrocytes is variable; the channel is expressed in the spinal cord (Olsen et al., 2006), deep cerebellar nuclei, Müller glia of the retina as well as a subset of the hippocampus, but not in all astrocytes found within the hippocampus and white matter (Poopalasundaram et al., 2000; Higashi et al., 2001; Rurak et al., 2020). In a comprehensive analysis of $K_{ir}4.1$ subtype expression in glial cells, $K_{ir}4.1$ immunoreactivity was enriched in astrocytic processes wrapped around blood vessels (Hibino et al., 2004) and at synapses. Enrichment of $K_{ir}4.1$ at blood vessels was also noted in human tissue (Tan et al., 2008).

The channel subtype was observed on astrocytes in several regions, including the forebrain, midbrain, and hindbrain, albeit to varying degrees (Higashi et al., 2001). The percentage of total synapses covered by $K_{ir}4.1$-positive processes varied substantially between brain regions, with over 60% of synapses covered in regions such as the entorhinal cortex, the superior and inferior colliculi and the pontine nucleus, but only 30%–60% of synapses covered in regions such as the anterior dorsal nucleus and lateral nuclei of the thalamus and the interpeduncular nucleus. Other regions, like the mitral cell layer of the olfactory bulb, exhibited very little $K_{ir}4.1$-positive processes surrounding synapses (Higashi et al., 2001).

The expression of the $K_{ir}4.1$ subtype is also variable within the cortex. Benesova et al. (2012) identified distinct subpopulations of astrocytes within the cortex that differed in their extent of swelling following oxygen-glucose deprivation. These subpopulations were (nearly) uniformly distributed across each layer of the cortex but varied significantly in gene expression of several K^+-related channels, including $K_{ir}4.1$. There was approximately a 1.5 log difference in gene expression between the subpopulations (Benesova et al., 2012). In contrast, another study found differences in $K_{ir}4.1$ immunoreactivity between layers of the cortex; there was greater $K_{ir}4.1$ subtype expression in cortical layers II and III compared to layers IV–VI, though this study did not distinguish between (possible) subtypes of astrocytes (Higashi et al., 2001).

The subregional diversity of astrocytic $K_{ir}4.1$ subtype expression has been noted in other regions including the olfactory bulb and the hippocampus (Higashi et al., 2001). Each layer of the olfactory bulb, for example, has varying expression of the $K_{ir}4.1$ subtype subunit, with high expression in layers such as the glomerular layer, and much lower expression in layers such as the olfactory nerve and mitral cell layers (Higashi et al., 2001). A similar pattern was seen in the hippocampal layers; almost no $K_{ir}4.1$ was seen in the dentate gyrus but there was astroglial expression of the channel in the CA layers (Higashi et al., 2001). Moreover, co-localization of the $K_{ir}4.1$ subtype with glial fibrillary acidic protein (GFAP), an intermediate filament protein commonly used as a marker for astrocytes, showed differences between each layer of the olfactory bulb (Higashi et al., 2001), further demonstrating the molecular and physiological heterogeneity of astrocytes.

There is some evidence to indicate heterogeneous subcellular localization of $K_{ir}4.1$ in astrocytes. One study of cerebellar glia found $K_{ir}4.1$ expression in the radial processes of Bergmann glia in the Purkinje cell layer, whereas astrocytes of the granule cell layer expressed $K_{ir}4.1$ in both the processes and somata (Brasko et al., 2017). In contrast, Muller glia of the retina preferentially express $K_{ir}4.1$ in their perivascular endfeet vessels (Kofuji et al., 2002). Similarly, $K_{ir}4.1$ is expressed in endfeet and fine processes of astrocytes within the rat optic nerve (Kalsi et al., 2004). The function of $K_{ir}4.1$ may be mediated by its subcellular localization; at perivascular endfeet, the ion channel may be important for regulating K^+ in the blood vessels, but those localized at the processes or somata may be more important for regulating K^+ levels of the astrocyte itself. Nonetheless, the heterogeneity of subcellular $K_{ir}4.1$ expression across different regions further emphasizes the extensive diversity of astrocyte electrophysiology.

The variability of astrocytic $K_{ir}4.1$ subtype expression further demonstrates the physiological heterogeneity of astrocytes. Whilst differing levels of the $K_{ir}4.1$ subtype are not necessarily indicative of differing capabilities of K^+ regulation, it does suggest, at the very least, that astrocytes of varying brain regions utilize alternative mechanisms to regulate K^+. It appears astrocytes of the *same* region may also exhibit alternative mechanisms for K^+ regulation as they also display differing

levels of the $K_{ir}4.1$ subtype; and since $K_{ir}4.1$ appears to be particularly important in generating the RMP of astrocytes, it is possible that astrocyte subtypes with different membrane potentials express different levels of this K^+ channel. That astrocytes might differ concomitantly in distinct features (i.e., morphological, physiological, functional) demonstrates the complexity of astrocyte heterogeneity, and the importance of further understanding the physiological diversity of this unique cell population.

Voltage-Independent K^+ Channels Contribute to Passive Conductance

The two-pore domain, voltage-independent K^+ channels (K_{2P}) are thought to contribute substantially to the electrophysiological properties of astrocytes (Ryoo and Park, 2016; Verkhratsky and Nedergaard, 2018). This group of "leak channels" is a 15-member family of which at least three channel subtypes have been identified in astrocytes (Seifert et al., 2009; Du et al., 2016). TREK 1, TREK 2, and TWIK 1 have been observed in astrocytes of the hippocampus (Seifert et al., 2009; Du et al., 2016), cortex (Gnatenco et al., 2002), and forebrain (Cahoy et al., 2008), though it is likely that these channels are expressed in astrocytes throughout the CNS.

Despite their voltage-independence, K_{2P} channels mediate currents at a wide range of membrane potentials and are believed to contribute to the RMP of neurons and astrocytes (Ryoo and Park, 2016; Verkhratsky and Nedergaard, 2018). In the hippocampus, passive conductance (that is a linear current-voltage relationship) in astrocytes was reduced following a pharmacological blockade and shRNA-mediated knockdown of TREK 1 and TWIK 1 (Zhou et al., 2009; Mi Hwang et al., 2014), suggesting a contributory role of these channels to the passive conductance and K^+ uptake observed in astrocytes (Seifert et al., 2009). However, there is some contradictory evidence to this as the genetic deletion of TWIK and/or TREK 1 did not alter passive conductance in hippocampal astrocytes (Du et al., 2016). If TWIK 1 and TREK 1 are involved in passive conductance, then differences in astrocytic conductance throughout the CNS suggests potential variability in the expression of these leak channels throughout the brain. Since the passive conductance of astrocytes is thought to be the reason for their ability to buffer K^+ (Tang et al., 2009), this suggests TREK 1 and TWIK 1 might also play a contributory role in the ability of astrocytes to buffer K^+. Further research is needed to determine if indeed the expression of TREK 1 and TWIK 1 influence K^+ buffering, and to what extent. It is also possible (and likely) these channels are important in determining other functions in astrocytes, further highlighting the need for more research.

Voltage-Dependent K^+ Channels Have Distinct Subcellular Localization

Beyond $K_{ir}4.1$, several other types of voltage-dependent K^+ (K_V) channels, with heterogeneous biophysical properties, have been identified in astrocytes (Verkhratsky and Nedergaard, 2018). As a first example, delayed rectifying K^+ currents have been observed in astrocytes from the spinal cord, hippocampus, cerebellum, and cortex (Bordey and Sontheimer, 2000). The delayed rectifying K^+ current ion channel subtype (K_D) that mediates these currents has outward rectification and a higher conductance capability at potentials more positive than −50 mV. Transient "A"-type currents are a second type of K^+ current present in astrocytes of the cerebrum, hippocampus, spinal cord, and the optic nerve (Sontheimer, 1994). The A-type channels are rapidly activating and inactivating and also require hyperpolarization to remove the tonic inactivation before they can activate (Sontheimer, 1994; Verkhratsky and Nedergaard, 2018). There are also additional subtypes of inward-rectifying K^+ channels beyond $K_{ir}4.1$ that have been characterized in astrocytes (Bekar et al., 2005). In astrocytes, these voltage-gated K^+ channels are thought to play a role in modulating membrane potential; blockade of K_v channels in cortical astrocytes diminished their ability to repolarize (Wu et al., 2015). Blockade of these channels also reduced the influx of Ca^{2+}, suggesting a role of these channels in the regulation of Ca^{2+} entry into astrocytes (Wu et al., 2015).

Various voltage-dependent K^+ channels are expressed in astrocytes; Kv1.1 and Kv1.6 are seen in cortical mouse astrocytes (Smart et al., 1997); Kv1.5 has been observed in the spinal cord and brains of rats, as well as in gliomas of human patients (Preussat et al., 2003). Kv1.3 is also expressed in human gliomas (Preussat et al., 2003). In addition, the subtype and subunit composition of voltage-gated K^+ channels differ across astrocyte subpopulations, at least in the hippocampus. One study found three families of K^+ channels, Kv4, Kv3, and Kv1 that each contributed a different percentage of the A-type currents observed in the hippocampus (about 70, 10 and 5%, respectively; Bekar et al., 2005). These K^+ channels also exhibit distinct subcellular localization in astrocytes; the Kv3.4 subtype was expressed primarily in the processes whereas the Kv4.3 was found localized to the somata (Bekar et al., 2005). The functional implications of this have not been fully elucidated, but do suggest that there may be distinct responses of the subcellular components in astrocytes to changes in voltage. Whether the differential expression of Kv families in hippocampal astrocytes is comparable to astrocytes of other brain regions has not yet been characterized. However, the variability in astrocytic membrane potential, which is partially modulated through voltage-gated K^+ channels, suggests there is likely variability in the expression of these channels across astrocytes of other areas.

Like Kv3.4 and Kv4.3, the Kv1.3 and Kv1.6 subtypes exhibit distinct subcellular localization. In rat astrocytes, Kv1.3 is expressed on the Golgi apparatus and the Kv1.6 subtype is on the endoplasmic reticulum (Zhu et al., 2014), thus reiterating the heterogeneous nature of astrocytes and astrocyte physiology.

At least one study has demonstrated that the cAMP/PKA pathway might influence the RMP of astrocytes (Bolton et al., 2006). It is possible that the cAMP pathway regulates RMP through the modulation of voltage-gated K^+ channels. In fact, one study did find that treating cultured astrocytes with activators of the cAMP pathway was sufficient to modulate the expression (both up-and downregulation) of several potassium channels (Paco et al., 2016). Activation of this pathway through neuronal input, intracellular (astrocyte) signals, environmental factors, or some combination of these, might influence the temporal and spatial expression of these channels, and ultimately

the RMP of an astrocyte. Particularly over the course of development, these neuronal inputs, signals and, environmental influences vary greatly from region to region, and this may (in part) explain the diversity of Kv expression and activity in astrocytes.

Potassium-dependent activity is an integral part of CNS function, and astrocytes play a key role in regulating its levels. Throughout the CNS, astrocytes express these K^+ channels to varying degrees, demonstrating the physiological heterogeneity and diversity of these cells. The functional outcomes of these channel profile differences have not been completely elucidated, but several studies have found a correlation between the expression of particular K^+ channels and cell proliferation (Bordey et al., 2001). Additionally, given that high extracellular K^+ has been linked to neuronal damage, the heterogeneity of astrocytic K^+ channels may represent regional and subregional susceptibility to K^+-induced neuronal damage. This susceptibility may be particularly exacerbated in times of stress or injury; it is possible that these functional differences may only be observed under reactive conditions, or when the system has been perturbed significantly.

Na^+ CHANNELS ARE NOT ONLY EXPRESSED IN NEURONS

A classic dogma is that voltage-dependent sodium (Na^+) channels are only associated with excitable cells, such as neurons, because of their role in driving an action potential. Upon membrane depolarization, these voltage-dependent Na^+ channels open and allow a transient inward Na^+ current, which marks the initiation of the action potential (Pappalardo et al., 2016). However, these voltage-dependent Na^+ channels have also been identified on non-excitable cells, such as Schwann cells, microglia, and astrocytes (Black and Waxman, 2013; Pappalardo et al., 2016). Though these voltage-dependent Na^+ channels are not responsible for action potential initiation in astrocytes, they are thought to play an important role in some astrocytic functions, particularly ion and neurotransmitter homeostasis and reactive astrogliosis (Parpura and Verkhratsky, 2012; Pappalardo et al., 2016; Verkhratsky et al., 2019). Intracellular sodium transients in hippocampal astrocytes have been observed following Schaffer collateral stimulation, suggesting sodium signaling in astrocytes occurs in response to excitatory synaptic activity (Langer and Rose, 2009). Thus, understanding the heterogenous nature of astrocytic Na^+ signaling and channel expression may provide critical insight into astrocyte function.

Voltage-dependent Na^+ channels consist of an α-subunit, of which there are nine isoforms ($Na_v1.1$–$Na_v1.9$) and a β-subunit of which there are only four isoforms (Pappalardo et al., 2016; Verkhratsky and Nedergaard, 2018). Astrocyte expression of these voltage-gated Na^+ channels has been noted in regions such as the spinal cord, cerebellum, optic nerve, cortex, and hippocampus (Sontheimer et al., 1991; Black et al., 1995; Kressin et al., 1995; Reese and Caldwell, 1999; Schaller and Caldwell, 2003; Ziemens et al., 2019; Rurak et al., 2020). Sodium signals have also been measured in astrocytes of the white matter (Moshrefi-Ravasdjani et al., 2017). In this study, Na^+ transients, as determined by changes in the fluorescence of the sodium indicator, SBFI, were observed following glutamate application (Moshrefi-Ravasdjani et al., 2017).

The (gene) expression of these Na_v subtypes has been noted to change across development, at least in cortical astrocytes (Rurak et al., 2020). In this study, the authors combined translating ribosome affinity purification with RNA sequencing (TRAPseq) to measure gene expression changes specifically in cortical astrocytes. Across development, there was significant differential expression of several genes that encode for voltage-gated Na^+ channels, including SCN1A (which encodes for the $Na_v1.1$ subtype), SCN3A ($Na_v1.3$), SCN8A ($Na_v1.6$), and SCN11A ($Na_v1.9$; Rurak et al., 2020). Though these differentially expressed genes were not validated using alternative methods (i.e., RT-qPCR), they do suggest that the physiological properties of astrocytes (such as Na^+ channels and signaling) are highly dynamic across development, and extrapolating data to other studies must be done with caution.

Na^+ Channel Subtype Expression Is Heterogenous in Astrocytes

Several of these Na^+ channel subtypes have been observed in this glial population, including $Na_v1.2$, $Na_v1.3$, $Na_v1.5$, and $Na_v1.6$ (Black et al., 1995; Schaller and Caldwell, 2003; Black and Waxman, 2013; Pappalardo et al., 2016). However, there is considerable heterogeneity in Na_v subtype expression in astrocytes across the CNS. For example, one study evaluated the expression of Na_v 1.2 and Na_v 1.3 in cultured astrocytes of the spinal cord and optic nerve (Black et al., 1995). Immunocytochemistry revealed higher levels of Na_v 1.2 and Na_v 1.3 in spinal cord astrocytes compared to those of the optic nerve (Black et al., 1995). Furthermore, the researchers noted varying expression of these Na^+ channels in morphological subtypes of astrocytes. In particular, spinal cord astrocytes classified as "stellate" had moderate levels of Na_v 1.2 but the "flat" astrocytes of this region expressed only low levels of the channel. Similarly, in the optic nerve, the "stellate" astrocytes expressed low levels of Na_v 1.2, but this expression was negligible in astrocytes classified as "flat" (Black et al., 1995). This study demonstrates the heterogeneity of some voltage-dependent Na^+ channel subtypes across the CNS and further demonstrates how there is heterogenous expression within astrocytes of a given region. Data from this study suggests astrocyte morphology may be correlated to the diversity of Na_v subtype expression.

Another study in the cerebellum found heterogeneity in Na_v expression amongst morphological subtypes of astrocytes in this region. In the cerebellum, $Na_v1.6$ expression has been noted in the processes of Bergmann glia, but the subtype was not identified in astrocytes of the granule cell layer (Schaller and Caldwell, 2003), suggesting again that morphological subtypes of astrocytes express different voltage-dependent Na^+ channels. Interestingly, high expression of $Na_v1.6$ was observed in cerebellar granule cells themselves (Schaller and Caldwell, 2003), implying that Na_v expression in astrocytes may, in part, be driven by the expression of these channels in neighboring neurons. Like with the K^+ channels discussed above, it is probable that the heterogenous expression of voltage-dependent

Na^+ channels in astrocytes is the result of the interplay between various intrinsic and extrinsic factors. Understanding all these different influences will help uncover the molecular and electrophysiological underpinnings of the functional differences across astrocytes.

The heterogenous expression of $Na_v1.6$ may have important implications about an astrocyte's ability to respond appropriately to injury. Zhu et al. (2016) demonstrated that $Na_v1.6$ expression is significantly upregulated in hippocampal astrocytes following status epilepticus in the kainic acid model of epilepsy and that this upregulation is strongly correlated to the severity of both the seizures and the reactive astrogliosis. Interestingly, the authors noted several lines of evidence demonstrating large voltage-dependent Na^+ currents in reactive astrocytes following seizure (de Lanerolle and Lee, 2005), suggesting that the increase in $Na_v1.6$ in reactive astrocytes may contribute to hyperexcitability in an epileptic brain (Zhu et al., 2016). This may be caused by a Ca^{2+}-mediated release of glutamate from astrocytes. Upregulation of $Na_v1.6$ could drive increases in Na^+ influx, which, *via* the Na^+/Ca^{2+} exchanger, could subsequently induce increases in intracellular Ca^{2+} levels, and Ca^{2+}-mediated activities like the release of glutamate (Zhu et al., 2016). In an epiletic brain, this mechanism might further drive hyperexcitability and epileptogenesis. It is therefore possible that baseline differences in $Na_v1.6$ expression in astrocytes might be indicative of the potential risk for hyperexcitability following seizure activity.

Like $Na_v1.6$, the $Na_v1.5$ subtype may play an important role in reactive astrogliosis. Knockdown of $Na_v1.5$ mRNA in primary rat cortical astrocytes resulted in impaired wound closure following a scratch injury (Pappalardo et al., 2014). Furthermore, the scratch injury induced an intracellular Ca^{2+} response that was attenuated by the $Na_{v1.5}$ knockdown (Pappalardo et al., 2014).

Changes in astrocytic $Na_v1.5$ expression have also been observed in other models of CNS injury. In one study, conditional knockouts lacking $Na_{v1.5}$ in astrocytes were generated. Compared to wildtype animals, the conditional knockouts developed more severe clinical outcomes in an EAE model of Multiple Sclerosis, though this effect was only observed in female mice (Pappalardo et al., 2018). This suggests that $Na_v1.5$ may be important in mediating the astrocytic response to pathological conditions, though these effects may be sex-specific. Interestingly, some of the astrocytes lacking $Na_v1.5$ appeared to have a more simple morphology compared to those of wildtype animals (Pappalardo et al., 2018).

Astrocytic Na^+ Currents Are Linked to Specific Morphologies

The differences in Na_v subtype expression likely underlies variation in astrocytic Na^+ currents and associated pharmacology. Several studies have demonstrated heterogeneity of Na^+ currents in two morphological subclasses of astrocytes (Sontheimer and Waxman, 1992; Sontheimer et al., 1994), suggesting different (morphological) subclasses of astrocytes may express different densities of the various Na_v subtypes. Fibrous astrocytes exhibit Na^+ currents comparable to neurons; they tend to activate at relatively depolarized potentials and inactivate rapidly. Protoplasmic astrocytes, on the other hand, tend to activate at relatively negative potentials and inactivate more slowly. Additionally, different morphological classes of astrocytes have distinct sensitivities to tetrodotoxin, a blocker of a subset of sodium channel isoforms including $Na_v1.1$–1.4, $Na_v1.6$, and $Na_v1.7$ (Sontheimer et al., 1994). In the spinal cord, the Na^+ currents of astrocytes characterized as "stellate" (with numerous processes) were highly sensitive to tetrodotoxin but those that had a flat or "pancake" morphology exhibited Na^+ currents that were largely resistant to the drug (Sontheimer and Waxman, 1992), highlighting the extensive diversity of the astrocyte population. This suggests morphological subtypes of astrocytes may express different Na^+ channel subtypes, further emphasizing the heterogeneity of this cell population.

Heterogeneous astrocytic Na^+ signals have also been observed in those from different regions, particularly the neocortex and hippocampus (Ziemens et al., 2019). Neocortical astrocytes exhibited larger intracellular Na^+ transients following glutamate application in slice compared to those of the hippocampus (Ziemens et al., 2019).

The full extent to which the expression of these sodium channels and currents vary between astrocytes throughout the CNS has not been fully delineated but is imperative given the current evidence which suggests voltage-dependent Na^+ channels are involved in several critical astrocytic functions such as the regulation of ion channels and in response to CNS injury such as epileptogenesis (Qiao et al., 2013; Zhu et al., 2016). It is already established that Na^+ currents appear to differ between morphological subtypes of astrocytes but whether these properties also differ between other subtypes of astrocytes remains to be explored. Nonetheless, the differences in Na_v subtype expression and the biophysical and pharmacological properties of Na^+ currents further demonstrate the electrophysiological heterogeneity of astrocytes.

MULTIPLE Ca^{2+} SIGNALING PATHWAYS IN ASTROCYTES, AN INTEGRAL PART OF ASTROCYTE PHYSIOLOGY

Traditionally, astrocytes were believed to be passive cells whose sole function was to provide support for neuronal function. However, seminal studies in the 1990s revealed that astrocytes are capable of responding to synaptic activity through increases in intracellular calcium $[Ca^{2+}]_i$ levels (Porter and McCarthy, 1995; Pasti et al., 1997; Kang et al., 1998; Agulhon et al., 2008). These effects are also seen in cultured human astrocytes (Navarrete et al., 2013; Hashioka et al., 2014). Since then, calcium signaling cascades have been recognized as an integral part of astrocyte physiology. Importantly, under physiological conditions, both spontaneous and receptor-activated Ca^{2+} signals have been observed in astrocytes (Shigetomi et al., 2019).

Astrocytes express a vast array of G-protein coupled receptors (GPCRs; Shigetomi et al., 2019). In particular, $G\alpha_q$-linked GPCRs (G_qPCRs) are coupled to internal Ca^{2+} stores and may be the specific link between changes in $[Ca^{2+}]_i$ in response to neurotransmitter release at the synapse (Agulhon et al.,

2008). Activation of a G_qPCRs leads to the hydrolysis of the membrane lipid phosphatidylinositol 4,5-biphosphate (PIP_2) *via* the enzyme phospholipase C (PLC; Agulhon et al., 2008). This produces diacylglycerol (DAG) and inositol 1,4,5-trisphosphate (IP_3), the latter which binds to and activates IP_3 receptors on the endoplasmic reticulum membrane, thereby releasing Ca^{2+} from intracellular stores (Agulhon et al., 2008).

There are three isoforms of the IP_3 receptor (IP_3R; Sherwood et al., 2017). In astrocytes, the IP_3R_2 subtype appears to be the primary receptor subtype driving the PLC/IP_3 pathway (Holtzclaw et al., 2002; Sheppard et al., 2002; Petravicz et al., 2008); deletion of IP_3R_2 resulted in a lack of spontaneous and G_qPCR-induced elevations in Ca^{2+} in astrocytes (Petravicz et al., 2008). However, some studies have demonstrated Ca^{2+} signals still occur in the astrocytes of mice lacking the IP_3R_2 subtype (Stobart et al., 2018b), suggesting other mechanisms contribute to intracellular Ca^{2+} astrocytic signaling. In fact, a recent study found that the first and third isoforms of IP_3R may also contribute to Ca^{2+} signaling in astrocytes, albeit to a lesser extent (Sherwood et al., 2017).

Nonetheless, the IP_3R_2 subtype plays a particularly important role in Ca^{2+} signaling. A study from Holtzclaw et al. (2002) demonstrated distinct regional astrocytic subcellular expression of IP_3R_2. Astrocytes of the hippocampus expressed IP_3R_2 in their somata and processes, though there appeared to be a higher density in the large and fine processes. This was also true for cerebellar Bergmann glia in the molecular layer, which had punctate expression of IP_3R_2 in their finer processes. In contrast, Bergmann glia of the Purkinje cell layer expressed IP_3R_2 primarily in their somata (Holtzclaw et al., 2002). The study also showed that IP_3R_2 is particularly enriched in astrocytic processes that encircle synapses, highlighting an important putative role of Ca^{2+} signaling in mediating the link between neurotransmission and astroglia.

Spontaneous Ca^{2+} Oscillations in Astrocytes

Spontaneous Ca^{2+} signaling events occur in the absence of neuronal activity (Parri et al., 2001) and have been observed in astrocytes throughout the CNS including in the hippocampus (Nett et al., 2002; Rungta et al., 2016), cortex, striatum, and thalamus (Parri et al., 2001; Aguado et al., 2002; Jiang et al., 2014); the presence of spontaneous Ca^{2+} signals have also been confirmed, at least *in vitro*, in human astrocytes (Navarrete et al., 2013). They have been observed in Bergmann glia of the cerebellum (Aguado et al., 2002) as well as in astrocytes of the olfactory bulb (Otsu et al., 2015). Both extracellular and intracellular Ca^{2+} levels are critical for driving these spontaneous oscillations (Aguado et al., 2002); removal of extracellular Ca^{2+} is sufficient to prevent spontaneous Ca^{2+} signals *in vitro* (Aguado et al., 2002) and the loss of the IP_3R_2 reduces spontaneous events *in vivo* (Petravicz et al., 2008; Jiang et al., 2016; Yu et al., 2018). However, some reports have noted spontaneous Ca^{2+} events even in the astrocytes of $IP_3R_2^{-/-}$ mice (Sherwood et al., 2017), suggesting that these mechanisms are not the only ones that drive spontaneous Ca^{2+} signals in astrocytes. Recent evidence from Wu et al. (2019) suggests that the morphology of astrocytes may be an important factor in driving these spontaneous Ca^{2+} signals- these events were more frequent in thin processes with a high surface-to-volume ratio. Given the extensive morphological heterogeneity of astrocytes, it is possible that the localization of transient Ca^{2+} events to thinner processes can explain some of the diversity in astroglial calcium signaling, particularly spontaneous events. The spontaneity of these Ca^{2+} signals fluctuate between astrocytes across the CNS, perhaps reflecting diversity in some of these processes. For example, hippocampal astrocytes, specifically of the CA1 *stratum radiatum* region, have a higher frequency of spontaneous Ca^{2+} events than those of the dorsolateral striatum (Chai et al., 2017), but fewer oscillations than those of the cortex (Navarrete et al., 2013), perhaps reflecting regional differences in the mechanisms that drive these spontaneous events.

In the hippocampus, a subset of astrocytes displayed no spontaneous Ca^{2+} signals, but of the astrocytes that did, there was significant variability in the frequency of these events (Nett et al., 2002). Some had fairly frequent Ca^{2+} oscillations at intervals between 0.5 and 2 min, whilst others had much more irregular intervals between oscillations, with intervals that exceeded 2 mins (Nett et al., 2002). Similar heterogeneity has been observed in the thalamus; the majority of thalamic astrocytes showed multiple spontaneous Ca^{2+} events over a 10-min period but several displayed only one spontaneous Ca^{2+} signal in the same time (Parri et al., 2001). In the somatosensory cortex, astrocytes from layer I had nearly double the frequency of spontaneous Ca^{2+} activity compared to those from layer II/III (Takata and Hirase, 2008).

Precisely what the differences in spontaneous Ca^{2+} signaling across astrocyte subpopulations mean has yet to be fully elucidated. One study found that hippocampal astrocytes which did not exhibit spontaneous Ca^{2+} signals did not differ in morphology or electrophysiology from those that did (Nett et al., 2002), demonstrating that the classification of astrocytes is not so straightforward as one morphological class displaying one set of electrophysiological properties, or molecular markers. Regardless, it is plausible that the differences in these spontaneous Ca^{2+} oscillations represent important distinctions between the various types of astrocytes. Astrocytes displaying no spontaneous Ca^{2+} are still able to respond to some neurotransmitter release (Nett et al., 2002), but the lack of spontaneous Ca^{2+} signals might indicate a decreased ability or less sensitive response to these types of events which normally evoke a Ca^{2+} response.

The mobilization of both intracellular and extracellular Ca^{2+} may be another important mechanism driving spontaneous Ca^{2+} events (Aguado et al., 2002). Removal of extracellular Ca^{2+} blocked spontaneous Ca^{2+} events in hippocampal astrocytes in slices (Aguado et al., 2002). Likewise, when thapsigargin, a drug which inhibits endoplasmic reticulum Ca^{2+}-ATPase activity and thus depletes ER Ca^{2+} stores, was applied to hippocampal slices, spontaneous Ca^{2+} activity in astrocytes was blocked. This suggests that intracellular Ca^{2+} stores are also necessary for spontaneous Ca^{2+} events in astrocytes (Aguado et al., 2002). The lack of spontaneous Ca^{2+} activity in astrocytes might therefore reflect a depletion of extracellular or intracellular

Ca^{2+} signaling capacity, highlighting the influence of both extrinsic and intrinsic factors in the development of astroglial spontaneous Ca^{2+} activity. As with the frequency, the amplitude of these spontaneous astrocyte Ca^{2+} transients are variable- both inter-and intra-regionally (Aguado et al., 2002). This is true in several regions including the cortex, hippocampus, thalamus, hypothalamus, and spinal cord (Aguado et al., 2002). The heterogeneity of these spontaneous events is likely the result of regional and subregional diversity in the presence of extracellular Ca^{2+} and the available intracellular Ca^{2+} stores in astrocytes.

It is clear that there are subtle differences between astrocytes displaying spontaneous Ca^{2+} oscillations and those that do not (Nett et al., 2002). Furthermore, it is clear that of the astrocytes that do exhibit spontaneous Ca^{2+} oscillations, they differ significantly in several of their properties including the frequency and the amplitude of these signals. It is possible these distinct spontaneous Ca^{2+} oscillations have extensive functional consequences, making the understanding of this heterogeneity pertinent to comprehending the role of astrocytes within the CNS.

Astrocytic Ca^{2+} Signals Differ in Subcellular Compartments

Initial studies into astrocytic Ca^{2+} signaling focused on cytosolic Ca^{2+} signals, primarily in the somata of astrocytes, but the use of genetic encoded calcium indicators (GECIs) have enabled higher resolution visualization of localized Ca^{2+} transients in the processes and finer processes of astrocytes (Shigetomi et al., 2013; Stobart et al., 2018a; for a comparison of calcium imaging techniques, see Smith et al., 2018). For example, spontaneous Ca^{2+} transients have been observed in the somata, processes, and fine processes of striatal astrocytes (Jiang et al., 2014). These cytosolic and local transients have also been observed in astrocytes of the cortex (Agarwal et al., 2017), hippocampus (Zur Nieden and Deitmer, 2006; Jiang et al., 2014), somatosensory cortex (Wang et al., 2006), and olfactory bulb (Otsu et al., 2015).

Like the extensive inter-and intraregional variability in the frequency and amplitude of astrocytic Ca^{2+} signals, there is substantial data suggesting that these events are also variable across the distinct subcellular compartments of astrocytes. In particular, it seems that spontaneous Ca^{2+} events occur more frequently in the processes compared to the somata of astrocytes. One study found the majority of Ca^{2+} events (∼85%) were localized to the processes, with a much smaller percentage (∼10%) in the endfeet, and an even smaller percentage (∼5%) in the somata (Bindocci et al., 2017). A very similar distribution of spontaneous Ca^{2+} events was seen in astrocytes within the somatosensory cortex, with approximately 80% of those signals occurring in the fine processes (Kanemaru et al., 2014). In astrocytes of the *stratum lucidum* region of the hippocampus, spontaneous Ca^{2+} signals were virtually absent in the somata but were frequently observed in the processes (in fact, there was about an 8-fold greater increase in these events in the processes compared to the somata; Haustein et al., 2014). The high frequency of spontaneous Ca^{2+} transients in the fine processes of astrocytes relative to their somata has also been observed in the visual cortex (Asada et al., 2015).

The spontaneous Ca^{2+} transients observed throughout the subcellular compartments of astrocytes also differ in their ability to spread from the source event. In the CA1 region, for example, researchers identified distinct Ca^{2+} fluctuations; one fluctuation produced a wave-like property, spreading to adjacent areas, whereas the other produced a restricted response which the authors referred to as a microdomain (Srinivasan et al., 2015). Both types of fluctuations were displayed in the processes, and each differed from fluctuations measured from the somata (Srinivasan et al., 2015).

Spontaneous Ca^{2} transients, while common in astrocytes, vary tremendously in the frequency, amplitude, and even type of fluctuation they produce. These properties differ at the regional, subregional, and subcellular levels. The current literature highlights the complexity of astroglial Ca^{2+} signaling at the regional, sub-regional, and cellular level.

This subcellular heterogeneity of Ca^{2+} signals, combined with the varied expression of voltage-dependent and voltage-independent ion channels (such as those discussed previously), suggests that astrocytes possess different electrophysiological profiles amongst distinct microdomains of the cell. Thus, permitting a localized response to environmental changes. These differences in subcellular compartments may also explain voltage-dependent ion channels in astrocytes; while the relatively low membrane resistance and hyperpolarized phenotype would (generally) require highly depolarizing events to activate these channels, the intracellular heterogeneity means there could be local variability in the membrane resistance and RMP of the processes, fine processes, and soma of the astrocyte.

ASTROCYTE PHYSIOLOGY INFLUENCES SYNAPTIC NETWORKS

Thus far, we have summarized the available data on the heterogeneity of astrocyte physiology. But what do these differences mean for the greater network? Does this heterogeneity translate to functional differences between other cells in the network such as neurons? If, and how, these differences may influence the network is not fully understood, but there is some evidence to suggest they can.

K^+ homeostasis is a critical function of astroglia, but they are not the sole cell type that can buffer this ion. Neurons, too, are able to buffer against K^+. Not all astrocytes may regulate K^+ equally; for example, the expression of the $K_{ir}4.1$, a key channel in buffering K^+, is highly variable amongst astrocytes. In areas where the K^+ buffering capacity of astrocytes is low, then neurons may need to be more active at regulating K^+ to help offset that deficit. This increased activity of neuronal transporters could drive higher energy and metabolic demands, which might, in turn, make these neurons more susceptible to electrical and chemical perturbations. The implications of this heterogeneity in K^+ buffering are not yet understood, but moving forward may be particularly important when considering why some neuronal populations are more susceptible to perturbations and damage than others.

Several studies have shown a "wave-like" phenomena between astrocytes; that is, a Ca^{2+} signal appears in one astrocyte followed

quickly by a Ca^{2+} signal in another nearby (Verkhratsky, 2006). This is mediated through the extensive gap junction coupling of astrocytes, forming the "net-like" structure of the glial syncytium and demonstrates how astrocytes can influence surrounding astrocytes. Of course, Ca^{2+} signals are only one way astrocytes can influence each other; ions (such as K^+—see "Astroglial K^+ Spatial Buffering Mediated Through $K_{ir}4.1$ Subtype" section) can also cross gap junctions as can energy substrates like glucose (Rouach et al., 2008) and lactate (Murphy-Royal et al., 2020).

It has also been theorized that astrocytic Ca^{2+} signals can influence synaptic activity. One study found that spontaneous Ca^{2+} signals in hippocampal astrocytes were localized to specific regions in their processes (Nett et al., 2002). These "microdomains" were typically asynchronous, leading the authors to believe the astrocytes might be influencing neurons in a synapse-specific manner. However, they did note some "wave-like" activity between processes of the same astrocyte, suggesting a potential larger influence on the greater synaptic field (Nett et al., 2002). A recent study did find a more direct effect of the glial syncytium on synaptic activity (Murphy-Royal et al., 2020). In this experiment, an acute stressor was sufficient to reduce gap junction coupling between astrocytes, leading to a decrease in energy substrate transport between astrocytes and subsequent impairment in LTP (Murphy-Royal et al., 2020), clearly demonstrating that an intact glia syncytium is necessary for synaptic plasticity.

OPTOGENETICS AND DREADDs: PHYSIOLOGICALLY RELEVANT FOR THE STUDY OF ASTROCYTES?

Understanding the physiology of astrocytes has been challenging partly because of a lack of technology sensitive enough to measure many of these properties. This has been compounded by the inability to directly target and manipulate select populations of astrocytes *in vivo*. In the past couple of decades, the advent of novel technologies has enabled specific cell populations, such as astrocytes, to be selectively targeted and manipulated, thus permitting more in-depth analysis of their function within the CNS. In particular, optogenetics and DREADDs have been frontrunners for targeting astrocytes.

With optogenetics, cells of interest are targeted with light-sensitive proteins, known as opsins, which generally exist as ion channels and pumps (Bang et al., 2016). The absorption of a specific wavelength by the opsin induces a conformational change, driving electrical changes across the plasma membrane (Bang et al., 2016). These cellular changes differ extensively depending on the type and variant of opsin used. Channelrhodopsin 2 (ChR2), for example, is a cation channel that is activated specifically by 473 nm (blue) light (Nagel et al., 2003), leading to an influx of cations (namely protons and Na^+) that produces membrane depolarization (Boyden et al., 2005). In astrocytes, the cation influx (particularly of Na^+) may be important for modulating neuron homeostasis and GABAergic transmission (Parpura and Verkhratsky, 2012). Na^+ signaling in astrocytes (particularly Na^+ influx mediated by voltage-dependent Na^+ channels) is thought to be necessary for the activity of the Na^+/K^+ ATPase pump (Verkhratsky et al., 2019), suggesting a role in the maintenance of ion homeostasis. Additionally, intracellular Na^+ is important in controlling GABA uptake *via* the GABA transporter (GAT) pathways; decreases in Na^+ can reverse GAT-dependent transport causing GABA to be released (Verkhratsky et al., 2019). However, ChR2 can also allow the influx of Ca^{2+}, which has been shown to cause the release of gliostransmitters like ATP (Gourine et al., 2010; Chen et al., 2013) and glutamate (Haydon and Carmignoto, 2006). ChR2 stimulation in astrocytes has been reliably shown to induce changes in intracellular Ca^{2+} (Li D. et al., 2012; Figueiredo et al., 2014; Perea et al., 2014; Mederos et al., 2019; Balachandar et al., 2020); these changes have been observed to enhance both excitatory and inhibitory synaptic transmission in the primary visual cortex (Perea et al., 2014). The use of ChR2 to activate astrocytes has also been shown to induce the release of ATP (Gourine et al., 2010; Figueiredo et al., 2014).

Halorhodopsin, on the other hand, is optimally activated by approximately 590 nm (yellow) light and drives hyperpolarization of cells through the influx of Cl^- ions (Bang et al., 2016). Cl^- has been shown to affect outward K^+ currents in cultured astrocytes (Bekar and Walz, 1999), showing that the ion has an important role in mediating astrocyte physiology. Intracellular Cl^- in astrocytes has also been theorized to play a role in mediating crosstalk between neurons and astrocytes because of its impact on several astrocytic transporters, including the excitatory amino acid transporters EAAT1 and EAAT 2 (GLAST and GLT-1 in rodents, respectively), GAT 1 and 3, and NKCC1 (Wilson and Mongin, 2019). Changes in astrocyte intracellular Cl^- levels are associated with EAAT activity and the movement of Cl^- across the membrane is necessary for GAT function (Wilson and Mongin, 2019). Given the apparent role of Cl^- signaling in astrocyte physiology, the manipulation of this ion may be important for deepening our understanding of Cl^- function within an astrocyte. Moving forward, the use of halorhodopsin in astrocytes will likely become an invaluable tool. As with neurons, the functional consequences of the use of different opsins will vary significantly in astrocytes.

Like halorhodopsin, archaerhodopsin (Arch) and archaerhodopsin-T (Arch-T) also respond to yellow or green light (around 532 nm) and drive hyperpolarization of a cell (El-Gaby et al., 2016). However, unlike halorhodopsin, Arch and Arch-T induce hyperpolarization through the efflux of protons (El-Gaby et al., 2016; Poskanzer and Yuste, 2016). This hyperpolarization is sufficient to induce changes in intracellular Ca^{2+} in astrocytes; work from Poskanzer and Yuste (2016) showed that Arch activation in cortical astrocytes evoked Ca^{2+} transients. These transients appeared primarily in the branches and lasted approximately the same length as those generated from spontaneous events in non-stimulated controls (Poskanzer and Yuste, 2016). However, a slight decrease in the amplitude of these Ca^{2+}transients was noted in the Arch-stimulated compared to the non-stimulated astrocytes (Poskanzer and Yuste, 2016), suggesting that optogenetic stimulation may recapitulate some, but not all, physiological properties of astrocytes. Which of these physiological properties are conserved may depend on

the type of opsin used, the region of interest, and the original physiological state of the astrocyte.

Melanopsin responds to shorter wavelengths of light and is optimally activated by light of about 420–450 nm (blue) light (Newman et al., 2003; Wang et al., 2019). It is slightly different from other opsins as it binds to a GPCR, leading to Ca^{2+} signaling *via* activation of the PLC/IP_3 pathway (Mederos et al., 2019). As such, it has been suggested as a good tool for investigating the physiological effects of astrocytes. One recent study transfected melanopsin into hippocampal astrocytes and found that stimulation resulted in robust IP_3-dependent Ca^{2+} signals in their fine processes and the release of ATP/adenosine at the synapse (Mederos et al., 2019).

Adaptations to these opsins (particularly ChR2) have been generated in recent years, including ChETA and step function opsins (SFO; Bang et al., 2016). In neurons, ChETA has been shown to induce ultrafast spiking and SFOs are known to produce prolonged, sub-threshold membrane depolarizations (Bang et al., 2016) but how these differences might translate to astrocyte activity is not well characterized.

Optogenetics provides precise spatial and temporal resolution for the manipulation of cells within the CNS. The high spatial resolution can be obtained *via* the viral (i.e., adeno-associated virus or lentivirus) transfection of the genetically engineered opsin to a targeted region of interest. Combined with a cell-type-specific promoter, a high degree of cell specificity is attainable. The ability to precisely modulate the frequency of light pulses delivered to these regions of interest allows extensive manipulation of these cells, and thus provides a high degree of temporal resolution that is not seen in many other technologies. Optogenetics has been particularly valuable for studying neuronal function throughout the CNS, and in more recent years, the technology is being applied to astrocytes. Since the effects of depolarization and hyperpolarization on astrocyte signaling are not as well understood as these effects in neurons, the relevance and generalizability of optogenetic approaches to manipulate and understand astrocytes remains to be fully elucidated.

The use of designer receptors exclusively activated by designer drugs (DREADDs) provides an alternative to target cells, particularly astrocytes. DREADDs represent one of the most commonly employed forms of chemogenetics, in which genetically engineered receptors selectively bind ligands to drive transient changes (usually activation or inactivation) in the region of interest (Roth, 2016; Smith et al., 2016). The genetically engineered GPCRs have little to no response to endogenous ligands but a strong response to synthetic ones that are otherwise biologically inert (Bang et al., 2016). When the ligand (or actuator) is introduced, it binds to and activates the receptor, activating the downstream Gq, Gi, or Gs pathways that are coupled with these receptors.

Activation of neuronal and non-neuronal cells is mediated through DREADDs targeting the Gq signaling pathway, of which the hM3Dq is most frequently used (Alexander et al., 2009; Roth, 2016). Inhibitory DREADDs, which silence neuronal activity, target the Gi pathway, the most common being the hM4Di receptor (Roth, 2016). Traditionally, clozapine-N-oxide (CNO) has been used as the chemical actuator for both hM3Dq and hM4Di (as well as several other DREADDs), but new evidence suggesting it can reverse-metabolize to its parent compound, clozapine (Manvich et al., 2018; Walker and Kullmann, 2020), and that it may have poor penetrance into the brain (Bonaventura et al., 2019) has led to the use of newer classes of chemical actuators including Compound 13, Compound 21, JHU37152, and JHU37160 (Bonaventura et al., 2019).

Like opsins, these receptors can be placed under the control of cell-specific promoters, restricting expression to a particular group of cells. The use of a fluorescent tag such as green fluorescent protein (GFP) allows for easy visualization of the cells expressing the opsin or DREADD of interest.

Since DREADDs use intracellular Ca^{2+} signaling to modulate cell activity, many have suggested they are particularly useful for studying astroglial activity given the integral role of Ca^{2+} signaling in astroglial function and communication; that is, the manipulation of astrocytes *via* the GPCR activation might be physiologically relevant. However, neither DREADDs nor optogenetics may be physiologically relevant for the study of astrocytes unless the unique physiological features of astrocytic subtypes are addressed in the experimental design.

Due to their low membrane resistance, astrocytes will likely elicit smaller current changes to optogenetic stimulation than neurons. As such, "stronger" or more "intense" stimulation may be needed to elicit a response in astrocytes. Fine-tuning of experimental guidelines is needed to determine what parameters would elicit a physiological response in astrocytes.

Another important consideration for the manipulation of $[Ca^{2+}]_i$ in astrocytes is that the mechanism which induces a rise in $[Ca^{2+}]_i$ can influence the speed of the change in these levels (Bazargani and Attwell, 2016). This suggests that the use of opsin variants (such as channelrhodopsin 2, ChR2, and its variant ChETA), which have similar, but differing mechanisms (ChETA has faster kinetics and in neurons has been proven to have more rapid repolarization than ChR2; Gunaydin et al., 2010), may induce changes in $[Ca^{2+}]_i$ at varying speeds, possibly contributing to alternative downstream effects. This is further compounded by the regional and subregional diversity of astrocyte physiology previously discussed in this review, rendering rigorous pilot studies essential prior to the use of DREADDs or optogenetics to target astrocytes (see **Figure 2**).

One study compared several ChR2 variants; all four variants evaluated were sufficient to induce large increases in $[Ca^{2+}]_i$ (Figueiredo et al., 2014). There were no significant differences in the overall $[Ca^{2+}]_i$ responses or in the dynamics of these responses between the ChR2 variants (Figueiredo et al., 2014). However, another study found the Ca^{2+}-translocating channelrhodopsin (CatCh) variant was more efficient than ChR2 in controlling Ca^{2+} elevations in astrocytes (Li D. et al., 2012). This implies that generalizing results from studies that employ different opsin variants may be difficult. Selecting the appropriate opsin variant to employ (i.e., to produce a particular/desired effect) will be further complicated by the diverse nature of astrocytic Ca^{2+} signaling.

Differences between opsin types rather than just opsin variants may also induce significantly different effects. A recent

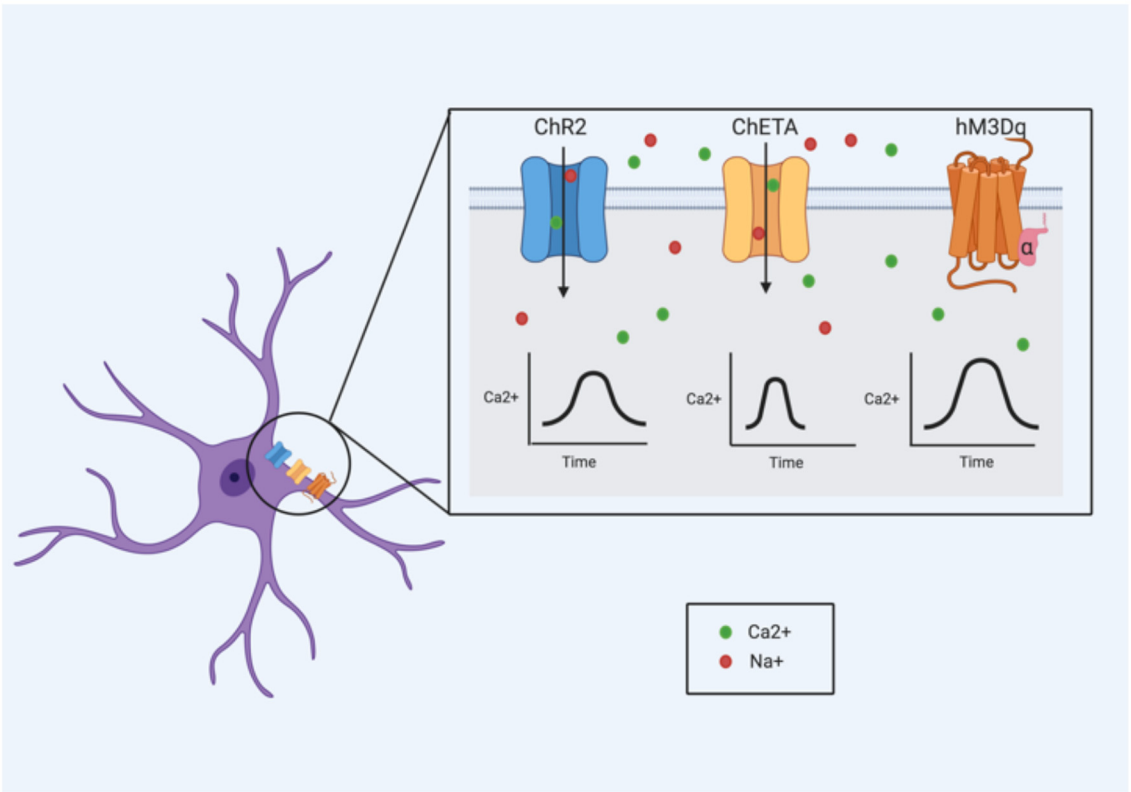

FIGURE 2 | Ca^{2+} signaling dynamics are influenced by the mechanism of Ca^{2+} induction. Therefore, opsin and designer receptors exclusively activated by designer drug (DREADD) variants that utilize alternative mechanisms to exert their effects may also show varying Ca^{2+} responses. These ion channel or receptor kinetics need to be considered when determining the best approach for targeting an astrocyte population.

study compared the effects of stimulating hippocampal astrocytes with ChR2 and melanopsin (Mederos et al., 2019). Although melanopsin was more efficient at inducing Ca^{2+} signals in both the soma and fine processes (referred to as microdomains in this study) of astrocytes, ChR2 stimulation elicited greater amplitude in miniature EPSCs of CA1 pyramidal neurons (Mederos et al., 2019). This effect on synaptic activity also persisted for longer following the ChR2 stimulation. However, these changes were only seen under certain stimulation parameters and not others (Mederos et al., 2019). Despite being "depolarizing" opsins, both melanopsin and ChR2 elicit different Ca^{2+} signals and ultimately, different downstream effects. This makes direct comparisons between studies that utilize different opsins difficult and also highlights how opsins may be physiologically relevant for some contexts, but not others. The effects that different opsins have on Ca^{2+} dynamics may be important for experimental design. Consideration of the effects that different opsins have on intracellular K^+ and Na^+ levels is also critical given their roles in numerous astrocyte functions.

In studies where the activity of select cell populations are directly targeted and modulated, it is essential to validate that the expression of the opsin or DREADD is restricted to that population only. Co-localization of the fluorescent tag with a cell-specific marker can confirm the specificity of this expression. Within astroglial cells, Ca^{2+} signals differ throughout their subcellular compartments, with potentially variable effects. Therefore, the precise subcellular localization of an opsin or DREADD receptor within an astrocyte may modulate the overall effect on that individual cell. Moving forward, it may be important to validate whether the subcellular expression does indeed alter functional outcomes, and what those functional outcomes might be. The physiological relevance of these technologies may therefore be better understood with the full knowledge of the cellular distribution of opsins and DREADD receptors in astrocytes.

Through gap junction proteins, astrocytes can create a network of interconnected cells. Several studies have demonstrated that calcium waves initiated in one astrocyte can propagate to others surrounding it (Verkhratsky, 2006). This phenomenon was first observed from *in vitro* culture work; these results were later confirmed in acute slices (Dani et al., 1992; Konietzko and Müller, 1994), and eventually with *in vivo* experiments (Kuga et al., 2011). Similar effects have been noted with Na^+ signals; several studies have demonstrated the ability of astrocytes to propagate these signals from one cell to another *via* these gap junctions (Rose and Ransom, 1997; Bernardinelli et al., 2004; Langer et al., 2012; Augustin et al., 2016; Moshrefi-Ravasdjani et al., 2017). What this means for studies in which

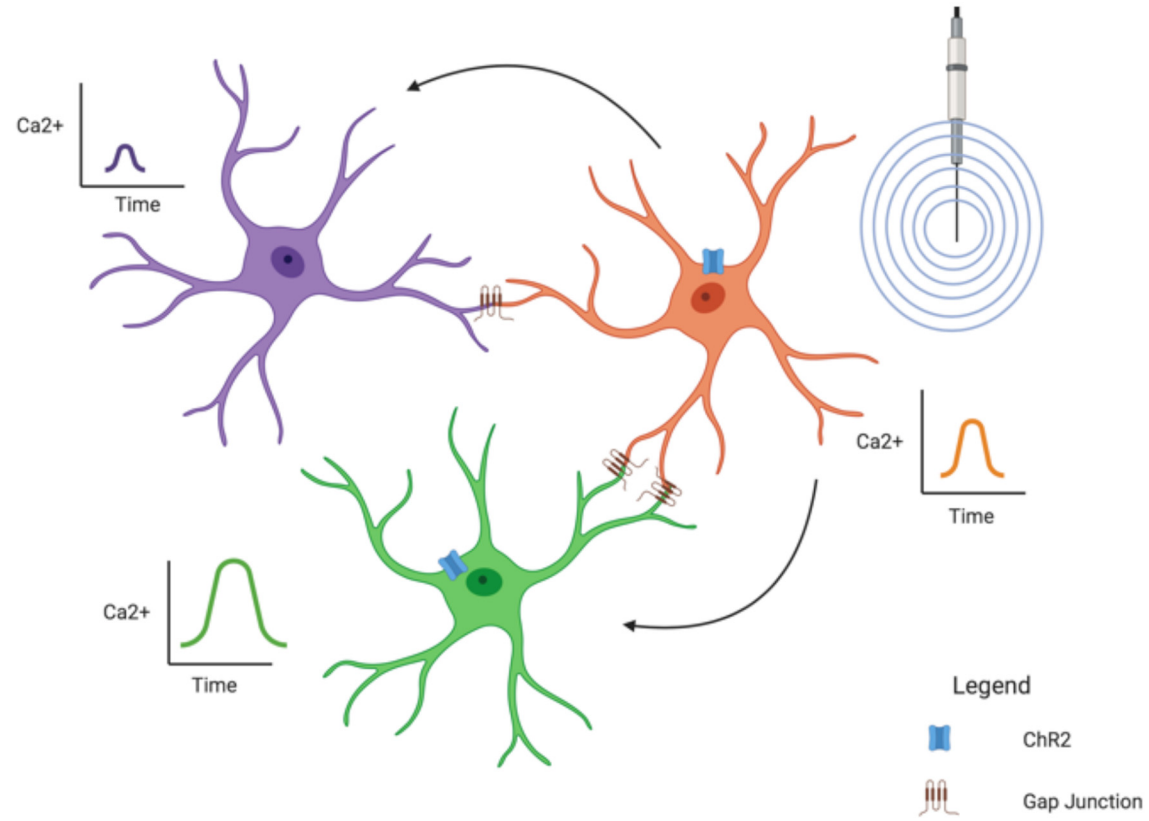

FIGURE 3 | The glial syncytium may impact the physiological effects of optogenetics and DREADD technologies (optogenetics illustrated above). The connection of astrocytes *via* gap junction proteins might produce a "double stimulation" or "spillover" effect. In the diagram above, only a portion of the astrocytes (orange and green) express the opsin of interest. The green astrocyte is first stimulated following the introduction of light into the system, and then again when a neighboring astrocyte (orange) is also stimulated, generating a larger than anticipated response. In the case of "spillover," astrocytes that do not express the opsin or DREADD in use nonetheless become "stimulated" from the activation of its neighboring astrocytes. In the image above, the purple astrocyte still exhibits a response following light stimulation despite the lack of ChR2 expression. The "stimulation" arises from the influence of the connected astrocyte (orange) that is stimulated *via* its ChR2 ion channels.

astroglial cells are manipulated remains to be seen. In most cases, it is unlikely that all astrocytes in a region of interest express the opsin or DREADD receptor. However, *via* the glial syncytium, it is possible that "activation" of one astrocyte leads to the activation of surrounding astrocytes. In one study, Ca^{2+} changes were restricted to only astrocytes expressing the opsin (Arch; Poskanzer and Yuste, 2016). However, only Ca^{2+} changes were measured, and it is possible that other ions/substrates were altered in coupled, Arch^{-} astrocytes. The potential of Ca^{2+} or other compounds to move from a stimulated astrocyte to its coupled neighbors needs to be studied under other parameters and with different opsin and DREADD variants. How far this effect could spread would likely depend on the extent of astroglial coupling within regions of interest. *In vivo* imaging of astrocytes during optogenetic stimulation or DREADD activation may help answer these questions.

Importantly, whether this stimulation of one astrocyte leads to the stimulation of other astrocytes will likely also depend on the integrity of the glial syncytium. The Murphy-Royal et al.'s (2020) study described in the previous section found acute stress was sufficient to reduce the amount of gap junction coupling between astrocytes. Therefore, the paradigm under which optogenetics is employed could significantly impact the extent to which the optogenetic stimulation of astrocytes "spreads" or influences astrocytes of the neighboring area. As such, optogenetic stimulation of astrocytes under normal, physiological conditions, when presumably the glial syncytium is intact, may have a greater impact than stimulation in a model of stress or injury where this may not be the case.

Another consideration is the potential of "double stimulation." An astroglial cell stimulated *via* optogenetics or DREADDs could, through gap junction coupling, stimulate a neighboring astrocyte. If this astrocyte is also stimulated *via* optogenetic or DREADD technology, this may result in a "double stimulation" effect, leading to a response much greater than physiological conditions. A stronger response could mean the stimulated astrocytes influence neighboring cells, in particular, neurons, in a manner incompatible with a normal physiological response. The strength of the glial syncytium in a given area may dictate the likelihood that this happens, further highlighting

the necessity of understanding the heterogeneous nature of astrocyte physiology and connectivity. As stress can influence the integrity of the glial syncytium (Murphy-Royal et al., 2020), this (potential) issue of "double stimulation" may be less of a concern in paradigms where the astrocytes are stimulated under conditions of stress or injury/disease. This demonstrates the importance of pilot studies to understand how optogenetics and DREADDs impact astoglial activity (see **Figure 3**).

In optogenetic and DREADD studies involving neurons, their heterogeneous nature is taken into consideration when designing experiments. The opsin variant or DREADD, for example, that is used to stimulate or inhibit a GABAergic neuron may differ from that of a glutamatergic or dopaminergic one. This same consideration needs to be taken for astrocytes. The literature shows that like neurons, astrocytes are a completely heterogenous population. They differ extensively in their morphology, electrophysiology, protein expression, and function. These subtypes are important to consider as each type may not respond in the same manner to different opsin and DREADD variants. Moving forward, understanding these subtypes will be crucial for informing experimental design. Greater knowledge of astrocyte electrophysiology will be an essential component for characterizing these astrocyte subtypes.

Similarly, in neurons, the use of an opsin or DREADD variant largely depends on the desired effect that researchers are looking to elicit. In neurons, these desired effects are typically the facilitation or inhibition of an action potential, driven by depolarization or hyperpolarization of the targeted cell. However, with astrocytes, a depolarization or hyperpolarization will not elicit these same effects. As such, understanding astrocyte physiology, and the heterogeneous nature of this physiology, will be critical for making knowledgeable and appropriate decisions regarding experimental design.

CONCLUSION

The research over the past few decades has demonstrated that astrocytes are a more "excitable" and heterogenous cell population than previously believed. They differ in morphology, function, and physiology, though the extent of physiological diversity has not been fully characterized. In this review, we discussed how astrocytes exhibit a wide range of basic electrophysiological properties under basal conditions. The mechanisms underlying homeostatic potassium regulation vary between and within brain regions, as do the specific variants of K^+ channels that mediate this K^+ buffering. Likewise, the Na^+ currents and Na^+ channel subtypes that mediate those currents are also heterogenous in astrocytes. Ca^{2+} signaling, a key component of astrocyte physiology is also highly variable. There are several different types of Ca^{2+} waves present in astrocytes, and these vary considerably amongst astrocytes across the CNS. Precisely how all these electrophysiological differences influence surrounding network activity is still unclear, but there is some evidence to indicate that they do. For example, asynchronous Ca^{2+} microdomains in astrocyte processes likely provides a synapse-specific influence of network activity. This heterogeneity is important to consider for optogenetic and DREADD technologies so that the limitations and generalization of each study can be fully assessed.

Astrocytes represent a very heterogenous cell population; we have highlighted some of the vast differences between the electrophysiological properties of these cells. Despite the available evidence, there is still a substantial amount of research needed in order to truly understand the extensive diversity of this unique cell population.

AUTHOR CONTRIBUTIONS

JM, MH, CR, and NS wrote the manuscript. JM and NS made the figures. All authors contributed to the article and approved the submitted version.

FUNDING

This work was supported by a Canadian Institute of Health Research Canada Research Chair to NS.

REFERENCES

Abney, E. R., Bartlett, P. P., and Raff, M. C. (1981). Astrocytes, ependymal cells, and oligodendrocytes develop on schedule in dissociated cell cultures of embryonic rat brain. *Dev. Biol.* 83, 301–310. doi: 10.1016/0012-1606(81)90476-0

Agarwal, A., Wu, P.-H., Hughes, E. G., Fukaya, M., Tischfield, M. A., Langseth, A. J., et al. (2017). Transient opening of the mitochondrial permeability transition pore induces microdomain calcium transients in astrocyte processes. *Neuron* 93, 587.e7–605.e7. doi: 10.1016/j.neuron.2016.12.034

Aguado, F., Espinosa-Parrilla, J. F., Carmona, M. A., and Soriano, E. (2002). Neuronal activity regulates correlated network properties of spontaneous calcium transients in astrocytes in situ. *J. Neurosci.* 22, 9430–9444. doi: 10.1523/JNEUROSCI.22-21-09430.2002

Agulhon, C., Petravicz, J., McMullen, A. B., Sweger, E. J., Minton, S. K., Taves, S. R., et al. (2008). What is the role of astrocyte calcium in neurophysiology? *Neuron* 59, 932–946. doi: 10.1016/j.neuron.2008.09.004

Alexander, G. M., Rogan, S. C., Abbas, A. I., Armbruster, B. N., Pei, Y., Allen, J. A., et al. (2009). Remote control of neuronal activity in transgenic mice expressing evolved G protein-coupled receptors. *Neuron* 63, 27–39. doi: 10.1016/j.neuron.2009.06.014

Allen, N. J., and Eroglu, C. (2017). Cell biology of astrocyte-synapse interactions. *Neuron* 96, 697–708. doi: 10.1016/j.neuron.2017.09.056

Anderson, S., Brismar, T., and Hansson, E. (1995). Effect of external K^+, Ca^{2+} and Ba^{2+} on membrane potential and ionic conductance in rat astrocytes. *Cell Mol. Neurobiol.* 15, 439–450. doi: 10.1007/BF02071879

Annunziato, L., Boscia, F., and Pignataro, G. (2013). Ionic transporter activity in astrocytes, microglia, and oligodendrocytes during brain ischemia. *J. Cereb. Blood Flow Metab.* 33, 969–982. doi: 10.1038/jcbfm.2013.44

Araque, A., Carmignoto, G., Haydon, P. G., Oliet, S. H. R., Robitaille, R., and Volterra, A. (2014). Gliotransmitters travel in space and time. *Neuorn* 81, 728–739. doi: 10.1016/j.neuron.2014.02.007

Asada, A., Ujita, S., Nakayama, R., Oba, S., Ishii, S., Matsuki, N., et al. (2015). Subtle modulation of ongoing calcium dynamics in astrocytic microdomains by sensory inputs. *Physiol. Rep.* 3:e12454. doi: 10.14814/phy2.12454

Augustin, V., Bold, C., Wadle, S. L., Langer, J., Jabs, R., Philippot, C., et al. (2016). Functional anisotropic panglial networks in the lateral superior olive. *Glia* 64, 1892–1911. doi: 10.1002/glia.23031

Balachandar, L., Montejo, K. A., Castano, E., Perez, M., Moncion, C., Chambers, J. W., et al. (2020). Simultaneous Ca^{2+} imaging and optogenetic stimulation of cortical astrocytes in adult murine brain slices. *Curr. Protoc. Neurosci.* 94:e110. doi: 10.1002/cpns.110

Bang, J., Kim, H. Y., and Lee, H. (2016). Optogenetic and chemogenetic approaches for studying astrocytes and gliotransmitters. *Exp. Neurobiol.* 25, 205–221. doi: 10.5607/en.2016.25.5.205

Bayraktar, O. A., Bartels, T., Holmqvist, S., Kleshchevnikov, V., Martirosyan, A., Polioudakis, D., et al. (2020). Astrocyte layers in the mammalian cerebral cortex revealed by a single-cell in situ transcriptomic map. *Nat. Neurosci.* 23, 500–509. doi: 10.1038/s41593-020-0602-1

Bazargani, N., and Attwell, D. (2016). Astrocyte calcium signaling: the third wave. *Nat. Neurosci.* 19, 182–189. doi: 10.1038/nn.4201

Bedner, P., Dupper, A., Hüttmann, K., Müller, J., Herde, M. K., Dublin, P., et al. (2015). Astrocyte uncoupling as a cause of human temporal lobe epilepsy. *Brain* 138, 1208–1222. doi: 10.1093/brain/awv067

Bedner, P., Jabs, R., and Steinhäuser, C. (2020). Properties of human astrocytes and NG2 glia. *Glia* 68, 756–767. doi: 10.1002/glia.23725

Bekar, L. K., Loewen, M. E., Cao, K., Sun, X., Leis, J., Wang, R., et al. (2005). Complex expression and localization of inactivating Kv channels in cultured hippocampal astrocytes. *J. Neurophysiol.* 93, 1699–1709. doi: 10.1152/jn.00850.2004

Bekar, L. K., and Walz, W. (1999). Evidence for chloride ions as intracellular messenger substances in astrocytes. *J. Neurophysiol.* 82, 248–254. doi: 10.1152/jn.1999.82.1.248

Bellot-Saez, A., Kékesi, O., Morley, J. W., and Buskila, Y. (2017). Astrocytic modulation of neuronal excitability through K^+ spatial buffering. *Neurosci. Biobehav. Rev.* 77, 87–97. doi: 10.1016/j.neubiorev.2017.03.002

Benesova, J., Rusnakova, V., Honsa, P., Pivonkova, H., Dzamba, D., Kubista, M., et al. (2012). Distinct expression/function of potassium and chloride channels contributes to the diverse volume regulation in cortical astrocytes of GFAP/EGFP mice. *PLoS One* 7:e29725. doi: 10.1371/journal.pone.0029725

Bernardinelli, Y., Magistretti, P. J., and Chatton, J.-Y. (2004). Astrocytes generate Na^+-mediated metabolic waves. *Proc. Natl. Acad. Sci. U S A* 101, 14937–14942. doi: 10.1073/pnas.0405315101

Bindocci, E., Savtchouk, I., Liaudet, N., Becker, D., Carriero, G., and Volterra, A. (2017). Three-dimensional Ca^{2+} imaging advances understanding of astrocyte biology. *Science* 356:eaai8185. doi: 10.1126/science.aai8185

Black, J. A., and Waxman, S. G. (2013). Noncanonical roles of voltage-gated sodium channels. *Neuron* 80, 280–291. doi: 10.1016/j.neuron.2013.09.012

Black, J. A., Westenbroek, R., Minturn, J. E., Ransom, B. R., Catterall, W. A., and Waxman, S. G. (1995). Isoform-specific expression of sodium channels in astrocytes *in vitro*: immunocytochemical observations. *Glia* 14, 133–144. doi: 10.1002/glia.440140208

Bolton, S., Greenwood, K., Hamilton, N., and Butt, A. M. (2006). Regulation of the astrocyte resting membrane potential by cyclic AMP and protein kinase A. *Glia* 54, 316–328. doi: 10.1002/glia.20384

Bonaventura, J., Eldridge, M. A. G., Hu, F., Gomez, J. L., Sanchez-Soto, M., Abramyan, A. M., et al. (2019). High-potency ligands for DREADD imaging and activation in rodents and monkeys. *Nat. Commun.* 10:4627. doi: 10.1038/s41467-019-12236-z

Bordey, A., Lyons, S. A., Hablitz, J. J., and Sontheimer, H. (2001). Electrophysiological characteristics of reactive astrocytes in experimental cortical dysplasia. *J. Neurophysiol.* 85, 1719–1731. doi: 10.1152/jn.2001.85.4.1719

Bordey, A., and Sontheimer, H. (1998). Electrophysiological properties of human astrocytic tumor cells in situ: enigma of spiking glial cells. *J. Neurophysiol.* 79, 2782–2793. doi: 10.1152/jn.1998.79.5.2782

Bordey, A., and Sontheimer, H. (2000). Ion channel expression by astrocytes in situ: comparison of different CNS regions. *Glia* 30, 27–38. doi: 10.1002/(sici)1098-1136(200003)30:1<27::aid-glia4>3.0.co;2-#

Boyden, E. S., Zhang, F., Bamberg, E., Nagel, G., and Deisseroth, K. (2005). Millisecond-timescale, genetically targeted optical control of neural activity. *Nat. Neurosci.* 8, 1263–1268. doi: 10.1038/nn1525

Brasko, C., Hawkins, V., De La Rocha, I. C., and Butt, A. M. (2017). Expression of Kir4.1 and Kir5.1 inwardly rectifying potassium channels in oligodendrocytes, the myelinating cells of the CNS. *Brain Struct. Funct.* 222, 41–59. doi: 10.1007/s00429-016-1199-8

Brockhaus, J., and Deitmer, J. W. (2002). Long-lasting modulation of synaptic input to Purkinje neurons by Bergmann glia stimulation in rat brain slices. *J. Physiol.* 545, 581–593. doi: 10.1113/jphysiol.2002.028423

Bushong, E. A., Martone, M. E., and Ellisman, M. H. (2004). Maturation of astrocyte morphology and the establishment of astrocyte domains during postnatal hippocampal development. *Int. J. Dev. Neurosci.* 22, 73–86. doi: 10.1016/j.ijdevneu.2003.12.008

Butt, A. M., and Jennings, J. (1994). Response of astrocytes to γ-aminobutyric acid in the neonatal rat optic nerve. *Neurosci. Lett.* 168, 53–56. doi: 10.1016/0304-3940(94)90414-6

Cahoy, J. D., Emery, B., Kaushal, A., Foo, L. C., Zamanian, J. L., Christopherson, K. S., et al. (2008). A transcriptome database for astrocytes, neurons, and oligodendrocytes: a new resource for understanding brain development and function. *J. Neurosci.* 28, 264–278. doi: 10.1523/JNEUROSCI.4178-07.2008

Chai, H., Diaz-castro, B., Shigetomi, E., Monte, E., Octeau, J. C., Yu, X., et al. (2017). Neural circuit-specialized astrocytes: transcriptomic, proteomic, morphological, and functional evidence. *Neuron* 95, 531–549. doi: 10.1016/j.neuron.2017.06.029

Chen, J., Tan, Z., Zeng, L. I., Zhang, X., He, Y., Gao, W., et al. (2013). Heterosynaptic long-term depression mediated by ATP released from astrocytes. *Glia* 61, 178–191. doi: 10.1002/glia.22425

Cotrina, M. L., Lin, J. H., López-García, J. C., Naus, C. C., and Nedergaard, M. (2000). ATP-mediated glia signaling. *J. Neurosci.* 20, 2835–2844. doi: 10.1523/JNEUROSCI.20-08-02835.2000

Dallérac, G., Chever, O., and Rouach, N. (2013). How do astrocytes shape synaptic transmission? Insights from electrophysiology. *Front. Cell. Neurosci.* 7:159. doi: 10.3389/fncel.2013.00159

Dani, J. W., Chernjavsky, A., and Smith, S. J. (1992). Neuronal activity triggers calcium waves in hippocampal astrocyte networks. *Neuron* 8, 429–440. doi: 10.1016/0896-6273(92)90271-e

de Lanerolle, N., and Lee, T.-S. (2005). New facets of the neuropathology and molecular profile of human temporal lobe epilepsy. *Epilepsy Behav.* 7, 190–203. doi: 10.1016/j.yebeh.2005.06.003

Deemyad, T., Lüthi, J., and Spruston, N. (2018). Astrocytes integrate and drive action potential firing in inhibitory subnetworks. *Nat. Commun.* 9:4336. doi: 10.1038/s41467-018-06338-3

Dossi, E., Vasile, F., and Rouach, N. (2018). Human astrocytes in the diseased brain. *Brain Res. Bull.* 136, 139–156. doi: 10.1016/j.brainresbull.2017.02.001

Du, Y., Kiyoshi, C. M., Wang, Q., Wang, W., Ma, B., Alford, C. C., et al. (2016). Genetic deletion of TREK-1 or TWIK-1/TREK-1 potassium channels does not alter the basic electrophysiological properties of mature hippocampal astrocytes in situ. *Front. Cell. Neurosci.* 10:13. doi: 10.3389/fncel.2016.00013

Du, Y., Ma, B., Kiyoshi, C. M., Alford, C. C., Wang, W., and Zhou, M. (2015). Freshly dissociated mature hippocampal astrocytes exhibit passive membrane conductance and low membrane resistance similarly to syncytial coupled astrocytes. *J. Neurophysiol.* 113, 3744–3750. doi: 10.1152/jn.00206.2015

El-Gaby, M., Zhang, Y., Wolf, K., Schwiening, C. J., Paulsen, O., and Shipton, O. A. (2016). Archaerhodopsin selectively and reversibly silences synaptic transmission through altered pH. *Cell Rep.* 16:2259. doi: 10.1016/j.celrep.2016.07.057

Fernandez, F. R., Noueihed, J., and White, J. A. (2019). Voltage-dependent membrane properties shape the size but not the frequency content of spontaneous voltage fluctuations in layer 2/3 somatosensory cortex. *J. Neurosci.* 39, 2221–2237. doi: 10.1523/JNEUROSCI.1648-18.2019

Figueiredo, M., Lane, S., Stout, R. F., Liu, B., Parpura, V., Teschemacher, A. G., et al. (2014). Comparative analysis of optogenetic actuators in cultured astrocytes. *Cell Calcium* 56, 208–214. doi: 10.1016/j.ceca.2014.07.007

Freeman, M. R. (2010). Specification and morphogenesis of astrocytes. *Science* 330, 774–778. doi: 10.1126/science.1190928

Gnatenco, C., Han, J., Snyder, A. K., and Kim, D. (2002). Functional expression of TREK-2 K^+ channel in cultured rat brain astrocytes. *Brain Res.* 931, 56–67. doi: 10.1016/s0006-8993(02)02261-8

Gourine, A. V., Kasymov, V., Marina, N., Tang, F., Figueiredo, M. F., Lane, S., et al. (2010). Astrocytes control breathing through pH-dependent release of ATP. *Science* 329, 571–575. doi: 10.1126/science.1190721

Guatteo, E., Stanness, K. A., and Janigro, D. (1996). Hyperpolarization-activated ion currents in cultured rat cortical and spinal cord astrocytes. *Glia* 16, 196–209. doi: 10.1002/(SICI)1098-1136(199603)16:3<196::AID-GLIA2>3.0.CO;2-0

Gunaydin, L. A., Yizhar, O., Berndt, A., Sohal, V. S., Deisseroth, K., and Hegemann, P. (2010). Ultrafast optogenetic control. *Nat. Neurosci.* 13, 387–392. doi: 10.1038/nn.2495

Hashioka, S., Wang, Y. F., Little, J. P., Choi, H. B., Klegeris, A., McGeer, P. L., et al. (2014). Purinergic responses of calcium-dependent signaling pathways in cultured adult human astrocytes. *BMC Neurosci.* 15:18. doi: 10.1186/1471-2202-15-18

Haustein, M. D., Kracun, S., Lu, X.-H., Shih, T., Jackson-Weaver, O., Tong, X., et al. (2014). Conditions and constraints for astrocyte calcium signaling in the hippocampal mossy fiber pathway. *Neuron* 82, 413–429. doi: 10.1016/j.neuron.2014.02.041

Haydon, P. G., and Carmignoto, G. (2006). Astrocyte control of synaptic transmission and neurovascular coupling. *Physiol. Rev.* 86, 1009–1031. doi: 10.1152/physrev.00049.2005

Henneberger, C., Papouin, T., Oliet, S. H. R., and Rusakov, D. A. (2010). Long-term potentiation depends on release of D-serine from astrocytes. *Nature* 463, 232–236. doi: 10.1038/nature08673

Hertz, L., and Chen, Y. (2016). Importance of astrocytes for potassium ion (K^+) homeostasis in brain and glial effects of K^+ and its transporters on learning. *Neurosci. Biobehav. Rev.* 71, 484–505. doi: 10.1016/j.neubiorev.2016.09.018

Hibino, H., Fujita, A., Iwai, K., Yamada, M., and Kurachi, Y. (2004). Differential assembly of inwardly rectifying K^+ channel subunits, Kir4.1 and Kir5.1, in brain astrocytes. *J. Biol. Chem.* 279, 44065–44073. doi: 10.1074/jbc.M405985200

Higashi, K., Fujita, A., Inanobe, A., Tanemoto, M., Doi, K., Kubo, T., et al. (2001). An inwardly rectifying K^+ channel, Kir4.1, expressed in astrocytes surrounds synapses and blood vessels in brain. *Am. J. Physiol. Cell Physiol.* 281, C922–C931. doi: 10.1152/ajpcell.2001.281.3.C922

Hinterkeuser, S., Schröder, W., Hager, G., Seifert, G., Blümcke, I., Elger, C. E., et al. (2000). Astrocytes in the hippocampus of patients with temporal lobe epilepsy display changes in potassium conductances. *Eur. J. Neurosci.* 12, 2087–2096. doi: 10.1046/j.1460-9568.2000.00104.x

Holtzclaw, L. A., Pandhit, S., Bare, D. J., Mignery, G. A., and Russell, J. T. (2002). Astrocytes in adult rat brain express type 2 inositol 1,4,5-trisphosphate receptors. *Glia* 39, 69–84. doi: 10.1002/glia.10085

Isokawa, M., and McKhann, G. M. (2005). Electrophysiological and morphological characterization of dentate astrocytes in the hippocampus. *J. Neurobiol.* 65, 125–134. doi: 10.1002/neu.20186

Jiang, R., Diaz-Castro, B., Looger, L. L., and Khakh, B. S. (2016). Dysfunctional calcium and glutamate signaling in striatal astrocytes from Huntington's disease model mice. *J. Neurosci.* 36, 3453–3470. doi: 10.1523/JNEUROSCI.3693-15.2016

Jiang, R., Haustein, M. D., Sofroniew, M. V., and Khakh, B. S. (2014). Imaging intracellular Ca^{2+} signals in striatal astrocytes from adult mice using genetically-encoded calcium indicators. *J. Vis. Exp.* 93:e51972. doi: 10.3791/51972

Kalsi, A. S., Greenwood, K., Wilkin, G., and Butt, A. M. (2004). Kir4.1 expression by astrocytes and oligodendrocytes in CNS white matter: a developmental study in the rat optic nerve. *J. Anat.* 204, 475–485. doi: 10.1111/j.0021-8782.2004.00288.x

Kanemaru, K., Sekiya, H., Xu, M., Satoh, K., Kitajima, N., Yoshida, K., et al. (2014). *in vivo* visualization of subtle, transient, and local activity of astrocytes using an ultrasensitive Ca^{2+} indicator. *Cell Rep.* 8, 311–318. doi: 10.1016/j.celrep.2014.05.056

Kang, J., Jiang, L., Goldman, S. A., and Nedergaard, M. (1998). Astrocyte-mediated potentiation of inhibitory synaptic transmission. *Nat. Neurosci.* 1, 683–692. doi: 10.1038/3684

Kofuji, P., Biedermann, B., Siddharthan, V., Raap, M., Iandiev, I., Milenkovic, I., et al. (2002). Kir potassium channel subunit expression in retinal glial cells: implications for spatial potassium buffering. *Glia* 39, 292–303. doi: 10.1002/glia.10112

Khakh, B. S., and Deneen, B. (2019). The emerging nature of astrocyte diversity. *Annu. Rev. Neurosci.* 42, 187–207. doi: 10.1146/annurev-neuro-070918-050443

Kofuji, P., and Newman, E. A. (2004). Potassium buffering in the central nervous system. *Neuroscience* 129, 1045–1056. doi: 10.1016/j.neuroscience.2004.06.008

Konietzko, U., and Müller, C. M. (1994). Astrocytic dye coupling in rat hippocampus: topography, developmental onset, and modulation by protein kinase C. *Hippocampus* 4, 297–306. doi: 10.1002/hipo.450040313

Kressin, K., Kuprijanova, E., Jabs, R., Seifert, G., and Steinhäuser, C. (1995). Developmental regulation of Na^+ and K^+ conductances in glial cells of mouse hippocampal brain slices. *Glia* 15, 173–187. doi: 10.1002/glia.440150210

Kuga, N., Sasaki, T., Takahara, Y., Matsuki, N., and Ikegaya, Y. (2011). Large-scale calcium waves traveling through astrocytic networks *in vivo*. *J. Neurosci.* 31, 2607–2614. doi: 10.1523/JNEUROSCI.5319-10.2011

Langer, J., and Rose, C. R. (2009). Synaptically induced sodium signals in hippocampal astrocytes in situ. *J. Physiol.* 587, 5859–5877. doi: 10.1113/jphysiol.2009.182279

Langer, J., Stephan, J., Theis, M., and Rose, C. R. (2012). Gap junctions mediate intercellular spread of sodium between hippocampal astrocytes in situ. *Glia* 60, 239–252. doi: 10.1002/glia.21259

Lanjakornsiripan, D., Pior, B. J., Kawaguchi, D., Furutachi, S., Tahara, T., Katsuyama, Y., et al. (2018). Layer-specific morphological and molecular differences in neocortical astrocytes and their dependence on neuronal layers. *Nat. Commun.* 9:1623. doi: 10.1038/s41467-018-03940-3

Li, D., Hérault, K., Isacoff, E. Y., Oheim, M., and Ropert, N. (2012). Optogenetic activation of LiGluR-expressing astrocytes evokes anion channel-mediated glutamate release. *J. Physiol.* 590, 855–873. doi: 10.1113/jphysiol.2011.219345

Li, Y.-K., Wang, F., Wang, W., Luo, Y., Wu, P.-F., Xiao, J.-L., et al. (2012). Aquaporin-4 deficiency impairs synaptic plasticity and associative fear memory in the lateral amygdala: involvement of downregulation of glutamate transporter-1 expression. *Neuropsychopharmacology* 37, 1867–1878. doi: 10.1038/npp.2012.34

Liddelow, S. A., Guttenplan, K. A., Clarke, L. E., Bennett, F. C., Bohlen, C. J., Schirmer, L., et al. (2017). Neurotoxic reactive astrocytes are induced by activated microglia. *Nature* 541, 481–487. doi: 10.1038/nature21029

Liedtke, W., Edelmann, W., Bieri, P. L., Chiu, F. C., Cowan, N. J., Kucherlapati, R., et al. (1996). GFAP is necessary for the integrity of CNS white matter architecture and long-term maintenance of myelination. *Neuron* 17, 607–615. doi: 10.1016/s0896-6273(00)80194-4

Ma, B., Xu, G., Wang, W., Enyeart, J. J., and Zhou, M. (2014). Dual patch voltage clamp study of low membrane resistance astrocytes in situ. *Mol. Brain* 7:18. doi: 10.1186/1756-6606-7-18

Mahmoud, S., Gharagozloo, M., Simard, C., and Gris, D. (2019). Astrocytes maintain glutamate homeostasis in the CNS by controlling the balance between glutamate uptake and release. *Cells* 8:184. doi: 10.3390/cells8020184

Manvich, D. F., Webster, K. A., Foster, S. L., Farrell, M. S., Ritchie, J. C., Porter, J. H., et al. (2018). The DREADD agonist clozapine N-oxide (CNO) is reverse-metabolized to clozapine and produces clozapine-like interoceptive stimulus effects in rats and mice. *Sci. Rep.* 8:3840. doi: 10.1038/s41598-018-22116-z

Mederos, S., Hernández-Vivanco, A., Ramírez-Franco, J., Martín-Fernández, M., Navarrete, M., Yang, A., et al. (2019). Melanopsin for precise optogenetic activation of astrocyte-neuron networks. *Glia* 67, 915–934. doi: 10.1002/glia.23580

Mi Hwang, E., Kim, E., Yarishkin, O., Ho Woo, D., Han, K.-S., Park, N., et al. (2014). A disulphide-linked heterodimer of TWIK-1 and TREK-1 mediates passive conductance in astrocytes. *Nat. Commun.* 5:3227. doi: 10.1038/ncomms4227

Miller, S. J. (2018). Astrocyte heterogeneity in the adult central nervous system. *Front. Cell. Neurosci.* 12:401. doi: 10.3389/fncel.2018.00401

Mishima, T., and Hirase, H. (2010). *in vivo* intracellular recording suggests that gray matter astrocytes in mature cerebral cortex and hippocampus are electrophysiologically homogeneous. *J. Neurosci.* 30, 3093–3100. doi: 10.1523/JNEUROSCI.5065-09.2010

Moore, Y. E., Conway, L. C., Wobst, H. J., Brandon, N. J., Deeb, T. Z., and Moss, S. J. (2019). Developmental regulation of KCC2 phosphorylation

has long-term impacts on cognitive function. *Front. Mol. Neurosci.* 12:173. doi: 10.3389/fnmol.2019.00173

Moshrefi-Ravasdjani, B., Hammel, E. L., Kafitz, K. W., and Rose, C. R. (2017). Astrocyte sodium signalling and panglial spread of sodium signals in brain white matter. *Neurochem. Res.* 42, 2505–2518. doi: 10.1007/s11064-017-2197-9

Murphy-Royal, C., Johnston, A. D., Boyce, A. K. J., Diaz-Castro, B., Institoris, A., Peringod, G., et al. (2020). Stress gates an astrocytic energy reservoir to impair synaptic plasticity. *Nat. Commun.* 11:2014. doi: 10.1038/s41467-020-15778-9

Nagel, G., Szellas, T., Huhn, W., Kateriya, S., Adeishvili, N., Berthold, P., et al. (2003). Channelrhodopsin-2, a directly light-gated cation-selective membrane channel. *Proc. Natl. Acad. Sci. U S A* 100, 13940–13945. doi: 10.1073/pnas.1936192100

Navarrete, M., Perea, G., Fernandez de Sevilla, D., Gómez-Gonzalo, M., Núñez, A., Martín, E. D., et al. (2012). Astrocytes mediate *in vivo* cholinergic-induced synaptic plasticity. *PLoS Biol.* 10:e1001259. doi: 10.1371/journal.pbio.1001259

Navarrete, M., Perea, G., Maglio, L., Pastor, J., Garcia de Sola, R., and Araque, A. (2013). Astrocyte calcium signal and gliotransmission in human brain tissue. *Cereb. Cortex* 23, 1240–1246. doi: 10.1093/cercor/bhs122

Neprasova, H., Anderova, M., Petrik, D., Vargova, L., Kubinova, S., Chvatal, A., et al. (2007). High extracellular K^+ evokes changes in voltage-dependent K^+ and Na^+ currents and volume regulation in astrocytes. *Pflugers Arch.* 453, 839–849. doi: 10.1007/s00424-006-0151-9

Nett, W. J., Oloff, S. H., and McCarthy, K. D. (2002). Hippocampal astrocytes in situ exhibit calcium oscillations that occur independent of neuronal activity. *J. Neurophysiol.* 87, 528–537. doi: 10.1152/jn.00268.2001

Newman, L. A., Walker, M. T., Brown, R. L., Cronin, T. W., and Robinson, P. R. (2003). Melanopsin forms a functional short-wavelength photopigment. *Biochemistry* 42, 12734–12738. doi: 10.1021/bi035418z

O'Connor, E. R., Sontheimer, H., Spencer, D. D., and De Lanerolle, N. C. (1998). Astrocytes from exhibit human hippocampal epileptogenic foci action potential-like responses. *Epilepsia* 39, 347–354. doi: 10.1093/cid/ciab196

Oberheim, N. A., Takano, T., Han, X., He, W., Lin, J. H. C., Wang, F., et al. (2009). Uniquely hominid features of adult human astrocytes. *J. Neurosci.* 29, 3276–3287. doi: 10.1523/JNEUROSCI.4707-08.2009

Oberheim, N. A., Wang, X., Goldman, S., and Nedergaard, M. (2006). Astrocytic complexity distinguishes the human brain. *Trends Neurosci.* 29, 547–553. doi: 10.1016/j.tins.2006.08.004

Olsen, M. L., Higashimori, H., Campbell, S. L., Hablitz, J. J., and Sontheimer, H. (2006). Functional expression of Kir4.1 channels in spinal cord astrocytes. *Glia* 53, 516–528. doi: 10.1002/glia.20312

Orkand, R. K., Nicholls, J. G., and Kuffler, S. W. (1966). Effect of nerve impulses on the membrane potential of glial cells in the central nervous system of amphibia. *J. Neurophysiol.* 29, 788–806. doi: 10.1152/jn.1966.29.4.788

Otsu, Y., Couchman, K., Lyons, D. G., Collot, M., Agarwal, A., Mallet, J.-M., et al. (2015). Calcium dynamics in astrocyte processes during neurovascular coupling. *Nat. Neurosci.* 18, 210–218. doi: 10.1038/nn.3906

Paco, S., Hummel, M., Plá, V., Sumoy, L., and Aguado, F. (2016). Cyclic AMP signaling restricts activation and promotes maturation and antioxidant defenses in astrocytes. *BMC Genomics* 17:304. doi: 10.1186/s12864-016-2623-4

Pappalardo, L. W., Black, J. A., and Waxman, S. G. (2016). Sodium channels in astroglia and microglia. *Glia* 64, 1628–1645. doi: 10.1002/glia.22967

Pappalardo, L. W., Samad, O. A., Black, J. A., and Waxman, S. G. (2014). Voltage-gated sodium channel Nav 1.5 contributes to astrogliosis in an *in vitro* model of glial injury *via* reverse Na^+/Ca^{2+} exchange. *Glia* 62, 1162–1175. doi: 10.1002/glia.22671

Pappalardo, L. W., Samad, O. A., Liu, S., Zwinger, P. J., Black, J. A., and Waxman, S. G. (2018). Nav1.5 in astrocytes plays a sex-specific role in clinical outcomes in a mouse model of multiple sclerosis. *Glia* 66, 2174–2187. doi: 10.1002/glia.23470

Parpura, V., Basarsky, T. A., Liu, F., Jeftinija, K., Jeftinija, S., and Haydon, P. G. (1994). Glutamate-mediated astrocyte-neuron signalling. *Nature* 369, 744–747. doi: 10.1038/369744a0

Parpura, V., Grubišić, V., and Verkhratsky, A. (2011). Ca^{2+} sources for the exocytotic release of glutamate from astrocytes. *Biochim. Biophys. Acta* 1813, 984–991. doi: 10.1016/j.bbamcr.2010.11.006

Parpura, V., and Verkhratsky, A. (2012). Homeostatic function of astrocytes: Ca^{2+} and Na^+ signalling. *Transl. Neurosci.* 3, 334–344. doi: 10.2478/s13380-012-0040-y

Parri, H. R., Gould, T. M., and Crunelli, V. (2001). Spontaneous astrocytic Ca^{2+} oscillations in situ drive NMDAR-mediated neuronal excitation. *Nat. Neurosci.* 4, 803–812. doi: 10.1038/90507

Pasti, L., Volterra, A., Pozzan, T., and Carmignoto, G. (1997). Intracellular calcium oscillations in astrocytes: a highly plastic, bidirectional form of communication between neurons and astrocytes in situ. *J. Neurosci.* 17, 7817–7830. doi: 10.1523/JNEUROSCI.17-20-07817.1997

Perea, G., Yang, A., Boyden, E. S., and Sur, M. (2014). Optogenetic astrocyte activation modulates response selectivity of visual cortex neurons *in vivo*. *Nat. Commun.* 5:3262. doi: 10.1038/ncomms4262

Perez, E. J., Tapanes, S. A., Loris, Z. B., Balu, D. T., Sick, T. J., Coyle, J. T., et al. (2017). Enhanced astrocytic d-serine underlies synaptic damage after traumatic brain injury. *J. Clin. Invest.* 127, 3114–3125. doi: 10.1172/JCI92300

Petravicz, J., Fiacco, T. A., and McCarthy, K. D. (2008). Loss of IP3 receptor-dependent Ca^{2+} increases in hippocampal astrocytes does not affect baseline CA1 pyramidal neuron synaptic activity. *J. Neurosci.* 28, 4967–4973. doi: 10.1523/JNEUROSCI.5572-07.2008

Poopalasundaram, S., Knott, C., Shamotienko, O. G., Foran, P. G., Dolly, J. O., Ghiani, C. A., et al. (2000). Glial heterogeneity in expression of the inwardly rectifying K^+ channel, Kir4.1, in adult rat CNS. *Glia* 30, 362–372. doi: 10.1002/(sici)1098-1136(200006)30:4<362::aid-glia50>3.0.co;2-4

Porter, J. T., and McCarthy, K. D. (1995). GFAP-positive hippocampal astrocytes in situ respond to glutamatergic neuroligands with increases in $[Ca^{2+}]i$. *Glia* 13, 101–112. doi: 10.1002/glia.440130204

Poskanzer, K. E., and Yuste, R. (2016). Astrocytes regulate cortical state switching *in vivo*. *Proc. Natl. Acad. Sci. U S A* 113, E2675–E2684. doi: 10.1073/pnas.1520759113

Prebil, M., Jensen, J., Zorec, R., and Kreft, M. (2011). Astrocytes and energy metabolism. *Arch. Physiol. Biochem.* 117, 64–69. doi: 10.3109/13813455.2010.539616

Preussat, K., Beetz, C., Schrey, M., Kraft, R., Wölfl, S., Kalff, R., et al. (2003). Expression of voltage-gated potassium channels Kv1.3 and Kv1.5 in human gliomas. *Neurosci. Lett.* 346, 33–36. doi: 10.1016/s0304-3940(03)00562-7

Qian, X., Shen, Q., Goderie, S. K., He, W., Capela, A., Davis, A. A., et al. (2000). Timing of CNS cell generation: a programmed sequence of neuron and glial cell production from isolated murine cortical stem cells. *Neuron* 28, 69–80. doi: 10.1016/s0896-6273(00)00086-6

Qiao, X., Werkman, T. R., Gorter, J. A., Wadman, W. J., and van Vliet, E. A. (2013). Expression of sodium channel α subunits 1.1, 1.2 and 1.6 in rat hippocampus after kainic acid-induced epilepsy. *Epilepsy Res.* 106, 17–28. doi: 10.1016/j.eplepsyres.2013.06.006

Reese, K. A., and Caldwell, J. H. (1999). Immunocytochemical localization of NaCh6 in cultured spinal cord astrocytes. *Glia* 26, 92–96. doi: 10.1002/(sici)1098-1136(199903)26:1<92::aid-glia10>3.0.co;2-4

Rose, C. R., and Ransom, B. R. (1997). Gap junctions equalize intracellular Na^+ concentration in astrocytes. *Glia* 20, 299–307. doi: 10.1002/(sici)1098-1136(199708)20:4<299::aid-glia3>3.0.co;2-1

Roth, B. L. (2016). DREADDs for neuroscientists. *Neuron* 89, 683–694. doi: 10.1016/j.neuron.2016.01.040

Rouach, N., Koulakoff, A., Abudara, V., Willecke, K., and Giaume, C. (2008). Astroglial metabolic networks sustain hippocampal synaptic transmission. *Science* 322, 1551–1555. doi: 10.1126/science.1164022

Rungta, R. L., Bernier, L.-P., Dissing-Olesen, L., Groten, C. J., LeDue, J. M., Ko, R., et al. (2016). Ca^{2+} transients in astrocyte fine processes occur *via* Ca^{2+} influx in the adult mouse hippocampus. *Glia* 64, 2093–2103. doi: 10.1002/glia.23042

Rurak, G. M., Simard, S., Charih, F., Van Geel, A., Stead, J., Woodside, B., et al. (2020). Translatomic database of cortical astroglia across male and female mouse development reveals two distinct developmental phenotypes. *bioRxiv* [Preprint]. doi: 10.1101/681684

Ryoo, K., and Park, J.-Y. (2016). Two-pore domain potassium channels in astrocytes. *Exp. Neurobiol.* 25, 222–232. doi: 10.5607/en.2016.25.5.222

Schaller, K. L., and Caldwell, J. H. (2003). Expression and distribution of voltage-gated sodium channels in the cerebellum. *Cerebellum* 2, 2–9. doi: 10.1080/14734220309424

Schröder, W., Hager, G., Kouprijanova, E., Weber, M., Schmitt, A. B., Seifert, G., et al. (1999). Lesion-induced changes of electrophysiological properties in astrocytes of the rat dentate gyrus. *Glia* 28, 166–174. doi: 10.1002/(sici)1098-1136(199911)28:2<166::aid-glia8 >3.0.co;2-t

Seifert, G., Hüttmann, K., Binder, D. K., Hartmann, C., Wyczynski, A., Neusch, C., et al. (2009). Analysis of astroglial K^+ channel expression in the developing hippocampus reveals a predominant role of the Kir4.1 subunit. *J. Neurosci.* 29, 7474–7488. doi: 10.1523/JNEUROSCI.3790-08.2009

Shen, Y., Kyu Han, S., and Dong Ryu, P. (2018). Comparison of electrophysiological properties of two types of pre-sympathetic neurons intermingled in the hypothalamic paraventricular nucleus. *J. Vet. Sci.* 19, 483–491. doi: 10.4142/jvs.2018.19.4.483

Sheppard, C. A., Simpson, P. B., Sharp, A. H., Nucifora, F. C., Ross, C. A., Lange, G. D., et al. (2002). Comparison of type 2 inositol 1,4,5-trisphosphate receptor distribution and subcellular Ca^{2+} release sites that support Ca^{2+} waves in cultured astrocytes. *J. Neurochem.* 68, 2317–2327. doi: 10.1046/j.1471-4159.1997.68062317.x

Sherwood, M. W., Arizono, M., Hisatsune, C., Bannai, H., Ebisui, E., Sherwood, J. L., et al. (2017). Astrocytic IP_3 Rs: contribution to Ca^{2+} signalling and hippocampal LTP. *Glia* 65, 502–513. doi: 10.1002/glia.23107

Shigetomi, E., Bushong, E. A., Haustein, M. D., Tong, X., Jackson-Weaver, O., Kracun, S., et al. (2013). Imaging calcium microdomains within entire astrocyte territories and endfeet with GCaMPs expressed using adeno-associated viruses. *J. Gen. Physiol.* 141, 633–647. doi: 10.1085/jgp.201210949

Shigetomi, E., Saito, K., Sano, F., and Koizumi, S. (2019). Aberrant calcium signals in reactive astrocytes: a key process in neurological disorders. *Int. J. Mol. Sci.* 20:996. doi: 10.3390/ijms20040996

Sloan, S. A., and Barres, B. A. (2014). Mechanisms of astrocyte development and their contributions to neurodevelopmental disorders. *Curr. Opin. Neurobiol.* 27, 75–81. doi: 10.1016/j.conb.2014.03.005

Smart, S. L., Bosma, M. M., and Tempel, B. L. (1997). Identification of the delayed rectifier potassium channel, Kv1.6, in cultured astrocytes. *Glia* 20, 127–134. doi: 10.1002/(sici)1098-1136(199706)20:2<127::aid-glia4>3.0.co;2-6

Smith, K. S., Bucci, D. J., Luikart, B. W., and Mahler, S. V. (2016). DREADDS: use and application in behavioral neuroscience. *Behav. Neurosci.* 130, 137–155. doi: 10.1037/bne0000135

Smith, N. A., Kress, B. T., Lu, Y., Chandler-Militello, D., Benraiss, A., and Nedergaard, M. (2018). Fluorescent Ca^{2+} indicators directly inhibit the Na,K-ATPase and disrupt cellular functions. *Sci. Signal.* 11:eaal2039. doi: 10.1126/scisignal.aal2039

Sofroniew, M. V., and Vinters, H. V. (2010). Astrocytes: biology and pathology. *Acta Neuropathol.* 119, 7–35. doi: 10.1007/s00401-009-0619-8

Somjen, G. G. (1979). Extracellular potassium in the mammalian central nervous system. *Annu. Rev. Physiol.* 41, 159–177. doi: 10.1146/annurev.ph.41.030179.001111

Sontheimer, H. (1994). Voltage-dependent ion channels in glial cells. *Glia* 11, 156–172. doi: 10.1002/glia.440110210

Sontheimer, H., Fernandez-Marques, E., Ullrich, I. N., Pappas, C. A., and Waxman, S. G. (1994). Astrocyte Na^+ channels are required for maintenance of Na^+/K^+-ATPase activity. *J. Neurosci.* 14, 2464–2475. doi: 10.1523/JNEUROSCI.14-05-02464.1994

Sontheimer, H., Minturn, J. E., Black, J. A., Ransom, B. R., and Waxman, S. G. (1991). Two types of Na^+-currents in cultured rat optic nerve astrocytes: changes with time in culture and with age of culture derivation. *J. Neurosci. Res.* 30, 275–287. doi: 10.1002/jnr.490300202

Sontheimer, H., and Waxman, S. G. (1992). Ion channels in spinal cord astrocytes *in vitro*. II. Biophysical and pharmacological analysis of two Na^+ current types. *J. Neurophysiol.* 68, 1001–1011. doi: 10.1152/jn.1992.68.4.1001

Srinivasan, R., Huang, B. S., Venugopal, S., Johnston, A. D., Chai, H., Zeng, H., et al. (2015). Ca^{2+} signaling in astrocytes from Ip3r2−/− mice in brain slices and during startle responses *in vivo*. *Nat. Neurosci.* 18, 708–717. doi: 10.1038/nn.4001

Stephan, J., Haack, N., Kafitz, K. W., Durry, S., Koch, D., Hochstrate, P., et al. (2012). Kir4.1 channels mediate a depolarization of hippocampal astrocytes under hyperammonemic conditions in situ. *Glia* 60, 965–978. doi: 10.1002/glia.22328

Stobart, J. L., Ferrari, K. D., Barrett, M. J. P., Glück, C., Stobart, M. J., Zuend, M., et al. (2018a). Cortical circuit activity evokes rapid astrocyte calcium signals on a similar timescale to neurons. *Neuron* 98, 726.e4–735.e4. doi: 10.1016/j.neuron.2018.03.050

Stobart, J. L., Ferrari, K. D., Barrett, M. J. P., Stobart, M. J., Looser, Z. J., Saab, A. S., et al. (2018b). Long-term *in vivo* calcium imaging of astrocytes reveals distinct cellular compartment responses to sensory stimulation. *Cereb. Cortex* 28, 184–198. doi: 10.1093/cercor/bhw366

Takata, N., and Hirase, H. (2008). Cortical layer 1 and layer 2/3 astrocytes exhibit distinct calcium dynamics *in vivo*. *PLoS One* 3:e2525. doi: 10.1371/journal.pone.0002525

Takata, N., Mishima, T., Hisatsune, C., Nagai, T., Ebisui, E., Mikoshiba, K., et al. (2011). Astrocyte calcium signaling transforms cholinergic modulation to cortical plasticity *in vivo*. *J. Neurosci.* 31, 18155–18165. doi: 10.1523/JNEUROSCI.5289-11.2011

Tan, G., Sun, S.-Q., and Yuan, D.-L. (2008). Expression of Kir 4.1 in human astrocytic tumors: correlation with pathologic grade. *Biochem. Biophys. Res. Commun.* 367, 743–747. doi: 10.1016/j.bbrc.2008.01.014

Tang, X., Taniguchi, K., and Kofuji, P. (2009). Heterogeneity of Kir4.1 channel expression in glia revealed by mouse transgenesis. *Glia* 57, 1706–1715. doi: 10.1002/glia.20882

Verkhratsky, A. (2006). Glial calcium signaling in physiology and pathophysiology 1. *Acta Pharmacol. Sin.* 27, 773–780. doi: 10.1111/j.1745-7254.2006.00396.x

Verkhratsky, A., and Nedergaard, M. (2018). Physiology of astroglia. *Physiol. Rev.* 98, 239–389. doi: 10.1152/physrev.00042.2016

Verkhratsky, A., Parpura, V., Vardjan, N., and Zorec, R. (2019). Physiology of astroglia. *Adv. Exp. Med. Biol.* 1175, 45–91. doi: 10.1007/978-981-13-9913-8_3

Walker, M. C., and Kullmann, D. M. (2020). Optogenetic and chemogenetic therapies for epilepsy. *Neuropharmacology* 168:107751. doi: 10.1016/j.neuropharm.2019.107751

Walz, W. (1982). Do neuronal signals regulate potassium flow in glial cells? Evidence from an invertebrate central nenrous system. *J. Neurosci. Res.* 7, 71–79. doi: 10.1002/jnr.490070108

Wang, X., Lou, N., Xu, Q., Tian, G.-F., Peng, W. G., Han, X., et al. (2006). Astrocytic Ca^{2+} signaling evoked by sensory stimulation *in vivo*. *Nat. Neurosci.* 9, 816–823. doi: 10.1038/nn1703

Wang, F., Smith, N. A., Xu, Q., Fujita, T., Baba, A., Matsuda, T., et al. (2012). Astrocytes modulate neural network activity by Ca^{2+}-dependent uptake of extracellular K^+. *Sci. Signal.* 5:ra26. doi: 10.1126/scisignal.2002334

Wang, M., Xu, Z., Liu, Q., Sun, W., Jiang, B., Yang, K., et al. (2019). Nongenetic optical modulation of neural stem cell proliferation and neuronal/glial differentiation. *Biomaterials* 225:119539. doi: 10.1016/j.biomaterials.2019.119539

Wilhelm, I., Nyúl-Tóth, Á., Suciu, M., Hermenean, A., and Krizbai, I. A. (2016). Heterogeneity of the blood-brain barrier. *Tissue Barriers* 4:e1143544. doi: 10.1080/21688370.2016.1143544

Wilson, C. S., and Mongin, A. A. (2019). The signaling role for chloride in the bidirectional communication between neurons and astrocytes. *Neurosci. Lett.* 689, 33–44. doi: 10.1016/j.neulet.2018.01.012

Wu, Y.-W., Gordleeva, S., Tang, X., Shih, P.-Y., Dembitskaya, Y., Semyanov, A., et al. (2019). Morphological profile determines the frequency of spontaneous calcium events in astrocytic processes. *Glia* 67, 246–262. doi: 10.1002/glia.23537

Wu, K.-C., Kuo, C.-S., Chao, C.-C., Huang, C.-C., Tu, Y.-K., Chan, P., et al. (2015). Role of voltage-gated K^+ channels in regulating Ca^{2+} entry in rat cortical astrocytes. *J. Physiol. Sci.* 65, 171–177. doi: 10.1007/s12576-015-0356-9

Xin, W., Schuebel, K. E., Jair, K.-W., Cimbro, R., De Biase, L. M., Goldman, D., et al. (2019). Ventral midbrain astrocytes display unique physiological features and sensitivity to dopamine D2 receptor signaling. *Neuropsychopharmacology* 44, 344–355. doi: 10.1038/s41386-018-0151-4

Yu, X., Taylor, A. M. W., Nagai, J., Golshani, P., Evans, C. J., Coppola, G., et al. (2018). Reducing astrocyte calcium signaling *in vivo* alters striatal microcircuits and causes repetitive behavior. *Neuron* 99, 1170.e9–1187.e9. doi: 10.1016/j.neuron.2018.08.015

Zaitzev, A. V., Povysheva, N. V., Gonzalez-Burgos, G., and Lewis, D. A. (2012). Electrophysiological classes of layer 2/3 pyramidal cells in monkey prefrontal cortex. *J. Neurophysiol.* 108, 595–609. doi: 10.1152/jn.00859.2011

Zhang, Y., Sloan, S. A., Clarke, L. E., Grant, G. A., Gephart, M. G. H., and Correspondence, B. A. B. (2016). Purification and characterization of progenitor and mature human astrocytes reveals transcriptional and functional differences with mouse. *Neuron* 89, 37–53. doi: 10.1016/j.neuron.2015.11.013

Zhong, S., Du, Y., Kiyoshi, C. M., Ma, B., Alford, C. C., Wang, Q., et al. (2016). Electrophysiological behavior of neonatal astrocytes in hippocampal stratum radiatum. *Mol. Brain* 9:34. doi: 10.1186/s13041-016-0213-7

Zhou, M., Schools, G. P., and Kimelberg, H. K. (2006). Development of $GLAST^+$ astrocytes and $NG2^+$ glia in rat hippocampus CA1: mature astrocytes are electrophysiologically passive. *J. Neurophysiol.* 95, 134–143. doi: 10.1152/jn.00570.2005

Zhou, M., Xu, G., Xie, M., Zhang, X., Schools, G. P., Ma, L., et al. (2009). TWIK-1 and TREK-1 are potassium channels contributing significantly to astrocyte passive conductance in rat hippocampal slices. *J. Neurosci.* 29, 8551–8564. doi: 10.1523/JNEUROSCI.5784-08.2009

Zhu, J., Yan, J., and Thornhill, W. B. (2014). The Kv1.3 potassium channel is localized to the cis-Golgi and Kv1.6 is localized to the endoplasmic reticulum in rat astrocytes. *FEBS J.* 281, 3433–3445. doi: 10.1111/febs.12871

Zhu, H., Zhao, Y., Wu, H., Jiang, N., Wang, Z., Lin, W., et al. (2016). Remarkable alterations of Nav1.6 in reactive astrogliosis during epileptogenesis. *Sci. Rep.* 6:38108. doi: 10.1038/srep38108

Ziemens, D., Oschmann, F., Gerkau, N. J., and Rose, C. R. (2019). Heterogeneity of activity-induced sodium transients between astrocytes of the mouse hippocampus and neocortex: mechanisms and consequences. *J. Neurosci.* 39, 2620–2634. doi: 10.1523/JNEUROSCI.2029-18.2019

Zur Nieden, R., and Deitmer, J. W. (2006). The role of metabotropic glutamate receptors for the generation of calcium oscillations in rat hippocampal astrocytes in situ. *Cereb. Cortex* 16, 676–687. doi: 10.1093/cercor/bhj013

Conflict of Interest: The authors declare that the research was conducted in the absence of any commercial or financial relationships that could be construed as a potential conflict of interest.

frontiers in Cellular Neuroscience

ORIGINAL RESEARCH
published: 20 May 2021
doi: 10.3389/fncel.2021.681066

Begonia—A Two-Photon Imaging Analysis Pipeline for Astrocytic Ca^{2+} Signals

*Daniel M. Bjørnstad[1†], Knut S. Åbjørsbråten[1†], Eivind Hennestad[2], Céline Cunen[3], Gudmund Horn Hermansen[3], Laura Bojarskaite[1,4], Klas H. Pettersen[1,5], Koen Vervaeke[2] and Rune Enger[1]**

[1]GliaLab at the Letten Centre, Division of Anatomy, Department of Molecular Medicine, Institute of Basic Medical Sciences, University of Oslo, Oslo, Norway, [2]Lab for Neural Computation, Division of Physiology, Department of Molecular Medicine, Institute of Basic Medical Sciences, University of Oslo, Oslo, Norway, [3]Statistics and Data Science Group, Department of Mathematics, Faculty of Mathematics and Natural Sciences, University of Oslo, Oslo, Norway, [4]Department of Neurology, Oslo University Hospital, Rikshospitalet, Oslo, Norway, [5]NORA—Norwegian Artificial Intelligence Research Consortium, Faculty of Mathematics and Natural Sciences, University of Oslo, Oslo, Norway

OPEN ACCESS

Edited by:
Yu-Wei Wu, Academia Sinica, Taiwan

Reviewed by:
Bernd Kuhn, Okinawa Institute of Science and Technology Graduate University, Japan
Janelle M. P. Pakan, Otto von Guericke University Magdeburg, Germany

***Correspondence:**
Rune Enger
rune.enger@medisin.uio.no

†These authors have contributed equally to this work and share first authorship

Specialty section:
This article was submitted to Non-Neuronal Cells, a section of the journal Frontiers in Cellular Neuroscience

Received: *15 March 2021*
Accepted: *21 April 2021*
Published: *20 May 2021*

Citation:
Bjørnstad DM, Åbjørsbråten KS, Hennestad E, Cunen C, Hermansen GH, Bojarskaite L, Pettersen KH, Vervaeke K and Enger R (2021) Begonia—A Two-Photon Imaging Analysis Pipeline for Astrocytic Ca^{2+} Signals. Front. Cell. Neurosci. 15:681066. doi: 10.3389/fncel.2021.681066

Imaging the intact brain of awake behaving mice without the dampening effects of anesthesia, has revealed an exceedingly rich repertoire of astrocytic Ca^{2+} signals. Analyzing and interpreting such complex signals pose many challenges. Traditional analyses of fluorescent changes typically rely on manually outlined static region-of-interests, but such analyses fail to capture the intricate spatiotemporal patterns of astrocytic Ca^{2+} dynamics. Moreover, all astrocytic Ca^{2+} imaging data obtained from awake behaving mice need to be interpreted in light of the complex behavioral patterns of the animal. Hence processing multimodal data, including animal behavior metrics, stimulation timings, and electrophysiological signals is needed to interpret astrocytic Ca^{2+} signals. Managing and incorporating these data types into a coherent analysis pipeline is challenging and time-consuming, especially if research protocols change or new data types are added. Here, we introduce Begonia, a MATLAB-based data management and analysis toolbox tailored for the analyses of astrocytic Ca^{2+} signals in conjunction with behavioral data. The analysis suite includes an automatic, event-based algorithm with few input parameters that can capture a high level of spatiotemporal complexity of astrocytic Ca^{2+} signals. The toolbox enables the experimentalist to quantify astrocytic Ca^{2+} signals in a precise and unbiased way and combine them with other types of time series data.

Keywords: two-photon (2P), image analysis, calcium imaging, ROA analysis, astrocyte

INTRODUCTION

Astrocytic Ca^{2+} signals have been shown to play important roles in a wide range of physiological and pathophysiological brain processes (Cornell-Bell et al., 1990; Rusakov et al., 2011; Verkhratsky and Parpura, 2013; Bazargani and Attwell, 2016). Until recently, studies on astrocytic Ca^{2+} signals were confined to *in vitro* experiments and *in vivo* experiments in anesthetized mice. With the development of genetically encoded Ca^{2+} sensors and

improvements in optical imaging, *in vivo* imaging without the dampening effects of anesthesia (Thrane et al., 2012) in behaving animals has become possible (Srinivasan et al., 2015; Enger et al., 2017; Stobart et al., 2018). This, in turn, has revealed an exceedingly rich palette of astrocytic Ca^{2+} signals coupled to behavior, ranging from small, short-lived events in subcellular compartments to long-lasting, global activations affecting large swaths of the cortical mantle (Srinivasan et al., 2015; Stobart et al., 2018; Bojarskaite et al., 2020).

High frame rates (e.g., ∼30 Hz) are needed to appropriately capture short-lasting Ca^{2+} signals and enable efficient movement correction of two-photon imaging data from awake mice (Pnevmatikakis and Giovannucci, 2017; Stobart et al., 2018). Moreover, to reliably quantify the relatively sparse astrocytic Ca^{2+} signals in behavioral quiescence, long acquisition times are also warranted. For these reasons, two-photon microscopy data for a given project could amount to tens of terabytes of data, and an analysis pipeline for such datasets needs to be optimized for speed and performance to avoid unacceptably long processing times.

Traditional analyses of astrocytic Ca^{2+} signals typically comprise manual or semi-automatic segmentation of regions-of-interest (ROIs) overlying astrocytic somata and processes (Eilert-Olsen et al., 2019; Semyanov et al., 2020). Even though such analyses are appropriate and to some level sufficient to describe the relatively sparse astrocytic Ca^{2+} activity in brain slices and the anesthetized brain, they are not adequate for capturing the true complexity of astrocytic Ca^{2+} signals in the unanesthetized brain (Wang et al., 2019; Bojarskaite et al., 2020; Semyanov et al., 2020): first, ROI analyses do not capture the dynamic spatial extent of these signals, as astrocytic Ca^{2+} signals can emerge from multiple point sources, merge, and spread throughout the gap junction coupled astrocyte syncytium (Semyanov, 2019). Second, as fluorescence from an ROI is typically measured as the mean gray value of the pixels within that ROI per time unit, events affecting a small proportion of the segmented area will typically not reach the threshold for event detection. Third, a static ROI analysis fails to capture separate concurrent events occurring within a single defined area (Wang et al., 2019; Bojarskaite et al., 2020). Lately, new algorithms have been proposed to appropriately address the dynamic nature of astrocytic Ca^{2+} signaling (Srinivasan et al., 2015; Barrett et al., 2018; Wang et al., 2019). One of these, the *Astrocyte Quantitative Analysis* (AQuA) algorithm, employs an event-based approach to detect astrocytic Ca^{2+} signals (Wang et al., 2019). AQuA has in our view prominently advanced the field of astroglial Ca^{2+} signal analyses, especially by its efforts to describe how astroglial Ca^{2+} signals dynamically change in time and space. Even so, AQuA is dependent on a wide range of tuning parameters, and the analysis pipeline is not optimized for high frame rate data (Bojarskaite et al., 2020).

Another challenge with analyzing astrocytic Ca^{2+} signaling data from unanesthetized awake–behaving mice is to properly align and interpret these in the context of rich animal behavior. Various time series data are acquired for studies in behaving animals that need to be integrated with astrocytic signaling. For example, locomotion and whisking activity are typically recorded. To properly collate and align such multimodal data is challenging as they are typically acquired by multiple recording devices with different sampling frequencies and data formats.

Here, we present a MATLAB toolbox tailored to analyze astrocytic Ca^{2+} signals from behaving animals in a timely manner. The toolbox comprises a data management pipeline from raw data to derived data in tables, is optimized for large datasets, and contains the following functions: (i) implementation of previously published image alignment algorithms (Pnevmatikakis and Giovannucci, 2017); (ii) an automatic Ca^{2+} signal analysis pipeline, the region-of-activity (ROA) method, that may be used without setting manual tuning parameters; (iii) an ROI segmentation graphical user interface that can combine hand-drawn ROIs with automatically detected Ca^{2+} signals; (iv) easy integration with other time series data such as electrophysiological recordings or movement data; and (v) an output module that can export data as tables for statistical analyses, or as plots and figures. The toolbox is programmed in MATLAB with modularity and flexibility in mind, enabling quick creation of graphical user interfaces and workflows when new analyses need to be established.

MATERIALS AND METHODS

The Begonia toolbox comprises multiple graphical and programmatic tools placed on top of a framework for the storage of metadata and derived data from image recordings, and a set of abstract base classes that offer a common application programming interface (API) for accessing image data in a source agnostic manner.

Metadata Storage With Data Locations

We define metadata as all data connected to the recording and analysis of a two-photon microscopy experiment except the actual imaging data. We developed Begonia around a metadata storage strategy we call *data locations* which is facilitated by the DataLocation class. Data locations offer a way for the software provided by Begonia to easily store and retrieve metadata as processing and manual steps take place on imaging data.

In simple terms, data locations are paths in the file directory that through the DataLocation class allow metadata variables to be associated with these paths. The system does not rely on a centralized database of any kind and does not enforce a strict schema of names and entities on the data being saved. Data locations by default store the metadata entries at the path they point to. A problem with using filesystem paths as identifiers is to keep track of the data if files and folders are moved. For this reason, data locations save a universal unique identifier (UUID) on first use so that data that are moved can be re-identified.

The data location system supports several ways of storing and retrieving metadata through the use of keywords, with abstract access to these mechanisms through a generic API on the DataLocation objects. We provide two such methods, or *engines*: the on-path engine, and the off-path engine. The on-path engine is the default, and stores metadata in a .mat file adjacent to the imaging data. The off-path engine stores all the metadata in a separate directory chosen by the user. Using the on-path engine,

data locations require no setup to attach additional data to the imaging data.

Data Import, Management, and On-Demand Reading

We offer an API for importing imaging data and metadata acquired by different microscopes into a standardized format. This is implemented through the TSeries class, which provides a gateway to use the functionality of Begonia, regardless of how the data are recorded. Begonia contains a +scantype namespace that contains classes that inherit from the TSeries class that can load multi-page TIFF files [an adaptation of the TIFFStack (Muir and Kampa, 2014) library for faster loading and alternative matrix indexing], PrairieView (Bruker) time series, and TIFFs created in ScanImage (Vidrio Technologies). The imaging classes also inherit the DataLocation class, allowing new metadata to be associated directly with a particular recording and granting access to the data management system.

We have frequently found that two-photon microscopy data from a single trial exceed the random-access memory size (RAM) on the analyst's computer. Moreover, we often want to review specific moments without waiting to load the whole recording. To allow faster and improved loading, we convert large data to the Hierarchical Data Format 5 (HDF5) whenever possible. HDF5 allows data to be retrieved on-demand, utilizing only the memory needed for the operation in question and retrieving only a subset of the recording of interest.

Analysts can use imported recordings directly in MATLAB. However, Begonia offers a data management tool, that lists recordings and displays associated metadata through the data location system (**Figure 1B**). The tool offers multiple features such as filtering, processing, and plotting through simple drop-down menus and buttons. The data manager is built on a base class called Editor that allows programmers to quickly develop one-shot graphical user interfaces (GUIs) with customized visualization of data and metadata as well as buttons for project-specific processing functions. We find that GUIs and the DataLocation system enable an efficient and flexible analysis pipeline that provides non-expert programmers with easy access to a complex processing pipeline. The GUIs are particularly useful for performing manual steps of the analyses, such as marking anatomical features and reviewing the data quality of individual recordings. Manually generated metadata can be used by processing functions that subsequently can be executed directly or added to a processing queue from the data manager.

Collation and Segmentation of Time Series Data

Once data is processed, it is often necessary to combine them with other data types, like for instance recordings of locomotion and whisking. Such additional data are typically acquired on a different computer than the imaging data and are often of different acquisition rates, starting times, and data formats than the microscopy data. It is useful to plot or analyze all these multimodal data in a collated fashion. To facilitate this, Begonia implements a class called MultiTable and an associated API that can collect data from multiple sources and group them by a custom entity such as an experiment or trial identifier. In this way, all data from a single experiment are connected using a common entity.

MultiTable is not a table of data, but a list of sources that provides data in a uniform tabular format on demand. It can additionally slice and resample the data based on user-given criteria. With this approach, the origin of the data can be hidden from the user and thus simplify the analysis. We provide sources for data locations out of the box, which simplifies adding data from ROI and ROA analyses. The sources must provide time information in addition to the data vectors themselves. With this requirement, analysts can resample and time-align MultiTable outputs. Additionally, all data provided to MultiTable can be added with time correction so that differences in starting time on different hardware can be compensated. The system provides a way to include any custom time series data alongside the data types provided by Begonia.

We frequently need to extract time series data from various data sources around a time point or in a specified time interval. The MultiTable API allows such segmentation using MATLAB categorical arrays. For example, it may be desirable to extract fluorescence values and whisking activity around the transition from quiet wakefulness to running. In this case, the categorical array in the MultiTable (**Figure 1D**) could contain the value "quiet wakefulness" in the time points where the mouse is still, and "running" when the mouse moves. MultiTable can then be asked to identify these transitions based on the categorical arrays and retrieve data from an interval relative to such a time point.

ROI Manager

In addition to metadata and data management features, Begonia provides a highly modular ROI management and time series viewer called ROI Manager. The software is designed to be extended for any type of markup a project might need, and to be a generic viewer for data loaded through Begonia.

Architecturally, ROI Manager uses a central concept of *Views* for windows that display data, and *Tools* for windows that provide tools to edit the data. It is designed with a hybrid object and data-oriented design. Each piece of data loaded—primarily two-photon microscopy time series data—can have multiple views of the same imaging data simultaneously. In this way, imaging data from multiple channels may be viewed simultaneously in different windows. *Views* provide a data-oriented approach to communication between the modules of the ROI Manager (tools, rendering layers, and, interaction modes) by offering a set of *key-value pairs* (KVPs) for each *View* that can be read and written by any module and periodically checked. The KVPs have non-strict semantics, meaning modules can read and write any data they want to the *Views*. E.g., an ROI editing tool can write a table of ROIs to the key "roi_table," and a tool for changing the colormap displayed can write these settings to a key called "channel_colormap," while both can write to a key "channel" to set what channel in the multi-channel data is currently displayed. The modules handling the rendering of the data in the figure window similarly check if keys they are

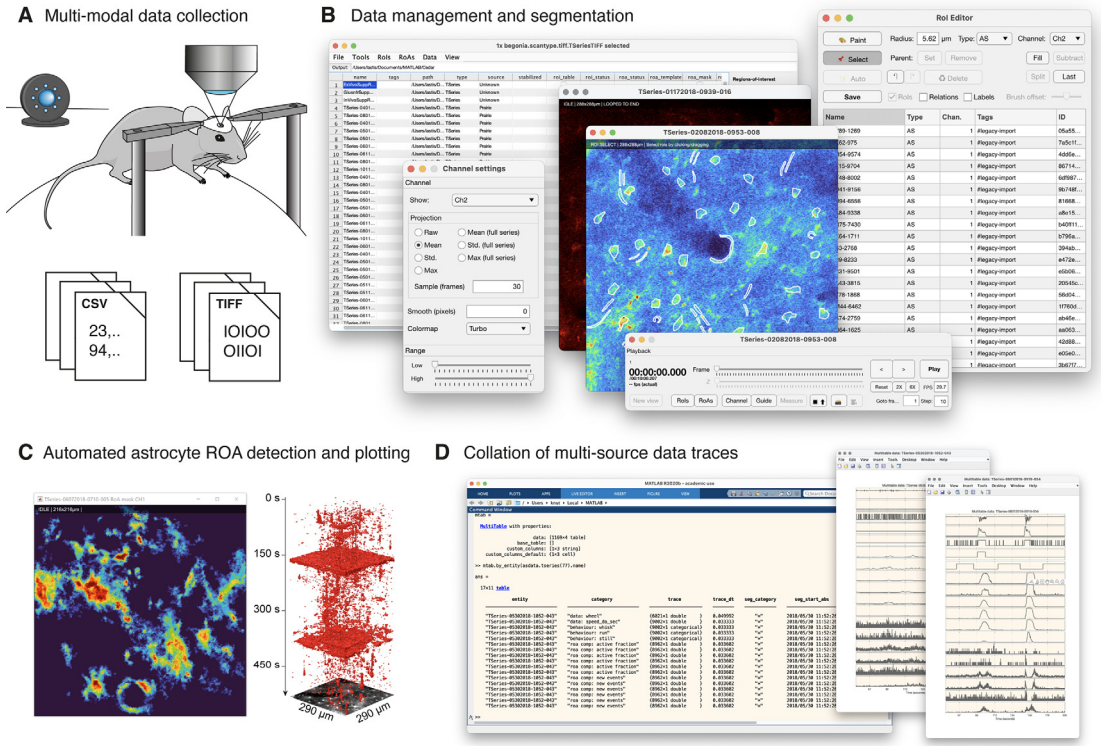

FIGURE 1 | Begonia workflow. **(A)** Acquisition of multi-modal data. Movement from a running wheel and surveillance video from an infrared-sensitive camera is typically recorded alongside two-photon imaging data. **(B)** Begonia provides an editor for project-specific manual tasks, data and metadata management, and manual ROI segmentation of the imaging data. **(C)** The region-of-activity (ROA) algorithm provides an automated or semi-automatic detection of astrocytic Ca^{2+} signals in the field-of-view or inside manually segmented ROIs or groups of manually segmented ROIs. **(D)** MultiTable provides a way to collate, synchronize and segment time series traces from ROIs, ROA, and custom sources on demand.

associated with are updated and then redraw the view of the data as needed.

Tools and various modules can be set up to load in any combination the user wants, allowing the ROI Manager to take roles beyond managing ROIs. For instance, a project measuring vascular diameters and flow of red blood cells might warrant a Tool window for marking the vessel, in combination with visible ROIs. In its simplest form, ROI Manager is just an image sequence viewer with no Tools, and Begonia offers this as well to allow viewing any 3D MATLAB arrays.

Begonia offers ROI signal extraction from ROIs in time series data through batch operations available in Data Manager. In addition, the ROIs from the ROI Manager may be used to filter the output of the ROA analysis to assign ROA activity to cells or subcellular structures.

ROA Algorithm

The ROA algorithm is a method that detects fluorescence signal events in a pixel-by-pixel fashion in two-photon microscopy time series data (**Figure 2**). The raw fluorescence time series (F) of each pixel is transformed into a binary time series where the ones indicate events. These events correspond to fluorescence values which exceed a certain pixel-specific threshold τ_i. The threshold is a function of the baseline gray values and standard deviation of the noise. The algorithm is tailor-made for noisy, high frame rate (∼30 Hz) recordings.

Finding Activity

We denote the raw fluorescence time series as $F_i(t)$, i.e., the gray value of pixel i at time t. Let $F_i'(t)$ denote a moving average smoothed version of $F_i(t)$; (see below for details on smoothing), and consider $F_i^*(t) = \sqrt{F_i'(t)}$ the square root transformed version of $F_i'(t)$. We determine events in our time series data, by binarizing $F_i^*(t)$ per pixel using a threshold (τ_i) defined as:

$$\tau_i = \hat{\mu}_i + \kappa \cdot \hat{\sigma},$$

where κ is a user-defined number (default $\kappa = 4$) which determines the height of the threshold, $\hat{\mu}_i$ is the estimated baseline value for each pixel, and $\hat{\sigma}$ is the estimated standard deviation of the noise as defined in the following sections.

Modeling Fluorescence Time Series

To accurately estimate the level of noise, one needs to model the underlying distribution of the fluorescence data. When the number of photons recorded per pixel is sufficiently high, fluorescence data from two-photon Ca^{2+} imaging may be

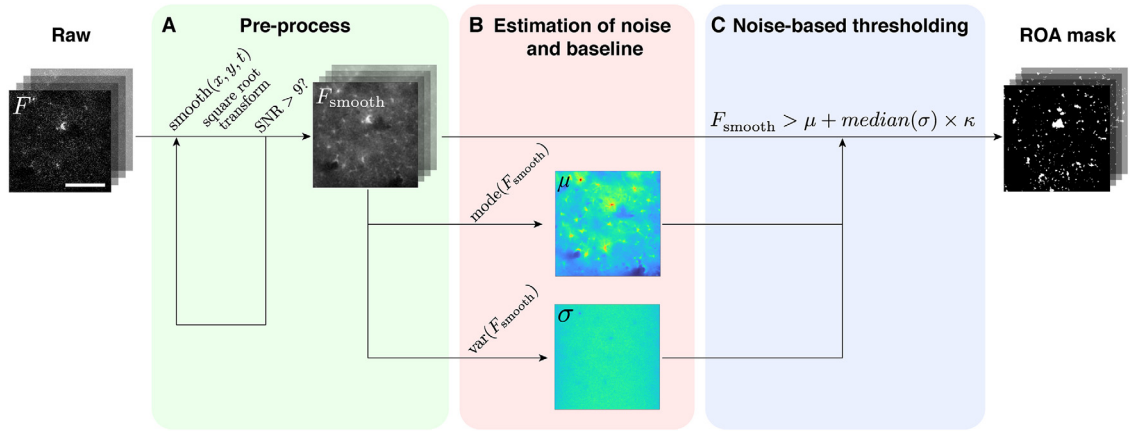

FIGURE 2 | The ROA algorithm. **(A)** The raw data (F) are spatiotemporally smoothed and transformed (F_{smooth}) until an acceptable SNR is attained. **(B)** In each pixel, the baseline value (μ) and the standard deviation (σ) of the root gray values are then estimated from F_{smooth} (temporal smoothing applied by merging frames). **(C)** F_{smooth} is then binarized by applying a threshold defined as the baseline value (μ) plus κ times the standard deviation of the noise (σ; temporal smoothing applied with a moving average).

considered approximately normally distributed with a particular relationship between the expected value and the variance; $Var_i(t) = aE_i(t) + b$, with unknown parameters a and b, due to the effect of the amplification of the signal by the photomultiplier tubes (Danielyan et al., 2014). Here $E_i(t)$ denotes the expected fluorescence value at time t and in a particular pixel i and $Var_i(t)$ the variance of the fluorescence. Our raw, high frame rate data ($F_i(t)$) have a highly non-normal distribution, with a high probability of observing values equal to zero and a heavy right tail. After smoothing (mainly in time), we observe that the distribution comes closer to normality. This is natural, since smoothing has a similar effect on the distribution of the pixel gray values as increasing the pixel integration time. At this level of the analysis, we perform spatiotemporal smoothing by averaging a specific number of frames and neighboring pixels and we denote this time series by $Z_i(t)$. The particular dependency between the expected value and variance in the model of Danielyan et al. (2014) may be essentially eliminated using the following transformation $X_i(t) = \sqrt{Z_i(t)}$. The transformed variable $X_i(t)$ will have a time-varying expected value $\mu_i(t) \approx \sqrt{E(Z_i(t))}$ and an (essentially) time-independent variance σ_i^2. In the following, E denotes the expected value and σ_i represents the standard deviation of the noise. The transformation above is occasionally referred to as a variance stabilization in the literature (Bartlett, 1947; Wang et al., 2019). Note that the variance after transformation will, in fact, be approximately equal to the following expression

$$Var(X_i(t)) \approx a/4 + b/[4E(Z_i(t))].$$

This expression can be derived using the delta method, see for instance Casella and Berger (2002). Clearly, the dependency between the variance and the expected value will be negligible if the expected value, $E(Z_i(t))$, is sufficiently large, and after the square root transformation, we observe that there is virtually no dependency between $\mu_i(t)$ and $Var(X_i(t))$, which suggests that b is an order of magnitude smaller than $E(Z_i(t))$. We therefore ignore b in the following.

Estimating Pixel-Specific Parameters

Estimating the time-varying expectation $\mu_i(t)$ requires additional assumptions and can be challenging. Furthermore we are primarily interested in estimating the baseline of $X_i(t)$, which we refer to as μ_i. We estimate this quantity by finding the mode of the observations in pixel i,

$$\hat{\mu}_i = Mode(X_i).$$

Intuitively, since the fluorescence signal in each pixel primarily takes values close to the baseline for most of the recording, it is natural to estimate the baseline by the most frequent value in the time series for pixel i. In our investigations, this estimate appears to work adequately.

Since we do not estimate the time-varying expected value $\mu_i(t)$, we cannot use the conventional sample variance formula. Instead, we use the following estimator for the variance of the noise,

$$\widehat{\sigma}_i^2 = \frac{1}{c} Median\left([X_i(t+1) - X_i(t)]^2\right),$$

for all pairs of successive observations. The number c is a constant which ensures that this is a consistent estimator for σ_i^2 under the assumption of normality. The value of c may be found by simulations or calculated theoretically, by

$$c = 2m_1 \approx 0.9099,$$

where m_1 is the median of the chi-squared distribution with 1 degree of freedom. This formula for c is an approximation that

holds when the number of time points is sufficiently large. This estimator was employed by Wang et al. (2019). Its theoretical properties have not been derived as far as we know, but its form and motivation is close to the mean squared successive difference (MSSD) estimator suggested by Neumann et al. (1941) and with a relatively widespread use (Ebner-Priemer et al., 2007, 2009; Garrett et al., 2013; Nomi et al., 2017).

Smoothing

The number of events detected with the ROA algorithm is dependent on the imaging quality, which can be assessed by the signal-to-noise ratio (SNR), which we define as

$$SNR = \hat{\mu}/\hat{\sigma},$$

where $\hat{\mu}$ and $\hat{\sigma}$ are estimates of the common baseline and standard deviation for all pixels in an image time series. We use the median of the pixel-specific estimates in order to be robust against extreme values,

$$\hat{\mu} = Median(\widehat{\mu}_i) \, and \, \hat{\sigma} = Median(\widehat{\sigma}_i).$$

We observed that for low SNRs there was a positive correlation between SNR and the number of events detected with the ROA algorithm. If a typical dataset was smoothed to attain at least an SNR of 9, this correlation disappeared. In order to attain this desired level of SNR of at least 9, we perform a parameter search of varying levels of spatiotemporal smoothing and apply spatial Gaussian smoothing and temporal boxcar smoothing. Although we cannot guarantee that an SNR of at least 9 is the optimal target for datasets acquired by different labs and hardware, an SNR of at least 9 worked well for the external datasets we tested. For the time series $X_i(t)$, the temporal smoothing is applied by binning frames and not as a moving average. The parameter search may be performed on all imaging trials independently or on a selected trial serving as a template for the rest of the analyses. For spatial smoothing, we perform a parameter search where the sigma of the Gaussian filter is increased from 0 to 2 pixels. If the desired SNR is not reached by spatial filtering alone, we keep the maximum spatial smoothing and do a parameter search for the number of averaged frames between one and 30 frames. If the target SNR is still not reached, the configurations are set to 2 pixels for the spatial smoothing and 30 frames for the temporal smoothing. We perform the parameters search for the number of frames to average by using the interval halving method. To limit the computation time in large time series data only the last 1,000 merged frames are used to compute the SNR in the parameter search. The spatial and temporal smoothing parameters can also be set manually. The parameters are estimated and stored for interactive threshold adjustment and filtering when the pre-process button in the GUI is pressed.

Optional Threshold Adjustment and Filtering Results

As the size and duration of two-photon microscopy of astrocytic Ca^{2+} events follow a power law distribution and the optical resolution of two-photon microscopy is an order of magnitude poorer than the smallest astrocytic processes, there is a continuum between signal and noise. Moreover, we do not have access to the ground truth of real-life data. Consequently, the threshold applied will be somewhat heuristic (we have chosen four times the standard deviation of the noise as default: $\kappa = 4$) and the events detected will be strongly dependent on the threshold applied. In addition, no matter the threshold applied, a large proportion of the true Ca^{2+} event will go undetected due to the limitations of (non-super-resolution) optical microscopy. For these reasons it is desirable to be somewhat conservative when deciding what is signal and what should be considered noise, and a tool is provided for interactively changing the threshold by adjusting κ and filtering out ROAs below a minimum size and duration.

Performance

The main outputs from Begonia can be found in **Table 1**. The ROA method and surrounding pipeline have been created to support the analysis of large datasets on moderate performance computers like a personal laptop. Two-photon recordings at high frame rates typically store data in integer formats at rates of ∼1 GB per minute. However, for many calculations, data need to be transformed to floating-point formats. These can be two to eight times more memory intensive and consequently exhaust the working memory of the computer even for shorter (5–10 min) recordings. For these reasons, in the pipeline where the sheer size of the file may exceed the capacity of a normally configured computer, data are chunked and analyzed in smaller segments. Moreover, data retrieval is implemented with lazy (on-demand) reading. On a personal laptop, with 16 GB RAM, it took 15, 31, 51, 143, and 267 s, to analyze 100, 500, 1,000, 2,500, and 5,000 frames of 512 × 512 pixels, respectively.

RESULTS

Workflow

We built Begonia with the flow of data in mind, and a high priority during development was to create responsive GUIs and speed up functions that have high computational demands. Furthermore, time-consuming steps can be queued and processed in batch operations. The workflow is outlined in **Figure 1**. The intended workflow is a step-by-step procedure where small chunks of the data are processed at a time and the results and intermediate data are stored with data locations associated with the imaging time series object. The chunking ensures that the software can be applied to (infinitely) large datasets whereas saving intermediate data adds flexibility. For example, if there is a failure during one or more processing steps, the fault can be troubleshot and the procedure can be started from the point where it stopped. Also, intermediate steps can easily be reprocessed using different parameters.

The first step of the workflow in Begonia is to identify imaging time series data and instantiate classes to interact with them. Begonia includes methods that search directories for supported two-photon imaging formats and returns a list of imaging objects. The objects are used to access the imaging time series data and microscope metadata in a standardized

way, even if the recordings are stored using heterogeneous file formats. Instructions on how to make new imaging classes for unsupported formats are provided in the documentation.

Begonia provides a general method to save data together with the imaging data in folders in the directory tree. The data in these folders can then be directly accessed via the imaging objects and are known in this toolbox as data locations. Data stored through the data locations system may be retrieved via the imaging time series objects using keywords.

We have provided a workflow GUI (**Figures 1B**, **3A**) that lists groups of data locations and associated metadata in a table and allows the user to select items and run procedures. It includes basic steps typically performed in the analysis of two-photon imaging data, and can easily be expanded or modified to allow for other types of analyses on the data. The user can select and pass single or multiple data objects to functions, other GUIs or to the batch processing queue (**Figure 3B**). Standard procedures that are currently implemented in the toolbox are image alignment using the NoRMCorre software package (Pnevmatikakis and Giovannucci, 2017), manual segmentation of ROIs in a GUI, and running the ROA algorithm.

The last step of the processing workflow is to combine imaging data with other types of data (e.g., behavioral data) and to export data. Begonia provides a way to easily combine the results from the analysis of the imaging data with other types of data (for instance electrophysiology or behavioral metrics) in a data class called MultiTable. The MultiTable enables you to resample, align and slice your dataset to export a desired subset of data for plotting or statistical analyses (**Figure 1D** and see "Materials and Methods" section). The main outputs from Begonia is listed in **Table 1**.

Data Management and Processing

Begonia is built around the concept of data locations to save metadata and derived data throughout the analyses (see "Materials and Methods" section). Begonia further provides a template GUI for working with these abstract representations of the data and metadata (**Figure 3**). Here, DataLocation objects, e.g., a two-photon microscopy time series with corresponding metadata, appear as an entity in a list. The GUI enables the user to selectively see metadata coupled to the data location objects in the same list, and gives quick access to pass these objects to the MATLAB workspace or functions represented by buttons and menu options. You may add new buttons and menus with associated functions to the GUI by passing anonymous functions as input arguments during the initialization of the GUI. The GUI also provides a processing queue (**Figure 3B**), where actions on the data location objects can be visualized before being executed in a batch-wise process.

Marking ROIs

The toolbox provides a multi-purpose GUI for visualization of imaging data, ROAs, and manual segmentation of ROIs (**Figure 4**). The GUI components may also be assembled for other types of analyses. Imaging data may be visualized as raw data, running average data, or projections of the whole time series. ROIs are manually drawn with a paintbrush tool and saved in a list where the type of ROI and relationships between ROIs may be defined.

Region of Activity (ROA) Analysis

The ROA algorithm is an event-based method to quantify astrocytic Ca^{2+} signals. An earlier iteration of the ROA algorithm was applied to two-photon microscopy data in Bojarskaite et al. (2020). In the current version, the noise estimation strategy has been adapted from Wang et al. (2019). The analysis comprises first a spatial and temporal filtering of two-dimensional time series data to attain an acceptable SNR, followed by a pixel-by-pixel quantification of noise over time, to define a threshold for signal detection. The steps of the method are shown in **Figure 2**. The appropriate level of smoothing is automatically found as the first step of the algorithm (see "Materials and Methods" section). This part of the algorithm enables the ROA method to be run with few input parameters and still give reproducible results.

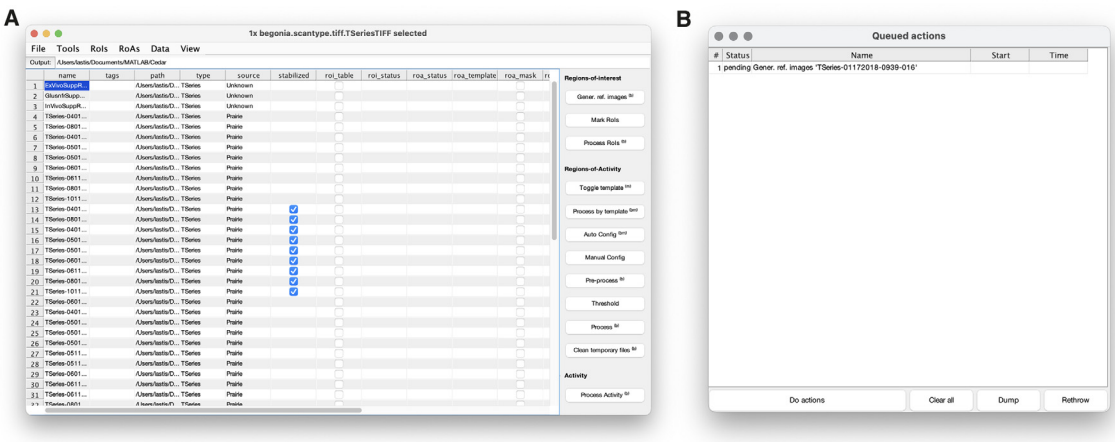

FIGURE 3 | Begonia includes a data management GUI with **(A)** a main window where rows represent data entities (typically imaging data) and columns contain corresponding metadata. Actions in the main window can be run immediately or be added as tasks to a processing queue **(B)** that can be loaded for time-consuming batch processing.

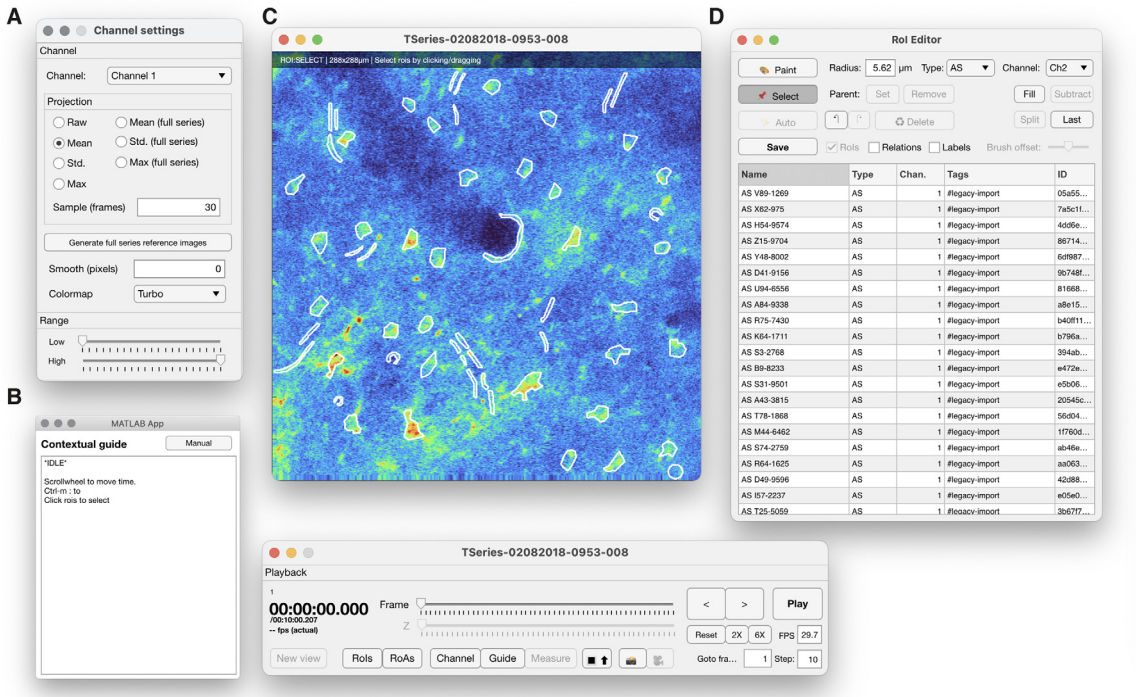

FIGURE 4 | The ROI manager provided in Begonia comprises the following features: **(A)** a view controller that determines what and how imaging data should be displayed, **(B)** a contextual guide window that informs the user of useful shortcuts and keyboard commands for the current mode. **(C)** The main image window, where raw imaging data or running averages or various projections of the imaging data can be displayed. Manually segmented ROIs are drawn into the overlay. **(D)** An ROI editor that organizes the ROIs and enables the user to classify, rename, delete or modify ROIs.

The ROA analysis can be executed by running a few functions in series and the results can be viewed in a similar fashion. The ROA analysis is simplified by using the data management GUI which guides the analyst through the following steps: (1) loading imaging data into the GUI by searching specified directories for supported imaging formats; (2) setting the two smoothing parameters by either clicking "Auto config" or "Manual config"; (3) running the pre-processing by clicking the "Pre-process" button; (4) previewing detected events and adjusting the detection threshold in the ROA GUI (**Figure 5**) by clicking the "Threshold" button. The GUI also enables filtering small and short events as well as ignoring regions around the edge of the FOV or other user-defined areas; and (5) converting the detected, filtered events to time series traces of (a) the density of Ca^{2+} signal events per time unit and (b) the number of new events per frame. Metrics about the events, such as size, duration, and timing, are saved in a table where each row represents one event.

This list of output of the ROA algorithm is less extensive than that of the AQuA algorithm (Wang et al., 2019). Most importantly, AQuA provides information about the spatial dynamics of every single Ca^{2+} event and applies a set of rules to separate Ca^{2+} events that may be splitting into several events, or merging into larger events. The overall performance of the ROA algorithm was compared to the AQuA algorithm using a downsampled dataset detecting the same trends in Ca^{2+} signaling across different sleep stages in Bojarskaite et al. (2020).

ROA Activity in ROIs Analysis

As there is substantial evidence that the astroglial subcompartments behave differently, separate analyses of anatomical subcompartments are warranted (Bazargani and Attwell, 2016). The ROA analysis output does not disclose the underlying anatomical structure of the tissue. Therefore the output of the ROA algorithm can be filtered based on manually defined ROIs providing the percentage of an ROI or subcompartment active at a given time.

Accessibility

The Begonia toolbox may be downloaded at https://github.com/GliaLab/Begonia. A detailed user manual and links to third party software packages and links to instructional videos are provided there as well as a user community discussion group.

DISCUSSION

Deciphering astroglial Ca^{2+} signals remains one of the biggest challenges for the field of glioscience (Semyanov et al., 2020). Even though a plethora of functions are thought to be supported by astroglial Ca^{2+} signals, the interpretation and importance of these signals are still somewhat controversial (Bazargani and Attwell, 2016; Shigetomi et al., 2016). When studying unanesthetized awake-behaving mice, a range of Ca^{2+} signals can be detected, from small events close to the level of noise

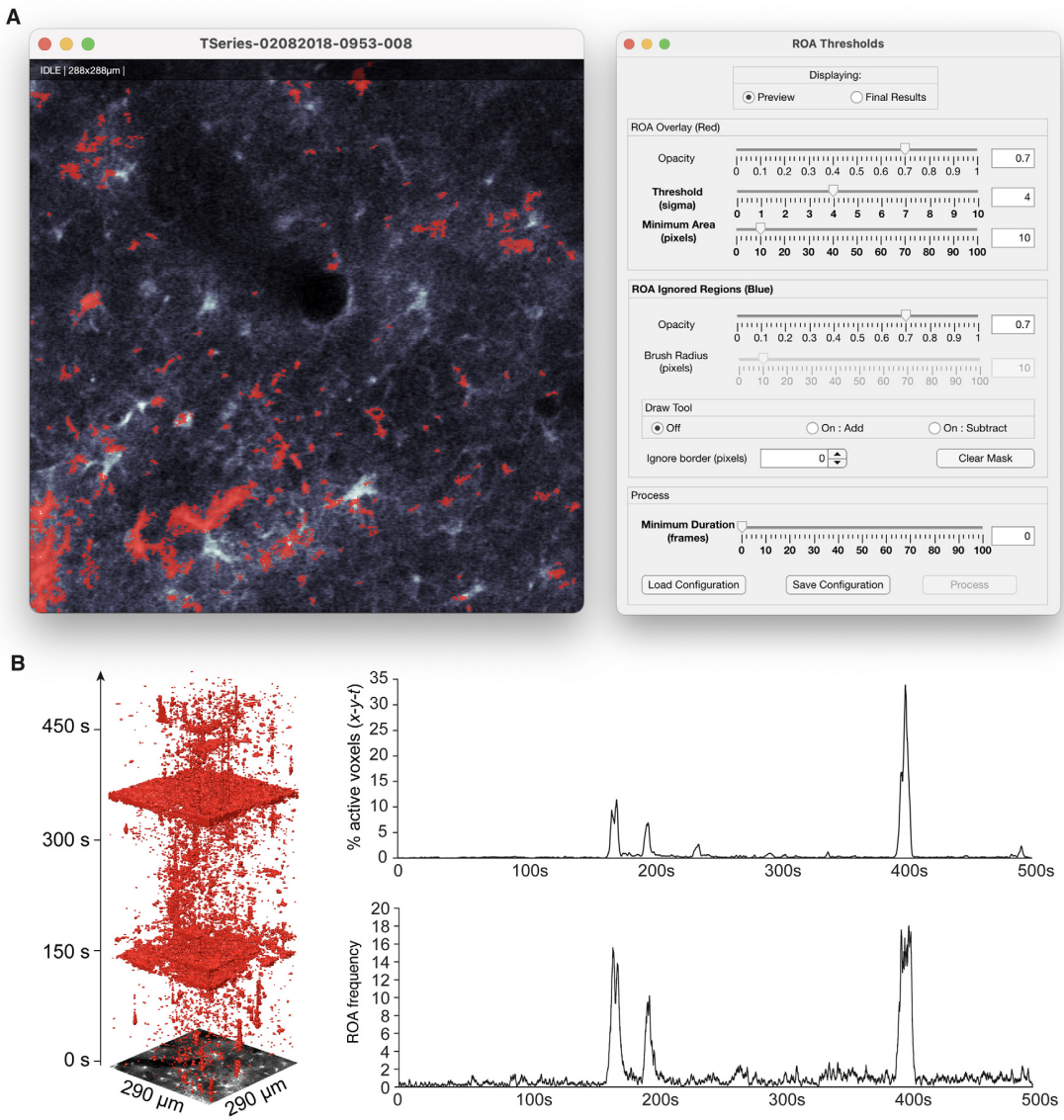

FIGURE 5 | ROA thresholding and output. **(A)** The thresholding step of the ROA algorithm is supported by a GUI that displays an overlay of the ROAs on top of the imaging data, and allows for interactive adjustment of the Ca^{2+} event detection threshold, adjusting the minimum size and duration of events, and defining regions that should be ignored. **(B)** An *x-y-t* volume rendering of a time series of astrocytic Ca^{2+} signals and corresponding traces of ROA density (% active voxels) and ROA frequency events per minute per μm^2.

to global increases in astrocytic Ca^{2+} signaling across the cortex in relation to neuromodulatory activity (Srinivasan et al., 2015; Bojarskaite et al., 2020). To better characterize this wide range of event types is a key first step in identifying their role in the circuitry, and may contribute to solving some of the controversies in this field. Here, we present a toolbox tailor-made for the analyses of two-photon microscopy data of astrocytic Ca^{2+} signals in conjunction with rich behavioral data, from raw data to aggregated results in tables.

A large proportion of astroglial Ca^{2+} signals are likely stochastic events (Semyanov et al., 2020), and under certain conditions, they are quite infrequent (Bojarskaite et al., 2020). In these cases, long acquisition times are warranted (e.g., time series of 10 min or more) to accurately quantify event rates and dynamics. Furthermore, when imaging awake mice, a high frame rate is warranted to be able to effectively remove movement artifacts (Pnevmatikakis and Giovannucci, 2017). For these reasons, astroglial Ca^{2+} imaging time series from awake mice are often large files up to tens of gigabytes. We have therefore gone to great lengths to optimize Begonia's processing to run quickly on large files even on moderate performance computers. The workflow has been organized in such a way that the time-consuming steps of the analyses can be performed unsupervised. Moreover, an important goal with

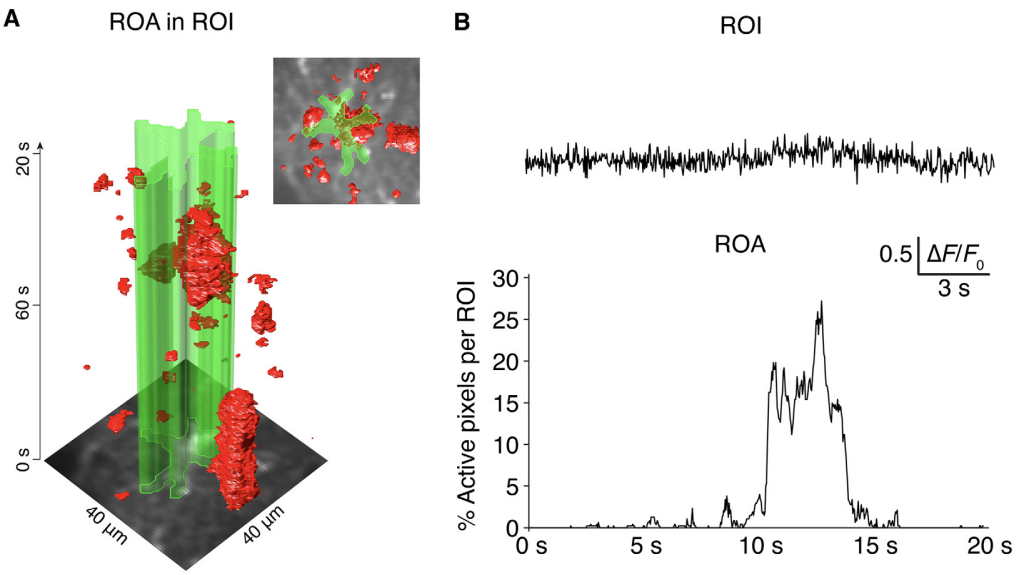

FIGURE 6 | ROA algorithm vs. ROI analyses. **(A)** The complex spatiotemporal distribution of astroglial Ca^{2+} signals presented as an *x-y-t* volume rendering. The outline of an astrocyte (ROI) is presented in green. **(B)** The ROA algorithm is considerably more sensitive than a standard ROI-based analysis, as evident when comparing the percentage of active pixels detected with the ROA algorithm within the ROI defined in **(A)**, compared to the extracted mean fluorescence from the ROI defined in **(A)** where no signals would be detected with a standard peak detection algorithm.

TABLE 1 | The primary outputs from Begonia and where to find them.

Output	Description
ROA event table	Each row represents one event. The table contains the center position, start frame, end frame, duration, size and duration. Saved with the key-value pair "roa_table" after processing.
ROA traces	Time series of roa frequency (new events per frame) and ROA density (active *x-y-t* voxels) key-value pair "roa_traces" after processing.
ROA mask	A binary 3D matrix representing the imaging time series, where 1's represent detected events. Saved with the key-value pair "roa_mask_chx" (*x* denoting the channel where ROAs have been detected).
ROA 3D plot	A GUI is provided to produce 3D ROA plots as in **Figure 5B**.
ROI table	A table containing the manually segmented ROIs. Each row represents one ROI and contains the size, location, channel, name and a unique identifier of the ROI. Saved with the key-value pair "roi_table."
ROI traces	Raw and $\Delta F/F_0$ normalized signals from ROIs. Saved with the key-value pair "roi_signals_raw" and "roi_signals_dff."
ROI active pixels	Fraction of ROI that has a ROA per time unit. Saved with the key-value pair "roi_signals_raw" and "roi_signal_rpa."

the toolbox is responsive behavior and a short waiting time when manually interacting with the data. Therefore all large data in the pipeline are loaded lazily, i.e., on request. Even so, some of the analyses provided in Begonia will be slow to execute with large recordings due to the sheer number of calculations performed. Incorporating hardware-accelerated analyses could hold great potential for some of these time-consuming steps in the future.

The first hurdle in the analyses of two-photon microscopy data is to import the imaging data in an efficient fashion to the analysis platform. Two-photon microscopy data are typically stored as TIFF files (either single-frame files or multi-page TIFFs). Even so the TIFF format allows for many variations and data from different channels, trials and most importantly metadata are saved in different ways by different setups. Consequently, there are no standardized ways to read two-photon microscopy data across platforms. ImageJ and FIJI offer a low threshold plug-and-play software that can handle many different TIFF implementations but has the drawback of confining the analyses to the ImageJ framework (Schindelin et al., 2012; Schneider et al., 2012). Begonia offers direct support for imaging data from ScanImage and PrarieView software as well as TIFF files read by the TIFFStack (Muir and Kampa, 2014) library, but just as important provides an API for easy adaptation of other imaging data formats to our pipeline.

In this article, we present an event-based Ca^{2+} signal detection tool for the unbiased quantification of astrocytic Ca^{2+} signals with a high level of detail. The algorithm separates Ca^{2+} signals from the noise for each individual pixel over time, before connecting the active *x-y-t* voxels to Ca^{2+} signal events. The ROA algorithm performs considerably better than static ROI analyses in terms of sensitivity and accuracy (see **Figure 6** and Bojarskaite et al., 2020). An earlier iteration of this algorithm was used for the analyses of Ca^{2+} signaling data in Bojarskaite et al. (2020). The present algorithm calculates the threshold for signal detection slightly differently, similar to that of the AQuA algorithm (Wang et al., 2019). The event

definition of the ROA algorithm and the first part of the AQuA algorithm share many similarities, but there are also noteworthy differences. In our hands, the AQuA method had some limitations that made it impractical or even impossible to use for our large files of high frame rate imaging data (Bojarskaite et al., 2020). The first issue was processing time. For our long (e.g., 18,000 frames), 30 Hz two-photon microscopy data, processing with the AQuA algorithm failed even on a high-performance computer (128 Gb RAM, 18 cores) due to running out of RAM. When run on a moderate performance computer, a moderately sized dataset of 5,000 frames recording that ran in 267 s with the ROA algorithm took ∼2 full days to analyze with the ROA algorithm. Moreover, the AQuA algorithm did not perform well in terms of separation of signal from the noise in our data, that had a poor SNR due to our high acquisition rates, resulting in high levels of artifactual events detected. The ROA algorithm is considerably less extensive than the AQuA algorithm as it does not analyze the spatiotemporal dynamics of each signaling event separately. Rather it only reports on the frequency of starting events and density of events per time unit in the full FOV or per manually segmented compartments, as well as descriptive measures of maximum spatial extent and duration of individual ROAs. This in part explains the large difference in processing times between the two algorithms—i.e., the ROA algorithm is a substantially more lightweight algorithm.

The size and duration of astrocytic Ca^{2+} events are known to follow a power law distribution (Jung et al., 1998; Wu et al., 2014; Semyanov et al., 2020), and Ca^{2+} signals in the smallest processes and leaflets are of considerably smaller spatial extent than the resolution limit of optical (non-super resolution) microscopy allows. Therefore, even minute changes in the settings and consequently the thresholds and filtering applied will profoundly change the distribution of Ca^{2+} signal events detected. These reasons call for being conservative when determining the threshold for separating signal and noise and is also an argument for not considering the smallest detected events in a given recording. An interactive tool is provided that enables easy adjustment of the threshold applied and the minimum sizes and durations allowed for a Ca^{2+} event.

One goal with the ROA method was to provide an algorithm that could be used without too many input parameters to enable a more direct comparison between datasets recorded with different hardware or settings. We have therefore provided a pre-processing method that evaluates the imaging data and determines what filtering is appropriate to: (a) ensure an accurate identification of events with few artifacts; and (b) to enable more direct comparisons between data from different datasets. The pre-processing will find suitable parameters for spatial and temporal smoothing until an empirically chosen level of SNR of at least nine is attained. We have tested the algorithm on datasets acquired in three different laboratories with different types of hardware and acquisition parameters. Even so we cannot be certain that the target SNR of nine is optimal for two-photon image recordings of all types, as photon statistics and data quality vary significantly across acquisition hardware, fluorophores, and experimental protocols.

In principle, other types of fluorescent data than astrocytic Ca^{2+} signals could be possible to analyze with Begonia. The pipeline already supports signal extraction and neuropil subtraction from neuronal ROIs (accessible through the API). Moreover, the ROA algorithm could prove useful in the future for quantifying both neuronal Ca^{2+} signals or other types of dynamic fluorescent sensors but has not been validated for this purpose yet.

To the best of our knowledge, no algorithm exists for automatically segmenting images of astroglial cells into their respective subcellular compartments of somata, processes, and endfeet. This is also true for our ROA method. Therefore, we provide the option of integrating manually segmented ROIs with the automatic ROA algorithm, such that subcompartment specific ROA signals can be described separately. Ideally ROIs should have been detected and correctly classified without manual intervention. Potentially, machine learning algorithms, using manually segmented ROIs as a training dataset could provide such functionality in the future.

Our toolbox requires imaging data to be adapted to standardized classes and be funneled through our data management pipeline. We believe this is a major strength for this toolbox as it allows for more efficient and flexible approaches to data management. This may, however, also be perceived as a potential drawback—the tools in our toolbox are not standalone pieces of software that take general image formats and directly outputs results—rather, the tools are embedded in a workflow pipeline that must be executed in a certain fashion. Consequently, the threshold to start using the toolbox could be somewhat higher. To mitigate these problems, we have made instructional videos and live script example cases to be run with example datasets to quickly familiarize potential users with the API. GUIs are also provided for users that are not comfortable scripting their analyses. The Begonia software published here is the first version of this package, built to be easily extendable, and we hope that the project will evolve both locally and in collaboration with potential external users through the GitHub repository and associated user community discussion group.

DATA AVAILABILITY STATEMENT

Publicly available datasets were analyzed in this study. Links to the example datasets can be found here: http://github.com/GliaLab/Begonia.

ETHICS STATEMENT

The animal study was reviewed and approved by the Norwegian Food Safety Authority.

AUTHOR CONTRIBUTIONS

KV and RE: conceptualization and funding acquisition. DB, KÅ, EH, KP, CC, GH, and RE: methodology. RE: resources. DB, KÅ, LB, CC, GH, and RE: writing—original draft. LB and EH: acquiring microscopy data and testing. DB, KÅ, EH, KP, KV, LB,

CC, GH, and RE: writing—review and editing. KP, KV, and RE: supervision. All authors contributed to the article and approved the submitted version.

FUNDING

We acknowledge the support by UNINETT Sigma2 AS for making data storage available through NIRD, project NS9021K.

This work was supported by the Research Council of Norway (Norges Forskningsråd; grants #249988, #240476, and #262552), the South-Eastern Norway Regional Health Authority (Helse Sør-Øst RHF; grant #2016070), the European Union's Seventh Framework Program for research, technological development, and demonstration under grant agreement no. 601055, The National Association of Public Health, The Olav Thon Foundation, and the Letten Foundation.

REFERENCES

Barrett, M. J. P., Ferrari, K. D., Stobart, J. L., Holub, M., and Weber, B. (2018). CHIPS: an extensible toolbox for cellular and hemodynamic two-photon image analysis. *Neuroinformatics* 16, 145–147. doi: 10.1007/s12021-017-9344-y

Bartlett, M. S. (1947). The use of transformations. *Biometrics* 3, 39–52. doi: 10.2307/3001536

Bazargani, N., and Attwell, D. (2016). Astrocyte calcium signaling: the third wave. *Nat. Neurosci.* 19, 182–189. doi: 10.1038/nn.4201

Bojarskaite, L., Bjørnstad, D. M., Pettersen, K. H., Cunen, C., Hermansen, G. H., Åbjørsbråten, K. S., et al. (2020). Astrocytic Ca signaling is reduced during sleep and is involved in the regulation of slow wave sleep. *Nat. Commun.* 11:3240. doi: 10.1038/s41467-020-17062-2

Casella, G., and Berger, R. L. (2002). *Statistical Inference*. Chicago, IL: Cengage Learning.

Cornell-Bell, A. H., Finkbeiner, S. M., Cooper, M. S., and Smith, S. J. (1990). Glutamate induces calcium waves in cultured astrocytes: long-range glial signaling. *Science* 247, 470–473. doi: 10.1126/science.1967852

Danielyan, A., Wu, Y.-W., Shih, P.-Y., Dembitskaya, Y., and Semyanov, A. (2014). Denoising of two-photon fluorescence images with block-matching 3D filtering. *Methods* 68, 308–316. doi: 10.1016/j.ymeth.2014.03.010

Ebner-Priemer, U. W., Eid, M., Kleindienst, N., Stabenow, S., and Trull, T. J. (2009). Analytic strategies for understanding affective (in)stability and other dynamic processes in psychopathology. *J. Abnorm. Psychol.* 118, 195–202. doi: 10.1037/a0014868

Ebner-Priemer, U. W., Kuo, J., Kleindienst, N., Welch, S. S., Reisch, T., Reinhard, I., et al. (2007). State affective instability in borderline personality disorder assessed by ambulatory monitoring. *Psychol. Med.* 37, 961–970. doi: 10.1017/S0033291706009706

Eilert-Olsen, M., Hjukse, J. B., Thoren, A. E., Tang, W., Enger, R., Jensen, V., et al. (2019). Astroglial endfeet exhibit distinct Ca signals during hypoosmotic conditions. *Glia* 67, 2399–2409. doi: 10.1002/glia.23692

Enger, R., Dukefoss, D. B., Tang, W., Pettersen, K. H., Bjørnstad, D. M., Helm, P. J., et al. (2017). Deletion of aquaporin-4 curtails extracellular glutamate elevation in cortical spreading depression in awake mice. *Cereb. Cortex* 27, 24–33. doi: 10.1093/cercor/bhw359

Garrett, D. D., Samanez-Larkin, G. R., MacDonald, S. W. S., Lindenberger, U., McIntosh, A. R., and Grady, C. L. (2013). Moment-to-moment brain signal variability: a next frontier in human brain mapping? *Neurosci. Biobehav. Rev.* 37, 610–624. doi: 10.1016/j.neubiorev.2013.02.015

Jung, P., Cornell-Bell, A., Madden, K. S., and Moss, F. (1998). Noise-induced spiral waves in astrocyte syncytia show evidence of self-organized criticality. *J. Neurophysiol.* 79, 1098–1101. doi: 10.1152/jn.1998.79.2.1098

Muir, D. R., and Kampa, B. M. (2014). FocusStack and StimServer: a new open source MATLAB toolchain for visual stimulation and analysis of two-photon calcium neuronal imaging data. *Front. Neuroinform.* 8:85. doi: 10.3389/fninf.2014.00085

Neumann, J., von Neumann, J., Kent, R. H., Bellinson, H. R., and Hart, B. I. (1941). The mean square successive difference. *Ann. Math. Stat.* 12, 153–162. doi: 10.1214/aoms/1177731746

Nomi, J. S., Bolt, T. S., Ezie, C. E. C., Uddin, L. Q., and Heller, A. S. (2017). Moment-to-moment BOLD signal variability reflects regional changes in neural flexibility across the lifespan. *J. Neurosci.* 37, 5539–5548. doi: 10.1523/JNEUROSCI.3408-16.2017

Pnevmatikakis, E. A., and Giovannucci, A. (2017). NoRMCorre: an online algorithm for piecewise rigid motion correction of calcium imaging data. *J. Neurosci. Methods* 291, 83–94. doi: 10.1016/j.jneumeth.2017.07.031

Rusakov, D. A., Zheng, K., and Henneberger, C. (2011). Astrocytes as regulators of synaptic function: a quest for the Ca^{2+} master key. *Neuroscientist* 17, 513–523. doi: 10.1177/1073858410387304

Schindelin, J., Arganda-Carreras, I., Frise, E., Kaynig, V., Longair, M., Pietzsch, T., et al. (2012). Fiji: an open-source platform for biological-image analysis. *Nat. Methods* 9, 676–682. doi: 10.1038/nmeth.2019

Schneider, C. A., Rasband, W. S., and Eliceiri, K. W. (2012). NIH image to imagej: 25 years of image analysis. *Nat. Methods* 9, 671–675. doi: 10.1038/nmeth.2089

Semyanov, A. (2019). Spatiotemporal pattern of calcium activity in astrocytic network. *Cell Calcium* 78, 15–25. doi: 10.1016/j.ceca.2018.12.007

Semyanov, A., Henneberger, C., and Agarwal, A. (2020). Making sense of astrocytic calcium signals—from acquisition to interpretation. *Nat. Rev. Neurosci.* 21, 551–564. doi: 10.1038/s41583-020-0361-8

Shigetomi, E., Patel, S., and Khakh, B. S. (2016). Probing the complexities of astrocyte calcium signaling. *Trends Cell Biol.* 26, 300–312. doi: 10.1016/j.tcb.2016.01.003

Srinivasan, R., Huang, B. S., Venugopal, S., Johnston, A. D., Chai, H., Zeng, H., et al. (2015). Ca^{2+} signaling in astrocytes from Ip3r2(−/−) mice in brain slices and during startle responses in vivo. *Nat. Neurosci.* 18, 708–717. doi: 10.1038/nn.4001

Stobart, J. L., Ferrari, K. D., Barrett, M. J. P., Glück, C., Stobart, M. J., Zuend, M., et al. (2018). Cortical circuit activity evokes rapid astrocyte calcium signals on a similar timescale to neurons. *Neuron* 98, 726–735.e4.doi: 10.1016/j.neuron.2018.03.050

Thrane, A. S., Rangroo Thrane, V., Zeppenfeld, D., Lou, N., Xu, Q., Nagelhus, E. A., et al. (2012). General anesthesia selectively disrupts astrocyte calcium signaling in the awake mouse cortex. *Proc. Natl. Acad. Sci. U S A* 109, 18974–18979. doi: 10.1073/pnas.1209448109

Verkhratsky, A., and Parpura, V. (2013). "Astroglial calcium signaling and calcium waves," in *Gap Junctions in the Brain*, ed E. Dere (Elsevier, Inc.), 51–68. doi: 10.1016/b978-0-12-415901-3.00004-9

Wang, Y., DelRosso, N. V., Vaidyanathan, T. V., Cahill, M. K., Reitman, M. E., Pittolo, S., et al. (2019). Accurate quantification of astrocyte and neurotransmitter fluorescence dynamics for single-cell and population-level physiology. *Nat. Neurosci.* 22, 1936–1944. doi: 10.1038/s41593-019-0492-2

Wu, Y.-W., Tang, X., Arizono, M., Bannai, H., Shih, P.-Y., Dembitskaya, Y., et al. (2014). Spatiotemporal calcium dynamics in single astrocytes and its modulation by neuronal activity. *Cell Calcium* 55, 119–129. doi: 10.1016/j.ceca.2013.12.006

Conflict of Interest: The authors declare that the research was conducted in the absence of any commercial or financial relationships that could be construed as a potential conflict of interest.

frontiers in Cellular Neuroscience

REVIEW
published: 07 June 2021
doi: 10.3389/fncel.2021.682888

Potential and Realized Impact of Astroglia Ca^{2+} Dynamics on Circuit Function and Behavior

Eunice Y. Lim[1,2], *Liang Ye*[1] *and Martin Paukert*[1,2]*

[1] Department of Cellular and Integrative Physiology, University of Texas Health Science Center at San Antonio, San Antonio, TX, United States, [2] Center for Biomedical Neuroscience, University of Texas Health Science Center at San Antonio, San Antonio, TX, United States

Astroglia display a wide range of spontaneous and behavioral state-dependent Ca^{2+} dynamics. During heightened vigilance, noradrenergic signaling leads to quasi-synchronous Ca^{2+} elevations encompassing soma and processes across the brain-wide astroglia network. Distinct from this vigilance-associated global Ca^{2+} rise are apparently spontaneous fluctuations within spatially restricted microdomains. Over the years, several strategies have been pursued to shed light on the physiological impact of these signals including deletion of endogenous ion channels or receptors and reduction of intracellular Ca^{2+} through buffering, extrusion or inhibition of release. Some experiments that revealed the most compelling behavioral alterations employed chemogenetic and optogenetic manipulations to modify astroglia Ca^{2+} signaling. However, there is considerable contrast between these findings and the comparatively modest effects of inhibiting endogenous sources of Ca^{2+}. In this review, we describe the underlying mechanisms of various forms of astroglia Ca^{2+} signaling as well as the functional consequences of their inhibition. We then discuss how the effects of exogenous astroglia Ca^{2+} modification combined with our knowledge of physiological mechanisms of astroglia Ca^{2+} activation could guide further refinement of behavioral paradigms that will help elucidate the natural Ca^{2+}-dependent function of astroglia.

Keywords: astroglia, behavioral state, calcium, astrocyte, neuromodulation, norepinephrine, Bergmann glia, vigilance

OPEN ACCESS

Edited by:
Rolf Sprengel,
Max Planck Institute for Medical Research (MPIMF), Germany

Reviewed by:
Fritjof Helmchen,
University of Zurich, Switzerland
Mazahir T. Hasan,
Achucarro Basque Center for Neuroscience, Spain
J. Troy Littleton,
Massachusetts Institute of Technology, United States

***Correspondence:**
Martin Paukert
paukertm@uthscsa.edu

Specialty section:
This article was submitted to Non-Neuronal Cells, a section of the journal Frontiers in Cellular Neuroscience

Received: *19 March 2021*
Accepted: *03 May 2021*
Published: *07 June 2021*

Citation:
Lim EY, Ye L and Paukert M (2021) Potential and Realized Impact of Astroglia Ca^{2+} Dynamics on Circuit Function and Behavior. Front. Cell. Neurosci. 15:682888. doi: 10.3389/fncel.2021.682888

INTRODUCTION

Astroglia are ubiquitous in the brain and exhibit a range of morphological structure adapted for each brain region. Star-shaped or protoplasmic astrocytes in gray matter possess minimal internal structure and are shaped by the surrounding neuropil, whereas fibrous astrocytes in white matter contain fibrils that assist integration within axon bundles (Köhler et al., 2019). Specialized astrocytes like retinal Müller cells and cerebellar Bergmann glia have distinct orientation that aligns with the stratification of nearby sensory cells and neurons, respectively (Siegel et al., 1991; Franze et al., 2007). Across all astroglia, their space-filling arrangement provides contact with a myriad of neural cell types including the vasculature (McCaslin et al., 2011). Astroglia perform dual functions of both isolating and modulating individual synaptic contacts, conceptualized in the tripartite synapse model (Araque et al., 1999), and also maintaining extensive intercellular communication through gap junctions producing an interconnected composition within the brain (Giaume and McCarthy, 1996; Theis and Giaume, 2012). Expression of numerous neurotransmitter receptors, ion channels, and transporters (Verkhratsky and Nedergaard, 2018) demonstrates that both anatomically and

functionally, astroglia are primed for a role in sensing and dynamically modulating brain-wide neural networks. Astroglia do not fire action potentials and rather display a large and selective permeability to potassium, conferring the exceptionally negative resting membrane potential of −85 to −90 mV (Kuffler, 1967; Ransom and Goldring, 1973). High potassium conductance underlies their ability to buffer extracellular ions and allows modulation of neuronal activity (Wang et al., 2015; Weiss et al., 2019).

Aside from a relatively simple electrical constitution, astroglia abundantly express receptors and molecular components that produce a range of dynamic fluctuations in intracellular Ca^{2+}. A list of many but not all membrane proteins enabling rise in astroglia intracellular Ca^{2+} is shown in **Table 1**. The following organizing principles were used: dependence on inositol-triphosphate receptor type 2 (IP_3R2 protein or *ITPR2* gene) – whether demonstrated or expected; *in vivo* characterization – a crucial factor given that even in the most conservative *ex vivo* preparation that is acute brain slice preparation, alterations in astroglia protein expression, morphology and Ca^{2+} dynamics can occur within less than 2 h of preparation (Takano et al., 2014); use of unanesthetized animal model – since general anesthesia strongly suppresses global astroglia Ca^{2+} elevations (Nimmerjahn et al., 2009; Thrane et al., 2012); and trigger of Ca^{2+} signal – to describe whether or not astroglia signaling pathways contributing to Ca^{2+} dynamics have been studied within their physiological dynamic range. Since in most cases it is very difficult if even possible to quantify the physiological dynamic range, for the tables we take a conservative approach and consider as "physiological" only astroglia Ca^{2+} dynamics that occur spontaneously or are driven by sensory stimulation or behavioral state, which we distinguish from electrical stimulation of an axonal fiber tract, application of a receptor agonist, or activation of an exogenously expressed receptor or channel. Various exogenous proteins for manipulation of astroglia intracellular Ca^{2+} are further explored in **Table 2**. We follow these concepts in order to emphasize the importance of using *in vivo* experimental paradigms that preserve or at least mimic the natural condition in order to understand which properties among the many purported abilities of astrocytes are physiologically employed. For each experiment, if concepts two or three are met, they are represented in green, and if not, they are represented in orange or without color. The more concepts are represented in green, we consider the respective finding to demonstrate a realized astroglia function. Conversely, the fewer concepts are represented in green, we consider that the respective finding may indicate a potential astroglia function.

We intentionally do not categorize astroglia Ca^{2+} dynamics by somatic or process location since, as we will discuss, a considerable portion of process Ca^{2+} elevations share the underlying mechanism with somatic Ca^{2+} elevations. Also, it is noted that astroglia Ca^{2+} signaling has been tightly associated with the concept of gliotransmission, which is the Ca^{2+}-dependent vesicular release of signaling molecules from astroglia (Araque et al., 2014). The existence and/or significance of this concept still faces controversy (Fiacco and McCarthy, 2018; Savtchouk and Volterra, 2018). It is beyond the reach of this review to resolve this controversy. Instead, we take an agnostic glial neuromodulation view at what has been found about astroglia Ca^{2+} dynamics in living animals and how it is or may be linked to neuronal activity and behavior.

In this review, we describe the various forms of astroglia Ca^{2+} signaling distinguishing between (i) whole-cell, behavior-associated signals as well as (ii) spatially localized microdomain activity, and (iii) the functional consequences of their inhibition. We then discuss (iv) what effects of exogenous astroglia Ca^{2+} activation have been identified that could guide further refinement of behavioral paradigms to study the natural function of astroglia.

MECHANISMS OF GLOBAL, BEHAVIOR-ASSOCIATED ASTROGLIA Ca^{2+} ACTIVATION

Relating mammalian astroglia Ca^{2+} dynamics directly to behavioral state became possible with the introduction of an approach that allows study of cellular brain activity in head-fixed awake mice on a spherical treadmill using two-photon microscopy (Dombeck et al., 2007). It was found that protoplasmic astrocytes in the somatosensory cortex produce Ca^{2+} transients that correlate with bouts of motor activity. The head-fixation two-photon microscopy paradigm was soon adopted to study cerebellar Bergmann glia (Nimmerjahn et al., 2009). Three distinct types of Ca^{2+} signals were defined in this seminal study. First, 'bursts' are spontaneous radially spreading Ca^{2+} elevations that depend on purinergic signaling and can also be detected in anesthetized rats and mice (Hoogland et al., 2009). Since they are not at all, or extremely rarely detected in awake mice through chronic cranial windows after sufficient tissue recovery from surgery (Paukert et al., 2014), they may be triggered by trauma-associated ATP release. Second, 'sparkles' are spontaneous, low-frequency Ca^{2+} elevations that occur asynchronously in individual Bergmann glia process domains and persist at lower frequency under isoflurane anesthesia. These events may correspond to microdomain Ca^{2+} activity in protoplasmic astrocytes which will be discussed below. Finally, 'flares' are a robust, whole-cell Ca^{2+} transient encompassing Bergmann glia in the entire field of view, are detectable only in awake mice, and relate to the onset of motor activity.

The underlying mechanism of this motor activity-associated astroglia Ca^{2+} elevation remained elusive in these initial studies. It is now known that locomotion is associated with sufficient arousal to trigger the release of norepinephrine and acetylcholine. In mouse primary visual cortex for example, noradrenergic signaling is responsible for tonic depolarization of the membrane potential of layer 2/3 and 4 excitatory neurons as well as interneurons during locomotion (Polack et al., 2013). Locomotion also evokes a Ca^{2+} rise in vasoactive intestinal peptide (VIP)-positive neurons, which depends on activation of nicotinic acetylcholine receptors (Fu et al., 2014). Finally, direct observation of terminal Ca^{2+} dynamics was accomplished by expression of the genetically-encoded Ca^{2+} indicator (GECI) GCaMP6s in mouse noradrenergic and cholinergic neurons,

TABLE 1 | Membrane proteins controlling *in situ* astroglia intracellular Ca^{2+}.

Protein	Biological function	IP_3R2-dependent proven/ expected	*In vivo* awake/ anesthesia	Behavior-induced* awake/ anesthesia
mGlu	Co-activated with mAChRs to induce LTP in hippocampal CA3-CA1 synapses (Navarrete et al., 2012)	proven	anesthesia	No
$mGlu_5$	Purported role in arteriole dilation (Takano et al., 2006;	expected	anesthesia	No
	Zonta et al., 2003)	expected	anesthesia	Yes
	Challenged by lack of mGluR5 in adult mouse cortical astrocytes (Sun et al., 2013)	N/A	N/A	N/A
	Lack of phenotype in IP_3R2 knockout mice (Nizar et al., 2013;	proven no	anesthesia	Yes
	Bonder and McCarthy, 2014)	proven no	awake	Yes
$mGlu_{2/3}$	Activated along with $GABA_B$ receptors in hippocampal astrocytes following mossy fiber stimulation (Haustein et al., 2014)	expected	No	No
GluA1/A4# (AMPAR)	Impairing Ca^{2+}-permeability by GluA2 overexpression in cerebellar Bergmann glia affects synaptic process coverage (Iino et al., 2001)#	No	awake	unresolved
	KO of GluA1 and GluA6, impairs fine motor control and associative conditioning in addition to affect synaptic process coverage in the adult (Saab et al., 2012)#	expected no	awake	unresolved
$P2Y_1$	Cortical astrocyte hyperactivity in Alzheimer's disease mouse model (Delekate et al., 2014)	expected	anesthesia	Spont**
	Spontaneous inner supporting cell activity in the developing cochlea (Babola et al., 2020);	expected	No	spont**
	Occurs also *in vivo* (Babola et al., 2018)	expected	awake	spont**
P2X1	Astrocytes contribute to functional hyperemia through capillary dilation (Mishra et al., 2016)	expected no	anesthesia	Yes
mAChR	Enables sensory-evoked plasticity in barrel cortex (Takata et al., 2011),	proven	anesthesia	No
	in primary visual cortex (Chen et al., 2012),	proven	anesthesia	No
	in hippocampus (Navarrete et al., 2012)	proven	anesthesia	No
α7nAChR#	Wakefulness-dependent release of D-serine from hippocampal astrocytes (Papouin et al., 2017)#	expected no	awake	Yes
$GABA_BR$#	Activated along with mGluR2/3 receptors in hippocampal astrocytes following mossy fiber stimulation (Haustein et al., 2014);	expected	No	No
	Participates in hippocampal theta and gamma oscillations (Perea et al., 2016)#;	proven	anesthesia	Yes
	Activated in prefrontal cortex astrocytes sustains goal-directed behaviors (Mederos et al., 2021)#	proven	awake	Yes
CB1R#	Endocannabinoids potentiate hippocampal CA3–CA1 synaptic transmission (Navarrete and Araque, 2010);	expected	No	No
	Enables recognition memory through control of D-serine availability (Robin et al., 2018)#;	expected	awake	Yes
	Exogenous cannabinoids disrupt spatial working memory (Han et al., 2012)#	expected	awake	No
α_1-AR	Vigilance-dependent Ca^{2+} activation of astroglia in somatosensory cortex (Ding et al., 2013);	expected	awake	Yes
	Simultaneous vigilance-dependent Ca^{2+} activation of astroglia in primary visual cortex and cerebellum (Paukert et al., 2014);	expected	awake	Yes
	Transcranial direct current stimulation-induced cortical plasticity (Monai et al., 2016)	proven	awake	No
Oct-TyrR#	Required for startle-induced Drosophila astroglia Ca^{2+} response and consecutive modulation of dopamine neuron activity (Ma et al., 2016)#	No	awake	Yes
α_{1A}-AR#	Activation on $Hes5^+$ spinal cord superficial dorsal horn astrocytes causes mechanical hypersensitivity (Kohro et al., 2020)#;	proven	awake	Yes
	Required on cerebellar Bergmann glia for vigilance-dependent Ca^{2+}activation (Ye et al., 2020)#	expected	awake	Yes
α_{1B}-AR	Drives behavioral inactivity in Zebrafish upon futile struggle (Mu et al., 2019)	proven (IP_3R)	awake	Yes
TRPA1	Microdomain Ca^{2+} activity in hippocampal astrocytes regulates GABAergic signaling (Shigetomi et al., 2011); however, see mPTP below	No	No	spont**
Wtrw# (Water witch)	Required for startle-induced *Drosophila* astroglia Ca^{2+} response and consecutive modulation of dopamine neuron activity (Ma et al., 2016)#	No	awake	Yes
TrpML#	Microdomain Ca^{2+} activity in *Drosophila* astroglia contribute to CNS gas exchange homeostasis (Ma and Freeman, 2020) #	No	awake	spont**
mPTP	Microdomain Ca^{2+} activity in astrocytes is caused by mitochondrial mPTP and is enhanced by norepinephrine (Agarwal et al., 2017)	enhanced	awake	spont**

(Continued)

TABLE 1 | Continued

Protein	Biological function	IP_3R2-dependent proven/ expected	*In vivo* awake/ anesthesia	Behavior-induced* awake/ anesthesia
eNOS	Endothelial nitric oxide production enhances astrocyte endfeet Ca^{2+} elevations (Tran et al., 2018)	expected no	awake	Yes
Not defined	Store-dependent astroglia Ca^{2+} signaling contributes to:			
	Motor-skill learning (Padmashri et al., 2015);	proven	awake	Yes
	Synapse elimination (Yang et al., 2016);	proven	awake	Yes
	Functional hyperemia at the capillary level (Biesecker et al., 2016);	proven	anesthesia	Yes
	Regulation of sleep phases (Foley et al., 2017);	proven (IP_3R)	awake	Yes
	Regulation of sleep phases (Bojarskaite et al., 2020);	proven	awake	Yes
	Regulation of sleep drive (Ingiosi et al., 2020);	expected	awake	Yes
	Remote memory formation (Pinto-Duarte et al., 2019);	proven	awake	Yes
	Regulation of sensory-evoked cortical neuron population activity (Lines et al., 2020)	proven	awake	Yes

*Proteins are described in terms of the following: biological function; proven or expected dependence on IP_3R2; whether experiments were conducted in vivo and if so, whether done in awake (green) or anesthetized (orange) mice; and whether the Ca^{2+} signal is behavior-induced and if so, whether this was validated in awake (green) or anesthetized (orange) mice. #, indicates proteins for which functional expression in astroglia has been demonstrated by conditional gene deletion or rescue, and the respective studies are indicated individually. *, "Behavior-induced" indicates that a Ca^{2+} signal is caused by any form of sensory stimulation or awake behavior. Accepted manipulations are forms of acute or chronic suppression of endogenous signaling pathways. Any form of electrical, optical, or chemical overactivation of a nerve fiber tract or an endogenous or exogenous signaling pathway does not qualify. **, "spont" or spontaneous indicates Ca^{2+} signal is unprovoked and not triggered by a specific behavioral state.*

mGlu, metabotropic glutamate receptor; GluA, AMPA-type glutamate receptor; $P2Y_1$, P2Y purinoceptor 1; P2X1, P2X purinoceptor 1; mAChR, muscarinic acetylcholine receptor; α7nAChR, α7 nicotinic acetylcholine receptor; $GABA_BR$, metabotropic $GABA_B$ receptor; CB1R, cannabinoid receptor 1; α_1-AR, α_1-adrenergic receptor; Oct/TyrR, tyramine/octopamine receptor; TRPA1, transient receptor potential A1 channel; Wtrw, transient receptor potential channel Water witch; TrpML, transient receptor potential mucolipin channel (vertebrate orthologs TRPML1-3 or mucolipins 1-3); mPTP, mitochondrial permeability transition pore; eNOS, endothelial nitric oxide synthase.

TABLE 2 | Exogenous proteins for manipulation of astroglia intracellular Ca^{2+}.

Protein	Biological function	IP_3R2- dependent proven/ expected	*In vivo* awake/ anesthesia	Behavior-induced* awake/ anesthesia
Ca^{2+} ↓				
CalEx	Profoundly reduced Ca^{2+} in striatal astrocytes reduces microcircuit tonic inhibition and is associated with repetitive behavior (Yu et al., 2018),	expected +/or microdomain	awake	Yes
	in cortical astrocytes, it reduces voluntary ethanol consumption (Erickson et al., 2020)	expected +/or microdomain	awake	Yes
hM4Di	Reduced Ca^{2+} in hippocampal CA1 astrocytes impairs remote memory (Kol et al., 2020); (but see hM4Di also below)	expected no	awake	Yes
Ca^{2+} ↑				
MrgA1 (Gq)	Enhanced Ca^{2+} in cerebellar Bergmann glia causes reduction of extracellular K^+ and increase in Purkinje cell up-state (Wang et al., 2012)	expected	anesthesia	No
Arch	Arch activation in cortical astrocytes facilitates neuronal synchrony (Poskanzer and Yuste, 2016)	expected no	awake	No
hM3Dq	Enhanced Ca^{2+} in hippocampal CA1 astrocytes enhances memory acquisition (Adamsky et al., 2018)	expected	awake	No
Opto-Gq	Enhanced Ca^{2+} in hippocampal CA1 astrocytes enhances memory acquisition (Adamsky et al., 2018)	expected	awake	No
hM4Di	Enhanced Ca^{2+} in striatal astrocytes enhances synaptogenesis leading to hyperactivity and disrupted attention (Nagai et al., 2019),	expected	awake	No
	in cortical astrocytes, it changes neuronal delta activity (Durkee et al., 2019),	proven	anesthesia	No
	in striatal astrocytes, it induces changes in gene expression profile which can be exploited to compensate for changes in a mouse model of Huntington's disease (Yu et al., 2020)	expected	awake	No

*Exogenous manipulations are described using the same principles as in **Table 1**: biological function; proven or expected dependence on IP_3R2; whether experiments were conducted in vivo and if so, whether done in awake (green) or anesthetized (orange) mice; and whether the Ca^{2+} signal is behavior-induced and if so, whether this was validated in awake (green) or anesthetized (orange) mice. * "Behavior-induced" indicates that a Ca^{2+} signal is caused by any form of sensory stimulation or awake behavior. Accepted manipulations are forms of acute or chronic suppression of endogenous signaling pathways. Any form of electrical, optical, or chemical overactivation of a nerve fiber tract or an endogenous or exogenous signaling pathway does not qualify.*

respectively. Locomotion is accompanied by Ca^{2+} elevations in both types of terminals in primary visual and auditory cortices (Reimer et al., 2016).

Electrical stimulation of brainstem nuclei in anesthetized mice revealed the powerful potential of neuromodulators for coordinated Ca^{2+} activation of astroglia. Stimulation of

locus coeruleus triggers norepinephrine release and leads to subsequent Ca^{2+} activation of somatosensory cortex astrocytes (Bekar et al., 2008). Stimulation of nucleus basalis of Meynert induces acetylcholine release and causes a Ca^{2+} activation of astrocytes in somatosensory cortex (Takata et al., 2011), primary visual cortex (Chen et al., 2012), and hippocampus (Navarrete et al., 2012). Consistent with the idea that vigilance-dependent astroglia Ca^{2+} activation may be mediated by norepinephrine, it was found that locomotion as well as isometric muscle contractions, such as during a freezing response, induce widespread Ca^{2+} elevations in mouse cerebellar Bergmann glia, an occurrence previously described as 'flares.' Vigilance-dependent Bergmann glia responses are highly correlated with astrocyte Ca^{2+} elevations in primary visual cortex (Paukert et al., 2014). In the same study, pharmacological experiments revealed the importance of α_1-adrenergic receptors for Bergmann glia Ca^{2+} activation. α_1-adrenergic receptors had been independently found to be required for whisker stimulation- and air puff-induced Ca^{2+} activation of mouse somatosensory cortex astrocytes (Ding et al., 2013). Notably, locomotion-induced widespread Bergmann glia Ca^{2+} elevations have been studied in the molecular layer of cerebellar cortex where cross-sections of Bergmann glia processes are captured (Nimmerjahn et al., 2009; Paukert et al., 2014). Consistent with this finding, locomotion/startle-induced Ca^{2+} elevations in cortical astrocytes encompass processes in addition to somata (Paukert et al., 2014; Srinivasan et al., 2015; Ye et al., 2017; King et al., 2020).

Recently, use of global as well as cell type-specific gene deletion revealed that α_{1A}-adrenergic receptors on Bergmann glia are required for vigilance-dependent Ca^{2+} activation (Ye et al., 2020). The generated conditional knockout mouse line in combination with the inducible *Aldh1l1-CreER*^{T2} mouse line (Srinivasan et al., 2016) led to a loss of >94% of *Adra1a* mRNA in the cerebellum, indicating that within the cerebellum, α_{1A}-adrenergic receptors are potentially exclusively expressed in astroglia. Despite almost complete loss of Bergmann glia Ca^{2+} elevations in the global *Adra1a* knockout mouse, the loss of responsiveness in the conditional mouse more than 1 month following Cre recombination was approximately 40%, suggesting an extended stability of some receptors and highlights an obstacle for the interpretation of negative behavioral data. An independent study found that knock-out of α_{1A}-adrenergic receptors in mouse *Hes5*-positive astrocytes of superficial laminae of the spinal dorsal horn strongly reduced Ca^{2+} elevations in those cells in response to intraplantar injection of capsaicin (Kohro et al., 2020).

Noradrenergic signaling to astroglia is evolutionarily highly conserved. Indeed, the first experimental evidence for direct signaling of neuromodulators through astroglia was obtained from studying *Drosophila* astrocytes (Ma et al., 2016). Olfactory-driven larval chemotaxis as well as touch-induced startle responses induce somatic Ca^{2+} elevations in astrocytes that are mediated by the release of the *Drosophila* norepinephrine analogs tyramine and octopamine from Tdc2-positive neurons through binding to their receptor on astrocytes. In zebrafish, radial astrocytes accumulate information about futile motor activity through α_{1B}-adrenergic receptors (Mu et al., 2019). Astroglia Ca^{2+} elevations encompassing whole cells can also occur spontaneously. In the developing mouse cochlea, clusters of supporting cells undergo Ca^{2+} elevations that depend on the activation of $P2Y_1$ receptors (Tritsch et al., 2007; Babola et al., 2020). Astroglia express many more G protein-coupled receptors (Kofuji and Araque, 2020). Most if not all of them contribute to the diverse pool of astroglia microdomain Ca^{2+} dynamics that will be discussed in the next section. It is currently unclear and awaits further investigation whether they also modulate norepinephrine-mediated, vigilance-dependent global astroglia Ca^{2+} elevations, independently cause global astroglia Ca^{2+} elevations in yet to be defined behavioral context, or exclusively contribute to microdomain activity.

MECHANISMS LEADING TO MICRODOMAIN Ca^{2+} DYNAMICS IN ASTROGLIA

The astroglia network is anatomically complex and dynamic. A single astroglia contacts multiple neuronal cell bodies, hundreds of processes, and tens of thousands of synapses (Ventura and Harris, 1999). In addition, a considerable body of experimental findings suggests functional interactions between astrocytes and neurons at the synaptic level, termed gliotransmission, most of which have been determined to depend on astrocyte Ca^{2+} elevations (Araque et al., 2014). This feature has inspired investigations in subcellular, localized Ca^{2+} dynamics restricted to small portions of astroglia processes. First observed in acute cerebellar slices, 'microdomain' Ca^{2+} transients in Bergmann glia processes occur spontaneously or in response to electrical stimulation of parallel fibers, which are glutamatergic axons of granule cells passing by Purkinje cell dendrites, molecular layer interneurons and Bergmann glia processes (Grosche et al., 1999). Bergmann glia express GluA2 lacking, Ca^{2+}-permeable α-amino-3-hydroxy-5-methyl-4-isoxazolepropionic acid (AMPA) type glutamate receptors (Burnashev et al., 1992; Müller et al., 1992) and the G_q protein-coupled purinergic receptor $P2Y_1$ (Rudolph et al., 2016). The fast component of Ca^{2+} elevation following parallel fiber stimulation has been ascribed to AMPA receptors (Piet and Jahr, 2007) and a second slower component of Ca^{2+} elevation depends on $mGlu_1$-dependent release of ATP from molecular layer interneurons (Beierlein and Regehr, 2006; Piet and Jahr, 2007).

In awake mice, the Bergmann glia Ca^{2+} signal equivalent of microdomain events was previously termed 'sparkles' (Nimmerjahn et al., 2009). They are spontaneous Ca^{2+} elevations spatially restricted to individual main process branches that anatomically appear as palisades. Sparkles persist at a lower frequency during inhibition of action potential firing with tetrodotoxin (TTX), during inhibition of glutamatergic receptors, and during isoflurane general anesthesia. These features suggest that a considerable portion of sparkles resemble intrinsically-generated Ca^{2+} elevations that have been previously described in cortical astrocytes of anesthetized mice (Takata and Hirase, 2008).

Two major experimental obstacles have limited the appreciation of microdomain Ca^{2+} dynamics. The paucity in cytosolic volume of the finest astroglia processes limits the availability of synthetic Ca^{2+} indicators as well as cytosolic GECIs in those compartments and reduces the signal-to-noise level. The other difficulty is in distinguishing between a microdomain Ca^{2+} event and global Ca^{2+} signaling events spreading into the microdomain's spatial territory. For instance, locomotion-associated 'flares' prevent determining if 'sparkles' are enhanced during locomotion (Nimmerjahn et al., 2009). A significant advancement came with the introduction of membrane-tethered GECIs (Shigetomi et al., 2010a,b), which detect miniature Ca^{2+} fluctuations in astroglia localized near the plasma membrane and within the finest processes with only minimum volume of cytoplasm. These 'spotty' Ca^{2+} transients have more variable kinetics including faster responses than global vigilance-dependent responses described above, and occur asynchronously (Srinivasan et al., 2015; Agarwal et al., 2017). Some asynchrony of microdomain Ca^{2+} events may be explained by the biochemical compartmentation of nodal structural elements often localized in proximity to dendritic spines, a discovery recently made with super-resolution microscopy within the meshwork of astrocyte fine processes (Arizono et al., 2020).

By expressing the membrane-anchored GECI in acute hippocampal slices and organotypic culture, respectively, it was deduced that TRPA1 is required for astrocyte microdomain responses and for setting the basal Ca^{2+} level (Shigetomi et al., 2011, 2013; Jackson and Robinson, 2015). Using transgenic mice expressing a membrane-anchored GECI in astrocytes confirmed that TRPA1 contributes to the basal hippocampal astrocyte Ca^{2+} level, but transient microdomain Ca^{2+} events are not sensitive to pharmacological inhibition of TRPA1, Ca^{2+} release-activated channels (CRACs), ryanodine receptors, voltage-dependent Ca^{2+} channels or Na^{+}-Ca^{2+} exchangers (Agarwal et al., 2017). Instead, consistent with the considerable subcellular co-localization of microdomain Ca^{2+} events and mitochondria (Jackson and Robinson, 2015; Agarwal et al., 2017), inhibition of the mitochondrial permeability transition pore (mPTP) dramatically reduces the frequency of microdomain Ca^{2+} events (Agarwal et al., 2017). Stochastic opening of the mPTP causes brief bursts of reactive oxygen species (ROS) production in mitochondria (Wang et al., 2008). In turn, excessive ROS production can open mPTP (Vercesi et al., 1997; Duchen, 2000). Remarkably, microdomain Ca^{2+} events, like global, vigilance-dependent Ca^{2+} responses, are also evolutionarily conserved. In *Drosophila* astrocytes, ROS-regulated TrpML is responsible for transient microdomain Ca^{2+} elevations (Ma and Freeman, 2020). ROS facilitate IP_3R-mediated Ca^{2+} release from stores (Bánsághi et al., 2014), and further promote mPTP opening (Agarwal et al., 2017).

IP_3R2 plays an important role for microdomain Ca^{2+} events because the frequency of those events is strongly reduced in *ITPR2*$^{-/-}$ mice (Srinivasan et al., 2015; Agarwal et al., 2017). In the absence of any circuit stimulation, IP_3R-dependent facilitation of microdomain Ca^{2+} events appears to be not dependent on vesicular neurotransmitter release since incubation with veratridine and bafilomycin A1, for depleting vesicle content, does not affect the frequency of those events (Agarwal et al., 2017). On the other hand, it has been demonstrated that electrical stimulation of individual hippocampal axons in acute slices can evoke microdomain Ca^{2+} elevations (Bindocci et al., 2017) and that whisker stimulation, air puff stimulation, and locomotion can facilitate microdomain Ca^{2+} events (Srinivasan et al., 2015; Agarwal et al., 2017; Stobart et al., 2018). Certainly, it needs to be noted that, as mentioned above, it may be difficult to distinguish between highly coordinated microdomain Ca^{2+} activity and predominantly IP_3R2-dependent global whole cell Ca^{2+} activity. Intriguingly, sensory stimulation and arousal can enhance microdomain activity even in *ITPR2*$^{-/-}$ mice, and norepinephrine can still enhance microdomain event frequency in the absence of IP_3R2 (Agarwal et al., 2017) but the α_1-adrenergic receptor antagonist prazosin does not inhibit this enhancement (Srinivasan et al., 2015). Thus, if this is a direct effect of norepinephrine on astrocytes through non-type 2 IP3 receptors (Sherwood et al., 2017), it is possible that α_{2A}-adrenergic receptors, whose mRNA is expressed in astrocytes (Zhang et al., 2014), could contribute to facilitation of microdomain Ca^{2+} events.

CONSEQUENCES OF ASTROGLIA-SPECIFIC DELETION OF ENDOGENOUS PLASMA MEMBRANE PROTEINS

The most convincing and complete evidence if and how astroglia Ca^{2+} dynamics influence circuit activity and behavior stems from experimental approaches that allow a combination of the following three components: (1) visualization of astroglia Ca^{2+} dynamics in awake organisms during behavior, (2) reduction or abolishment of the behavior-dependence of Ca^{2+} dynamics through astroglia-specific genetic deletion of a signaling pathway component, and (3) the detection of consequences for circuit activity and/or behavior.

Noradrenergic Signaling

Employing such a three-component approach has revealed the crucial role of noradrenergic signaling in the context of widespread whole-astrocyte Ca^{2+} elevations. Its importance is further demonstrated by its evolutionary conservation. Sensory stimulation (olfaction) or startling touch of *Drosophila* larvae triggers release of the *Drosophila* adrenergic transmitter analogs octopamine and tyramine from Tdc2-positive neurons (Ma et al., 2016). Octopamine/tyramine (Oct/Tyr) bind directly to astrocyte Oct/TyrR causing extracellular Ca^{2+} influx through the transient receptor potential (TRP) channel Water witch (Wtrw). Somatic astrocyte Ca^{2+} elevation, through an unknown mechanism, potentially causes release of ATP, which following breakdown to adenosine, activates the inhibitory AdoR on dopaminergic neurons, relieving chemotaxis and startle-induced reversal behaviors from dopaminergic inhibition (Ma et al., 2016). Notably, this study provided the first experimental evidence that neuromodulators can signal directly through

astroglia. In addition to *Drosophila*, futile motor activity in zebrafish causes incremental Ca^{2+} elevations in radial astrocytes ultimately leading to a 'giving up' change in behavioral state (Mu et al., 2019). Mismatch between swimming as motor action and visual virtual feedback, a paradigm previously employed in studies of mouse primary visual cortex (Keller et al., 2012), activates noradrenergic neurons and leads to a delayed global Ca^{2+} elevation in radial astrocytes. This astrocyte Ca^{2+} activation is dependent on α_{1B}-adrenergic receptors and through the combination of opto-/chemogenetics and laser cell ablation it has been found that astrocyte Ca^{2+} activation, through a yet unknown mechanism, activates inhibitory neurons that trigger a cessation of swimming attempts (Mu et al., 2019).

In mouse cerebellar Bergmann glia, it is α_{1A}-adrenergic receptors that are responsible for vigilance-dependent Ca^{2+} activation (Ye et al., 2020). Remarkably, despite almost complete loss of locomotion-induced Bergmann glia Ca^{2+} elevations in global *Adra1a* knockout mice, the mice do not display any motor coordination deficit. Consistent with this finding, acute exposure to ethanol (2 g/kg i.p.), which suppresses locomotion-induced norepinephrine release, results in considerable loss of Bergmann glia Ca^{2+} responsiveness that lasts for more than 45 min whereas ataxic motor coordination, present 15 min after onset of exposure to ethanol, is completely recovered 30 min later (Ye et al., 2020). These findings suggest that vigilance-dependent Bergmann glia global Ca^{2+} elevations may play a role in cognitive function of the cerebellum rather than motor coordination; however, it needs to be noted that direct evidence for this is still missing.

An independently developed *Adra1a* conditional knockout mouse line was used to investigate the role of α_{1A}-adrenergic receptors in *Hes5*-positive astrocytes in superficial laminae of the spinal dorsal horn (supSDH) (Kohro et al., 2020). Although the completeness of reduction of ipsilateral, intraplantar capsaicin-induced *Hes5*-positive supSDH astrocyte Ca^{2+} elevation in *Adra1a* conditional knockout mice was not tested, strikingly, it was found that mechanosensory hypersensitivity was abolished. The precise mechanism how α_{1A}-adrenergic receptor activation in *Hes5*-positive supSDH astrocytes triggers mechanosensory hypersensitivity remains elusive. One possible mechanism is based on the concept of gliotransmission where D-serine, besides glutamate and ATP, is the most frequently proposed signaling molecule (Yang et al., 2003; Panatier et al., 2006; Henneberger et al., 2010), but see Wolosker et al. (2016), Mothet et al. (2019). D-serine may function as a diffusible messenger following exogenous activation of $P2Y_1$ receptors on lamina I SDH astrocytes to spread gliogenic long-term potentiation (LTP) beyond individual synapses (Kronschläger et al., 2016). It is conceivable that α_{1A}-adrenergic receptors in *Hes5*-positive supSDH astrocytes could substitute the experimental role of $P2Y_1$ receptors and control D-serine signaling. Indeed, Kohro et al. (2020) found that exogenously administered D-serine is sufficient to cause mechanosensory hypersensitivity. However, they did not detect extracellular elevations of D-serine in *Hes5*-positive supSDH astrocytes even following the drastic activation of a Designer Receptors Exclusively Activated by Designer Drugs (DREADD), specifically the humanized G_q protein-coupled muscarinic receptor type 3-based DREADD (hM3Dq). This finding could either mean that even excessive Ca^{2+} elevation in *Hes5*-positive supSDH astrocytes does not modulate extracellular D-serine signaling, or it could suggest that the detection method was not sensitive enough to take advantage of the *Adra1a* conditional knockout mouse line to imperatively link capsaicin-induced, noradrenergic Ca^{2+} activation of *Hes5*-positive supSDH astrocytes to D-serine signaling.

Robust noradrenergic signaling to astroglia in awake mice establishes a translational potential. Monai et al. (2016) found that a 10 min episode of transcranial direct current stimulation (tDCS), which is employed to ameliorate symptoms in patients of major depression among other neuropsychiatric and neurological conditions, when applied to mouse visual cortex, induces an α_1-adrenergic receptor-dependent widespread, global Ca^{2+} elevation in astrocytes but not in neurons (Monai et al., 2016). Despite the absence of tDCS-induced neuronal Ca^{2+} elevation, a single 10 min tDCS application is sufficient for IP_3R2-dependent induction of an hours-lasting potentiation of visually evoked potentials.

Cholinergic Signaling

For many astroglia receptors it remains to be defined in which awake behavioral context they are activated. This requires investigation of whether they lead to global astroglia Ca^{2+} activation like noradrenergic receptors, whether they potentiate noradrenergic responses, or whether they exclusively contribute to microdomain Ca^{2+} events. For example, there is strong evidence that electrical stimulation of cholinergic nuclei and fibers in anesthetized mice leads to muscarinic receptor-dependent global Ca^{2+} elevation in somatosensory cortex, primary visual cortex and hippocampal astrocytes affecting local circuit plasticity (Takata et al., 2011; Chen et al., 2012; Navarrete et al., 2012). Given that cholinergic signaling is engaged during states of heightened vigilance (Polack et al., 2013; Fu et al., 2014; Reimer et al., 2016), it is somewhat surprising that no widespread, heightened vigilance-dependent global cortical astrocyte Ca^{2+} elevations persist following pharmacological inhibition of α_1-adrenergic receptors (Ding et al., 2013; Srinivasan et al., 2015). Also, indirect evidence from a detailed study of sleep states suggests that acetylcholine may not directly lead to a Ca^{2+} rise in cortical astrocytes (Bojarskaite et al., 2020) though a fraction of somatosensory cortex astrocyte microdomain Ca^{2+} events in awake mice is sensitive to the muscarinic receptor antagonist atropine (Stobart et al., 2018). This highlights that caution is warranted when electrical stimulation of fiber tracts is employed. For instance, with cerebellar granule cell-Purkinje cell glutamatergic synapses, whether one stimulates bundles of neighboring axons in the molecular layer or whether one excites dispersed axons by stimulating in the granule cell layer determines if glutamate spillover leads to endocannabinoid-dependent short-term plasticity (Marcaggi and Attwell, 2005). For this reason, in **Tables 1**, **2** we emphasize the difference between behavior-induced (sensory stimulation or behavioral state) versus electrical stimulation- or excitatory opto- or chemogenetic stimulation-induced astroglia Ca^{2+} dynamics.

A very elegant study revealed that wakefulness/vigilance-dependent release of acetylcholine leads to circadian oscillations in hippocampal extracellular D-serine levels (Papouin et al., 2017). D-serine circadian oscillations were abolished when the gene for α7 nicotinic acetylcholine receptors (nAChRs) was specifically deleted from hippocampal CA1 astrocytes. Extracellular L-serine does not follow circadian oscillations, indicating that circadian D-serine fluctuations originate from astrocytes. Remarkably, α7nAChR-dependent D-serine release causes the glycine-binding site of *N*-methyl D-aspartate receptors (NMDARs) to reach saturation during the active/wakeful phase of the mouse. This finding raises the possibility that transient vigilance-independent D-serine release may be less impactful during the active phase, when NMDAR glycine-binding sites appear to be saturated, than during sleep, and may offer an explanation why several phenotypes arising from astroglia-selective reductions in Ca^{2+} dynamics have been found linked to the regulation of sleep (Halassa et al., 2009; Foley et al., 2017; Bojarskaite et al., 2020; Ingiosi et al., 2020).

Glutamatergic Signaling

Glutamatergic signaling to astrocytes has been intensively studied in juvenile rodent hippocampus initially with a significant emphasis on metabotropic glutamate receptor $mGlu_5$ signaling (Rose et al., 2018). *In vivo* topical pharmacology experiments have suggested that $mGlu_5$ activation on somatosensory cortex astrocytes contributes to contralateral forepaw stimulation- or local electrical stimulation-induced arteriole dilation leading to functional hyperemia (Zonta et al., 2003; Takano et al., 2006). However, while this does not exclude $mGlu_5$ signaling in astrocytic endfeet where microdomain Ca^{2+} events are spared, it has been demonstrated that in *ITPR2*$^{-/-}$ mice where the majority of Ca^{2+} elevations in soma and main processes as well as a considerable portion of fine process microdomain events are abolished, functional hyperemia is not impaired (Nizar et al., 2013; Bonder and McCarthy, 2014). More recent work has even revealed the reverse flow of information: cortical astrocyte endfeet in contact with arterioles sense functional hyperemia-associated vasodilation and endothelial nitric oxide production and respond with enhanced Ca^{2+} elevations (Tran et al., 2018).

Developmental expression analysis of rodent $mGlu_5$ in mouse cortical astrocytes revealed steep downregulation during the third and fourth postnatal weeks leaving the $G_{i/o}$ protein-coupled receptor $mGlu_{2/3}$ as the predominant astrocyte metabotropic glutamate receptor (Sun et al., 2013). The developmental downregulation of cortical astrocyte $mGlu_5$ expression is also subject to pathological dysregulation. In a mouse model of Fragile X syndrome, microRNA miR-128-3p is expressed at an elevated level in astroglia and causes accelerated loss of $mGlu_5$ function (Men et al., 2020). Similar to cortical astrocyte downregulation of $mGlu_5$ expression, adult mouse hippocampal mossy fiber stimulation-evoked astrocyte Ca^{2+} elevations as well as the frequency of spontaneous microdomain Ca^{2+} events are not inhibited by the antagonist for $mGlu_5$ but are sensitive to antagonists for $mGlu_{2/3}$ and for the metabotropic γ-amino butyric acid (GABA) receptor $GABA_BR$ (Haustein et al., 2014). In contrast to their action in neurons, $G_{i/o}$ protein-coupled receptors in astroglia often enhance Ca^{2+} elevations, most likely through direct initiation and/or facilitation of IP_3R opening by the βγ subunit (Zeng et al., 2003; Durkee et al., 2019; Nagai et al., 2019), but see (Kol et al., 2020).

Regarding *in vivo* consequences of glutamatergic signaling to astroglia, AMPA receptor function in cerebellar Bergmann glia is among the better understood examples. Two distinct strategies have been pursued to reduce or eliminate AMPA receptor-mediated Ca^{2+} influx. As demonstrated in one study, viral overexpression of the GluA2 subunit in Bergmann glia renders AMPA receptors Ca^{2+} impermeable, impairs the close ensheathment of glutamatergic synapses onto Purkinje cells by Bergmann glia processes and consequently, slows glutamate clearance (Iino et al., 2001). Developmental pruning of the climbing fiber, one of the two major excitatory inputs to the cerebellar cortex, is also impaired. The second strategy was use of conditional knockout of the two predominant AMPA receptor subunits expressed in Bergmann glia, GluA1 and GluA4. Twelve weeks after inducing gene deletion, Bergmann glia processes were morphologically altered, synaptic glutamate clearance impaired, and miniature excitatory postsynaptic currents in Purkinje cells were less frequent (Saab et al., 2012). Moreover, the mice exhibited a higher propensity toward missteps on the Erasmus Ladder, which is a fine motor coordination task, and impaired eyeblink conditioned responses. Together, these findings indicate that Ca^{2+} influx through AMPA receptors is an important signal for establishment and maintenance of proper synaptic function in the cerebellar cortex.

Purinergic Signaling

ATP is among the most reliable agonists to trigger global Ca^{2+} elevations as well as enhance microdomain Ca^{2+} events in astroglia *in vitro*. *In vivo*, some of the best understood mechanisms of purinergic signaling through astroglia are during development, pathological reactivity and functional hyperemia. Before hearing onset, astroglia-like inner supporting cells (ISCs) spontaneously release ATP which activates $P2Y_1$ autoreceptors and together with intense gap junction coupling among ISCs, intracellular Ca^{2+} rises in clusters of neighboring cells (Babola et al., 2020). The Ca^{2+} elevation leads to opening of Ca^{2+}-activated chloride channel TMEM16A which extrudes chloride, drives potassium efflux, and causes transient depolarization of neighboring inner hair cells (Wang et al., 2015). Bursts of action potentials in spiral ganglion neuron (SGN) afferents that innervate neighboring inner hair cells propagate throughout the pre-hearing auditory pathway preserving later tonotopic representation (Babola et al., 2018). ISC-initiated transient potassium elevations can even excite neighboring SGN afferents directly when inner hair cell-SGN afferent synaptic transmission is impaired (Babola et al., 2018). It is thought that this astroglia-mediated spontaneous and transient activation of the auditory pathway allows for circuit maturation so that sensory processing may begin when the ear canal opens.

In adult rodents, $P2Y_1$ receptors participate in astrocyte-to-neuron signaling in brainstem-mediated baroreception and response. It has been found that experimentally increasing intracranial pressure leads to increased venous pressure, reduced difference in brain arterio-venous pressure, and decreases the

brain blood flow, which ultimately causes a Ca^{2+} elevation in brainstem astrocytes that are in proximity to central sympathetic autonomous nervous system centers (Marina et al., 2020). In response, the heart rate and the mean arterial pressure increase for homeostatic regulation of brain blood flow. This astrocytic regulatory response was impaired when vesicular release was hampered by overexpressing dominant-negative soluble *N*-ethyl-maleimide-sensitive factor attachment protein receptor (dn-SNARE). The Gourine laboratory studied the pressure sensing mechanism in more detail in an *in vitro* preparation and proposed a model for the initial pressure-dependent ATP release mechanism based on an interaction between TRPV4 ion channels and connexin 43. After finding that $P2Y_1$ autoreceptors appear to serve as signal amplifiers, they deduced that vesicular release of ATP from brainstem astrocytes is the signal that excites central sympathetic centers (Turovsky et al., 2020). Astrocyte $P2Y_1$ receptors have also been found to account for the enhanced microdomain Ca^{2+} event frequency in cortical astrocytes of anesthetized mouse models of Alzheimer's disease (Kuchibhotla et al., 2009; Delekate et al., 2014).

Ionotropic receptors are likewise utilized by astrocytes to receive purinergic signals. Functional hyperemia occurs differently at the capillary level, which is controlled by astroglia Ca^{2+} dynamics, and the arteriole level, which occurs through interneuron nitric oxide release (Mishra et al., 2016). Astroglia-mediated, neuronally evoked dilation of capillaries occurs when Ca^{2+} influx through P2X1 receptors activates phospholipase D2 and diacylglycerol lipase to generate arachidonic acid. The regulation of functional hyperemia in the rat retina (Biesecker et al., 2016) is consistent with the concept of astroglia mediation of functional hyperemia at the level of capillaries (Mishra et al., 2016) but not arterioles (Nizar et al., 2013; Bonder and McCarthy, 2014). Light flickering induces Ca^{2+} elevations in Müller cell fine processes in contact with capillaries and in those in contact with arterioles. In *ITPR2*$^{-/-}$ mice with impaired light flickering-induced Ca^{2+} elevations in both types of fine processes, vasodilation is impaired only with capillaries (Biesecker et al., 2016).

Cannabinergic Signaling

Circuit and behavior analysis following astroglia-specific gene deletion of the cannabinoid receptor type 1 (CB1R) settled an earlier controversy about the expression of this receptor in astrocytes (Stella, 2004; Han et al., 2012). In addition to $mGlu_{2/3}$ receptors and $GABA_B$ receptors, $G_{i/o}$ protein-coupled CB1R activation also leads to astrocyte Ca^{2+} elevations (Navarrete and Araque, 2008, 2010; Robin et al., 2018). It still remains to be determined whether in awake behaving mice CB1R activation leads to global, whole-cell Ca^{2+} elevation as seen in slice experiments following neuronal depolarization or CB1R agonist application, or to increased frequency of microdomain Ca^{2+} events.

Depending on intensity and duration of hippocampal astrocyte CB1R activation, different effects on local circuit activity and behavior have been observed. Han et al. (2012) tested the hypothesis that astrocyte CB1Rs could account for the known detrimental effect of acute cannabinoid exposure for spatial working memory (Lichtman and Martin, 1996). They found that acute cannabinoid exposure is required during induction, but not for expression of *in vivo* hippocampal CA3-CA1 long-term depression (LTD) (Han et al., 2012). Cannabinoids cause LTD through astrocyte CB1R but not through glutamatergic or GABAergic neuron CB1R. LTD occurs through internalization of postsynaptic AMPA receptors that is independent of mGlu1 activation but dependent on NMDA receptor activation. The impairment in spatial working memory follows the same pharmacological profile as the impairment of astrocyte CB1R-mediated LTD (Han et al., 2012). A recent study on NMDA receptor-dependent, postsynaptic expression of CA3-CA1 hippocampal LTD further demonstrated that this circuit phenomenon depends on the astrocytic activation of the p38α variant of mitogen-activated protein kinase (MAPK) (Navarrete et al., 2019).

In contrast, endogenous activation of astrocyte CB1Rs leads to synaptic potentiation. The retrograde diffusion of endogenous cannabinoids following postsynaptic depolarization-induced production causes inhibition of subsequent neurotransmitter release from presynaptic terminals that express CB1Rs, a phenomenon known as depolarization-induced suppression of inhibition (DSI) or excitation (DSE) (Maejima et al., 2001; Wilson and Nicoll, 2001; Alger, 2002; Kreitzer et al., 2002; Ohno-Shosaku et al., 2002). An investigation for a role of hippocampal astrocytes in endocannabinoid-mediated short-term plasticity found that while a 5 s depolarization of CA1 pyramidal neurons to 0 V induces homoneuronal DSE of Schaffer collateral input, neighboring pyramidal neurons experience heteroneuronal synaptic potentiation (Navarrete and Araque, 2010). Several lines of evidence pointed at astrocyte CB1Rs being responsible for the tens of seconds lasting synaptic potentiation. This was abolished following depletion of intracellular Ca^{2+} stores with thapsigargin, while DSE was not. Also, it was inhibited by loading astrocytes with the high-affinity Ca^{2+} chelator BAPTA or the G-protein inhibitor GDPβS, a procedure leading toward enhanced DSE. While pyramidal neuron depolarization-induced astrocyte Ca^{2+} elevations were insensitive to inhibition of $mGlu_1$, synaptic potentiation was inhibited, suggesting presynaptic $mGlu_1$ activation downstream of astrocyte Ca^{2+} elevation is responsible for synaptic potentiation (Navarrete and Araque, 2010).

Recently, it has been demonstrated that novel object recognition is strongly impaired in astroglia-specific CB1R knockout mice (Robin et al., 2018). Hippocampal NMDA receptor function was found to be required for novel object recognition, and both NMDA receptors as well as astrocyte CB1Rs were required for *in vivo* high-frequency stimulation-induced long-term potentiation (LTP). Consistent with the dependence on NMDA receptors, high-frequency stimulation-induced LTP as well as novel object recognition could be rescued in astroglia-specific CB1R knockout mice by substituting with saturating concentration of D-serine (Robin et al., 2018). This finding suggests that astrocyte CB1R signaling is important for hippocampal LTP and novel object recognition via controlling the availability of extracellular D-serine. This conclusion,

however, may have some interesting implications. As discussed earlier, it has recently been found that circadian/wakefulness-dependent cholinergic signaling through hippocampal astrocytes controls mean extracellular availability of D-serine (Papouin et al., 2017). Six hours into the active phase in environmental enrichment housing, extracellular D-serine levels saturate the glycine binding site of NMDA receptors, whereas the occupancy of this site reaches a minimum toward the end of the sleep phase (Papouin et al., 2017). The novel object recognition study here was conducted 7–10 h into the sleep phase, and indeed NMDA receptors were not saturated with endogenous D-serine (Robin et al., 2018). Therefore, it will also be important to explore the impact of hippocampal astrocyte CB1R signaling on novel object recognition during the active phase when animals are more likely to encounter object recognition challenges.

GABAergic Signaling

In the hippocampal CA3-CA1 microcircuit, astrocyte $GABA_B$ receptor signaling plays a role in counterbalancing GABAergic interneuron-mediated inhibition of Shaffer collateral glutamate release (Perea et al., 2016). At states of low interneuron excitation (individual action potential firing) Shaffer collateral glutamate release is inhibited in a $GABA_A$ receptor-dependent manner. In contrast, when interneurons fire bursts of action potentials, $GABA_B$ receptors on astrocytes are recruited, as astrocyte-specific knockout experiments confirmed, leading to enhanced Ca^{2+} signaling and group 1 mGlu receptor-dependent enhancement of Shaffer collateral glutamate release. Astrocyte-specific $GABA_B$ receptor knockout was sufficient to reduce the power of hippocampal theta and low gamma oscillations (30–60 Hz) in anesthetized mice (Perea et al., 2016). The contribution of astrocyte-dependent Ca^{2+} signaling to low gamma oscillations is consistent with findings from transgenic mice with astrocyte-selective overexpression of tetanus toxin (Lee et al., 2014). Here the reduction of low gamma oscillations was, however, only significant in awake mice, not during sleep.

A recent study explored the circuit and behavioral consequences of astrocyte-specific knockout of $GABA_B$ receptors in prefrontal cortex (Mederos et al., 2021). They also found a reduction of low gamma oscillations in active awake mice, but not in resting mice. Low gamma oscillations may reflect synchronization of the neuronal population and has been associated with working memory processing in prefrontal cortex (Buzśaki and Wang, 2012). Indeed, mice lacking $GABA_B$ receptors in prefrontal cortex astrocytes have difficulty making correct decisions during the T-maze alternating behavioral task, a paradigm testing working memory performance (Mederos et al., 2021). A more detailed cellular analysis of the circuit function revealed that astrocyte $GABA_B$ receptors, IP_3R2-dependently, potentiate parvalbumin-positive interneuron-driven inhibitory postsynaptic currents in local neurons. Using astrocyte-specific overexpression of melanopsin[1] for optical control of G_q protein-coupled receptor activation exclusively in astrocytes (Mederos et al., 2019), they not only rescued goal-directed behavior in astrocyte-$GABA_B$ receptor knockout mice but further enhanced goal-directed behavior in wildtype mice (Mederos et al., 2021). This observation is in contrast with disruptive consequences of astrocyte-specific activation of exogenous Gi protein-coupled receptors in striatal astrocytes, which also enhances Ca^{2+} dynamics but leads to hyperactivity of the mice (Nagai et al., 2019). It indicates that brain region, subcellular location of receptors within astroglia, and duration of activation likely all have inherent importance.

[1]https://www.addgene.org/122630/

INTRINSIC MICRODOMAIN SIGNALING

The mitochondrial PTP appears to be a major determinant of spontaneous, intrinsically regulated astroglia microdomain Ca^{2+} fluctuations (Agarwal et al., 2017). The intrinsic nature of these signaling events likely stems from metabolic control (Jackson and Robinson, 2015; Agarwal et al., 2017; Oheim et al., 2018). In addition, the promiscuous regulation of mPTP activity by ROS, Ca^{2+}, and IP3R among others suggests that stochastic activation of the many G protein-coupled astrocyte receptors in the presence of ambient receptor ligands at low basal concentrations or in their absence may account for the considerable bafilomycin A1-insensitive, IP_3R2-dependent portion of microdomain Ca^{2+} events (Agarwal et al., 2017). To further this complexity, vigilance/arousal-dependent, predominantly noradrenergic signaling, which is critical for whole-cell, widespread Ca^{2+} elevations (Ding et al., 2013; Paukert et al., 2014; Ye et al., 2020), also contributes to microdomain events (Agarwal et al., 2017), as does local neuronal activity through activation of various receptors or ion channels (Agarwal et al., 2017; Bindocci et al., 2017; Stobart et al., 2018). The complexity of astroglia microdomain Ca^{2+} dynamics so far has made it impossible to genetically manipulate selectively microdomain activity while leaving basal Ca^{2+} as well as whole-cell Ca^{2+} elevations intact. More refined mechanistic insight into what happens in astroglia mitochondria during distinct behavioral and environmental states will be required to design gentle but highly specific genetic manipulations.

In the midst of this challenge, the *Drosophila* model system offers an opportunity to selectively target astrocyte microdomain Ca^{2+} events (Ma and Freeman, 2020). In contrast to mammalian microdomain events, apart from the ineffective neurotransmitters including glutamate, acetylcholine, GABA and octopamine, only tyramine, which corresponds to mammalian dopamine, enhances the frequency of *Drosophila* TrpML-mediated Ca^{2+} transients by approximately 40%. Around half of the microdomain events are associated with the tracheal system, which in *Drosophila*, consists of a network that terminates in filopodia throughout the nervous system and facilitates oxygen delivery. Retractions of tracheal filopodia are often preceded by astrocyte microdomain events. Inhibiting or genetically deleting TrpML in astrocytes eliminates microdomain Ca^{2+} events and increases ROS concentration and results in growth of the tracheal system, suggestive of reduced filopodia retractions (Ma and Freeman, 2020). Together, these findings suggest that astroglia microdomain Ca^{2+} dynamics are not only an evolutionary conserved phenomenon, but may serve a conserved functional

role as homeostatic element within the metabolic state of the microenvironment. As we will discuss below, a way of studying preferentially microdomain Ca^{2+} events in mammalian astroglia could be represented by sleep studies, where vigilance/arousal-dependent whole cell Ca^{2+} events, like under general anesthesia, are strongly reduced, if not absent (Bojarskaite et al., 2020; Ingiosi et al., 2020).

IMPLICATIONS OF ASTROGLIA BASAL CA^{2+} FOR LOCAL CIRCUIT EXCITABILITY

Drosophila astroglia have granted insight into diverse mechanisms of how basal Ca^{2+} controls local circuit excitability and behavior. In cortex glia, which are located in brain areas densely populated with cell bodies but no synapses, the genetic deletion of the Na^+/Ca^{2+}, K^+ exchanger *zydeco* leads to elevation of intracellular Ca^{2+} accompanied by a proneness to seizure activity (Melom and Littleton, 2013). The constant elevation of Ca^{2+} causes the intrinsic microdomain Ca^{2+} activity to disappear, possibly through masking it. Intracellular Ca^{2+} elevation in cortex glia is mechanistically linked to seizure activity by activation of calcineurin, subsequent endocytosis of two-pore K^+ channel *sandman*, and impaired extracellular buffering of K^+ (Weiss et al., 2019). The elevated extracellular K^+ will depolarize surrounding excitable cells and bring their membrane potential closer to the threshold of excitation.

In *Drosophila* astrocytes, which are located in areas containing synapses, intracellular Ca^{2+} elevation triggers a different signaling pathway resulting in paralysis (Zhang et al., 2017). It was found that Ca^{2+} elevation increases the expression of Rab11, a GABA plasma membrane transporter (GAT) regulator, facilitating endocytosis of GAT, impairing synaptic GABA clearance, and leading to paralysis (Zhang et al., 2017). An analogous mechanism was uncovered in mouse striatal astrocytes where experimental reduction of intracellular Ca^{2+} leads to enhanced GABA clearance and reduced tonic inhibition of the surrounding microcircuitry, ultimately causing excessive self-grooming (Yu et al., 2018). Mouse astroglia can also control tonic inhibition through GABA release via Ca^{2+}-activated anion channel bestrophin-1. This mechanism has been proposed for cerebellar Bergmann glia controlling excitability of granule cells (Lee et al., 2010) and for astrocytes in the striatum controlling excitability of medium spiny neurons (Yoon et al., 2014). Astroglia-mediated tonic inhibition has been associated with limited performance on the rotarod paradigm (Woo et al., 2018). Also, bestrophin-1 has been implicated in vesicle-independent astrocytic release of glutamate and D-serine (Oh and Lee, 2017).

CONSEQUENCES OF DELETION OF IP_3R2 SIGNALING

IP_3R2 is an astroglia Ca^{2+} signaling junction point. It is by far the most abundant IP_3R subtype in astroglia (Sharp et al., 1999; Holtzclaw et al., 2002; Petravicz et al., 2008). Upon gene deletion, whole-cell Ca^{2+} elevations are almost completely abolished and also the frequency of microdomain events is considerably reduced (Fiacco et al., 2007; Srinivasan et al., 2015; Agarwal et al., 2017), suggesting that through its interaction with mPTP, it is a major pathway how G protein-coupled receptors facilitate microdomain events. The importance of IP_3R2 for astroglia Ca^{2+} dynamics is further emphasized by the finding that it serves not only G_q protein-coupled receptors but also $G_{i/o}$ protein-coupled receptors for intracellular Ca^{2+} release (Durkee et al., 2019). Given the apparent importance of IP_3R2 for astroglia Ca^{2+} dynamics, it came as a surprise that a series of acute hippocampal slice studies of baseline and stimulated synaptic function and synaptic plasticity found no consequences of IP_3R2 gene deletion (Fiacco et al., 2007; Petravicz et al., 2008; Agulhon et al., 2010). These findings triggered more refined slice physiology studies that applied astrocyte-specific knockout of endogenous receptors and the dissection of concomitant excitatory as well as inhibitory or potentiating as well as depressing circuit mechanisms (e.g., Perea et al., 2016). In addition, the study of spontaneous as well as agonist-induced hippocampal astrocyte Ca^{2+} dynamics from acute slices of mice carrying a combined gene deletion of IP_3R2 and IP_3R3 suggests that non-type 2 IP_3Rs may contribute to astroglia Ca^{2+} elevations (Sherwood et al., 2017). Not only at the level of slice physiology, also at the behavioral level the consequences of IP_3R2 gene deletion have been less impressive than one might have expected. A battery of behavioral tests with astrocyte-specific IP_3R2 gene deletion mice revealed no significant difference to wildtype littermates when testing anxiety, depressive behavior, motor coordination, exploratory behavior, sensory motor gating with the acoustic startle response and prepulse inhibition, and with learning and memory using the Morris water maze (Petravicz et al., 2014).

On the other hand, recent years have also seen a considerable number of findings demonstrating how loss of IP_3R2 function does affect developmental synaptic pruning, neurovascular coupling, cortical plasticity and memory, and the regulation of sleep. Similar to the climbing fiber synapse in the cerebellum mentioned earlier (Iino et al., 2001), the principal trigeminal nucleus-ventral posteromedial thalamic nucleus synapse serves as a model of developmental synaptic pruning since between postnatal day 7 (P7) and P16, 7–8 inputs are refined into a single mature input (Yang et al., 2016). Using a combination of acute slice electrophysiology and immunocytochemistry it has been found that this synapse elimination is incomplete in *ITPR2*$^{-/-}$ mice, leaving on average more than two functional inputs at P16. Local administration of ATP or the $P2Y_1$ receptor agonist MRS-2365 rescued synapse elimination, but global $P2Y_1$ receptor gene deletion made all rescue attempts fail (Yang et al., 2016). This suggests a model where IP_3R2-dependent astrocytic ATP release acts through $P2Y_1$ receptors to facilitate synapse elimination.

In awake behaving mice, learning and memory can be controlled by astroglia Ca^{2+} dynamics at different time scales. Padmashri et al. (2015) used an inducible astroglia-specific IP_3R2 gene deletion approach to test whether motor skill learning is affected. Even though the conditional knockout approach reduced astrocyte Ca^{2+} responses to the application of ATP only by approximately 50%, knockout mice reached an earlier

ceiling of the success rate in a forelimb reaching-task after 3 of 5 days. They also found a linear relationship between residual Ca^{2+} responsiveness and preservation in motor skill learning (Padmashri et al., 2015). Pinto-Duarte et al. (2019) did not find an effect of global IP_3R2 gene deletion on novel object recognition, fear memory, or spatial memory within 2–5 days. But in all three tests, they found a considerable impairment 2–4 weeks later. Since such a remote memory deficit might represent impaired memory consolidation, they investigated hippocampal Schaffer collateral-to-CA1 field potential LTD in acute slices. They found impaired LTD in *ITPR2*$^{-/-}$ mice, which could be rescued with exogenous D-serine, but not when preincubated with the degrading enzyme D-amino acid oxidase (DAAO) or with NMDA receptor inhibition (Pinto-Duarte et al., 2019). Astroglia Ca^{2+} dynamics can also acutely shape cortical neuronal population activity in response to sensory stimulation (Lines et al., 2020). Monitoring somatosensory cortex gamma activity revealed that sensory stimulation induces a transient increase in power that attenuates to a steady-state level for the duration of the stimulation. In *ITPR2*$^{-/-}$ mice, the attenuation is diminished. This is unlikely due to developmental changes, since acute elevation of astroglia Ca^{2+} via astroglia-specific activation of hM3Dq reduces the gamma activity (Lines et al., 2020).

Several studies have focused on the role of astroglia Ca^{2+} signaling during sleep. A very elegant recent study combined monitoring of somatosensory cortex astrocyte Ca^{2+} dynamics, locomotion activity of head-fixed mice, whisking activity, as well as cortical electrical activity and muscle activity in *ITPR2*$^{-/-}$ mice and wildtype littermates (Bojarskaite et al., 2020). In the analysis of sleep states, they distinguished between slow wave sleep with a further distinction between non-rapid eye movement (NREM) sleep and intermediate state (IS) sleep, and rapid eye movement (REM) sleep. As expected for a behavioral state lacking significant arousal, astrocyte Ca^{2+} dynamics during sleep are dominated by microdomain events. Preceding the state transition from either of the two slow wave sleep states (NREM or IS) to wakefulness, there is an enhanced IP_3R2-dependent Ca^{2+} elevation. This finding is consistent with an independent recent astroglia Ca^{2+} imaging study where intracellular Ca^{2+} release was attenuated by astroglia-specific gene deletion of stromal interaction molecule 1 (STIM1) (Ingiosi et al., 2020). The transition from slow wave sleep to wakefulness is when enhanced norepinephrine release is expected (Takahashi et al., 2010). Surprisingly, neither study found a Ca^{2+} elevation during REM sleep (Bojarskaite et al., 2020; Ingiosi et al., 2020) when elevated levels of extracellular acetylcholine are expected (Jasper and Tessier, 1971). This finding, together with the inhibition of global widespread cortical astroglia Ca^{2+} elevations during awake states of heightened vigilance by α_1-adrenergic receptor antagonists (Ding et al., 2013; Srinivasan et al., 2015) raise the possibility that acetylcholine cannot directly cause significant cortical astroglia Ca^{2+} elevations. Another finding in *ITPR2*$^{-/-}$ mice was increased frequency of sleep spindles during IS sleep, which may cause impaired memory consolidation (Bojarskaite et al., 2020). This finding may provide a mechanistic explanation for impaired remote memory in *ITPR2*$^{-/-}$ mice discussed above (Pinto-Duarte et al., 2019) or for impaired remote memory in consequence of manipulation of astroglia Ca^{2+} dynamics using the humanized G_i protein-coupled muscarinic receptor type 4 DREADD (hM4Di) discussed below (Kol et al., 2020). Bojarskaite et al. (2020) also found considerably reduced delta electrocorticogram power during NREM sleep in *ITPR2*$^{-/-}$ mice, which indicates reduced sleep pressure, which is consistent with the first study that reported astrocyte control of sleep pressure and the impact of sleep deprivation (Halassa et al., 2009). This study by Halassa et al. (2009) used astrocyte-specific overexpression of dn-SNARE to impair the proposed vesicular release of ATP and to reduce occupancy of adenosine A1 receptors, which are important for mediating sleep pressure. Consistent findings on sleep pressure and sleep deprivation were obtained by Ingiosi et al. (2020). Finally, Bojarskaite et al. (2020) found that loss of IP_3R2 function reduces the dwell time but increases the frequency of both slow wave sleep states, leaving REM sleep unaltered. This finding is almost opposite to the outcome of a study where IP3 signaling was directly attenuated by astroglia-specific overexpression of the venus-tagged IP3 5'phosphatase (VIPP) (Foley et al., 2017). There they found an increased number of REM sleep bouts with no difference in dwell time and no change in NREM sleep. The discrepancy in results may be explained by the fact that IP_3R2 gene deletion will considerably attenuate intracellular Ca^{2+} release mediated by possibly all astrocyte G protein-coupled receptors. In contrast, hydrolysis of IP3 is not expected to interfere with Gi/o $\beta\gamma$ subunit binding to IP3R2. Therefore, it is tempting to speculate that activation of α_2-adrenergic receptors, or of any other astrocyte Gi/o protein-coupled receptor in the study by Foley et al. (2017) could account for the difference in sleep regulation among these two studies.

CONSEQUENCES OF ASTROGLIA-SPECIFIC MANIPULATION OF Ca^{2+} DYNAMICS VIA EXOGENOUS ACTUATORS

In recent years, astroglia-specific overexpression of exogenous actuators for manipulation and interrogation of astroglia physiology has become very popular (**Table 2**). The advantages of such approaches are immediately clear since almost all receptors on astroglia are also present on neurons and other neural cells. Limitations of the utility of exogenous actuators need to be considered in light of the downstream signaling events that follow the astroglia-specific initiation. Actuators which remove an endogenous signal may arguably be regarded as less invasive. One example is the CalEx constitutively active plasmalemmal Ca^{2+} pump and will be discussed below. For actuators that represent the overexpression of an exogenous G protein-coupled receptor that elevates Ca^{2+}, one needs to consider the physiological dynamic range of the expected signal regarding expression level, its subcellular location, and duration/pattern of ligand application. Predictions of the consequences of overexpression of ion channels, some with ion selectivity for which no physiological counterpart is known in astroglia, a cell type

with ion buffering function, are most complex. Nevertheless, these are very powerful tools that may inform follow-up studies focused on the physiological role of specific endogenous astroglia signaling pathways.

To inhibit microdomain events despite their mechanistic diversity, Yu et al. (2018) modified human plasma membrane Ca^{2+} ATPase pump (hPMCA) isoform 2, w/b splice variant with excised cytosolic interaction domains (hPMCA2w/b), resulting in a modified pump that constitutively extrudes cytosolic Ca^{2+}. The model was coined "CalEx" due to its function in Ca^{2+} extrusion[2] (Yu et al., 2018). Behavioral assays of mice expressing CalEx in striatal astrocytes revealed that reducing whole-cell and microdomain Ca^{2+} dynamics results in excessive self-grooming behavior indicative of an obsessive-compulsive disorder phenotype. The underlying circuit mechanism was identified as low astrocyte Ca^{2+} leading to reduced expression of Rab11a, which leads to less internalization of the GABA transporter GAT-3, more GABA uptake, lower ambient GABA concentration and less tonic inhibition (Yu et al., 2018). This mechanism is conserved in *Drosophila* astrocytes (Zhang et al., 2017), but the relationship between basal mouse astrocyte Ca^{2+} set by TRPA1 and surface expression of GAT-3 in co-culture with neurons is reversed (Shigetomi et al., 2011). CalEx overexpressed in mouse prefrontal cortex astrocytes was used in comparison with hM3Dq[3], the G_q protein-coupled DREADD, to study the effects of manipulating astrocyte Ca^{2+} on ethanol's motivational, stimulatory and sedating impact (Erickson et al., 2020). It was found that while boosting astrocyte Ca^{2+} dynamics enhances all negative effects such as ethanol consumption, excessive locomotor stimulation in response to low dose ethanol and prolonged loss of righting reflex (LORR) due to high dose ethanol sedation, reducing astrocyte Ca^{2+} dynamics with CalEx has protective, opposite effects. The aggravated sedating effect of enhanced astrocyte Ca^{2+} could be reversed by inhibiting adenosine A1 receptors (Erickson et al., 2020), suggesting that hM3Dq activation in prefrontal cortex astrocytes may trigger ATP release. In the light of these findings it is interesting to note that the suppression of vigilance-dependent astroglia Ca^{2+} activation by ethanol inhibition of norepinephrine release (Ye et al., 2020) may play a homeostatic protective role during acute ethanol intoxication.

The Goshen group recently expressed hM4Di[4] in hippocampal CA1 astrocytes to inhibit their Ca^{2+} elevations (Kol et al., 2020). This is remarkable, because Gi/o protein-coupled receptors usually enhance Ca^{2+} dynamics in astroglia. Others indeed found that hM4Di when expressed in hippocampal CA1 astrocytes enhances Ca^{2+} signals (Durkee et al., 2019), and this is consistent with striatal astrocytes (Nagai et al., 2019). One could imagine two possible explanations for this discrepancy. It is possible that the expression level, which could then also affect the subcellular location, was different. Or, since they used the mode in order to present the quantification of Ca^{2+} events, which represents the global maximum in the amplitude frequency distribution but completely ignores local maxima, it may be interesting to see the full distribution in response sizes. Nevertheless, in this elegant study they found that the CA1-to-anterior cingulate cortex (ACC) projection is critical for remote memory but not for recent memory. Inhibiting CA1 astrocyte Ca^{2+} dynamics then disrupts remote memory (Kol et al., 2020). These results are consistent with the recent finding that IP_3R2 gene deletion impairs remote but not recent memory (Pinto-Duarte et al., 2019).

The mas-related genes G_q protein-coupled orphan receptor MrgA1, which is naturally only expressed in some nociceptive neurons (Han et al., 2002), was the first xenoreceptor used for astroglia-specific Ca^{2+} activation (Fiacco et al., 2007). When expressed in cerebellar Bergmann glia of anesthetized mice, it was found that application of its peptide ligand, the Phe-Met-Arg-Phe (FMRF)amide, a whole-cell Ca^{2+} elevation is accompanied by extracellular reduction in potassium concentration leading to a temporary hyperexcitability of Purkinje cells, the cerebellar principal neurons (Wang et al., 2012); however, see Smith et al. (2018). A different study used the hyperpolarizing optogenetic actuator Archaerhodopsin (Arch)[5] in cortical astrocytes of awake mice and found that Arch light-activation causes Ca^{2+} elevations that, in terms of their spatial restriction, resemble microdomain events, but last tens of seconds (Poskanzer and Yuste, 2016). The mechanism of how Arch leads to Ca^{2+} elevation remains elusive. As a consequence of astrocyte Arch activation, extracellular glutamate spikes can be detected accompanying slow oscillatory and more synchronized neuronal activity (Poskanzer and Yuste, 2016).

Activation of hM3Dq and the α_1-adrenergic receptor-based opsin Opto-Gq (Airan et al., 2009) in hippocampal CA1 astrocytes to elevate Ca^{2+} has been demonstrated to be sufficient to induce NMDA receptor-dependent LTP and contextual memory (Adamsky et al., 2018). In contrast, hM3Dq activation in neurons has a detrimental effect on memory performance (Adamsky et al., 2018). Activation of hM4Di in striatal astrocytes leads to enhanced Ca^{2+} elevations and hyperactivity (Nagai et al., 2019). Transcriptomic analysis of activated astrocytes revealed the reactivation of thrombospondin 1, which is an important factor during developmental synaptogenesis (Christopherson et al., 2005). Treatment with gabapentin, antagonist of the thrombospondin 1 receptor, rescues all morphological as well as all functional changes (Nagai et al., 2019). They further demonstrated that hM4Di activation in astrocytes can be used to compensate phenotypically for mouse disease models which display reduced astrocytic Ca^{2+} activity, such as the Huntington's disease mouse model (Yu et al., 2020). Durkee et al. (2019) conducted a systematic comparison of the effects of hM3Dq and hM4Di when expressed in neurons or astrocytes. They found that hM4Di, like $GABA_BR$ activation, elevates Ca^{2+} levels in astrocytes in an IP_3R2-dependent manner. Yet, the phospholipase C inhibitor U73122 failed to inhibit hM4Di as well as $GABA_BR$ responses in astrocytes. This suggests the possibility that in general, Gi/o protein-coupled receptors in astroglia couple via the $\beta\gamma$ subunit to the IP_3R2 (Zeng et al., 2003; Durkee et al., 2019).

[2]http://www.addgene.org/111568/

[3]https://www.addgene.org/50478/

[4]https://www.addgene.org/50479/

[5]https://www.addgene.org/28307/

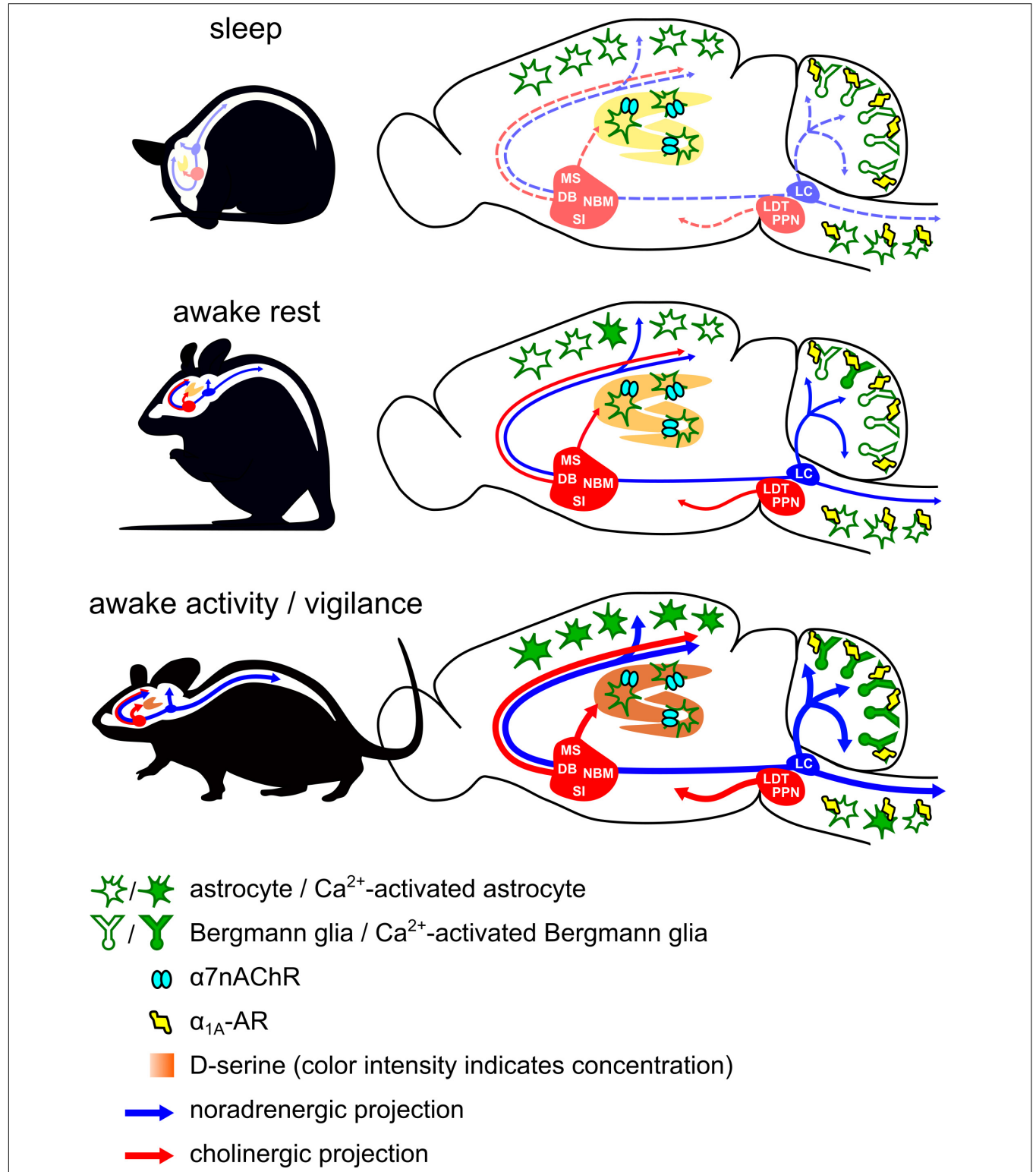

FIGURE 1 | Diagram of behavioral state-dependent activation of noradrenergic and cholinergic systems and their modulation of astroglia Ca^{2+} dynamics during sleep, rest, and vigilance. Astrocytes in primary visual cortex and somatosensory cortex, *Hes5*-positive astrocytes in spinal dorsal horn, and cerebellar Bergmann glia exhibit norepinephrine-dependent global Ca^{2+} rises during states of heightened vigilance. In Bergmann glia and *Hes5*-positive astrocytes of spinal dorsal horn, this arousal-associated Ca^{2+} signal is mediated by α_{1A}-adrenergic receptors. Cholinergic activation of hippocampal astrocytes through α7 nicotinic acetylcholine receptors has been found to modulate D-serine concentration depending on the sleep-wake state. LC, locus coeruleus; LDT, laterodorsal tegmental nucleus; PPN, pedunculopontine nucleus; MS, medial septal nucleus; DB, diagonal band of Broca; NBM, nucleus basalis of Meynert; SI, substantia innominata.

OUTLOOK

Considerable progress has been made in our understanding of the role of astroglia Ca^{2+} dynamics for the processing of information in the brain. Behavioral state transitions occur constantly, ranging from different sleep states to various levels of vigilance during wakefulness and are disrupted in psychiatric disease. Emerging experimental findings, which are schematized in **Figure 1**, emphasize the importance of the particular behavioral state that determines which molecular mechanisms predominate the respective astroglia Ca^{2+} signal, what spatial and temporal pattern it assumes, and how it feeds back to behavior. While the precise astroglia Ca^{2+} signals in unanesthetized animals have not yet been defined *in vivo* for many of the discussed receptors, it appears that a significant portion of astroglia Ca^{2+} dynamics are representations of neuromodulator signaling and are primed for a role in informing neural populations about the behavioral and environmental context. Since dependence of astroglia Ca^{2+} activation on behavioral state relies on variable release of neuromodulator and not on variable intrinsic responsiveness of astroglia, it is possible that exogenous astroglia-specific actuators have led to more robust phenotypes because the limited spatial and temporal precision of this approach allows the recruitment of astroglia Ca^{2+} activation out of behavioral or environmental context. On the other hand, it is encouraging that several similarities in phenotypes have been independently defined. For example, the importance of astroglia Ca^{2+} dynamics in memory consolidation allowing remote memory formation has been discovered using the IP_3R2 gene deletion model as well as independently using inhibitory DREADD overexpression in hippocampal astrocytes. Similarly, a role for astroglia Ca^{2+} dynamics in developmental synapse elimination was discovered using the same IP_3R2 gene deletion model, and independently it was found that developmental synaptogenic cues can be reactivated by exogenous enhancement of astroglia Ca^{2+} dynamics in adult mice. It will be important to combine insight from exogenous activation studies with our increasing understanding of the behavioral and environmental context when endogenous astroglia signaling pathways are naturally engaged to revise and customize conventional behavioral paradigms for testing the physiological impact of astroglia Ca^{2+} dynamics. This will be a prerequisite for recognizing alterations in astroglia Ca^{2+} dynamics and for understanding how they can contribute to nervous system disease.

AUTHOR CONTRIBUTIONS

All authors listed have made a substantial, direct and intellectual contribution to the work, and approved it for publication.

FUNDING

EL was supported by a T32NS082145 fellowship. This work was supported by R01AA025128, R01MH113780, and The Robert J. Kleberg, Jr. and Helen C. Kleberg Foundation to MP.

ACKNOWLEDGMENTS

Astroglia Ca^{2+} dynamics and their consequences for neural circuit function and behavior has become a rapidly proliferating research area. Many important contributions could not be covered in this review. However, we hope that the organization of this review will help to place other studies in context.

REFERENCES

Adamsky, A., Kol, A., Kreisel, T., Doron, A., Ozeri-Engelhard, N., Melcer, T., et al. (2018). Astrocytic activation generates De Novo neuronal potentiation and memory enhancement. *Cell* 174, 59.e14–71.e14. doi: 10.1016/j.cell.2018.05.002

Agarwal, A., Wu, P.-H., Hughes, E. G., Fukaya, M., Tischfield, M. A., Langseth, A. J., et al. (2017). Transient opening of the mitochondrial permeability transition pore induces microdomain calcium transients in astrocyte processes. *Neuron* 93, 587.e7–605.e7. doi: 10.1016/j.neuron.2016.12.034

Agulhon, C., Fiacco, T. A., and McCarthy, K. D. (2010). Hippocampal short- and long-term plasticity are not modulated by astrocyte Ca2+ signaling. *Science* 327, 1250–1254. doi: 10.1126/science.1184821

Airan, R. D., Thompson, K. R., Fenno, L. E., Bernstein, H., and Deisseroth, K. (2009). Temporally precise in vivo control of intracellular signalling. *Nature* 458, 1025–1029. doi: 10.1038/nature07926

Alger, B. E. (2002). Retrograde signaling in the regulation of synaptic transmission: focus on endocannabinoids. *Prog. Neurobiol.* 68, 247–286. doi: 10.1016/S0301-0082(02)00080-1

Araque, A., Carmignoto, G., Haydon, P. G., Oliet, S. H. R., Robitaille, R., and Volterra, A. (2014). Gliotransmitters travel in time and space. *Neuron* 81, 728–739. doi: 10.1016/j.neuron.2014.02.007

Araque, A., Parpura, V., Sanzgiri, R. P., and Haydon, P. G. (1999). Tripartite synapses: glia, the unacknowledged partner. *Trends Neurosci.* 22, 208–215. doi: 10.1016/S0166-2236(98)01349-6

Arizono, M., Inavalli, V. V. G. K., Panatier, A., Pfeiffer, T., Angibaud, J., Levet, F., et al. (2020). Structural basis of astrocytic Ca2+ signals at tripartite synapses. *Nat. Commun.* 11:1906. doi: 10.1038/s41467-020-15648-4

Babola, T. A., Kersbergen, C. J., Wang, H. C., and Bergles, D. E. (2020). Purinergic signaling in cochlear supporting cells reduces hair cell excitability by increasing the extracellular space. *eLife* 9:e52160. doi: 10.7554/eLife.52160

Babola, T. A., Li, S., Gribizis, A., Lee, B. J., Issa, J. B., Wang, H. C., et al. (2018). Homeostatic control of spontaneous activity in the developing auditory system. *Neuron* 99, 511.e5–524.e5. doi: 10.1016/j.neuron.2018.07.004

Bánsághi, S., Golenár, T., Madesh, M., Csordás, G., RamachandraRao, S., Sharma, K., et al. (2014). Isoform- and species-specific control of inositol 1,4,5-trisphosphate (IP3) receptors by reactive oxygen species. *J. Biol. Chem.* 289, 8170–8181. doi: 10.1074/jbc.M113.504159

Beierlein, M., and Regehr, W. G. (2006). Brief bursts of parallel fiber activity trigger calcium signals in bergmann glia. *J. Neurosci.* 26, 6958–6967.

Bekar, L. K., He, W., and Nedergaard, M. (2008). Locus coeruleus alpha-adrenergic-mediated activation of cortical astrocytes in vivo. *Cereb. Cortex* 18, 2789–2795. doi: 10.1093/cercor/bhn040

Biesecker, K. R., Srienc, A. I., Shimoda, A. M., Agarwal, A., Bergles, D. E., Kofuji, P., et al. (2016). Glial cell calcium signaling mediates capillary regulation of blood flow in the retina. *J. Neurosci.* 36, 9435–9445. doi: 10.1523/JNEUROSCI.1782-16.2016

Bindocci, E., Savtchouk, I., Liaudet, N., Becker, D., Carriero, G., and Volterra, A. (2017). Three-dimensional Ca $^{2+}$ imaging advances understanding of astrocyte biology. *Science* 356:eaai8185. doi: 10.1126/science.aai8185

Bojarskaite, L., Bjørnstad, D. M., Pettersen, K. H., Cunen, C., Hermansen, G. H., Åbjørsbråten, K. S., et al. (2020). Astrocytic Ca2+ signaling is reduced during sleep and is involved in the regulation of slow wave sleep. *Nat. Commun.* 11:3240. doi: 10.1038/s41467-020-17062-2

Bonder, D. E., and McCarthy, K. D. (2014). Astrocytic Gq-GPCR-linked IP3R-dependent Ca2+ signaling does not mediate neurovascular coupling in mouse visual cortex in vivo. *J. Neurosci.* 34, 13139–13150. doi: 10.1523/JNEUROSCI.2591-14.2014

Burnashev, N., Khodorova, A., Jonas, P., Helm, P. J., Wisden, W., Monyer, H., et al. (1992). Calcium-permeable AMPA-kainate receptors in fusiform cerebellar glial cells. *Science* 256, 1566–1570. doi: 10.1126/science.1317970

Buzśaki, G., and Wang, X. J. (2012). Mechanisms of gamma oscillations. *Annu. Rev. Neurosci.* 35, 203–225. doi: 10.1146/annurev-neuro-062111-150444

Chen, N., Sugihara, H., Sharma, J., Perea, G., Petravicz, J., Le, C., et al. (2012). Nucleus basalis-enabled stimulus-specific plasticity in the visual cortex is mediated by astrocytes. *Proc. Natl. Acad. Sci. U.S.A.* 109, E2832–E2841. doi: 10.1073/pnas.1206557109

Christopherson, K. S., Ullian, E. M., Stokes, C. C. A., Mullowney, C. E., Hell, J. W., Agah, A., et al. (2005). Thrombospondins are astrocyte-secreted proteins that promote CNS synaptogenesis. *Cell* 120, 421–433. doi: 10.1016/j.cell.2004.12.020

Delekate, A., Füchtemeier, M., Schumacher, T., Ulbrich, C., Foddis, M., and Petzold, G. C. (2014). Metabotropic P2Y1 receptor signalling mediates astrocytic hyperactivity in vivo in an Alzheimer's disease mouse model. *Nat. Commun.* 5:5422. doi: 10.1038/ncomms6422

Ding, F., O'Donnell, J., Thrane, A. S., Zeppenfeld, D., Kang, H., Xie, L., et al. (2013). α1-Adrenergic receptors mediate coordinated Ca2+ signaling of cortical astrocytes in awake, behaving mice. *Cell Calcium* 54, 387–394. doi: 10.1016/j.ceca.2013.09.001

Dombeck, D. A., Khabbaz, A. N., Collman, F., Adelman, T. L., and Tank, D. W. (2007). Imaging large-scale neural activity with cellular resolution in awake, mobile mice. *Neuron* 56, 43–57. doi: 10.1016/j.neuron.2007.08.003

Duchen, M. R. (2000). Mitochondria and Ca2+ in cell physiology and pathophysiology. *Cell Calcium* 28, 339–348. doi: 10.1054/ceca.2000.0170

Durkee, C. A., Covelo, A., Lines, J., Kofuji, P., Aguilar, J., and Araque, A. (2019). $G_{i/o}$ protein-coupled receptors inhibit neurons but activate astrocytes and stimulate gliotransmission. *Glia* 67, 1076–1093. doi: 10.1002/glia.23589

Erickson, E. K., DaCosta, A. J., Mason, S. C., Blednov, Y. A., Mayfield, R. D., and Harris, R. A. (2020). Cortical astrocytes regulate ethanol consumption and intoxication in mice. *Neuropsychopharmacology* 46, 500–508. doi: 10.1038/s41386-020-0721-0

Fiacco, T. A., Agulhon, C., Taves, S. R., Petravicz, J., Casper, K. B., Dong, X., et al. (2007). Selective stimulation of astrocyte calcium in situ does not affect neuronal excitatory synaptic activity. *Neuron* 54, 611–626. doi: 10.1016/j.neuron.2007.04.032

Fiacco, T. A., and McCarthy, K. D. (2018). Multiple lines of evidence indicate that gliotransmission does not occur under physiological conditions. *J. Neurosci.* 38, 3–13. doi: 10.1523/JNEUROSCI.0016-17.2017

Foley, J., Blutstein, T., Lee, S., Erneux, C., Halassa, M. M., and Haydon, P. (2017). Astrocytic IP3/Ca2+ signaling modulates theta rhythm and REM Sleep. *Front. Neural Circuits* 11:3. doi: 10.3389/fncir.2017.00003

Franze, K., Grosche, J., Skatchkov, S. N., Schinkinger, S., Foja, C., Schild, D., et al. (2007). Müller cells are living optical fibers in the vertebrate retina. *Proc. Natl. Acad. Sci. U.S.A.* 104, 8287–8292. doi: 10.1073/pnas.0611180104

Fu, Y., Tucciarone, J. M., Espinosa, J. S., Sheng, N., Darcy, D. P., Nicoll, R. A., et al. (2014). A cortical circuit for gain control by behavioral state. *Cell* 156, 1139–1152. doi: 10.1016/j.cell.2014.01.050

Giaume, C., and McCarthy, K. D. (1996). Control of gap-junctional communication in astrocytic networks. *Trends Neurosci.* 19, 319–325. doi: 10.1016/0166-2236(96)10046-1

Grosche, J., Matyash, V., Möller, T., Verkhratsky, A., Reichenbach, A., and Kettenmann, H. (1999). Microdomains for neuron-glia interaction: parallel fiber signaling to Bergmann glial cells. *Nat. Neurosci.* 2, 139–143.

Halassa, M. M., Florian, C., Fellin, T., Munoz, J. R., Lee, S.-Y., Abel, T., et al. (2009). Astrocytic modulation of sleep homeostasis and cognitive consequences of sleep loss. *Neuron* 61, 213–219. doi: 10.1016/j.neuron.2008.11.024

Han, J., Kesner, P., Metna-Laurent, M., Duan, T., Xu, L., Georges, F., et al. (2012). Acute cannabinoids impair working memory through astroglial CB1 receptor modulation of hippocampal LTD. *Cell* 148, 1039–1050. doi: 10.1016/j.cell.2012.01.037

Han, S. K., Dong, X., Hwang, J. I., Zylka, M. J., Anderson, D. J., and Simon, M. I. (2002). Orphan G protein-coupled receptors Mrga1 and Mrgc11 are distinctively activated by RF-amide-related peptides through the Gαq/11 pathway. *Proc. Natl. Acad. Sci. U.S.A.* 99, 14740–14745. doi: 10.1073/pnas.192565799

Haustein, M. D., Kracun, S., Lu, X.-H., Shih, T., Jackson-Weaver, O., Tong, X., et al. (2014). Conditions and constraints for astrocyte calcium signaling in the hippocampal mossy fiber pathway. *Neuron* 82, 413–429. doi: 10.1016/j.neuron.2014.02.041

Henneberger, C., Papouin, T., Oliet, S. H. R., and Rusakov, D. A. (2010). Long-term potentiation depends on release of d-serine from astrocytes. *Nature* 463, 232–236. doi: 10.1038/nature08673

Holtzclaw, L. A., Pandhit, S., Bare, D. J., Mignery, G. A., and Russell, J. T. (2002). Astrocytes in adult rat brain express type 2 inositol 1,4,5-trisphosphate receptors. *Glia* 39, 69–84. doi: 10.1002/glia.10085

Hoogland, T. M., Kuhn, B., Göbel, W., Huang, W., Nakai, J., Helmchen, F., et al. (2009). Radially expanding transglial calcium waves in the intact cerebellum. *Proc. Natl. Acad. Sci. U.S.A.* 106, 3496–3501.

Iino, M., Goto, K., Kakegawa, W., Okado, H., Sudo, M., Ishiuchi, S., et al. (2001). Glia-synapse interaction through Ca2+-permeable AMPA receptors in Bergmann glia. *Science* 292, 926–929.

Ingiosi, A. M., Hayworth, C. R., Harvey, D. O., Singletary, K. G., Rempe, M. J., Wisor, J. P., et al. (2020). A role for astroglial calcium in mammalian sleep and sleep regulation. *Curr. Biol.* 30, 1–11. doi: 10.1016/j.cub.2020.08.052

Jackson, J. G., and Robinson, M. B. (2015). Reciprocal regulation of mitochondrial dynamics and calcium signaling in astrocyte processes. *J. Neurosci.* 35, 15199–15213. doi: 10.1523/JNEUROSCI.2049-15.2015

Jasper, H. H., and Tessier, J. (1971). Acetylcholine liberation from cerebral cortex during paradoxical (REM) sleep. *Science* 172, 601–602. doi: 10.1126/science.172.3983.601

Keller, G. B., Bonhoeffer, T., and Hübener, M. (2012). Sensorimotor mismatch signals in primary visual cortex of the behaving mouse. *Neuron* 74, 809–815. doi: 10.1016/j.neuron.2012.03.040

King, C. M., Bohmbach, K., Minge, D., Delekate, A., Zheng, K., Reynolds, J., et al. (2020). Local Resting Ca2+ controls the scale of astroglial Ca2+ Signals. *Cell Rep.* 30, 3466.e5–3477.e5. doi: 10.1016/j.celrep.2020.02.043

Kofuji, P., and Araque, A. (2020). G-Protein-Coupled receptors in astrocyte–neuron communication. *Neuroscience* 456, 71–84. doi: 10.1016/j.neuroscience.2020.03.025

Köhler, S., Winkler, U., and Hirrlinger, J. (2019). Heterogeneity of astrocytes in grey and white matter. *Neurochem. Res.* 46, 3–14. doi: 10.1007/s11064-019-02926-x

Kohro, Y., Matsuda, T., Yoshihara, K., Kohno, K., Koga, K., Katsuragi, R., et al. (2020). Spinal astrocytes in superficial laminae gate brainstem descending control of mechanosensory hypersensitivity. *Nat. Neurosci.* 23, 1376–1387. doi: 10.1038/s41593-020-00713-4

Kol, A., Adamsky, A., Groysman, M., Kreisel, T., London, M., and Goshen, I. (2020). Astrocytes contribute to remote memory formation by modulating hippocampal–cortical communication during learning. *Nat. Neurosci.* 23, 1229–1239. doi: 10.1038/s41593-020-0679-6

Kreitzer, A. C., Carter, A. G., and Regehr, W. G. (2002). Inhibition of interneuron firing extends the spread of endocannabinoid signaling in the cerebellum. *Neuron* 34, 787–796. doi: 10.1016/S0896-6273(02)00695-5

Kronschläger, M. T., Drdla-Schutting, R., Gassner, M., Honsek, S. D., Teuchmann, H. L., and Sandkühler, J. (2016). Gliogenic LTP spreads widely in nociceptive pathways. *Science* 354, 1144–1148. doi: 10.1126/science.aah5715

Kuchibhotla, K. V., Lattarulo, C. R., Hyman, B. T., and Bacskai, B. J. (2009). Synchronous hyperactivity and intercellular calcium waves in astrocytes in Alzheimer mice. *Science* 323, 1211–1215. doi: 10.1126/science.1169096

Kuffler, S. W. (1967). Neuroglial cells: physiological properties and a potassium mediated effect of neuronal activity on the glial membrane potential. *Proc. R. Soc. Lond. Ser. B Biol. Sci.* 168, 1–21. doi: 10.1098/rspb.1967.0047

Lee, H. S., Ghetti, A., Pinto-Duarte, A., Wang, X., Dziewczapolski, G., Galimi, F., et al. (2014). Astrocytes contribute to gamma oscillations and recognition

memory. *Proc. Natl. Acad. Sci. U.S.A.* 111, E3343–E3352. doi: 10.1073/pnas.1410893111

Lee, S., Yoon, B.-E., Berglund, K., Oh, S.-J., Park, H., Shin, H.-S., et al. (2010). Channel-mediated tonic GABA release from glia. *Science* 330, 790–796. doi: 10.1126/science.1184334

Lichtman, A. H., and Martin, B. R. (1996). Δ9-Tetrahydrocannabinol impairs spatial memory through a cannabinoid receptor mechanism. *Psychopharmacology* 126, 125–131. doi: 10.1007/BF02246347

Lines, J., Martin, E. D., Kofuji, P., Aguilar, J., and Araque, A. (2020). Astrocytes modulate sensory-evoked neuronal network activity. *Nat. Commun.* 11:3689. doi: 10.1038/s41467-020-17536-3

Ma, Z., and Freeman, M. R. (2020). TrpML-mediated astrocyte microdomain Ca2+ transients regulate astrocyte-tracheal interactions. *eLife* 9:e58952. doi: 10.7554/eLife.58952

Ma, Z., Stork, T., Bergles, D. E., and Freeman, M. R. (2016). Neuromodulators signal through astrocytes to alter neural circuit activity and behaviour. *Nature* 539, 428–432. doi: 10.1038/nature20145

Maejima, T., Hashimoto, K., Yoshida, T., Aiba, A., and Kano, M. (2001). Presynaptic inhibition caused by retrograde signal from metabotropic glutamate to cannabinoid receptors. *Neuron* 31, 463–475. doi: 10.1016/S0896-6273(01)00375-0

Marcaggi, P., and Attwell, D. (2005). Endocannabinoid signaling depends on the spatial pattern of synapse activation. *Nat. Neurosci.* 8, 776–781. doi: 10.1038/nn1458

Marina, N., Christie, I. N., Korsak, A., Doronin, M., Brazhe, A., Hosford, P. S., et al. (2020). Astrocytes monitor cerebral perfusion and control systemic circulation to maintain brain blood flow. *Nat. Commun.* 11:131. doi: 10.1038/s41467-019-13956-y

McCaslin, A. F. H., Chen, B. R., Radosevich, A. J., Cauli, B., and Hillman, E. M. C. (2011). In vivo 3D morphology of astrocyte-vasculature interactions in the somatosensory cortex: Implications for neurovascular coupling. *J. Cereb. Blood Flow Metab.* 31, 795–806. doi: 10.1038/jcbfm.2010.204

Mederos, S., Hernández-Vivanco, A., Ramírez-Franco, J., Martín-Fernández, M., Navarrete, M., Yang, A., et al. (2019). Melanopsin for precise optogenetic activation of astrocyte-neuron networks. *Glia* 67, 915–934. doi: 10.1002/glia.23580

Mederos, S., Sánchez-Puelles, C., Esparza, J., Valero, M., Ponomarenko, A., and Perea, G. (2021). GABAergic signaling to astrocytes in the prefrontal cortex sustains goal-directed behaviors. *Nat. Neurosci.* 24, 82–92. doi: 10.1038/s41593-020-00752-x

Melom, J. E., and Littleton, J. T. (2013). Mutation of a NCKX eliminates glial microdomain calcium oscillations and enhances seizure susceptibility. *J. Neurosci.* 33, 1169–1178. doi: 10.1523/JNEUROSCI.3920-12.2013

Men, Y., Ye, L., Risgaard, R. D., Promes, V., Zhao, X., Paukert, M., et al. (2020). Astroglial FMRP deficiency cell-autonomously up-regulates miR-128 and disrupts developmental astroglial mGluR5 signaling. *Proc. Natl. Acad. Sci. U.S.A.* 117, 25092–25103. doi: 10.1073/pnas.2014080117

Mishra, A., Reynolds, J. P., Chen, Y., Gourine, A. V., Rusakov, D. A., and Attwell, D. (2016). Astrocytes mediate neurovascular signaling to capillary pericytes but not to arterioles. *Nat. Neurosci.* 19, 1619–1627. doi: 10.1038/nn.4428

Monai, H., Ohkura, M., Tanaka, M., Oe, Y., Konno, A., Hirai, H., et al. (2016). Calcium imaging reveals glial involvement in transcranial direct current stimulation-induced plasticity in mouse brain. *Nat. Commun.* 7:11100. doi: 10.1038/ncomms11100

Mothet, J. P., Billard, J. M., Pollegioni, L., Coyle, J. T., and Sweedler, J. V. (2019). Investigating brain d-serine: advocacy for good practices. *Acta Physiol.* 226:e13257. doi: 10.1111/apha.13257

Mu, Y., Bennett, D. V., Rubinov, M., Narayan, S., Yang, C.-T., Tanimoto, M., et al. (2019). Glia accumulate evidence that actions are futile and suppress unsuccessful behavior. *Cell* 178, 27.e19–43.e19. doi: 10.1016/j.cell.2019.05.050

Müller, T., Möller, T., Berger, T., Schnitzer, J., and Kettenmann, H. (1992). Calcium entry through kainate receptors and resulting potassium-channel blockade in Bergmann glial cells. *Science* 256, 1563–1566.

Nagai, J., Rajbhandari, A. K., Gangwani, M. R., Hachisuka, A., Coppola, G., Masmanidis, S. C., et al. (2019).). Hyperactivity with disrupted attention by activation of an astrocyte synaptogenic cue. *Cell* 177, 1280.e20–1292.e20. doi: 10.1016/j.cell.2019.03.019

Navarrete, M., and Araque, A. (2008). Endocannabinoids mediate neuron-astrocyte communication. *Neuron* 57, 883–893. doi: 10.1016/j.neuron.2008.01.029

Navarrete, M., and Araque, A. (2010). Endocannabinoids potentiate synaptic transmission through stimulation of astrocytes. *Neuron* 68, 113–126. doi: 10.1016/j.neuron.2010.08.043

Navarrete, M., Cuartero, M. I., Palenzuela, R., Draffin, J. E., Konomi, A., Serra, I., et al. (2019). Astrocytic p38α MAPK drives NMDA receptor-dependent long-term depression and modulates long-term memory. *Nat. Commun.* 10:2968. doi: 10.1038/s41467-019-10830-9

Navarrete, M., Perea, G., de Sevilla, D. F., Gómez-Gonzalo, M., Núñez, A., Martín, E. D., et al. (2012). Astrocytes mediate in vivo cholinergic-induced synaptic plasticity. *PLoS Biol.* 10:e1001259. doi: 10.1371/journal.pbio.1001259

Nimmerjahn, A., Mukamel, E. A., and Schnitzer, M. J. (2009). Motor behavior activates Bergmann glial networks. *Neuron* 62, 400–412.

Nizar, K., Uhlirova, H., Tian, P., Saisan, P. A., Cheng, Q., Reznichenko, L., et al. (2013). In vivo stimulus-induced vasodilation occurs without IP3 receptor activation and may precede astrocytic calcium increase. *J. Neurosci.* 33, 8411–8422. doi: 10.1523/JNEUROSCI.3285-12.2013

Oh, S. J., and Lee, C. J. (2017). Distribution and function of the Bestrophin-1 (Best1) channel in the brain. *Exp. Neurobiol.* 26, 113–121. doi: 10.5607/en.2017.26.3.113

Oheim, M., Schmidt, E., and Hirrlinger, J. (2018). Local energy on demand: are 'spontaneous' astrocytic Ca2+-microdomains the regulatory unit for astrocyte-neuron metabolic cooperation? *Brain Res. Bull.* 136, 54–64. doi: 10.1016/j.brainresbull.2017.04.011

Ohno-Shosaku, T., Tsubokawa, H., Mizushima, I., Yoneda, N., Zimmer, A., and Kano, M. (2002). Presynaptic cannabinoid sensitivity is a major determinant of depolarization-induced retrograde suppression at hippocampal synapses. *J. Neurosci.* 22, 3864–3872. doi: 10.1523/jneurosci.22-10-03864.2002

Padmashri, R., Suresh, A., Boska, M. D., and Dunaevsky, A. (2015). Motor-skill learning is dependent on astrocytic activity. *Neural Plast* 2015:938023. doi: 10.1155/2015/938023

Panatier, A., Theodosis, D. T., Mothet, J. P., Touquet, B., Pollegioni, L., Poulain, D. A., et al. (2006). Glia-Derived d-Serine controls NMDA receptor activity and synaptic memory. *Cell* 125, 775–784. doi: 10.1016/j.cell.2006.02.051

Papouin, T., Dunphy, J. M., Tolman, M., Dineley, K. T., and Haydon, P. G. (2017). Septal cholinergic neuromodulation tunes the astrocyte-dependent gating of hippocampal NMDA Receptors to wakefulness. *Neuron* 94, 840.e7–854.e7. doi: 10.1016/j.neuron.2017.04.021

Paukert, M., Agarwal, A., Cha, J., Doze, V. A., Kang, J. U., and Bergles, D. E. (2014). Norepinephrine controls astroglial responsiveness to local circuit activity. *Neuron* 82, 1263–1270. doi: 10.1016/j.neuron.2014.04.038

Perea, G., Gómez, R., Mederos, S., Covelo, A., Ballesteros, J. J., Schlosser, L., et al. (2016). Activity-dependent switch of GABAergic inhibition into glutamatergic excitation in astrocyte-neuron networks. *eLife* 5:e20362. doi: 10.7554/eLife.20362

Petravicz, J., Boyt, K. M., and McCarthy, K. D. (2014). Astrocyte IP3R2-dependent Ca2+ signaling is not a major modulator of neuronal pathways governing behavior. *Front. Behav. Neurosci.* 8:384. doi: 10.3389/fnbeh.2014.00384

Petravicz, J., Fiacco, T. A., and McCarthy, K. D. (2008). Loss of IP3 receptor-dependent Ca2+ increases in hippocampal astrocytes does not affect baseline CA1 pyramidal neuron synaptic activity. *J. Neurosci.* 28, 4967–4973. doi: 10.1523/JNEUROSCI.5572-07.2008

Piet, R., and Jahr, C. E. (2007). Glutamatergic and purinergic receptor-mediated calcium transients in Bergmann glial cells. *J. Neurosci.* 27, 4027–4035.

Pinto-Duarte, A., Roberts, A. J., Ouyang, K., and Sejnowski, T. J. (2019). Impairments in remote memory caused by the lack of Type 2 IP3 receptors. *Glia* 67, 1976–1989. doi: 10.1002/glia.23679

Polack, P.-O., Friedman, J., and Golshani, P. (2013). Cellular mechanisms of brain state-dependent gain modulation in visual cortex. *Nat. Neurosci.* 16, 1331–1339. doi: 10.1038/nn.3464

Poskanzer, K. E., and Yuste, R. (2016). Astrocytes regulate cortical state switching in vivo. *Proc. Natl. Acad. Sci. U.S.A.* 113, E2675–E2684. doi: 10.1073/pnas.1520759113

Ransom, B. R., and Goldring, S. (1973). Ionic determinants of membrane potential of cells presumed to be glia in cerebral cortex of cat. *J. Neurophysiol.* 36, 855–868. doi: 10.1152/jn.1973.36.5.855

Reimer, J., McGinley, M. J., Liu, Y., Rodenkirch, C., Wang, Q., McCormick, D. A., et al. (2016). Pupil fluctuations track rapid changes in adrenergic and cholinergic activity in cortex. *Nat. Commun.* 7:13289. doi: 10.1038/ncomms13289

Robin, L. M., Oliveira da Cruz, J. F., Langlais, V. C., Martin-Fernandez, M., Metna-Laurent, M., Busquets-Garcia, A., et al. (2018). Astroglial CB1 receptors determine synaptic d-serine availability to enable recognition memory. *Neuron* 98, 935.e5–944.e5. doi: 10.1016/j.neuron.2018.04.034

Rose, C. R., Felix, L., Zeug, A., Dietrich, D., Reiner, A., and Henneberger, C. (2018). Astroglial glutamate signaling and uptake in the hippocampus. *Front. Mol. Neurosci.* 10:451. doi: 10.3389/fnmol.2017.00451

Rudolph, R., Jahn, H. M., Courjaret, R., Messemer, N., Kirchhoff, F., and Deitmer, J. W. (2016). The inhibitory input to mouse cerebellar Purkinje cells is reciprocally modulated by Bergmann glial P2Y1 and AMPA receptor signaling. *Glia* 64, 1265–1280. doi: 10.1002/glia.22999

Saab, A. S., Neumeyer, A., Jahn, H. M., Cupido, A., Šimek, A. A. M., Boele, H.-J., et al. (2012). Bergmann glial AMPA receptors are required for fine motor coordination. *Science* 337, 749–753. doi: 10.1126/science.1221140

Savtchouk, I., and Volterra, A. (2018). Gliotransmission: beyond black-and-white. *J. Neurosci.* 38, 14–25. doi: 10.1523/JNEUROSCI.0017-17.2017

Sharp, A. H., Nucifora, F. C., Blondel, O., Sheppard, C. A., Zhang, C., Snyder, S. H., et al. (1999). Differential cellular expression of isoforms of inositol 1,4,5-triphosphate receptors in neurons and glia in brain. *J. Comp. Neurol.* 406, 207–220. doi: 10.1002/(SICI)1096-9861(19990405)406:2<207:AID-CNE6>3.0.CO;2-7

Sherwood, M. W., Arizono, M., Hisatsune, C., Bannai, H., Ebisui, E., Sherwood, J. L., et al. (2017). Astrocytic IP3Rs: contribution to Ca2+ signalling and hippocampal LTP. *Glia* 65, 502–513. doi: 10.1002/glia.23107

Shigetomi, E., Jackson-Weaver, O., Huckstepp, R. T., O'Dell, T. J., and Khakh, B. S. (2013). TRPA1 channels are regulators of astrocyte basal calcium levels and long-term potentiation via constitutive d-serine release. *J. Neurosci.* 33, 10143–10153. doi: 10.1523/JNEUROSCI.5779-12.2013

Shigetomi, E., Kracun, S., and Khakh, B. S. (2010a). Monitoring astrocyte calcium microdomains with improved membrane targeted GCaMP reporters. *Neuron Glia Biol.* 6, 183–191. doi: 10.1017/S1740925X10000219

Shigetomi, E., Kracun, S., Sofroniew, M. V., and Khakh, B. S. (2010b). A genetically targeted optical sensor to monitor calcium signals in astrocyte processes. *Nat. Neurosci.* 13, 759–766. doi: 10.1038/nn.2557

Shigetomi, E., Tong, X., Kwan, K. Y., Corey, D. P., and Khakh, B. S. (2011). TRPA1 channels regulate astrocyte resting calcium and inhibitory synapse efficacy through GAT-3. *Nat. Neurosci.* 15, 70–80. doi: 10.1038/nn.3000

Siegel, A., Reichenbach, A., Hanke, S., Senitz, D., Brauer, K., and Smith, T. G. (1991). Comparative morphometry of Bergmann glial (Golgi epithelial) cells - A Golgi study. *Anat. Embryol.* 183, 605–612. doi: 10.1007/BF00187909

Smith, N. A., Kress, B. T., Lu, Y., Chandler-Militello, D., Benraiss, A., and Nedergaard, M. (2018). Fluorescent Ca2+ indicators directly inhibit the Na,K-ATPase and disrupt cellular functions. *Sci. Signal.* 11:eaal2039. doi: 10.1126/scisignal.aal2039

Srinivasan, R., Huang, B. S., Venugopal, S., Johnston, A. D., Chai, H., Zeng, H., et al. (2015). Ca2+ signaling in astrocytes from Ip3r2−/− mice in brain slices and during startle responses in vivo. *Nat. Neurosci.* 18, 708–717. doi: 10.1038/nn.4001

Srinivasan, R., Lu, T.-Y., Chai, H., Xu, J., Huang, B. S., Golshani, P., et al. (2016). New transgenic mouse lines for selectively targeting astrocytes and studying calcium signals in astrocyte processes In Situ and In Vivo. *Neuron* 92, 1181–1195. doi: 10.1016/j.neuron.2016.11.030

Stella, N. (2004). Cannabinoid signaling in glial cells. *Glia* 48, 267–277. doi: 10.1002/glia.20084

Stobart, J. L., Ferrari, K. D., Barrett, M. J. P., Glück, C., Stobart, M. J., Zuend, M., et al. (2018). Cortical circuit activity evokes rapid astrocyte calcium signals on a similar timescale to neurons. *Neuron* 98, 726.e4–735.e4. doi: 10.1016/j.neuron.2018.03.050

Sun, W., McConnell, E., Pare, J.-F., Xu, Q., Chen, M., Peng, W., et al. (2013). Glutamate-dependent neuroglial calcium signaling differs between young and adult brain. *Science* 339, 197–200. doi: 10.1126/science.1226740

Takahashi, K., Kayama, Y., Lin, J. S., and Sakai, K. (2010). Locus coeruleus neuronal activity during the sleep-waking cycle in mice. *Neuroscience* 169, 1115–1126. doi: 10.1016/j.neuroscience.2010.06.009

Takano, T., He, W., Han, X., Wang, F., Xu, Q., Wang, X., et al. (2014). Rapid manifestation of reactive astrogliosis in acute hippocampal brain slices. *Glia* 62, 78–95. doi: 10.1002/glia.22588

Takano, T., Tian, G. F., Peng, W., Lou, N., Libionka, W., Han, X., et al. (2006). Astrocyte-mediated control of cerebral blood flow. *Nat. Neurosci.* 9, 260–267. doi: 10.1038/nn1623

Takata, N., and Hirase, H. (2008). Cortical layer 1 and layer 2/3 astrocytes exhibit distinct calcium dynamics in vivo. *PLoS One* 3:e0002525. doi: 10.1371/journal.pone.0002525

Takata, N., Mishima, T., Hisatsune, C., Nagai, T., Ebisui, E., Mikoshiba, K., et al. (2011). Astrocyte calcium signaling transforms cholinergic modulation to cortical plasticity in vivo. *J. Neurosci.* 31, 18155–18165. doi: 10.1523/JNEUROSCI.5289-11.2011

Theis, M., and Giaume, C. (2012). Connexin-based intercellular communication and astrocyte heterogeneity. *Brain Res.* 1487, 88–98. doi: 10.1016/j.brainres.2012.06.045

Thrane, A. S., Rangroo Thrane, V., Zeppenfeld, D., Lou, N., Xu, Q., Nagelhus, E. A., et al. (2012). General anesthesia selectively disrupts astrocyte calcium signaling in the awake mouse cortex. *Proc. Natl. Acad. Sci. U.S.A.* 109, 18974–18979. doi: 10.1073/pnas.1209448109

Tran, C. H. T., Peringod, G., and Gordon, G. R. (2018). astrocytes integrate behavioral state and vascular signals during functional hyperemia. *Neuron* 100, 1133.e3–1148.e3. doi: 10.1016/j.neuron.2018.09.045

Tritsch, N. X., Yi, E., Gale, J. E., Glowatzki, E., and Bergles, D. E. (2007). The origin of spontaneous activity in the developing auditory system. *Nature* 450, 50–55. doi: 10.1038/nature06233

Turovsky, E. A., Braga, A., Yu, Y., Esteras, N., Korsak, A., Theparambil, S. M., et al. (2020). Mechanosensory signaling in astrocytes. *J. Neurosci.* 40, 9364–9371. doi: 10.1523/JNEUROSCI.1249-20.2020

Ventura, R., and Harris, K. M. (1999). Three-dimensional relationships between hippocampal synapses and astrocytes. *J. Neurosci.* 19, 6897–6906. doi: 10.1523/jneurosci.19-16-06897.1999

Vercesi, A. E., Kowaltowski, A. J., Grijalba, M. T., Meinicke, A. R., and Castilho, R. F. (1997). The role of reactive oxygen species in mitochondrial permeability transition. *Biosci. Rep.* 17, 43–52. doi: 10.1023/A:1027335217774

Verkhratsky, A., and Nedergaard, M. (2018). Physiology of astroglia. *Physiol. Rev.* 98, 239–389. doi: 10.1152/physrev.00042.2016

Wang, F., Xu, Q., Wang, W., Takano, T., and Nedergaard, M. (2012). Bergmann glia modulate cerebellar Purkinje cell bistability via Ca2+-dependent K+ uptake. *Proc. Natl. Acad. Sci. U.S.A.* 109, 7911–7916. doi: 10.1073/pnas.1120380109

Wang, H. C., Lin, C. C., Cheung, R., Zhang-Hooks, Y., Agarwal, A., Ellis-Davies, G., et al. (2015). Spontaneous activity of cochlear hair cells triggered by fluid secretion mechanism in adjacent support cells. *Cell* 163, 1348–1359. doi: 10.1016/j.cell.2015.10.070

Wang, W., Fang, H., Groom, L., Cheng, A., Zhang, W., Liu, J., et al. (2008). Superoxide flashes in single mitochondria. *Cell* 134, 279–290. doi: 10.1016/j.cell.2008.06.017

Weiss, S., Melom, J. E., Ormerod, K. G., Zhang, Y. V., and Littleton, J. T. (2019). Glial Ca2+signaling links endocytosis to K+buffering around neuronal somas to regulate excitability. *eLife* 8:e44186. doi: 10.7554/eLife.44186

Wilson, R. I., and Nicoll, R. A. (2001). Endogenous cannabinoids mediate retrograde signalling at hippocampal synapses. *Nature* 410, 588–592. doi: 10.1038/35069076

Wolosker, H., Balu, D. T., and Coyle, J. T. (2016). The rise and fall of the D-Serine-mediated gliotransmission hypothesis. *Trends Neurosci.* 39, 712–721. doi: 10.1016/j.tins.2016.09.007

Woo, J., Min, J. O., Kang, D. S., Kim, Y. S., Jung, G. H., Park, H. J., et al. (2018). Control of motor coordination by astrocytic tonic GABA release through modulation of excitation/inhibition balance in cerebellum. *Proc. Natl. Acad. Sci. U.S.A.* 115, 5004–5009. doi: 10.1073/pnas.1721187115

Yang, J., Yang, H., Liu, Y., Li, X., Qin, L., Lou, H., et al. (2016). Astrocytes contribute to synapse elimination via type 2 inositol 1,4,5-trisphosphate receptor-dependent release of ATP. *eLife* 5:e15043. doi: 10.7554/eLife.15043

Yang, Y., Ge, W., Chen, Y., Zhang, Z., Shen, W., Wu, C., et al. (2003). Contribution of astrocytes to hippocampal long-term potentiation through release of D-serine. *Proc. Natl. Acad. Sci. U.S.A.* 100, 15194–15199. doi: 10.1073/pnas.2431073100

Ye, L., Haroon, M. A., Salinas, A., and Paukert, M. (2017). Comparison of GCaMP3 and GCaMP6f for studying astrocyte Ca2+ dynamics in the awake mouse brain. *PLoS One* 12:e0181113. doi: 10.1371/journal.pone.0181113

Ye, L., Orynbayev, M., Zhu, X., Lim, E. Y., Dereddi, R. R., Agarwal, A., et al. (2020). Ethanol abolishes vigilance-dependent astroglia network activation in mice by inhibiting norepinephrine release. *Nat. Commun.* 11:6157. doi: 10.1038/s41467-020-19475-5

Yoon, B. E., Woo, J., Chun, Y. E., Chun, H., Jo, S., Bae, J. Y., et al. (2014). Glial GABA, synthesized by monoamine oxidase B, mediates tonic inhibition. *J. Physiol.* 592, 4951–4968. doi: 10.1113/jphysiol.2014.278754

Yu, X., Nagai, J., Marti-Solano, M., Soto, J. S., Coppola, G., Babu, M. M., et al. (2020). Context-specific striatal astrocyte molecular responses are phenotypically exploitable. *Neuron* 108, 1146.e10–1162.e10. doi: 10.1016/j.neuron.2020.09.021

Yu, X., Taylor, A. M. W., Nagai, J., Golshani, P., Evans, C. J., Coppola, G., et al. (2018). Reducing astrocyte calcium signaling in vivo alters striatal microcircuits and causes repetitive behavior. *Neuron* 99, 1170.e9–1187.e9. doi: 10.1016/j.neuron.2018.08.015

Zeng, W., Mak, D. O. D., Li, Q., Shin, D. M., Foskett, J. K., and Muallem, S. (2003). A new mode of Ca2+ signaling by G protein-coupled receptors: gating of IP3 receptor Ca2+ release channels by Gβγ. *Curr. Biol.* 13, 872–876. doi: 10.1016/S0960-9822(03)00330-0

Zhang, Y., Chen, K., Sloan, S. A., Bennett, M. L., Scholze, A. R., O'Keeffe, S., et al. (2014). An RNA-Sequencing transcriptome and splicing database of glia, neurons, and vascular cells of the cerebral cortex. *J. Neurosci.* 34, 11929–11947. doi: 10.1523/JNEUROSCI.1860-14.2014

Zhang, Y. V., Ormerod, K. G., and Littleton, J. T. (2017). Astrocyte Ca2+ influx negatively regulates neuronal activity. *eNeuro* 4:ENEURO.0340-16.2017. doi: 10.1523/ENEURO.0340-16.2017

Zonta, M., Angulo, M. C., Gobbo, S., Rosengarten, B., Hossmann, K. A., Pozzan, T., et al. (2003). Neuron-to-astrocyte signaling is central to the dynamic control of brain microcirculation. *Nat. Neurosci.* 6, 43–50. doi: 10.1038/nn980

Conflict of Interest: The authors declare that the research was conducted in the absence of any commercial or financial relationships that could be construed as a potential conflict of interest.

frontiers in Cellular Neuroscience

MINI REVIEW
published: 15 July 2021
doi: 10.3389/fncel.2021.695380

Astrocytic Ca^{2+} Signaling in Epilepsy

Kjell Heuser[1]* *and Rune Enger*[2]*

[1] Department of Neurology, Oslo University Hospital, Rikshospitalet, Oslo, Norway, [2] Letten Centre and GliaLab, Division of Anatomy, Department of Molecular Medicine, Institute of Basic Medical Sciences, University of Oslo, Oslo, Norway

Epilepsy is one of the most common neurological disorders – estimated to affect at least 65 million worldwide. Most of the epilepsy research has so far focused on how to dampen neuronal discharges and to explain how changes in intrinsic neuronal activity or network function cause seizures. As a result, pharmacological therapy has largely been limited to symptomatic treatment targeted at neurons. Given the expanding spectrum of functions ascribed to the non-neuronal constituents of the brain, in both physiological brain function and in brain disorders, it is natural to closely consider the roles of astrocytes in epilepsy. It is now widely accepted that astrocytes are key controllers of the composition of the extracellular fluids, and may directly interact with neurons by releasing gliotransmitters. A central tenet is that astrocytic intracellular Ca^{2+} signals promote release of such signaling substances, either through synaptic or non-synaptic mechanisms. Accruing evidence suggests that astrocytic Ca^{2+} signals play important roles in both seizures and epilepsy, and this review aims to highlight the current knowledge of the roles of this central astrocytic signaling mechanism in ictogenesis and epileptogenesis.

Keywords: astrocyte, epilepsy, calcium signaling, IP3, epileptogenesis, ictogenesis, astrogliosis

OPEN ACCESS

Edited by:
Leonid Savtchenko, University College London, United Kingdom

Reviewed by:
Ulyana Lalo, Immanuel Kant Baltic Federal University, Russia
Reno Cervo Reyes, Holy Names University, United States

***Correspondence:**
Kjell Heuser
kheuser@ous-hf.no;
dr.heuser@gmail.com
Rune Enger
rune.enger@medisin.uio.no

Specialty section:
This article was submitted to Non-Neuronal Cells, a section of the journal Frontiers in Cellular Neuroscience

Received: *14 April 2021*
Accepted: *16 June 2021*
Published: *15 July 2021*

Citation:
Heuser K and Enger R (2021) Astrocytic Ca^{2+} Signaling in Epilepsy. Front. Cell. Neurosci. 15:695380. doi: 10.3389/fncel.2021.695380

INTRODUCTION

Epilepsy is one of the most common neurological disorders – estimated to affect around 1% of the world's population (Hesdorffer et al., 2011; Neligan et al., 2012; Beghi, 2016). It is a chronic disorder, characterized by sudden, violent perturbations of normal brain function, causing social stigma, morbidity, and risk of premature death. In spite of a multitude of drugs for the treatment of epilepsy, about 30% of patients are not able to control their seizures with seizure suppressing medication (French, 2007; Perucca and Gilliam, 2012).

There is a striking lack of knowledge of the pathophysiological cellular mechanisms at play in epilepsy. For instance, the process transforming normal brain matter to a focus for epileptic seizures – the process of epileptogenesis – is not well understood. Also, the central question of what sets in motion an epileptic seizure – ictogenesis – remains unanswered. Most of the epilepsy research has so far focused on how to dampen neuronal discharges and to explain how changes in intrinsic neuronal activity or neuronal network function cause seizures. As a result, pharmacological therapy has been limited to symptomatic treatment aiming at neuronal targets. Given the expanding spectrum of roles ascribed to the non-neuronal constituents of the brain, it is natural to take a closer look at astrocytes as potential targets for epilepsy treatment.

Astrocytes are critical homeostatic controllers of extracellular glutamate and K^+ levels (Rothstein et al., 1996; Larsen et al., 2014; Danbolt et al., 2016). Numerous studies have also demonstrated that astrocytes have important roles in supporting the neurons metabolically

(Pellerin and Magistretti, 1994; Lundgaard et al., 2015) and that they have the capability of altering the vascular tone (Mulligan and MacVicar, 2004; Haydon and Carmignoto, 2006; Gordon et al., 2008). Increasing evidence suggests that astrocytes play important roles in brain state transitions and maintenance (Paukert et al., 2014; Poskanzer and Yuste, 2016; Szabó et al., 2017; Bojarskaite et al., 2020). Notably, astrocytes seem to also directly partake in brain signaling by releasing substances that affect neurons at the so-called tripartite synapse (Perea et al., 2009; Bindocci et al., 2017; Martin-Fernandez et al., 2017). A central tenet is that astroglial intracellular Ca^{2+} signals promote such "gliotransmitter" release, either through synaptic or non-synaptic mechanisms (Perea et al., 2014; Bazargani and Attwell, 2016). Glutamate, purines and D-serine are examples of transmitter substances that are thought to be released from astrocytes in a Ca^{2+} dependent manner (ibid.).

Perturbation of astrocytic Ca^{2+} signaling has been demonstrated in seizures and in epileptic tissue, potentially affecting both the homeostatic functions and signaling functions of astrocytes. These downstream mechanisms are largely speculative in the context of epilepsy but reflect the knowledge of roles of astrocytic Ca^{2+} signaling in physiology. Here, we discuss the relatively limited body of studies directly assessing astrocytic Ca^{2+} signaling in epilepsy, and briefly discuss potential downstream effects (**Table 1**). For the sake of structure and simplification, we arrange the topic into paragraphs on ictogenesis (i.e., the emergence of seizure activity), and epileptogenesis (i.e., the process by which the brain develops the predisposition of generating spontaneous seizures). These two processes are highly interconnected (Blauwblomme et al., 2014), but animal studies are often designed to study one of these two facets of epilepsy, and hence provide a framework for the further discussion.

ASTROCYTIC Ca^{2+} SIGNALING AND ICTOGENESIS

Ictogenesis describes the emergence of seizure activity (Blauwblomme et al., 2014). The interaction between astrocytes and neurons in ictogenesis has only sparsely been investigated and findings are to some extent ambiguous or contradictory, potentially due to different experimental models (**Table 1**; Tian et al., 2005; Fellin et al., 2006; Gómez-Gonzalo et al., 2010; Baird-Daniel et al., 2017; Heuser et al., 2018; Diaz Verdugo et al., 2019). Astrocytes express a plethora of functionally important receptors, transporters and channels, and a role of these cells in ictogenesis is highly suggestive (Agulhon et al., 2008; Patel et al., 2019; Caudal et al., 2020). Several known astrocyte-neuron interactions involving Ca^{2+} signaling can partake in ictogenesis or in the maintenance of hypersynchronous neuronal activity, possibly by creating excitatory feedback loops (**Figure 1**; Gómez-Gonzalo et al., 2010; Henneberger, 2017).

Building upon seminal studies demonstrating that astrocytes are able to directly interact with neurons (Nedergaard, 1994; Parpura et al., 1994; Araque et al., 1998; Parpura and Haydon, 2000; Parri et al., 2001; Angulo et al., 2004), Fellin et al. (2006), found that eliciting astrocytic Ca^{2+} signals by photolysis of caged Ca^{2+} and by application of ATP agonist and mGluR5 agonist triggered slow inward currents (SICs) in nearby neurons that were unaffected by application of the neuronal sodium channel blocker tetrodotoxin (Fellin et al., 2004). Soon thereafter, Tian et al. (2005) demonstrated that Ca^{2+} mediated glutamate release from astrocytes during experimentally induced seizure activity triggered slow inward currents (SICs) in neurons. These findings proposed a role for astrocytes in synchronizing neuronal activity and contributing to seizure generation (Tian et al., 2005). Further exploring which astrocytic Ca^{2+} signaling mechanisms were involved in this context, Kang et al. applied IP_3 into astrocytes of the CA1 hippocampal region in rats, and were able to trigger epileptiform discharges in adjacent neurons (Kang et al., 2005). Later, Ding et al. (2007) were able to demonstrate increased astrocytic Ca^{2+} signaling in an *in vivo* pilocarpine epilepsy model. They proposed that this increase in Ca^{2+} signaling was due to activation of astrocytic metabotropic glutamate receptors, and that this activation led to the release of glutamate from astrocytes that could contribute to neuronal SICs through the activation of extrasynaptic neuronal NMDA receptors. By applying simultaneous patch-clamp recordings and Ca^{2+} imaging in cortical slices of the rat entorhinal cortex, Gómez-Gonzalo et al. (2010) found that Ca^{2+} elevations in astrocytes correlate with initiation and maintenance of focal seizure-like discharges, and postulated a recurrent excitatory loop between neurons and astrocytes in ictogenesis, where astrocytes play a role in recruiting neurons to ictal events, possibly through the release of gliotransmitters (Gómez-Gonzalo et al., 2010).

By using two-photon microscopy and simultaneous astrocyte and neuron Ca^{2+} imaging in the hippocampal CA1 region of awake mice, we were able to show that prominent astrocytic Ca^{2+} transients preceded local hypersynchronous neuronal activity in the emergence of kainate induced generalized epileptic seizures (Heuser et al., 2018). These findings were in agreement with the earlier results from the study of Tian et al. (2005), who also observed stereotypical astrocytic Ca^{2+} signals typically preceding local neurons in the spread of cortical seizure activity. A later work by Diaz Verdugo et al. (2019) similarly demonstrated large and synchronized astrocytic Ca^{2+} signals preceding ictal onset in zebrafish, and proposed that this signaling modulated neural excitation through glutamate release, by gap junction dependent mechanisms. In another *in vivo* study, Zhang et al. (2019), provided evidence, although correlative, that increased Ca^{2+} concentration in astrocytic endfeet governed precapillary arteriole dilation during epileptic events, suggesting a role for astrocytes in the metabolic support of neurons in seizures. In contrast to these previously mentioned studies, data from another model for focal neocortical seizures in anesthetized rats using bulk-loaded synthetic Ca^{2+} indicators found the astrocytic Ca^{2+} activation to lag behind neuronal activation and to be unnecessary for ictogenesis and the accompanying vascular dynamics (Baird-Daniel et al., 2017).

An extensive array of stimuli and corresponding signaling pathways have been shown to trigger intracellular Ca^{2+} signals in astrocytes (Zhang et al., 2019; Caudal et al., 2020). To

TABLE 1 | Key publications investigating the roles of astrocytic Ca^{2+} signalling in ictogenesis and epileptogenesis.

Publication	Model	Ca^{2+} indicator	Main findings
Astrocytic Ca^{2+} signaling in ictogenesis			
Kang et al., 2005	Rat hippocampal slices, 4-AP	Fluo-4 AM	Adding IP_3 in astrocytes causes epileptiform activity due to glutamate, and that astrocytic Ca^{2+} signals occur during 4-AP seizures
Tian et al., 2005	Rat hippocampal slices: 4-AP, zero-Mg^{2+}, bicuculline, penicillin Mouse cortex, *in vivo*, anesthetized: local injection of 4-AP	Fluo-4 AM	Increased astrocytic Ca^{2+} signaling *in vivo* during spread of 4-AP seizures, as well as showing that uncaging Ca^{2+} in astrocytes and extrasynaptic sources of glutamate triggered paroxysmal depolarization shifts
Fellin et al., 2006	Mouse cortical-hippocampal slices: zero-Mg^{2+} and picrotoxin, or 0.5 mM Mg^{2+} and 8.5 mM K^+	Indo-1 AM or OGB-1 AM	A correlation between astrocytic Ca^{2+} and SICs, but activation of extrasynaptic NMDA activation by astrocytes is not necessary for either ictal or interictal epileptiform events
Ding et al., 2007	Mouse, *in vivo*, anesthetized. Pilocarpine s.c., 350 mg/kg	Fluo-4 AM	Increase in astrocytic Ca^{2+} signals during SE. See also under "Epileptogenesis"
Gómez-Gonzalo et al., 2010	Mouse entorhinal cortex slice: Picrotoxin/ zero-Mg^{2+} Whole guinea pig: Bicuculline	OGB-1 AM / Rhod-2	Astrocytic Ca^{2+} signals are triggered by ictal but not interictal events, and can be inhibited by blocking mGluRs and purinergic receptors. Astrocytic Ca^{2+} signals contribute to the excitation of neurons, and blocking of early ictal astrocytic Ca^{2+} signals prevent spread of ictal activity.
Baird-Daniel et al., 2017	Rat cortex, *in vivo*, anesthetized. 4-AP. Blocking astrocytic Ca^{2+} signals and gap junctions with fluoroacetate and carbenoxolone, respectively	OGB-1 AM or Rhod-2 AM	Increased Ca^{2+} signals in astrocytes during seizures, but blocking of these did not affect epileptiform discharges or vascular dynamics associated with the seizures
Heuser et al., 2018	Mouse hippocampus, *in vivo*, unanesthetized, "dual color" Ca^{2+} imaging of hippocampal neurons and astrocytes	GCaMP6f in astrocytes	Prominent astrocytic Ca^{2+} activity preceding local neuronal recruitment to seizure activity in hippocampus
Diaz Verdugo et al., 2019	Zebra fish: PTZ	GCaMP6s in astrocytes	Large activations of astrocytic Ca^{2+} signals in the pre-ictal state and that astrocytic Ca^{2+} signals contribute to excitation of neurons
Zhang et al., 2019	Mouse cortex, *in vivo*, anesthetized: local injection of 4-AP	OGB-1 AM	Absolute levels of Ca^{2+} in the astrocytic endfeet correlates with vascular tone during seizures
Astrocytic calcium signaling in epileptogenesis			
Ding et al., 2007	Mouse cortex, *in vivo*, anesthetized: Pilocarpine s.c. 350 mg/kg. 3D post SE	Fluo-4 AM	An increase in astrocytic Ca^{2+} signals at day 3 after SE due to mGluR5 signaling. Blocking this hyperactivity attenuated neuronal death
Szokol et al., 2015	Mouse hippocampal slices: intracortical kainate injection. Early epileptogenesis (1, 3, and 7 days after SE)	GCaMP5E	Increased Ca^{2+} signaling in hippocampal astrocytes upon schaffer collateral stimulation at days 1 and 3 after SE mediated by mGluR
Umpierre et al., 2019	Mouse hippocampal slices, at 1–3, 7–9, or 28–30 days after SE	GCaMP5G	mGluR5-mediated Ca^{2+} signaling re-emerges in epileptogenesis
Mentioned in Shigetomi et al. (2019): Sato et al.: unpublished report	4 weeks after pilocarpine induced SE	Not known	Increased Ca^{2+} signaling in reactive astrocytes
Enger et al., 2015 conference proceedings, American Epilepsy Society conference	Mouse hippocampus, *in vivo*, unanesthetized. Chronic MTLE model of deep cortical kainate injection, imaging at 3 months after SE	GCaMP6f	Episodic spontaneous hyperactivity of reactive astrocytes within/close to the sclerotic hippocampus
Plata et al., 2018	Rat, hippocampal slices, Lithium-pilocarpine	OGB-1 AM	A reduction in large size astrocytic Ca^{2+} events in atrophic astrocytes

discuss all of them would go beyond the scope of this review. One important pathway is mediated by the Inositol 1,4,5-trisphosphate (IP_3) receptor in the endoplasmic reticulum, of which the isoform 2 (IP_3R2) is thought to be the key functional IP_3 receptor in astrocytes (**Figure 1**; Sharp et al., 1999; Parri and Crunelli, 2003; Volterra and Steinhäuser, 2004; Scemes and Giaume, 2006; Foskett et al., 2007). Lack of IP_3R2 has been shown to abolish a large proportion of astrocytic Ca^{2+} signals (Petravicz et al., 2008; Guerra-Gomes et al., 2020). In spite of the importance of IP_3 as a second messenger involved in astrocytic Ca^{2+} dynamics, mice lacking this receptor are overtly normal (Petravicz et al., 2008). Accordingly, studies have questioned the physiological importance of IP_3-mediated astrocytic Ca^{2+} signaling, by for instance demonstrating normal synaptic transmission and plasticity in mice devoid of IP_3R2 (Agulhon et al., 2010; Nizar et al., 2013; Petravicz et al., 2014).

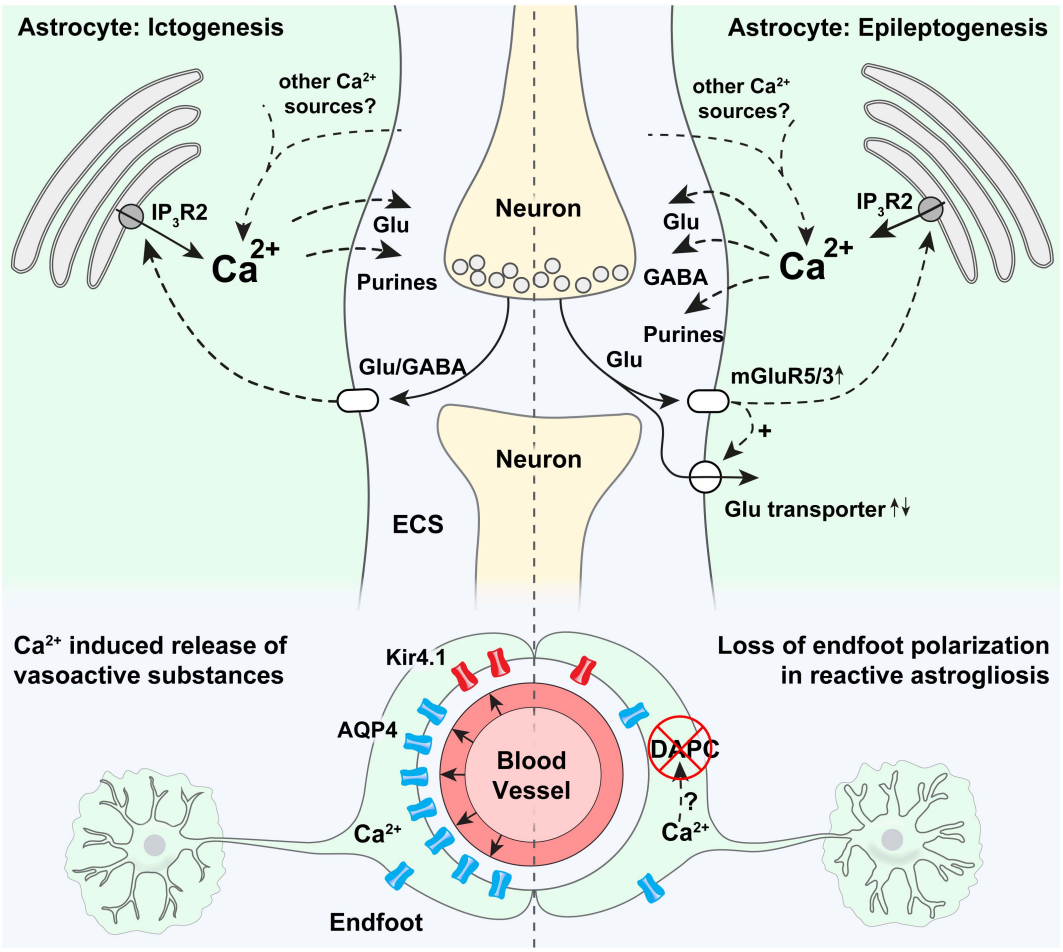

FIGURE 1 | Potential roles of astrocytic Ca^{2+} signaling in epilepsy. Strong astrocytic Ca^{2+} signals have been shown to occur in the emergency of acute seizures (in ictogenesis), that are probably triggered by neurotransmitters released by neurons. Ca^{2+} increases at the onset of seizures are known to be partly mediated by release through IP_3R2 from the endoplasmic reticulum, even though pronounced Ca^{2+} signaling is present also in mice devoid of IP_3R2. It is thought that intracellular Ca^{2+} increases may trigger proconvulsive gliotransmitter release. In astrocytic endfeet, increased Ca^{2+} signaling has been shown to correlate with ictal vasodilation. Epileptogenesis triggers a pronounced increase in mGluR5 expression, mGluR5-mediated Ca^{2+} signaling, and increased glutamate uptake. An increase in astrocytic Ca^{2+} signaling has been demonstrated in the days after status epilepticus, and aberrant Ca^{2+} signaling at later time points in the epileptogenesis has been anecdotally reported. Increased Ca^{2+} signaling could potentially cause both the release of glutamate (pro-convulsive), purines (pro-convulsive), and GABA (anti-convulsive, through Bestrophin-1 channels). In astrocytic endfeet in epileptic tissue a pronounced loss of aquaporin-4 (AQP4) and the K^+ inwardly rectifying channel Kir4.1 can potentially be due to Ca^{2+} activated proteases causing a disassembly of the dystrophin associated protein complex (DAPC) tethering AQP4 and Kir4.1 to perivascular endfeet.

Conversely, we have demonstrated attenuated seizure activity in mice devoid of IP_3R2 compared to WT mice following low dose intraperitoneal kainate, suggesting a proconvulsant role of astrocytic IP_3R2 mediated Ca^{2+} elevations (Heuser et al., 2018). However, seizure activity in this study was only collected for 1 h after initiation of seizures, encouraging further investigation of the role of IP_3R2 at later time points during epileptogenesis and in chronic epilepsy. Interestingly, even though a sizable amount of Ca^{2+} signals were still present in the knockout mice, we found that the early activation of astrocytic Ca^{2+} signals in the emergence of seizures, as discussed above, was dependent on IP_3R2 (Heuser et al., 2018). These two observations underscore the potential importance of IP_3R2 in ictogenesis.

Another pathway involved in astrocytic Ca^{2+} signaling attracting increasing attention for a role in epilepsy is glial purinergic signaling (Ding et al., 2007; Wellmann et al., 2018; Alves et al., 2019; Nikolic et al., 2020). Activation of astrocytic purinergic receptors triggers intracellular Ca^{2+} signals that could promote astrocytic release of gliotransmitters like glutamate or ATP, which acts on neurons and modulates excitation [reviewed in Nikolic et al. (2020)]. Importantly, Nikolic et al. (2018) provided evidence for TNFα-driven autocrine astrocyte purinergic signaling as a trigger of glutamatergic gliotransmission in a model of mesial temporal lobe epilepsy (mTLE), highlighting the complex interplay between astrocytes and microglia in epilepsy pathogenesis, discussed elsewhere (Bedner and Steinhäuser, 2019).

Most of the studies above explored the role for astrocytic Ca^{2+} signals in seizures in relation to gliotransmission, i.e., that astrocytes release transmitters that directly signal to neurons. A growing body of evidence suggests that astrocytic Ca^{2+} signals also play important roles in the control of the homeostatic functions of astrocytes. For instance they have been shown to be involved in the uptake of extracellular K^+ through modulation of the Na^+/K^+ ATPase, and through the breakdown of glycogen (Wang et al., 2012; Müller et al., 2014). These mechanisms remain poorly explored in the context of epilepsy but could be important downstream effects of astrocytic Ca^{2+} signaling.

ASTROCYTIC Ca^{2+} SIGNALING AND EPILEPTOGENESIS

Epileptogenesis refers to the gradual process by which a normal brain develops a propensity for recurrent seizure activity. A range of pathophysiological changes have been shown to occur during epileptogenesis, including inflammation, neurodegeneration, aberrant neurogenesis and dendritic plasticity, impaired blood-brain-barrier, epigenetic changes and alterations of the molecular composition and function of ion channels, receptors and transporters, and more (van Vliet et al., 2007; Vezzani et al., 2011; Steinhäuser and Seifert, 2012; Dingledine et al., 2014; Jessberger and Parent, 2015; Hauser et al., 2018; Escartin et al., 2021).

A common denominator of astrocytic pathophysiology associated with epileptogenesis is the process of reactive astrogliosis (Burda and Sofroniew, 2014; Pekny and Pekna, 2016). This is a graded response to a wide array of insults, which is a hallmark of many neurological disorders (Burda and Sofroniew, 2014; Ferlazzo et al., 2016; Glushakov et al., 2016; Pekny and Pekna, 2016; Fordington and Manford, 2020; Galovic et al., 2021).

Reactive astrocytes are characterized by morphological and molecular changes (**Figure 1**). Specifically they proliferate, undergo hypertrophy and increase their expression of intermediary filament proteins like glial fibrillary acid protein (GFAP) and vimentin (Yang et al., 1994; Pekny and Nilsson, 2005; Sofroniew, 2009; Cregg et al., 2014; Escartin et al., 2021). *In extremis*, these changes may lead to the formation of a glial scar (Miller, 2005; Barres, 2008; Sofroniew, 2009; Burda and Sofroniew, 2014; Ferlazzo et al., 2016; Glushakov et al., 2016; Pekny and Pekna, 2016; Fordington and Manford, 2020; Galovic et al., 2021). Reactive astrogliosis can be observed in several acquired forms of epilepsy but has mostly been investigated in the context of mTLE (Wieser and ILAE Commission on Neurosurgery of Epilepsy., 2004; Blümcke et al., 2013; Cendes et al., 2014).

There is ample evidence that reactive astrocytes display aberrant Ca^{2+} signaling at least in the early phase of epileptogenesis (**Table 1**). Ding et al. (2007) found increased astrocytic Ca^{2+} activity in the days following pilocarpine-induced SE in mice. In the same study both *in vitro* and *in vivo* pharmacological approaches demonstrated that these Ca^{2+} signals could contribute to neuronal death, linking astrocytic hyperactivity to a key hallmark of epileptogenesis (Ding et al., 2007). We confirmed the astrocytic hyperactivity following SE by employing genetically encoded Ca^{2+} indicators in acute hippocampal slices from a mouse model of mTLE, and found that stimulation-evoked Ca^{2+} transients in astrocytic endfeet even outlasted those in cell bodies during the latent phase of epileptogenesis (Szokol et al., 2015).

Increased astrocytic Ca^{2+} activity has been anecdotally reported at even later time points after the initial insult (Enger et al., 2015; Shigetomi et al., 2019). These increased Ca^{2+} signals are likely stimuli- and stage specific and may reflect the degree of the reactive astrogliosis (Kuchibhotla et al., 2009; Fordsmann et al., 2019), as others have shown attenuated astrocytic Ca^{2+} activity in atrophic astrocytes in chronic epilepsy (Plata et al., 2018).

The degree, development and underlying mechanisms involved in aberrant Ca^{2+} signaling in epileptogenesis are still unknown, but it is plausible that several of the physiological signaling pathways involved in astrocytic Ca^{2+} dynamics (Caudal et al., 2020), could be perturbed. A major pathway for eliciting astrocytic Ca^{2+} signals is the activation of the Gq G-protein coupled receptors (GqPCRs) and subsequent release of Ca^{2+} from the endoplasmic reticulum via IP_3R2 as discussed in "Astrocyte Ca^{2+} signaling and Ictogenesis" (**Figure 1**; Foskett et al., 2007). Astrocytes express several GqPCRs, of which mGluR5 has attracted most attention due to an upregulation in epileptic tissue and potential involvement in an excitatory loop comprising glutamate induced Ca^{2+} dependent glutamate release from astrocytes (Umpierre et al., 2019). While astrocytes in the adult brain are almost depleted of mGluR5 (Sun et al., 2013), the receptor is consistently expressed in chronic epilepsy models and resected tissue from patients with epilepsy (Aronica et al., 2000, 2003), and a recent study has shown that mGluR5 expression and mGluR5-dependent Ca^{2+} transients reemerge during epileptogenesis along with an increase in glutamate uptake (Umpierre et al., 2019). This reemergence of astrocytic mGluR5 could potentially be a compensatory anti-epileptic mechanism to handle the elevated glutamate levels in epileptic tissue but could possibly also represent a pro-epileptic feature triggering downstream Ca^{2+} mediated gliotransmission.

Apart from these perturbations in glutamate dynamics, it has been shown that reactive astrocytes exhibit a tonic release of GABA, presumably through Bestrophin-1 channels (Pandit et al., 2020). Bestrophin-1 channels are Ca^{2+} activated anion channels, and increased GABA release could hence be a downstream effect of increased Ca^{2+} signaling in reactive astrocytes (Lee et al., 2010). In support of this conjecture is the finding of an accumulation of GABA in reactive astrocytes in a model of mTLE (Müller et al., 2020). Potentially, this is a protective aspect of reactive astrocytes to curb epileptiform activity in this pathological tissue.

Moreover, as mentioned in "Ictogenesis" astrocytic Ca^{2+} signaling has been suggested to be involved in homeostatic mechanisms of astrocytes. These mechanisms could be important downstream effects of astrocytic Ca^{2+} dyshomeostasis in

epileptic tissue, but these effects are so far rudimentarily investigated in epilepsy.

Loss of astrocytic gap junction coupling has been shown to occur during early epileptogenesis in experimental models of mTLE and in specimens of resected hippocampi from patients with mTLE (Bedner et al., 2015; Deshpande et al., 2017, 2020; Henning et al., 2021). It is believed that this loss of astrocytic coupling in epilepsy may perturb the ability of astrocytes to remove K^+ from the extracellular space through the process of K^+ spatial buffering (Nwaobi et al., 2016). Notably, astrocytic gap junctions may also allow Ca^{2+} signals to propagate from cell to cell, at least during pathological conditions like seizure activity (Scemes and Giaume, 2006). It is tempting to hypothesize that such propagating Ca^{2+} waves could play a role in neuronal synchronization and seizure generation. Potentially a loss of astrocytic gap junctions as seen in epileptic tissue, may be a compensatory mechanism to prevent intercellular spread of astrocytic Ca^{2+} waves. Even so, to the best of our knowledge, no direct study of astrocytic Ca^{2+} signaling in gap junction deficient mice has been performed.

Loss of the highly concentrated expression of key membrane channels in astrocytic endfoot processes, i.e., loss of astrocyte polarization, is another pathological hallmark, which could be a consequence of perturbed glial Ca^{2+} dynamics (**Figure 1**). For instance AQP4 and Kir4.1 are normally densely expressed in astrocytic endfeet, kept in place by the so-called dystrophin associated protein complex (DAPC) (Nagelhus et al., 1998; Enger et al., 2012), and in tissue resectates from patients with mTLE, a striking loss of this polarized expression of both AQP4 and Kir4.1 have been shown (Eid et al., 2005; Heuser et al., 2012). It is possible that prolonged epileptic activity and increased Ca^{2+} signaling in astrocytic endfeet, as we demonstrated in Szokol et al. (2015), activate Ca^{2+} dependent proteases like calpain (Nagelhus and Ottersen, 2013), that shows affinity to dystrophin and could cleave the DAPC (**Figure 1**; Shields et al., 2000).

Even though the evidence is indirect, it has been suggested that this loss of astrocyte endfoot polarization could contribute to epileptogenesis and hyperexcitation (Binder et al., 2012; Binder and Carson, 2013; Crunelli et al., 2015). Notably, the loss of the astrocyte endfoot Kir4.1 channels in tissue from mTLE patients (Heuser et al., 2012) is expected to cause impaired K^+ handling and resultant neuronal hyperexcitation due to the role of Kir4.1 in K^+ homeostasis (Bordey and Sontheimer, 1998; Hinterkeuser et al., 2000; Kivi et al., 2000; Neusch et al., 2001; Djukic et al., 2007; Bockenhauer et al., 2009; Scholl et al., 2009; Steinhäuser et al., 2012).

CONCLUSION AND FUTURE PERSPECTIVES

Here we have discussed the role of astrocyte Ca^{2+} signaling in *ictogenesis* and *epileptogenesis*. These terms are used to describe two different features of epilepsy, but do not necessarily imply two separate processes, as mechanisms crucial in ictogenesis could also be an integral part of epileptogenesis, or vice versa. While we often associate astrocytic dysfunction in *epileptogenesis* with the appearance of *reactive astrogliosis* (Escartin et al., 2021), the term *ictogenesis* seems typically to be used when studying the interplay between neurons and astrocytes independent of pre-existing tissue pathology. Therefore, we may overlook the fact that ictogenesis most often would occur in tissue that has undergone pathological transformation typical for *epileptogenesis,* i.e., not normal, healthy tissue. On the other hand, *epileptogenesis* comprises many pathological changes beyond *reactive astrogliosis*, like alterations in transcriptional regulation, morphological, biochemical, metabolic and physiological remodeling ultimately resulting in gain or loss of function (Escartin et al., 2021).

Astrocytic Ca^{2+} signals are today considered a main readout of astrocytic activity and there are reasons to believe that they play important roles in epilepsy. Evidence suggests that such signals are neither necessary nor sufficient to maintain epileptiform activity, but rather should be seen as modulators of the pathophysiological process. The literature directly investigating the role of astrocytic Ca^{2+} signaling in epilepsy is still sparse and at some points contradictory, and for most proposed mechanisms only a small subset of the signaling pathways involved are identified. A major challenge will be to disentangle the potentially beneficial from detrimental consequences of the different modes of astrocyte Ca^{2+} signaling in reactive astrogliosis. It is even probable that astrocyte Ca^{2+} signaling may carry different roles in the large variety of epileptic entities. To decipher the roles of astrocyte Ca^{2+} signaling in epilepsy, next steps should include a rigorous study of the mechanisms mentioned above *in vivo* in adult mice, leveraging new developments in both imaging and genetics, with the aim of identifying promising targets for future pharmacological therapy of epilepsy.

AUTHOR CONTRIBUTIONS

KH and RE reviewed the literature, conceptualized the manuscript, and wrote the manuscript. Both authors contributed to the article and approved the submitted version.

FUNDING

KH has received funding from the European Union's Horizon 2020 research and innovation programme under the Marie Sklodowska-Curie grant agreement no. 722053.

ACKNOWLEDGMENTS

We would like to thank the Department of Neurology, Oslo University Hospital, and especially Erik Taubøll, leader of the Epilepsy Research Group, Oslo, https://www.ous-research.no/ergo/, for constant support. We would also like to thank all members of the EU Glia Ph.D. Consortium, http://www.eu-gliaphd.eu for long-lasting friendship and discussions on glial pathology in epilepsy, and the Letten Foundation.

REFERENCES

Agulhon, C., Fiacco, T. A., and McCarthy, K. D. (2010). Hippocampal short- and long-term plasticity are not modulated by astrocyte Ca2 signaling. *Science* 327, 1250–1254. doi: 10.1126/science.1184821

Agulhon, C., Petravicz, J., McMullen, A. B., Sweger, E. J., Minton, S. K., Taves, S. R., et al. (2008). What is the role of astrocyte *calcium* in neurophysiology? *Neuron* 59, 932–946. doi: 10.1016/j.neuron.2008.09.004

Alves, M., De Diego Garcia, L., Conte, G., Jimenez-Mateos, E. M., D'Orsi, B., Sanz-Rodriguez, A., et al. (2019). Context-specific switch from anti- to pro-epileptogenic function of the P2Y receptor in experimental epilepsy. *J. Neurosci.* 39, 5377–5392. doi: 10.1523/jneurosci.0089-19.2019

Angulo, M. C., Kozlov, A. S., Charpak, S., and Audinat, E. (2004). Glutamate released from glial cells synchronizes neuronal activity in the hippocampus. *J. Neurosci.* 24, 6920–6927. doi: 10.1523/jneurosci.0473-04.2004

Araque, A., Sanzgiri, R. P., Parpura, V., and Haydon, P. G. (1998). Calcium elevation in astrocytes causes an NMDA receptor-dependent increase in the frequency of miniature synaptic currents in cultured hippocampal neurons. *J. Neurosci.* 18, 6822–6829. doi: 10.1523/jneurosci.18-17-06822.1998

Aronica, E., Gorter, J. A., Jansen, G. H., van Veelen, C. W. M., van Rijen, P. C., Ramkema, M., et al. (2003). Expression and cell distribution of group I and group II metabotropic glutamate receptor subtypes in taylor-type focal cortical dysplasia. *Epilepsia* 44, 785–795. doi: 10.1046/j.1528-1157.2003.54802.x

Aronica, E., van Vliet, E. A., Mayboroda, O. A., Troost, D., da Silva, F. H., and Gorter, J. A. (2000). Upregulation of metabotropic glutamate receptor subtype mGluR3 and mGluR5 in reactive astrocytes in a rat model of mesial temporal lobe epilepsy. *Eur. J. Neurosci.* 12, 2333–2344. doi: 10.1046/j.1460-9568.2000.00131.x

Baird-Daniel, E., Daniel, A. G. S., Wenzel, M., Li, D., Liou, J.-Y., Laffont, P., et al. (2017). Glial calcium waves are triggered by seizure activity and not essential for initiating ictal onset or neurovascular coupling. *Cereb. Cortex* 27, 3318–3330. doi: 10.1093/cercor/bhx072

Barres, B. A. (2008). The mystery and magic of glia: a perspective on their roles in health and disease. *Neuron* 60, 430–440. doi: 10.1016/j.neuron.2008.10.013

Bazargani, N., and Attwell, D. (2016). Astrocyte calcium signaling: the third wave. *Nat. Neurosci.* 19, 182–189. doi: 10.1038/nn.4201

Bedner, P., Dupper, A., Hüttmann, K., Müller, J., Herde, M. K., Dublin, P., et al. (2015). Astrocyte uncoupling as a cause of human temporal lobe epilepsy. *Brain* 138, 1208–1222. doi: 10.1093/brain/awv067

Bedner, P., and Steinhäuser, C. (2019). TNFα-driven astrocyte purinergic signaling during epileptogenesis. *Trends Mol. Med.* 25, 70–72. doi: 10.1016/j.molmed.2018.12.001

Beghi, E. (2016). Addressing the burden of epilepsy: many unmet needs. *Pharmacol. Res.* 107, 79–84. doi: 10.1016/j.phrs.2016.03.003

Binder, D. K., and Carson, M. J. (2013). Glial cells as primary therapeutic targets for epilepsy. *Neurochem. Int.* 63, 635–637. doi: 10.1016/j.neuint.2013.09.004

Binder, D. K., Nagelhus, E. A., and Ottersen, O. P. (2012). Aquaporin-4 and epilepsy. *Glia* 60, 1203–1214. doi: 10.1002/glia.22317

Bindocci, E., Savtchouk, I., Liaudet, N., Becker, D., Carriero, G., and Volterra, A. (2017). Three-dimensional Ca imaging advances understanding of astrocyte biology. *Science* 356:eaai8185. doi: 10.1126/science.aai8185

Blauwblomme, T., Jiruska, P., and Huberfeld, G. (2014). Mechanisms of ictogenesis. *Int. Rev. Neurobiol.* 114, 155–185. doi: 10.1016/b978-0-12-418693-4.00007-8

Blümcke, I., Thom, M., Aronica, E., Armstrong, D. D., Bartolomei, F., Bernasconi, A., et al. (2013). International consensus classification of hippocampal sclerosis in temporal lobe epilepsy: a Task Force report from the ILAE commission on diagnostic methods. *Epilepsia* 54, 1315–1329. doi: 10.1111/epi.12220

Bockenhauer, D., Feather, S., Stanescu, H. C., Bandulik, S., Zdebik, A. A., Reichold, M., et al. (2009). Epilepsy, ataxia, sensorineural deafness, tubulopathy, and KCNJ10 mutations. *N. Engl. J. Med.* 360, 1960–1970.

Bojarskaite, L., Bjørnstad, D. M., Pettersen, K. H., Cunen, C., Hermansen, G. H., Åbjørsbråten, K. S., et al. (2020). Astrocytic Ca signaling is reduced during sleep and is involved in the regulation of slow wave sleep. *Nat. Commun.* 11:3240.

Bordey, A., and Sontheimer, H. (1998). Properties of human glial cells associated with epileptic seizure foci. *Epilepsy Res.* 32, 286–303. doi: 10.1016/s0920-1211(98)00059-x

Burda, J. E., and Sofroniew, M. V. (2014). Reactive gliosis and the multicellular response to CNS damage and disease. *Neuron* 81, 229–248. doi: 10.1016/j.neuron.2013.12.034

Caudal, L. C., Gobbo, D., Scheller, A., and Kirchhoff, F. (2020). The paradox of astroglial Ca^{2+} signals at the interface of excitation and inhibition. *Front. Cell. Neurosci.* 14:609947. doi: 10.3389/fncel.2020.609947

Cendes, F., Sakamoto, A. C., Spreafico, R., Bingaman, W., and Becker, A. J. (2014). Epilepsies associated with hippocampal sclerosis. *Acta Neuropathol.* 128, 21–37. doi: 10.1007/s00401-014-1292-0

Cregg, J. M., DePaul, M. A., Filous, A. R., Lang, B. T., Tran, A., and Silver, J. (2014). Functional regeneration beyond the glial scar. *Exp. Neurol.* 253, 197–207. doi: 10.1016/j.expneurol.2013.12.024

Crunelli, V., Carmignoto, G., and Steinhäuser, C. (2015). Novel astrocyte targets: new avenues for the therapeutic treatment of epilepsy. *Neuroscientist* 21, 62–83. doi: 10.1177/1073858414523320

Danbolt, N. C., Furness, D. N., and Zhou, Y. (2016). Neuronal vs glial glutamate uptake: resolving the conundrum. *Neurochem. Int.* 98, 29–45. doi: 10.1016/j.neuint.2016.05.009

Deshpande, T., Li, T., Henning, L., Wu, Z., Müller, J., Seifert, G., et al. (2020). Constitutive deletion of astrocytic connexins aggravates kainate−induced epilepsy. *Glia* 68, 2136–2147. doi: 10.1002/glia.23832

Deshpande, T., Li, T., Herde, M. K., Becker, A., Vatter, H., Schwarz, M. K., et al. (2017). Subcellular reorganization and altered phosphorylation of the astrocytic gap junction protein connexin43 in human and experimental temporal lobe epilepsy. *Glia* 65, 1809–1820. doi: 10.1002/glia.23196

Diaz Verdugo, C., Myren-Svelstad, S., Aydin, E., Van Hoeymissen, E., Deneubourg, C., Vanderhaeghe, S., et al. (2019). Glia-neuron interactions underlie state transitions to generalized seizures. *Nat. Commun.* 10: 3830.

Ding, S., Fellin, T., Zhu, Y., Lee, S.-Y., Auberson, Y. P., Meaney, D. F., et al. (2007). Enhanced astrocytic Ca^{2+} signals contribute to neuronal excitotoxicity after status epilepticus. *J. Neurosci.* 27, 10674–10684. doi: 10.1523/jneurosci.2001-07.2007

Dingledine, R., Varvel, N. H., and Dudek, F. E. (2014). When and how do seizures kill neurons, and is cell death relevant to epileptogenesis? *Adv. Exp. Med. Biol.* 813, 109–122. doi: 10.1007/978-94-017-8914-1_9

Djukic, B., Casper, K. B., Philpot, B. D., Chin, L.-S., and McCarthy, K. D. (2007). Conditional knock-out of Kir4.1 leads to glial membrane depolarization, inhibition of potassium and glutamate uptake, and enhanced short-term synaptic potentiation. *J. Neurosci.* 27, 11354–11365. doi: 10.1523/jneurosci.0723-07.2007

Eid, T., Lee, T.-S. W., Thomas, M. J., Amiry-Moghaddam, M., Bjornsen, L. P., Spencer, D. D., et al. (2005). Loss of perivascular aquaporin 4 may underlie deficient water and K homeostasis in the human epileptogenic hippocampus. *Proc. Natl. Acad. Sci. U.S.A.* 102, 1193–1198. doi: 10.1073/pnas.0409308102

Enger, R., Gundersen, G. A., Haj-Yasein, N. N., Eilert-Olsen, M., Thoren, A. E., Vindedal, G. F., et al. (2012). Molecular scaffolds underpinning macroglial polarization: an analysis of retinal Müller cells and brain astrocytes in mouse. *Glia* 60, 2018–2026. doi: 10.1002/glia.22416

Enger, R., Heuser, K., Nome, C., Tang, W., Jensen, V., Helm, P. J., et al. (2015). "Abnormal astrocytic Ca^{2+} signaling in the sclerotic hippocampus of awake mice: a two-photon imaging study using the unilateral intracortical kainate injection model of mesial temporal lobe epilepsy," in *Proceedings of the AES 2015 Annual Meeting Abstract Database*, (Chicago: American epilepsy society).

Escartin, C., Galea, E., Lakatos, A., O'Callaghan, J. P., Petzold, G. C., Serrano-Pozo, A., et al. (2021). Reactive astrocyte nomenclature, definitions, and future directions. *Nat. Neurosci.* 24, 312–325.

Fellin, T., Gomez-Gonzalo, M., Gobbo, S., Carmignoto, G., and Haydon, P. G. (2006). Astrocytic glutamate is not necessary for the generation of epileptiform neuronal activity in hippocampal slices. *J. Neurosci.* 26, 9312–9322. doi: 10.1523/jneurosci.2836-06.2006

Fellin, T., Pascual, O., Gobbo, S., Pozzan, T., Haydon, P. G., and Carmignoto, G. (2004). Neuronal synchrony mediated by astrocytic glutamate through activation of extrasynaptic NMDA receptors. *Neuron* 43, 729–743. doi: 10.1016/j.neuron.2004.08.011

Ferlazzo, E., Gasparini, S., Beghi, E., Sueri, C., Russo, E., Leo, A., et al. (2016). Epilepsy in cerebrovascular diseases: review of experimental and clinical data

with meta-analysis of risk factors. *Epilepsia* 57, 1205–1214. doi: 10.1111/epi.13448

Fordington, S., and Manford, M. (2020). A review of seizures and epilepsy following traumatic brain injury. *J. Neurol.* 267, 3105–3111. doi: 10.1007/s00415-020-09926-w

Fordsmann, J. C., Murmu, R. P., Cai, C., Brazhe, A., Thomsen, K. J., Zambach, S. A., et al. (2019). Spontaneous astrocytic Ca activity abounds in electrically suppressed ischemic penumbra of aged mice. *Glia* 67, 37–52. doi: 10.1002/glia.23506

Foskett, J. K., White, C., Cheung, K.-H., and Mak, D.-O. D. (2007). Inositol trisphosphate receptor Ca2+ release channels. *Physiol. Rev.* 87, 593–658. doi: 10.1152/physrev.00035.2006

French, J. A. (2007). Refractory epilepsy: clinical overview. *Epilepsia* 48(Suppl. 1), 3–7. doi: 10.1111/j.1528-1167.2007.00992.x

Galovic, M., Ferreira-Atuesta, C., Abraira, L., Döhler, N., Sinka, L., Brigo, F., et al. (2021). Seizures and epilepsy after stroke: epidemiology, biomarkers and management. *Drugs Aging.* 38, 285–299. doi: 10.1007/s40266-021-00837-7

Glushakov, A. V., Glushakova, O. Y., Doré, S., Carney, P. R., and Hayes, R. L. (2016). Animal Models of Posttraumatic Seizures and Epilepsy. *Methods Mol. Biol.* 1462, 481–519.

Gómez-Gonzalo, M., Losi, G., Chiavegato, A., Zonta, M., Cammarota, M., Brondi, M., et al. (2010). An excitatory loop with astrocytes contributes to drive neurons to seizure threshold. *PLoS Biol.* 8:e1000352. doi: 10.1371/journal.pbio.1000352

Gordon, G. R. J., Choi, H. B., Rungta, R. L., Ellis-Davies, G. C. R., and MacVicar, B. A. (2008). Brain metabolism dictates the polarity of astrocyte control over arterioles. *Nature* 456, 745–749. doi: 10.1038/nature07525

Guerra-Gomes, S., Cunha-Garcia, D., Marques Nascimento, D. S., Duarte-Silva, S., Loureiro-Campos, E., Morais Sardinha, V., et al. (2020). IP R2 null mice display a normal acquisition of somatic and neurological development milestones. *Eur. J. Neurosci.* doi: 10.1111/ejn.14724 [Epub ahead of print].

Hauser, R. M., Henshall, D. C., and Lubin, F. D. (2018). The Epigenetics of Epilepsy and Its Progression. *Neuroscientist* 24, 186–200. doi: 10.1177/1073858417705840

Haydon, P. G., and Carmignoto, G. (2006). Astrocyte control of synaptic transmission and neurovascular coupling. *Physiol. Rev.* 86, 1009–1031. doi: 10.1152/physrev.00049.2005

Henneberger, C. (2017). Does rapid and physiological astrocyte-neuron signalling amplify epileptic activity? *J. Physiol.* 595, 1917–1927. doi: 10.1113/jp271958

Henning, L., Steinhäuser, C., and Bedner, P. (2021). Initiation of experimental temporal lobe epilepsy by early astrocyte uncoupling is independent of TGFβR1/ALK5 signaling. *Front. Neurol.* 12:660591. doi: 10.3389/fneur.2021.660591

Hesdorffer, D. C., Logroscino, G., Benn, E. K. T., Katri, N., Cascino, G., and Hauser, W. A. (2011). Estimating risk for developing epilepsy: a population-based study in Rochester, Minnesota. *Neurology* 76, 23–27. doi: 10.1212/wnl.0b013e318204a36a

Heuser, K., Eid, T., Lauritzen, F., Thoren, A. E., Vindedal, G. F., Taubøll, E., et al. (2012). Loss of perivascular Kir4.1 potassium channels in the sclerotic hippocampus of patients with mesial temporal lobe epilepsy. *J. Neuropathol. Exp. Neurol.* 71, 814–825. doi: 10.1097/nen.0b013e318267b5af

Heuser, K., Nome, C. G., Pettersen, K. H., Åbjørsbråten, K. S., Jensen, V., Tang, W., et al. (2018). Ca^{2+} Signals in astrocytes facilitate spread of epileptiform activity. *Cereb. Cortex* 28, 4036–4048. doi: 10.1093/cercor/bhy196

Hinterkeuser, S., Schröder, W., Hager, G., Seifert, G., Blümcke, I., Elger, C. E., et al. (2000). Astrocytes in the hippocampus of patients with temporal lobe epilepsy display changes in potassium conductances. *Eur. J. Neurosci.* 12, 2087–2096. doi: 10.1046/j.1460-9568.2000.00104.x

Jessberger, S., and Parent, J. M. (2015). Epilepsy and adult neurogenesis. *Cold Spring Harb. Perspect. Biol.* 7:a020677. doi: 10.1101/cshperspect.a020677

Kang, N., Xu, J., Xu, Q., Nedergaard, M., and Kang, J. (2005). Astrocytic glutamate release-induced transient depolarization and epileptiform discharges in hippocampal CA1 pyramidal neurons. *J. Neurophysiol.* 94, 4121–4130. doi: 10.1152/jn.00448.2005

Kivi, A., Lehmann, T.-N., Kovács, R., Eilers, A., Jauch, R., Meencke, H. J., et al. (2000). Effects of barium on stimulus-induced rises of [K]oin human epileptic non-sclerotic and sclerotic hippocampal area CA1. *Eur. J. Neurosci.* 12, 2039–2048. doi: 10.1046/j.1460-9568.2000.00103.x

Kuchibhotla, K. V., Lattarulo, C. R., Hyman, B. T., and Bacskai, B. J. (2009). Synchronous hyperactivity and intercellular calcium waves in astrocytes in Alzheimer mice. *Science* 323, 1211–1215. doi: 10.1126/science.1169096

Larsen, B. R., Assentoft, M., Cotrina, M. L., Hua, S. Z., Nedergaard, M., Kaila, K., et al. (2014). Contributions of the Na^+/K^+-ATPase, NKCC1, and Kir4.1 to hippocampal K^+ clearance and volume responses. *Glia* 62, 608–622. doi: 10.1002/glia.22629

Lee, S., Yoon, B.-E., Berglund, K., Oh, S.-J., Park, H., Shin, H.-S., et al. (2010). Channel-mediated tonic GABA release from glia. *Science* 330, 790–796. doi: 10.1126/science.1184334

Lundgaard, I., Li, B., Xie, L., Kang, H., Sanggaard, S., Haswell, J. D. R., et al. (2015). Direct neuronal glucose uptake heralds activity-dependent increases in cerebral metabolism. *Nat. Commun.* 6:6807.

Martin-Fernandez, M., Jamison, S., Robin, L. M., Zhao, Z., Martin, E. D., Aguilar, J., et al. (2017). Synapse-specific astrocyte gating of amygdala-related behavior. *Nat. Neurosci.* 20, 1540–1548. doi: 10.1038/nn.4649

Miller, G. (2005). Neuroscience. The dark side of glia. *Science* 308, 778–781. doi: 10.1126/science.308.5723.778

Müller, J., Timmermann, A., Henning, L., Müller, H., Steinhäuser, C., and Bedner, P. (2020). Astrocytic GABA accumulation in experimental temporal lobe epilepsy. *Front. Neurol.* 11:614923. doi: 10.3389/fneur.2020.614923

Müller, M. S., Fox, R., Schousboe, A., Waagepetersen, H. S., and Bak, L. K. (2014). Astrocyte glycogenolysis is triggered by store-operated calcium entry and provides metabolic energy for cellular calcium homeostasis. *Glia* 62, 526–534. doi: 10.1002/glia.22623

Mulligan, S. J., and MacVicar, B. A. (2004). Calcium transients in astrocyte endfeet cause cerebrovascular constrictions. *Nature* 431, 195–199. doi: 10.1038/nature02827

Nagelhus, E. A., and Ottersen, O. P. (2013). Physiological roles of aquaporin-4 in brain. *Physiol. Rev.* 93, 1543–1562. doi: 10.1152/physrev.00011.2013

Nagelhus, E. A., Veruki, M. L., Torp, R., Haug, F. M., Laake, J. H., Nielsen, S., et al. (1998). Aquaporin-4 water channel protein in the rat retina and optic nerve: polarized expression in Müller cells and fibrous astrocytes. *J. Neurosci.* 18, 2506–2519. doi: 10.1523/jneurosci.18-07-02506.1998

Nedergaard, M. (1994). Direct signaling from astrocytes to neurons in cultures of mammalian brain cells. *Science* 263, 1768–1771. doi: 10.1126/science.8134839

Neligan, A., Hauser, W. A., and Sander, J. W. (2012). The epidemiology of the epilepsies. *Handb. Clin. Neurol.* 107, 113–133. doi: 10.1016/b978-0-444-52898-8.00006-9

Neusch, C., Rozengurt, N., Jacobs, R. E., Lester, H. A., and Kofuji, P. (2001). Kir4.1 potassium channel subunit is crucial for oligodendrocyte development and in vivo myelination. *J. Neurosci.* 21, 5429–5438. doi: 10.1523/jneurosci.21-15-05429.2001

Nikolic, L., Nobili, P., Shen, W., and Audinat, E. (2020). Role of astrocyte purinergic signaling in epilepsy. *Glia* 68, 1677–1691. doi: 10.1002/glia.23747

Nikolic, L., Shen, W., Nobili, P., Virenque, A., Ulmann, L., and Audinat, E. (2018). Blocking TNFα-driven astrocyte purinergic signaling restores normal synaptic activity during epileptogenesis. *Glia* 66, 2673–2683. doi: 10.1002/glia.23519

Nizar, K., Uhlirova, H., Tian, P., Saisan, P. A., Cheng, Q., Reznichenko, L., et al. (2013). In vivo stimulus-induced vasodilation occurs without IP3 receptor activation and may precede astrocytic calcium increase. *J. Neurosci.* 33, 8411–8422. doi: 10.1523/jneurosci.3285-12.2013

Nwaobi, S. E., Cuddapah, V. A., Patterson, K. C., Randolph, A. C., and Olsen, M. L. (2016). The role of glial-specific Kir4.1 in normal and pathological states of the CNS. *Acta Neuropathol.* 132, 1–21. doi: 10.1007/s00401-016-1553-1

Pandit, S., Neupane, C., Woo, J., Sharma, R., Nam, M.-H., Lee, G.-S., et al. (2020). Bestrophin1-mediated tonic GABA release from reactive astrocytes prevents the development of seizure-prone network in kainate-injected hippocampi. *Glia* 68, 1065–1080. doi: 10.1002/glia.23762

Parpura, V., Basarsky, T. A., Liu, F., Jeftinija, K., Jeftinija, S., and Haydon, P. G. (1994). Glutamate-mediated astrocyte-neuron signalling. *Nature* 369, 744–747. doi: 10.1038/369744a0

Parpura, V., and Haydon, P. G. (2000). Physiological astrocytic calcium levels stimulate glutamate release to modulate adjacent neurons. *Proc. Natl. Acad. Sci. U.S.A.* 97, 8629–8634. doi: 10.1073/pnas.97.15.8629

Parri, H. R., and Crunelli, V. (2003). The role of Ca2+ in the generation of spontaneous astrocytic Ca2+ oscillations. *Neuroscience* 120, 979–992. doi: 10.1016/s0306-4522(03)00379-8

Parri, H. R., Gould, T. M., and Crunelli, V. (2001). Spontaneous astrocytic Ca2+ oscillations in situ drive NMDAR-mediated neuronal excitation. *Nat. Neurosci.* 4, 803–812. doi: 10.1038/90507

Patel, D. C., Tewari, B. P., Chaunsali, L., and Sontheimer, H. (2019). Neuron-glia interactions in the pathophysiology of epilepsy. *Nat. Rev. Neurosci.* 20, 282–297. doi: 10.1038/s41583-019-0126-4

Paukert, M., Agarwal, A., Cha, J., Doze, V. A., Kang, J. U., and Bergles, D. E. (2014). Norepinephrine controls astroglial responsiveness to local circuit activity. *Neuron* 82, 1263–1270. doi: 10.1016/j.neuron.2014.04.038

Pekny, M., and Nilsson, M. (2005). Astrocyte activation and reactive gliosis. *Glia* 50, 427–434. doi: 10.1002/glia.20207

Pekny, M., and Pekna, M. (2016). Reactive gliosis in the pathogenesis of CNS diseases. *Biochim. Biophys. Acta* 1862, 483–491. doi: 10.1016/j.bbadis.2015.11.014

Pellerin, L., and Magistretti, P. J. (1994). Glutamate uptake into astrocytes stimulates aerobic glycolysis: a mechanism coupling neuronal activity to glucose utilization. *Proc. Natl. Acad. Sci. U.S.A.* 91, 10625–10629. doi: 10.1073/pnas.91.22.10625

Perea, G., Navarrete, M., and Araque, A. (2009). Tripartite synapses: astrocytes process and control synaptic information. *Trends Neurosci.* 32, 421–431. doi: 10.1016/j.tins.2009.05.001

Perea, G., Sur, M., and Araque, A. (2014). Neuron-glia networks: integral gear of brain function. *Front. Cell. Neurosci.* 8:378. doi: 10.3389/fncel.2014.00378

Perucca, P., and Gilliam, F. G. (2012). Adverse effects of antiepileptic drugs. *Lancet Neurol.* 11, 792–802. doi: 10.1016/s1474-4422(12)70153-9

Petravicz, J., Boyt, K. M., and McCarthy, K. D. (2014). Astrocyte IP3R2-dependent Ca^{2+} signaling is not a major modulator of neuronal pathways governing behavior. *Front. Behav. Neurosci.* 8:384. doi: 10.3389/fnbeh.2014.00384

Petravicz, J., Fiacco, T. A., and McCarthy, K. D. (2008). Loss of IP3 receptor-dependent Ca^{2+} increases in hippocampal astrocytes does not affect baseline CA1 pyramidal neuron synaptic activity. *J. Neurosci.* 28, 4967–4973. doi: 10.1523/jneurosci.5572-07.2008

Plata, A., Lebedeva, A., Denisov, P., Nosova, O., Postnikova, T. Y., Pimashkin, A., et al. (2018). Astrocytic atrophy following parallels reduced Ca^{2+} activity and impaired synaptic plasticity in the rat hippocampus. *Front. Mol. Neurosci.* 11:215. doi: 10.3389/fnmol.2018.00215

Poskanzer, K. E., and Yuste, R. (2016). Astrocytes regulate cortical state switching in vivo. *Proc. Natl. Acad. Sci. U.S.A.* 113, E2675–E2684.

Rothstein, J. D., Dykes-Hoberg, M., Pardo, C. A., Bristol, L. A., Jin, L., Kuncl, R. W., et al. (1996). Knockout of glutamate transporters reveals a major role for astroglial transport in excitotoxicity and clearance of glutamate. *Neuron* 16, 675–686. doi: 10.1016/s0896-6273(00)80086-0

Scemes, E., and Giaume, C. (2006). Astrocyte calcium waves: what they are and what they do. *Glia* 54, 716–725. doi: 10.1002/glia.20374

Scholl, U. I., Choi, M., Liu, T., Ramaekers, V. T., Häusler, M. G., Grimmer, J., et al. (2009). Seizures, sensorineural deafness, ataxia, mental retardation, and electrolyte imbalance (SeSAME syndrome) caused by mutations in KCNJ10. *Proc. Natl. Acad. Sci. U. S. A.* 106, 5842–5847. doi: 10.1073/pnas.0901749106

Sharp, A. H., Nucifora, F. C. Jr., Blondel, O., Sheppard, C. A., Zhang, C., Snyder, S. H., et al. (1999). Differential cellular expression of isoforms of inositol 1,4,5-triphosphate receptors in neurons and glia in brain. *J. Comp. Neurol.* 406, 207–220. doi: 10.1002/(sici)1096-9861(19990405)406:2<207::aid-cne6>3.0.co;2-7

Shields, D. C., Schaecher, K. E., Hogan, E. L., and Banik, N. L. (2000). Calpain activity and expression increased in activated glial and inflammatory cells in penumbra of spinal cord injury lesion. *J. Neurosci. Res.* 61, 146–150. doi: 10.1002/1097-4547(20000715)61:2<146::AID-JNR5>3.0.CO;2-C

Shigetomi, E., Saito, K., Sano, F., and Koizumi, S. (2019). Aberrant calcium signals in reactive astrocytes: a key process in neurological disorders. *Int. J. Mol. Sci.* 20, 996. doi: 10.3390/ijms20040996

Sofroniew, M. V. (2009). Molecular dissection of reactive astrogliosis and glial scar formation. *Trends Neurosci.* 32, 638–647. doi: 10.1016/j.tins.2009.08.002

Steinhäuser, C., and Seifert, G. (2012). "Astrocyte dysfunction in epilepsy," in *Jasper's Basic Mechanisms of the Epilepsies*, eds J. L. Noebels, M. Avoli, M. A. Rogawski, R. W. Olsen, and A. V. Delgado-Escueta (Bethesda, MD: National Center for Biotechnology Information).

Steinhäuser, C., Seifert, G., and Bedner, P. (2012). Astrocyte dysfunction in temporal lobe epilepsy: K^+ channels and gap junction coupling. *Glia* 60, 1192–1202. doi: 10.1002/glia.22313

Sun, W., McConnell, E., Pare, J.-F., Xu, Q., Chen, M., Peng, W., et al. (2013). Glutamate-dependent neuroglial calcium signaling differs between young and adult brain. *Science* 339, 197–200. doi: 10.1126/science.1226740

Szabó, Z., Héja, L., Szalay, G., Kékesi, O., Füredi, A., Szebényi, K., et al. (2017). Extensive astrocyte synchronization advances neuronal coupling in slow wave activity in vivo. *Sci. Rep.* 7:6018.

Szokol, K., Heuser, K., Tang, W., Jensen, V., Enger, R., Bedner, P., et al. (2015). Augmentation of Ca^{2+} signaling in astrocytic endfeet in the latent phase of temporal lobe epilepsy. *Front. Cell. Neurosci.* 9:49. doi: 10.3389/fncel.2015.00049

Tian, G.-F., Azmi, H., Takano, T., Xu, Q., Peng, W., Lin, J., et al. (2005). An astrocytic basis of epilepsy. *Nat. Med.* 11, 973–981.

Umpierre, A. D., West, P. J., White, J. A., and Wilcox, K. S. (2019). Conditional knock-out of mGluR5 from astrocytes during epilepsy development impairs high-frequency glutamate uptake. *J. Neurosci.* 39, 727–742. doi: 10.1523/jneurosci.1148-18.2018

van Vliet, E. A., da Costa Araújo, S., Redeker, S., van Schaik, R., Aronica, E., and Gorter, J. A. (2007). Blood-brain barrier leakage may lead to progression of temporal lobe epilepsy. *Brain* 130, 521–534. doi: 10.1093/brain/awl318

Vezzani, A., French, J., Bartfai, T., and Baram, T. Z. (2011). The role of inflammation in epilepsy. *Nat. Rev. Neurol.* 7, 31–40.

Volterra, A., and Steinhäuser, C. (2004). Glial modulation of synaptic transmission in the hippocampus. *Glia* 47, 249–257. doi: 10.1002/glia.20080

Wang, F., Smith, N. A., Xu, Q., Fujita, T., Baba, A., Matsuda, T., et al. (2012). Astrocytes modulate neural network activity by Ca2 -dependent uptake of extracellular K^+. *Sci. Signal.* 5:ra26. doi: 10.1126/scisignal.2002334

Wellmann, M., Álvarez-Ferradas, C., Maturana, C. J., Sáez, J. C., and Bonansco, C. (2018). Astroglial Ca-dependent hyperexcitability requires P2Y purinergic receptors and pannexin-1 channel activation in a chronic model of epilepsy. *Front. Cell. Neurosci.* 12:446. doi: 10.3389/fncel.2018.00446

Wieser, H.-G., and ILAE Commission on Neurosurgery of Epilepsy. (2004). ILAE Commission Report. Mesial temporal lobe epilepsy with hippocampal sclerosis. *Epilepsia* 45, 695–714. doi: 10.1111/j.0013-9580.2004.09004.x

Yang, H. Y., Lieska, N., Shao, D., Kriho, V., and Pappas, G. D. (1994). Proteins of the intermediate filament cytoskeleton as markers for astrocytes and human astrocytomas. *Mol. Chem. Neuropathol.* 21, 155–176. doi: 10.1007/bf02815349

Zhang, C., Tabatabaei, M., Bélanger, S., Girouard, H., Moeini, M., Lu, X., et al. (2019). Astrocytic endfoot Ca correlates with parenchymal vessel responses during 4-AP induced epilepsy: an in vivo two-photon lifetime microscopy study. *J. Cereb. Blood Flow Metab.* 39, 260–271. doi: 10.1177/0271678x17725417

Conflict of Interest: The authors declare that the research was conducted in the absence of any commercial or financial relationships that could be construed as a potential conflict of interest.

frontiers in Cellular Neuroscience

MINI REVIEW
published: 30 July 2021
doi: 10.3389/fncel.2021.695817

Astrocytic IP_3Rs: Beyond IP_3R2

Mark W. Sherwood[1†], Misa Arizono[2*†], Aude Panatier[1], Katsuhiko Mikoshiba[3,4,5] and Stéphane H. R. Oliet[1]*

[1] University of Bordeaux, INSERM, Neurocentre Magendie, U1215, Bordeaux, France, [2] University of Bordeaux, CNRS, Interdisciplinary Institute for Neuroscience, IINS, UMR 5297, Bordeaux, France, [3] ShanghaiTech University, Shanghai, China, [4] Faculty of Science, Toho University, Funabashi, Japan, [5] RIKEN CLST, Kobe, Japan

Astrocytes are sensitive to ongoing neuronal/network activities and, accordingly, regulate neuronal functions (synaptic transmission, synaptic plasticity, behavior, etc.) by the context-dependent release of several gliotransmitters (e.g., glutamate, glycine, D-serine, ATP). To sense diverse input, astrocytes express a plethora of G-protein coupled receptors, which couple, via $G_{i/o}$ and G_q, to the intracellular Ca^{2+} release channel IP_3-receptor (IP_3R). Indeed, manipulating astrocytic IP_3R-Ca^{2+} signaling is highly consequential at the network and behavioral level: Depleting IP_3R subtype 2 (IP_3R2) results in reduced GPCR-Ca^{2+} signaling and impaired synaptic plasticity; enhancing IP_3R-Ca^{2+} signaling affects cognitive functions such as learning and memory, sleep, and mood. However, as a result of discrepancies in the literature, the role of GPCR-IP_3R-Ca^{2+} signaling, especially under physiological conditions, remains inconclusive. One primary reason for this could be that IP_3R2 has been used to represent all astrocytic IP_3Rs, including IP_3R1 and IP_3R3. Indeed, IP_3R1 and IP_3R3 are unique Ca^{2+} channels in their own right; they have unique biophysical properties, often display distinct distribution, and are differentially regulated. As a result, they mediate different physiological roles to IP_3R2. Thus, these additional channels promise to enrich the diversity of spatiotemporal Ca^{2+} dynamics and provide unique opportunities for integrating neuronal input and modulating astrocyte–neuron communication. The current review weighs evidence supporting the existence of multiple astrocytic-IP_3R isoforms, summarizes distinct sub-type specific properties that shape spatiotemporal Ca^{2+} dynamics. We also discuss existing experimental tools and future refinements to better recapitulate the endogenous activities of each IP_3R isoform.

Keywords: astrocyte, inositol triphosphate (IP3) receptor, IP_3R subtypes, calcium, GPCR, tripartite synapse, gliotransmission

OPEN ACCESS

Edited by:
Yu-Wei Wu, Academia Sinica, Taiwan

Reviewed by:
Dmitri A. Rusakov, University College London, United Kingdom
Vladimir Grubišiæ, Michigan State University, United States

***Correspondence:**
Mark W. Sherwood
MWSherwood@protonmail.com
Misa Arizono
arizono0202@gmail.com

†These authors have contributed equally to this work and share first authorship

Specialty section:
This article was submitted to Non-Neuronal Cells, a section of the journal Frontiers in Cellular Neuroscience

Received: *15 April 2021*
Accepted: *30 June 2021*
Published: *30 July 2021*

Citation:
Sherwood MW, Arizono M, Panatier A, Mikoshiba K and Oliet SHR (2021) Astrocytic IP_3Rs: Beyond IP_3R2. Front. Cell. Neurosci. 15:695817. doi: 10.3389/fncel.2021.695817

INTRODUCTION

Over the last three decades, Ca^{2+} imaging has revealed new roles for astrocytes. Indeed, astrocytic Ca^{2+} signaling was shown to regulate synaptic transmission, synaptic plasticity, and to influence behavior (Araque et al., 2014; Park and Lee, 2020). Inositol 1,4,5-trisphosphate receptors (IP_3Rs) mediated Ca^{2+} signaling (IP_3R-Ca^{2+}) is regarded a primary generator of astrocytic Ca^{2+} signaling. Upon activation of G_q-GPCRs, the main input pathway of astrocytes, phospholipase C breaks down PIP_2 into DAG and IP_3, activating IP_3R predominantly located on the membrane of endoplasmic reticulum (ER) resulting in Ca^{2+} release (Bootman et al., 2001). This IP_3R-mediated Ca^{2+} signaling is considered to trigger the activity-dependent and selective release of chemical transmitters (gliotransmitters) such as glutamate, D-serine, and ATP, which have distinct influences

over neuronal activity. Initially, IP_3R subtype 2 (IP_3R2) was the only recognized Ca^{2+} channel in astrocytes; However, advanced Ca^{2+} imaging techniques have since identified novel Ca^{2+} sources, including mitochondria (Agarwal et al., 2017), transient receptor potential ankyrin 1 (Shigetomi et al., 2012, 2013b), L-type voltage gated Ca^{2+} channels (Letellier et al., 2016), sodium/calcium exchanger (Kirischuk et al., 1997; Boddum et al., 2016; Rose et al., 2020), and transient receptor potential canonical (Shiratori-Hayashi et al., 2020) amongst others, thereby expanding the known Ca^{2+} signaling toolkit of astrocytes. Doubtlessly additional Ca^{2+} channels and sources will emerge in the future.

While the field's focus has moved on from understanding IP_3Rs to identifying new Ca^{2+} sources, understanding IP_3R signaling in astrocytes remains highly relevant. Indeed, IP_3Rs are the primary target for manipulating astrocytic activity, and such manipulations have proven to be very consequential in many studies. Since most of these manipulations indiscriminately influence all IP_3R subtypes, this could reflect the key role played by IP_3R subtypes other than IP_3R2, namely IP_3R1 and IP_3R3, which were mostly overlooked. In this review, we summarize the evidence for different subtypes of IP_3R and discuss how we can better study the role of IP_3R-Ca^{2+} signaling in astrocytes which is one of the core issues in understanding astrocyte physiology.

EVIDENCE FOR THREE SUBTYPES

The Dogma: IP_3R2 the Sole Functional Astrocytic IP_3R

There are three mammalian IP_3R subtypes, i.e., IP_3R1 (Furuichi et al., 1989; Mignery et al., 1989; Yamada et al., 1994), IP_3R2 (Mignery et al., 1990; Südhof et al., 1991; Yamamoto-Hino et al., 1994; Iwai et al., 2005), and IP_3R3 (Blondel et al., 1993; Yamamoto-Hino et al., 1994; Iwai et al., 2005). Among them, IP_3R2 has widely been accepted as the only functional IP_3R subtype present in astrocytes, and consequently, the IP_3R2KO model mouse has been at the center of numerous important studies (Agulhon et al., 2010; Takata et al., 2011; Chen et al., 2012; Navarrete et al., 2012, 2019; Cao et al., 2013; Perez-Alvarez et al., 2014; Petravicz et al., 2014; Gómez-Gonzalo et al., 2015, 2017; Mariotti et al., 2016; Monai et al., 2016; Perea et al., 2016; Martin-Fernandez et al., 2017; Tanaka et al., 2017). Although an important model in the astrocyte field, the belief that knocking out IP_3R type-2 abolishes IP_3 induced Ca^{2+} release (IICR) entirely appears to need remedying. This section considers the historical data from which the dogmatic view of astrocytic-IP_3R2 has flowed and reviews the evidence for other IP_3R subtypes.

Astrocyte Proteome

Several studies explored IP_3Rs using immunohistochemistry which provided a consensus over the expression of IP_3R2 in hippocampal/cortical astrocytes and Bergmann glia (Sharp et al., 1999; Holtzclaw et al., 2002; Hertle and Yeckel, 2007; Takata et al., 2011; Chen et al., 2012). While there are some conflicting reports over the immunoreactivity of IP_3R3 in astrocytes and Bergmann glia (Sugiyama et al., 1994; Yamamoto-Hino et al., 1995; Hamada et al., 1999; Sharp et al., 1999; Holtzclaw et al., 2002), IP_3R1 immunoreactivity was not initially observed in glia (Nakanishi et al., 1991; Dent et al., 1996; Hamada et al., 1999; Sharp et al., 1999; Holtzclaw et al., 2002; Hertle and Yeckel, 2007). These findings supported the view that IP_3R2 is the predominant astrocytic IP_3R. However, these results may also reflect limitations of the available IP_3R antibodies or the difficulty of accurately assigning proteins located within ultrathin astrocyte processes, which are below the resolution limit of conventional microscopy (Panatier et al., 2014; Arizono et al., 2020) and buried amongst neuronal dendrites.

IP_3R1 immunoreactivity was recently detected in spinal dorsal horn astrocytes (Shiratori-Hayashi et al., 2020) and, albeit with low stringency, in isolated astrocytes from adult mice (Chai et al., 2017). Using a state of the art TurboID construct to biotinylate proteins in the immediate proximity of tripartite synapses, Takano et al. (2020) report enrichment of IP_3R1 protein in the peri-synaptic astrocytic compartment (Takano et al., 2020). This finding, however, should be interpreted with some caution as identified proteins were assigned to astrocytes based on published mRNA datasets (Zhang et al., 2014, 2016). Nevertheless, IP_3R1 protein enrichment in fine astrocytic processes is consistent with Ca^{2+} imaging studies (Sherwood et al., 2017) and could account for the poor detection in various assays which favor detection in large subcellular compartments, i.e., major processes and soma of astrocytes. Notably, IP_3R2, which is reported to be in the soma and main branches (Chen et al., 2012), was not enriched in peri-synaptic astrocytic compartments (Takano et al., 2020), likely reflecting the different subcellular distribution of IP_3R1 and IP_3R2 (**Figure 1A** and **Table 1**).

Astrocyte Transcriptome

IP_3R1, IP_3R2, and IP_3R3 are encoded by the respective genes ITPR1, ITPR2, and ITPR3. Notably, mRNA for all three genes have been detected in astrocytes isolated from young and aged mouse brain (Cahoy et al., 2008; Zhang et al., 2014; Chai et al., 2017; Clarke et al., 2018) as well as humans (Zhang et al., 2016). Furthermore, ITPR1 and ITPR2 are actively translated in astrocytes of adult mice (Srinivasan et al., 2016; Chai et al., 2017; Clarke et al., 2018; Yu et al., 2018) indicating that their proteins are produced in astrocytes. In astrocytes the isoform transcript abundance is generally ITPR2 > ITPR1 >>> ITPR3 (ITPR3 mRNA is present in very small amounts and may be negligible). However, these transcripts are developmentally and differentially regulated across brain regions and in some instances ITPR1 mRNA appears to be more abundant than ITPR2 mRNA (Yu et al., 2018; **Table 1**).

Ca^{2+} Imaging

Over the last decade, studies show that deletion of IP_3R2 does not abolish Ca^{2+} signaling in astrocytes. It is now generally agreed that bulk/somatic cytosolic Ca^{2+} responses are hard to detect in IP_3R2KO astrocytes (Petravicz et al., 2008, 2014; Agulhon et al., 2010, 2013; Takata et al., 2011, 2013; Nizar et al., 2013). However, with a detailed examination, rich Ca^{2+} activity can be observed within fine astrocyte processes (Di Castro et al., 2011; Haustein et al., 2014; Kanemaru et al., 2014; Srinivasan et al., 2015;

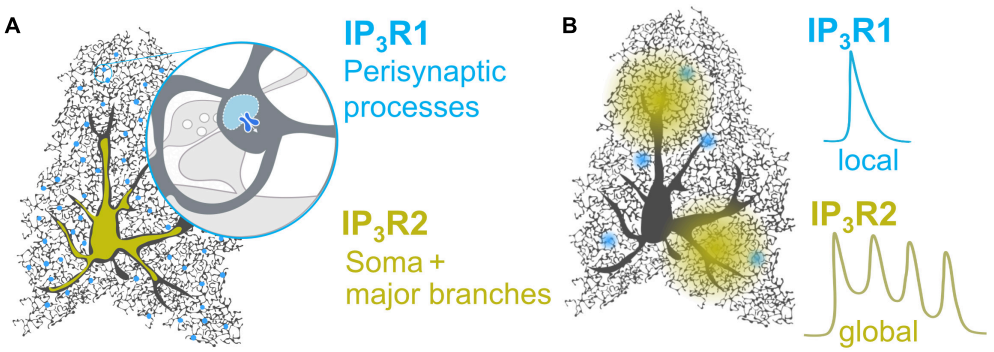

FIGURE 1 | Proposed distribution and Ca^{2+} profiles of IP_3R1 and IP_3R2 in astrocytes. **(A)** While IP_3R2 is distributed in the soma and major branches (Takata et al., 2011; Chen et al., 2012; Petravicz et al., 2014), IP_3R1 may be enriched in the peri-synaptic processes (Sherwood et al., 2017; Takano et al., 2020), for instance in the nodes which were recently shown to host 2-APB-sensitive local Ca^{2+} signals at the tripartite synapse (Arizono et al., 2020). **(B)** IP_3R2 generates global Ca^{2+} waves and oscillations in both astrocytes (Srinivasan et al., 2015; Sherwood et al., 2017) and model cells (Miyakawa, 1999). IP_3R1 mediated Ca^{2+} dynamics in astrocytes have not been observed directly, but may resemble IP_3R1-dependent monophasic Ca^{2+} transients observed in model cells (Miyakawa, 1999) and dendritic spines of pyramidal neurons (Holbro et al., 2009).

Rungta et al., 2016; Agarwal et al., 2017; Sherwood et al., 2017). Non-IP_3R2 Ca^{2+} activity has largely been interpreted as evidence for non-IP_3R Ca^{2+} stores, nevertheless, these activities could equally arise from IP_3R1 and or IP_3R3 (Tamamushi et al., 2012; Sherwood et al., 2017). Indeed, Ca^{2+} release from the ER was recently reported for IP_3R2KO astrocytes (Okubo et al., 2019). In Bergmann glia, while IP_3R2 was shown to be a dominant subtype, IP_3R1 and IP_3R3 were also shown to contribute to rapid Ca^{2+} events in the processes (Tamamushi et al., 2012). Similarly, using IP_3R2KO and $IP_3R2/3$ double KO mice, we found that IP_3R2 is involved in global Ca^{2+} release, whereas local Ca^{2+} signals involve IP_3R1 and IP_3R3 (**Figure 1B**) (Sherwood et al., 2017) in hippocampal astrocytes. Knock-down of IP_3R1 in dorsal spinal cord astrocytes of IP_3R2KO mice also unmasked IP_3R1 mediated Ca^{2+} signals (Shiratori-Hayashi et al., 2020). Furthermore, the selective activation of G_q-GPCR/IP_3R/Ca^{2+} signaling in astrocytes, using DREADDs (designer receptor exclusively activated by designer drug, see section "Activation of IP_3 Induced Ca^{2+} Release in Astrocytes"), triggered Ca^{2+} events in the astrocytic processes of IP_3R2KO mice (Wang et al., 2021) indicating the presence of $IP_3R1/3$.

2-APB was introduced as an antagonist of IP_3Rs (Maruyama et al., 1997) and has been widely used to investigate the contribution of IP_3Rs to cellular Ca^{2+} signaling. 2-APB appears to preferentially block IP_3R1 and IP_3R3, whereas cells predominantly expressing IP_3R2 seem largely insensitive (Kukkonen et al., 2001; Bootman et al., 2002; Saleem et al., 2014). Thus, the fact that 2-APB reduces astrocyte Ca^{2+} amplitude and responsiveness in diverse brain regions (Sul et al., 2004; Young et al., 2010; Tamura et al., 2014; Tang et al., 2015; Arizono et al., 2020) and spinal dorsal horn (Shiratori-Hayashi et al., 2020) may support the presence of functional IP_3R1 and IP_3R3 in astrocytes. The functional role of non-IP_3R2 in astrocytic Ca^{2+} signaling remains to be determined, it is possible that some membrane receptors are functionally coupled solely to IP_3R1 or IP_3R3 and generate local Ca^{2+} events, which may or may not be involved in triggering IP_3R2 dependent Ca^{2+} waves (Petravicz et al., 2008). Alternatively, it is possible that IP_3Rs exist as heterotetramers (Wojcikiewicz and He, 1995; Nucifora et al., 1996).

Phenotypic Comparison

Comparison of WT and total IP_3R2KO mice has revealed some important physiological roles of IP_3R2 signaling in astrocytes, i.e., motor learning (Padmashri et al., 2015) modulating depressive-like behaviors (Cao et al., 2013) but this remains controversial (Petravicz et al., 2014). The possible roles of astrocytic IP_3R1 and IP_3R3 may be gleaned by comparing WT and IP_3R2KOs with manipulations that impair all IP_3R subtypes. For example, while IP_3R2KO has no impact on sleep (Cao et al., 2013) overexpressing a transgene for the IP_3 hydrolyzing enzyme, IP_3-5-phosphatase, in astrocytes, suppresses Ca^{2+} release from all IP_3R subtypes and disrupts sleep (Foley et al., 2017). Similarly, although IP_3R2KO had no impact on hippocampal LTP (Agulhon et al., 2010), we showed that loading a single astrocyte with the membrane-impermeable pan-IP_3R antagonist, heparin, blocks long-term synaptic potentiation (Sherwood et al., 2017). These studies, taken together, indicate that non-IP_3R2 IP_3Rs regulate sleep and hippocampal LTP.

Summary

The expression of multiple IP_3R subtypes in astrocytes has a wide-reaching implication in the field. Studies using IP_3R2KO as a model for blocked IICR would need to be re-assessed to include the possibility of IICR mediated by IP_3R1 and IP_3R3.

PROSPECTUS/ADVANTAGE OF MULTIPLE IP_3R ISOFORMS

Different Properties of IP_3R Subtypes

The three IP_3R subtypes share only 65–85% homology accounting for many of the subtype-specific properties leading to particular spatiotemporal features of Ca^{2+} responses. Although

TABLE 1 | Dissecting IP_3R subtypes.

Transcriptome/translatome

Species	Age (weeks)	Region	ITPR1 (FPKM)	ITPR2 (FPKM)	ITPR3 (FPKM)	Comment	References
Mouse	1	Str	1.4	7.6	0.1	Translatome	Clarke et al., 2018
	4.6		7.8	4.5	0.3		
	9		28.5; 85.0	17.4; 6.4	0.2; 0.1		Yu et al., 2018
	9		27.1	10.1			Chai et al., 2017
	10		10.9	2.6	0.1		
	38		13.1	2.5	0.1		
	96		16.1	4.4	0.0		Clarke et al., 2018
	0–2.4	Forebrain	Present	Present	Absent	Transcriptome	Cahoy et al., 2008
	1	Ctx	0.4	12.6	0.1		Zhang et al., 2014
	1		1.5	4.2	0.1	Translatome	Clarke et al., 2018
	Adult		2.6	7.1			Srinivasan et al., 2016
	4.6		5.4	6.0	0.6		Clarke et al., 2018
	10		13.7	5.3	0.1		
	38		12.3	4.6	0.0		
	96		17.5	4.5	0.0		
	1	Hc	0.8	4.8	0.1		Clarke et al., 2018
	4.6		3.0	5.4	0.3		
	9		6.7	11.7			Chai et al., 2017
	10		8.6	4.0	0.1		Clarke et al., 2018
	38		4.4	4.8	0.0		
	96		4.4	6.9	0.1		
Human	8–63 years	Ctx	0.7	13.7	0.1	Transcriptome	Zhang et al., 2016
	17–20 gw	Brain	0.4	2.6	0.2		

Proteome

Species	Age (weeks)	Region	IP_3R1	IP_3R2	IP_3R3	References
Rat	Adult	Hc, Cb, Cc, ScNu	No	Yes	No	Holtzclaw et al., 2002
	>8	Hc	No	Yes	No	Hertle and Yeckel, 2007
	8	Cb, Ht, Hc	No	No	Yes	Yamamoto-Hino et al., 1995
		ScNu, Ht, Ctx	No	–	Yes	Hamada et al., 1999
Mouse		SDH	Yes	–	–	Shiratori-Hayashi et al., 2020
		Hc, Str	Yes	Yes	No	Chai et al., 2017
	7	Ctx	Yes	–	–	Takano et al., 2020
	>6	Ctx	–	Yes	–	Chen et al., 2012
	8–12	Ctx	–	Yes	–	Takata et al., 2011
Human		Ctx	Yes	Yes	Yes	Hur et al., 2010

Available pharmacological/genetic tools

	Tool	IP_3R	References
Transgenic mice	IP_3R1 KO	1	Tamamushi et al., 2012
	IP_3R2 KO	2	Fiacco et al., 2007; Petravicz et al., 2008; Agulhon et al., 2010; Takata et al., 2011, 2013; Navarrete et al., 2012; Tamamushi et al., 2012; Cao et al., 2013; Nizar et al., 2013; Bonder and McCarthy, 2014; Gómez-Gonzalo et al., 2015, 2017; Mariotti et al., 2016; Monai et al., 2016; Perea et al., 2016; Martin-Fernandez et al., 2017; Sherwood et al., 2017; Tanaka et al., 2017; Wang et al., 2021
	IP_3R3 KO	3	Tamamushi et al., 2012
	$IP_3R2/3KO$	2 and 3	Tamamushi et al., 2012; Sherwood et al., 2017
	IP_3R1 cKO	1	# Sugawara et al., 2013
	IP_3R2 cKO	2	Chen et al., 2012; Petravicz et al., 2014; Padmashri et al., 2015; Wang et al., 2021
Genetic tools for inhibition	IP_3 sponge	1, 2, and 3	Xie et al., 2010; Tanaka et al., 2013
	5ppase	1, 2, and 3	Kanemaru et al., 2007; Foley et al., 2017
	IP_3R1 shRNA	1	Shiratori-Hayashi et al., 2020

(Continued)

TABLE 1 | Continued

Available pharmacological/genetic tools			
	Tool	**IP_3R**	**References**
	IP_3R2 shRNA	2	#
	IP_3R3 shRNA	3	#
Pharmacology	IP_3R1 Ab	1	#$ Miyazaki et al., 1992; Inoue et al., 1998; Nishiyama et al., 2000
	IP_3R2 Ab	2	#$ Gerasimenko et al., 2009
	IP_3R3 Ab	3	#$ Gerasimenko et al., 2009
	Heparin	1, 2, and 3	$ Sherwood et al., 2017
	(1,2,3,4,6)IP_5 dimer	1; 2/3?	#$ Konieczny et al., 2016
Genetic tools for activation	MrgA1 (G_q GPCR)	?	Fiacco et al., 2007; Agulhon et al., 2010; Cao et al., 2013
	hM3Dq	2 and 1 or 3	Agulhon et al., 2013; Bonder and McCarthy, 2014; Yang et al., 2015; Martin-Fernandez et al., 2017; Adamsky et al., 2018; Wang et al., 2021
	hM4Di	?	Yang et al., 2015
	Opto-α_1AR	?	Figueiredo et al., 2014; Adamsky et al., 2018; Iwai et al., 2021
	Melanopsin	?	Mederos et al., 2019

 # Untested in astrocytes; $ requires loading using an astrocytic patch-pipette; ?, unknown; FPKM, fragments per kilobase of transcript per million mapped reads; Ctx, cortex; Str, striatum; Hc, hippocampus; Ht, hypothalamus; Cb, cerebellum; Cc, corpus callosum; ScNu, suprachiasmatic nucleus; SDH, spinal dorsal horn; gw, gestational weeks. Darker shades of blue represents higher FPKM values.

high homology is observed in regions critical for forming the IP_3−gated Ca^{2+} channel, each subtype has a different IP_3 affinity; $IP_3R2 > IP_3R1 > IP_3R3$ (Zhang et al., 2011). High IP_3 affinity of IP_3R2 has been associated with slower kinetics and more prolonged duration of IP_3R2-mediated Ca^{2+} microdomains, or Ca^{2+} puffs (Mataragka and Taylor, 2018).

Importantly, IP_3R channel activity is not only regulated by IP_3 but also by Ca^{2+} (Finch et al., 1991). The synergy between IP_3 and Ca^{2+} creates repetitive IP_3R activation and inhibition, resulting in Ca^{2+} oscillations. Such oscillations are crucial to protect cells from extended Ca^{2+} elevation that can often be toxic to the cell (Berridge et al., 2000). The oscillatory pattern is considered necessary for many cellular processes, such as fertilization (Miyazaki et al., 1992). IP_3R2 mediates long-lasting, regular Ca^{2+} oscillations, whereas IP_3R1 or IP_3R3 tend to exhibit mono-phasic transients or very rapidly dampened Ca^{2+} oscillations (Miyakawa, 1999).

The difference in IP_3R subtype properties is further characterized by various binding partners, including kinase and phosphatases, which can further fine-tune Ca^{2+} profiles. Interestingly, while there are many interacting partners common to all three IP_3R subtypes, the nature of their regulation can be subtype-specific. For instance, protein kinase C, depending on the IP_3R subtype, can either be stimulatory or inhibitory; this difference likely reflects isoform-specific phosphorylation sites. Further detailed biochemical study (Hamada et al., 2017) is required to investigate how various IP_3R binding molecules specifically regulate each IP_3R isoform (Hamada and Mikoshiba, 2020).

Different Distribution and Role of IP_3R Subtypes Within Various Tissues

One important feature that defines the subtype-specific role of IP_3Rs *in vivo* is the tissue distribution patterns. While IP_3R1 is mostly expressed in the central nervous system, IP_3R2 and IP_3R3 are broadly expressed in various organs such as the heart, pancreas, liver, and salivary glands (Hisatsune and Mikoshiba, 2017). This distribution pattern is tightly linked to the physiological role of IP_3R subtypes. Reflecting its rich expression in Purkinje cells, mice lacking IP_3R1 exhibit severe cerebellar ataxia, a seizure−like posture, impaired cerebellar LTD. (Inoue et al., 1998), and die within 3–4 weeks of birth (Matsumoto et al., 1996). The dysregulation of IP_3R1 is linked with other brain disorders such as Huntington's disease and Alzheimer's disease (Hisatsune and Mikoshiba, 2017). IP_3R2 is associated with sweating (Klar et al., 2014), bone formation (Kuroda et al., 2008), and heart hypertrophy (Nakayama et al., 2010; Drawnel et al., 2012; Vervloessem et al., 2015). IP_3R3 plays a role in taste sensing (Hisatsune et al., 2007) and hair cycle (Sato-Miyaoka et al., 2012). IP_3R2 and IP_3R3 together are associated with the heart's development (Uchida et al., 2010, 2016) and secretion of saliva and tears (Futatsugi, 2005; Inaba et al., 2014).

Different Distribution and Role of IP_3R Subtypes Within a Cell

Some cells express multiple IP_3R subtypes, enabling each subtype to uniquely contribute to Ca^{2+} profiles and cellular functions. For instance, in HeLa cells, knock-down of IP_3R1 terminates Ca^{2+} oscillations, whereas knock-down of IP_3R3 results in more robust and long-lasting Ca^{2+} oscillations (Hattori et al., 2004). The specific contribution of IP_3R subtypes can also depend on their distinct subcellular distribution, as seen in pancreatic acinar cells (Lur et al., 2011), COS cells (Pantazaka and Taylor, 2011), and DT40 cells (Bartok et al., 2019). In Bergmann glia, knocking out IP_3R2 resulted in decreased agonist-induced Ca^{2+} release while knocking out IP_3R1 and IP_3R3 resulted in delaying the peak of agonist-induced Ca^{2+} release specifically in astrocytic processes (Tamamushi et al., 2012), suggesting their subtype-specific distribution. It is likely that astrocytes, which

express multiple IP_3R subtypes, also take advantage of subtype-specific distribution.

In astrocytes, IP_3Rs are predominantly located on thapsigargin sensitive ER Ca^{2+} store. The ER in astrocytes may be found throughout the cell in the soma, major processes (Okubo et al., 2019, 2020), and peri-synaptic astrocytic processes (Bergersen et al., 2012), in close association with adhesion junctions (puncta adherentia) between dendritic spines and astrocytic processes (Spacek and Harris, 1998). Although recent studies indicate that ER and other membrane-bound organelles are absent from peri-synaptic processes (Patrushev et al., 2013) this likely reflects their sensitivity to chemical fixation (Korogod et al., 2015). The ER store in astrocytes is heterogeneous and organized into sub-compartments that can release Ca^{2+} independently (Golovina and Blaustein, 1997, 2000). It would be fascinating to see if IP_3R subtypes are located to specific functional domains, e.g., signaling domains of membrane receptors, ER-mitochondria contacts (Bartok et al., 2019), and ER-plasma membrane junctions (Thillaiappan et al., 2017). In addition to the ER, astrocytic IP_3Rs can also be found on other Ca^{2+} stores, with unique properties, i.e., the large dense-core vesicles (Hur et al., 2010), which may be comparable to the thapsigargin insensitive, Bafilomycin A1 sensitive, acidic Ca^{2+} stores previously described in secretory cells (Gerasimenko et al., 1996, 2009, 2011; Hur et al., 2010). Notably, compared to the ER, acidic Ca^{2+} stores can exhibit enhanced sensitivity to IP_3 (Yoo, 2010). Other potential IP_3-sensitive Ca^{2+} stores include the nuclear envelope (Gerasimenko et al., 1995; Petersen et al., 1998), nucleoplasm (Echevarría et al., 2003), Golgi (Pinton et al., 1998), and plasma membrane (Dellis et al., 2006).

Summary

While IP_3R subtypes are regulated by IP_3 and Ca^{2+} and have many common interacting partners, they differ in how they are affected by these regulators. Such differences enrich the diversity of spatio-temporal Ca^{2+} profiles created by IP_3Rs. The IP_3R subtype expression pattern, *in vivo*, is tissue specific and their subcellular localization is highly variable and dependent on cell types, and this carries important functional implications. Together with recent reports showing the distinct role of IP_3R1 and IP_3R3 in Bergmann glia and astrocytes, these facts support the view that IP_3R isoforms 1 and 3 are unique Ca^{2+} channels that need to be addressed independently of IP_3R2.

TOOLS TO DISSECT THE ROLE OF IP_3R ISOFORMS

Experimental and Analytical Tools

To understand the role of the various Ca^{2+} signals in astrocyte physiology, it will be necessary to make quantitative measurements (Neher, 2008). Progress in this direction has been frustrated by the unique astrocyte morphology and difficulties in interpreting recorded Ca^{2+}-dependent fluorescent signals (Rusakov, 2015). To accurately capture Ca^{2+} dynamics in sub-cellular compartments, there is a need to adopt imaging techniques with improved resolution and to develop tools for efficient analysis in three-dimensional (Bindocci et al., 2017; Romanos et al., 2019). Because of our poor understanding of functional compartments, analysis of astrocytic Ca^{2+} dynamics has been moving toward state-of-the-art event-based analysis (Romanos et al., 2019; Wang et al., 2019; Bjørnstad et al., 2021), nevertheless ROI (region-of-interest) based analysis, informed by cellular anatomy (functional compartments) and molecular architecture, has been critical for understanding neuron physiology (e.g., spines and boutons). To this end, the identification of morphologically distinct subcellular compartments are promising targets for classical ROI based analysis, i.e., "glial microdomains" on Bergmann glial processes (Grosche et al., 1999) and "astrocytic compartments" on major branches (Panatier et al., 2011), both revealed using confocal microscopy, and astrocytic nodes and shafts within the spongiform structure visualized using live STED microscopy (Arizono et al., 2020). The ultimate goal of extracting quantitative Ca^{2+} dynamics from fluorescent data is non-trivial but achievable using realistic biophysical cell models (Rusakov, 2015; Denizot et al., 2019), a task simplified by the recent development of the open-source flexible model builder ASTRO (Savtchenko et al., 2018). For an accurate understanding of Ca^{2+} dynamics, it will be necessary to constrain models further using empirically determined details, e.g., receptor kinetics, expression patterns, endogenous Ca^{2+} buffering, etc.

Pharmacological Tools

It is difficult to disentangle the physiological roles of IP_3R subtypes in cells that typically express complex mixtures of homo- and hetero-tetrameric IP_3Rs. There are no ligands that usefully distinguish among IP_3R subtypes (Saleem et al., 2013a,b) and nor are there effective antagonists that lack serious side effects (Michelangeli et al., 1995). Of the available antagonists, heparin is currently the most useful. Heparin is a membrane impermeant pan-IP_3R inhibitor that may be selectively loaded into astrocytes using a whole-cell patch-pipette (Sherwood et al., 2017). Recent developments report small impermeant competitive antagonists of IP_3R1, which, compared to heparin, are likely to have fewer off-targets (Konieczny et al., 2016). Well-characterized function-blocking monoclonal antibodies are powerful tools to specifically inhibit IP_3R subtypes (Miyazaki et al., 1992; Inoue et al., 1998; Nishiyama et al., 2000; Gerasimenko et al., 2009). This technology has not yet been applied to astrocytes.

Genetic Tools

Inhibition of IP_3 Induced Ca^{2+} Release

IP_3R2KO and conditional-KO (cKO) mice (Petravicz et al., 2014; Padmashri et al., 2015; Wang et al., 2021) are widely used, however, as highlighted above, deletion of IP_3R2 does not abolish IICR. IICR can be suppressed, irrespective of the underlying receptor, using an IP_3-sponge to buffer IP_3 (Xie et al., 2010; Tanaka et al., 2013), or an IP_3-5′-phospatase transgene to enhance IP_3 metabolism

(Kanemaru et al., 2007; Foley et al., 2017). To study the physiological role of IP_3R subtypes it is necessary to develop inducible cKO for IP_3R1 (Sugawara et al., 2013) and IP_3R3. Specific knock-down of IP_3R subtypes can also be achieved using viruses to introduce short hairpin RNA into astrocytes (Shiratori-Hayashi et al., 2020).

Activation of IP_3 Induced Ca^{2+} Release in Astrocytes

Pharmacogenetics

DREADDs (designer receptor exclusively activated by designer drug) enable the selective activation of GPCR-IP_3R-Ca^{2+} signaling in astrocytes. The most used DREADDs are the excitatory Gq or inhibitory G_i-coupled receptors, hM3Dq and hM4Di, respectively (derived from human M3/M4 muscarinic receptor). Both receptors are activated by a pharmacologically inert but bioavailable ligand clozapine-N-oxide (CNO) while being non-responsive to endogenous GPCR ligands (Agulhon et al., 2013). hM3Dq has been used to demonstrate an astrocytic role in behaviors such as food intake (Yang et al., 2015), fear response (Martin-Fernandez et al., 2017), and memory recall (Adamsky et al., 2018). While the DREADDs enables selective activation of astrocytes, they have two major drawbacks: Firstly, the exogenous receptors have not been targeted to specific signaling domains and are likely to be spatially uncoupled from signaling nanodomains critical to IP_3R physiology (Bootman et al., 2001); Secondly, because of the sustained (hour-long) activation by exogenous ligands (Iwai et al., 2021), temporal features of astrocyte signaling are lost. While perhaps mimicking global Ca^{2+} surges, the available DREADDs are unlikely to recapitulate many of the local Ca^{2+} transients typically observed within fine astrocytic processes (Shigetomi et al., 2013a; Arizono et al., 2020).

Optogenetics

To achieve temporal control, an optogenetic approach has been developed for the reliable stimulation of endogenous GPCR-IP_3R-Ca^{2+} signaling cascade using light. Light activation has been achieved by introducing to astrocytes either a mammalian light-sensitive $G_q/G_{i/o}$-protein-coupled photopigment, Melanopsin (Panda, 2005; Bailes and Lucas, 2013; Mederos et al., 2019), or light-activated chimeric GPCRs, termed OptoXRs. OptoXRs are generated by replacing the intracellular loops of a light-sensitive GPCR, e.g., rhodopsin, with those of a donor GPCR, e.g., G_q-coupled human adrenergic receptor α_{1a} (Airan et al., 2009; Figueiredo et al., 2014; Tang et al., 2014; Adamsky et al., 2018; Iwai et al., 2021).

Summary – Future Developments

While having great potential for controlling astrocytic activation, a central question is to what extent do the chimeras mimic the signaling of wild-type receptors. GPCRs can have multiple signaling axis, e.g., multiple G-protein axes, β-arrestins, wnt-frizzled, or the hedgehog-smoothened axes (Bailes and Lucas, 2013; Tichy et al., 2019), and the signaling axes bias is often not characterized but can have profound side effects on physiology (Agulhon et al., 2013; Tichy et al., 2019). Indeed, the functional outcome of activating G_q in astrocytes using different exogenous receptor (i.e., hM3Dq and MrgA1) is not reproducible (Agulhon et al., 2010; Adamsky et al., 2018). While multiple signaling axis could confuse the role of IICR, they may be required to obtain an optimal IP_3R response (Konieczny et al., 2017). Another primary concern is that DREADDs and optoXRs likely activate IP_3Rs from cellular compartments distinct from those of the endogenous receptors, limiting their ability to recreate physiologically relevant Ca^{2+} profiles. To address this, next-generation activation tools are being engineered to mimic the subcellular distribution of endogenous receptors (Oh et al., 2010; Masseck et al., 2014; Spoida et al., 2014; Tichy et al., 2019).

In the last decade, substantial progress has been made revealing diverse spatio-temporal Ca^{2+} signaling in astrocytes. Understanding the subtleties of these signals will require detailed knowledge of the astrocytic Ca^{2+} signaling toolbox along with the generation and characterization of more sophisticated tools to control and accurately recapitulate the physiologically relevant Ca^{2+} signals.

AUTHOR CONTRIBUTIONS

MS and MA performed the literature survey, wrote the manuscript, and prepared the figures and tables. MS, MA, AP, KM, and SHRO reviewed, finalized, and approved the final version.

FUNDING

This review was funded by the CNRS, INSERM, LabEx BRAIN, and the Agence Nationale de la Recherche, grant numbers ANR-17-CE16-0002 to SHRO, and ANR-16-CE16-0001-0 to AP. MS was supported by a Takeda Science Foundation fellowship (Japan), and MA was supported by postdoctoral fellowships from RIKEN and JSPS (Japan). KM was supported by Scientific Research S (25221002) of JSPS and ICORP; ICORP-SORST of Japan Science and Technology Agency.

REFERENCES

Adamsky, A., Kol, A., Kreisel, T., Doron, A., Ozeri-Engelhard, N., Melcer, T., et al. (2018). Astrocytic activation generates de novo neuronal potentiation and memory enhancement. *Cell* 174, 59–71.e14. doi: 10.1016/j.cell.2018.05.002

Agarwal, A., Wu, P.-H., Hughes, E. G., Fukaya, M., Tischfield, M. A., Langseth, A. J., et al. (2017). Transient opening of the mitochondrial permeability transition pore induces microdomain calcium transients in astrocyte processes. *Neuron* 93, 587–605.e7. doi: 10.1016/j.neuron.2016.12.034

Agulhon, C., Boyt, K. M., Xie, A. X., Friocourt, F., Roth, B. L., and McCarthy, K. D. (2013). Modulation of the autonomic nervous system and behaviour by acute glial cell G q protein-coupled receptor activation in vivo: Glial GPCR signalling in physiology and behaviour in vivo. *J. Physiol.* 591, 5599–5609. doi: 10.1113/jphysiol.2013.261289

Agulhon, C., Fiacco, T. A., and McCarthy, K. D. (2010). hippocampal short- and long-term plasticity are not modulated by astrocyte Ca2+ signaling. *Science* 327, 1250–1254. doi: 10.1126/science.1184821

Airan, R. D., Thompson, K. R., Fenno, L. E., Bernstein, H., and Deisseroth, K. (2009). Temporally precise in vivo control of intracellular signalling. *Nature* 458, 1025–1029. doi: 10.1038/nature07926

Araque, A., Carmignoto, G., Haydon, P. G., Oliet, S. H. R., Robitaille, R., and Volterra, A. (2014). Gliotransmitters travel in time and space. *Neuron* 81, 728–739. doi: 10.1016/j.neuron.2014.02.007

Arizono, M., Inavalli, V. V. G. K., Panatier, A., Pfeiffer, T., Angibaud, J., Levet, F., et al. (2020). Structural basis of astrocytic Ca2+ signals at tripartite synapses. *Nat. Commun.* 11:1906. doi: 10.1038/s41467-020-15648-4

Bailes, H. J., and Lucas, R. J. (2013). Human melanopsin forms a pigment maximally sensitive to blue light (λ max $\approx$ 479 nm) supporting activation of G q /11 and G i/o signalling cascades. *Proc. R. Soc. B Biol. Sci.* 280:20122987. doi: 10.1098/rspb.2012.2987

Bartok, A., Weaver, D., Golenár, T., Nichtova, Z., Katona, M., Bánsághi, S., et al. (2019). IP3 receptor isoforms differently regulate ER-mitochondrial contacts and local calcium transfer. *Nat. Commun.* 10:3726. doi: 10.1038/s41467-019-11646-3

Bergersen, L. H., Morland, C., Ormel, L., Rinholm, J. E., Larsson, M., Wold, J. F. H., et al. (2012). Immunogold detection of L-glutamate and D-serine in small synaptic-like microvesicles in adult hippocampal astrocytes. *Cereb. Cortex* 22, 1690–1697. doi: 10.1093/cercor/bhr254

Berridge, M. J., Lipp, P., and Bootman, M. D. (2000). The versatility and universality of calcium signalling. *Nat. Rev. Mol. Cell Biol.* 1, 11–21. doi: 10.1038/35036035

Bindocci, E., Savtchouk, I., Liaudet, N., Becker, D., Carriero, G., and Volterra, A. (2017). Three-dimensional Ca 2+ imaging advances understanding of astrocyte biology. *Science* 356:eaai8185. doi: 10.1126/science.aai8185

Bjørnstad, D. M., Åbjørsbråten, K. S., Hennestad, E., Cunen, C., Hermansen, G. H., Bojarskaite, L., et al. (2021). Begonia-A two-photon imaging analysis pipeline for astrocytic Ca2+ signals. *Front. Cell. Neurosci.* 15:681066. doi: 10.3389/fncel.2021.681066

Blondel, O., Takeda, J., Janssen, H., Seino, S., and Bell, G. I. (1993). Sequence and functional characterization of a third inositol trisphosphate receptor subtype, IP3R-3, expressed in pancreatic islets, kidney, gastrointestinal tract, and other tissues. *J. Biol. Chem.* 268, 11356–11363. doi: 10.1016/s0021-9258(18)82132-9

Boddum, K., Jensen, T. P., Magloire, V., Kristiansen, U., Rusakov, D. A., Pavlov, I., et al. (2016). Astrocytic GABA transporter activity modulates excitatory neurotransmission. *Nat. Commun.* 7:13572. doi: 10.1038/ncomms13572

Bonder, D. E., and McCarthy, K. D. (2014). Astrocytic Gq-GPCR-linked IP3R-dependent Ca^{2+} signaling does not mediate neurovascular coupling in mouse visual cortex *in vivo*. *J. Neurosci.* 34, 13139–13150. doi: 10.1523/JNEUROSCI.2591-14.2014

Bootman, M. D., Collins, T. J., Mackenzie, L., Roderick, H. L., Berridge, M. J., and Peppiatt, C. M. (2002). 2-Aminoethoxydiphenyl borate (2-APB) is a reliable blocker of store-operated Ca 2+ entry but an inconsistent inhibitor of InsP 3 -induced Ca 2+ release. *FASEB J.* 16, 1145–1150. doi: 10.1096/fj.02-0037rev

Bootman, M. D., Lipp, P., and Berridge, M. J. (2001). The organisation and functions of local Ca(2+) signals. *J. Cell Sci.* 114, 2213–2222. doi: 10.1242/jcs.114.12.2213

Cahoy, J. D., Emery, B., Kaushal, A., Foo, L. C., Zamanian, J. L., Christopherson, K. S., et al. (2008). A transcriptome database for astrocytes, neurons, and oligodendrocytes: a new resource for understanding brain development and function. *J. Neurosci.* 28, 264–278. doi: 10.1523/JNEUROSCI.4178-07.2008

Cao, X., Li, L.-P., Wang, Q., Wu, Q., Hu, H.-H., Zhang, M., et al. (2013). Astrocyte-derived ATP modulates depressive-like behaviors. *Nat. Med.* 19, 773–777. doi: 10.1038/nm.3162

Chai, H., Diaz-Castro, B., Shigetomi, E., Monte, E., Octeau, J. C., Yu, X., et al. (2017). Neural circuit-specialized astrocytes: transcriptomic, proteomic, morphological, and functional evidence. *Neuron* 95, 531–549.e9. doi: 10.1016/j.neuron.2017.06.029

Chen, N., Sugihara, H., Sharma, J., Perea, G., Petravicz, J., Le, C., et al. (2012). Nucleus basalis-enabled stimulus-specific plasticity in the visual cortex is mediated by astrocytes. *Proc. Natl. Acad. Sci. U.S.A.* 109, E2832–E2841. doi: 10.1073/pnas.1206557109

Clarke, L. E., Liddelow, S. A., Chakraborty, C., Münch, A. E., Heiman, M., and Barres, B. A. (2018). Normal aging induces A1-like astrocyte reactivity. *Proc. Natl. Acad. Sci. U.S.A.* 115, E1896–E1905. doi: 10.1073/pnas.1800165115

Dellis, O., Dedos, S. G., Tovey, S. C., Taufiq-Ur-Rahman, Dubel, S. J., and Taylor, C. W. (2006). Ca2+ entry through plasma membrane IP3 receptors. *Science* 313, 229–233. doi: 10.1126/science.1125203

Denizot, A., Arizono, M., Nägerl, U. V., Soula, H., and Berry, H. (2019). Simulation of calcium signaling in fine astrocytic processes: effect of spatial properties on spontaneous activity. *PLoS Comput. Biol.* 15:e1006795. doi: 10.1371/journal.pcbi.1006795

Dent, M. A., Raisman, G., and Lai, F. A. (1996). Expression of type 1 inositol 1,4,5-trisphosphate receptor during axogenesis and synaptic contact in the central and peripheral nervous system of developing rat. *Dev. Camb. Engl.* 122, 1029–1039. doi: 10.1242/dev.122.3.1029

Di Castro, M. A., Chuquet, J., Liaudet, N., Bhaukaurally, K., Santello, M., Bouvier, D., et al. (2011). Local Ca2+ detection and modulation of synaptic release by astrocytes. *Nat. Neurosci.* 14, 1276–1284. doi: 10.1038/nn.2929

Drawnel, F. M., Wachten, D., Molkentin, J. D., Maillet, M., Aronsen, J. M., Swift, F., et al. (2012). Mutual antagonism between IP3RII and miRNA-133a regulates calcium signals and cardiac hypertrophy. *J. Cell Biol.* 199, 783–798. doi: 10.1083/jcb.201111095

Echevarría, W., Leite, M. F., Guerra, M. T., Zipfel, W. R., and Nathanson, M. H. (2003). Regulation of calcium signals in the nucleus by a nucleoplasmic reticulum. *Nat. Cell Biol.* 5, 440–446. doi: 10.1038/ncb980

Fiacco, T. A., Agulhon, C., Taves, S. R., Petravicz, J., Casper, K. B., Dong, X., et al. (2007). Selective stimulation of astrocyte calcium in situ does not affect neuronal excitatory synaptic activity. *Neuron* 54, 611–626. doi: 10.1016/j.neuron.2007.04.032

Figueiredo, M., Lane, S., Stout, R. F., Liu, B., Parpura, V., Teschemacher, A. G., et al. (2014). Comparative analysis of optogenetic actuators in cultured astrocytes. *Cell Calcium* 56, 208–214. doi: 10.1016/j.ceca.2014.07.007

Finch, E., Turner, T., and Goldin, S. (1991). Calcium as a coagonist of inositol 1,4,5-trisphosphate-induced calcium release. *Science* 252, 443–446. doi: 10.1126/science.2017683

Foley, J., Blutstein, T., Lee, S., Erneux, C., Halassa, M. M., and Haydon, P. (2017). Astrocytic IP3/Ca2+ signaling modulates theta rhythm and REM sleep. *Front. Neural Circuits* 11:3. doi: 10.3389/fncir.2017.00003

Furuichi, T., Yoshikawa, S., Miyawaki, A., Wada, K., Maeda, N., and Mikoshiba, K. (1989). Primary structure and functional expression of the inositol 1,4,5-trisphosphate-binding protein P400. *Nature* 342, 32–38. doi: 10.1038/342032a0

Futatsugi, A. (2005). IP3 receptor types 2 and 3 mediate exocrine secretion underlying energy metabolism. *Science* 309, 2232–2234. doi: 10.1126/science.1114110

Gerasimenko, J. V., Lur, G., Ferdek, P., Sherwood, M. W., Ebisui, E., Tepikin, A. V., et al. (2011). Calmodulin protects against alcohol-induced pancreatic trypsinogen activation elicited via Ca2+ release through IP3 receptors. *Proc. Natl. Acad. Sci. U.S.A.* 108, 5873–5878. doi: 10.1073/pnas.1016534108

Gerasimenko, J. V., Lur, G., Sherwood, M. W., Ebisui, E., Tepikin, A. V., Mikoshiba, K., et al. (2009). Pancreatic protease activation by alcohol metabolite depends on Ca2+ release via acid store IP3 receptors. *Proc. Natl. Acad. Sci. U.S.A.* 106, 10758–10763. doi: 10.1073/pnas.0904818106

Gerasimenko, O. V., Gerasimenko, J. V., Belan, P. V., and Petersen, O. H. (1996). Inositol trisphosphate and cyclic ADP-ribose-mediated release of Ca2+ from single isolated pancreatic zymogen granules. *Cell* 84, 473–480. doi: 10.1016/s0092-8674(00)81292-1

Gerasimenko, O. V., Gerasimenko, J. V., Tepikin, A. V., and Petersen, O. H. (1995). ATP-dependent accumulation and inositol trisphosphate- or cyclic ADP-ribose-mediated release of Ca2+ from the nuclear envelope. *Cell* 80, 439–444. doi: 10.1016/0092-8674(95)90494-8

Golovina, V. A., and Blaustein, M. P. (1997). Spatially and functionally distinct Ca2+ stores in sarcoplasmic and endoplasmic reticulum. *Science* 275, 1643–1648. doi: 10.1126/science.275.5306.1643

Golovina, V. A., and Blaustein, M. P. (2000). Unloading and refilling of two classes of spatially resolved endoplasmic reticulum Ca(2+) stores in astrocytes. *Glia* 31, 15–28. doi: 10.1002/(sici)1098-1136(200007)31:1<15::aid-glia20>3.0.co;2-h

Gómez-Gonzalo, M., Martin-Fernandez, M., Martínez-Murillo, R., Mederos, S., Hernández-Vivanco, A., Jamison, S., et al. (2017). Neuron-astrocyte signaling

is preserved in the aging brain: neuron-astrocyte signaling in aging brain. *Glia* 65, 569–580. doi: 10.1002/glia.23112

Gómez-Gonzalo, M., Navarrete, M., Perea, G., Covelo, A., Martín-Fernández, M., Shigemoto, R., et al. (2015). Endocannabinoids induce lateral long-term potentiation of transmitter release by stimulation of gliotransmission. *Cereb. Cortex* 25, 3699–3712. doi: 10.1093/cercor/bhu231

Grosche, J., Matyash, V., Möller, T., Verkhratsky, A., Reichenbach, A., and Kettenmann, H. (1999). Microdomains for neuron-glia interaction: parallel fiber signaling to Bergmann glial cells. *Nat. Neurosci.* 2, 139–143. doi: 10.1038/5692

Hamada, K., and Mikoshiba, K. (2020). IP 3 receptor plasticity underlying diverse functions. *Annu. Rev. Physiol.* 82, 151–176. doi: 10.1146/annurev-physiol-021119-034433

Hamada, K., Miyatake, H., Terauchi, A., and Mikoshiba, K. (2017). IP 3 -mediated gating mechanism of the IP 3 receptor revealed by mutagenesis and X-ray crystallography. *Proc. Natl. Acad. Sci. U.S.A.* 114, 4661–4666. doi: 10.1073/pnas.1701420114

Hamada, T., Niki, T., Ziging, P., Sugiyama, T., Watanabe, S., Mikoshiba, K., et al. (1999). Differential expression patterns of inositol trisphosphate receptor types 1 and 3 in the rat suprachiasmatic nucleus. *Brain Res.* 838, 131–135. doi: 10.1016/s0006-8993(99)01719-9

Hattori, M., Suzuki, A. Z., Higo, T., Miyauchi, H., Michikawa, T., Nakamura, T., et al. (2004). Distinct roles of inositol 1,4,5-Trisphosphate receptor types 1 and 3 in Ca2+ signaling. *J. Biol. Chem.* 279, 11967–11975. doi: 10.1074/jbc.M311456200

Haustein, M. D., Kracun, S., Lu, X.-H., Shih, T., Jackson-Weaver, O., Tong, X., et al. (2014). Conditions and constraints for astrocyte calcium signaling in the hippocampal mossy fiber pathway. *Neuron* 82, 413–429. doi: 10.1016/j.neuron.2014.02.041

Hertle, D. N., and Yeckel, M. F. (2007). Distribution of inositol-1,4,5-trisphosphate receptor isotypes and ryanodine receptor isotypes during maturation of the rat hippocampus. *Neuroscience* 150, 625–638. doi: 10.1016/j.neuroscience.2007.09.058

Hisatsune, C., and Mikoshiba, K. (2017). IP 3 receptor mutations and brain diseases in human and rodents. *J. Neurochem.* 141, 790–807. doi: 10.1111/jnc.13991

Hisatsune, C., Yasumatsu, K., Takahashi-Iwanaga, H., Ogawa, N., Kuroda, Y., Yoshida, R., et al. (2007). Abnormal taste perception in mice lacking the Type 3 Inositol 1,4,5-trisphosphate receptor. *J. Biol. Chem.* 282, 37225–37231. doi: 10.1074/jbc.M705641200

Holbro, N., Grunditz, A., and Oertner, T. G. (2009). Differential distribution of endoplasmic reticulum controls metabotropic signaling and plasticity at hippocampal synapses. *Proc. Natl. Acad. Sci. U.S.A.* 106, 15055–15060. doi: 10.1073/pnas.0905110106

Holtzclaw, L. A., Pandhit, S., Bare, D. J., Mignery, G. A., and Russell, J. T. (2002). Astrocytes in adult rat brain express type 2 inositol 1,4,5-trisphosphate receptors. *Glia* 39, 69–84. doi: 10.1002/glia.10085

Hur, Y. S., Kim, K. D., Paek, S. H., and Yoo, S. H. (2010). Evidence for the existence of secretory granule (dense-core vesicle)-based inositol 1,4,5-trisphosphate-dependent Ca2+ signaling system in astrocytes. *PLoS One* 5:e11973. doi: 10.1371/journal.pone.0011973

Inaba, T., Hisatsune, C., Sasaki, Y., Ogawa, Y., Ebisui, E., Ogawa, N., et al. (2014). Mice lacking inositol 1,4,5-trisphosphate receptors exhibit dry eye. *PLoS One* 9:e99205. doi: 10.1371/journal.pone.0099205

Inoue, T., Kato, K., Kohda, K., and Mikoshiba, K. (1998). Type 1 inositol 1,4,5-trisphosphate receptor is required for induction of long-term depression in cerebellar purkinje neurons. *J. Neurosci.* 18, 5366–5373. doi: 10.1523/JNEUROSCI.18-14-05366.1998

Iwai, M., Tateishi, Y., Hattori, M., Mizutani, A., Nakamura, T., Futatsugi, A., et al. (2005). Molecular cloning of mouse type 2 and type 3 inositol 1,4,5-trisphosphate receptors and identification of a novel type 2 receptor splice variant. *J. Biol. Chem.* 280, 10305–10317. doi: 10.1074/jbc.M413824200

Iwai, Y., Ozawa, K., Yahagi, K., Mishima, T., Akther, S., Vo, C. T., et al. (2021). Transient astrocytic Gq signaling underlies remote memory enhancement. *Front. Neural. Circuits*, 15:658343 doi: 10.3389/fncir.2021.658343

Kanemaru, K., Okubo, Y., Hirose, K., and Iino, M. (2007). Regulation of neurite growth by spontaneous Ca2+ oscillations in astrocytes. *J. Neurosci.* 27, 8957–8966. doi: 10.1523/JNEUROSCI.2276-07.2007

Kanemaru, K., Sekiya, H., Xu, M., Satoh, K., Kitajima, N., Yoshida, K., et al. (2014). In vivo visualization of subtle, transient, and local activity of astrocytes using an ultrasensitive Ca2+ indicator. *Cell Rep.* 8, 311–318. doi: 10.1016/j.celrep.2014.05.056

Kirischuk, S., Kettenmann, H., and Verkhratsky, A. (1997). Na+/Ca2+ exchanger modulates kainate-triggered Ca2+ signaling in Bergmann glial cells in situ. *FASEB J. Off. Publ. Fed. Am. Soc. Exp. Biol.* 11, 566–572. doi: 10.1096/fasebj.11.7.9212080

Klar, J., Hisatsune, C., Baig, S. M., Tariq, M., Johansson, A. C. V., Rasool, M., et al. (2014). Abolished InsP3R2 function inhibits sweat secretion in both humans and mice. *J. Clin. Invest.* 124, 4773–4780. doi: 10.1172/JCI70720

Konieczny, V., Stefanakis, J. G., Sitsanidis, E. D., Ioannidou, N.-A. T., Papadopoulos, N. V., Fylaktakidou, K. C., et al. (2016). Synthesis of inositol phosphate-based competitive antagonists of inositol 1,4,5-trisphosphate receptors. *Org. Biomol. Chem.* 14, 2504–2514. doi: 10.1039/C5OB02623G

Konieczny, V., Tovey, S. C., Mataragka, S., Prole, D. L., and Taylor, C. W. (2017). Cyclic AMP recruits a discrete intracellular Ca 2+ store by unmasking hypersensitive IP 3 receptors. *Cell Rep.* 18, 711–722. doi: 10.1016/j.celrep.2016.12.058

Korogod, N., Petersen, C. C. H., and Knott, G. W. (2015). Ultrastructural analysis of adult mouse neocortex comparing aldehyde perfusion with cryo fixation. *eLife* 4:e05793. doi: 10.7554/eLife.05793

Kukkonen, J. P., Lund, P.-E., and Åkerman, K. E. O. (2001). 2-aminoethoxydiphenyl borate reveals heterogeneity in receptor-activated Ca2+discharge and store-operated Ca2+influx. *Cell Calcium* 30, 117–129. doi: 10.1054/ceca.2001.0219

Kuroda, Y., Hisatsune, C., Nakamura, T., Matsuo, K., and Mikoshiba, K. (2008). Osteoblasts induce Ca2+ oscillation-independent NFATc1 activation during osteoclastogenesis. *Proc. Natl. Acad. Sci. U.S.A.* 105, 8643–8648. doi: 10.1073/pnas.0800642105

Letellier, M., Park, Y. K., Chater, T. E., Chipman, P. H., Gautam, S. G., Oshima-Takago, T., et al. (2016). Astrocytes regulate heterogeneity of presynaptic strengths in hippocampal networks. *Proc. Natl. Acad. Sci. U.S.A.* 113, E2685–E2694. doi: 10.1073/pnas.1523717113

Lur, G., Sherwood, M. W., Ebisui, E., Haynes, L., Feske, S., Sutton, R., et al. (2011). InsP3 receptors and Orai channels in pancreatic acinar cells: co-localization and its consequences. *Biochem. J.* 436, 231–239. doi: 10.1042/BJ20110083

Mariotti, L., Losi, G., Sessolo, M., Marcon, I., and Carmignoto, G. (2016). The inhibitory neurotransmitter GABA evokes long-lasting Ca(2+) oscillations in cortical astrocytes. *Glia* 64, 363–373. doi: 10.1002/glia.22933

Martin-Fernandez, M., Jamison, S., Robin, L. M., Zhao, Z., Martin, E. D., Aguilar, J., et al. (2017). Synapse-specific astrocyte gating of amygdala-related behavior. *Nat. Neurosci.* 20, 1540–1548. doi: 10.1038/nn.4649

Maruyama, T., Kanaji, T., Nakade, S., Kanno, T., and Mikoshiba, K. (1997). 2APB, 2-aminoethoxydiphenyl borate, a membrane-penetrable modulator of Ins(1,4,5)P3-induced Ca2+ release. *J. Biochem. (Tokyo)* 122, 498–505. doi: 10.1093/oxfordjournals.jbchem.a021780

Masseck, O. A., Spoida, K., Dalkara, D., Maejima, T., Rubelowski, J. M., Wallhorn, L., et al. (2014). Vertebrate cone opsins enable sustained and highly sensitive rapid control of G i/o signaling in anxiety circuitry. *Neuron* 81, 1263–1273. doi: 10.1016/j.neuron.2014.01.041

Mataragka, S., and Taylor, C. W. (2018). All three IP 3 receptor subtypes generate Ca 2+ puffs, the universal building blocks of IP 3 -evoked Ca 2+ signals. *J. Cell Sci.* 131:jcs220848. doi: 10.1242/jcs.220848

Matsumoto, M., Nakagawa, T., Inoue, T., Nagata, E., Tanaka, K., Takano, H., et al. (1996). Ataxia and epileptic seizures in mice lacking type 1 inositol 1,4,5-trisphosphate receptor. *Nature* 379, 168–171. doi: 10.1038/379168a0

Mederos, S., Hernández-Vivanco, A., Ramírez-Franco, J., Martín-Fernández, M., Navarrete, M., Yang, A., et al. (2019). Melanopsin for precise optogenetic activation of astrocyte-neuron networks. *Glia* 67, 915–934. doi: 10.1002/glia.23580

Michelangeli, F., Mezna, M., Tovey, S., and Sayers, L. G. (1995). Pharmacological modulators of the inositol 1,4,5-trisphosphate receptor. *Neuropharmacology* 34, 1111–1122. doi: 10.1016/0028-3908(95)00053-9

Mignery, G. A., Newton, C. L., Archer, B. T., and Südhof, T. C. (1990). Structure and expression of the rat inositol 1,4,5-trisphosphate receptor. *J. Biol. Chem.* 265, 12679–12685. doi: 10.1016/s0021-9258(19)38397-8

Mignery, G. A., Südhof, T. C., Takei, K., and De Camilli, P. (1989). Putative receptor for inositol 1,4,5-trisphosphate similar to ryanodine receptor. *Nature* 342, 192–195. doi: 10.1038/342192a0

Miyakawa, T. (1999). Encoding of Ca2+ signals by differential expression of IP3 receptor subtypes. *EMBO J.* 18, 1303–1308. doi: 10.1093/emboj/18.5.1303

Miyazaki, S., Yuzaki, M., Nakada, K., Shirakawa, H., Nakanishi, S., Nakade, S., et al. (1992). Block of Ca2+ wave and Ca2+ oscillation by antibody to the inositol 1,4,5-trisphosphate receptor in fertilized hamster eggs. *Science* 257, 251–255. doi: 10.1126/science.1321497

Monai, H., Ohkura, M., Tanaka, M., Oe, Y., Konno, A., Hirai, H., et al. (2016). Calcium imaging reveals glial involvement in transcranial direct current stimulation-induced plasticity in mouse brain. *Nat. Commun.* 7:11100. doi: 10.1038/ncomms11100

Nakanishi, S., Maeda, N., and Mikoshiba, K. (1991). Immunohistochemical localization of an inositol 1,4,5-trisphosphate receptor, P400, in neural tissue: studies in developing and adult mouse brain. *J. Neurosci.* 11, 2075–2086. doi: 10.1523/JNEUROSCI.11-07-02075.1991

Nakayama, H., Bodi, I., Maillet, M., DeSantiago, J., Domeier, T. L., Mikoshiba, K., et al. (2010). The IP 3 receptor regulates cardiac hypertrophy in response to select stimuli. *Circ. Res.* 107, 659–666. doi: 10.1161/CIRCRESAHA.110.220038

Navarrete, M., Cuartero, M. I., Palenzuela, R., Draffin, J. E., Konomi, A., Serra, I., et al. (2019). Astrocytic p38α MAPK drives NMDA receptor-dependent long-term depression and modulates long-term memory. *Nat. Commun.* 10:2968. doi: 10.1038/s41467-019-10830-9

Navarrete, M., Perea, G., de Sevilla, D. F., Gómez-Gonzalo, M., Núñez, A., Martín, E. D., et al. (2012). Astrocytes mediate in vivo cholinergic-induced synaptic plasticity. *PLoS Biol.* 10:e1001259. doi: 10.1371/journal.pbio.1001259

Neher, E. (2008). Details of Ca2+ dynamics matter. *J. Physiol.* 586:2031. doi: 10.1113/jphysiol.2008.153080

Nishiyama, M., Hong, K., Mikoshiba, K., Poo, M. M., and Kato, K. (2000). Calcium stores regulate the polarity and input specificity of synaptic modification. *Nature* 408, 584–588. doi: 10.1038/35046067

Nizar, K., Uhlirova, H., Tian, P., Saisan, P. A., Cheng, Q., Reznichenko, L., et al. (2013). In vivo stimulus-induced vasodilation occurs without IP3 receptor activation and may precede astrocytic calcium increase. *J. Neurosci.* 33, 8411–8422. doi: 10.1523/JNEUROSCI.3285-12.2013

Nucifora, F. C., Sharp, A. H., Milgram, S. L., and Ross, C. A. (1996). Inositol 1,4,5-trisphosphate receptors in endocrine cells: localization and association in hetero- and homotetramers. *Mol. Biol. Cell* 7, 949–960. doi: 10.1091/mbc.7.6.949

Oh, E., Maejima, T., Liu, C., Deneris, E., and Herlitze, S. (2010). Substitution of 5-HT1A Receptor Signaling by a Light-activated G Protein-coupled Receptor. *J. Biol. Chem.* 285, 30825–30836. doi: 10.1074/jbc.M110.147298

Okubo, Y., Iino, M., and Hirose, K. (2020). Store-operated Ca2+ entry-dependent Ca2+ refilling in the endoplasmic reticulum in astrocytes. *Biochem. Biophys. Res. Commun.* 522, 1003–1008. doi: 10.1016/j.bbrc.2019.12.006

Okubo, Y., Kanemaru, K., Suzuki, J., Kobayashi, K., Hirose, K., and Iino, M. (2019). Inositol 1,4,5-trisphosphate receptor type 2-independent Ca 2+ release from the endoplasmic reticulum in astrocytes. *Glia* 67, 113–124. doi: 10.1002/glia.23531

Padmashri, R., Suresh, A., Boska, M. D., and Dunaevsky, A. (2015). Motor-Skill learning is dependent on astrocytic activity. *Neural Plast.* 2015:938023. doi: 10.1155/2015/938023

Panatier, A., Arizono, M., and Nägerl, U. V. (2014). Dissecting tripartite synapses with STED microscopy. *Philos. Trans. R. Soc. B Biol. Sci.* 369:20130597. doi: 10.1098/rstb.2013.0597

Panatier, A., Vallée, J., Haber, M., Murai, K. K., Lacaille, J.-C., and Robitaille, R. (2011). Astrocytes are endogenous regulators of basal transmission at central synapses. *Cell* 146, 785–798. doi: 10.1016/j.cell.2011.07.022

Panda, S. (2005). Illumination of the Melanopsin Signaling Pathway. *Science* 307, 600–604. doi: 10.1126/science.1105121

Pantazaka, E., and Taylor, C. W. (2011). Differential distribution, clustering, and lateral diffusion of subtypes of the inositol 1,4,5-trisphosphate receptor. *J. Biol. Chem.* 286, 23378–23387. doi: 10.1074/jbc.M111.236372

Park, K., and Lee, S. J. (2020). Deciphering the star codings: astrocyte manipulation alters mouse behavior. *Exp. Mol. Med.* 52, 1028–1038. doi: 10.1038/s12276-020-0468-z

Patrushev, I., Gavrilov, N., Turlapov, V., and Semyanov, A. (2013). Subcellular location of astrocytic calcium stores favors extrasynaptic neuron-astrocyte communication. *Cell Calcium* 54, 343–349. doi: 10.1016/j.ceca.2013.08.003

Perea, G., Gómez, R., Mederos, S., Covelo, A., Ballesteros, J. J., Schlosser, L., et al. (2016). Activity-dependent switch of GABAergic inhibition into glutamatergic excitation in astrocyte-neuron networks. *eLife* 5:e20362. doi: 10.7554/eLife.20362

Perez-Alvarez, A., Navarrete, M., Covelo, A., Martin, E. D., and Araque, A. (2014). Structural and functional plasticity of astrocyte processes and dendritic spine interactions. *J. Neurosci.* 34, 12738–12744. doi: 10.1523/JNEUROSCI.2401-14.2014

Petersen, O. H., Gerasimenko, O. V., Gerasimenko, J. V., Mogami, H., and Tepikin, A. V. (1998). The calcium store in the nuclear envelope. *Cell Calcium* 23, 87–90. doi: 10.1016/s0143-4160(98)90106-3

Petravicz, J., Boyt, K. M., and McCarthy, K. D. (2014). Astrocyte IP3R2-dependent Ca2+ signaling is not a major modulator of neuronal pathways governing behavior. *Front. Behav. Neurosci.* 8:384. doi: 10.3389/fnbeh.2014.00384

Petravicz, J., Fiacco, T. A., and McCarthy, K. D. (2008). Loss of IP3 receptor-dependent Ca2+ increases in hippocampal astrocytes does not affect baseline CA1 pyramidal neuron synaptic activity. *J. Neurosci.* 28, 4967–4973. doi: 10.1523/JNEUROSCI.5572-07.2008

Pinton, P., Pozzan, T., and Rizzuto, R. (1998). The Golgi apparatus is an inositol 1,4,5-trisphosphate-sensitive Ca2+ store, with functional properties distinct from those of the endoplasmic reticulum. *EMBO J.* 17, 5298–5308. doi: 10.1093/emboj/17.18.5298

Romanos, J., Thieren, L., and Santello, M. (2019). Diving into new depths of astrocyte signaling. *Nat. Neurosci.* 22, 1749–1750. doi: 10.1038/s41593-019-0513-1

Rose, C. R., Ziemens, D., and Verkhratsky, A. (2020). On the special role of NCX in astrocytes: translating Na+-transients into intracellular Ca2+ signals. *Cell Calcium* 86:102154. doi: 10.1016/j.ceca.2019.102154

Rungta, R. L., Bernier, L.-P., Dissing-Olesen, L., Groten, C. J., LeDue, J. M., Ko, R., et al. (2016). Ca 2+ transients in astrocyte fine processes occur via Ca 2+ influx in the adult mouse hippocampus: Ca 2+ Transients in Astrocyte Fine Processes. *Glia* 64, 2093–2103. doi: 10.1002/glia.23042

Rusakov, D. A. (2015). Disentangling calcium-driven astrocyte physiology. *Nat. Rev. Neurosci.* 16, 226–233. doi: 10.1038/nrn3878

Saleem, H., Tovey, S. C., Molinski, T. F., and Taylor, C. W. (2014). Interactions of antagonists with subtypes of inositol 1,4,5-trisphosphate (IP 3) receptor. *Br. J. Pharmacol.* 171, 3298–3312. doi: 10.1111/bph.12685

Saleem, H., Tovey, S. C., Rahman, T., Riley, A. M., Potter, B. V. L., and Taylor, C. W. (2013a). Stimulation of inositol 1,4,5-trisphosphate (IP3) receptor subtypes by analogues of IP3. *PLoS One* 8:e54877. doi: 10.1371/journal.pone.0054877

Saleem, H., Tovey, S. C., Riley, A. M., Potter, B. V. L., and Taylor, C. W. (2013b). Stimulation of inositol 1,4,5-trisphosphate (IP3) receptor subtypes by adenophostin A and its analogues. *PLoS One* 8:e58027. doi: 10.1371/journal.pone.0058027

Sato-Miyaoka, M., Hisatsune, C., Ebisui, E., Ogawa, N., Takahashi-Iwanaga, H., and Mikoshiba, K. (2012). Regulation of hair shedding by the Type 3 IP3 receptor. *J. Invest. Dermatol.* 132, 2137–2147. doi: 10.1038/jid.2012.141

Savtchenko, L. P., Bard, L., Jensen, T. P., Reynolds, J. P., Kraev, I., Medvedev, N., et al. (2018). Disentangling astroglial physiology with a realistic cell model in silico. *Nat. Commun.* 9:3554. doi: 10.1038/s41467-018-05896-w

Sharp, A. H., Nucifora, F. C., Blondel, O., Sheppard, C. A., Zhang, C., Snyder, S. H., et al. (1999). Differential cellular expression of isoforms of inositol 1,4,5-triphosphate receptors in neurons and glia in brain. *J. Comp. Neurol.* 406, 207–220. doi: 10.1002/(sici)1096-9861(19990405)406:2<207::aid-cne6>3.0.co;2-7

Sherwood, M. W., Arizono, M., Hisatsune, C., Bannai, H., Ebisui, E., Sherwood, J. L., et al. (2017). Astrocytic IP 3 Rs: contribution to Ca 2+ signalling and hippocampal LTP: astrocytic IP 3 Rs: Ca 2+ Signalling and LTP. *Glia* 65, 502–513. doi: 10.1002/glia.23107

Shigetomi, E., Bushong, E. A., Haustein, M. D., Tong, X., Jackson-Weaver, O., Kracun, S., et al. (2013a). Imaging calcium microdomains within entire astrocyte territories and endfeet with GCaMPs expressed using adeno-associated viruses. *J. Gen. Physiol.* 141, 633–647. doi: 10.1085/jgp.201210949

Shigetomi, E., Jackson-Weaver, O., Huckstepp, R. T., O'Dell, T. J., and Khakh, B. S. (2013b). TRPA1 channels are regulators of astrocyte basal calcium levels and long-term potentiation via constitutive D-serine release. *J. Neurosci.* 33, 10143–10153. doi: 10.1523/JNEUROSCI.5779-12.2013

Shigetomi, E., Tong, X., Kwan, K. Y., Corey, D. P., and Khakh, B. S. (2012). TRPA1 channels regulate astrocyte resting calcium and inhibitory synapse efficacy through GAT-3. *Nat. Neurosci.* 15, 70–80. doi: 10.1038/nn.3000

Shiratori-Hayashi, M., Yamaguchi, C., Eguchi, K., Shiraishi, Y., Kohno, K., Mikoshiba, K., et al. (2020). Astrocytic STAT3 activation and chronic itch require IP3R1/TRPC-dependent Ca2+ signals in mice. *J. Allergy Clin. Immunol.* 147, 1341–1353. doi: 10.1016/j.jaci.2020.06.039

Spacek, J., and Harris, K. M. (1998). Three-dimensional organization of cell adhesion junctions at synapses and dendritic spines in area CA1 of the rat hippocampus. *J. Comp. Neurol.* 393, 58–68. doi: 10.1002/(sici)1096-9861(19980330)393:1<58::aid-cne6>3.0.co;2-p

Spoida, K., Masseck, O. A., Deneris, E. S., and Herlitze, S. (2014). Gq/5-HT2c receptor signals activate a local GABAergic inhibitory feedback circuit to modulate serotonergic firing and anxiety in mice. *Proc. Natl. Acad. Sci. U.S.A.* 111, 6479–6484. doi: 10.1073/pnas.1321576111

Srinivasan, R., Huang, B. S., Venugopal, S., Johnston, A. D., Chai, H., Zeng, H., et al. (2015). Ca2+ signaling in astrocytes from Ip3r2-/- mice in brain slices and during startle responses in vivo. *Nat. Neurosci.* 18, 708–717. doi: 10.1038/nn.4001

Srinivasan, R., Lu, T.-Y., Chai, H., Xu, J., Huang, B. S., Golshani, P., et al. (2016). New transgenic mouse lines for selectively targeting astrocytes and studying calcium signals in astrocyte processes in situ and in vivo. *Neuron* 92, 1181–1195. doi: 10.1016/j.neuron.2016.11.030

Südhof, T. C., Newton, C. L., Archer, B. T., Ushkaryov, Y. A., and Mignery, G. A. (1991). Structure of a novel InsP3 receptor. *EMBO J.* 10, 3199–3206. doi: 10.1002/j.1460-2075.1991.tb04882.x

Sugawara, T., Hisatsune, C., Le, T. D., Hashikawa, T., Hirono, M., Hattori, M., et al. (2013). Type 1 inositol trisphosphate receptor regulates cerebellar circuits by maintaining the spine morphology of purkinje cells in adult mice. *J. Neurosci.* 33, 12186–12196. doi: 10.1523/JNEUROSCI.0545-13.2013

Sugiyama, T., Furuya, A., Monkawa, T., Yamamoto-Hino, M., Satoh, S., Ohmori, K., et al. (1994). Monoclonal antibodies distinctively recognizing the subtypes of inositol 1,4,5-trisphosphate receptor: application to the studies on inflammatory cells. *FEBS Lett.* 354, 149–154. doi: 10.1016/0014-5793(94)01099-4

Sul, J.-Y., Orosz, G., Givens, R. S., and Haydon, P. G. (2004). Astrocytic connectivity in the hippocampus. *Neuron Glia Biol.* 1, 3–11. doi: 10.1017/S1740925X04000031

Takano, T., Wallace, J. T., Baldwin, K. T., Purkey, A. M., Uezu, A., Courtland, J. L., et al. (2020). Chemico-genetic discovery of astrocytic control of inhibition in vivo. *Nature* 588, 296–302. doi: 10.1038/s41586-020-2926-0

Takata, N., Mishima, T., Hisatsune, C., Nagai, T., Ebisui, E., Mikoshiba, K., et al. (2011). Astrocyte Calcium signaling transforms cholinergic modulation to cortical plasticity in vivo. *J. Neurosci.* 31, 18155–18165. doi: 10.1523/JNEUROSCI.5289-11.2011

Takata, N., Nagai, T., Ozawa, K., Oe, Y., Mikoshiba, K., and Hirase, H. (2013). Cerebral blood flow modulation by Basal forebrain or whisker stimulation can occur independently of large cytosolic Ca2+ signaling in astrocytes. *PLoS One* 8:e66525. doi: 10.1371/journal.pone.0066525

Tamamushi, S., Nakamura, T., Inoue, T., Ebisui, E., Sugiura, K., Bannai, H., et al. (2012). Type 2 inositol 1,4,5-trisphosphate receptor is predominantly involved in agonist-induced Ca2+ signaling in Bergmann glia. *Neurosci. Res.* 74, 32–41. doi: 10.1016/j.neures.2012.06.005

Tamura, A., Yamada, N., Yaguchi, Y., Machida, Y., Mori, I., and Osanai, M. (2014). Both neurons and astrocytes exhibited tetrodotoxin-resistant metabotropic glutamate receptor-dependent spontaneous Slow Ca2+ oscillations in striatum. *PLoS One* 9:e85351. doi: 10.1371/journal.pone.0085351

Tanaka, M., Shih, P.-Y., Gomi, H., Yoshida, T., Nakai, J., Ando, R., et al. (2013). Astrocytic Ca2+ signals are required for the functional integrity of tripartite synapses. *Mol. Brain* 6:6. doi: 10.1186/1756-6606-6-6

Tanaka, M., Wang, X., Mikoshiba, K., Hirase, H., and Shinohara, Y. (2017). Rearing-environment-dependent hippocampal local field potential differences in wild-type and inositol trisphosphate receptor type 2 knockout mice. *J. Physiol.* 595, 6557–6568. doi: 10.1113/JP274573

Tang, F., Lane, S., Korsak, A., Paton, J. F. R., Gourine, A. V., Kasparov, S., et al. (2014). Lactate-mediated glia-neuronal signalling in the mammalian brain. *Nat. Commun.* 5:284. doi: 10.1038/ncomms4284

Tang, W., Szokol, K., Jensen, V., Enger, R., Trivedi, C. A., Hvalby, O., et al. (2015). Stimulation-evoked Ca2+ signals in astrocytic processes at hippocampal CA3-CA1 synapses of adult mice are modulated by glutamate and ATP. *J. Neurosci.* 35, 3016–3021. doi: 10.1523/JNEUROSCI.3319-14.2015

Thillaiappan, N. B., Chavda, A. P., Tovey, S. C., Prole, D. L., and Taylor, C. W. (2017). Ca2+ signals initiate at immobile IP3 receptors adjacent to ER-plasma membrane junctions. *Nat. Commun.* 8:1505. doi: 10.1038/s41467-017-01644-8

Tichy, A.-M., Gerrard, E. J., Sexton, P. M., and Janovjak, H. (2019). Light-activated chimeric GPCRs: limitations and opportunities. *Curr. Opin. Struct. Biol.* 57, 196–203. doi: 10.1016/j.sbi.2019.05.006

Uchida, K., Aramaki, M., Nakazawa, M., Yamagishi, C., Makino, S., Fukuda, K., et al. (2010). Gene knock-outs of inositol 1,4,5-trisphosphate receptors types 1 and 2 result in perturbation of cardiogenesis. *PLoS One* 5:e12500. doi: 10.1371/journal.pone.0012500

Uchida, K., Nakazawa, M., Yamagishi, C., Mikoshiba, K., and Yamagishi, H. (2016). Type 1 and 3 inositol trisphosphate receptors are required for extra-embryonic vascular development. *Dev. Biol.* 418, 89–97. doi: 10.1016/j.ydbio.2016.08.007

Vervloessem, T., Yule, D. I., Bultynck, G., and Parys, J. B. (2015). The type 2 inositol 1,4,5-trisphosphate receptor, emerging functions for an intriguing Ca2+-release channel. *Biochim. Biophys. Acta BBA Mol. Cell Res.* 1853, 1992–2005. doi: 10.1016/j.bbamcr.2014.12.006

Wang, Q., Kong, Y., Wu, D.-Y., Liu, J.-H., Jie, W., You, Q.-L., et al. (2021). Impaired calcium signaling in astrocytes modulates autism spectrum disorder-like behaviors in mice. *Nat. Commun.* 12:3321. doi: 10.1038/s41467-021-23843-0

Wang, Y., DelRosso, N. V., Vaidyanathan, T. V., Cahill, M. K., Reitman, M. E., Pittolo, S., et al. (2019). Accurate quantification of astrocyte and neurotransmitter fluorescence dynamics for single-cell and population-level physiology. *Nat. Neurosci.* 22, 1936–1944. doi: 10.1038/s41593-019-0492-2

Wojcikiewicz, R. J., and He, Y. (1995). Type I, II and III inositol 1,4,5-trisphosphate receptor co-immunoprecipitation as evidence for the existence of heterotetrameric receptor complexes. *Biochem. Biophys. Res. Commun.* 213, 334–341. doi: 10.1006/bbrc.1995.2134

Xie, Y., Wang, T., Sun, G. Y., and Ding, S. (2010). Specific disruption of astrocytic Ca2+ signaling pathway in vivo by adeno-associated viral transduction. *Neuroscience* 170, 992–1003. doi: 10.1016/j.neuroscience.2010.08.034

Yamada, N., Makino, Y., Clark, R. A., Pearson, D. W., Mattei, M. G., Guénet, J. L., et al. (1994). Human inositol 1,4,5-trisphosphate type-1 receptor, InsP3R1: structure, function, regulation of expression and chromosomal localization. *Biochem. J.* 302, 781–790. doi: 10.1042/bj3020781

Yamamoto-Hino, M., Miyawaki, A., Kawano, H., Sugiyama, T., Furuichi, T., Hasegawa, M., et al. (1995). Immunohistochemical study of inositol 1,4,5-trisphosphate receptor type 3 in rat central nervous system. *NeuroReport* 6, 273–276. doi: 10.1097/00001756-199501000-00012

Yamamoto-Hino, M., Sugiyama, T., Hikichi, K., Mattei, M. G., Hasegawa, K., Sekine, S., et al. (1994). Cloning and characterization of human type 2 and type 3 inositol 1,4,5-trisphosphate receptors. *Recept. Channels* 2, 9–22.

Yang, L., Qi, Y., and Yang, Y. (2015). Astrocytes control food intake by inhibiting AGRP neuron activity via adenosine A1 receptors. *Cell Rep.* 11, 798–807. doi: 10.1016/j.celrep.2015.04.002

Yoo, S. H. (2010). Secretory granules in inositol 1,4,5-trisphosphate-dependent Ca2+ signaling in the cytoplasm of neuroendocrine cells. *FASEB J. Off. Publ. Fed. Am. Soc. Exp. Biol.* 24, 653–664. doi: 10.1096/fj.09-132456

Young, S. Z., Platel, J., Nielsen, J. V., Jensen, N., and Bordey, A. (2010). GABAA increases calcium in subventricular zone astrocyte-like cells through L- and T-type voltage-gated calcium channels. *Front. Cell. Neurosci.* 4:8. doi: 10.3389/fncel.2010.00008

Yu, X., Taylor, A. M. W., Nagai, J., Golshani, P., Evans, C. J., Coppola, G., et al. (2018). Reducing astrocyte calcium signaling in vivo alters striatal microcircuits and causes repetitive behavior. *Neuron* 99, 1170–1187.e9. doi: 10.1016/j.neuron.2018.08.015

Zhang, S., Fritz, N., Ibarra, C., and Uhlén, P. (2011). Inositol 1,4,5-trisphosphate receptor subtype-specific regulation of calcium oscillations. *Neurochem. Res.* 36, 1175–1185. doi: 10.1007/s11064-011-0457-7

Zhang, Y., Chen, K., Sloan, S. A., Bennett, M. L., Scholze, A. R., O'Keeffe, S., et al. (2014). An RNA-sequencing transcriptome and splicing database of glia, neurons, and vascular cells of the cerebral cortex. *J. Neurosci.* 34, 11929–11947. doi: 10.1523/JNEUROSCI.1860-14.2014

Zhang, Y., Sloan, S. A., Clarke, L. E., Caneda, C., Plaza, C. A., Blumenthal, P. D., et al. (2016). Purification and characterization of progenitor and mature human astrocytes reveals transcriptional and functional differences with mouse. *Neuron* 89, 37–53. doi: 10.1016/j.neuron.2015.11.013

Conflict of Interest: The authors declare that the research was conducted in the absence of any commercial or financial relationships that could be construed as a potential conflict of interest.

frontiers in Cellular Neuroscience

HYPOTHESIS AND THEORY
published: 03 September 2021
doi: 10.3389/fncel.2021.693095

Review and Hypothesis: A Potential Common Link Between Glial Cells, Calcium Changes, Modulation of Synaptic Transmission, Spreading Depression, Migraine, and Epilepsy—H^+

Robert Paul Malchow[1,2], Boriana K. Tchernookova[1], Ji-in Vivien Choi[1,3], Peter J. S. Smith[4,5], Richard H. Kramer[6] and Matthew A. Kreitzer[7]*

[1]Department of Biological Sciences, University of Illinois at Chicago, Chicago, IL, United States, [2]Department of Ophthalmology and Visual Sciences, University of Illinois at Chicago, Chicago, IL, United States, [3]Stritch School of Medicine, Loyola University, Maywood, IL, United States, [4]Institute for Life Sciences, University of Southampton, Highfield Campus, Southampton, United Kingdom, [5]Bell Center, Marine Biological Laboratory, Woods Hole, MA, United States, [6]Department of Molecular and Cell Biology, University of California, Berkeley, Berkeley, CA, United States, [7]Department of Biology, Indiana Wesleyan University, Marion, IN, United States

OPEN ACCESS

Edited by:
Wannan Tang,
University of Oslo, Norway

Reviewed by:
Ana Lucia Marques Ventura,
Fluminense Federal University, Brazil
Erik B. Malarkey,
Vertex Pharmaceuticals (United States), United States

***Correspondence:**
Robert Paul Malchow
paulmalc@uic.edu

Specialty section:
This article was submitted to Non-Neuronal Cells, a section of the journal Frontiers in Cellular Neuroscience

Received: *09 April 2021*
Accepted: *25 June 2021*
Published: *03 September 2021*

Citation:
Malchow RP, Tchernookova BK, Choi JV, Smith PJS, Kramer RH and Kreitzer MA (2021) Review and Hypothesis: A Potential Common Link Between Glial Cells, Calcium Changes, Modulation of Synaptic Transmission, Spreading Depression, Migraine, and Epilepsy—H^+. Front. Cell. Neurosci. 15:693095. doi: 10.3389/fncel.2021.693095

There is significant evidence to support the notion that glial cells can modulate the strength of synaptic connections between nerve cells, and it has further been suggested that alterations in intracellular calcium are likely to play a key role in this process. However, the molecular mechanism(s) by which glial cells modulate neuronal signaling remains contentiously debated. Recent experiments have suggested that alterations in extracellular H^+ efflux initiated by extracellular ATP may play a key role in the modulation of synaptic strength by radial glial cells in the retina and astrocytes throughout the brain. ATP-elicited alterations in H^+ flux from radial glial cells were first detected from Müller cells enzymatically dissociated from the retina of tiger salamander using self-referencing H^+-selective microelectrodes. The ATP-elicited alteration in H^+ efflux was further found to be highly evolutionarily conserved, extending to Müller cells isolated from species as diverse as lamprey, skate, rat, mouse, monkey and human. More recently, self-referencing H^+-selective electrodes have been used to detect ATP-elicited alterations in H^+ efflux around individual mammalian astrocytes from the cortex and hippocampus. Tied to increases in intracellular calcium, these ATP-induced extracellular acidifications are well-positioned to be key mediators of synaptic modulation. In this article, we examine the evidence supporting H^+ as a key modulator of neurotransmission, review data showing that extracellular ATP elicits an increase in H^+ efflux from glial cells, and describe the potential signal transduction pathways involved in glial cell—mediated H^+ efflux. We then examine the potential role that extracellular H^+ released by glia might play in regulating synaptic transmission within the vertebrate retina, and then expand the focus to discuss potential roles in spreading depression, migraine, epilepsy, and alterations in

brain rhythms, and suggest that alterations in extracellular H^+ may be a unifying feature linking these disparate phenomena.

Keywords: glia, Müller cell, pH, H^+, ATP, epilepsy, migraine, spreading depression

INTRODUCTION

An ever-increasing number of studies suggest that cells christened by Rudolf Virchow as "glue"—glial cells—are more than the "passive" or "filler" elements originally envisaged years ago. In addition to providing nutrients and scaffolding critical for neuronal growth, proper development and continued function (see Barres et al., 2015; von Bernhardi, 2016), glia are now recognized as active participants in the "tripartite synapse," modulating and regulating signal transmission between neurons and among themselves (Halassa et al., 2007, 2009; Papouin et al., 2017). It has long been suspected that elevations in glial intracellular calcium play a role in the modulation of synaptic transfer at synapses, but the nature and molecular mechanism(s) of such regulation is currently an area of contentious debate (see Khakh and McCarthy, 2015; Bazargani and Attwell, 2016; Guerra-Gomes et al., 2017; Fiacco and McCarthy, 2018; Savtchouk and Volterra, 2018; Ashhad and Narayanan, 2019; Semyanov et al., 2020; Kofuji and Araque, 2021). In addition, a number of "gliotransmitters" have been identified as potential modulators of neuronal activity, among them glutamate, ATP, serine, and GABA (Petrelli and Bezzi, 2016). The degree to which these contribute to the modulation of neurotransmitter release by neurons and the mechanisms regulating the release of these gliotransmitters remains controversial (Sahlender et al., 2014; Durkee and Araque, 2019).

A potent but commonly overlooked regulator of synaptic transmission is simple H^+—that is, small changes in levels of extracellular acidity around sites of neurotransmitter release. Recent studies have shown that activation of glial cells inducing increased intracellular calcium also promotes the release of H^+ from glia, and it has been proposed that this may play a key role in regulating synaptic transmission (Tchernookova et al., 2018, 2021; Choi et al., 2021). In this review and hypothesis article, we first review studies demonstrating the potency of extracellular H^+ as a modulator of synaptic transmission and then describe techniques used and studies conducted to show calcium-dependent extrusion of H^+ from glial cells activated by extracellular ATP. The potential implications of such glial-mediated H^+ extrusion in the regulation of normal nervous system function as well as in such maladies as epilepsy and migraines are then discussed, followed by a perspective on challenges facing further advances in the field.

H^+—A POTENT MODULATOR OF SYNAPTIC TRANSMISSION

Alterations in extracellular H^+ can affect many channels and other proteins within the nervous system with consequent significant effects on its function. In this article, we restrict our examination to the effects of altered levels of extracellular H^+ on mechanisms underlying synaptic transmission.

Just how potent small alterations in extracellular H^+ are in affecting neurotransmitter release is perhaps best illustrated in **Figure 1**, a modification of a figure first published by Kleinschmidt (1991). This figure shows electrical responses from a neuron in the retina of a salamander made using a high resistance intracellular pipette. The cell recorded is a horizontal cell that receives direct input from photoreceptors and whose primary response to a flash of light is a hyperpolarization, shown as a downward deflection in the figure. In the dark, vertebrate photoreceptors sit depolarized and are thought to continuously release glutamate onto postsynaptic neurons (for review, see Wu, 1994; Barnes, 1995). Glutamate binds to ionotropic channels on horizontal cells, allowing sodium and calcium influx, and horizontal cells thus sit relatively depolarized in the dark. Absorption of light induces a hyperpolarization of photoreceptors, which closes voltage-gated calcium channels present on photoreceptor axon terminals. The reduction in calcium influx decreases the calcium-dependent release of glutamate from photoreceptors. The glutamate-sensitive channels on horizontal cells close when extracellular glutamate is not present, inducing a hyperpolarization of the horizontal cell. The figure shows the multiple downward hyperpolarizations

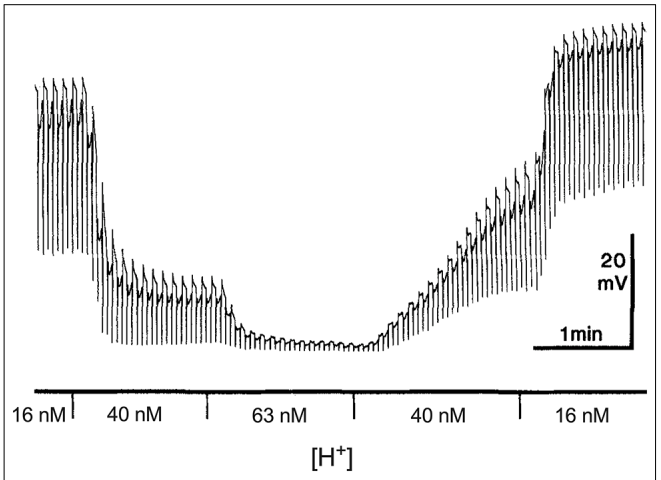

FIGURE 1 | Dependence of the dark resting potential and light-evoked responses of a retinal horizontal cell of the salamander to alterations in extracellular H^+. Modified from Kleinschmidt (1991). An intracellular sharp electrode was used to monitor membrane potential in a single horizontal cell impaled in an isolated retinal preparation superfused with the pH of the solution buffered with 20 mM HEPES. Alternating red (600 nm) and green (555 nm) 100 ms full field flashes, separated by 3 s and adjusted to give equal cone responses were used to stimulate the cell. The author notes that the responses to the different lights can be distinguished by the small rod-driven tails found only in responses to green stimuli.

in a horizontal cell resulting from repetitive bright light stimuli.

The first responses shown in the figure were obtained with the isolated retina superfused with a Ringer's solution containing 16 nM H^+ using the pH buffer HEPES. In this condition, the cell sits at a depolarized level and light-induced hyperpolarizations are large. The solution was then switched to one containing 40 nM H^+, and there are two clear effects of this modest increase in extracellular H^+ concentration. First, a large hyperpolarization of the cell is observed, and second, a significant decrease occurs in hyperpolarizations induced by light. A third change to a solution containing 63 nM H^+ results in a further hyperpolarization of the cell and the virtual elimination of hyperpolarizations induced by light. The effects of altered levels of H^+ on the baseline level of polarization and hyperpolarizations induced by light were fully and rapidly reversible, as the second portion of the recording makes clear.

To emphasize how sensitive both the resting membrane potential and responses to light are to levels of extracellular H^+, the concentration of H^+ in the solutions used—16 nM, 40 nM and 63 nM—have been converted from the equivalent levels of pH listed in the original figure (pH_o values of 7.8, 7.4 and 7.2, respectively). But it is not only the low concentration of H^+ relative to that of other neurotransmitters/neuromodulators that is worth noting; Kleinschmidt also emphasized how extraordinarily steep the relation between altered levels of extracellular H^+ and resting membrane potential is, estimating a Hill coefficient of about 4 with an inflection point of 23 nM (pH = 7.64). The sensitivity of horizontal cells to direct application of glutamate was unchanged by these alterations in extracellular H^+, implicating a presynaptic localization for the effect, and light-induced hyperpolarizations of photoreceptors were only weakly altered, leading to a conclusion that the dramatic effects of altered H^+ resulted from inhibition in the release of neurotransmitter from photoreceptors to second order cells. The steep dependence of horizontal cell membrane potential and light-induced responses on alterations of extracellular H^+ has been noted by others; for example, in recordings from horizontal cells of goldfish, increasing the H^+ concentration of a solution superfusing the retina from 25 nM to 40 nM, which reduced the value of extracellular pH by 0.1 unit within the retina as measured by H^+-selective microelectrodes, reduced cone horizontal cell light responses by about 50% (Harsanyi and Mangel, 1993; Dmitriev and Mangel, 2000; Mangel, 2001).

Barnes et al. (1993) provided data that the effect of altered levels of H^+ occurred largely at voltage-gated calcium channels of photoreceptors. The exponential dependence on extracellular H^+ of both L-type calcium channel currents and light-induced responses of second order neurons was characterized, and the authors noted that changing the extracellular H^+ concentration to 115 nM, close to neutral (pH = 6.94), was as effective in blocking calcium influx through voltage-gated calcium channels and responses from second order neurons as was the addition of 100 μM cadmium, which blocked virtually all synaptic transmission. Increased levels of extracellular H^+ reduced the maximal current through calcium channels and shifted the activation voltage needed to open the channels to significantly more positive transmembrane potentials. In examining the molecular basis of the block of L-type calcium channels by H^+, Chen et al. (1996) demonstrated that protons exerted their action on calcium channels by binding to four glutamate residues located within the channel pore. They further noted that because of the high degree of conservation of the glutamate residues in the pore region of all voltage-gated calcium channels, the pronounced sensitivity to extracellular H^+ was likely to be a universal characteristic of this family of membrane proteins. Confirmation of this prediction came from work by Doering and McRory (2007) examining the effects of extracellular H^+ on nine different subtypes of voltage gated calcium channels, observing that in all cases, acidification of the extracellular solution resulted in a significant depolarizing shift in the activation curve and reduction in peak current amplitudes. Thus, increases in H^+ around the physiological range are likely to reduce the influx of calcium into neuronal terminals and decrease significantly calcium-dependent neurotransmitter release at virtually all chemical synapses within the nervous system.

Alterations in extracellular H^+ also have potent effects at several other steps in the process of synaptic transmission. For example, although the AMPA subtype of glutamate receptors present on horizontal cells examined by Kleinschmidt and Barnes were not particularly sensitive to physiologically relevant changes in extracellular H^+, NMDA glutamate receptors are highly sensitive to small extracellular acidifications around the physiological range (Traynelis and Cull-Candy, 1990; Traynelis et al., 1995, 2010; Jalali-Yazdi et al., 2018). These receptors, believed to be critically important in learning and memory and expressed widely in neurons throughout the nervous system, have an IC_{50} for inhibition by H^+ of about 50 nM (pH of 7.3), a value close to normal levels of extracellular interstitial pH of many organisms. Indeed, the size of postsynaptic NMDA receptor currents of hippocampal pyramidal neurons was boosted by approximately one third through extracellular alkalinization elicited by activation of the same cell's PMCA calcium pump, which extrudes one calcium while transporting two protons into the cell during each cycle of transport (Chen and Chesler, 2015).

Additionally, the reuptake of neurotransmitters from the extracellular space into cells adjacent to release sites significantly influences the overall impact of neurotransmitters released during synaptic transmission. Removal of neurotransmitters from the extracellular space surrounding the release site often requires co-transport with extracellular H^+. For example, hippocampal astrocytes possess transport proteins for glutamate that ferry three sodium ions and one proton along with glutamate into the cell while also exporting one potassium ion (Nicholls and Attwell, 1990; Owe et al., 2006; Vandenberg and Ryan, 2013; Rose et al., 2017). In an examination of flux coupling of the EAAT3 glutamate transporter, Zerangue and Kavanaugh (1996) reported an affinity constant for H^+ of 26 nM during glutamate transport, corresponding to an extracellular pH of 7.58. This value implies that small

changes of extracellular H^+ around normal physiological levels could significantly impact the transport of glutamate and thus alter the extent of effects induced by neurotransmitters on post-synaptic cells. The removal of glutamate by uptake into astrocytes leads to an extracellular alkalinization, and if extracellular levels of H^+ remained depressed, the remaining glutamate could potentially linger longer and exert more pronounced effects.

Thus, several critical components of the process of synaptic transmission—the initial calcium-dependent release of neurotransmitters, its effects on certain post-synaptic receptors, and removal of neurotransmitters from the synaptic cleft—are all susceptible to small changes in extracellular H^+ concentrations around the physiological range.

H^+ EFFLUX FROM GLIAL CELLS ELICITED BY ATP

Recent studies using self-referencing H^+-selective electrodes have demonstrated clear rises in extracellular H^+ adjacent to radial glial cells isolated from the vertebrate retina and from astrocytes cultured from mice and rat hippocampus and cortex upon activation by extracellular ATP. In this section, we first describe the method used to detect H^+ fluxes from individual cells, then show the nature of responses and finally describe what is known about the signal transduction process underlying the efflux of H^+ from glia.

Attempts to definitively ascribe changes in extracellular levels of H^+ to a particular cell type such as glia in the nervous system, with its extraordinarily complex web of processes, cell types, and panoply of H^+-coupled transport proteins and channels, are exceptionally difficult. To ensure that measured changes in extracellular H^+ come specifically from glial cells, therefore, initial characterizations are best carried out in cell culture preparations where responses can be obtained from cells unambiguously identified as glia and which sit isolated from neurons or other cell types present in the culture. While this approach ensures that measured signals emanate solely from cells identified as glia, the disruption of the normal extracellular architecture presents its own new technical hurdle: protons released by cells no longer can accumulate in the very small extracellular spaces and microdomains that allow small alterations in H^+ activity to result in large overall changes in concentration in a small volume. A major challenge in measuring changes in extracellular H^+ induced by activation of single isolated glial cells is that protons released by glia under such conditions diffuse quickly into the vast ocean of fluid surrounding the cells, making it quite difficult to measure changes in extracellular H^+. Self-referencing H^+-selective microelectrodes provide the needed spatial and temporal sensitivity and stability over time to make such measurements. A detailed description of the construction, use, advantages, and limitations of self-referencing electrodes is beyond the scope of this article; detailed reviews can be found in Smith (1995), Smith et al. (1999), Smith and Trimarchi (2001), Messerli et al. (2006), Smith et al. (2007), and Messerli and Smith (2010). Here, we provide a brief overview of the technique, highlighting how it works, why it greatly increases the useful sensitivity of H^+-selective microelectrodes, and describe concerns and limitations to be kept in mind when using the technique.

In experiments using self-referencing electrodes to measure H^+ fluxes from isolated glial cells, silanized glass pipettes with dimensions similar to patch pipettes are filled with an ∼30 μm column of a liquid cocktail possessing high selectivity for H^+ ions. The tips of the pipettes are then positioned 1–2 μm from the membrane of a cell. Ion-selective potentiometric electrodes report a voltage at the tip that varies as H^+ ion activity changes as defined by the Nernst equation—a 10-fold change in concentration (or more strictly, activity) of H^+ induces a 58 mV change at standard room temperatures. A major challenge encountered with the use of liquid cocktail-based ion-selective electrodes is random electrical slow-frequency baseline drift of the signal with time, drift more than large enough to swamp H^+-generated signals expected from single isolated cells. The problem is schematically illustrated in **Figure 2**, along with the solution afforded by using the electrodes in a self-referencing configuration. A key facet of the electrical drift in the output signal is that while it is random, it is relatively slow, and is present regardless of whether the electrode is adjacent to a cell or a location far away. If the sensor is translated quickly enough—from a point adjacent to a cell to a second point away from the cell (in our experiments, 30 μm), the voltage contributed by drift will be essentially the same, or common, to the two points. External membrane-associated voltage gradients are too small to be detected by the H^+-selective electrode, a very different situation from operating ion-selective electrodes in an intracellular environment. The possible but unlikely impact of surface charge influencing measurements is discussed in detail in Smith et al. (2010). An example of the actual size and time-dependence of electrical drift associated with ion-selective electrodes is shown in **Figures 2C,D** (note that this signal was generated by creating a steep artificial gradient from a source pipette far larger than would be expected when recording responses from a single cell, which generate signals in the microvolt range). Subtracting the output signal at the location distant from the cell (the far pole) from the voltage measured close to the cell (near pole) then minimizes the signal contributed by the slow electrical drift or common interferents. The subtraction results in a differential voltage that reflects the difference in H^+ ion activity measured between the two points—that is, close to the cell compared to the value obtained 30 μm away, with a greatly reduced contribution associated with electrical drift. This simple process enhances the detection limits of liquid cocktail-based ion-selective electrodes by more than 1,000× (Somieski and Nagel, 2001), and enables the stable measurement of H^+ fluxes from individual isolated cells (Smith and Trimarchi, 2001). It is worth noting that attempts to use two separate electrodes at the two positions will not work in this framework, since the electrical drift present in the two electrodes will vary independently and so cannot be subtracted out meaningfully to yield a stable baseline.

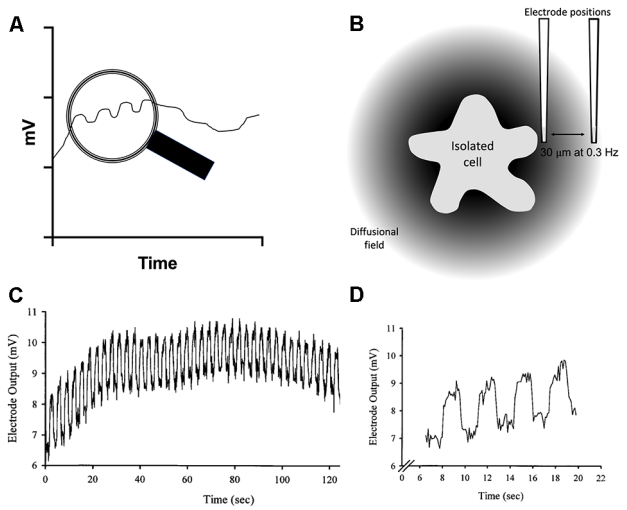

FIGURE 2 | Schematic diagram and sample data illustrating the challenge imposed in using liquid cocktail-based ion-selective microelectrodes to measure changes in extracellular ion levels adjacent to cells, and the solution provided by using the electrode in a self-referencing fashion. **(A)** Drawing showing the electrical drift typical of such ion-selective electrodes as a function of time. The voltage output signal can wander several millivolts over several minutes. The view within the magnifying glass shows the small voltages one would expect to obtain by monitoring the electrode output at two positions, one close to the source of the ion, and the other a defined distance away from the cell. **(B)** Illustration of the diffusional field of an ion emanating from a cell and its decline with distance, along with the positioning of a self-referencing ion-selective electrode at the near pole, close to the source of ion efflux from the cell, and again at a position 30 μm away from the cell. **(C)** Experimental demonstration of electrical voltage drift from an ion-selective electrode; from Smith et al. (1999). The trace shows the output from a calcium-selective microelectrode while recording the response at both the near- and far-pole position from a source pipette filled with calcium. Note that the electrical drift is in the millivolt range; in biological preparations, differential voltages induced by physiological stimuli would be expected to be in the microvolt range. **(D)** An expanded section from **(C)** to more clearly illustrate the signal and the drift. Note how the electrical drift is common to both measuring positions in the electrical output signal.

The enhanced sensitivity provided by self-referencing comes with its own challenges and limitations. First, the method is relatively slow. Electrodes are typically translated in an approximate square wave between the poles with an interval of 0.3 Hz, with data collected at each position for around 1 s. The electrode must be moved quickly enough so that the contribution from electrical drift is roughly the same at both locations, but not so quickly as to significantly stir the solution and thus potentially disrupt the differential H^+ gradient at the heart of the measurement. With these operating parameters and dimensions, and taking into account the diffusion constant of H^+, mixing is not seen as a problem (Messerli et al., 2006; Smith et al., 2010).

Second, the differential flux signal depends critically on the distance of the electrode from the source, with the signal from a point source declining exponentially due to diffusion. The electrode must be placed close enough to an H^+ source to measure a differential signal, but not so close as to touch the membrane of the cell, which would result in the silanized glass and liquid cocktail disrupting the plasma membrane. Thus, the absolute magnitude of the differential signal will vary significantly with the distance of the electrode away from the cell and must be kept constant.

Third, as the electrode tip surface area is exposed to the external medium, pharmacological agents added to the medium could affect the performance of the H^+-selective liquid cocktail. It is essential to conduct control experiments to ensure that the addition of a drug at an experimental concentration, does not alter the selectivity or sensitivity of the electrodes. Another technical matter when applying pharmacological modulators is the instability of the baseline during application, which tends to rule out continuous superfusion. Modulators are either applied by bulk replacement of the medium or as aliquots at a distance from the cell.

Fourth, perhaps the most significant modulator of recorded H^+ flux is the pH buffer in the solution. Messerli et al. (2006) deal with this in-depth and discuss how the proportion of protonated vs. unprotonated buffer can be taken into account. Frequently, however, results are presented in a qualitative manner without attempting conversion to a flux value.

Finally, self-referencing H^+-selective electrodes report an ion flux—that is, an alteration in H^+-activity as it changes over a specified period of time and distance, typically given in units of $\mu mol\ cm^{-2}s^{-1}$. As noted above, an exact determination of the flux value is dependent on distance, response times, buffering capacity, the source strength, and *in vivo*, on the intracellular volume and tortuosity (Syková and Nicholson, 2008; Smith et al., 2010). Given these considerations, we have opted to present results simply as the difference in the voltage reported between the two poles of translation, i.e., $\Delta\ \mu V$.

The application of self-referencing H^+-selective electrodes to detect H^+ fluxes from isolated retinal glial cells is shown in **Figure 3**. To obtain isolated glia, retinae from tiger salamanders were dissociated using a commonly used and well-characterized papain-based enzymatic dissociation protocol. The radial glia referred to as Müller cells, possess a distinct morphology that allows ready and precise identification, with cells possessing an apical tuft and a thick stalk connecting cell body and basal end foot regions, along with fine processes extruding from the plasma membrane (see Newman, 1985). **Figure 3A** shows a self-referencing H^+ sensor placed adjacent to the junction of the apical tuft and cell body region of the cell, a location likely to correspond with what would be the outer plexiform layer (OPL) of the intact retina. **Figure 3B** shows a typical recording obtained from a single Müller cell using an H^+-selective microelectrode (Tchernookova et al., 2018). A small initial standing H^+ flux is first observed, indicating that the reading obtained adjacent to the cell is more acidic than the point 30 μm away, revealing a small basal efflux of H^+. A bolus of ATP resulting in a final concentration of 100 μM induced a large increase in H^+ flux from the cell. At the point marked with an asterisk, the electrode was moved to a control location 200 μm above the cell. At this location, the concentration of H^+ should be roughly identical at the two electrode positions, and consequently, the differential voltage should be close to zero; this is an important control incorporated

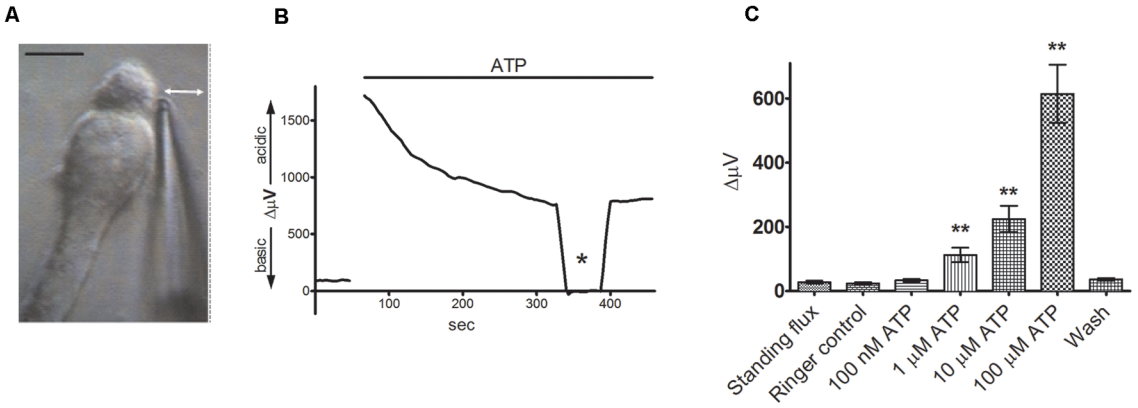

FIGURE 3 | Extracellular ATP induces a significant increase in extracellular H^+ flux from isolated Müller cells. From Tchernookova et al. (2018). **(A)** An example of an isolated Müller cell with a self-referencing H^+-selective microelectrode positioned next to the apical end of the cell. Scale bar: 20 μm; double-headed arrow depicts the direction of electrode movement as it alternately records the potential established by protons adjacent to the cell and 30 μm away. **(B)** Response from a single isolated Müller cell to 100 μM ATP. The top bar represents the duration of drug application. Asterisk represents a background control reading taken 200 μm above the cell. **(C)** Mean data from eight trials in response to various extracellular ATP concentrations: error bars represent standard errors of the mean. The double asterisks indicate statistical *P*-values of 0.01 or less.

in virtually every experiment to ensure the self-referencing system is operating correctly. Returning the self-referencing H^+-selective electrode to its position adjacent to the cell results in a restoration of the H^+ flux differential signal. **Figure 3C** shows the dose-response relation of H^+ flux to changes in extracellular ATP, and it is notable that concentrations of extracellular ATP as low as 1 μM initiate significant H^+ efflux. At high doses of extracellular ATP, the size of the H^+ flux signal was on the same order of magnitude as that detected from cells and tissues known to be potent proton pumpers, such as in the vas deferens, where changes in extracellular H^+ concentration play an essential role in the activation of sperm cells (Breton et al., 1998). The extracellular H^+ fluxes induced by ATP from Müller cells were mimicked by the P2Y1 agonist MRS 2365 and were significantly reduced by the P2 receptor blockers suramin and PPADS, suggesting activation of P2Y receptors. ADP, UTP, and the non-hydrolyzable analog ATPγs were also potent stimulators of extracellular H^+ fluxes, but 100 μM adenosine had no effect.

The alterations in H^+ flux induced by extracellular ATP did not appear to result from sodium-coupled bicarbonate transporters. The experiments described above were carried out in solutions in which the primary extracellular H^+ buffer was 1 mM HEPES, with no bicarbonate added. ATP-elicited increases in H^+ flux from Müller cells also persisted unchanged when solutions were bubbled for 15 min before use with 100% oxygen, to remove trace amounts of CO_2 from the atmosphere that could potentially be used by very high affinity bicarbonate transporters (Theparambil et al., 2014; Tchernookova et al., 2021).

Significant increases in extracellular H^+ flux induced by extracellular ATP were also detected when the normal complex web of cellular connections within the retina was preserved in retinal slice preparations. **Figure 4** shows results with a self-referencing H^+-selective electrode placed over the outer plexiform (synaptic) layer of a tiger salamander retinal slice and then alternately translated to a position 30 μm above the retinal slice to obtain a differential signal (**Figure 4A**). The application of 100 μM extracellular ATP gave a robust increase in H^+ flux that was substantially reduced by the P2 receptor inhibitors PPADS and suramin (**Figures 4B,C**). Similar increases in extracellular H^+ flux induced by ATP were observed when the H^+-selective microelectrode was placed above the inner plexiform (synaptic) layer of the retina and were also reduced by application of PPADS and suramin. Recordings from isolated Müller cells made adjacent to the side of the basal end-foot of cells revealed extracellular ATP-induced increases in H^+ flux as well, consistent with increased H^+ flux detected at the inner synaptic layer of the retina.

ATP-elicited increases in H^+ flux from retinal radial glial cells appear to be mediated by activation of a G-protein cascade that induces an increase in calcium release from intracellular stores. Inhibition of the G-protein-coupled PLC linked to metabotropic ATP receptors by U-73122 reduced both the amplitude of ATP-elicited H^+ efflux from isolated Müller cells as well as increases in intracellular calcium so commonly elicited in many glial cells by application of ATP. Both ATP-elicited increases in H^+ efflux from Müller cells and concomitant increases in intracellular calcium were also reduced by the IP3 receptor inhibitor 2-APB. Finally, as shown in **Figure 5**, thapsigargin, an agent which depletes intracellular calcium by preventing reuptake into intracellular stores, potently reduced both the ATP-elicited increase in intracellular calcium (**Figure 5A**) as well as the ATP-initiated increase in H^+ flux (**Figure 5B**). These data demonstrate that ATP-mediated increases in H^+ flux from Müller cells are critically dependent upon increases in intracellular calcium released from intracellular stores.

Additional experiments demonstrated that about 75% of the ATP-elicited increase in H^+ flux likely resulted from the extrusion of protons *via* Na^+/H^+ exchange (Tchernookova et al., 2021). The complete removal of extracellular sodium

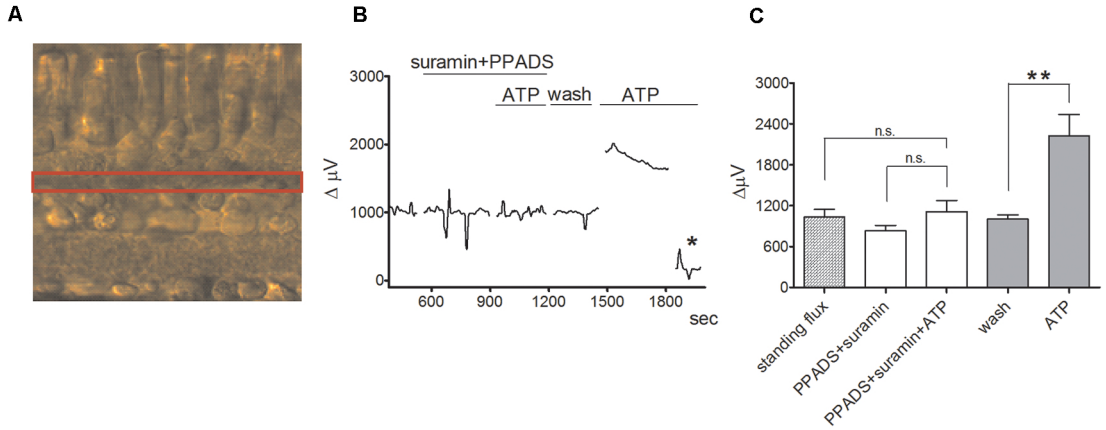

FIGURE 4 | ATP induces an increase in extracellular H^+ flux at the outer plexiform layer (OPL) in retinal slices that is markedly reduced by PPADS and suramin. From Tchernookova et al. (2018). **(A)** Retinal slice preparation obtained using a 200 μm section of a tiger salamander retina. The red box highlights the outer plexiform (synaptic) layer (OPL). **(B)** A representative trace showing the response observed to the application of 100 μM ATP from an individual self-referencing recording from a retinal slice with the microelectrode positioned just above the OPL; asterisk indicates a background control reading taken 600 μm above the retinal slice. **(C)** Mean data from eight slices. ATP induced a significantly smaller increase in extracellular H^+ flux in the background of suramin and PPADS than it did in plain Ringer's solution. The double asterisks indicate statistical *P*-values of 0.01 or less. n.s., not significantly different.

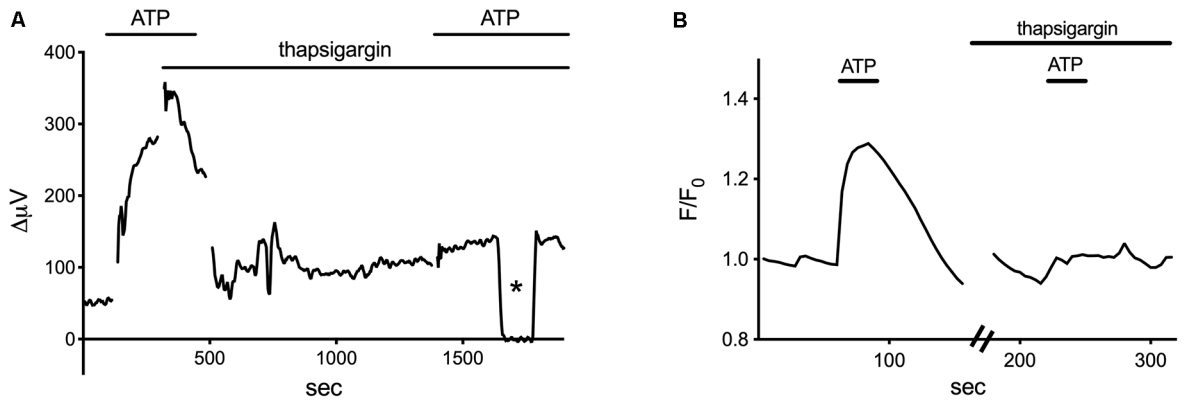

FIGURE 5 | Thapsigargin, an inhibitor of calcium reuptake into intracellular stores, blocks both the ATP-elicited increase in H^+ and the ATP-elicited increase in calcium from isolated Müller cells. Modified from Tchernookova et al. (2018). **(A)** A representative self-referencing recording from an isolated Müller cell demonstrating an initial increase in H^+ flux induced by 1 μM ATP; after soaking the cell for about 15 min with 1 μM thapsigargin, the ATP-induced alteration in H^+ flux was largely blocked. Asterisk indicates a control reading taken 200 μm from the cell. **(B)** Changes in intracellular calcium induced by ATP as reported by alterations in fluorescence of the calcium indicator Oregon Green. 1 μM ATP produced a robust increase in intracellular calcium. Subsequent ATP-induced alterations in Oregon Green fluorescence were blocked by soaking the cell in 1 μM thapsigargin for 15 min.

coupled with replacement by choline reduced ATP-elicited increases in H^+ efflux by 75%, and ATP-initiated H^+ efflux was also significantly reduced by pharmacological agents known to inhibit Na^+/H^+ exchange, including amiloride, cariporide, and zoniporide. Additional unpublished data implicate activation of calmodulin and PKC in this process, examples of which are provided in **Figure 6**. The calmodulin inhibitors W-7 and chlorpromazine (CLP) at 100 μM and trifluoperazine (TFP) at 50 μM were all potent inhibitors of the ATP-initiated increase in H^+ flux from tiger salamander Müller cells. The response from one cell to the application of ATP in the presence of a calmodulin inhibitor is shown in **Figure 6A**; in eight cells tested, the total H^+ flux from isolated tiger salamander Müller cells by 10 μM ATP was 36 ± 12 μV in 100 μM CLP compared to a value of 239 ± 46 μV obtained from six separate cells in response to 10 μM ATP without CLP present. The block of H^+ flux by these calmodulin inhibitors occurred without any noticeable effect on ATP-induced rises of intracellular calcium reported by the calcium indicator Oregon Green. The increase in H^+ efflux from isolated tiger salamander Müller cells in response to 10 μM ATP was also significantly reduced by 10 μM of the PKC inhibitor chelerythrine, as shown in **Figure 6B**, which charts the H^+ flux signal from a single cell first to 10 μM ATP, then with ATP in the presence of chelerythrine,

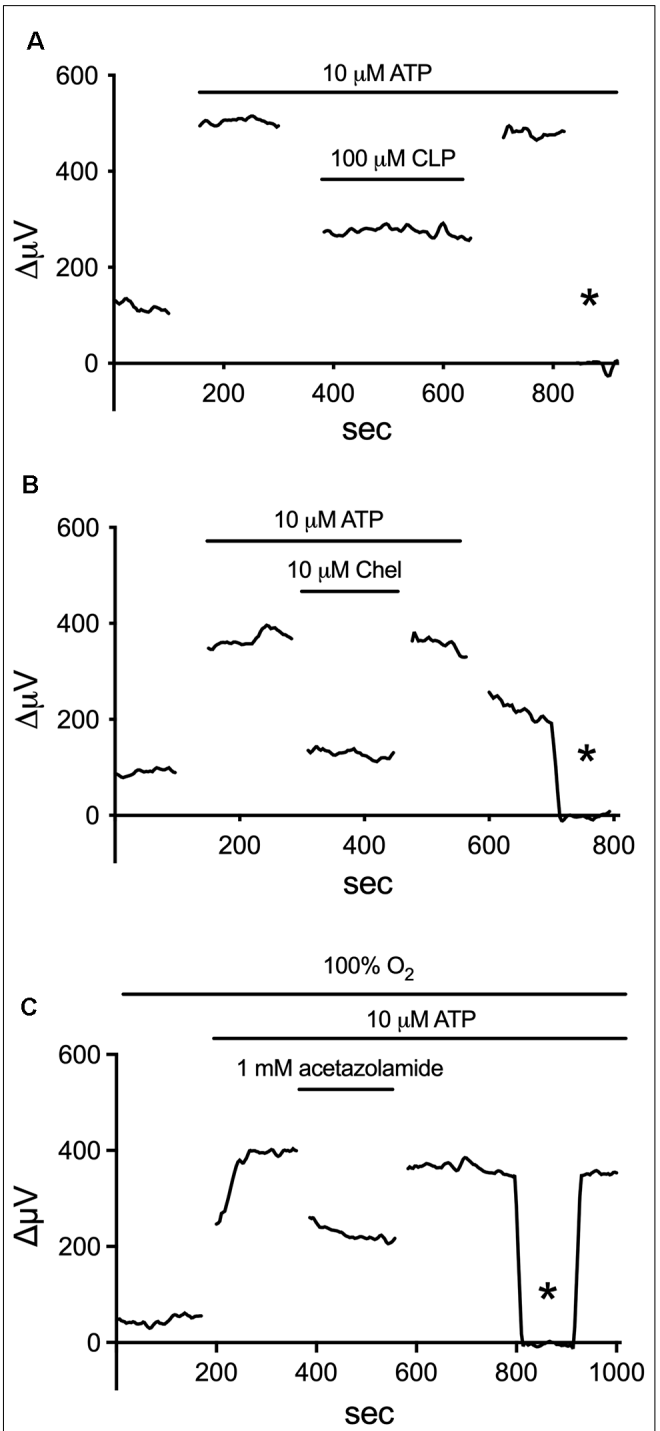

FIGURE 6 | Inhibitors of calmodulin, PKC, and carbonic anhydrase (CA) reduce the ATP-elicited increase in H^+ flux from retinal Müller cells isolated from the retina of the tiger salamander. **(A)** 100 μM of the calmodulin inhibitor CLP potently inhibited the rise in H^+ flux from an isolated Müller cell induced by 10 μM ATP. **(B)** Reduction of ATP-elicited increase in H^+ flux from a single tiger salamander Müller cell induced by 10 μM ATP upon the addition of 10 μM of the PKC inhibitor chelerythrine. **(C)** Inhibition of H^+ efflux from a single Müller cell by 1 mM of the carbonic anhydrase inhibitor acetazolamide. Asterisk represents a background control reading taken 200 μm above the cell.

and then with chelerythrine removed but ATP still present. A similar reduction of H^+ efflux in response to ATP was observed in seven cells. The block of the ATP-elicited increase in H^+ by chelerythrine also occurred without significant alteration in ATP-elicited increases in intracellular calcium as measured by Oregon Green fluorescence, suggesting a direct effect of chelerythrine on PKC. These data suggest that one important consequence of increased intracellular calcium initiated by ATP in retinal radial glia may be to activate calmodulin and PKC, which then promote an increase in Na^+/H^+ exchange activity.

The H^+ flux initiated by extracellular ATP from Müller cells is also significantly reduced by compounds that inhibit the activity of carbonic anhydrase (CA). **Figure 6C** shows the effect of one such compound, acetazolamide, on ATP-initiated H^+ efflux. Previous studies have shown that methazolamide and acetazolamide significantly inhibit the activity of intracellular CA of isolated Müller cells (Newman, 1994). CAs play a key role in the production of H^+ from the interaction of CO_2 and water, increasing the speed of the chemical reaction by as much as a million times from its basal rate (Maren, 1988). Many glial cells, including the Müller cells of the retina, have high concentrations of CA intracellularly (see Cammer and Tansey, 1988; Nagelhus, 2005; Theparambil et al., 2017, 2020). The ability of membrane-permeant CA inhibitors to reduce H^+ efflux initiated by extracellular ATP suggests that the rise in intracellular calcium induced by extracellular ATP facilitates the conversion of water and CO_2 to H^+ and HCO_3. We hypothesize that the rise of intracellular calcium activates mitochondria and enhances metabolic activity within the cell (for review, see Boyman et al., 2020), leading to the production of CO_2, effectively providing an increase in the substrate for the reaction facilitated by CA. This would result in increases in intracellular levels of H^+, which would then be exported from the cell largely *via* Na^+/H^+ exchange. A schematic diagram illustrating our current thoughts regarding the signal transduction process leading to the increase in H^+ efflux initiated by extracellular ATP is shown in **Figure 7**.

Increases in extracellular H^+ efflux in response to small increases in extracellular ATP appear to be a common and highly conserved response detectable in Müller cells isolated from a wide range of other organisms. In addition to Müller cells of the tiger salamander, self-referencing H^+-selective recordings from Müller cells isolated from such distantly related animals as lamprey, skate, catfish, rat, two species of monkey, as well as from human donor retinal tissue, all showed significant increases in H^+ efflux by 100 μM ATP (Tchernookova et al., 2018). The high degree of conservation of ATP-elicited increase in H^+ efflux across such disparate species speaks of a highly important biological function conserved across organisms.

Extracellular ATP also elicits increases in extracellular H^+ fluxes from astrocytes cultured from mouse hippocampus and rat cortex (Choi et al., 2021). Cultured cells were identified as astrocytes by high levels of the intermediate filament protein glial fibrillary acidic protein (GFAP). **Figure 8A** shows the high level of GFAP staining typically observed in such cultures using an antibody specific to GFAP, and **Figure 8B** shows the placement

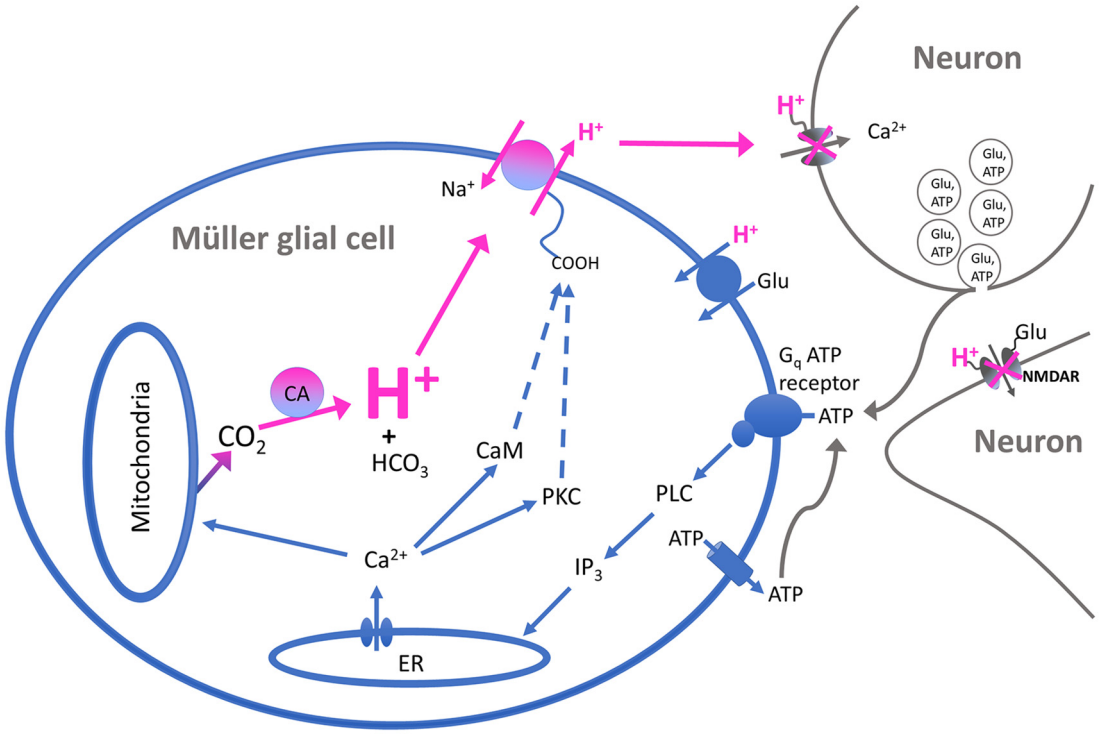

FIGURE 7 | Schematic of the proposed signal transduction pathway underlying ATP-elicited H^+ efflux from Müller cells of the tiger salamander. Extracellular ATP binds to a G-protein-coupled P2 receptor (labeled Gq ATP receptor) and activates the enzyme phospholipase C (PLC). This results in the production of inositol triphosphate (IP3) which promotes the release of calcium from intracellular stores such as the endoplasmic reticulum (ER). The rise in intracellular calcium leads to activation of calmodulin and protein kinase C (PKC), which in turn stimulate the activity of Na^+/H^+ exchange and the extrusion of H^+ into the extracellular space. The rise in intracellular calcium is also postulated to stimulate mitochondria to produce a cloud of CO_2 within the cell, serving as the substrate for the production of H^+ and HCO_3 by CA within the cell and providing continued high levels of intracellular H^+ for export by transporters in the plasma membrane. The exported H^+ ions act to bind to and inhibit voltage-gated calcium channels regulating neurotransmitter release from presynaptic neurons, as well as binding to and inhibiting NMDA-glutamate receptors on post-synaptic cells. The increased concentration of extracellular H^+ is also postulated to facilitate the removal of neurotransmitters such as glutamate by H^+-dependent transport proteins present on neurons and glia. The source of the extracellular ATP as shown in the model is proposed to come from co-release with neurotransmitters upon fusion of synaptic vesicles with the plasma membranes of presynaptic neurons; extracellular ATP can also arise from release by the glia themselves.

of an H^+-selective electrode adjacent to a cell identified as an astrocyte. The ATP-elicited increase in H^+ efflux from cultured astrocytes appeared to be independent of bicarbonate transport activity since ATP increased H^+ flux regardless of whether the primary extracellular pH buffer was 26 mM bicarbonate or 1 mM HEPES, and persisted when atmospheric levels of CO_2 were replaced by oxygen. Like retinal Müller cells, 100 μM adenosine did not alter extracellular H^+ flux from baseline levels, and ATP-mediated increases in H^+ flux were inhibited by the P2 antagonists suramin and PPADS, again suggesting activation of ATP receptors. Also like Müller cells, the increased level of H^+ flux initiated by extracellular ATP appeared to depend critically on increases in intracellular calcium released from intracellular stores. Consistent with many earlier findings, extracellular ATP induced an intracellular rise in calcium in cultured astrocytes, and ATP-induced rises in both calcium and H^+ efflux were significantly attenuated when calcium re-loading into internal stores was inhibited by thapsigargin. **Figure 8C** shows an ATP-elicited increase in H^+ efflux from one astrocyte first in ordinary Ringer's solution and then from the same cell after application of 1 μM thapsigargin. The response in thapsigargin was virtually abolished, while the response to a second application of 100 μM ATP in plain Ringer's solution without thapsigargin present elicited an increase in H^+ flux that was statistically indistinguishable from an initial application of ATP in control cells.

One interesting difference between ATP-elicited increases in H^+ flux from astrocytes compared to Müller cells was the relative lack of dependence of increases in H^+ flux from astrocytes on extracellular sodium. Replacement of extracellular sodium with choline did not significantly reduce the ATP-induced increases in H^+ flux from cultured astrocytes, and increases in H^+ flux were not significantly affected by the addition of EIPA, a blocker of Na^+/H^+ transport activity. One attractive alternative mechanism is the activity of monocarboxylate transporters, thought to play an important role in enabling astrocytes to provide lactate to neurons for their energy needs and which require co-transport of lactate with H^+ (Pierre and Pellerin, 2005; Jha and Morrison, 2018, 2020). The release of lactate would likely be greatest when neuronal activity is highest, coinciding with the highest levels

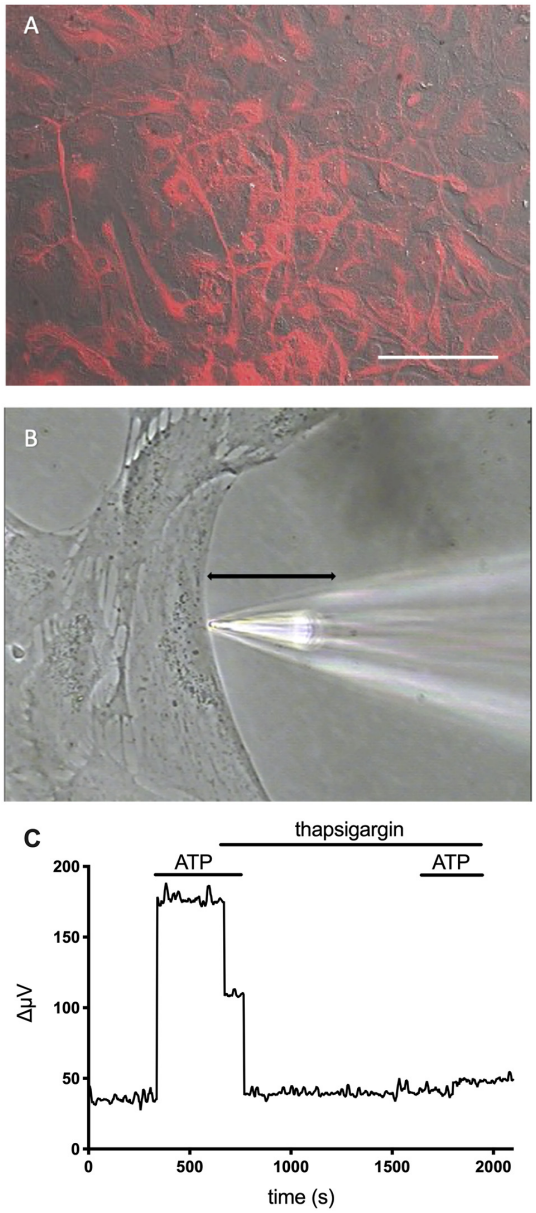

FIGURE 8 | Cells cultured from the hippocampus of mice and identified as astrocytes show ATP-mediated increases in H^+ efflux that are greatly reduced by the calcium reuptake blocker thapsigargin. Modified from Choi et al. (2021). **(A)** Low power photomicrograph combining DIC image with fluorescent staining for glial fibrillary acidic protein (GFAP) in a confluent dish of cells cultured for 11 days from mouse hippocampus. Red indicates signal from GFAP. The signal was not observed in negative controls (not shown). Scale bar = 100 μm. **(B)** High power photomicrograph showing the positioning of an H^+ selective microelectrode adjacent to a cell cultured from mouse hippocampus. The black line indicates the 30 μm lateral movement the H^+ selective electrode would travel from the near pole adjacent to the plasma membrane (pictured) to a background location 30 μm away. **(C)** H^+ efflux from a single hippocampal astrocyte induced by 100 μM ATP first under normal conditions and then after soaking the cell in 1 μM thapsigargin. As is apparent, thapsigargin virtually abolished the increase in H^+ flux initiated by ATP. In control cells, responses to a second application of ATP in plain Ringer's solution without thapsigargin present were not significantly different from initial responses to ATP (data not shown).

of extracellular ATP co-released with neurotransmitters when numerous vesicles fuse. Another potential mechanism involves calcium-stimulated fusion of vesicles with the plasmalemma of glia (see Malarkay and Parpura, 2011); H^+ ions present in such vesicles could contribute to an extracellular acidification. V-ATPases appear not to be major contributors, as the addition of bafilomycin A_1 failed to significantly alter ATP-induced increases in astrocytes. In 11 astrocytes tested, application of 100 μM ATP increased H^+ flux to 183 ± 29 μV from an initial H^+ standing flux of 87 ± 26 μV ($P < 0.0001$). The same cells were then exposed to 2 μM bafilomycin for several minutes, which has been reported to inhibit vacuolar ATPases with an IC_{50} of about 0.5 nM (Al-Fifi et al., 1998). 100 μM ATP again significantly increased the size of the H^+ flux signal to 167 ± 26 μV from an initial standing flux in the presence of bafilomycin of 96 ± 26 μV ($P = 0.0006$). Neither the standing flux ($P = 0.1854$) nor the ATP response ($P = 0.0768$) was significantly different in bath solutions with and without bafilomycin A_1. A previous study examining acid efflux from astrocytes cultured from the neopallium of 1 day old rats using microphysiometry, an entirely different technique (McConnell et al., 1992), also indicated that extracellular ATP induces acid efflux (Dixon et al., 2004). In that study, it was noted that cariporide, an inhibitor of Na^+/H^+ exchange, suppressed the initial portion of ATP-induced H^+ efflux, and the authors argued for a role for Na^+/H^+ transport. However, the 5 μM cariporide used depressed ATP-elicited H^+ efflux measured by microphysiometry by only about 30%, indicating that the majority of H^+ release was not due to NHE1 exchange. Given the nature of microphysiometry experiments (measuring the sum of acid released by all cells present in a culture dish), it is possible that some of the measured H^+ release might have come from cells other than astrocytes. One advantage of self-referencing H^+ microelectrodes is the ability to restrict measurements to single cells possessing a clear astrocytic morphology. On the other hand, the high spatial resolution of H^+-selective microelectrodes also means that H^+-selective microelectrodes may have been consistently positioned at regions of the cell low in Na^+/H^+ activity and might have missed higher levels at other locations. Another difference in methodology is that experiments conducted with microphysiometry were done on confluent cell cultures grown for 11 days, while those employing self-referencing were done on cells examined at earlier times prior to confluence, and the physiological properties of the astrocytes might differ in the two sets of culturing conditions. Nevertheless, the main conclusion—that ATP elicits increases in H^+ flux from cultured astrocytes—is supported by both the earlier microphysiometry studies as well as studies using self-referencing H^+-selective electrodes.

DISCUSSION

Implications of ATP-Elicited H^+ Efflux From Glial Cells

We have seen above that H^+ is one of the most potent modulators of synaptic transmission occurring naturally in the

nervous system, acting as an inhibitor of voltage-gated calcium channels, an inhibitor of such post-synaptic receptor proteins as NMDA glutamate receptors, and facilitating removal of neurotransmitters from the synaptic cleft. We have also seen that extracellular ATP induces H^+ release from retinal radial glial cells as well as astrocytes cultured from several areas of the brain. In this section, we examine several hypotheses for the role of alterations in extracellular H^+ in regulating synaptic transmission within the vertebrate retina and then broaden our scope to discuss implications of ATP-elicited H^+ efflux from glial cells for such phenomena as epilepsy, migraines, and electrical patterns of brain rhythms.

The high sensitivity of photoreceptor calcium channels to changes in extracellular H^+ has led to the hypothesis that the surround portion of the classic center-surround receptive field of retinal neurons may result from alterations in extracellular acidity—but mediated by retinal horizontal cells (Thoreson and Mangel, 2012; Kramer and Davenport, 2015). In one common version of this hypothesis, glutamate released by photoreceptors depolarizes horizontal cells, leading to increased release of H^+ from horizontal cells and inhibition of photoreceptor calcium channels with the consequent reduction in glutamate release. Strong evidence supporting this hypothesis comes from experiments employing CalipHlourin, a novel sensor developed to detect changes in extracellular H^+ at synaptic terminals of vertebrate photoreceptors (Wang et al., 2014). CalipHluorin is a pH-sensitive form of GFP (pHluorin) attached to the extracellular N terminus of the α2δ4 subunit of L-type calcium channels that is selectively expressed in cone photoreceptors, allowing measurements of extracellular H^+ at the level of photoreceptor synaptic terminals. Extracellular levels of H^+ were highest with retinal slices in the dark, and light stimuli induced an extracellular alkalinization. The light-induced effects on extracellular H^+ became larger as light stimuli were varied from small to a larger diameter, a characteristic expected from the large receptive field size of horizontal cells. In addition, activation by FMRF-amide of genetically modified zebrafish horizontal cells containing FMRF-amide receptors induced an extracellular acidification reported by alterations in CalipHlourin fluorescence.

However, experiments measuring changes in extracellular H^+ flux from horizontal cells with self-referencing H^+-selective electrodes consistently reveal that depolarization of isolated horizontal cells by glutamate or high extracellular potassium induces an extracellular alkalinization, not the expected acidification called for by the original hypothesis (Molina et al., 2004; Kreitzer et al., 2007, 2012; Jacoby et al., 2012). Data suggest that the extracellular alkalinization stems from activation of plasma membrane calcium pumps (PMCA), which take in two extracellular H^+ for each calcium extruded. In this model, depolarization of horizontal cells promotes the influx of calcium through voltage-gated calcium channels and calcium-permeable AMPA glutamate receptors, with consequent activation of PMCA pumps to extrude accumulated intracellular calcium, resulting in an extracellular alkalinization. Experiments examining changes in fluorescence of the H^+ reporter HAF when restricted to the plasma membrane of horizontal cells confirmed that activation of horizontal cells by potassium and glutamate induced an extracellular alkalinization, and further demonstrated that this alkalinization occurred over the entire external cell surface, with no isolated hot spots of acidification (Jacoby et al., 2014). It is also worth noting that the maximal size of the ATP-elicited extracellular acidification measured from isolated Müller cells is almost an order of magnitude larger than the biggest extracellular alkalinization detected from activated horizontal cells using identical methods.

At the time the original experiments with CalipHluorin were done (Wang et al., 2014), it was not known that extracellular ATP could induce alterations in extracellular H^+ via activation of Müller cells. Another explanation for the observed alterations in extracellular H^+ previously reported by CalipHluorin, then, is that activation of retinal neurons leads to release of neurotransmitter as well as ATP, leading to ATP-elicited activation of Müller cells and consequent release of H^+ from the radial glial cells of the retina. Synaptic vesicles possess high concentrations of ATP which can be released to the extracellular space by fusion of vesicles with the plasma membrane (for review, see Pankratov et al., 2006; Abbracchio et al., 2009; Burnstock and Verkhratsky, 2012), and the higher levels of H^+ observed in the dark may reflect H^+ extrusion by Müller cells in response to ATP released upon fusion of synaptic vesicles with the plasma membrane. Activation of genetically modified horizontal cells with FMRF-amide would likely result in a strong depolarization and greatly increased intracellular calcium levels inside these cells with consequent stimulation of fusion of synaptic vesicles and release of vesicular ATP, which again would result in increased stimulation of ATP-induced release of H^+ from Müller cells. The increase in the size of the extracellular acidification with increasing size of light stimulus, while consistent with the relatively large receptive field of horizontal cells, might reflect activation of glial cells adjacent to horizontal cells, effectively mimicking the receptive field size of horizontal cells. Additional evidence in support of the contention that the extracellular changes in H^+ reported by CalipHluorin might come from radial glial cells is illustrated in **Figure 9**. The left-hand portion of the figure shows staining of CalipHluorin seen at the level of synaptic terminals of photoreceptors (**Figure 9A**), while the right shows data that application of 1 mM extracellular ATP on to zebrafish retinal slices induces extracellular acidification at the synaptic terminal as reported by CalipHlorin (**Figure 9B**; presented in abstract form in Malchow et al., 2018). The extracellular acidification detected by CalipHluorin is consistent with increases in extracellular levels of H^+ induced by ATP as detected using self-referencing H^+-selective electrodes at the level of the outer plexiform (synaptic) layer of retinal slices of the tiger salamander as shown in **Figure 4**.

We envision, then, that "feedback" is being provided continually at photoreceptor synaptic terminals by the release of H^+ from radial glial cell processes activated by extracellular ATP likely co-released with glutamate during fusion of synaptic vesicles. Thus, many of the findings examining feedback onto vertebrate photoreceptors initially ascribed to neurons may reflect at least in part glial-mediated inhibition of synaptic

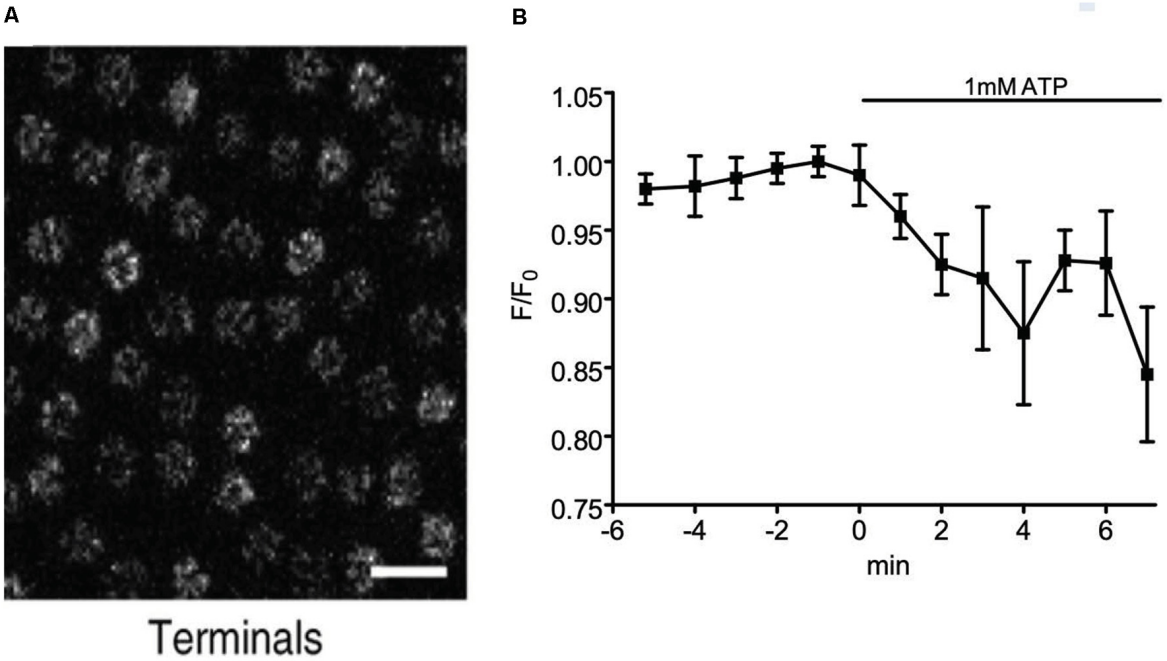

FIGURE 9 | Changes in extracellular H^+ at the level of the synaptic terminals in the retinal slice of a zebrafish. **(A)** Fluorescent micrograph showing the pattern of expression of the extracellular pH indicator CalipHluorin at the level of the synaptic terminals of cone photoreceptors of the zebrafish retina. To produce CalipHluorin, the H^+-sensitive GFP pHlourin is fused to the extracellular N terminus of the α2δ4 subunit of the L-type calcium channel. From Wang et al. (2014). **(B)** Addition of 1 mM extracellular ATP induced a decrease in fluorescence reported by CalipHluorin indicative of extracellular acidification at the level of the outer synaptic (plexiform) layer from five zebrafish retinal slices. Measurements were made as described in detail in Wang et al. (2014). From data presented in abstract form by Malchow et al. (2018).

transmission *via* release of H^+. To be sure, the evidence that H^+ plays a role in regulating synaptic transmission at the OPL is strong. DeVries (2001) and Hosoi et al. (2005) have presented compelling data that H^+ co-released from photoreceptor synaptic vesicles acts as a highly transient (several msec) but quite potent inhibitor of neurotransmitter release from photoreceptors. On a greater scale of time and space, Hirasawa and Kaneko (2003) and Cadetti and Thoreson (2006) demonstrated alterations in the voltage-dependent calcium conductance of cone photoreceptors consistent with effects mediated by extracellular H^+. Initially attributed to horizontal cells, we propose an effect secondarily mediated by activation of Müller cells *via* extracellular ATP with consequent extrusion of H^+, in part through activation of Na^+/H^+ exchange activity.

Measurements of extracellular H^+ flux in retinal slices indicate that extracellular ATP induces extracellular acidification not only at the outer synaptic layer of the retina but also at the more complex inner plexiform (synaptic) layer, where bipolar cells make synaptic connections with amacrine and ganglion cells. This suggests that inhibition of synaptic transmission by ATP-elicited changes in extracellular H^+ may extend to this area of extensive signal processing as well. Modulation of neuronal responses in the inner retina by activation of glial cells has been reported previously (Newman and Zahs, 1998; Newman, 2003). At least part of the modulation resulting from activation of Müller cells was ascribed to the actions of adenosine converted from extracellular ATP by extracellular ATPases acting on receptors present on the neurons (Newman, 2003). In this latter study, extracellular recording solutions contained 10 mM HEPES, a concentration expected to significantly blunt changes in extracellular H^+ that might result from stimulation of Müller cells and reduce the impact of H^+-dependent inhibition of synaptic transmission. We hypothesize that under conditions in which normal concentrations of the physiological buffer bicarbonate are used, alterations in H^+ resulting from release *via* stimulation of Müller cells might further contribute to the modulation of neuronal signals within the inner synaptic layer of the retina.

Circadian rhythms in levels of extracellular H^+ in the retina have been detected as well as circadian changes in the gain of synaptic transfer at the outer synaptic layer of the retina. Measurements of extracellular H^+ in isolated retinae of goldfish and rabbits using H^+-selective microelectrodes revealed a significantly higher level of H^+ in the subjective night compared to subjective daytime (Dmitriev and Mangel, 2000, 2001; Mangel, 2001). Additional experiments examining light-induced responses of goldfish horizontal cells demonstrated that during the subjective day, the cone photoreceptor-to-cone-driven horizontal cell transfer function exhibited an asymptotic synaptic gain of about 1.5, while the gain at subjective night decreased to about 0.3 (Ribelayga and Mangel, 2019). In the

dark of subjective night, photoreceptors would be expected to be in their most depolarized state, and theoretically constantly liberating high amounts of glutamate. It has always been a mystery as to why the release of neurotransmitters from photoreceptors should be highest in the dark, when we are asleep, and why this expected continuous release of neurotransmitters would not induce glutamate-mediated neuronal excitotoxicity, as observed in other areas of the brain when high levels of glutamate are present. We propose that glutamate release from tonically depolarized photoreceptors and other neurons is accompanied by co-release of ATP, leading to extracellular acidification mediated by activation of Müller cells. We further hypothesize that this release of H^+ from Müller cells acts as a form of automatic gain control, decreasing calcium influx into synaptic terminals and limiting neurotransmitter release from retinal neurons, and decreasing synaptic gain without significantly altering the ability of light to alter the voltage of photoreceptive cells themselves.

A circadian rhythm in levels of extracellular adenosine has been reported in the retina as well, with the highest levels occurring at night under dark adapted conditions (Ribelayga and Mangel, 2005; Cao et al., 2020). This distribution would be consistent with high levels of extracellular ATP at the same time—at subjective night and in the dark—since the enzymatic breakdown of ATP by extracellular ectonucleases would result in the production of extracellular adenosine. Circadian patterns in levels of adenosine have also been detected in other areas of the brain (Huston et al., 1996; Murillo-Rodriguez et al., 2004). Both adenosine and astrocytes have long been implicated with the regulation of sleep (see Bjorness and Greene, 2009; Blutstein and Haydon, 2013; Bjorness et al., 2016; Greene et al., 2017; Haydon, 2017). There is also evidence for a circadian rhythm associated with ATP in the suprachiasmatic nucleus as well as with cultured astrocytes; moreover, levels of extracellular ATP are associated with increases in intracellular calcium in astrocytes (Womac et al., 2009; Burkeen et al., 2011; Marpegan et al., 2011). Based on our data demonstrating ATP-induced H^+ efflux from cultured astrocytes from rat cortex and mouse hippocampus and their dependence upon intracellular calcium, it seems reasonable to hypothesize that alterations in extracellular acidity mediated by glial cells could play an important role in inducing sleep. Sleep and wakefulness are highly complex processes involving large networks of neurons and also appear to involve a large number of transmitter chemicals and modulators (see Luppi and Fort, 2011; Holst and Landolt, 2018; Landolt and Dijk, 2019). Given that glial cells are widely distributed and embedded in all of these networks with their fine processes wrapping and enveloping virtually every synapse, and further given the exceptional sensitivity of synaptic transmission to changes in extracellular H^+, it may be that glial release of H^+ plays a role in regulating waking and sleeping and driving the transitions between these behavioral states.

The various stages of sleep are well known to be accompanied by alterations in brain rhythms measured with extracellular electrodes (EEG). Increases in the efflux of extracellular H^+ mediated by alterations in intracellular calcium within glial cells might provide the physical link by which glial cells could induce changes in both brain states as well as corresponding electrical activity measured with an EEG. The altered threshold for initiation of neurotransmitter release anticipated when levels of extracellular H^+ are varied, as well as alterations in postsynaptic receptor activation and the speed with which released neurotransmitters are taken up, could influence the rhythmic pattern of firing of ensembles of neurons, leading to changes noted in EEG recordings. Alterations in brain rhythms measured by an EEG are also well known to occur upon administration of anesthetics; indeed, the dose, strength, and impact of an anesthetic are often assessed by the variation in EEG signals that are recorded. While the cellular and molecular mechanism of action of some anesthetics are well known, there remain a number of questions about the mode of action of some important and widely used compounds such as general anesthetics, for which the mechanism is not yet entirely clear. While most studies have naturally focused on the direct effects of anesthetics on neurons, it is plausible that some of the effects of some anesthetics might result from effects at the level of the glial cells. Given the high sensitivity of synaptic transmission to alterations in extracellular H^+, anesthetic actions resulting in the release of H^+ from glia could account for some of the sedative effects of such compounds.

We also hypothesize that release of H^+ from glia elicited by extracellular ATP provides the physical link underpinning the profound inhibition of electrical activity encountered in the phenomenon commonly referred to as spreading depression. Characterized in part by a slowly expanding wave of profound depression of spontaneous and evoked electrical activity in the nervous system that can last minutes at any one point, the phenomenon of spreading depression has been detected in the cortex, hippocampus, cerebellum, and other areas and has also received extensive study in the retina, where it is marked by readily observed optical changes (for review, see Martins-Ferreira et al., 2000; Gorji, 2001; Cozzolino et al., 2018). Large changes in the extracellular concentrations of a number of different ions including H^+ occur during spreading depression (Mutch and Hansen, 1984; Nicholson, 1984; Rice and Nicholson, 1988; Martins-Ferreira et al., 2000; Menna et al., 2000; Tong and Chesler, 2000). **Figure 10** shows an example of changes in extracellular levels of potassium, calcium, and H^+ detected during spreading depression in the rat cerebellum. Unlike the monophasic changes in extracellular potassium and calcium, alterations in extracellular H^+ during spreading depression are biphasic, with an initial small transient alkalinization followed by a larger and more long-lasting extracellular acidification. The slow wave of profound inhibition during spreading depression is preceded by a slow "spreading depolarization" accompanied by a burst of neuronal electrical activity (Charles and Baca, 2013; Cozzolino et al., 2018). This initial high level of neuronal activation should induce large increases in calcium entering neurons through activation of voltage-gated calcium channels in presynaptic neuronal terminals as well as through activation of receptors that are calcium-permeant such as NMDA receptors in postsynaptic processes. Indeed, another hallmark of ionic changes occurring during spreading depression is depletion of extracellular calcium, as illustrated in **Figure 10**,

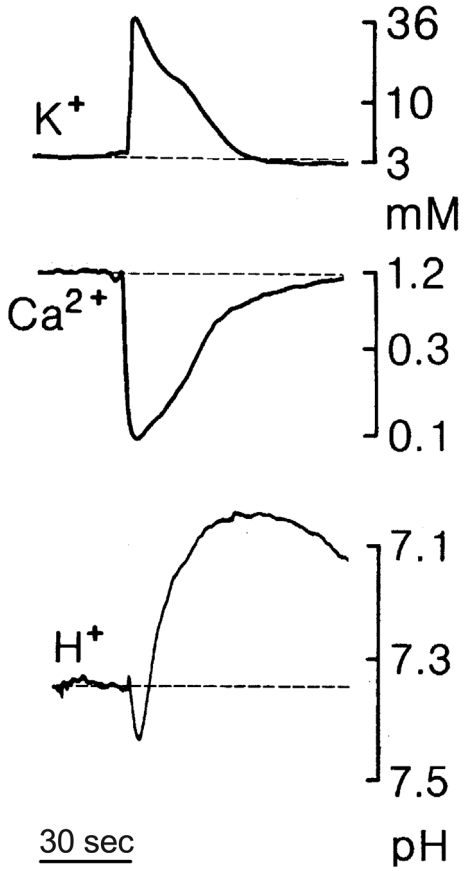

FIGURE 10 | Changes in extracellular levels of potassium (K^+), calcium (Ca^{2+}), and H^+ during spreading depression in the rat cerebellum measured using ion-selective microelectrodes; based on data by Charles Nicholson presented in Martins-Ferreira et al. (2000). Spreading depression was initiated by brief trains of local surface stimuli. Notice the biphasic change in extracellular levels of H^+, with an initial small transient alkalinization followed by a larger and more prolonged extracellular acidification.

consistent with calcium entering neurons during the initial depolarization event (Kraig and Nicholson, 1978; Nicholson, 1984; Martins-Ferreira and do Carmo, 1987; Martins-Ferreira et al., 2000). The contribution of Na^+/Ca^{2+} exchange to the restoration of normal levels of intracellular calcium in neurons is likely to be compromised since extracellular sodium also plummets during spreading depression. The reestablishment of pre-stimulus levels of intracellular calcium in neurons is thus likely to depend critically upon the activity of the plasmalemma calcium pump, which takes in two extracellular H^+ for each calcium extruded (Thomas, 2009). We envision that the initial extracellular alkalinization detected in spreading depression results from increased activity of PMCA pumps on neurons accumulating extracellular protons while extruding calcium ions following the burst of neuronal activity at the beginning of the event. Increases in extracellular ATP by as much as 100 μM have also been reported to occur during spreading depression (Schock et al., 2007), which based on our studies should activate pronounced H^+ extrusion from glial cells into the extracellular space, likely resulting in the secondary prolonged acidification observed during spreading depression. We further hypothesize that glial-mediated extrusion of H^+ is essential in restoring calcium levels in neurons to pre-stimulus conditions. Thus, rather than reflecting a nebulous and hazy increase in extracellular H^+ attributed in the past to general increases in overall cellular metabolism, we propose that the secondary increase in extracellular H^+ is mediated specifically by glial extrusion of H^+ initiated by high levels of extracellular ATP, and is likely essential for providing extracellular H^+ needed for restoration of normal calcium levels in neurons *via* the action of PMCA pumps. This same glial-mediated increase in H^+ would also depress additional neurotransmission by blocking voltage-gated calcium channels and certain post-synaptic responses, and enhance the uptake of neurotransmitters from the extracellular space, leading to the profound inhibition of spontaneous and evoked responses observed during spreading depression.

Spreading depression has long been associated with slow waves of increased intracellular calcium in glial cells (Basarsky et al., 1998; Kunkler and Kraig, 1998; Peters et al., 2003; Chuquet et al., 2007; Charles and Brennan, 2009), consistent with the calcium-dependence observed for increases in glial cell-mediated H^+ extrusion. Glial calcium waves have also been tied to increases in extracellular ATP, and it has been proposed that glial-mediated release of extracellular ATP may play a role in the generation and propagation of such spreading waves (Newman and Zahs, 1997; Guthrie et al., 1999; Newman, 2001; Weissman et al., 2004; Hoogland et al., 2009). Slow propagating waves of cortical activity have also been associated with migraines, and a link between the phenomenon of spreading depression and the occurrence of certain migraines has long been suspected (see Gorji, 2001; Rogawski, 2008; Eikermann-Haerter and Ayata, 2010; Charles and Baca, 2013; Eikermann-Haerter et al., 2013; Cozzolino et al., 2018; Harriott et al., 2019; Takizawa et al., 2020). Migraines are a heterogenous set of headache-related maladies reported to occur in many different parts of the brain and appear to involve widespread changes in multiple neuronal pathways and involve a number of neurochemical mediators [Davidoff, 2002; Charles, 2013; Headache Classification Committee of the International Headache Society (IHS) (2013)]. The aura perceived in certain migraines has been suggested to result from the initial spreading depolarizing wave that precedes the profound suppression of neuronal responses characteristic of spreading depression (Lauritzen, 1994; Cui et al., 2014; Charles, 2018; Major et al., 2020; Harriott et al., 2021). The pain in certain migraines following an aura might then result in part from the excessive and prolonged release of H^+ from glia during the period of synaptic inhibition occurring during the depression that follows the spreading depolarization. H^+ has been strongly implicated in pain pathways, and an excess of released H^+ from glial cells could potentially act on ASICs (acid sensing ion channels) and TRP (transient receptor potential) receptors to induce pain; indeed, both ASICs and TRP channels have specifically been proposed as targets for pharmacological approaches to reduce pain associated with migraine headaches (see Holland et al., 2012; Dussor, 2015, 2019; Benemei and Dussor, 2019; Takizawa et al., 2020).

A potential association between migraine and epilepsy has also long been suspected (see Post and Silberstein, 1994; De Simone et al., 2007; Parisi et al., 2008; Rogawski, 2008; Kasteleijn-Nolst Trenité et al., 2010; Keezer et al., 2015; Zarcone and Corbetta, 2017; Çilliler et al., 2017). Indeed, as pointed out by a number of investigators, the original description of spreading depression by Leão (1944) was done in the context of studies designed to induce experimental epilepsy (see Somjen, 2005; Teive et al., 2005; Cozzolino et al., 2018). We propose that the release of H^+ by glial cells constitutes a key and essential protective mechanism by which the nervous system normally prevents the development and spread of excessive neuronal stimulation that is a hallmark of epileptiform activity. In this view, the application of supra-normal stimulation such as that employed by Leão induces an initial massive depolarization of large numbers of neurons that in turn leads to high levels of extracellular ATP and consequent increases in intracellular calcium in neighboring glial cells. The high calcium in glial cells promotes the release of H^+ into the extracellular milieu, inhibiting further synaptic transmission by H^+-induced inhibition of voltage-gated calcium channels and certain post-synaptic receptors, as well as accelerating the removal of neurotransmitters *via* H^+-dependent uptake and also facilitating removal of intracellular calcium from over-activated neurons. Thus, we envision a negative feedback loop—a reset switch, if one will—whereby ATP-elicited H^+ extrusion by glial cells shuts down and prevents excess neuronal activity for a time while promoting a restoration of pre-stimulus levels of extracellular and intracellular ions and neurotransmitters. We hypothesize that the initial high levels of extracellular ATP stimulating H^+ release from glial cells likely come from ATP co-packaged with neurotransmitters in synaptic vesicles and that this is then augmented by ATP released by glial cells themselves, resulting in the wave of spreading depression mediated by extracellular H^+. The wave of spreading depolarization elicited by supra-normal stimuli, or that might occur in certain epilepsies upon excessive neuronal activity in potentially sensitive foci, would be expected to elicit a following wave of profound neuronal depression mediated by H^+ release from glial cells.

Epilepsies, like migraines, are a diverse set of nervous system abnormalities likely to have a number of different etiologies (see Chang and Lowenstein, 2003; Stafstrom and Carmant, 2015). With that important caveat in mind, it is notable that a sizable literature links astrocytes with epileptiform activity (see de Lanerolle et al., 2010; Carmignoto and Haydon, 2012; Vargas-Sánchez et al., 2018; Patel et al., 2019; Binder and Steinhäuser, 2021), and with purinergic signaling (Kumaria et al., 2008; Engel et al., 2016; Nikolic et al., 2020) as well as Na^+/H^+ transport (Gu et al., 2001; Zhao et al., 2016; Fliegel, 2020). We propose that excessive levels of neuronal activity associated with certain epilepsies might occur in conditions in which the signal transduction pathway leading to H^+ release from glial cells has been compromised, or when glial processes are aberrantly too far away from sites of synaptic activity for H^+ released by glia to inhibit neuronal activity. Tuberous sclerosis complex is one such epileptic condition in which this may be the case. This is a genetic disorder associated with the mTOR signaling pathway that results in epileptic activity in most individuals afflicted with the disease and is characterized by significant alterations in the relationships between glia and neurons (reviewed in Curatolo et al., 2002, 2015; Chu-Shore et al., 2010; Sofroniew and Vinters, 2010; Zimmer et al., 2020). The morphological and functional properties of the glial cells themselves are significantly distorted in this disease; for example, giant glial cells with exceptionally large cell bodies possessing relatively sparse fine processes are common (see Mizuguchi and Takashima, 2001; Boer et al., 2008; Grajkowska et al., 2010; Zimmer et al., 2020). Tuberous sclerosis complex has also been associated with disruptions in the balance of synaptic excitation and inhibition (Dooves et al., 2021). We hypothesize that the aberrant positioning and properties of glial cell fine processes in this condition leads to an inability of these cells to provide essential H^+-mediated inhibition of synaptic activity needed to prevent epileptiform activity, as well as inhibiting adequate removal by H^+-dependent transporters of neurotransmitters released into the synaptic cleft. We also predict that epileptic foci in other epilepsies might result from similar abnormalities in H^+-mediated regulation of synaptic activity and neurotransmitter uptake by glial cells. Excessive excitation at such foci could result either from compromises in the signal transduction pathway leading to H^+ release or alterations in the spatial relationship between glial cells and neurons that prevent H^+ released from glial cells from reaching synaptic terminals. A previous study observed close correlations of neuronal bursting with changes in intracellular calcium in glial cells and concluded that increases in calcium in glial cells were the cause of epileptic-like behavior resulting from glial-mediated release of glutamate (Tian et al., 2005). However, others have presented data demonstrating that astrocytic glutamate is not necessary for the generation of epileptiform activity in hippocampal slices and have argued that the discharge of action potentials in neurons, rather than astrocytic release of glutamate, is the key driver of epileptiform activity (Fellin et al., 2006). More recent studies have suggested that glial calcium waves are triggered by seizure activity and are not essential for epileptogenesis (Baird-Daniel et al., 2017). Our model would predict close correlations of glial cell increases in intracellular calcium with increases in neuronal activity, but with the calcium-dependent release of H^+ from glia acting as a response to reduce neuronal activity to suppress excessive stimulation.

It is interesting to note that CA inhibitors have long been employed in the treatment of epilepsy (see Bergstom et al., 1952; Ansell and Clarke, 1956; Reiss and Oles, 1996; Thiry et al., 2007; Mishra et al., 2021). Indeed, intravenous administration of the CA inhibitor acetazolamide induced a significant extracellular acidosis in the brains of anesthetized cats (Heuser et al., 1975). Extracellular CAs are known to be present in the brain interstitial space and have been suggested to play important roles in regulating extracellular H^+ levels (Chen and Chesler, 1992, 2015; Tong et al., 2000; Makani and Chesler, 2010). We envision that CA inhibitors crossing the blood-brain barrier, entering the brain, and reaching synapses

in sufficient concentrations might exert their salutary actions primarily by inhibiting extracellular CA activity. Drugs that inhibit the activity of extracellular CAs near synaptic terminals could significantly impact the magnitude and time course of synaptic inhibition mediated by H^+ released from glial cells. If a little is beneficial, however, more may not be better, since, at higher concentrations, acetazolamide and comparable CA inhibitors would likely cross the plasma membrane of glial cells and compromise the activity of intracellular CAs, reducing the amount of intracellular H^+ produced and secreted. This expected inverted U-shaped dose-response relationship, along with side effects resulting from these drugs on CAs present throughout the body, may be why such drugs are not the first choice for the treatment of epilepsy.

In response to injury and disease, glial cells undergo reactive gliosis, a complex and broad term that includes a host of morphological, molecular, and functional alterations (Escartin et al., 2021). The phenomenon has been described as a finely graded continuum of alterations that range from reversible changes in gene expression and cell hypertrophy to scar formation with permanent alterations in overall morphological arrangements (see Anderson et al., 2014; Burda and Sofroniew, 2014; Pekny et al., 2014; Robel and Sontheimer, 2016; Liddelow and Barres, 2017). In conditions where glial cells form scar-like structures, such as occurs in transection of the spinal cord, it has proven difficult to encourage neurons to grow through the scar. A number of studies have suggested that reactive glia have increases in the frequency and amplitude of alterations in intracellular calcium (for review, see Agulhon et al., 2012; Shigetomi et al., 2019; Verkhratsky, 2019). If such increased levels of glial intracellular calcium also result in increased extrusion of H^+, consequent elevations in overall extracellular H^+ could be one factor limiting the growth and extension of neurons through glial scars. The influx of calcium into specific portions of neurites is thought to play a key role in guiding the growth and extension of neurites in specific directions (Kater and Mills, 1991; Henley and Poo, 2004; Rosenberg and Spitzer, 2011; Gasperini et al., 2017). High levels of extracellular H^+ at the site of a glial scar would then be expected to prevent calcium channels in nearby neurites from opening, thus impeding neurite outgrowth. Thus, enhanced extrusion of H^+ by reactive glial cells could be one mechanism hindering the reestablishment of neuronal connections in injured or diseased states, and treatments designed to reduce extracellular levels of H^+ could potentially improve the reestablishment of neuronal growth and connectivity.

TOWARDS THE FUTURE

To sum up, small alterations in H^+ are exceptionally potent inhibitors of synaptic transmission, inhibiting voltage-gated calcium channels in presynaptic cells and certain neurotransmitter receptors on postsynaptic cells, and playing a critical role in the uptake of neurotransmitters as well as facilitating extrusion of intracellular calcium *via* PMCA pumps. Quite low concentrations of extracellular ATP promote H^+ extrusion from retinal radial glial cells. The ATP-elicited H^+ efflux is observed in Müller cells isolated from organisms as evolutionarily distant as lamprey, skate, tiger salamander, rat, monkey, and human, implying an important role conserved throughout vertebrate evolution. Extracellular ATP also elicits H^+ efflux from astrocytes cultured from mouse hippocampus and rat cortex, suggesting that ATP-elicited H^+ efflux is likely a general property of radial glia and astroglial cells. The fine processes of glial cells wrap and extensively envelop nervous system synapses, and thus release of H^+ by glia upon activation by extracellular ATP is well poised to regulate synaptic activity. This leads us to postulate an important role for glial cell-released H^+ in modulating neuronal activity in both normal and aberrant conditions. We envision that ATP-elicited H^+ flux from glia provides essential inhibition throughout the nervous system, and this inhibition prevents overexcitation of synaptic circuits. We also postulate that the release of H^+ by glia is the molecular mechanism underpinning the phenomenon of spreading depression and is a key and essential factor in preventing epileptiform activity. If this is correct, the broad extent of spreading depression and its observation in many areas of the nervous system would be consistent with our contention that ATP-elicited H^+ release is a general property of many glia. The similarity in the characteristics of spreading depression and migraine noted by others also leads us to suggest a potentially causative role for excessive glial cell-mediated H^+ release in the etiology of migraine. We further propose that disruptions in either the signal transduction pathway leading to H^+ efflux from glia or the positioning of glial processes away from the synapse, may prevent adequate inhibition of synaptic activity by H^+ efflux from glia and lead to the development of epileptiform activity.

We hypothesize that under normal levels of neuronal activity, synaptic activity is adjusted by the glial cell-mediated release of H^+ on a synapse-by-synapse basis. This would imply that the fine processes of individual glial cells act independently, with local variations of intracellular calcium leading to localized alterations in H^+ flux. Studies examining the three- dimensional pattern of calcium dynamics in awake animals and brain slices have demonstrated that calcium increases in astrocytes are scattered throughout the cell, are highly compartmentalized within predominantly local regions, and are heterogeneously distributed regionally and locally (Bindocci et al., 2017; Savtchouk et al., 2018). Additionally, these studies indicate that astrocytes can respond locally to quite minimal axonal firing with time-correlated changes in intracellular calcium. This suggests that potential regulation of neurotransmitter release by H^+ extruded from glia could be highly localized and that inhibition provided by H^+ release initiated by local increases in calcium may modulate synaptic strength at a synapse-by-synapse scale. The thousands of fine processes from astrocytes wrapping various separate synapses could thus potentially act independently from one another, with ATP released at just that synapse acting to locally influence synaptic strength by the highly localized release of H^+.

When excitation is intense, we hypothesize that waves of calcium throughout glial cells are generated that induce increases in extracellular H^+ at many synapses simultaneously, resulting in

the coordinated shutdown of neuronal activity so characteristic of spreading depression. Such waves of calcium may also induce the release of ATP by glial cells themselves, leading to further lateral spread of ATP-elicited H^+ inhibition. An important question to address in future experiments will be the mechanism by which local H^+-mediated inhibition provided by calcium changes in the fine processes of glial cells, transitions to waves of calcium within and across glial cells, leading to inhibition over larger spatial and temporal scales. One possibility is that excess neuronal stimulation in a local area leads to large increases in extracellular potassium and perhaps glutamate, and a concomitantly significant decrease in extracellular calcium as it enters neurons through voltage-gated calcium channels on presynaptic terminals and calcium-permeant receptors on post-synaptic neurons. The high level of extracellular potassium and glutamate resulting from the excessive neuronal activity then might lead to depolarization of neighboring neurons, consistent with the wave of spreading depolarization that precedes the profound depression of responses in the later stage of spreading depression. Low levels of extracellular calcium induce, almost paradoxically, significant increases in levels of intracellular calcium in astrocytes, as well as enhancing the intracellular calcium changes elicited by extracellular ATP (Zanotti and Charles, 1997). The increases in intracellular calcium in astrocytes induced by decreases in extracellular calcium may be mediated by store-operated Ca^{2+} release-activated Ca^{2+} (CRAC) channels (Toth et al., 2019). The lowered levels of extracellular calcium induced by excessive neuronal activation might then act as a signal that leads to increases in intracellular calcium in glial cells and an increase in calcium-dependent H^+ efflux from glial cells.

The overall impact of H^+ released by glial cells on transmission at synaptic terminals will depend on a complex number of factors, including the amount and duration of release of H^+, the distance of H^+ extrusion sites on glia from synaptic terminals, the concentration, strength, and nature of buffers for H^+ present, the location and amount of bicarbonate transporters, and the location and amount of CA present. Our model for activation of H^+ efflux by extracellular ATP in retinal Müller cells calls in part for the production of both H^+ and HCO_3 *via* enzymatic conversion of CO_2 mediated by the high concentrations of intracellular CA present in glia. Studies have shown that the bulk of HCO_3 transport activity occurs at the basal end foot of Müller cells, significantly removed from the sites of most synaptic terminals (Newman, 1991; Kreitzer et al., 2017). Thus, bicarbonate that is produced within Müller cells would be largely secreted into the vitreous humor of the eye. On the other hand, ATP-elicited alterations in extracellular H^+ measured using self-referencing electrodes show prominent extracellular acidifications at both the outer and inner synaptic layers of the retina (Tchernookova et al., 2018). We envision that activation of Müller cells by extracellular ATP leads to the production of both H^+ and HCO_3 and that a significant portion of the H^+ generated is extruded by Na^+/H^+ exchange near synaptic terminals. The sodium internalized in this process, along with increased concentrations of HCO_3 generated within the cells, would facilitate extrusion of HCO_3 at the basal end-foot of the cells by Na-HCO_3 cotransporters present in the end-foot; other types of HCO_3 transporters might also facilitate extrusion of HCO_3. We hypothesize, then, that generation of H^+ and HCO_3 occur together, but are exported largely at different locations in Müller cells, helping to preserve the overall level of intracellular pH inside the cell. It will be important in future studies to determine the relative spatial relationships between H^+ extrusion and HCO_3 transport within astroglial cells, as the overall effect of H^+ extrusion on alteration of synaptic activity will likely be significantly different if HCO_3 is secreted at the same location. The presence or absence of extracellular CA, and its precise localization, will also likely have a significant impact on the effects of H^+ extruded by the glia. Even if H^+ and HCO_3 are extruded at the same site, the slow kinetics of the conversion of H^+ and HCO_3 to CO_2 and water could result in a significant transient effect of H^+ on synaptic transmission if extracellular CAs are low in number around the release site.

In future experiments to examine the effects of glial-released H^+ on synaptic transmission, it will be critical to measure alterations in extracellular H^+ upon selective stimulation of glia at the precise location where H^+ is expected to exert its effects on synaptic transmission. The development of molecular sensors such as CalipHluorin—calcium channels engineered to express extracellular pHluorins as extracellular H^+ sensors—now offers the opportunity to make such measurements (Wang et al., 2014). One can imagine the development of similar H^+-sensitive tags expressed selectively in various cells and attached to other transporters or postsynaptic receptors to report alterations in extracellular H^+ at these locations. A remaining challenge will be to selectively stimulate just the glia in various experimental preparations since many neurons possess receptors for extracellular ATP, and simple addition of ATP is thus likely to have multiple effects resulting from activation of many different sets of cells and cellular signaling transduction pathways. The use of DREADDS (designer receptors exclusively activated by designer drugs) offers one possible approach to solving this challenge, and these have successfully been incorporated into glial cells (see Xie et al., 2015; Bang et al., 2016; Losi et al., 2017; Yu et al., 2020). However, the use of DREADDS and the interpretations of data obtained from such experiments come with their own set of important caveats and concerns. One major concern is how closely the activation of DREADDS mimic the response initiated by naturally occurring receptors activated by normal physiological activators, in this case, the initiation of H^+ flux by extracellular ATP. Our hypothesis that H^+ release from fine branches and extensions of glial cells modulates synaptic activity at the level of individual synapses suggests a crucial role for microdomains in glial-mediated regulation of synaptic transmission by H^+. It will be essential to ensure that the pattern of activation of, say, intracellular calcium by DREADDS expressed in glial cells mimics the natural alteration in calcium by ATP as closely as possible in both time and space.

Modulation of neuronal excitability by glial-induced changes in extracellular H^+ has been hypothesized by

others previously (see Ransom, 1992, 2000). The calcium-dependent increase in extracellular H^+ flux initiated by extracellular ATP provides a straightforward molecular mechanism by which such modulation can take place. Our hypothesis calls for a broad, powerful, and essential regulation of synaptic transmission by H^+ released by glia throughout the nervous system, with too little inhibition by glial H^+ efflux leading potentially to epileptiform behavior, and too much leading to the misery of migraine. Our recent work demonstrating ATP-elicited H^+ efflux from radial glia and astrocytes provides a specific molecular mechanism by which glia might provide feedback inhibition to limit synaptic transmission, and also provides a specific potential molecular link to spreading depression, migraine, and epilepsy. If this hypothesis is correct, it will be remarkable that an ion (H^+), which generally receives little consideration from neurobiologists, released from a cell type that historically has been underappreciated in the area of neuroscience (glial cells), might have such an important and impactful role in the functioning of the nervous system that has been overlooked for so long.

DATA AVAILABILITY STATEMENT

The raw data supporting the conclusions of this article will be made available by the authors, without undue reservation.

ETHICS STATEMENT

All animals were treated in accordance with the protocols approved by the Institutional Animal Care and Use Committees (IACUC) of the University of Illinois at Chicago, Indiana Wesleyan University, Marine Biological Laboratory, and University of California Berkeley as well as the federal guidelines listed in the Public Health Service Policy on Humane Care and Use of Laboratory Animals.

AUTHOR CONTRIBUTIONS

RM, BT, JC, PS, RK, and MK all contributed to the writing, content and editing of this article and approved the submitted version.

FUNDING

This work was supported by National Science Foundation (NSF) Grants 1557725 (to RM) and 1557820 (to MK), National Institute of Health (NIH) Award P30 EY003176 (to RK), NCRR P41 RR001395 (to PS), an LAS award for Faculty in the Natural Sciences from the University of Illinois at Chicago (to RM), an Indiana Wesleyan University Hodson Research Institute award (to MK), an Indiana Wesleyan University Scholar award (to MK), and a gift from the estate of John C. Hagensick (to RM).

REFERENCES

Abbracchio, M. P., Burnstock, G., Verkhratsky, A., and Zimmermann, H. (2009). Purinergic signalling in the nervous system: an overview. *Trends Neurosci.* 32, 19–29. doi: 10.1016/j.tins.2008.10.001

Agulhon, C., Sun, M.-Y., Murphy, T., Myers, T., Lauderdale, K., and Fiacco, T. A. (2012). Calcium signaling and gliotransmission in normal vs. reactive astrocytes. *Front. Pharmacol.* 3:139. doi: 10.3389/fphar.2012.00139

Al-Fifi, Z. I., Marshall, S. L., Hyde, D., Anstee, J. H., and Bowler, K. (1998). Characterization of ATPases of apical membrane fractions from Locusta migratoria Malpighian tubules. *Insect. Biochem. Mol. Biol.* 28, 201–211. doi: 10.1016/s0965-1748(98)00025-3

Anderson, M. A., Ao, Y., and Sofroniew, M. V. (2014). Heterogeneity of reactive astrocytes. *Neurosci. Lett.* 565, 23–29. doi: 10.1016/j.neulet.2013.12.030

Ansell, B., and Clarke, E. (1956). Acetazolamide in treatment of epilepsy. *Br. Med. J.* 1, 650–654. doi: 10.1136/bmj.1.4968.650

Ashhad, S., and Narayanan, R. (2019). Stores, channels, glue, and trees: active glial and active dendritic physiology. *Mol. Neurobiol.* 56, 2278–2299. doi: 10.1007/s12035-018-1223-5

Baird-Daniel, E., Daniel, A. G. S., Wenzel, M., Li, D., Liou, J.-Y., Laffont, P., et al. (2017). Glial calcium waves are triggered by seizure activity and not essential for initiating ictal onset or neurovascular coupling. *Cereb. Cortex* 27, 3318–3330. doi: 10.1152/ajpregu.00048.2021

Bang, J., Kim, H. Y., and Lee, H. (2016). Optogenetic and chemogenetic approaches for studying astrocytes and gliotransmitters. *Exp. Neurobiol.* 25, 205–221. doi: 10.5607/en.2016.25.5.205

Barnes, S. (1995). "Photoreceptor synaptic output: neurotransmitter release and photoreceptor coupling," in *Neurobiology and Clinical Aspects of the Outer Retina*, eds M. B. Djamgoz, S. N. Archer and S. Vallerga (Dordrecht: Springer), 133–154.

Barnes, S., Merchant, V., and Mahmud, F. (1993). Modulation of transmission gain by protons at the photoreceptor output synapse. *Proc. Natl. Acad. Sci. U S A* 90, 10081–10085. doi: 10.1073/pnas.90.21.10081

Barres, B. A., Freeman, M. R., and Stevens, B. (eds). (2015). *Glia*. New York, NY: Cold Spring Harbor Laboratory Press.

Basarsky, T. A., Duffy, S. N., Andrew, R. D., and MacVicar, B. A. (1998). Imaging spreading depression and associated intracellular calcium waves in brain slices. *J. Neurosci.* 18, 7189–7199. doi: 10.1523/JNEUROSCI.18-18-07189.1998

Bazargani, N., and Attwell, D. (2016). Astrocyte calcium signaling: the third wave. *Nat. Neurosci.* 19, 182–189. doi: 10.1038/nn.4201

Benemei, S., and Dussor, G. (2019). TRP channels and migraine: recent developments and new therapeutic opportunities. *Pharmaceuticals* 12:54. doi: 10.3390/ph12020054

Bergstom, W. H., Carzoli, R. F., Lombroso, C., Davidson, D. T., and Wallace, W. M. (1952). Observations on the metabolic and clinical effects of carbonic-anhydrase inhibitors in epileptics. *AMA Am. J. Dis. Child* 84, 771–772.

Binder, D. K., and Steinhäuser, C. (2021). Astrocytes and epilepsy. *Neurochem. Res.* doi: 10.1007/s11064-021-03236-x [Epub ahead of print].

Bindocci, E., Savtchouk, I., Liaudet, N., Becker, D., Carriero, G., and Volterra, A. (2017). Three-dimensional Ca^{2+} imaging advances understanding of astrocyte biology. *Science* 356:eaai8185. doi: 10.1126/science.aai8185

Bjorness, T. E., Dale, N., Mettlach, G., Sonneborn, A., Sahin, B., Fienberg, A. A., et al. (2016). An adenosine-mediated glial-neuronal circuit for homeostatic sleep. *J. Neurosci.* 36, 3709–3721. doi: 10.1523/JNEUROSCI.3906-15.2016

Bjorness, T. E., and Greene, R. W. (2009). Adenosine and sleep. *Curr. Neuropharmacol.* 7, 238–245. doi: 10.2174/157015909789152182

Blutstein, T., and Haydon, P. G. (2013). The importance of astrocyte-derived purines in the modulation of sleep. *Glia* 61, 129–139. doi: 10.1002/glia.22422

Boer, K., Troost, D., Jansen, F., Nellist, M., van den Ouweland, A. M. W., Geurts, J. J. G., et al. (2008). Clinicopathological and immunohistochemical findings in an autopsy case of tuberous sclerosis complex. *Neuropathology* 28, 577–590. doi: 10.1111/j.1440-1789.2008.00920.x

Boyman, L., Karbowski, M., and Lederer, W. J. (2020). Regulation of mitochondrial ATP production: Ca^{2+} signaling and quality control. *Trends Mol. Med.* 26, 21–39. doi: 10.1016/j.molmed.2019.10.007

Breton, S., Hammar, K., Smith, P. J., and Brown, D. (1998). Proton secretion in the male reproductive tract: involvement of Cl—independent HCO_3^- transport. *Am. J. Physiol.* 275, C1134–C1142. doi: 10.1152/ajpcell.1998.275.4.C1134

Burda, J. E., and Sofroniew, M. V. (2014). Reactive gliosis and the multicellular response to CNS damage and disease. *Neuron* 81, 229–248. doi: 10.1016/j.neuron.2013.12.034

Burkeen, J. F., Womac, A. D., Earnest, D. J., and Zoran, M. J. (2011). Mitochondrial calcium signaling mediates rhythmic extracellular ATP accumulation in suprachiasmatic nucleus astrocytes. *J. Neurosci.* 31, 8432–8440. doi: 10.1523/JNEUROSCI.6576-10.2011

Burnstock, G., and Verkhratsky, A. (2012). *Purinergic Signalling and the Nervous System*. Berlin, Heidelberg: Springer Verlag.

Cadetti, L., and Thoreson, W. B. (2006). Feedback effects of horizontal cell membrane potential on cone calcium currents studied with simultaneous recordings. *J. Neurophysiol.* 95, 1992–1995. doi: 10.1152/jn.01042.2005

Cammer, W., and Tansey, F. A. (1988). Carbonic anhydrase immunostaining in astrocytes in the rat cerebral cortex. *J. Neurochem.* 50, 319–322. doi: 10.1111/j.1471-4159.1988.tb13267.x

Cao, J., Ribelayga, C. P., and Mangel, S. C. (2020). A circadian clock in the retina regulates rod-cone gap junction coupling and neuronal light responses *via* activation of adenosine A2A receptors. *Front. Cell. Neurosci.* 14:605067. doi: 10.3389/fncel.2020.605067

Carmignoto, G., and Haydon, P. G. (2012). Astrocyte calcium signaling and epilepsy. *Glia* 60, 1227–1233. doi: 10.1002/glia.22318

Chang, B. S., and Lowenstein, D. H. (2003). Epilepsy. *N. Engl. J. Med.* 349, 1257–1266. doi: 10.1056/NEJMra022308

Charles, A. (2013). Migraine: a brain state. *Curr. Opin. Neurol.* 26, 235–239. doi: 10.1097/WCO.0b013e32836085f4

Charles, A. (2018). The migraine aura. *Continuum* 24, 1009–1022. doi: 10.1212/CON.0000000000000627

Charles, A. C., and Baca, S. M. (2013). Cortical spreading depression and migraine. *Nat. Rev. Med.* 9, 637–644. doi: 10.1038/nrneurol.2013.192

Charles, A., and Brennan, K. (2009). Cortical spreading depression-new insights and persistent questions. *Cephalalgia* 29, 1115–1124. doi: 10.1111/j.1468-2982.2009.01983.x

Chen, X. H., Bezprozvanny, I., and Tsien, R. W. (1996). Molecular basis of proton block of L-type Ca^{2+} channels. *J. Gen. Physiol.* 108, 363–374. doi: 10.1085/jgp.108.5.363

Chen, J. C., and Chesler, M. (1992). pH transients evoked by excitatory synaptic transmission are increased by inhibition of extracellular carbonic anhydrase. *Proc. Natl. Acad. Sci. U S A* 89, 7786–7790. doi: 10.1073/pnas.89.16.7786

Chen, H.-Y., and Chesler, M. (2015). Autocrine boost of NMDAR current in hippocampal CA1 pyramidal neurons by a PMCA-dependent, perisynaptic, extracellular pH shift. *J. Neurosci.* 35, 873–877. doi: 10.1523/JNEUROSCI.2293-14.2015

Choi, J. V., Tchernookova, B. K., Kumar, W., Kiedrowski, L., Goeke, C., Guizzetti, M., et al. (2021). Extracellular ATP induced alterations in extracellular H^+ fluxes from cultured cortical and hippocampal astrocytes. *Front Cell Neurosci.* 15:640217. doi: 10.3389/fncel.2021.640217

Chuquet, J., Hollender, L., and Nimchinsky, E. A. (2007). High-resolution *in vivo* imaging of the neurovascular unit during spreading depression. *J. Neurosci.* 27, 4036–4044. doi: 10.1523/JNEUROSCI.0721-07.2007

Chu-Shore, C. J., Major, P., Camposano, S., Muzykewicz, D., and Thiele, E. A. (2010). The natural history of epilepsy in tuberous sclerosis complex. *Epilepsia* 51, 1236–1241. doi: 10.1111/j.1528-1167.2009.02474.x

Çilliler, A. E., Güven, H., and Çomoğlu, S. S. (2017). Epilepsy and headaches: further evidence of a link. *Epilepsy Behav.* 70, 161–165. doi: 10.1016/j.yebeh.2017.03.009

Cozzolino, O., Marchese, M., Trovato, F., Pracucci, E., Ratto, G. M., Buzzi, M. G., et al. (2018). Understanding spreading depression from headache to sudden unexpected death. *Front. Neurol.* 9:19. doi: 10.3389/fneur.2018.00019

Cui, Y., Kataoka, Y., and Watanabe, Y. (2014). Role of cortical spreading depression in the pathophysiology of migraine. *Neurosci. Bull.* 30, 812–822. doi: 10.1007/s12264-014-1471-y

Curatolo, P., Moavero, R., and de Vries, P. J. (2015). Neurological and neuropsychiatric aspects of tuberous sclerosis complex. *Lancet Neurol.* 14, 733–745. doi: 10.1016/S1474-4422(15)00069-1

Curatolo, P., Verdecchia, M., and Bombardieri, R. (2002). Tuberous sclerosis complex: a review of neurological aspects. *Eur. J. Paediatr. Neurol.* 6, 15–23. doi: 10.1053/ejpn.2001.0538

Davidoff, R. A. (2002). *Migraine: Manifestations, Pathogenesis, and Management*. 2nd Edn. Oxford: Oxford University Press.

de Lanerolle, N. C., Lee, T.-S., and Spencer, D. D. (2010). Astrocytes and epilepsy. *Neurotherapeutics* 7, 424–438. doi: 10.1016/j.nurt.2010.08.002

De Simone, R., Ranieri, A., Marano, E., Beneduce, L., Ripa, P., Bilo, L., et al. (2007). Migraine and epilepsy: clinical and pathophysiological relations. *Neurol. Sci.* 28, S150–S155. doi: 10.1007/s10072-007-0769-1

DeVries, S. H. (2001). Exocytosed protons feedback to suppress the Ca^{2+} current in mammalian cone photoreceptors. *Neuron* 32, 1107–1117. doi: 10.1016/s0896-6273(01)00535-9

Dixon, S. J., Yu, R., Panupinthu, N., and Wilson, J. X. (2004). Activation of P2 nucleotide receptors stimulates acid efflux from astrocytes. *Glia* 47, 367–376. doi: 10.1002/glia.20048

Dmitriev, A. V., and Mangel, S. C. (2000). A circadian clock regulates the pH of the fish retina. *J. Physiol.* 522, 77–82. doi: 10.1111/j.1469-7793.2000.0077m.x

Dmitriev, A. V., and Mangel, S. C. (2001). Circadian clock regulation of pH in the rabbit retina. *J. Neurosci.* 21, 2897–2902. doi: 10.1523/JNEUROSCI.21-08-02897.2001

Doering, C. J., and McRory, J. E. (2007). Effects of extracellular pH on neuronal calcium channel activation. *Neuroscience* 146, 1032–1043. doi: 10.1016/j.neuroscience.2007.02.049

Dooves, S., van Velthoven, A. J. H., Suciati, L. G., and Heine, V. M. (2021). Neuron-glia interactions in tuberous sclerosis complex affect the synaptic balance in 2D and organoid cultures. *Cells* 10:134. doi: 10.3390/cells10010134

Durkee, C. A., and Araque, A. (2019). Diversity and specificity of astrocyte-neuron communication. *Neuroscience* 396, 73–78. doi: 10.1016/j.neuroscience.2018.11.010

Dussor, G. (2015). ASICs as therapeutic targets for migraine. *Neuropharmacol* 94, 64–71. doi: 10.1016/j.neuropharm.2014.12.015

Dussor, G. (2019). New discoveries in migraine mechanisms and therapeutic targets. *Curr. Opin. Physiol.* 11, 116–124. doi: 10.1016/j.cophys.2019.10.013

Eikermann-Haerter, K., and Ayata, C. (2010). Cortical spreading depression and migraine. *Curr. Neurol. Neurosci. Rep.* 10, 167–173. doi: 10.1007/s11910-010-0099-1

Eikermann-Haerter, K., Negro, A., and Ayata, C. (2013). Spreading depression and the clinical correlates of migraine. *Rev. Neurosci.* 24, 353–363. doi: 10.1515/revneuro-2013-0005

Engel, T., Alves, M., Sheedy, C., and Henshall, D. C. (2016). ATPergic signalling during seizures and epilepsy. *Neuropharmacol* 104, 140–153. doi: 10.1016/j.neuropharm.2015.11.001

Escartin, C., Galea, E., Lakatos, A., O'Callaghan, J. P., Petzold, G. C., Serrano-Pozo, A., et al. (2021). Reactive astrocyte nomenclature, definitions and future directions. *Nat. Neurosci.* 24, 312–325. doi: 10.1038/s41593-020-00783-4

Fellin, T., Gomez-Gonzalo, M., Gobbo, S., Carmignoto, G., and Haydon, P. G. (2006). Astrocytic glutamate is not necessary for the generation of epileptiform neuronal activity in hippocampal slices. *J. Neurosci.* 26, 9312–9322. doi: 10.1523/JNEUROSCI.2836-06.2006

Fiacco, T. A., and McCarthy, K. D. (2018). Multiple lines of evidence indicate that gliotransmission does not occur under physiological conditions. *J. Neurosci.* 38, 3–13. doi: 10.1523/JNEUROSCI.0016-17.2017

Fliegel, L. (2020). Role of genetic mutations of the Na^+/H^+ exchanger isoform 1, in human disease and protein targeting and activity. *Mol. Cell. Biochem.* 476, 1221–1232. doi: 10.1007/s11010-020-03984-4

Gasperini, R. J., Pavez, M., Thompson, A. C., Mitchell, C. B., Hardy, H., Young, K. M., et al. (2017). How does calcium interact with the cytoskeleton to regulate growth cone motility during axon pathfinding? *Mol. Cell. Neurosci.* 84, 29–35. doi: 10.1016/j.mcn.2017.07.006

Gorji, A. (2001). Spreading depression: a review of the clinical relevance. *Brain Res. Brain Res. Rev.* 38, 33–60. doi: 10.1016/s0165-0173(01)00081-9

Grajkowska, W., Kotulska, K., Jurkiewicz, E., and Matyja, E. (2010). Brain lesions in tuberous sclerosis complex. Review. *Folia Neuropathol.* 48, 139–149.

Greene, R. W., Bjorness, T. E., and Suzuki, A. (2017). The adenosine-mediated, neuronal-glial, homeostatic sleep response. *Curr. Opin. Neurobiol.* 44, 236–242. doi: 10.1016/j.conb.2017.05.015

Gu, X. Q., Yao, H., and Haddad, G. G. (2001). Increased neuronal excitability and seizures in the Na^+/H^+ exchanger null mutant mouse. *Am. J. Physiol. Cell Physiol.* 281, C496–C503. doi: 10.1152/ajpcell.2001.281.2.C496

Guerra-Gomes, S., Sousa, N., Pinto, L., and Oliveira, J. F. (2017). Functional roles of astrocyte calcium elevations: from synapses to behavior. *Front. Cell. Neurosci.* 11:427. doi: 10.3389/fncel.2017.00427

Guthrie, P. B., Knappenberger, J., Segal, M., Bennett, M. V., Charles, A. C., and Kater, S. B. (1999). ATP released from astrocytes mediates glial calcium waves. *J. Neurosci.* 19, 520–528. doi: 10.1523/JNEUROSCI.19-02-00520.1999

Halassa, M. M., Fellin, T., and Haydon, P. G. (2007). The tripartite synapse: roles for gliotransmission in health and disease. *Trends Mol. Med.* 13, 54–63. doi: 10.1016/j.molmed.2006.12.005

Halassa, M. M., Fellin, T., and Haydon, P. G. (2009). Tripartite synapses: roles for astrocytic purines in the control of synaptic physiology and behavior. *Neuropharmacol* 57, 343–346. doi: 10.1016/j.neuropharm.2009.06.031

Harriott, A. M., Chung, D. Y., Uner, A., Bozdayi, R. O., Morais, A., Takizawa, T., et al. (2021). Optogenetic spreading depression elicits trigeminal pain and anxiety behavior. *Ann. Neurol.* 89, 99–110. doi: 10.1002/ana.25926

Harriott, A. M., Takizawa, T., Chung, D. Y., and Chen, S.-P. (2019). Spreading depression as a preclinical model of migraine. *J. Headache Pain* 20:45. doi: 10.1186/s10194-019-1001-4

Harsanyi, K., and Mangel, S. C. (1993). Modulation of cone to horizontal cell transmission by calcium and pH in the fish retina. *Vis. Neurosci.* 10, 81–91. doi: 10.1017/s0952523800003242

Haydon, P. G. (2017). Astrocytes and the modulation of sleep. *Curr. Opin. Neurobiol.* 44, 28–33. doi: 10.1016/j.conb.2017.02.008

Headache Classification Committee of the International Headache Society (IHS). (2013). The international classification of headache disorders, 3rd edition. *Cephalalgia* 33, 1–211. doi: 10.1177/0333102413485658

Henley, J., and Poo, M.-M. (2004). Guiding neuronal growth cones using Ca^{2+} signals. *Trends Cell Biol.* 14, 320–330. doi: 10.1016/j.tcb.2004.04.006

Heuser, D., Astrup, J., Lassen, N. A., and Betz, B. E. (1975). Brain carbonic acid acidosis after acetazolamide. *Acta Physiol. Scand.* 93, 385–390. doi: 10.1111/j.1748-1716.1975.tb05827.x

Hirasawa, H., and Kaneko, A. (2003). pH changes in the invaginating synaptic cleft mediate feedback from horizontal cells to cone photoreceptors by modulating Ca^{2+} channels. *J. Gen. Physiol.* 122, 657–671. doi: 10.1085/jgp.200308863

Holland, P. R., Akerman, S., Andreou, A. P., Karsan, N., Wemmie, J. A., and Goadsby, P. J. (2012). Acid-sensing ion channel 1: a novel therapeutic target for migraine with aura. *Ann. Neurol.* 72, 559–563. doi: 10.1002/ana.23653

Holst, S. C., and Landolt, H.-P. (2018). Sleep-wake neurochemistry. *Sleep Med. Clin.* 13, 137–146. doi: 10.1016/j.jsmc.2018.03.002

Hoogland, T. M., Kuhn, B., Göbel, W., Huang, W., Nakai, J., Helmchen, F., et al. (2009). Radially expanding transglial calcium waves in the intact cerebellum. *Proc. Natl. Acad. Sci. U S A* 106, 3496–3501. doi: 10.1073/pnas.0809269106

Hosoi, N., Arai, I. and Tachibana, M. (2005). Group III metabotropic glutamate receptors and exocytosed protons inhibit L-type calcium currents in cones but not in rods. *J. Neurosci.* 25, 4062–4072. doi: 10.1523/JNEUROSCI.2735-04.2005

Huston, J. P., Haas, H. L., Boix, F., Pfister, M., Decking, U., Schrader, J., et al. (1996). Extracellular adenosine levels in neostriatum and hippocampus during rest and activity periods of rats. *Neuroscience* 73, 99–107. doi: 10.1016/0306-4522(96)00021-8

Jacoby, J., Kreitzer, M. A., Alford, S., and Malchow, R. P. (2014). Fluorescent imaging reports an extracellular alkalinization induced by glutamatergic activation of isolated retinal horizontal cells. *J. Neurophysiol.* 111, 1056–1064. doi: 10.1152/jn.00768.2013

Jacoby, J., Kreitzer, M. A., Alford, S., Qian, H., Tchernookova, B. K., Naylor, E. R., et al. (2012). Extracellular pH dynamics of retinal horizontal cells examined using electrochemical and fluorometric methods. *J. Neurophysiol.* 107, 868–879. doi: 10.1152/jn.00878.2011

Jalali-Yazdi, F., Chowdhury, S., Yoshioka, C., and Gouaux, E. (2018). Mechanisms for zinc and proton inhibition of the GluN1/GluN2A NMDA receptor. *Cell* 175, 1520.e15–1532.e15. doi: 10.1016/j.cell.2018.10.043

Jha, M. K., and Morrison, B. M. (2018). Glia-neuron energy metabolism in health and diseases: new insights into the role of nervous system metabolic transporters. *Exp. Neurol.* 309, 23–31. doi: 10.1016/j.expneurol.2018.07.009

Jha, M. K., and Morrison, B. M. (2020). Lactate transporters mediate glia-neuron metabolic crosstalk in homeostasis and disease. *Front. Cell. Neurosci.* 14:589582. doi: 10.3389/fncel.2020.589582

Kasteleijn-Nolst Trenité, D. G. A., Verrotti, A., Di Fonzo, A., Cantonetti, L., Bruschi, R., Chiarelli, F., et al. (2010). Headache, epilepsy and photosensitivity: how are they connected? *J. Headache Pain* 11, 469–476. doi: 10.1007/s10194-010-0229-9

Kater, S. B., and Mills, L. R. (1991). Regulation of growth cone behavior by calcium. *J. Neurosci.* 11, 891–899. doi: 10.1523/JNEUROSCI.11-04-00891.1991

Keezer, M. R., Bauer, P. R., Ferrari, M. D., and Sander, J. W. (2015). The comorbid relationship between migraine and epilepsy: a systematic review and meta-analysis. *Eur. J. Neurol.* 22, 1038–1047. doi: 10.1111/ene.12612

Khakh, B. S., and McCarthy, K. D. (2015). Astrocyte calcium signaling: from observations to functions and the challenges therein. *Cold Spring Harb. Perspect. Biol.* 7:a020404. doi: 10.1101/cshperspect.a020404

Kleinschmidt, J. (1991). Signal transmission at the photoreceptor synapse. Role of calcium ions and protons. *Ann. N Y Acad. Sci.* 635, 468–470. doi: 10.1111/j.1749-6632.1991.tb36529.x

Kofuji, P., and Araque, A. (2021). G-protein-coupled receptors in astrocyte-neuron communication. *Neuroscience* 456, 71–84. doi: 10.1016/j.neuroscience.2020.03.025

Kraig, R. P., and Nicholson, C. (1978). Extracellular ionic variations during spreading depression. *Neuroscience* 3, 1045–1059. doi: 10.1016/0306-4522(78)90122-7

Kramer, R. H., and Davenport, C. M. (2015). Lateral inhibition in the vertebrate retina: the case of the missing neurotransmitter. *PLoS Biol.* 13:e1002322. doi: 10.1371/journal.pbio.1002322

Kreitzer, M. A., Collis, L. P., Molina, A. J. A., Smith, P. J. S., and Malchow, R. P. (2007). Modulation of extracellular proton fluxes from retinal horizontal cells of the catfish by depolarization and glutamate. *J. Gen. Physiol.* 130, 169–182. doi: 10.1085/jgp.200709737

Kreitzer, M. A., Jacoby, J., Naylor, E., Baker, A., Grable, T., Tran, E., et al. (2012). Distinctive patterns of alterations in proton efflux from goldfish retinal horizontal cells monitored with self-referencing H^+-selective electrodes. *Eur. J. Neurosci.* 36, 3040–3050. doi: 10.1111/j.1460-9568.2012.08226.x

Kreitzer, M. A., Swygart, D., Osborn, M., Skinner, B., Heer, C., Kaufman, R., et al. (2017). Extracellular H^+ fluxes from tiger salamander Müller (glial) cells measured using self-referencing H^+-selective microelectrodes. *J. Neurophysiol.* 118, 3132–3143. doi: 10.1152/jn.00409.2017

Kumaria, A., Tolias, C. M., and Burnstock, G. (2008). ATP signalling in epilepsy. *Purinergic Signal.* 4, 339–346. doi: 10.1007/s11302-008-9115-1

Kunkler, P. E., and Kraig, R. P. (1998). Calcium waves precede electrophysiological changes of spreading depression in hippocampal organ cultures. *J. Neurosci.* 18, 3416–3425. doi: 10.1523/JNEUROSCI.18-09-03416.1998

Landolt, H.-P., and Dijk, D.-J. (2019). *Sleep-Wake Neurobiology and Pharmacology*. Cham: Springer International Publishing.

Lauritzen, M. (1994). Pathophysiology of the migraine aura. The spreading depression theory. *Brain* 117, 199–210. doi: 10.1093/brain/117.1.199

Leão, A. A. (1944). Spreading depression of activity in the cerebral cortex. *J. Neurophysiol.* 7, 359–390.

Liddelow, S. A., and Barres, B. A. (2017). Reactive astrocytes: production, function and therapeutic potential. *Immunity* 46, 957–967. doi: 10.1016/j.immuni.2017.06.006

Losi, G., Mariotti, L., Sessolo, M., and Carmignoto, G. (2017). New tools to study astrocyte Ca^{2+} signal dynamics in brain networks *in vivo*. *Front. Cell. Neurosci.* 11:134. doi: 10.3389/fncel.2017.00134

Luppi, P.-H., and Fort, P. (2011). Neurochemistry of sleep an overview of animal experimental work. *Handb. Clin. Neurol.* 98, 173–190. doi: 10.1016/B978-0-444-52006-7.00011-3

Major, S., Huo, S., Lemale, C. L., Siebert, E., Milakara, D., Woitzik, J., et al. (2020). Direct electrophysiological evidence that spreading depolarization-induced spreading depression is the pathophysiological correlate of the migraine aura and a review of the spreading depolarization continuum of acute neuronal mass injury. *Geroscience* 42, 57–80. doi: 10.1007/s11357-019-00142-7

Makani, S., and Chesler, M. (2010). Rapid rise of extracellular pH evoked by neural activity is generated by the plasma membrane calcium ATPase. *J. Neurophysiol.* 103, 667–676. doi: 10.1152/jn.00948.2009

Malarkay, E. B., and Parpura, V. (2011). Temporal characteristics of vesicular fusion in astrocytes: examination of synaptobrevin 2-laden vesicles at single vesicle resolution. *J. Physiol.* 589, 4271–4300. doi: 10.1113/jphysiol.2011.210435

Malchow, R. P., Tchernookova, B. K., Holzhausen, L. C., Kramer, R. H., and Kreitzer, M. A. (2018). ATP-induced alterations in extracellular H^+: a potent potential mechanism for modulation of neuronal signals by Müller (glial) cells in the vertebrate retina. *Invest Ophthalmol. Visual Sci.* 59:1863.

Mangel, S. C. (2001). Circadian clock regulation of neuronal light responses in the vertebrate retina. *Prog. Brain Res.* 131, 505–518. doi: 10.1016/s0079-6123(01)31040-3

Maren, T. H. (1988). The kinetics of HCO_3^- synthesis related to fluid secretion, pH control and CO_2 elimination. *Annu. Rev. Physiol.* 50, 695–717. doi: 10.1146/annurev.ph.50.030188.003403

Marpegan, L., Swanstrom, A. E., Chung, K., Simon, T., Haydon, P. G., Khan, S. K., et al. (2011). Circadian regulation of ATP release in astrocytes. *J. Neurosci.* 31, 8342–8350. doi: 10.1523/JNEUROSCI.6537-10.2011

Martins-Ferreira, H., and do Carmo, R. J. (1987). Retinal spreading depression and the extracellular milieu. *Can. J. Physiol. Pharmacol.* 65, 1092–1098. doi: 10.1139/y87-171

Martins-Ferreira, H., Nedergaard, M., and Nicholson, C. (2000). Perspectives on spreading depression. *Brain Res. Brain Res. Rev.* 32, 215–234. doi: 10.1016/s0165-0173(99)00083-1

McConnell, H. M., Owicki, J. C., Parce, J. W., Miller, D. L., Baxter, G. T., Wada, H. G., et al. (1992). The cytosensor microphysiometer: biological applications of silicon technology. *Science* 257, 1906–1912. doi: 10.1126/science.1329199

Menna, G., Tong, C. K., and Chesler, M. (2000). Extracellular pH changes and accompanying cation shifts during ouabain-induced spreading depression. *J. Neurophysiol.* 83, 1338–1345. doi: 10.1152/jn.2000.83.3.1338

Messerli, M. A., Robinson, K. R., and Smith, P. J. S. (2006). "Electrochemical sensor applications to the study of molecular physiology and analyte flux in plants," in *Plant electrophysiology–Theory and Methods*, eds A. G. Volkov (Berlin, Heidelberg: Springer), 73–104.

Messerli, M. A., and Smith, P. J. S. (2010). Construction, theory and practical considerations for using self-referencing of Ca^{2+}-selective microelectrodes for monitoring extracellular Ca^{2+} gradients. *Methods Cell Biol.* 99, 91–111. doi: 10.1016/B978-0-12-374841-6.00004-9

Mishra, C. B., Kumari, S., Angeli, A., Bua, S., Mongre, R. K., Tiwari, M., et al. (2021). Discovery of potent carbonic anhydrase inhibitors as effective anticonvulsant agents: drug design, synthesis and *in vitro* and *in vivo* investigations. *J. Med. Chem.* 64, 3100–3114. doi: 10.1021/acs.jmedchem.0c01889

Mizuguchi, M., and Takashima, S. (2001). Neuropathology of tuberous sclerosis. *Brain Dev.* 23, 508–515. doi: 10.1016/s0387-7604(01)00304-7

Molina, A. J. A., Verzi, M. P., Birnbaum, A. D., Yamoah, E. N., Hammar, K., Smith, P. J. S., et al. (2004). Neurotransmitter modulation of extracellular H^+ fluxes from isolated retinal horizontal cells of the skate. *J. Physiol.* 560, 639–657. doi: 10.1113/jphysiol.2004.065425

Murillo-Rodriguez, E., Blanco-Centurion, C., Gerashchenko, D., Salin-Pascual, R. J., and Shiromani, P. J. (2004). The diurnal rhythm of adenosine levels in the basal forebrain of young and old rats. *Neuroscience* 123, 361–370. doi: 10.1016/j.neuroscience.2003.09.015

Mutch, W. A., and Hansen, A. J. (1984). Extracellular pH changes during spreading depression and cerebral ischemia: mechanisms of brain pH regulation. *J. Cereb. Blood Flow. Metab.* 4, 17–27. doi: 10.1038/jcbfm.1984.3

Nagelhus, E. A. (2005). Carbonic anhydrase XIV is enriched in specific membrane domains of retinal pigment epithelium, Müller cells and astrocytes. *Proc. Natl. Acad. Sci. U S A* 102, 8030–8035. doi: 10.1073/pnas.0503021102

Newman, E. A. (1985). Membrane physiology of retinal glial (Müller) cells. *J. Neurosci.* 5, 2225–2239. doi: 10.1523/JNEUROSCI.05-08-02225.1985

Newman, E. A. (1991). Sodium-bicarbonate cotransport in retinal Müller (glial) cells of the salamander. *J. Neurosci.* 11, 3972–3983. doi: 10.1523/JNEUROSCI.11-12-03972.1991

Newman, E. A. (1994). A physiological measure of carbonic anhydrase in Müller cells. *Glia* 11, 291–299. doi: 10.1002/glia.440110402

Newman, E. A. (2001). Propagation of intercellular calcium waves in retinal astrocytes and Müller cells. *J. Neurosci.* 21, 2215–2223. doi: 10.1523/JNEUROSCI.21-07-02215.2001

Newman, E. A. (2003). Glial cell inhibition of neurons by release of ATP. *J. Neurosci.* 23, 1659–1666. doi: 10.1523/JNEUROSCI.23-05-01659.2003

Newman, E. A., and Zahs, K. R. (1997). Calcium waves in retinal glial cells. *Science* 275, 844–847. doi: 10.1126/science.275.5301.844

Newman, E. A., and Zahs, K. R. (1998). Modulation of neuronal activity by glial cells in the retina. *J. Neurosci.* 18, 4022–4028. doi: 10.1523/JNEUROSCI.18-11-04022.1998

Nicholls, D., and Attwell, D. (1990). The release and uptake of excitatory amino acids. *Trends Pharmacol. Sci.* 11, 462–468. doi: 10.1016/0165-6147(90)90129-v

Nicholson, C. (1984). Comparative neurophysiology of spreading depression in the cerebellum. *An. Acad. Bras. Cienc.* 56, 481–494.

Nikolic, L., Nobili, P., Shen, W., and Audinat, E. (2020). Role of astrocyte purinergic signaling in epilepsy. *Glia* 68, 1677–1691. doi: 10.1002/glia.23747

Owe, S. G., Marcaggi, P., and Attwell, D. (2006). The ionic stoichiometry of the GLAST glutamate transporter in salamander retinal glia. *J. Physiol.* 577, 591–599. doi: 10.1113/jphysiol.2006.116830

Pankratov, Y., Lalo, U., Verkhratsky, A., and North, R. A. (2006). Vesicular release of ATP at central synapses. *Pflugers Arch.* 452, 589–597. doi: 10.1007/s00424-006-0061-x

Papouin, T., Dunphy, J., Tolman, M., Foley, J. C., and Haydon, P. G. (2017). Astrocytic control of synaptic function. *Philos. Trans. R. Soc. Lond. B Biol. Sci.* 372, 20160154–20160158. doi: 10.1098/rstb.2016.0154

Parisi, P., Piccioli, M., Villa, M. P., Buttinelli, C., and Kasteleijn-Nolst Trenité, D. G. A. (2008). Hypothesis on neurophysiopathological mechanisms linking epilepsy and headache. *Med. Hypotheses* 70, 1150–1154. doi: 10.1016/j.mehy.2007.11.013

Patel, D. C., Tewari, B. P., Chaunsali, L., and Sontheimer, H. (2019). Neuron-glia interactions in the pathophysiology of epilepsy. *Nat. Rev. Neurosci.* 20, 282–297. doi: 10.1038/s41583-019-0126-4

Pekny, M., Wilhelmsson, U., and Pekna, M. (2014). The dual role of astrocyte activation and reactive gliosis. *Neurosci. Lett.* 565, 30–38. doi: 10.1016/j.neulet.2013.12.071

Peters, O., Schipke, C. G., Hashimoto, Y., and Kettenmann, H. (2003). Different mechanisms promote astrocyte Ca^{2+} waves and spreading depression in the mouse neocortex. *J. Neurosci.* 23, 9888–9896. doi: 10.1523/JNEUROSCI.23-30-09888.2003

Petrelli, F., and Bezzi, P. (2016). Novel insights into gliotransmitters. *Curr. Opin. Pharmacol.* 26, 138–145. doi: 10.1016/j.coph.2015.11.010

Pierre, K., and Pellerin, L. (2005). Monocarboxylate transporters in the central nervous system: distribution, regulation and function. *J. Neurochem.* 94, 1–14. doi: 10.1111/j.1471-4159.2005.03168.x

Post, R. M., and Silberstein, S. D. (1994). Shared mechanisms in affective illness, epilepsy and migraine. *Neurology* 44, S37–47.

Ransom, B. R. (1992). Glial modulation of neural excitability mediated by extracellular pH: a hypothesis. *Prog. Brain Res.* 94, 37–46. doi: 10.1016/s0079-6123(08)61737-9

Ransom, B. R. (2000). Glial modulation of neural excitability mediated by extracellular pH: a hypothesis revisited. *Prog. Brain Res.* 125, 217–228. doi: 10.1016/S0079-6123(00)25012-7

Reiss, W. G., and Oles, K. S. (1996). Acetazolamide in the treatment of seizures. *Ann. Pharmacother.* 30, 514–519. doi: 10.1177/106002809603000515

Ribelayga, C., and Mangel, S. C. (2005). A circadian clock and light/dark adaptation differentially regulate adenosine in the mammalian retina. *J. Neurosci.* 25, 215–222. doi: 10.1523/JNEUROSCI.3138-04.2005

Ribelayga, C., and Mangel, S. C. (2019). Circadian clock regulation of cone to horizontal cell synaptic transfer in the goldfish retina. *PLoS One* 14:e0218818. doi: 10.1371/journal.pone.0218818

Rice, M. E., and Nicholson, C. (1988). Behavior of extracellular K^+ and pH in skate (Raja erinacea) cerebellum. *Brain Res.* 461, 328–334. doi: 10.1016/0006-8993(88)90263-6

Robel, S., and Sontheimer, H. (2016). Glia as drivers of abnormal neuronal activity. *Nat. Neurosci.* 19, 28–33. doi: 10.1038/nn.4184

Rogawski, M. A. (2008). Common pathophysiologic mechanisms in migraine and epilepsy. *Arch. Neurol.* 65, 709–714. doi: 10.1001/archneur.65.6.709

Rose, C. R., Felix, L., Zeug, A., Dietrich, D., Reiner, A., and Henneberger, C. (2017). Astroglial glutamate signaling and uptake in the hippocampus. *Front. Mol. Neurosci.* 10:451. doi: 10.3389/fnmol.2017.00451

Rosenberg, S. S., and Spitzer, N. C. (2011). Calcium signaling in neuronal development. *Cold Spring Harb. Perspect. Biol.* 3:a004259. doi: 10.1101/cshperspect.a004259

Sahlender, D. A., Savtchouk, I., and Volterra, A. (2014). What do we know about gliotransmitter release from astrocytes? *Philos. Trans. R. Soc. Lond. B Biol. Sci.* 369:20130592. doi: 10.1098/rstb.2013.0592

Savtchouk, I., and Volterra, A. (2018). Gliotransmission: beyond black-and-white. *J. Neurosci.* 38, 14–25. doi: 10.1523/JNEUROSCI.0017-17.2017

Savtchouk, I., Carriero, G., and Volterra, A. (2018). Studying axon-astrocyte functional interactions by 3D two-photon Ca^{2+} imaging: a practical guide to experiments and "big data" analysis. *Front. Cell. Neurosci.* 12:98. doi: 10.3389/fncel.2018.00098

Schock, S. C., Munyao, N., Yakubchyk, Y., Sabourin, L. A., Hakim, A. M., Ventureyra, E. C. G., et al. (2007). Cortical spreading depression releases ATP into the extracellular space and purinergic receptor activation contributes to the induction of ischemic tolerance. *Brain Res.* 1168, 129–138. doi: 10.1016/j.brainres.2007.06.070

Semyanov, A., Henneberger, C., and Agarwal, A. (2020). Making sense of astrocytic calcium signals-from acquisition to interpretation. *Nat. Rev. Neurosci.* 19:182. doi: 10.1038/s41583-020-0361-8

Shigetomi, E., Saito, K., Sano, F., and Koizumi, S. (2019). Aberrant calcium signals in reactive astrocytes: a key process in neurological disorders. *Int. J. Mol. Sci.* 20, 20–996. doi: 10.3390/ijms20040996

Smith, P. J. (1995). Non-invasive ion probes–tools for measuring transmembrane ion flux. *Nature* 378, 645–646. doi: 10.1038/378645a0

Smith, P. J. S., Collis, L. P., and Messerli, M. A. (2010). Windows to cell function and dysfunction: signatures written in the boundary layers. *Bioessays* 32, 514–523. doi: 10.1002/bies.200900173

Smith, P., Hammar, K., and Porterfield, D. M. (1999). Self-referencing, non-invasive, ion selective electrode for single cell detection of trans-plasma membrane calcium flux. *Microsc. Res. Tech.* 46, 398–417. doi: 10.1002/(SICI)1097-0029(19990915)46:6<398::AID-JEMT8>3.0.CO;2-H

Smith, P., Sanger, R. H., and Messerli, M. A. (2007). "Principles, development and applications of self-referencing electrochemical microelectrodes to the determination of fluxes at cell membranes," in *Electrochemical Methods for Neuroscience*, eds A. C. Michael, and L. M. Borland (Boca Raton, FL: Electrochemical Methods for Neuroscience), 373–405.

Smith, P., and Trimarchi, J. (2001). Noninvasive measurement of hydrogen and potassium ion flux from single cells and epithelial structures. *Am. J. Physiol., Cell Physiol.* 280, C1–C11. doi: 10.1152/ajpcell.2001.280.1.C1

Sofroniew, M. V., and Vinters, H. V. (2010). Astrocytes: biology and pathology. *Acta Neuropathol.* 119, 7–35. doi: 10.1007/s00401-009-0619-8

Somieski, P., and Nagel, W. (2001). Measurement of pH gradients using an ion-sensitive vibrating probe technique (IP). *Pflugers Arch.* 442, 142–149. doi: 10.1007/s004240000505

Somjen, G. G. (2005). Aristides Leão's discovery of cortical spreading depression. *J. Neurophysiol.* 94, 2–4. doi: 10.1152/classicessays.00031.2005

Stafstrom, C. E., and Carmant, L. (2015). Seizures and epilepsy: an overview for neuroscientists. *Cold Spring Harb. Perspect. Med.* 5:a022426. doi: 10.1101/cshperspect.a022426

Syková, E., and Nicholson, C. (2008). Diffusion in brain extracellular space. *Physiol. Rev.* 88, 1277–1340. doi: 10.1152/physrev.00027.2007

Takizawa, T., Ayata, C., and Chen, S.-P. (2020). Therapeutic implications of cortical spreading depression models in migraine. *Prog. Brain Res.* 255, 29–67. doi: 10.1016/bs.pbr.2020.05.009

Tchernookova, B. K., Gongwer, M. W., George, A., Goeglein, B., Powell, A. M., Caringal, H. L., et al. (2021). ATP-mediated increase in H^+ flux from retinal Müller cells: a role for Na^+/H^+ exchange. *J. Neurophysiol.* 125, 184–198. doi: 10.1152/jn.00546.2020

Tchernookova, B. K., Heer, C., Young, M., Swygart, D., Kaufman, R., Gongwer, M., et al. (2018). Activation of retinal glial (Müller) cells by extracellular ATP induces pronounced increases in extracellular H^+ flux. *PLoS One* 13:e0190893. doi: 10.1371/journal.pone.0190893

Teive, H. A. G., Kowacs, P. A., Maranhão Filho, P., Piovesan, E. J., and Werneck, L. C. (2005). Leao's cortical spreading depression: from experimental 'artifact' to physiological principle. *Neurology* 65, 1455–1459. doi: 10.1212/01.wnl.0000183281.12779.cd

Theparambil, S. M., Hosford, P. S., Ruminot, I., Kopach, O., Reynolds, J. R., Sandoval, P. Y., et al. (2020). Astrocytes regulate brain extracellular pH *via* a neuronal activity-dependent bicarbonate shuttle. *Nat. Commun.* 11:5073. doi: 10.1038/s41467-020-18756-3

Theparambil, S. M., Naoshin, Z., Defren, S., Schmaelzle, J., Weber, T., Schneider, H.-P., et al. (2017). Bicarbonate sensing in mouse cortical astrocytes during extracellular acid/base disturbances. *J. Physiol.* 595, 2569–2585. doi: 10.1113/JP273394

Theparambil, S. M., Ruminot, I., Schneider, H. P., Shull, G. E., and Deitmer, J. W. (2014). The electrogenic sodium bicarbonate cotransporter NBCe1 is a high-affinity bicarbonate carrier in cortical astrocytes. *J. Neurosci.* 34, 1148–1157. doi: 10.1523/JNEUROSCI.2377-13.2014

Thiry, A., Dogné, J.-M., Supuran, C. T., and Masereel, B. (2007). Carbonic anhydrase inhibitors as anticonvulsant agents. *Curr. Top Med. Chem.* 7, 855–864. doi: 10.2174/156802607780636726

Thomas, R. C. (2009). The plasma membrane calcium ATPase (PMCA) of neurones is electroneutral and exchanges 2 H^+ for each Ca^{2+} or Ba^{2+} ion extruded. *J. Physiol.* 587, 315–327. doi: 10.1113/jphysiol.2008.162453

Thoreson, W. B., and Mangel, S. C. (2012). Lateral interactions in the outer retina. *Prog. Retin. Eye Res.* 31, 407–441. doi: 10.1016/j.preteyeres.2012.04.003

Tian, G.-F., Azmi, H., Takano, T., Xu, Q., Peng, W., Lin, J., et al. (2005). An astrocytic basis of epilepsy. *Nat. Med.* 11, 973–981. doi: 10.1038/nm1277

Tong, C. K., Brion, L. P., Suarez, C., and Chesler, M. (2000). Interstitial carbonic anhydrase (CA) activity in brain is attributable to membrane-bound CA type IV. *J. Neurosci.* 20, 8247–8253. doi: 10.1523/JNEUROSCI.20-22-08247.2000

Tong, C. K., and Chesler, M. (2000). Modulation of spreading depression by changes in extracellular pH. *J. Neurophysiol.* 84, 2449–2457. doi: 10.1152/jn.2000.84.5.2449

Toth, A. B., Hori, K., Novakovic, M. M., Bernstein, N. G., Lambot, L., and Prakriya, M. (2019). CRAC channels regulate astrocyte Ca^{2+} signaling and gliotransmitter release to modulate hippocampal GABAergic transmission. *Sci. Signal* 12:eaaw5450. doi: 10.1126/scisignal.aaw5450

Traynelis, S. F., and Cull-Candy, S. G. (1990). Proton inhibition of N-methyl-D-aspartate receptors in cerebellar neurons. *Nature* 345, 347–350. doi: 10.1038/345347a0

Traynelis, S. F., Hartley, M., and Heinemann, S. F. (1995). Control of proton sensitivity of the NMDA receptor by RNA splicing and polyamines. *Science* 268, 873–876. doi: 10.1126/science.7754371

Traynelis, S. F., Wollmuth, L. P., McBain, C. J., Menniti, F. S., Vance, K. M., Ogden, K. K., et al. (2010). Glutamate receptor ion channels: structure, regulation and function. *Pharmacol. Rev.* 62, 405–496. doi: 10.1124/pr.109.002451

Vandenberg, R. J., and Ryan, R. M. (2013). Mechanisms of glutamate transport. *Physiol. Rev.* 93, 1621–1657. doi: 10.1152/physrev.00007.2013

Vargas-Sánchez, K., Mogilevskaya, M., Rodríguez-Pérez, J., Rubiano, M. G., Javela, J. J., and González-Reyes, R. E. (2018). Astroglial role in the pathophysiology of status epilepticus: an overview. *Oncotarget* 9, 26954–26976. doi: 10.18632/oncotarget.25485

Verkhratsky, A. (2019). Astroglial calcium signaling in aging and Alzheimer's disease. *Cold Spring Harb. Perspect. Biol.* 11:a035188. doi: 10.1101/cshperspect.a035188

von Bernhardi, R. (ed.). (2016). *Glial Cells in Health and Disease of the CNS.* Cham: Springer International Publishing.

Wang, T.-M., Holzhausen, L. C., and Kramer, R. H. (2014). Imaging an optogenetic pH sensor reveals that protons mediate lateral inhibition in the retina. *Nat. Neurosci.* 17, 262–268. doi: 10.1038/nn.3627

Weissman, T. A., Riquelme, P. A., Ivic, L., Flint, A. C., and Kriegstein, A. R. (2004). Calcium waves propagate through radial glial cells and modulate proliferation in the developing neocortex. *Neuron* 43, 647–661. doi: 10.1016/j.neuron.2004.08.015

Womac, A. D., Burkeen, J. F., Neuendorff, N., Earnest, D. J., and Zoran, M. J. (2009). Circadian rhythms of extracellular ATP accumulation in suprachiasmatic nucleus cells and cultured astrocytes. *Eur. J. Neurosci.* 30, 869–876. doi: 10.1111/j.1460-9568.2009.06874.x

Wu, S. M. (1994). Synaptic transmission in the outer retina. *Annu. Rev. Physiol.* 56, 141–168. doi: 10.1146/annurev.ph.56.030194.001041

Xie, A. X., Petravicz, J., and McCarthy, K. D. (2015). Molecular approaches for manipulating astrocytic signaling *in vivo*. *Front. Cell. Neurosci.* 9:144. doi: 10.3389/fncel.2015.00144

Yu, X., Nagai, J., and Khakh, B. S. (2020). Improved tools to study astrocytes. *Nat. Rev. Neurosci.* 21, 121–138. doi: 10.1038/s41583-020-0264-8

Zanotti, S., and Charles, A. (1997). Extracellular calcium sensing by glial cells: low extracellular calcium induces intracellular calcium release and intercellular signaling. *J. Neurochem.* 69, 594–602. doi: 10.1046/j.1471-4159.1997.69020594.x

Zarcone, D., and Corbetta, S. (2017). Shared mechanisms of epilepsy, migraine and affective disorders. *Neurol. Sci.* 38, 73–76. doi: 10.1007/s10072-017-2902-0

Zerangue, N., and Kavanaugh, M. P. (1996). Flux coupling in a neuronal glutamate transporter. *Nature* 383, 634–637. doi: 10.1038/383634a0

Zhao, H., Carney, K. E., Falgoust, L., Pan, J. W., Sun, D., and Zhang, Z. (2016). Emerging roles of Na^+/H^+ exchangers in epilepsy and developmental brain disorders. *Prog. Neurobiol.* 138, 19–35. doi: 10.1016/j.pneurobio.2016.02.002

Zimmer, T. S., Broekaart, D. W. M., Gruber, V.-E., van Vliet, E. A., Mühlebner, A., and Aronica, E. (2020). Tuberous sclerosis complex as disease model for investigating mTOR-related gliopathy during epileptogenesis. *Front. Neurol.* 11:1028. doi: 10.3389/fneur.2020.01028

Conflict of Interest: The authors declare that the research was conducted in the absence of any commercial or financial relationships that could be construed as a potential conflict of interest.

Publisher's Note: All claims expressed in this article are solely those of the authors and do not necessarily represent those of their affiliated organizations, or those of the publisher, the editors and the reviewers. Any product that may be evaluated in this article, or claim that may be made by its manufacturer, is not guaranteed or endorsed by the publisher.

Advantages of publishing in Frontiers

OPEN ACCESS
Articles are free to read for greatest visibility and readership

FAST PUBLICATION
Around 90 days from submission to decision

HIGH QUALITY PEER-REVIEW
Rigorous, collaborative, and constructive peer-review

TRANSPARENT PEER-REVIEW
Editors and reviewers acknowledged by name on published articles

Frontiers
Avenue du Tribunal-Fédéral 34
1005 Lausanne | Switzerland

Visit us: www.frontiersin.org
Contact us: frontiersin.org/about/contact

REPRODUCIBILITY OF RESEARCH
Support open data and methods to enhance research reproducibility

DIGITAL PUBLISHING
Articles designed for optimal readership across devices

FOLLOW US
@frontiersin

IMPACT METRICS
Advanced article metrics track visibility across digital media

EXTENSIVE PROMOTION
Marketing and promotion of impactful research

LOOP RESEARCH NETWORK
Our network increases your article's readership